MODELLING THE IMPACTS OF CLIMATE CHANGE ON SEDIMENT YIELD IN THE SONGWE RIVER SUB-BASIN, TANZANIA

LUPAKISYO GEORGE MWALWIBA

A THESIS SUBMITTED IN FULFILMENT OF THE REQUIREMENTS FOR THE DEGREE OF DOCTOR OF PHILOSOPHY IN CIVIL ENGINEERING OF THE MBEYA UNIVERSITY OF SCIENCE AND TECHNOLOGY

DECEMBER, 2025

MBEYA UNIVERSITY OF SCIENCE AND TECHNOLOGY

MODELLING THE IMPACTS OF CLIMATE CHANGE ON SEDIMENT YIELD IN THE SONGWE RIVER SUB-BASIN, TANZANIA

LUPAKISYO GEORGE MWALWIBA

DECEMBER, 2025

CERTIFICATION

The Undersigned certify that we have read and hereby recommend for acceptance by the Mbeya University of Science and Technology the thesis entitled "**Modelling the Impacts of Climate Change on Sediment Yield in the Songwe River Sub-basin, Tanzania**" in fulfillment of the requirements for the degree of Doctor of Philosophy in Civil Engineering of the Mbeya University of Science.

Dr. GISLAR E. KIFANYI, Date 03/12/2025, Signature .....

(Major Supervisor)

DR. EDMUND MUTAYOBA, Date 3/12/2025, Signature .....

(Co-Supervisor)

PROF. JULIUS M. NDAMBUKI, Date 3/12/2025, Signature .....

(Co-Supervisor)

Accepted by Senate, Name ..... Date 03/12/2025

Signature .....

DECLARATION

AND

COPYRIGHT

I, **Lupakisyo George Mwalwiba**, declare that this thesis is my original work and that it has not been presented and will not be presented to any other University for a similar or any other degree award.

Signature .....

Date 03/12/2025

ACKNOWLEDGEMENT

I am profoundly thankful to the Almighty God, my source of strength and knowledge, for giving upon me this chance and enabling me to successfully complete this journey. I wish to convey my profound appreciation to the Mbeya University of Science and Technology for its comprehensive sponsorship and financial assistance which facilitated my PhD research endeavours. The trip begun with a solitary step and progressively developed into a substantial undertaking, and finally to the conclusions. My excitement and sense of achievement would be incomplete without recognising the contributions and support of everyone who helped me during my PhD studies. This concise acknowledgement does not reduce the significance of the assistance I have received from both those named and those unnamed. I wish to convey my sincere gratitude to my supervisors, Dr Gislar E. Kifanyi, Dr Edmund Mutayoba, and the late Prof. Julius M. Ndambuki whose scientific counsel, guidance, constructive recommendations, exceptional patience, and unwavering support over the past five years have been pivotal to the successful completion of my study. I shall forever recall their scholarly prowess, kindness, and optimistic disposition in assisting me with every obstacle. I extend my heartfelt gratitude to the Postgraduate Committee panel members of the Department of Civil Engineering for their insightful input at each level of the thesis development which significantly improved the quality of the work. Gratitude is extended to Dr Patrice Nyangi, the Head of Civil Department for his generous assistance and steadfast support during this process. I express my gratitude to the Civil Engineering Department staff member and the entire Mbeya University of Science and Technology (MUST) for their support. To my fellow postgraduate students for their encouragement throughout mystudy. I wish to express my gratitude to the Lake Rukwa Water Basin office for providing with data essential for my study. I express my profound gratitude to Mr. Nyemo Chillagane and Mr. Willfred Molla for their assistance in collecting data. I extend my sincere gratitude to my family for their enduring love and encouragement, and unwavering support during the whole period of my study.

DEDICATION

I dedicate this research to my family and those who supported and assisted me throughout the execution of this study**.**

ABBREVIATIONS AND ACRONYMS

AGNPS	Agricultural Non-Point Source Pollution Model
ALOS PALSAR	Advanced Land Observing Satellite Phased Array L-band Synthetic Aperture Radar
AR5	Fifth Assessment Report
CA	Cellular Automata (CA) – Markov Model
CC	Correlation Coefficient
CCI	Climate Change Initiative
CDF	Cumulative Distribution Function
CH4	Methane
CO2	Carbon dioxide
CORDEX	Coordinated Regional Climate Downscaling Experiment
CS	Curve Number
CV	Coefficient of Variation
DCM	Delta Change Method
DEM	Digital Elevation Model
DEMs	Digital Elevation Models
EOF	Empirical Orthogonal Function
EQM	Empirical Quantile Mapping
ESGF	Earth System Grid Federation
EUROSEM	European Soil Erosion Model
FAO	Food and Agriculture Organization
GCMs	General Circulation Models
GHGS	Greenhouse Gases
GIS	Geographic Information System
HRU	Hydrologic Response Units
HSPF	Hydrological Simulation Program Fortran
IPCC	Intergovernmental Penelon Climate Change
ISODATA	Iterative Self-Organizing Data Analysis
K	Kappa Coefficient

LH-OAT	Latin Hypercube One Factor-At-A-Time
LHS	Latin Hypercube Sampling
LULC	Land Use Land Cover
MAE	Mean Absolute Error
MLC	Maximum Likelihood Classification
MUSLE	Modified Universal Soil Loss Equation
N2O	Nitrous Oxide
NSE	Nash-Sutcliffe Efficiency
PA	Producer's Accuracy (PA),
PBIAS	Percent Bias
PQM	Parametric Quantile Mapping
QGIS	Quantum Geographic Information System
QM	Quantile Mapping
QSWAT	QGSI Interface for SWAT
R^2	Coefficient of Determination
RCMs	Regional Climate Models
RCPs	Representative Concentration Pathways
RMSE	Root Mean Square Error
RS	Remote Sensing
RUSLE	Revised Universal Soil Loss Equation
SRES	Special Report on Emission Scenarios
SUFI	Sequential Uncertainty Fitting
SWAT	Soil and Water Assessment Tool
UA	User's Accuracy
USDA – ARS Service	United States Department of Agriculture, Agricultural Research
USGS	United States Geological Survey
USLE	Universal Soil Loss Equation
UTM	Universal Transverse Mercator
WCRP	World Climate Research Program

WEPP	Water Erosion Prediction Project

ABSTRACT

Environmental decline driven by climate change affects hydrological and sedimentation processes, eventually, resulting to variations in sediment transport. The changes in temperature and precipitation are evident in developing countries including Tanzania. The Songwe River sub-basin is one of the areas climate changes which has experienced an increase in sediment production. However, there limited modelling studies that assess the impacts of climate change on sediment yield in the Songwe River sub-basin. This study aimed to model the impacts of climate change on sediment yield in the Songwe River sub-basin. The Soil and Water Assessment Tool (SWAT) model and QGIS software were used to simulate sediment yield under historical climate conditions (1984–2005) and future climate projections (2011–2040, 2041–2070 and 2071–2100) for RCP4.5 and RCP8.5. Precipitation and temperature data were obtained from four selected CORDEX regional climate models (CCLM4, HIRHAM5, RACMO22T and RCA4) driven by different General Circulation Models (GCMs). Bias correction of regional climate models (RCMs) output was done by using linear scaling method. Land use and land cover (LULC) maps for 1990, 2000 and 2020 were created from Landsat TM and OLI_TIRS imagery with supervised classification using the Maximum Likelihood Algorithm and Kappa statistics for accuracy assessment. Future LULC changes for 2040, 2070 and 2100 were projected using the Cellular Automata (CA) – Markov Model. The bias-corrected RCM outputs and LULC maps for 2020, 2040, 2070 and 2100 were input into the calibrated SWAT model to simulate sediment yield with results compared across the RCMs. The Soil Conservation Service (SCS) Curve Number for Moisture Condition II (CN2) was identified as the most sensitive parameter for simulating sediment yield. The findings indicate an increase in sediment yield over time with the most significant rise under the RCP8.5 scenario particularly in the late century where sediment yield could increase by 35–50%. The models projected a 10–15% increase in sediment yield by 2040, rising to 20–35% by 2070 with HIRHAM5 showing the largest increase. The study emphasizes the importance of a multi-model approach and highlights the vulnerability of elevated sub-basins near agricultural areas to increased sedimentation. The findings support incorporating climate change adaptation strategies into national and regional water and land management policies.

TABLE OF CONTENTS

LIST OF FIGURES

LIST OF APPENDINCES

LIST OF TABLES

CHAPTER ONE

INTRODUCTION

1.1 Background

Global rivers and streams are experiencing heightened pollution from sediments and nutrient (Hailu et al., 2023; Ijaz et al., 2022; Kolli et al., 2021). The East African Rift Valley lakes, among the largest and most ecologically diversified aquatic systems worldwide, furnish vital resources such as water, food, and livelihoods for millions of individuals (Amasi et al., 2021). Increased sediment influx from adjacent catchments has resulted in siltation and eutrophication of rivers and lakes (Ang & Oeurng, 2018; Hailu et al., 2023; Kolli et al., 2021), rendering the water unfit for human consumption and detrimental to aquatic ecosystems (Echogdali et al., 2022; Guzman et al., 2017; J. Kimwaga, 2012). Environmental deterioration has garnered international focus as climate change impacts natural systems including hydrological and sedimentation processes (Chen et al., 2019; Guzman et al., 2017; Luhunga et al., 2018; Shrestha & Wang, 2018) These mechanisms are responsive to alterations in temperature, precipitation and evapotranspiration due to the climate (Chapman et al., 2021; Theron et al., 2021). Anthropogenic sediment retention, socio-economic advancement and impacts of climate change have resulted in variations in river sediment transport to floodplains and lakes consequently impairing downstream ecosystems worldwide (Jilo et al., 2019; Wynants et al., 2021). These problems are particularly evident in many catchments notably in Asia and Africa (Daniel & Abate, 2022; Jilo et al., 2019; Parajuli & Risal, 2021). Climate change has become one of the most pressing environmental issues of the 21st century mainly affecting natural and human systems. Increasing levels of greenhouse gases including CO_2, CH_4, and N_2O are principal catalysts of global warming (M. T. Assfaw et al., 2023; Azari et al., 2016; Gadissa et al., 2018; Kido et al., 2023). Human activities such as fossil fuel burning, deforestation and industrial processes have intensified greenhouse effect and increased global temperatures(Assfaw et al., 2023; Azari et al., 2016; Gitima et al., 2023; Luhunga et al., 2018; Mnyali & Materu, 2021). Global temperatures are anticipated to rise by 1.5°C to 4.5°C by the end of the century (Assfaw, 2019; Azari et al., 2016; Gadissa et al., 2018). Climate change modifies hydrological cycles, affecting precipitation

patterns, intensity and frequency which significantly impacts sediment yield due to an increased aggregate quantity of eroded material conveyed from terrestrial surfaces to rivers and downstream aquatic systems (Assfaw et al., 2023; Chen et al., 2019; Theron et al., 2021; Tibangayuka et al., 2022).

Multiple research studies have examined impacts of climate change on sediment yield in diverse places by utilising hydrological and climate models (Feyissa Negewo & Kumar Sarma, 2022; Lazaro et al., 2023; Mbungu, Heatwole, et al., 2016; Mfwango et al., 2022; Shinhu et al., 2023). These studies demonstrated that sediment yield varies in response to climatic changes across different locations underscoring the necessity for location-specific assessments to forecast and alleviate these impacts (Feyissa Negewo & Kumar Sarma, 2022; Gadissa et al., 2018; Masson-Delmotte et al., 2019; Parajuli & Risal, 2021). For example, in the Upper Blue Nile Basin of Ethiopia climate change projections indicate a substantial rise in sediment flow influenced by high precipitation and alterations in land use and land cover (Tekalegn and Diekkrüger, 2017). These alterations intensify soil erosion adversely affecting agricultural productivity and lifetime of reservoirs (Chapman et al., 2021; Echogdali et al., 2022; Marko et al., 2023; Melesse & Abtew, 2015). Similar patterns have been noted in the Loess Plateau of China where increased precipitation has augmented sediment yield notwithstanding persistent soil conservation initiatives (Shrestha et al., 2012; Zhang et al., 2016). A study in the Mekong River Basin illustrates the impacts of climate and land-use alterations on sediment discharge, highlighting necessity for tailored management approaches (Zhang et al., 2016) The diverse outcomes illustrate importance of regional research in understanding the impact of climate change and land use/land cover alterations on local sediment dynamics.

In Tanzania, climate change and alterations in land use and land cover have greatly affected sediment production. Alterations in precipitation patterns, increasing temperatures and severe weather phenomena are transforming natural environment (Kassian et al., 2017; Lalika et al., 2015; Mbungu, Easton, et al., 2016; Melchioly, 2021; Mfwango et al., 2022). Climate change in Tanzania has modified precipitation patterns resulting in intensified and erratic rainfall in certain regions of the country while others endure extended droughts (Luhunga et al., 2018; Nachmany, 2018;

Shemsanga et al., 2010). Elevated rainfall intensity has led to augmented surface runoff hence, facilitating sediment transfer from upstream regions to rivers and lakes (Gnitou et al., 2019; Kido et al., 2023; Theron et al., 2021; Xu et al., 2021). In contrast, diminished precipitation in some regions has led to a decline in plant cover rendering soil more vulnerable to erosion during sporadic rainfall events (Amasi et al., 2021; Kahimba et al., 2015; Kassian et al., 2017). In the Pangani River Basin for instance, increased sedimentation in reservoirs has been ascribed to erratic precipitation and alterations in land use induced by climatic changes (Lalika et al., 2015). Increasing temperatures have resulted in extended droughts succeeded by heavy rainfall which undermines soil integrity and hastens erosion (Amasi et al., 2021; Feger et al., 2017; Kangalawe, 2017; Mbungu, Easton, et al., 2016). Soil erosion in the Usangu Plains in southwestern Tanzania has intensified leading to increased sediment discharge into adjacent rivers (Mollel et al., 2023). This process has been further intensified by deforestation and unsustainable agricultural practices hastening land degradation (Mutayoba et al., 2018b).

The Songwe River sub-basin of the Lake Rukwa basin is vulnerable to climate change and alterations in land use and land cover (Mwalwiba et al., 2023). This sub-basin provides water for agricultural irrigation, energy generation, industrial operations, mining and home consumption rendering sediment yield a vital element for sustainable development and environmental stability (Amasi et al., 2021; Egberts, 2020; John et al., 2020; Valimba, 2019). The sediment production in the sub-basin is affected by diverse climatic factors and alterations in land use and land cover encompassing variations in precipitation and temperature changes (Augustsson et al., 2013; Luo et al., 2018; Mbungu, Easton, et al., 2016; Noel, 2014; Zhang et al., 2019). Climate change and alterations in land use and land cover have led to a rise in the frequency and severity of extreme events including intense rainfall, soil erosion and sediment yield (Guilyardi et al., 2018). In the Songwe River sub-basin these occurrences result in flash floods substantially increasing sediment output over brief periods which may harm infrastructure and impact downstream ecosystem (Jcu, 2016; Mtelela, 2018; Valimba, 2019). The sub-basin is also confronted with deforestation, land degradation, soil erosion, sedimentation and deteriorated water quality as a result of climate change

and alterations in land use and land cover (Amasi et al., 2021; John et al., 2020; Mwalwiba et al., 2023). These issues exacerbate water resource management, heightening flooding, erosion, sedimentation and land degradation.

Although extensive research on climate change, land use/land cover change and sediment yield has been undertaken in temperate regions where terrain, climate and land use patterns diverge from those in sub-Saharan Africa (Chen et al., 2020; Chiphang et al., 2022; Zhou et al., 2017), the distinctive attributes of the Songwe River sub-basin necessitate targeted investigations. The interplay between climate change, hydrological processes and sediment transport in this area has been the subject of limited research (Valimba, 2019). While it is well acknowledged that climate change and land use alterations affect sediment yield (Kangalawe, 2017; Leta et al., 2023), there is a lack of studies investigating the interaction of these elements with climatic variability and land use/land cover changes in the Songwe River sub-basin. The lack of long-term sediment yield data impedes thorough trend analysis and scenario planning (FAO, 2014).

Consequently, assessing the hydrological impacts of climatic variability and alterations in land use/land cover within the sub-basin is crucial given the lack of study on these topics in the Songwe River sub-basin (Kassian et al., 2017; Miller & Doyle, 2014; Mrad et al., 2024; Shemsanga et al., 2010).

This study models the impacts of climate change on sediment yield in the Songwe River sub-basin by using high-resolution climate projections and SWAT model for the first time in this region. This study was aimed to augment the geographical resolution of climate data and sediment yield modelling to elucidate the potential impacts of future climate scenarios on sub-basin sediment dynamics facilitating the development of effective management strategies to offset these impacts.

1.2 Statement of the Problem

Environmental degradation driven by climate change has emerged as a pressing global concern significantly affecting hydrological and sedimentation processes. The alterations marked by variations in temperature and precipitation impact water systems particularly in river basins. The rising occurrence of extreme weather events in

Tanzania including floods and droughts coupled with rising temperatures and modified rainfall patterns interrupt river flows and increase sediment discharge. The Songwe River sub-basin has witnessed increasing sediment yield and soil erosion as a result of climate change which threatens its water supplies, agricultural productivity and ecological integrity. Despite the increasing acknowledgement of these threats there is a significant gap in modelling studies that specifically model the impacts of climate change on sediment yield in the sub-basin.

Previous studies have concentrated on hydrology and water resources with no emphasis on how climate change affects sediment dynamics in the sub-basin. The lack in understanding is vital as the interaction among altered precipitation patterns, increasing temperatures and extreme weather phenomena intensify soil erosion and sediment discharge. These changes present considerable difficulties for water resource management, land management and agricultural activities. Acquiring a thorough understanding of the impact of climate changes on sediment yield is crucial for formulating effective management methods and mitigating soil erosion and sedimentation in the sub-basin.

Addressing this gap is vital for shaping future land and water management policies which are essential for sustaining the long-term viability of ecosystems and agricultural output of the Songwe River sub-basin. Therefore, this study aims to model the impacts of climate change on sediment yield in the Songwe River sub-basin under two future climate scenarios. The study investigates how temperature fluctuations and changes in precipitation influence sedimentation. The findings help policymakers and resource managers in developing adaptive measures to reduce the impacts of climate change and guarantee long-term management.

1.3 Objectives

1.3.1 Main Objective

The main objective of this research is to model impacts of climate change on sediment yield in the Songwe River sub-basin, Tanzania.

1.3.2 Specific Objectives

i. To characterize and map sediment sources in the Songwe River sub-basin

ii. To determine sediment yield under different climate scenarios in the Songwe River sub-basin
iii. To evaluate impacts of climate change under different scenarios on sediment yield in the Songwe River sub-basin

1.4 Research Questions

i. What are the characteristics of sediment sources, and where are the principal sources situated in the Songwe River sub-basin?
ii. In what ways have past climate patterns (precipitation and temperature) affected sediment yield in the Songwe River sub-basin?
iii. What are the anticipated impacts of forthcoming climate change scenarios on sediment yield in the Songwe River sub-basin?

1.5 Justification

Climate variability and future climate change are anticipated to progressively influence sediment production in the most susceptible sub-basins of developing countries (Ddamulira, 2016; Parajuli & Risal, 2021; Serpa et al., 2015; Stone, 2015). The Songwe River sub-basin similar to other river basins worldwide is vulnerable to these alterations. Changes in precipitation patterns, increasing temperatures and extreme weather events can disrupt hydrological cycles and accelerate soil erosion resulting in elevated sedimentation (Azim et al., 2016; Parajuli & Risal, 2021). This alteration consequently risks the basin's agricultural output, water quality and essential infrastructure such as reservoirs and irrigation systems (Chen et al., 2020; Neverman et al., 2023).

This study utilized remote sensing, geographic information systems (GIS), regional climatic models and the SWAT (Soil and Water Assessment Tool) model to improve comprehension of process evolution across various climatic conditions. This study examines variations in sediment yield and predicts future patterns for three specific periods: 2011–2040, 2041–2070 and 2071–2100. The SWAT model forecasts the impacts of climate change on sediment yield and supplying essential data to guide policy formulation and risk mitigation methods.

The study uses historical and predictive data to investigate the impacts of climate change on sediment yield in the Songwe River sub-basin by providing critical insights for sustainable water resource management and environmental planning in Tanzania. This study is one of the initial thorough evaluations of the correlation between climatic change and sediment yield in the Songwe River sub-basin, filling a notable gap in the current literature. The results of this study enhance worldwide comprehension of the impacts of climate-induced alterations in precipitation, temperature and extreme weather phenomena on sediment dynamics in sub-Saharan Africa.

The study is relevant not just to the Songwe River Sub-Basin but also to areas with similar climatic and socio-economic characters. The study enhances global discourse on climate change adaptation by presenting a case from a region especially vulnerable to climate change impacts. This research promotes sustainable development by providing techniques to mitigate soil erosion and manage sedimentation as well as essential elements of integrated watershed management. It underscores the pressing necessity for revised water policy in Tanzania particularly, in the Songwe River sub-basin, to tackle the intensifying problem of amplified sediment yield resulting from climate change.

1.6 Scope and Limitations of the Research

This research concentrates on the Songwe River sub-basin in Tanzania a significant area within the broader Lake Rukwa Basin. The study examines modelling impacts of climate change on sediment yield in relation to present and future climate scenarios. The study uses hydrological modelling tools specifically the Soil and Water Assessment Tool (SWAT) model to simulate sediment yield dynamics under varying climate conditions. SWAT is an effective instrument for assessing the impacts of land use, climate variability, and water management practices on sediment transport.

The research employs projections from four regional climate models (RCMs) based on two representative concentration pathways, namely RCP4.5 and RCP8.5, to analyze the impacts of temperature and precipitation on sediment dynamics in the Songwe River sub-basin over time. The research recognizes the impact of climate change and examines how these changes intensify or mitigate sediment yield. Although the

research includes a wide range of topics related to climate change and different future land use scenarios, it primarily highlights the direct impacts of climate change on sediment transport mechanisms.

This research also possesses drawbacks. The geographic scope is limited to the Songwe River sub-basin indicating that the results may not be immediately relevant to other river basins in Tanzania or similar areas in sub-Saharan Africa that may encounter different climatic and land use conditions. Therefore, we should carefully view the study's results within the Songwe River sub-basin and extrapolate them to other areas.

Furthermore, the research is significantly dependent on SWAT model which although thorough is basically dependent on the quality and accuracy of the input data. These models might not account for all complex environmental variables or local socio-economic factors that could potentially influence sediment yield. The research is limited by the accessibility of historical climatic data and long-term sediment yield data potentially hindering the comprehensive calibration and validation of the model. As a result, projections of future sediment yield could be somewhat uncertain especially in regions with scarce data.

1.7 The Significance of the Research and Its Contribution to the Body of Knowledge.

This research is significant as it addresses a crucial knowledge gap regarding the interaction between climate change and sediment yield in the Songwe River sub-basin of Tanzania a region vulnerable to the impacts of climate variability. It offers vital information for water resource managers, regulators and environmental planners clarifying the impacts of shifting climate patterns and human activities on sediment dynamics with considerable implications for sustainable watershed management. By identifying these interconnections, the study lays the groundwork for developing adaptive strategies that can mitigate the adverse impacts of climate change. Ultimately, such insights can enhance resilience in the region's ecosystems and support the livelihoods of communities reliant on these vital resources.

The research is particularly relevant given the intensifying challenges posed by climate change in East Africa a region marked by unpredictable rainfall patterns, extreme weather events and increasing temperatures. This study focuses on the Songwe River sub-basin providing a vital regional assessment of climate changes in sediment yield. It aims to help in the development of strategies to mitigate the adverse impacts of climate change, such as soil erosion, declining water quality and infrastructure damage. The findings are expected to contribute to the creation of effective management strategies that take into account both current and future climate scenarios, thereby strengthening the resilience of local ecosystems and communities.

1.8 Organization of the Thesis

This thesis comprises five chapters, each concentrating on a fundamental aspect of the research process. The structure and content of each chapter are described as follows:

Chapter One presents the introduction of the research, covering the research background, problem statement, research objectives and research questions that direct the research and provides the justification for the analysis. It emphasizes the study's significance, highlighting its relevance to sustainable watershed management and climate change adaptation in the sub basin. This chapter outlines the scope and limitations of the research and concludes with an examination of its contribution to the current body of knowledge in sediment production and climate change.

Chapter Two presents a literature review; it offers an extensive examination of global and regional studies regarding the impacts of climate change on sediment yield, sediment transport models, and the hydrological dynamics of river basins. It examines essential subjects, such as sediment source characterization, hydrological models (notably the SWAT model), climatic models and land-use/land-cover dynamics. This chapter analyses the impacts of land use change, emphasizing future forecasts using the CA-Markov model. Furthermore, it illustrates the importance of sensitivity analysis and model calibration especially for data-scarce catchments in forecasting sediment yield across diverse climatic and land-use scenarios.

Chapter Three outlines the methods and materials employed for this research. It describes the research area, it outlines the research design approach and data sources,

encompassing satellite data, climate forecasts, topography data, soil data and land use data. The chapter also explains the rationale for selecting the SWAT model to simulate sediment yield under diverse climatic situations. The chapter examines the integration of climate change scenarios (using the RCP4.5 and RCP8.5 pathways) with estimates of land-use and land-cover changes and how these variables are employed to construct sediment transport dynamics. The process includes data validation, model calibration, and scenario analysis techniques, guaranteeing that the research produces strong results.

Chapter Four presents the results and discussion pertaining to each specific objective. It explains the results from the SWAT model simulations, highlighting the impacts of climate change on sediment yield within the Songwe River sub-basin. This aspect includes an examination of alterations in precipitation patterns, temperature variations, sediment generation, and extreme weather events. The chapter analyses the results across various climate scenarios and changes in land use/land cover, assessing their cumulative impacts on sediment dynamics. It further evaluates the characterization of sediment sources and its geographical distribution, helping estimate how variability and land use changes affect different regions of the sub basin. Additionally, the chapter includes results from the sensitivity analysis, model calibration, and validation.

Chapter Five presents the conclusion and recommendations. It summarizes the principal findings of the study, addressing their significance in relation to the theoretical framework and practical implementations within the designated location. This chapter examines the policy implications of the research and underscores its contributions to the discipline. Furthermore, it provides recommendations derived from the study's findings and identifies future research areas.

1.9 Concluding Remarks

In summary, Chapter One offers a detailed introduction to the study, establishing the background for understanding the impacts of climate change on sediment yield in the Songwe River Sub-basin. This chapter highlights the soil erosion and sedimentation issues which have been intensified by climate change. It also highlights the gap in existing research specific to the sub-basin. The chapter outlines the research

objectives, research questions, clearly addresses the significance and scope of the study, and provides an overview of the organization of the thesis. Overall, chapter one serves as the foundation for investigating the impacts of climate change on sediment yield in the Songwe River Sub-Basin, with the aim of informing sustainable water management practices and policy development to address the challenges posed by climate change.

CHAPTER TWO

LITERATURE REVIEW

2.1 General Overview

The review begins by examining the concepts and theories pertaining to sediment yield in river catchments, emphasizing the impscts of climate change on sediment yield. The study initiates by examining sediment yield in river catchments, highlighting the impacts of climate variability and land-use alterations on sediment transport dynamics within the basin. This chapter explores techniques for detecting sediment sources and analyzing sediment transport in the sub-basins. It also examines the function of climate models and scenarios in predicting future sediment yield trends especially concerning the potential impacts of climate change on precipitation patterns, temperature fluctuations and extreme weather occurrences. The chapter additionally examines the application of hydrological models particularly the SWAT model to simulate sediment dynamics including their calibration and validation procedures. The chapter ultimately delineates study deficiencies and offers suggestions for next investigations particularly with the incorporation of climate scenarios and their consequences for sediment yield management in the area.

2.2 Sediment Yield in River Sub-basins

Sediment yield refers the total quantity of sediment conveyed by a river or stream during a defined timeframe usually expressed as mass or volume per unit area (Ndomba, 2013). This information is a crucial factor in understanding erosion, sedimentation processes and the general condition of watersheds (Amasi et al., 2021; Appiah, 2015; Shinhu et al., 2023). Sediment yield is crucial for environmental management, infrastructure development and the conservation of riverine ecosystems (Based et al., 2018; Gharibdousti et al., 2019; Marco NDOMBA, 2010; Wynants et al., 2021). Complex interactions between natural and human-induced processes affect the extent of sediment yields (Bussi et al., 2016; Huong & Son, 2020; Ngo Thanh et al., 2020).

A multitude of studies have investigated sediment yield across various catchments using models like the Soil and Water Assessment Tool (SWAT) to forecast future scenarios (Chawanda et al., 2024; Chelkeba Tumsa, 2023; Feyissa Negewo & Kumar

Sarma, 2022; Ndulue & Mbajiorgu, 2018a; Nkwasa et al., 2022). In Tanzania and many African countries climate change has induced considerable alterations in precipitation and temperature mainly impacting river flow, soil erosion, sediment transport and watershed hydrology (Feyissa Negewo & Kumar Sarma, 2022; Luhunga et al., 2018; Tibangayuka et al., 2022). The varied topography, soil characteristics, climatic variations and land-use patterns in Tanzania result in significant river flows and sediment discharges (Amasi et al., 2021; Chilagane et al., 2020; Clement et al., 2016; Mfwango et al., 2022). Nevertheless, investigations concerning sediment yield in Tanzania, namely inside the Songwe River Sub-Basin are limited.

2.3 Factors Affecting Sediment Yield in River Sub-basins

Various factors including climate, land use, soil characteristics, terrain, plant cover and anthropogenic activities influence sediment yield in river catchments (Lahunga et al., 2016a; Luhunga et al., 2018; Mbungu, Easton, et al., 2016; Serdeczny et al., 2017). The Soil and Water Assessment Tool (SWAT) are extensively employed to simulate sediment production in river basins primarily due to its capacity to model complex interactions (Catchments, 2005; Chelkeba Tumsa, 2023; Marco & van, 2011). By utilizing SWAT researchers can obtain helpful information about how modifications in land management practices or climate conditions may affect sediment transport and erosion rates (Akoko et al., 2021; Chelkeba Tumsa, 2023; Chen et al., 2020; Marco & van, 2011; Memarian et al., 2014). This information is important when creating effective strategies to address sediment-related challenges in aquatic ecosystems. This section examines the key elements that influence sediment yield and discusses their integration into the SWAT model for sediment yield simulation.

2.3.1 Climate Variables

Climate is an important factor in determining sediment yield as variations in rainfall intensity, duration and frequency influence sediment transport dynamics (Djunarsjah et al., 2023; Lazaro et al., 2023; Mbungu, Heatwole, et al., 2016; Tian et al., 2016). Intense rainfall events lead to increased surface runoff thereby exacerbating soil erosion and facilitating the transfer of sediment into river systems. The SWAT model incorporates climatic data including precipitation and temperature to simulate hydrological processes, runoff and sediment movement (Gemechu et al., 2021; Mueller-

Warrant et al., 2019; Ndulue & Mbajiorgu, 2018b). It utilises rainfall-runoff correlations to evaluate surface runoff which directly impacts sediment yield. Furthermore, changes in climate patterns such as increased rainfall intensity or shifts in the timing of rainfall can substantially affect sediment yield (Kido et al., 2023) SWAT has been widely used to model sediment dynamics across various climate scenarios making it a vital tool for predicting future changes in sediment yield as a result of climate change (C. N. Chen et al., 2020; Ercan et al., 2020; Ndulue & Mbajiorgu, 2018a).

2.3.2 Land Use and Land Cover (LULC) Changes

Changes in land use and land cover (LULC) are pivotal determinants of sediment production as anthropogenic land use modifications can either intensify or mitigate erosion (Gobry et al., 2023; Memarian et al., 2014; X. ke Zhang et al., 2015). Deforestation, urbanisation and agricultural developments can diminish vegetation coverage and make the soil more susceptible to erosion. SWAT simulates these effects by integrating land use and land cover data to estimate the influence of changes in vegetation, impervious surface and agricultural practices on sediment generation (Bussi et al., 2016; Nguyen, 2019; Nyatuame et al., 2023). The model allocates distinct parameters for vegetation cover, soil erosion potential, and runoff characteristics to various land use categories. Agricultural operations like tilling and deforestation contribute to heightened sediment output by diminishing soil stability and increasing surface runoff. Several studies have been conducted to simulate the impacts of crop varieties, cultivation techniques and land management strategies on sediment production in agricultural regions by using the SWAT model (Bussi et al., 2016; Huon et al., 2017; Mfwango et al., 2022; Nguyen, 2019; Zhang et al., 2015).

2.3.3 Soil Properties

Soil parameters are crucial in influencing sediment yield as they regulate the volume of runoff and erosion during precipitation events. Soils having distinct textures, including clay, silt or sand demonstrate differing levels of erosion vulnerability. SWAT uses soil erodibility parameters obtained from the Universal Soil Loss Equation (USLE) to assess sediment yield based on soil texture, structure and permeability. Soil erodibility is directly correlated with the model's sediment yield forecasts (Hussain et al., 2019; Marko et al., 2023; Melesse & Abtew, 2015). Soils with elevated clay

concentration have less permeability and hence produce greater runoff resulting in enhanced erosion (Chen et al., 2020; Efthimiou et al., 2017; Sime & Abebe, 2022). Sandy soils are more susceptible to wind erosion in arid places but may not significantly contribute to water-related sediment output in areas with greater rainfall (Chapman et al., 2021; Wynants et al., 2021). By including soil texture structure and erodibility into the model SWAT can more precisely simulate sediment processes across various soil types.

2.3.4 Topography

Topographic characteristics, including slope, elevation and catchment morphology are vital determinants of sediment yield (Ndulue & Mbajiorgu, 2018a; Tenaw et al., 2024). Steeper gradients enhance runoff velocity and accelerate erosion thereby increasing sediment yield. The SWAT model integrates topography by employing digital elevation models (DEMs) to define slope and catchment characteristics (Ndulue & Mbajiorgu, 2018a). It simulates the impacts of topographic features on water movement across the terrain and their role in sediment transport. Steep slopes are associated with higher runoff coefficients and greater sediment mobilization. Additionally, SWAT can simulate the impact of topographical elements such as channels, gullies and valleys which collect runoff and contribute to heightened sediment yield in certain areas (Tenaw et al., 2024). SWAT is capable to incorporate topographic data significantly enhanced the model's effectiveness in predicting sediment processes in complex terrain.

2.3.5 Vegetation Cover

Vegetation plays a crucial role in reducing sediment production by protecting the soil from the direct impacts of rain and minimizing surface runoff (Bussi et al., 2016; Zhang et al., 2015). It helps intercept rainwater which decreases runoff velocity and enhances soil stability. The SWAT model incorporates vegetation cover into its simulations through various land cover types which influence the calculations of surface runoff and erosion (Nguyen, 2019). Different types of vegetation such as forests, grasslands and agricultural crops have specific criteria that affect erosion rates and sediment yield (Based et al., 2018; Huon et al., 2017; Mfwango et al., 2022; Worku et al., 2017). For instance, forests with dense canopy cover significantly reduce both

runoff and soil erosion whereas areas that are bare or have sparse vegetation are more susceptible to erosion. The SWAT model also simulates changes in plant cover due to factors such as deforestation, agricultural expansion or climate change by adjusting land cover parameters, thereby allowing predictions regarding the effects of shifts in vegetation on sediment dynamics (Belay & Mengistu, 2021; Chilagane et al., 2021).

2.3.6 Human Activities

Human activities, including deforestation, urbanization, agricultural practices and infrastructure development significantly influence sediment yield (Huong & Son, 2020; Yao et al., 2015). These activities often lead to soil degradation, increased runoff and heightened silt generation. The Soil and Water Assessment Tool (SWAT) simulate these human impacts by incorporating data on changes in land use, management strategies and infrastructure such as dams, roads and urban expansion (Addis et al., 2016; Chelkeba Tumsa, 2023; Himanshu et al., 2019). For instance, the construction of dams can trap sediments which reduces sediment output downstream while potentially causing sedimentation problems upstream. SWAT has been extensively employed to model the effects of such actions on sediment transport. In agricultural settings, SWAT can assess how different tillage methods, crop rotations, and irrigation practices affect sediment yields (Himanshu et al., 2019). Furthermore, urbanization which is characterized by the spread of impermeable surfaces tends to increase runoff and sediment production. Accurate modelling of human interventions within SWAT offers useful information about the consequences of land management and policy decisions on sediment dynamics (Parajuli & Risal, 2021; Xu et al., 2021).

2.4 Characterization and Mapping of Sediment Sources in River Sub-basins

Mapping sediment production and identifying sediment sources are essential elements of efficient catchment management directly influencing environmental health and the sustainability of water supplies (Cavalli et al., 2019; Sime & Abebe, 2022; Smetanová et al., 2020). Sediment source mapping identifies the origins of sediment in a river basin offering vital insights into sediment dynamics and crucial for managing soil erosion, sediment transport and their environmental impacts especially regarding climate change and land-use alterations (Getachew Abebe & Woldemariam, 2024; Sime & Abebe, 2022; Smetanová et al., 2020). Understanding these processes is

essential for sustainable watershed management since they affect water quality, aquatic ecosystems and infrastructural resilience (Getachew Abebe & Woldemariam, 2024; Zhou et al., 2017).

2.4.1 Methods for Characterizing Sediment Sources

The characterization of sediment sources employs empirical and process-based models along with sophisticated remote sensing and Geographic Information Systems (GIS) technology (Chen et al., 2020; Khawaldah et al., 2020; Sime & Abebe, 2022; Tsegaye & Bharti, 2021). These methodologies offer significant insights into sediment dynamics by including diverse environmental and anthropogenic elements.

2.4.1.1 Empirical Models

Empirical models such as the Revised Universal Soil Loss Equation (RUSLE) are extensively employed to quantify soil erosion and sediment yield. RUSLE integrates variables like precipitation, soil composition, topography and land utilization offering a streamlined approach for calculating sediment loss over time. While RUSLE is useful in numerous scenarios it fails to incorporate the complete complexity of sediment transport processes especially the hydrological cycles that affect sediment dynamics (Tsegaye & Bharti, 2021).

2.4.1.2 Models Based on Processes

Process-based models such as the Soil and Water Assessment Tool (SWAT) provide more thorough simulations of sediment yield by incorporating hydrological cycles, land use alterations, climate changes and sediment transport mechanisms (Chelkeba Tumsa, 2023; Tesfahunegn et al., 2012). SWAT simulates sediment dynamics at the watershed level considering many environmental and land-use variables that influence sediment movement. Research has shown that SWAT effectively simulates sediment yield and forecasts the effects of various land management techniques on sedimentation (Bekele & Abate, 2020; Kumar et al., 2012). The use to predict sediment dynamics in Tanzanian river basins such as the Rufiji Basin has produced essential insights into the interplay between land use, climate change and sediment yield (Nkwasa et al., 2022).

2.4.2 Remote Sensing and Geographic Information System Technologies

Remote sensing (RS) and GIS technology have transformed sediment yield research by facilitating the mapping and monitoring of sediment generation and movement across extensive regions (Kanito et al., 2023; Tsegaye & Bharti, 2021). The combination of satellite images with GIS-based models facilitates the examination of spatial and temporal fluctuations in sediment yield throughout landscapes (Worku et al., 2017). The application of GIS and RS data in mapping sediment sources and quantifying sediment loads over extensive river basins offering essential information for watershed management (Kanito et al., 2023; Liping et al., 2018; Tsegaye & Bharti, 2021). In Tanzania, GIS and RS have been employed to evaluate land use alterations and pinpoint regions most vulnerable to erosion providing critical insights for sediment management (Chilagane et al., 2020; K, 2025; Mnyali & Materu, 2021).

2.4.3 Mapping and Fingerprinting of Sediment Sources

Determining the origins of sediment is essential for comprehending sediment dynamics and controlling erosion. Sediment source fingerprinting is a widely employed method for tracing sediment to its origins through the use of physical, chemical or isotopic markers (Haddadchi et al., 2005; Raigani et al., 2019). This method has been employed in several studies to ascertain the primary sources of sediment in river basins including agricultural fields, riverbanks and forested regions (Walling & Collins, 2005). Researchers can assess the relative contributions of various sediment sources within a catchment by analyzing the mineral composition, particle size and isotopic concentration of the sediment (Haddadchi et al., 2019; Pedrosa-Pàmies et al., 2015; Schuller et al., 2021).

The combination of GIS and SWAT has improved the precision of mapping sediment sources and estimating sediment loads (Worku et al., 2017). Various studies used GIS and RS data to ascertain sediment sources in the catchments illustrating the synthesis of topography, land use and hydrological data to enhance comprehension of sediment dynamics (Imani et al., 2014; Kanito et al., 2023; Tsegaye & Bharti, 2021). In Tanzania, GIS and SWAT have been employed to examine sediment source distribution yielding critical insights for erosion prevention and watershed management (Mbungu, Easton, et al., 2016; Mnyali & Materu, 2021).

2.5 Climate Change Impacts on Sediment Yield

2.5.1 Climate Change

Climate change mostly caused by human activities signifies enduring changes in global temperature, precipitation and extreme weather patterns (Feyissa Negewo & Kumar Sarma, 2022; Guilyardi et al., 2018; Masson-Delmotte et al., 2019). These transformations have become progressively apparent since the mid-20th century and are associated with both natural and anthropogenic influences (IPCC, 2021). Notable changes identified include a decline in cold temperature extremes, an increase in warm temperature extremes, raised sea levels and an increase in the occurrence of extreme precipitation events (Daba & You, 2020). These shifts are exerting immediate impacts on ecosystems, sediment movement, erosion rates and the overall sediment yield in river catchments worldwide. Climate change represents the continuous change of the climate system, influenced by both natural phenomena (e.g., volcanic eruptions, solar radiation) and human activities especially the release of greenhouse gases (GHGs) from fossil fuel combustion (IPCC, 2021).

The Industrial Revolution represented a significant juncture defined by amplified fossil fuel use that led to the buildup of greenhouse gases such as carbon dioxide (CO_2), methane (CH_4) and nitrous oxide (N_2O) in the atmosphere (Masson-Delmotte et al., 2019). These gases trap heat and exacerbate global warming thereby amplifying the "greenhouse effect." Natural climatic drivers such as volcano eruptions and solar activity certainly impact the climate; yet, their effects are significantly eclipsed by anthropogenic alterations (IPCC, 2021). The continuous emission of greenhouse gases is anticipated to cause additional warming increasing the probability of severe, widespread and irreversible impacts on human societies and ecosystems, such as heightened sedimentation and erosion resulting from modified precipitation patterns and extreme weather events (Guilyardi et al., 2018; Masson-Delmotte et al., 2019).

Climate change primarily induced by human activities represents one of the most urgent global challenges resulting in continuing alterations in weather patterns and temperatures (Feyissa Negewo & Kumar Sarma, 2022; Mbungu, Heatwole, et al., 2016). The alterations, evident in elevated temperatures, increasing sea levels, modified precipitation patterns and variations in snow cover significantly impact water

resources and sediment dynamics (Daba & You, 2020; IPCC, 2021). The main catalysts of these alterations are elevated levels of greenhouse gases particularly CO_2, CH_4 and N_2O predominantly associated with fossil fuel consumption (IPCC, 2021; Masson-Delmotte et al., 2019). These gases retain heat in the atmosphere leading to a warming impact that is a primary contributor to the climate changes observed worldwide.

Human activities, including deforestation and fossil fuel combustion not only intensify global warming but also increase atmospheric greenhouse gas concentrations hence intensifying the greenhouse effect (Luhunga et al., 2018; Ndulue & Mbajiorgu, 2018a). The IPCC projects a worldwide temperature increase of 1.5°C between 2030 and 2052 with East Africa anticipated to experience temperature rises of 1-4°C by the 2090s (Guilyardi et al., 2018; IPCC, 2021). The rise in temperature may result in more severe rainfall patterns perhaps increasing precipitation by as much as 48% (Guilyardi et al., 2018). These alterations are exacerbating the increasing frequency and severity of extreme weather events which directly affect sediment movement, erosion and sediment yield in river catchments (Guilyardi et al., 2018; IPCC, 2021). In areas highly susceptible to climate change like sub-Saharan Africa, the impacts are expected to be severe and complex (Kahimba et al., 2015; Nachmany, 2018; Shemsanga et al., 2010).

2.5.2 The Representative Concentration Pathways (RCPs)

The Representative Concentration Pathways (RCPs) are climatic scenarios formulated by the Intergovernmental Panel on Climate Change (IPCC) to forecast future climate conditions depending on different levels of greenhouse gas emissions (Das et al., 2021; IPCC, 2021; Masson-Delmotte et al., 2019). Introduced in the Fifth Assessment Report (AR5), Representative Concentration Pathways (RCPs) replace the earlier Special Report on Emission Scenarios (SRES) and provide a framework for climate modelling and the evaluation of impacts. Each RCP is characterised by a specific level of radiative forcing projected for the year 2100 measured in watts per square metre (W/m^2) (Figure 2.1). This measurement reflects the changes in energy balance resulting from greenhouse gases and aerosols." The RCPs provide a framework for understanding the impact of varying greenhouse gas concentrations on critical climatic variables, including temperature, precipitation and extreme weather events (IPCC,

2021). These elements are basically connected to sediment dynamics in river basins, as climatic changes modify precipitation patterns, temperature and extreme weather occurrences subsequently affecting sediment transport, erosion rates and sediment yield in river catchments (Masson-Delmotte et al., 2019; Nilawar & Waikar, 2019; Y. Zhang et al., 2016).

The four principal RCPs are:

RCP2.6: A low-emission scenario designed to restrict radiative forcing to 2.6 W/m² by the year 2100. This scenario presumes strong mitigation measures limiting global temperature increase to around 1.5°C by the conclusion of the century.

RCP4.5 is a moderate-emission scenario in which radiative forcing stabilises at 4.5 W/m by the year 2100. In this scenario, moderate mitigation efforts are implemented resulting in a global temperature rise of roughly 2.4°C by the century's end.

RCP6.0: An intermediate scenario in which radiative forcing attains 6.0 W/m² by the year 2100. This trajectory presumes certain mitigation measures while maintaining elevated emissions in the end part of the century.

RCP8.5: A high-emission scenario resulting in a radiative forcing of 8.5 W/m^2 by the year 2100. This scenario marked by elevated emissions and limited mitigation efforts forecasts a temperature increase of up to 4.5°C in the end part of the century.

RCPs are vital tools for predicting future climate changes which have considerable implications for temperature, precipitation and extreme weather events (Basheer et al., 2016; Gulakhmadov et al., 2020; Nilawar & Waikar, 2019). Under RCP2.6, the global mean surface temperature is expected to rise by approximately 1.0°C by 2100 reflecting strict mitigation strategies aimed at limiting global warming. In contrast, RCP8.5 which assumes little to no mitigation efforts, is projected to lead to a global temperature increase of about 4.8°C by the end of the century (IPCC, 2021) Temperature variations significantly affect the hydrological cycle, influencing precipitation patterns, rainfall intensity, and the frequency of extreme weather events such as floods and droughts (Daba & You, 2020) Increasing temperatures lead to higher evaporation rates and alter precipitation patterns resulting in increased runoff

and changes in sediment transport dynamics within river catchments (Mbungu, Heatwole, et al., 2016; Mfwango et al., 2022; S. Zhang et al., 2019). These changes are crucial for understanding sediment yield particularly in vulnerable regions where the impacts of fluctuating rainfall and temperature are expected to be pronounced such as sub-Saharan Africa (Feyissa Negewo & Kumar Sarma, 2022; Kahimba et al., 2015; Mbungu, Heatwole, et al., 2016).

The impact of RCP scenarios on sediment yield is more pronounced in regions susceptible to soil erosion, land degradation, and water scarcity (Nilawar & Waikar, 2019; Zhang et al., 2016) With rising temperatures under elevated emission scenarios such as RCP8.5 the intensity and frequency of precipitation events are anticipated to escalate resulting in increased runoff and, therefore, enhanced sediment movement (Nilawar & Waikar, 2019). In areas with previously compromised or vulnerable ecosystems, such as East Africa, these alterations may intensify soil erosion and increase sediment loads in rivers and lakes (C & M, 2024; Chapman et al., 2021). A complex interplay of elements, including climate, geography, land use and socio-economic situations affects sediment output in Africa (Chapman et al., 2021; Tesfahunegn et al., 2012). Reseachers conducted the studies that aggregated sediment yield data throughout the continent and underscored the necessity for region-specific models to fully comprehend sediment dynamics (Vanmaercke et al., 2014). In areas such as East Africa, where climatic changes are anticipated to produce more severe weather phenomena, sediment output is estimated to rise substantially under elevated RCP scenarios (Chapman et al., 2021).

Research in South Africa using the Soil and Water Assessment Tool (SWAT) suggested that RCP8.5 may result in a 10% annual increase in sediment yield by the century's end with peak sediment transport potentially tripling over time due to more frequent and intense storms (Theron et al., 2021). The impacts of climate change on sediment output in East Africa, namely inside the Songwe River Sub-Basin in Tanzania are particularly alarming. Forecasts for the region under RCP8.5 indicate that sediment output may rise by up to 47% by 2100 (Mwalwiba et al., 2025). The rise in sedimentation is predominantly caused by intensified rainfall and increased precipitation variability which exacerbates soil erosion and sediment transport in

susceptible terrains. The alteration in sediment dynamics is particularly vital for the management of water quality in rivers and lake as increased sediment loads can diminish water storage capacity in reservoirs, pollute water supplies and disturb aquatic ecosystems (Jilo et al., 2019; Mbungu, Easton, et al., 2016).

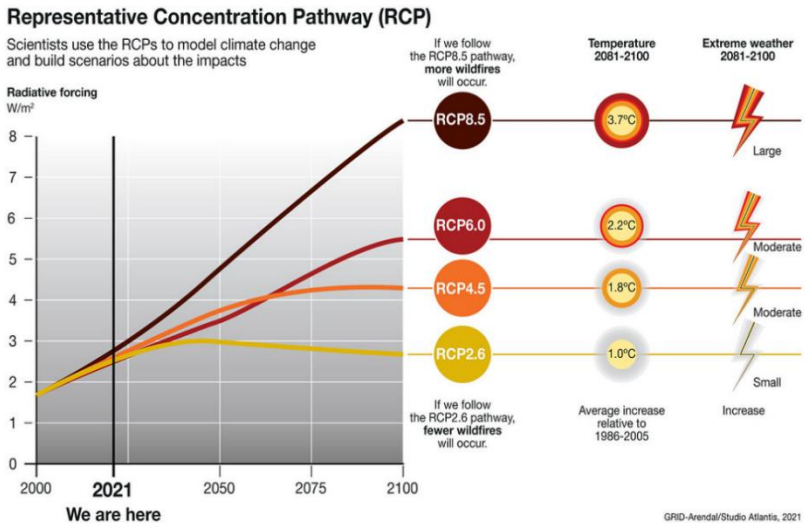

Figure 2.1: The four Representative Concentration Pathways (RCPs) showing projected trajectories of radiative forcing (W/m²) through to 2100 (IPCC, 2021)

2.5.3 Climate Change and sediment yield in Tanzania

Tanzania and the wider East African region are undergoing substantial climate change impacts marked by elevated temperatures, modified precipitation patterns and a heightened occurrence and severity of extreme weather events (John et al., 2020; Kassian et al., 2017; Melchioly, 2021; Näschen et al., 2019; Ojija et al., 2017). These alterations are especially harmful to water supplies, soil erosion, sediment transport, agriculture and ecosystems (Clement et al., 2016; Mbungu, Heatwole, et al., 2016; Mfwango et al., 2022). In Tanzania, climate change is manifesting through escalating temperatures, diminished and unreliable precipitation and changes in the intensity and distribution of rainfall across both wet and dry seasons. These climatic anomalies have resulted in significant alterations in hydrology, land productivity and socio-economic activities with grave implications for the nation's environmental and agricultural stability (Chapman et al., 2021; Jilo et al., 2019).

Tanzania's geographical position, varied topography and significant dependence on rain-fed agriculture render the nation exceedingly susceptible to the impacts of climate

change (Ojija et al., 2017). A restricted ability to adjust to climate-induced disturbances, such as droughts, floods and sedimentation exacerbates this vulnerability. Climate change in Tanzania intensifies soil erosion and sediment yield in river basins as modified rainfall patterns and more severe weather events result in elevated flow and augmented soil loss (Mbungu, Easton, et al., 2016). The country's diverse topography encompassing mountainous and lowland regions leads to considerable disparities in the impact of climate change across various places especially for sediment transport and erosion rates east Africa (Blake et al., 2018; Chapman et al., 2021; Imani et al., 2014).

The impacts of climate change are particularly evident in rural regions, where agriculture serves as the primary source of income and food security for most of the population (Setti et al., 2024). As precipitation becomes increasingly unpredictable and unreliable, agricultural production declines resulting in food poverty and economic instability. The rise in extreme weather phenomena including intense precipitation and droughts intensifies the susceptibility of these rural communities. Poverty and insufficient infrastructure hinder adaptation efforts rendering numerous locations unprepared to confront the adverse impacts of climate change such as increasing soil erosion and sedimentation in rivers and lakes (Feyissa Negewo & Kumar Sarma, 2022; Mbungu, Heatwole, et al., 2016). Fluctuations in sediment output influenced by changing climate patterns may impact river systems, water storage and hydropower potential in the region (Mbungu, Heatwole, et al., 2016; Mfwango et al., 2022; Zhang et al., 2019).

Although much research exists on climate change consequences, only a few studies in Tanzania examine the impacts of climate change on hydrological features, erosion and sediment output. Significant research conducted in Tanzania by employing the SWAT model alongside climate models to investigate these matters; however, the inadequate spatial resolution of these models constrains their efficiency in accurately forecasting the impacts of climate change on soil erosion and sediment yield (Mbungu, Easton, et al., 2016; Mutayoba et al., 2018b). Climate change and heightened land degradation attributed to modified precipitation patterns, increasing temperatures and a rise in extreme weather occurrences (Chawanda et al., 2024; Nguyen, 2019). These causes

intensify prevailing environmental challenges, including deforestation and overgrazing, rendering the region increasingly susceptible to soil erosion and elevated sediment yields.

(Mbungu, Easton, et al., 2016) evaluated the effects of land use, land cover alterations, and climatic variability on hydrology and soil erosion in the Upper Ruvu watershed in Tanzania. The research indicated that landscapes in the upper watershed are especially susceptible to significant soil erosion as a result of anthropogenic pressures on forested areas. The variability in precipitation severely affected the watershed's hydrology. The research indicated that sediment yield escalated in direct correlation with alterations in land use and cover within the catchment area.

2.5.3 Climate Change and Erosion in Designated Tanzanian Regions

In areas such as the Uluguru Mountains intense precipitation events induced by climate change have led to heightened erosion rates and sediment production (Mbungu, Easton, et al., 2016). As the frequency of severe storms increases significant amounts of silt enter river systems, thereby enhancing sediment production. Climate change significantly affects the Rufiji, Pangani and Songwe rivers making their adjacent landscapes vulnerable to erosion after intense precipitation (Lalika et al., 2015; Mwalwiba et al., 2025; Nobert, 2022). In regions such as Dodoma and Singida where droughts frequently occur, the interplay of extended dry periods and heavy rainfall has exacerbated sediment transport. In river basins like the Rufiji Basin and Lake Rukwa Basin where the Songwe River runs, climate-induced erosion is already influencing water resource management (Mwalwiba et al., 2023).

Agricultural practices in marginal areas act as both a catalyst and a result of heightened sediment yield. Unsustainable land management practices, including overgrazing, deforestation, and agricultural development, intensify soil erosion and sedimentation (Mfwango et al., 2022; Nguyen, 2019) Climate change exacerbates these consequences by altering precipitation patterns and increasing temperatures, undermining soil integrity and moisture retention capabilities (Chawanda et al., 2024; Gobry et al., 2023). Despite elevated levels of soil erosion and sediment yield, research

regarding the prospective effects of climate change on sediment yield in Tanzania is constrained by insufficient comprehensive data.

2.5.4 The Songwe River Sub-Basin Susceptibility to Climate Change and Sediment Yield

The Songwe River sub-basin in the Lake Rukwa Basin in southwestern Tanzania is vulnerable to climate fluctuation and change (Mwalwiba et al., 2023a). This region, similar to much of East Africa is undergoing substantial alterations in temperature, precipitation and extreme weather events which have extensive impacts for local ecosystems, agriculture, water resources, and livelihoods (Feyissa Negewo & Kumar Sarma, 2022; Lazaro et al., 2023; Mbungu, Heatwole, et al., 2016; Mwalwiba et al., 2023). Historical temperature records for the region reveal that the mean annual temperature in the Songwe River Sub-Basin has risen by roughly 1–1.5°C over the last 50 years, with notable warming trends evident since the 1970s (Mwalwiba et al., 2023). Anthropogenic climate change particularly the accumulation of greenhouse gases in the atmosphere is primarily responsible for the rise in temperatures (Chapman et al., 2021). Climate models forecast a temperature increase of 1.5–2°C in the region by 2050 intensifying current issues of water management, agriculture and ecosystems (Lahunga et al., 2016a).

Precipitation patterns in the Songwe River sub-basin demonstrate significant variability with alterations in the time, intensity and distribution of rainfall becoming increasingly apparent. Climate change has presented additional concerns such as increased frequency of droughts and severe rainfall events. Trends suggest a decline in total annual precipitation marked by abbreviated and less predictable rainy seasons. The fluctuation in precipitation coupled with extended dry periods heightens the likelihood of hydrological extremes like droughts and floods hence, intensifying soil erosion and sedimentation in the area (Feyissa Negewo & Kumar Sarma, 2022; Mbungu, Heatwole, et al., 2016; Serdeczny et al., 2017).

Recent studies indicate a reduction in precipitation during the extended rainy season, although brief yet powerful downpour events have increased in frequency(Jilo et al., 2019; Mbungu, Heatwole, et al., 2016). The alterations have exacerbated soil erosion

and elevated sediment output in the Songwe River sub-basin, resulting in enhanced sedimentation rates in Lake Rukwa (Mbungu, Heatwole, et al., 2016; Mtelela, 2018; Valimba, 2019). The interplay of extended droughts and heavy precipitation intensifies soil fertility decline leading to the loss of arable land and the deterioration of water quality. This highlights the necessity of integrating climate change forecasts into regional water management policies to foresee and alleviate the impacts of heightened sediment yield and soil erosion (Chapman et al., 2021).

While research has demonstrated the substantial impacts of climate change on sediment yield in Tanzania, investigations assessing future implications are few. The absence of extensive, high-quality data on sediment generation, climate variability and hydrological alterations obstruct the formulation of comprehensive models for reliably predicting the future impacts of climate change. The lack of such data restricts the capacity to make educated decisions on water and land management, especially in areas like the SongweRiver Sub-Basin where sediment yield is an increasing issue.

2.6 Land use Land Cover Change

2.6.1 Changes in Land Use and Land Cover (LULC) and Their Effects on Sediment Yield

Alterations in land use and land cover (LULC) are critical factors contributing to environmental deterioration, threatening sustainability and long-term development (Lazaro et al., 2023; Selmy et al., 2023). Land use and land cover changes are among the most significant alterations to the land surface impacting ecosystems and environmental processes. These alterations impact hydrology, soil erosion, sedimentation, ecosystem dynamics, biodiversity, climate and biogeochemical cycles (Leta et al., 2021). Both biophysical elements and anthropogenic activity influence land use change and climate alteration (Sigalla et al., 2024). Human-induced alterations in land use frequently stem from an imbalanced interaction between humanity and the natural environment, a phenomenon that has intensified with the growth of the world population and agricultural practices (Huong & Son, 2020; Yao et al., 2015). Understanding land use and land cover dynamics is essential for understanding the dynamics of environmental change. Deforestation, urbanization and agricultural expansion affect land use and land cover (LULC) resulting in adverse

impacts on biodiversity, soil erosion, climate change, environmental conservation, pollution and water resources (Gemmechis, 2022).

Deforestation eliminates essential tree cover which stabilizes soil via root networks and enhances rainwater absorption. In the absence of this natural barrier precipitation directly affects the soil increasing surface runoff and compromising soil stability (Chawanda et al., 2024; Gobry et al., 2023). Consequently, silt transport into neighbouring rivers and streams intensifies (Shrestha et al., 2013).

In Tanzania and several African countries land use and land cover (LULC) have experienced substantial alterations greatly affecting ecosystem services, hydrological processes and environmental stability (Gobry et al., 2023; Mbungu, Heatwole, et al., 2016; Mutayoba et al., 2018b). These alterations have resulted in heightened soil erosion, silt accumulation, water shortages and the pollution of water sources, consequently obstructing sustainable socio-economic development (Beroho et al., 2023). Several studies have associated soil erosion, sedimentation and variations in water quality and quantity with land use and land cover changes at the watershed level, highlighting the necessity to comprehend the interplay between human activities and global environmental changes (Based et al., 2018; Beroho et al., 2023; da Fonseca et al., 2022).

In Tanzania's Uluguru Mountains, agricultural expansion-induced deforestation has been demonstrated to elevate sediment loads in rivers leading to reservoir siltation and diminishing the efficiency of hydroelectric power generation (Chilagane et al., 2021; Mbungu, Heatwole, et al., 2016). Agricultural practices, notably tillage, compromise soil structure and increase susceptibility to erosion particularly after heavy rainfall events. Unsustainable practices such as monocropping and overgrazing diminish soil cohesion and organic matter; hence, they intensify soil erosion. In regions devoid of effective irrigation methods, excessive water runoff transports substantial quantities of sediment into rivers and lakes (Xu et al., 2017) The conversion of wetlands and forests to agricultural land in the Lake Victoria Basin has resulted in heightened sedimentation, nutrient enrichment, and eutrophication, adversely affecting water quality and fisheries (Kimwaga, 2012).

Urbanization markedly transforms landscapes by substituting permeable surfaces with impermeable ones such as highways and buildings; hence, it diminishes water penetration and amplifies surface runoff (Gondwe et al., 2021; Ssewankambo et al., 2023). This flow, frequently saturated with sediment can elevate sediment concentrations in nearby water bodies (Chelkeba Tumsa, 2023). Construction operations associated with urban expansion expose vast regions to soil erosion hence, augmenting sediment transport into rivers and lakes.

Significant land use and land cover changes, including deforestation and agricultural intensification have transpired in the Songwe River Sub-Basin of the Lake Rukwa Basin (Kalisa et al., 2013). The aforementioned changes, along with climate unpredictability have intensified sediment yield in the region. The transformation of vegetated regions particularly on hillslopes, into agricultural land reduces the ground's capacity to retain soil resulting in heightened soil erosion and sediment movement. Intense precipitation events exacerbate this issue by moving loose soil into rivers. The Songwe River has undergone significant bank erosion, particularly during flood events resulting in increased silt influx into Lake Rukwa. These modifications have adversely impacted water quality and local ecosystems, underscoring the complex relationship between land use and land cover, climate variability and sediment yield. Nevertheless, no research has explicitly examined land use and land cover (LULC) alterations in the Songwe River Sub-Basin highlighting the necessity for thorough investigation that integrates historical transformations and anticipates prospective LULC situations. The region necessitates a comprehensive LULC study to comprehend long-term trends and patterns and guide sustainable development and environmental conservation initiatives.

2.6.2 Modelling Land Use and Land Cover Changes to Forecast Sediment Yield

Diverse modelling methodologies have been used to forecast and regulate the effects of land use and land cover changes on sediment yield (Azizi et al., 2016; Barbosa de Souza et al., 2023). Various models are employed for predicting land use including Markov Chain models, Cellular Automata (CA) models and System Dynamics models (Azizi et al., 2016; Gondwe et al., 2021; Khawaldah et al., 2020). The Cellular Automata-Markov (CA-Markov) model is particularly popular for simulating the

spatial and temporal dynamics of land use changes (Khawaldah et al., 2020). It combines spatial simulation with the Markov process to forecast temporal transitions making it effective for depicting alterations in landscapes. Alternative methodologies, such as machine learning and GIS-based models are also used for complex land use projections especially when extensive data is available (Worku et al., 2017). Although these models have shown promising results, they heavily depend on high-quality, accurate data and may face challenges with accuracy when data is scarce or inadequately calibrated.

A commonly employed instrument is the Cellular Automata (CA)-Markov Model, renowned for its efficiency in simulating the spatial and temporal dynamics of land use and land cover (LULC) alterations (Azizi et al., 2016; Khawaldah et al., 2020). This model integrates the spatial modelling features of cellular automata with the temporal forecasting functions of the Markov process establishing a comprehensive framework for the analysis and prediction of LULC transitions (Atef et al., 2024).

The combination of Geographic Information Systems (GIS), Remote Sensing (RS), and the CA-Markov model has demonstrated efficacy in delineating the spatiotemporal dynamics of land use and land cover (LULC) change across varied landscapes (Khawaldah et al., 2020; Selmy et al., 2023). This model integrates biophysical, socioeconomic and remote sensing data to elucidate the determinants of land use and land cover transitions and to predict future land use alterations (Atef et al., 2024; Nyatuame et al., 2023; Tadese et al., 2021). The CA-Markov model has been widely employed in Africa to examine deforestation, land degradation and urban growth which are essential for understanding environmental changes in fast-evolving areas (Tadese et al., 2021). With the ongoing rise in urbanization, population density, and agricultural demands throughout the continent, the model functions as a crucial instrument for policymakers aiming to tackle these transformations and develop sustainable land management methods (Op de Hipt et al., 2019).

In Tanzania, the CA-Markov model has been utilized to analyze the effects of agricultural practices and urbanization on ecosystems (Chilagane et al., 2020; Gobry et al., 2023; Kitalika et al., 2018). Insufficient historical data frequently impede the

implementation of the CA-Markov model in Africa, thereby compromising the accuracy of future forecasts (Azizi et al., 2016; Selmy et al., 2023). Nevertheless, it is a crucial instrument for long-term environmental planning and the formulation of climate change adaptation strategies in Tanzania and other African nations.

2.6.2.1 Assessment of Land Use/Land Cover Classification Accuracy (LULC)

Land Use/Land Cover (LULC) classification is an essential technique in remote sensing and geographic information systems (GIS) facilitating the examination of temporal land changes (Azizi et al., 2016; Chang et al., 2018; Selmy et al., 2023). The accuracy of LULC classifications is essential for guaranteeing the dependability of outcomes particularly in environmental management, urban planning, and climate change evaluations. The Kappa coefficient is a prevalent statistical tool for assessing classification accuracy as it quantifies the concordance between classed data and reference data (Chilagane et al., 2020; Selmy et al., 2023).

2.6.2.2 Kappa Coefficient and Confusion Matrix

The Kappa coefficient (K) is a reliable metric that measures the extent of concordance between predicted classifications and actual ground-truth data. In contrast to basic accuracy metrics which may be influenced by class imbalance the Kappa statistic considers the likelihood of chance agreement providing a more stringent assessment of classification efficiency (Chilagane et al., 2020; Nyatuame et al., 2023; Osman et al., 2023). The Kappa value spans from -1 to 1 with values approaching 1 denoting robust concordance between anticipated and actual classifications while values nearing 0 imply no superior agreement than random chance. A Kappa value exceeding 0.85 indicates excellent accuracy in classification results deemed suitable for dependable analysis (Chilagane et al., 2021). This property renders it especially advantageous for assessing distant sensing photos when individual inspection of each pixel is impractical.

The Kappa statistic is obtained from the confusion matrix, which was created by juxtaposing the categorized image with reference data. The matrix offers a comparative analysis of the alignment between each classification category and the ground-truth data, highlighting both correct classifications and errors among various land cover types (Azizi et al., 2016; Beroho et al., 2023). The confusion matrix is

crucial for calculating several classification accuracy metrics such as overall accuracy, producer's accuracy, user's accuracy and the Kappa coefficient.

The equation for the Kappa statistic is as shown in equation 2.1

$$K = \frac{N \sum_{i=1}^{r} x_{ii} - \sum_{i=1}^{r}(x_{i+} \times x_{+i})}{N^2 - \sum_{i=1}^{r}(x_{i+} \times x_{+i})} \quad (2.1)$$

Where N is the total number of sites in the matrix, r is the number of rows in the matrix, xii is the number in row i and column i, x_{+i} is the total for row i, and x_{i+} is the total for column.

(a) Temporal Consistency and Validation of Ground Truth

Precise ground-truth data is crucial for the validation of land use and land cover classification outcomes. Ground-truthing entails the acquisition of field data establishing a benchmark for comparison with remotely sensed data. Temporal consistency is essential, as alterations in land use and cover transpire over time, necessitating the collection of reference data for each pertinent time under examination (Beroho et al., 2023). Numerous studies calculate the Kappa coefficient across various time epochs (e.g., 1990, 2000, 2010 and 2020) to guarantee consistency in assessing classification accuracy over distinct timeframes (Chilagane et al., 2021). The ground-truthing data for each time period guarantees that the categorization accurately represents actual changes in the landscape and aids in evaluating the model's accuracy throughout the years. The accuracy of LULC classification can vary over time due to the influence of several environmental, technological and methodological factors. The utilization of higher-resolution satellite imagery and advancements in classification algorithms may enhance accuracy over time but environmental factors such as cloud cover and seasonal fluctuations in land cover could introduce data noise (Selmy et al., 2023).

(b) Assessment Criteria for Land Use and Land Cover Classification

The Kappa coefficient is a highly regarded tool for evaluating LULC classification accuracy since it accounts for chance agreement. Researchers have utilized the

Kappa statistic in several situations such as urbanization monitoring, deforestation research and agricultural land use evaluations (Selmy et al., 2023). Numerous studies indicate that Kappa values exceeding 0.85 often signify satisfactory accuracy in land use and land cover classifications. In the assessment of land use and land cover changes in the Amazon Basin a Kappa value of 0.92 was achieved signifying robust concordance between the classification outcomes and ground-truth data (Azizi et al., 2016). Likewise, research in agricultural areas has revealed Kappa values of 0.90 indicating substantial reliability in remote sensing-derived land use and land cover classification (Chang et al., 2018; Selmy et al., 2023).

(c) Limitations and Considerations

The Kappa coefficient, although a robust instrument for assessing classification accuracy possesses inherent limitations. A key concern is its reliance on the quality and amount of ground-truth data. Insufficient or biased reference data may result in the Kappa statistic failing to adequately represent the genuine classification accuracy (Atef et al., 2024; Khawaldah et al., 2020). The Kappa coefficient presupposes a homogeneous distribution of errors across courses which may not reflect real-world conditions resulting in potential misinterpretation of outcomes. Researchers have proposed alterations to the Kappa coefficient including the implementation of weighted Kappa to mitigate class imbalances and to enhance the importance of misclassifications within analogous classes (Selmy et al., 2023). A further barrier is the intricacy of integrating dynamic land cover alterations in multi-temporal land use and land cover classification. The Kappa statistic evaluates the accuracy of individual classifications but does not directly measure the extent to which the classification reflects actual land cover changes over time. Additionally, alternative metrics such as change detection accuracy may be used in conjunction with Kappa to enhance knowledge of classification performance (Beroho et al., 2023; Chilagane et al., 2020).

2.7 Role of Climate Models and Scenarios in Forecasting Future Trends in Sediment Yield

Climate models are computer instruments that simulate the Earth's climate system, offering understandings into historical, current and prospective climate conditions (Lahunga et al., 2016b). They are important for understanding climatic variability and change, as well as for guiding policy decisions about climate adaptation and mitigation.

Climate models employ quantitative techniques to simulate the interactions of essential climate drivers such as the atmosphere, oceans, land surface and ice (Figure 2.2). These models are crucial for various applications including the analysis of climate system dynamics and the forecasting of future climate scenarios (Lahunga et al., 2016b; Mengistu et al., 2021; Tessema et al., 2021). General Circulation Models (GCMs) are among the most sophisticated instruments for modelling the global climate system's reaction to increased greenhouse gas concentrations (Lahunga et al., 2016a; Luhunga et al., 2018; Mengistu et al., 2021). General Circulation Models (GCMs) employ an array of fluid dynamical, chemical and biological equations to depict significant physical processes within many components of the climate system including the atmosphere, seas, cryosphere and terrestrial surface (Luhunga et al., 2018). These models are essential for evaluating relative alterations in the climate system resulting from diverse radiative forcings and are employed for seasonal to decadal climate forecasts and future projections (Guilyardi et al., 2018). GCMs, considered highly effective instruments for understanding the physical processes of the Earth's surface-atmosphere system have thoroughly examined the influence of climate change. General Circulation Models (GCMs) provide reliable data on past, present and future climate conditions (Lahunga et al., 2016b).

Despite the progress made in GCMs, issues remain regarding spatial resolution and parameterization. The simulation of precipitation at regional and national levels continues to provide a difficulty for General Circulation Models (Mengistu et al., 2021; Tessema et al., 2021). Furthermore, GCMs with low spatial resolutions fail to represent extreme climatic events accurately especially in areas with diverse topography. Reducing these models to regional spatial scales is essential for obtaining precise data

for localised climate impact analyses (Luhunga et al., 2018; Mengistu et al., 2021; Tessema et al., 2021). Regional Climate Models (RCMs) are designed to fulfil this requirement providing improved spatial resolution to represent climate variability at regional levels (Luhunga et al., 2018; Mengistu et al., 2021). RCMs have demonstrated their use as effective instruments for regional climate downscaling (Dibaba et al., 2019), notably in mid-latitude areas, and are increasingly being used in climate research throughout several African regions. The application of high-resolution regional climate models has increasingly become prominent recently particularly for examining the hydrological effects of climate change as they provide a more accurate representation of local climates (Mengistu et al., 2021; Mutayoba et al., 2018b). These models are regarded as conventional instruments for refining climate predictions to more granular spatial dimensions.

Initiatives to generate extensive collections of RCM simulations are under progress to improve evaluations of the impacts of climate change on regional climates. The Coordinated Regional Climate Downscaling Experiment (CORDEX) established by the World Climate Research Program (WCRP) seeks to downscale outputs from multiple General Circulation Models (GCMs) to produce an ensemble of high-resolution historical and future climate projections for regions including Africa (Luhunga et al., 2018c). CORDEX models offer enhanced utility compared to GCMs, particularly in their precise depiction of the annual rainfall cycle and high rainfall occurrences throughout several African regions (Mutayoba et al., 2018b). Numerous CORDEX Regional Climate Models (RCMs) are frequently used in Africa including the Consortium for Small-scale Modelling (COSMO), the Climate Limited-Area Model (CCLM), the SMHI Rossby Centre Regional Climate Model (RCA4), the Max Planck Institute Regional Model (REMO), the KNMI Regional Atmospheric Climate Model (RACMO22T), and the High-Resolution Limited Area Model (HIRHAM5) (Dibaba et al., 2019; Lahunga et al., 2016b; Mengistu et al., 2021). In Tanzania, researchers have used four CORDEX regional climate models CCLM4, RACMO22T, HIRHAM5 and RCA4 to forecast the future impacts of climate change on hydrological processes and watershed features (Lahunga et al., 2016a; Luhunga et al., 2018; Mutayoba et al., 2018b), (Table 2.1).

Nonetheless, ambiguities remain in RCM models especially regarding precipitation, temperature, wind and other phenomena (Luhunga et al., 2018; Tessema et al., 2021). The origins of these uncertainties are challenging to identify as they may stem from either the initial boundary conditions supplied by GCMs or the parameterizations of the RCMs themselves. Another concern with RCMs is their variable performance across diverse regions and seasons which requires careful selection of RCMs when examining certain regions or timeframes (Dibaba et al., 2019; Luhunga et al., 2018). The inconsistency is vital in choosing suitable climate models for impact assessments as the efficiency of dynamically downscaled data differs by location and regional climate model (Lahunga et al., 2016b). Evaluating climate projections derived from distinct climate models introduces uncertainty originating from either the Regional Climate Model (RCM) or the driving General Circulation Model (GCM). Nonetheless, ambiguities in climate model outputs can be mitigated by using diverse lateral boundary conditions from numerous GCMs incorporating various RCM results, and implementing robust downscaling techniques (Luhunga et al., 2018).

Recent advancements in climate modelling seek to rectify numerous existing deficiencies especially uncertainty and predictive accuracy. A significant advancement in this domain has been the application of emergent constraints which mitigate inaccuracies in climate sensitivity predictions. Incorporating observable data into model simulations refines the range of potential future climatic (Dibaba et al., 2019). This methodological improvement has improved the dependability of climate predictions by reducing the uncertainty related to climate sensitivity and hence, strengthening long-term estimates. The integration of deep learning techniques in climate modelling signifies a significant advancement. Neural networks are progressively used to replicate sub grid processes such as cloud formation which have proven challenging to predict explicitly in conventional general circulation models (GCMs). This method has emerged as a valuable instrument for enhancing climate forecasts especially in accurately representing the variability intrinsic to climate systems.

Recent research has highlighted advancements in climate modelling demonstrating that models created over the previous fifty years have been exceptionally proficient in

forecasting following alterations in global mean surface temperatures (Dibaba et al., 2019; Mengistu et al., 2021). The analysis revealed that most of the models examined had warming tendencies that closely corresponded with observable data. This discovery substantiates the increasing trust in climate models as dependable instruments for understanding long-term temperature variations while also bolstering their application in policy formulation and adaptation strategies. Substantial advancements in model evaluation procedures have significantly improved the accuracy of climate predictions.

Climate change dramatically impacts sediment yield by modifying precipitation, temperature and land use; hence, it affects hydrological processes and soil erosion (Feyissa Negewo & Kumar Sarma, 2022). Research employing multiple climate models has demonstrated varied effects across different locations (Luhunga et al., 2018). Simulations using the SWAT model in Ethiopia's Watersheds indicated substantial increases in sediment output under the RCP4.5 and RCP8.5 scenarios underscoring the escalating erosion processes attributable to climate change (Daba & You, 2020; Gemechu et al., 2021). Models such as the Soil and Water Assessment Tool (SWAT) have proven essential in estimating sediment yield under climate change scenarios offering significant insights into hydrological responses and sediment dynamics (Addis et al., 2016; Ndulue & Mbajiorgu, 2018a; Qi et al., 2020). SWAT integrates climate data with land use and topographic information facilitating precise predictions of sediment flow and deposition (Hallouz et al., 2018; Ndulue & Mbajiorgu, 2018a). Recent developments in modelling have integrated climate models with sediment yield evaluations, highlighting the necessity of region-specific methodologies. Future research should concentrate on enhancing these models integrating localised data and formulating appropriate mitigation techniques to address the problems presented by climate-induced sedimentation and erosion. These initiatives are essential for sustainable watershed management and alleviating the effects of soil erosion on water resources and infrastructure.

In Tanzania, little research has examined the impacts of climate change on hydrological features, soil erosion and sediment yield using both SWAT and climate models (Lahunga et al., 2016a; Mbungu, Heatwole, et al., 2016; Mutayoba et al.,

2018b). A multitude of this research has used SWAT models and GCMs characterized by low spatial resolution hence, constraining their capacity to deliver significant insights regarding the effects of climate change on soil erosion and sediment production (Mbungu, Easton, et al., 2016). The low resolution of GCMs in this research hinders the ability to capture the detailed climate impacts essential for effective planning and control.

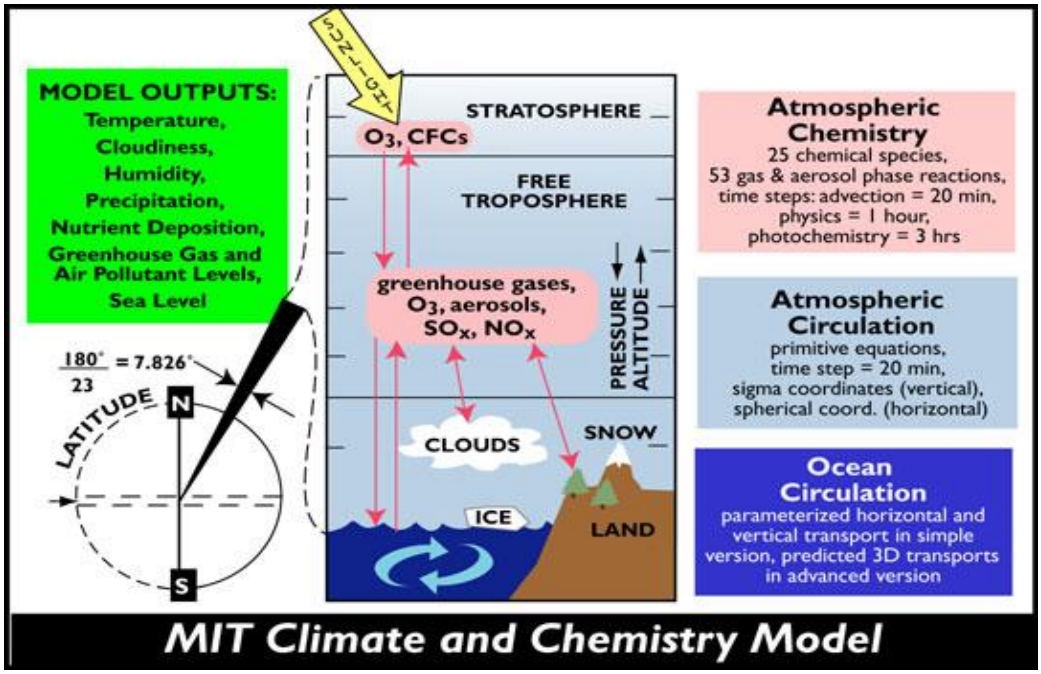

Figure 2.2: Climate Model Framework for Simulating Interactions (Jacoby et al., 1999)

Table 2.1: The CORDEX-RCMs and their driving GCMs used in Tanzania

S/N	RCM	Mode Center	Short name	GCMs
1	DMI HIRHAM5	Denmarks Meteoroliske Institute (DMI), Denmark	HIRHAM5	ICHEC
2	CLMcom COSMO-CLM (CCLM4)	Climate Limited-Area Modelling (CLM) Community	CCLM4	MPI ICHEC CNRM
3	KNMI Regional Atmospheric Climate Model, Version (RACMO2.2T)	Kininklijk Nederlands Meteorologisch Institute (SMHI), Swiden	RACMO22T	ICHEC
4	SMHIRossby Center Regional Atmospheric Model (RCA4)	Sweriges Meteorologiska OchHydrologiska Institut (SMHI), Sweden	RCA4	MPI ICHEC CNRM

Source:(Lahunga et al., 2016a)

2.7.1 The Bias Correction of Regional Climate Models (RCMs)

2.7.1.1 Overview of Bias in Regional Climate Models

Regional Climate Models (RCMs) are vital instruments for simulating climate at higher spatial resolutions providing critical insights into regional and local climate dynamics. Nevertheless, these models frequently display biases relative to observed climate data resulting in disparities between model projections and actual conditions (Lahunga et al., 2016a; Mengistu et al., 2021). These biases may originate from multiple sources such as inaccuracies in model physics, resolution constraints, boundary conditions and the intrinsic complexity of the model's internal mechanisms (Luhunga et al., 2018; Luo et al., 2018). With the growing utilization of RCMs in climate impact studies particularly for analyzing regional disparities in temperature, precipitation and extreme weather phenomena rectifying these biases has emerged as an essential measure to enhance the dependability of model outputs (Luo et al., 2018).

2.7.1.2 Categories of Bias in Regional Climate Models

Biases in Regional Climate Models (RCMs) can manifest in various forms including mean, variability, spatial and temporal biases. Mean bias denotes the model's propensity to consistently overestimate or underestimate the mean value of climate variables like temperature or precipitation over a certain duration (Luhunga et al., 2018; Luo et al., 2018). Variability bias occurs when the model does not accurately replicate the observed range or variability of climatic variables especially regarding extremes or seasonal variations (Mengistu et al., 2021). Spatial bias arises when the model fails to effectively depict the spatial distribution of climate variables particularly in regions characterised by intricate terrain or significant climatic (Mengistu et al., 2021). Temporal bias occurs when the model does not accurately replicate observed temporal patterns, including seasonal timing daily variability or long-term trends (Lahunga et al., 2016a).

2.7.1.3 Bias Mitigation Techniques

Numerous methods have been devised to rectify biases in RCM outputs which can be categorised into statistical, dynamical and hybrid approaches (Dibaba et al., 2019; Luo et al., 2018; Mengistu et al., 2021).

(a) Statistical Techniques

Quantile Mapping (QM) is a prevalent statistical bias correction technique that modifies model output by aligning its cumulative distribution function (CDF) with the observed CDF. The model output is adjusted to align with the observed distribution of climatic variables mitigating biases in mean and variability (Lahunga et al., 2016a; Luo et al., 2018). Various variants of Quantile Mapping (QM) including Empirical Quantile Mapping (EQM) and Parametric Quantile Mapping (PQM) exhibit distinctions in the estimation and application of cumulative distribution functions (CDFs) (Luo et al., 2018; Mengistu et al., 2021). The application of QM to precipitation data markedly enhanced the simulation of extreme occurrences in climate forecasts.

Linear scaling is a direct bias correction technique in which model outputs are modified by a linear factor, often the ratio of observed to modelled values for a certain climatic variable (Luo et al., 2018). This method is computationally cheap and straightforward to implement; nevertheless, it is constrained in its capacity to rectify more intricate biases especially those related to the variability of climatic data. Linear scaling can modify temperature and precipitation forecasts, thereby enhancing the model's depiction of seasonal cycles and average climatic trends (Luo et al., 2018).

The Delta Change Method (DCM) entails computing the discrepancy (or delta) between observed and modelled climatic values and incorporating this discrepancy into future climate projections. This methodology is particularly advantageous in situations where the observed data serves as the baseline or reference climate, emphasizing the projection of alterations in climate variables rather than their absolute values (Luhunga et al., 2018; Luo et al., 2018). DCM can modify precipitation and temperature forecasts for hydrological impact evaluations, demonstrating substantial enhancements in the projected climate alterations over the 21st century (Luo et al., 2018).

Unlike simpler methods, polynomial fitting entails modelling the relationship between observed and modelled climate variables as a polynomial function hence, offering greater flexibility in bias correction. This technique effectively addresses non-linear

biases and is especially beneficial for modifying extreme events or seasonal fluctuations (Luhunga et al., 2018; Luo et al., 2018; Nguyen, 2019). Polynomial fitting rectifies temperature and precipitation biases in a regional climate model (RCM) resulting in enhanced accuracy in reproducing extreme weather phenomena (Dibaba et al., 2019; Luo et al., 2018).

Another advanced statistical method is Empirical Orthogonal Function (EOF) decomposition which separates the model and observed time series of climate variables into orthogonal modes. The biases are subsequently rectified for each mode, facilitating a more precise depiction of the observed climate variability (Luo et al., 2018). Different studies used this strategy to rectify regional temperature forecasts, resulting in enhancements in the model's representation of seasonal cycles and long-term trends (Luhunga et al., 2018; Luo et al., 2018).

(b) Dynamical Approaches\Regional Downscaling

Dynamical bias correction techniques including regional downscaling employ high-resolution regional models to modify the outputs of course-resolution regional climate models (RCMs). These methods provide a more physically grounded approach to bias correction by dynamically applying corrections that consider the atmospheric processes responsible for biases in model outputs (Luhunga et al., 2018).

Stochastic weather generators produce synthetic weather sequences that align with the statistical characteristics (e.g., daily precipitation or temperature) of actual data, while integrating climate model forecasts. These generators are especially effective in rectifying biases associated with the temporal distribution of climatic variables, including the frequency and intensity of extreme occurrences (Luo et al., 2018).

(c) Hybrid Approaches

Recent methodologies have integrated statistical and dynamical techniques to capitalize on the advantages of both. Hybrid techniques provide thorough bias correction by combining statistical adjustments with physically-based corrections derived from regional downscaling or weather generation (Dibaba et al., 2019). These hybrid methodologies can rectify various biases, enhancing both the mean and variability of the model outputs (Mutayoba et al., 2018b).

Despite the progress in bias correction methodologies, difficulties persist in effectively rectifying biases in RCM outputs. A primary challenge is reconciling the spatial and temporal scale discrepancies between observed data and model outputs. This is especially troublesome in areas with complex topography or when observational data is limited (Kishiwa et al., 2018; Lahunga et al., 2016a; Luo et al., 2018). Moreover, model reliance is a considerable problem since many RCMs display distinct bias characteristics necessitating diverse corrective methodologies (Lahunga et al., 2016a). The assessment of bias-corrected data poses difficulties, necessitating extensive metrics to evaluate not only mean biases but also the representation of severe occurrences, seasonal patterns, and long-term (Luhunga et al., 2018; Mengistu et al., 2021).

2.8 Hydrological and Sedimentological Models

Simulation models are essential for understanding and forecasting the effects of climate change on sediment yields in river basins. These models enable researchers to evaluate the impact of variations in climatic factors such as precipitation and temperature on hydrological processes and sediment movement (Nguyen, 2019; Tessema et al., 2021) Simulation models fulfil two main functions: (1) to assess assumptions about real-world systems, and (2) to forecast the behaviour of these systems under realistic situations (Mbungu, Easton, et al., 2016). Hydrological and eroding models vary considerably in various aspects including process characterization, temporal and spatial resolution, solution techniques, land use and specific applications of the models (Mcnulty et al., 1995). In recent decades, numerous models and relationships have been established to characterize and predict soil erosion induced by water and its associated sediment formation. These models differ significantly in their aims, the temporal and spatial scales they encompass and their theoretical underpinnings. The formulation of models has predominantly concentrated on three principal categories: empirical or regression models, physical deterministic models and physics-based models (Vanmaercke et al., 2014). Depending on the complexity of the system under analysis and the available data each group offers specific advantages and disadvantages.

2.8.1 Empirical Models

Empirical models have been progressively developed, especially for watershed-scale applications, and are extensively employed for their simplicity and capacity to provide swift estimates of sediment yield. These models encompass approaches including the rational method, the unit hydrograph, the SCS method, the Universal Soil Loss Equation (USLE) and the Modified Universal Soil Loss Equation (MUSLE) (Efthimiou et al., 2017; Jamshidi et al., 2014). Empirical or regression models employ statistical techniques to forecast outcomes based on observed input-output correlations rather than recreating the underlying physical mechanisms that dictate the system. These models utilise approaches including regression analysis, statistical methods or neural networks to generate their predictions (Efthimiou et al., 2017; Tabarestani et al., 2022).

Empirical models are prevalent for estimating sediment yield in data-deficient regions; however, they frequently depend on oversimplified correlations and neglect to encompass the comprehensive array of physical factors affecting sediment yield, flow and the hydrological cycle (Mbungu, Easton, et al., 2016; Tabarestani et al., 2022). This constraint makes them less appropriate for long-term predictions, as they fail to include the complexities and variabilities that could influence future situations (Sulaiman et al., 2021). Nevertheless, these limitations empirical models continue to be favoured for their simplicity and minimal data requirements making them an appealing choice in areas with scarce physical data.

2.8.2 Deterministic Models

Deterministic models depend on the numerical resolution of partial differential equations that characterise physical phenomena including hydrological flow, sediment transport and erosion (Loague & Vanderkwaak, 2002). These models provide a more comprehensive depiction of physical processes and are especially beneficial for forecasting sediment transport in both steady and turbulent flow scenarios. Deterministic models include the European Soil Erosion Model (EUROSEM) (Morgan et al., 1998) and the Water Erosion Prediction Project (WEPP) . These models offer a more thorough comprehension of sediment yield and erosion by simulating the interactions among precipitation, runoff, soil characteristics and plant cover.

Nonetheless, a notable constraint of deterministic models is their requirement for substantial input data and tremendous computational resources. These prerequisites render them computationally demanding and potentially unfeasible for extensive or prolonged forecasts particularly in data-deficient areas (Haregeweyn et al., 2013). Notwithstanding these obstacles, deterministic models are essential for understanding complex hydrological processes and forecasting the impacts of diverse environmental and land use alterations on sediment transport.

2.8.3 Physics-Based Models

Semi-distributed physics-based models have gained prominence in hydrological research for their capacity to depict the spatial heterogeneity of hydrological processes. These models are exceptionally proficient at simulating the effects of climate change and anthropogenic activities on water supplies and sediment dynamics. In contrast to empirical or deterministic models, physics-based models incorporate physical representations of essential characteristics that affect water velocity and sediment movement. Prominent physics-based models are the Agricultural Non-Point Source Pollution Model (AGNPS), the Soil and Water Assessment Tool (SWAT) (Arnold et al., 2012) and the Hydrological Simulation Program FORTRAN (HSPF).

These models provide complex simulations of the impacts of land use alterations, climate fluctuations and soil management techniques on water resources rendering them especially useful for assessing the long-term consequences of climate change and land use on hydrology and sediment generation (Addis et al., 2016; Chelkeba Tumsa, 2023; Memarian et al., 2014). Due to its computing efficiency the SWAT model has gained widespread use allowing for effective operation on extensive basins within realistic time constraints. Furthermore, it excels at simulating the impacts of management options on long-term water quality and sediment yield (Marco & van, 2011; Sisay et al., 2017).

The growing application of physics-based models in sediment yield research has enhanced the comprehension of sediment dynamics particularly in regions affected by climate change and human activities. These models offer essential insights into how alterations in climate and land use such as deforestation and agricultural expansion

exacerbate soil erosion and sedimentation processes (Mbungu, Easton, et al., 2016). They are progressively employed to simulate complex water resource systems, encompassing river basins that undergo fluctuating hydrological conditions resulting from both climatic and anthropogenic factors. These models assist policymakers and land managers in formulating more efficient watershed management and erosion control methods assuring resource sustainability while alleviating the adverse effects of erosion and sedimentation on ecosystems and infrastructure (Chen et al., 2020).

2.9 The Utilization of the SWAT Model in Assessing the Impacts of Climate Change on Sediment Yield

2.9.1 Soil and Water Assessment Tool (SWAT) Model

2.9.1.1 General Overview

The Soil and Water Assessment Tool (SWAT) model is a semi-distributed, lumped-parameter hydrological model intended to simulate the impacts of land use, soil characteristics, climate and management methods on the movement of water, sediment and nutrients across extensive complex watersheds. The SWAT model, created by researchers at the U.S. Department of Agriculture Agricultural Research Service (USDA-ARS) (Arnold et al., 2012) is extensively used for the analysis of hydrological processes and sediment transport (Akoko et al., 2021; Catchments, 2005; Chelkeba Tumsa, 2023). In recent years, its use has broadened to assess the impacts of climate change on river flow and sediment transport. Research has shown SWAT's efficiency in modelling the impact of changes in climate variables including precipitation and temperature on sediment dynamics and river flow patterns (Ndulue & Mbajiorgu, 2018a; Ngo Thanh et al., 2020; Strauch et al., 2012). A key advantage is its capacity to forecast the long-term consequences of erosion in extensive basins rendering it especially valuable for understanding the timing of agricultural practices throughout the year and their influence on sediment dynamics (Feyissa Negewo & Kumar Sarma, 2022; Lazaro et al., 2023; Zhang et al., 2019). These characteristics have facilitated SWAT's prevalent application in watershed management and environmental research.

The SWAT model partitions a watershed into sub-basins which are subsequently categorized as Hydrologic Response Units (HRUs) according to land use, soil type and slope (Al-Khafaji & Al-Mukhtar, 2017; Maref et al., 2022). This split facilitates a more

nuanced depiction of spatial heterogeneity in hydrological processes hence, enhancing the model's capacity to simulate water, sediment and nutrient dynamics across diverse terrain characteristics (Gemechu et al., 2021; Lèye et al., 2020). The sub-basin approach offers a framework for capturing discrepancies in runoff and sediment yield over various sections of the watershed allowing the model to simulate hydrological processes at many scales ranging from small catchments to extensive river basins. In each sub-basin, Hydrologic Response Units (HRUs) are delineated as regions exhibiting similar land use, soil characteristics and topographical features hence, enhancing the model's capacity to properly reflect the impact of various climate change and land management strategies on hydrological results (Kimwaga, 2012). By integrating these spatially explicit units, SWAT can more accurately model the impacts of climate change, land use and land cover alterations on watershed hydrology and water quality (Echogdali et al., 2022; Karakoyun & Kaya, 2022; Zettam et al., 2017). This spatial resolution facilitates improved management of water resources by identifying crucial regions for erosion prevention and water conservation within a watershed (Marco Ndomba & Mtalo, 2016; Ngo Thanh et al., 2020). The adaptability in delineating Hydrological Response Units (HRUs) according to regional variability renders SWAT a potent instrument for understanding the complex relationships that connect land use, soil characteristics and hydrological processes across extensive and heterogeneous watersheds (Zettam et al., 2017).

The SWAT model necessitates certain critical data inputs to accurately simulate hydrological and environmental processes. This includes meteorological data (including precipitation, temperature, wind speed, humidity and solar radiation), land use/land cover (LULC) information, soil attributes (such as texture, hydraulic conductivity and water retention capacity) and topographical data obtained from a Digital Elevation Model (DEM) (Kimwaga et al., 2012; Lèye et al., 2020). A fundamental element in the management and processing of this data is geographic information systems (GIS) which are essential for organizing, analyzing and visualizing spatial data for watershed modelling (Getachew Abebe & Woldemariam, 2024; Tsegaye & Bharti, 2021; Worku et al., 2017). GIS facilitates the integration of diverse spatial variables essential for SWAT including land use, soil characteristics and

topography under a unified spatial framework (Kolli et al., 2021). It facilitates the precise definition of sub-basins, Hydrologic Response Units (HRUs) and flow paths within a watershed according to the geographical distribution of land use and soil types. The capacity to manage extensive regionally distributed datasets and execute complex spatial analyses is a fundamental advantage of GIS in hydrological modelling (Arnold et al., 2012; Gassman et al., 2007). GIS tools are employed to extract topographic features from the DEM including slope, aspect and flow direction which are essential for modelling runoff and sediment transport processes (Arnold et al., 2012; Worku et al., 2017).

GIS facilitates the categorisation of land use and cover which is essential for assessing the impact of various land management methods on sediment yield, water quality and hydrological processes (Arnold et al., 2012). When integrated with SWAT, GIS facilitates the visualization of model outputs including sediment distributions, hydrological flow patterns and regions susceptible to erosion. These visualizations facilitate the identification of key locations for management interventions and enable decision-makers to evaluate the efficiency of diverse land management practices.

The integration of GIS with SWAT augments the model's capacity to simulate complex spatially diverse hydrological processes and furnishes watershed managers with robust instruments for the analysis and management of water resources, sediment dynamics and ecosystem health across extensive heterogeneous landscapes (Gassman et al., 2007).

The SWAT model quantifies the impacts of climate and vegetation changes on environmental variables including water quantity, water quality and physical processes including soil and groundwater water flows (Arnold et al., 2012; Gassman et al., 2007). The fundamental aspect of SWAT's hydrological simulations is the water balance equation which underpins the modelling of the hydrologic cycle (Arnold et al., 2012). This enables the model to evaluate the impact of various climate and land-use scenarios on the transportation and distribution of water within a watershed.
Water Balance Equation shown in equation 2.2:

$$SW_t = SW_o + \sum_{i=1}^{t}\left(R_{day} - Q_{surf} - E_a - W_{sweep} - W_{gw}\right)t \quad (2.2)$$

Where SW_t is the final soil water content; SW_o is the initial soil water content on day i in mm; R_{day} is the amount of precipitation on day in mm; Q_{surf} is the amount of surface runoff on day i in mm; E_a is the amount of evapotranspiration on day i in mm; W_{sweep} is the amount of water entering the vadose zone from the soil profile on day i in mm; W_{gw} is the amount of return flow on day i in mm; and t Is the time in da

Furthermore, SWAT integrates complex hydrological processes, including infiltration, evaporation, plant uptake, lateral fluxes, percolation and groundwater flows using integrated equations. A graphical representation of the hydrologic cycle in SWAT delineates essential catchment parameters such as precipitation, runoff, infiltration, evapotranspiration and groundwater flow emphasizing their interconnectedness. Typically illustrated in Figure 2.3, this figure depicts the processes of water movement and storage within the watershed, thereby aiding in the understanding of water partitioning across various phases and compartments. It demonstrates how SWAT integrates these systems to replicate the hydrological dynamics of a watershed under diverse land use, climatic, and management scenarios (Arnold et al., 2012; Gassman et al., 2007).

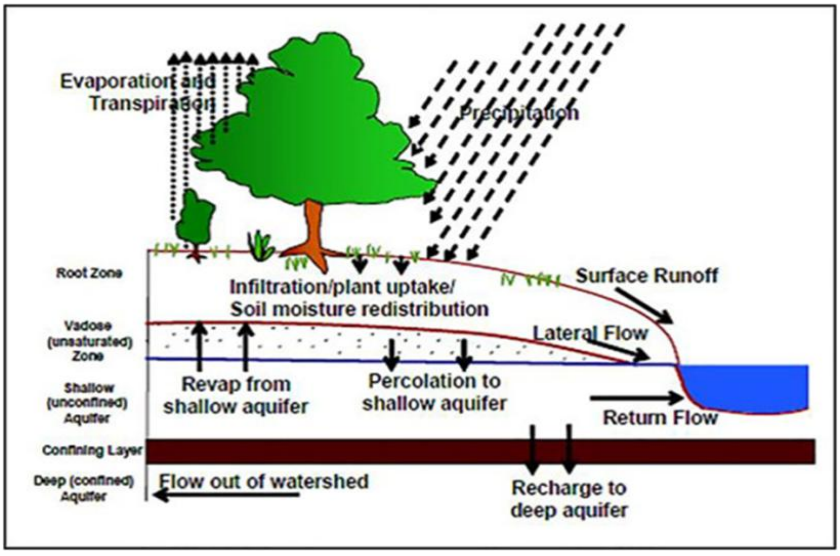

Figure 2.3: Graphical representation of the hydrologic cycle in SWAT (Janjić & Tadić, 2023)

The SWAT model simulates several hydrological and water quality processes such as surface runoff, evapotranspiration, infiltration, sediment transport, nutrient cycling and pesticide dynamics (Arnold et al., 2012). The Modified Universal Soil Loss Equation

(MUSLE) is used to simulate sediment yield and describe soil erosion processes whereas the Bagnold Equation characterizes sediment flow in channels (Akoko et al., 2021; Chelkeba Tumsa, 2023; Gwapedza et al., 2021). The MUSLE is very effective for calculating sediment yield in relation to runoff events, considering both the runoff volume and the peak discharge.

The MUSLE sediment model is as shown in equation 2.3:

$$Sed = 11.8 \times \left(Q_{surf} \times q_{peak} \times Area_{HRU}\right)^{0.56} \times K_{USLE} \times C_{USLE} \times P_{USLE} \times LS_{USLE} \times CFRG \quad .(2.3)$$

Where Sed is the sediment yield (metric ton day^{-1}); Q_{surf} is the surface runoff volume (mm ha^{-1}); q_{peak} is the peak runoff rate in m^3 s^{-1}; Area HRU is the area of HRU in ha; K_{USLE} is the soil erodibility factor; C_{USLE} is the cover and management factor; P_{USLE} is the support practice factor; LS is topographic factor; and CFRG is the course fragment factor in the universal soil loss equation (USLE).

This equation calculates sediment yield by considering the interplay of runoff volume, peak discharge, soil erodibility, plant cover and topography, when estimating the sediment generated from land surface erosion. The MUSLE in SWAT integrates these parameters to simulate sediment dynamics across diverse land use, climate and management scenarios rendering it an effective instrument for watershed management and soil conservation (Arnold et al., 2012; Bekele & Abate, 2020; Toma et al., 2023).

2.9.1.2 Calibration and Validation of the SWAT Model

The calibration and validation of the SWAT model are essential for guaranteeing its accuracy and dependability when modelling hydrological and sedimentary processes within watersheds (Akoko et al., 2021; Arnold et al., 2012). Calibration involves modifying model parameters to align with observed data whereas validation assesses the model's prediction ability using independent datasets. The effective calibration and validation of the SWAT model are essential for delivering reliable forecasts of hydrological dynamics and sediment output which are vital for watershed management and land use planning (Akoko et al., 2021; Arnold et al., 2012; Srinivasan et al., 2012). Flow data (streamflow) and sediment data (sediment concentration and sediment yield) are crucial for calibrating the SWAT model. Flow data is used to calibrate hydrological processes such as runoff, evapotranspiration and groundwater dynamics.

In contrast, sediment data is essential for calibrating parameters related to soil erosion and sediment transport including the soil erodibility factor (K_USLE) and the cover management factor (C_USLE). Within hydrological models like SWAT, calibrating sediment yield focuses on adjusting parameters to ensure that simulated sediment yields align with observed sediment movement and deposition within the watershed (Srinivasan, 2009; Srinivasan et al., 2012).

The calibration and validation of the Soil and Water Assessment Tool (SWAT) are essential procedures for confirming the model's ability to accurately simulate hydrological processes and sediment production. These methods entail modifying model parameters to optimally align with observed data (calibration) and evaluating the model using separate datasets (validation). Calibration and validation are essential to verify the model's prediction efficiency and guarantee its applicability in decision-making for watershed management (Arnold et al., 2012; Qi et al., 2020).

2.9.1.2.3 Calibration and Validation Methods in SWAT

The Sequential Uncertainty Fitting (SUFI-2) algorithm incorporated inside the SWAT-CUP (Calibration and Uncertainty Procedures) framework is a prevalent technique for model calibration and validation. SUFI-2 seeks to reduce prediction uncertainty by calibrating model parameters to minimize differences between observed and simulated data (Arnold et al., 2012; Hussain et al., 2019). This approach employs Latin Hypercube Sampling (LHS) to generate distinct parameter sets, facilitating the efficient investigation of the parameter space. Through the optimization of various parameter sets, SUFI-2 enables sensitization, validation and uncertainty analysis within a unified iterative framework.

Recent studies have proven the efficiency of SUFI-2 across diverse hydrological situations. Previous studies highlight the efficiency of SUFI-2 in optimizing hydrological model parameters across various areas and hydrologic conditions (A. T. Assfaw, 2019; Gyamfi et al., 2016; Narsimlu et al., 2015; Shivhare et al., 2018).

2.9.1.2.4 Sensitivity Analysis in SWAT Calibration

Before calibration begins, a sensitivity analysis is performed to identify which model parameters have the most significant influence on the model's outputs for a specific

basin or sub-basin (Arnold et al., 2012). This analysis evaluates how changes in model inputs affect the model's outputs allowing researchers to focus their calibration efforts on the most impactful factors. The SWAT model employs multiple methodologies for sensitivity analysis, notably the Latin Hypercube One Factor-At-A-Time (LH-OAT) method which methodically examines the influence of individual parameters on the model's output while keeping other parameters fixed. This approach effectively identifies essential factors for calibration and elucidates the influence of various input variables on the simulation of runoff and sediment dynamics (Assfaw, 2019; Gyamfi et al., 2016; Mengistu et al., 2019).

In SWAT, factors such as the soil erodibility factor (K_USLE), the cover management factor (C_USLE) and the topography factor (LS) are often recognised as sensitive and influential for hydrological outcomes (Nagireddy et al., 2023; Srinivasan, 2009; Srinivasan et al., 2012). River flow is a crucial output in hydrological models and understanding its sensitivity is vital during the calibration process. A river flow sensitivity study specifically examines the elements that influence the flow dynamics within a watershed including precipitation, runoff, infiltration and evapotranspiration. The sensitivity of river flow is essential for accurately replicating streamflow which frequently serves as the primary observed data for model calibration.

River flow sensitivity analysis involves investigating how variations in factors such as the SCS-CN, soil moisture capacity and curve number affect streamflow forecasts (Gyamfi et al., 2016). Runoff generation and streamflow response intricately link these factors. In regions characterized by significant precipitation variability, the SCS-CN parameter plays a critical role in river flow forecasts by controlling the volume of rainfall that translates into surface runoff (Arnold et al., 2012; Srinivasan et al., 2012). Additionally, characteristics related to infiltration such as soil hydraulic conductivity and soil depth are crucial for influencing the movement of water through the watershed and its eventual arrival in the river system.

2.9.1.2.5 Model Performance and Evaluation Metrics

Various statistical measures evaluate the performance of SWAT during calibration and validation assessing the model's accuracy in simulating observed data (Assfaw, 2019;

Shivhare et al., 2018; Yu et al., 2022). We include the following essential performance indicators:

Nash-Sutcliffe Efficiency (NSE): An indicator of the degree to which the model's predictions correspond with observable data with values spanning from -∞ to 1 (Negussie et al., 2022). A score of 1 signifies flawless prediction but values beyond 0.5 often denote commendable model performance (Assfaw, 2019; Maref et al., 2022). NSE is shown in equation 2.4:

$$Nash - Sutcliffe\ Efficiency\ \ (NSE) = \frac{\sum_{i=1}^{n}(O_{i-}\ S_i)^2}{\sum_{i=1}^{n}(O_i - \overline{O_i})^2} \qquad (2.4)$$

O_i: Observed Values; S_i: Simulated values; $\overline{O_i}$: Mean observed values; $\overline{S_i}$: Mean of mean simulated values; and n: is total number of time steps

The Coefficient of Determination (R^2) evaluates the fraction of variance in the observed data accounted for by the model. R^2 values approaching 1 signify a superior alignment between observed and simulated data (Moriasi et al., 1983). R^2 is shown in equation 2.5:

$$The\ Coefficient\ of\ Determination\ (R^2) = \frac{\sum_{i=1}^{n}(O_i - \overline{O_i})(S_i - \overline{S_i})}{\left[\sum_{i=1}^{n}(O_i - \overline{O_i})^2\right]^{0.5}\left[\sum_{i=1}^{n}(S_i - \overline{S_i})^2\right]^{0.5}} \qquad (2.5)$$

Percent Bias (PBIAS): This metric measures the discrepancy between observed and simulated data expressed as a percentage of the observed value. A negative PBIAS signifies under-prediction, whereas a positive PBIAS denotes over-prediction (Negussie et al., 2022). PBIAS is shown in equation 2.6:

$$Percent\ Bias\ (PBIAS) = \frac{\sum_{i=1}^{n}(O_{i-}\ S_i)}{\sum_{i=1}^{n} O_i} \times 100 \qquad (2.6)$$

Root Mean Square Error (RMSE) and Mean Absolute Error (MAE) quantify the average magnitude of model discrepancies between observed and simulated values. Reduced RMSE and MAE values signify superior model performance. RMSE is shown in equation 2.7:

$$Root\ Mean\ Square\ Error\ (RMSE) = \sqrt{\frac{1}{n}\sum_{i=1}^{n}(O_i - S_i)^2} \qquad (2.7)$$

An NSE over 0.5, an R^2 approaching 1, and a PBIAS within ±25% are generally regarded as acceptable benchmarks for effective model performance in river flow (Moriasi et al., 1983; Negussie et al., 2022). These limits guarantee that the model can consistently replicate river flow dynamics and deliver precise streamflow estimates for watershed management and planning purposes.

2.9.1.3 Challenges in Calibration and Validation

A significant challenge in calibrating and testing the SWAT model is the frequent lack of direct sediment data, particularly in regions where sediment monitoring stations are either sparse or entirely absent. In the absence of such data, Researchers face substantial difficulties in evaluating the accuracy of sediment production predictions. Consequently, researchers often resort to utilizing surrogate data to estimate sediment yield and facilitate calibration.

Surrogate data, including turbidity measurements and sediment rating curves, provide indirect estimates of sediment yield. Turbidity, which indicates water cloudiness caused by suspended particles is commonly linked to sediment concentration making it an effective proxy for sediment yield (Krysanova & White, 2015; Negussie et al., 2022). Similarly, sediment rating curves which establish a relationship between river discharge and sediment content can be employed to estimate sediment yields when direct data is unavailable. These rating curves are often derived from nearby catchments that share similar hydrological characteristics thereby assisting reseachers in estimating sediment transport within the targeted watershed (da Silva et al., 2021; Haque et al., 2024; Krysanova & White, 2015).

Flow data can serve as an effective proxy for sediment calibration due to the strong correlation between streamflow and sediment transport. Given that sediment transport is often influenced by runoff calibrating the SWAT model with observed streamflow data can indirectly replicate sediment dynamics even when direct sediment data is not available (Krysanova & White, 2015). By aligning simulated flow with observed streamflow, the model can be trained to forecast sediment yield as sediment response is typically associated with streamflow events.

Remote sensing and Geographic Information Systems (GIS) are crucial tools for addressing data limitations especially in areas with sparse field data. Satellite imagery, vegetation indices (such as NDVI) and digital elevation models (DEMs) provide essential spatial data on changes in land cover, erosion trends and river flow dynamics which are vital for model calibration in the absence of direct field observations (Krysanova & White, 2015; Theron et al., 2021). Remote sensing data allows for the monitoring of temporal changes in land use and land cover, both of which directly impact runoff and sediment production. GIS technologies further enhance the simulation of sediment transport by supplying spatial data on topography and hydrological networks (Kolli et al., 2021; Tsegaye & Bharti, 2021; Worku et al., 2017). By integrating remote sensing and GIS data researchers can address the lack of comprehensive field observations and improve their calibration processes thereby enhancing the accuracy of sediment yield simulations and increasing model efficiency in data-scarce contexts (Krysanova & White, 2015).

An alternative method for addressing the issue of missing data is the use of proxy catchment data. A proxy catchment is defined as an adjacent or comparable watershed that shares similar hydrological, topographical and land use characteristics with the target catchment (Msadala & Basson, 2017; Theron et al., 2021). Data from these proxy catchments can serve as a substitute during the calibration and validation phases. By utilizing proxy data Researchers can derive initial estimations of the model parameters for the target catchment particularly when data from the target catchment is limited or inaccessible. Following the initial calibration of the model with proxy catchment data further refinements can be made by adjusting model parameters based on the available flow or sediment data from the target catchment. This approach facilitates model calibration in catchments lacking direct sediment data by leveraging insights obtained from analogous catchments (Gassman et al., 2007; Gassman & Yingkuan, 2015).

Empirical sediment data derived from frequently used empirical equations provide a reliable alternative for model calibration and validation. Two commonly employed empirical equations are the Universal Soil Loss Equation (USLE) and the Modified Universal Soil Loss Equation (MUSLE). These equations estimate sediment yield

based on variables such as rainfall intensity, runoff volume, soil erodibility, and land cover. Both the USLE and the MUSLE have been extensively utilized in soil erosion research, producing significant sediment yield estimations, particularly in contexts with limited data (Sulaiman et al., 2021; Tabarestani et al., 2022).

2.9.2 The Role of the SWAT Model in Evaluating the Impacts of Climate Change on Sediment Yield

The SWAT (Soil and Water Assessment Tool) model is a crucial instrument for assessing the impacts of climate change on sediment yield in diverse global, African and Tanzanian watersheds. Numerous research investigations have demonstrated the model's efficacy in forecasting sediment dynamics under prospective climate scenarios, offering essential insights for watershed management and soil conservation strategies.

The SWAT model has been used worldwide to evaluate hydrological dynamics and sediment yield in response to changing climate conditions (Ercan et al., 2020; Ndulue & Mbajiorgu, 2018a). Various studies employed the SWAT model to assess the effects of anticipated climatic changes, including elevated temperatures and less precipitation, on water production and sediment load (Mueller-Warrant et al., 2019). The research indicated that these alterations would probably result in a reduction of both water supply and sediment transport across multiple climate models (Echogdali et al., 2022; Ngo Thanh et al., 2020). The findings underscored the necessity of comprehending these processes to properly manage water resources and soil erosion (Echogdali et al., 2022; Ndulue & Mbajiorgu, 2018a). The SWAT model was employed in various catchments to forecast fluctuations in sediment yield under climate change scenarios. The findings revealed that, climate change may intensify sediment transport, thereby aggravating soil erosion problems (Echogdali et al., 2022; Ndulue & Mbajiorgu, 2018a; Ngo Thanh et al., 2020). The SWAT model was used to evaluate sediment fluxes in the Mekong Basin of Laos. The research found that, under diverse climate change scenarios, sediment output might rise substantially, with some forecasts predicting an increase of up to 160% (Shrestha et al., 2013). These findings demonstrate the ability of climate-induced alterations to significantly modify sediment dynamics, exacerbating sedimentation challenges in the area.

The SWAT model has proved crucial in analysing the impact of climate change on sediment yields across many watersheds in Africa (Blake et al., 2018; Gwapedza et al., 2021). Research indicates that climate change is expected to increase both the frequency and intensity of precipitation events, thereby increasing sediment yields due to heightened flow and soil erosion. The studies employed the SWAT model to evaluate the possible impacts of climate change on sediment yields in the watersheds. The findings indicated that, if climate change persists unabated, sediment yields may rise each year with possible maximum increase over the next century (Hailu et al., 2023; Msadala & Basson, 2017; Theron et al., 2021). This underscores the considerable threat that climate change presents to sedimentation challenges highlighting the necessity for adaptive management strategies (Chapman et al., 2021). The SWAT model used in the Upper Abay Catchment, Ethiopia, to simulate soil erosion and sediment yields under projected climatic conditions (Gemechu et al., 2021). Their research indicated a significant increase in sediment production resulting from alterations in precipitation and temperature patterns, showcasing the model's capacity to forecast future soil erosion issues caused by climate change.

The SWAT model has been employed in Tanzania to evaluate sediment yields in data-scarce regions (Kimwaga, 2012; Mbungu, Heatwole, et al., 2016; Msaghaa, 2012; Ndomba et al., 2008; Wynants et al., 2021). A study in the Simiyu River sub-catchment illustrated the model's efficacy in ungauged catchments. The model adjusted using daily flow data, estimated sediment production at 0.523 tonnes per hectare per year, demonstrating SWAT's efficacy in sediment yield modelling even in data-deficient areas (Kimwaga, 2012). A distinct study in Tanzania examined the model's capacity to replicate the effects of land-use alterations and climate variability on sediment transport. The study demonstrated the model's ability to replicate the long-term impacts of climate change-induced land cover variations on erosion rates and sediment output over time (Mbungu, Easton, et al., 2016).

2.9.3 SWAT for Watershed Management and Soil Conservation

In addition to predicting the effects of climate change on sediment output, the SWAT model is essential for watershed management. A fundamental attribute of the model is its capacity to detect erosion hotspots via spatial analysis which allows land managers

to prioritize regions necessitating soil conservation initiatives (Addis et al., 2016; Akoko et al., 2021; Catchments, 2005; Tesfahunegn et al., 2012). This skill facilitates the formulation of targeted management strategies for regions most susceptible to soil erosion resulting from changing climatic conditions. Furthermore, SWAT is capable of simulating diverse land management strategies, including afforestation, reforestation and modifications in agricultural techniques, to evaluate their efficacy in reducing silt generation (Himanshu et al., 2019; Leta et al., 2023; Mrad et al., 2024). The model assesses various conservation measures to determine the best effective methods for mitigating the effects of climate change on sediment yield (Mrad et al., 2024). Consequently, SWAT is an essential instrument for formulating adaptive management plans to tackle the issues presented by climate change and sedimentation (Gharibdousti et al., 2019).

In conclusion, the SWAT model provides a comprehensive and adaptable instrument for evaluating the impacts of climate change on sediment yield in several geographical locations including Africa and Tanzania. The model simulates sediment movement under varying climatic circumstances, offering critical insights into future alterations in sediment dynamics vital for successful watershed management and soil protection (Leta et al., 2023; Mrad et al., 2024). The model's precision in forecasting sediment yield under climate change scenarios is contingent upon the quality of input data, calibration methodologies and uncertainty assessment. Consequently, it is imperative to meticulously assess the model's constraints to guarantee its practical utility. As climate change increasingly affects sediment dynamics, SWAT's role in formulating adaptive management techniques and soil conservation policies will be essential for safeguarding water resources and reducing erosion hazards.

2.10 Research Gap

A notable research gap exists in the examination of sediment yield specifically in the SongweRiver Sub-Basin. Despite extensive research on sediment transport in many African river basins this specific sub-basin has received relatively few studies. The existing research fails to adequately tackle the impacts of climate change on sediment dynamics in this region underscoring the need for more focused studies.

The incorporation of climatic scenarios in sediment yield management is yet to be adequately examined in the Songwe River Sub-Basin. The implications of climate change, including modified precipitation patterns, increased temperatures and extreme weather events, have not been sufficiently modelled to evaluate their influence on sediment dynamics in this region. Further research is required to model various climate change scenarios and their possible impacts on sediment movement and erosion in the Songwe River Sub-Basin particularly on the basin's susceptibility to climatic variations.

To address the shortcoming of low-resolution models, this research utilizes bias-corrected, high-resolution RCM data from CORDEX-Africa. The SWAT model and other climate models employed in the region frequently exhibit insufficient spatial resolution limiting their capacity to forecast the localised effects of climate change on soil erosion and sediment generation. High-resolution models are essential for accurately representing the intricacies of local climate and terrain and, hence, facilitating more precise predictions of sediment dynamics.

A notable research gap exists due to the absence of comprehensive and high-quality data regarding sediment generation, climate variability and hydrological changes specific to the Songwe River Sub-Basin. The lack of such data constrains the capacity to formulate dependable predictive models for sediment output. Augmented data-gathering initiatives and the implementation of enduring monitoring systems are essential for surmounting this obstacle and enhancing the precision of subsequent investigations.

Research on the impacts of climate alterations on sediment yield in the Songwe River sub-basin is relatively sparse. This study fills this gap by applying high-resolution CORDEX climate projections to the SWAT model to quantify future sediment yield in the Songwe Sub-Basin The document addresses the implications of climate changes for sediment dynamics; however, further targeted studies are required to investigate the impact of specific climate alterations and erosion patterns in the region. Comprehending the direct correlation between climate patterns and sediment yield is essential for formulating efficient water resource management and land management plans.

Ultimately, although numerous sediment management solutions have been suggested there is a deficiency of comprehensive studies assessing the efficiency of these measures in the Songwe River sub-basin. Further research is required to evaluate the viability and effectiveness of erosion control strategies, vegetation restoration approaches and sediment retention techniques in alleviating the consequences of heightened sediment yield resulting from climate changes. Addressing these research deficiencies is essential for formulating sustainable and effective sediment management strategies in the Songwe River sub-basin.

2.11 Concluding Remarks

This chapter provides an overview of various aspects of sediment yield and climate change. It begins by examining the factors that affect sediment yield in river sub-basins and the methods used for characterizing and mapping sediment sources. The chapter then discusses the impacts of climate change on sediment yield under different climate scenarios. It further highlights the use of climate and SWAT models for modelling future climate data and sediment yield. Finally, the chapter provides a description of the existing situation in the study area and identified the research gaps.

CHAPTER THREE

METHODS AND MATERIALS

3.1 Overview

Chapter three outlines the methodologies and materials employed to examine the impacts of climate change on sediment yield in the Songwe River sub-basin. The chapter outlines the use of the SWAT model with QGIS for simulating and visualizing sediment yield across climatic scenarios and different future land use scenarios. The study aimed to predict the impacts of climate change on future sediment dynamics under various climate scenarios by using four climate models' output. It also examines the impacts of climate change under different scenarios on sediment production. The study predicts effects of these elements emphasizing their difficulties in regulating erosion and sedimentation. The chapter also offers a comprehensive description of the study area establishing the background for the investigation.

3.2 Research Design

This research uses a quantitative research approach that combines hydrological modelling, climatic predictions and spatial analysis to evaluate the impacts of climate change and land use/land cover (LULC) changes on sediment production in the Songwe River Sub-Basin. Quantitative research is crucial for this study as it facilitates the numerical assessment of sediment dynamics under diverse environmental conditions providing accurate forecasts of future sediment fluxes. This approach is especially beneficial in hydrological research as model-based simulations provide understandings that are challenging to gain by conventional field techniques (Arnold et al., 2012; Gassman et al., 2007). The research employs a multi-method strategy integrating recognised hydrological models including the Soil and Water Assessment Tool (SWAT) with geospatial technologies such as remote sensing (RS) and geographic information systems (GIS) to simulate variations in sediment production within the sub-basin (Kolli et al., 2021; Tsegaye & Bharti, 2021; Worku et al., 2017).

The Soil and Water Assessment Tool (SWAT) Model was used for modelling sediment transport an advanced process-oriented model capable at simulating the relationships of land use, climate and hydrological cycles throughout extensive and complex

watersheds (Chelkeba Tumsa, 2023; Memarian et al., 2014; Srinivasan et al., 2012). The SWAT model was chosen for its capacity to simulate sediment transport and erosion processes across diverse climatic conditions essential for understanding sediment yield dynamics in relation to climate change in data scarce basins (Arnold et al., 2012; Gassman et al., 2007). The river flow data was used to calibrate the SWAT model for river flow (Krysanova & White, 2015). SWAT's ability to incorporate historical and projected climate data, land use/land cover maps and additional watershed characteristics renders it particularly suitable at assessing the increasing impacts of climate and land use/land cover changes on sediment dynamics. This benefit is significant in areas such as the Songwe River Sub-Basin where data are limited and extensive modelling methodologies are infrequently employed (Abbaspour et al., 2007; Hussain et al., 2019). The model's capacity to analyze extensive data while considering geographical and temporal variability in climate and land use makes it an optimal instrument for simulating the long-term impacts of climate change on sediment dynamics within the sub-basin (Feyissa Negewo & Kumar Sarma, 2022; Mbungu, Heatwole, et al., 2016; Zhang et al., 2019).

The research design and methods employed in this study are summarized in the conceptual framework presented in Figure 3.1.

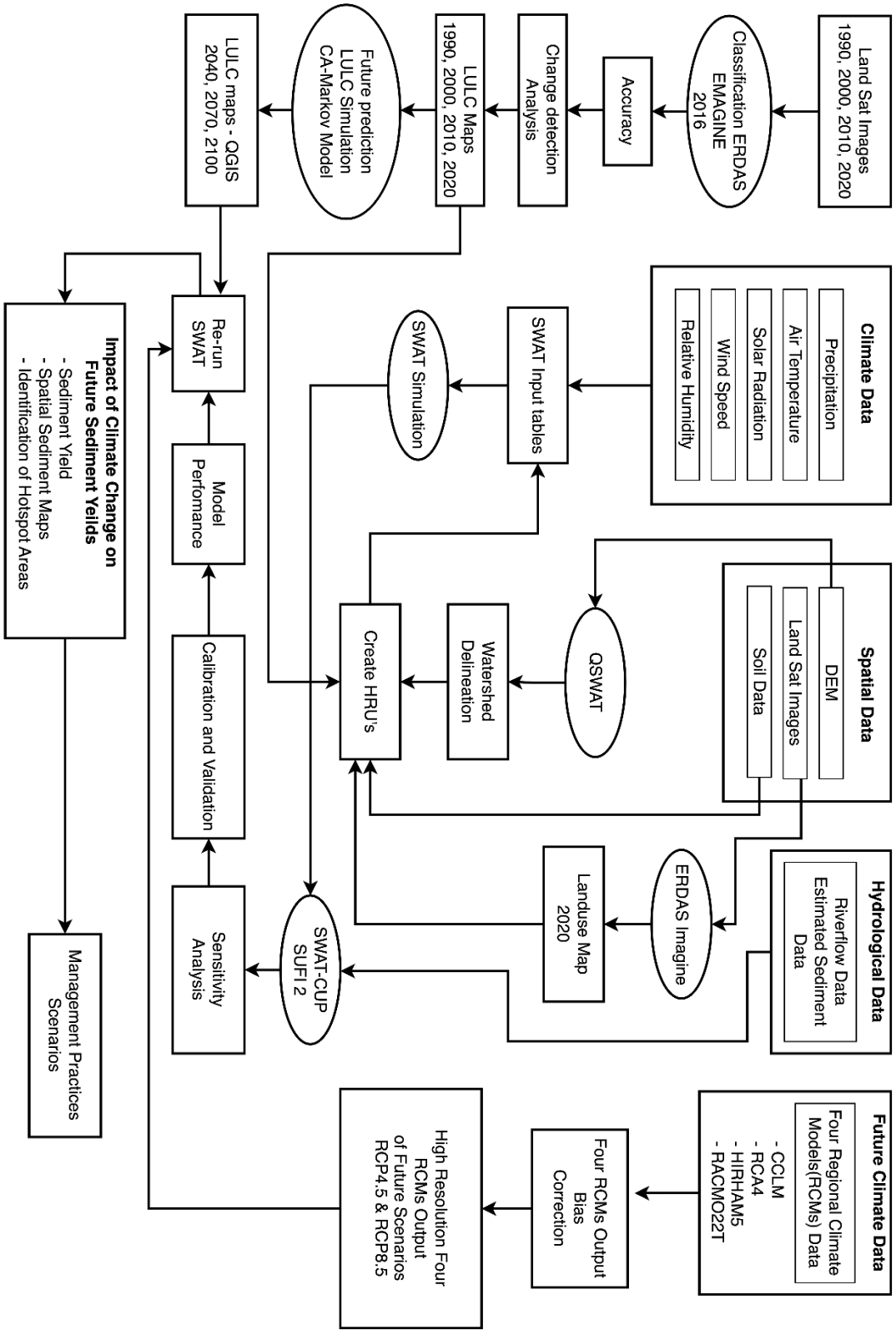

Figure 3.1: Schematic Representation of the Methodological Framework

3.3 Description of the Study Area

3.3.1 Location of the study Area

The Songwe River Sub-Basin is in the eastern region of the Lake Rukwa Basin in southwestern Tanzania, between latitudes 07°40'S and 09°20'S and longitudes 33°00'E and 33°50'E. The region encompasses around 10,800 km² (Figure 3.2) and has numerous districts including Chunya, Mbeya DC, Mbeya Urban, Mbozi, Mbarali, Songwe and Rungwe. The sub-basin is a crucial component of Tanzania's southern highlands including the middle Mbeya Plain and the Poroto Highlands. The Lake Rukwa Basin situated inside the East African Rift Valley, operates as an internal drainage system indicating that the rivers flowing into the lake do not discharge into the sea but remain contained within the basin. The Songwe River originating in the Poroto Mountains and is the principal river of the sub-basin.

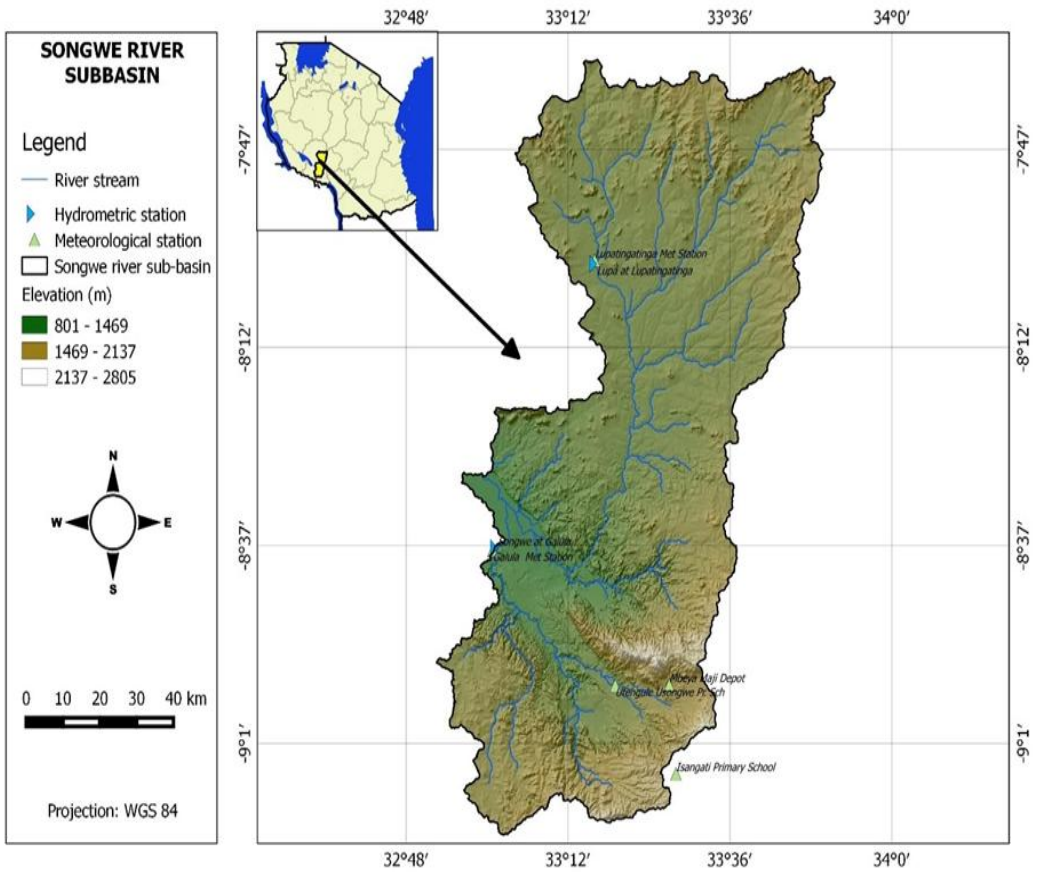

Figure 3.2: Location map of the Songwe River sub-basin, Tanzania created in QGIS 2.6.1

3.3.2 Topography

The Songwe River sub-asin has a diverse and dynamic topography with altitudes varying from 600 to 2,400 meters above sea level (masl) (Figure 3.3). The region features a combination of hills and valleys which significantly influence the sub-basin's hydrology, climate and land use patterns. The sub-basin's geography ascends sharply in the highlands with elevations attaining up to 2,400 meters above sea level, encompassing the Poroto Highlands and other mountainous regions of southern Tanzania (Kalisa et al., 2013). The highland regions are crucial for supplying water to the rivers via quick runoff particularly during the rainy season hence, enhancing the flow in the Songwe River and its tributaries (Addis et al., 2016). The steep inclines in these regions are frequently susceptible to soil erosion especially during heavy rainfall rendering them subject to degradation (Kalisa et al., 2013; Mbungu, Easton, et al., 2016). Conversely, the low-lying areas of the sub-basin including the Mbeya Plain are located at around 600 meters above sea level. These regions are generally defined by moderate inclines and nutrient-rich soils rendering them optimal for agricultural endeavours. The fertile valleys within the sub-basin facilitate the cultivation of crops such as maize, beans and vegetables which are essential for the local economy (Kalisa et al., 2013). Nonetheless, the lower regions have difficulties including seasonal floods, which are intensified by the swift runoff from the highland areas during the rainy season (Chen et al., 2020; Kido et al., 2023). The Songwe River sub-basin's topographical diversity directly influences land utilization. The highlands are primarily designated for forests, natural vegetation and restricted grazing but the fertile valleys are intensively employed for agriculture and habitation (Kalisa et al., 2013). This allocation of land use illustrates the inherent appropriateness of the topography for various occupations while also highlighting the difficulties of addressing erosion in the highlands and flooding in the valleys. Alterations in land use in both the highlands and lowlands significantly affect sediment movement, water quality and comprehensive land management techniques in the region.

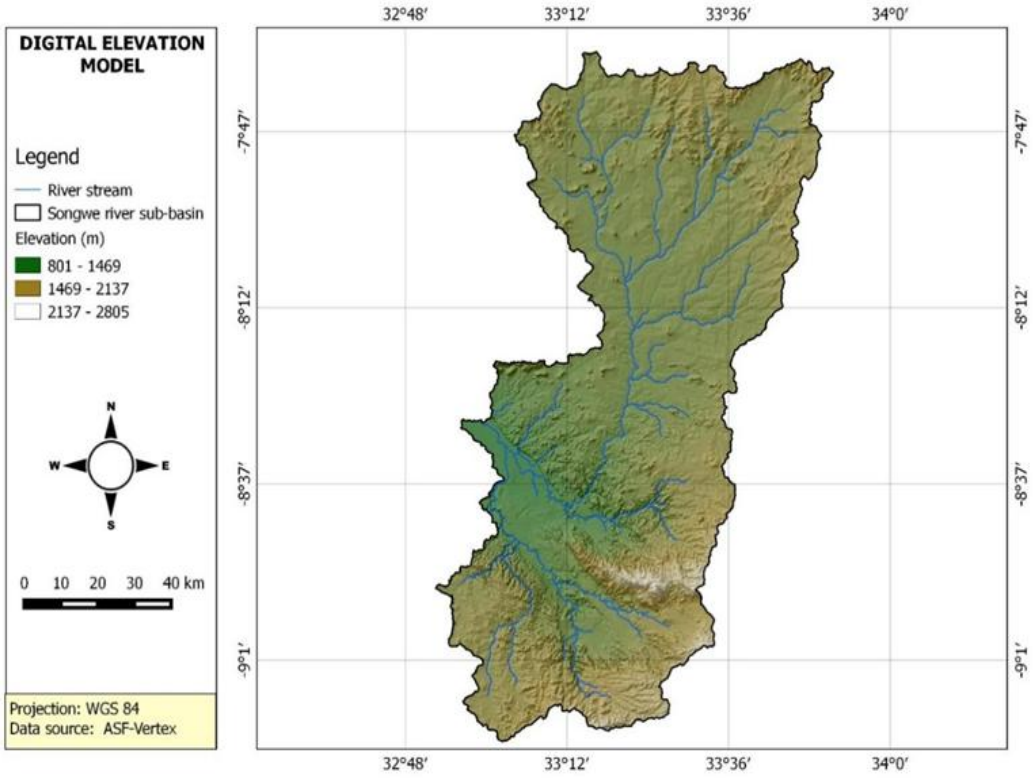

Figure 3.3: Digital Elevation Model (DEM) of the Songwe River sub-basin created in QGIS 2.6.1.

3.3.3 Climate

The Songwe River sub-basin exhibits a tropical climate marked by an extended rainy season from October to May which constitutes the majority of the region's yearly precipitation. This interval is vital for agricultural endeavours and the restoration of water resources in the region (Kalisa et al., 2013). The dry season which generally occurs from June to September is characterised by less precipitation resulting in water scarcity especially in lowland regions (Valimba, 2019). The sub-basin undergoes considerable climate variability chiefly influenced by its topographical diversity and periodic weather swings. This variability is evident in regional and temporal fluctuations in precipitation, temperature and hydrological dynamics (IPCC, 2021; Luhunga et al., 2018; Melesse & Abtew, 2015; Shrestha & Wang, 2018). Climate variability in the region is projected to escalate due to climate change leading to more frequent irregular precipitation patterns and temperature extremes (Mutayoba et al., 2018b; Stone, 2015). These changes may lead to heightened occurrences of floods during the rainy season along with intensified soil erosion and sediment displacement

especially on the steep inclines of the highland regions (Mbungu, Easton, et al., 2016). In contrast, the dry season may see extended droughts intensify water scarcity and adversely affect agricultural output (Gharibdousti et al., 2019).

Climate-induced alterations present considerable challenges to natural ecosystems and human lives in the river sub-basin potentially impacting water supply, food security and overall socio-economic stability (IPCC, 2021; Magang et al., 2024; Mbungu, Heatwole, et al., 2016).

3.3.4 Rainfall

The Songwe River sub-basin undergoes a prolonged rainy season from October to May followed by a dry season from June to September. The annual precipitation in the river sub-basin fluctuates considerably with elevation which is essential to the region's hydrology. The lowland regions generally receive approximately 650 mm of yearly precipitation although the elevated places such as the Poroto Highlands may receive up to 2,600 mm per year (Kalisa et al., 2013). The fluctuation in precipitation is essential for the sub-basin's hydrological equilibrium and river flow dynamics especially during the rainy season when rivers like the Songwe River reach peak discharge (Feyissa Negewo & Kumar Sarma, 2022; Mbungu, Heatwole, et al., 2016). The region's dependence on seasonal rainfall is essential for sustaining agriculture, water supplies and local ecosystems. The escalating unpredictability of precipitation patterns attributable to climate change engenders apprehensions regarding the future. Inconsistent precipitation may result in a higher frequency of severe rainstorm events henc, elevating the danger of floods and sedimentation (Mbungu, Heatwole, et al., 2016). In contrast, diminished precipitation in the dry season may intensify water shortage, impacting agricultural output and water accessibility for both humans and ecosystems (Ojija et al., 2017). The alterations in precipitation patterns may deeply affect the region's economy and ecological stability necessitating the formulation of adaptation solutions for water resource management and the protection of agricultural practices (Feyissa Negewo & Kumar Sarma, 2022; Lazaro et al., 2023; Mbungu, Heatwole, et al., 2016; Serdeczny et al., 2017).

3.3.5 Temperature

The Songwe River sub-basin exhibits a diverse variety of mean temperatures that fluctuate considerably with altitude. The average temperature in the highland sections of the sub-basin is roughly 16°C; however, in the lowland areas it can rise to 30°C (Kalisa et al., 2013; Valimba, 2019). The temperature variance is predominantly affected by the region's geography exhibiting milder temperatures in elevated altitudes such as the Poroto Highlands and warmer conditions in the lowland plains (Kalisa et al., 2013; Valimba, 2019). The river sub-basin experiences significant seasonal temperature variations influenced by elevation and the disparity between the rainy and dry seasons. In the rainy season (October to May) temperatures are often colder particularly in the highland regions where they average approximately 16°C. Conversely, the lowland regions exhibit elevated temperatures varying between 25°C and 28°C (Kalisa et al., 2013; Valimba, 2019). The dry season occurring from June to September results in elevated temperatures especially in the lowlands where temperatures can exceed 30°C. The highlands however exhibit cooler temperatures, generally between 18°C and 24°C (Kalisa et al., 2013). This temperature volatility has significant ramifications for agriculture, water supplies and local ecosystems. The lower temperatures in the highlands can benefit specific crops and forest ecosystems, while the warmer lowlands may aid the growth of heat-tolerant crops. The intense heat in the dry season especially in the lowlands can result in water scarcity and impact crop yields highlighting the necessity for efficient water management measures.

3.3.6 Hydrology

The Songwe River sub-basin, in the Lake Rukwa Basin in southern Tanzania, is predominantly fed by three main rivers. These rivers are Lupa, Songwe, and Zira. The rivers emanate from the eastern plains and the Poroto Mountains traversing territories that encompass gold mining sites and flat lowlands before uniting and discharging into Lake Rukwa. The hydrological dynamics of these rivers exhibit significant seasonality with peak flows during the rainy season (February to March) and diminished flows in the dry season (July to November). September is often recognised as the driest month of the year (Kalisa et al., 2013; Mwalwiba et al., 2023). The sub-basin is essential for supplying water for agriculture, supporting wetlands and preserving the water

equilibrium of Lake Rukwa. The region encounters considerable hydrological difficulties notably water scarcity in the dry season which limits agricultural and domestic water supply (Adhikari & Nejadhashemi, 2016; Mbungu, Easton, et al., 2016; Mutayoba et al., 2018b). Furthermore, substantial precipitation during the rainy season frequently results in flooding especially in lowland areas, intensifying soil erosion and sedimentation problems (Mbungu, Easton, et al., 2016). Environmental deterioration exacerbated by land use practices like gold mining and deforestation complicates the region's water management diminishing the sub-basin's ecosystems' capacity to regulate water flow and quality (Gobry et al., 2023; Marhaento et al., 2018). Climate variability progressively affects the sub-basin's hydrology intensifying water scarcity during the dry season and causing flooding during the wet season. The convergence of these difficulties highlights the necessity of adopting adaptive water management systems to reconcile agricultural demands, environmental conservation and the sustainable use of water resources.

3.3.7 Geology and Soil

The geology of the Songwe River sub-basin is shaped by its location within the East African Rift System which is characterized by a mixture of volcanic and sedimentary rocks in the highlands and alluvial deposits in the lowlands (Kalisa et al., 2013; Valimba, 2019). The region is abundant in mineral resources especially gold which is prevalent around the Lupa and Songwe Rivers. These mineral reserves substantially enhance the local economy; yet, they also pose concerns including environmental deterioration resulting from mining operations. The soil parameters of the sub-basin exhibit significant variation between the highlands and lowlands. Highland soils are often shallow and highly prone to erosion particularly when subjected to heavy rainfall and agricultural practices (Wynants et al., 2021). Conversely, the lowland regions possess fertile alluvial soils conducive to agricultural output; yet, they are susceptible to waterlogging and erosion especially following significant rainfall events (Kumar et al., 2012; Parajuli & Risal, 2021). The Songwe River sub-basin comprises nine predominant soil types: Eutric Fluvisol, Chromic Cambisols, Mollic Andosols, Vitric Andosols, Haplic Lixisols, Eutric Leptosols, Haplic Solonetz, Ferralic Cambisol and Umbric Nitisol (Figure 3.4). Eutric Leptosols and Mollic Andosols are shallow and

very susceptible to erosion regardless of their presence on hard rock or in unconsolidated gravelly substrates (Tenaw et al., 2024). These soil types are essential for comprehending the agricultural potential of the sub-basin and the environmental issues it encounters especially regarding erosion and soil degradation. The primary difficulties confronting the sub-basin encompass soil erosion, land degradation due to mining operations and insufficient water retention during dry spells. These difficulties impact agricultural output and the ecological health of the sub-basin rendering sustainable land management strategies vital for addressing these challenges.

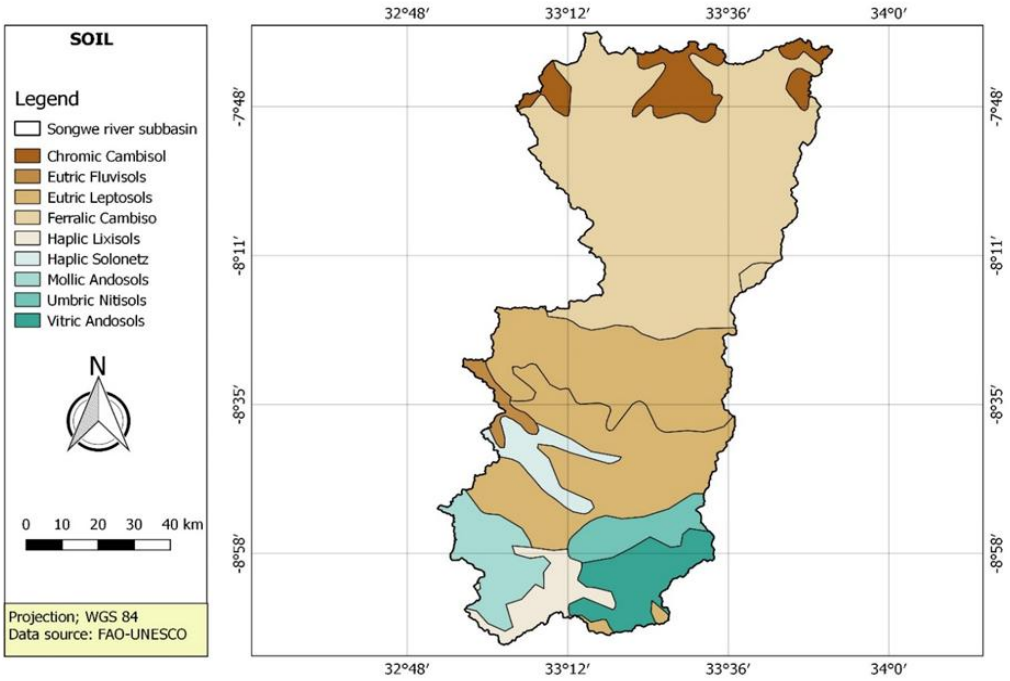

Figure 3.4: Soil map of the Songwe River sub-basin created in QGIS 2.6.1

3.3.8 Land Use Land Cover

The land use and land cover in the Songwe River sub-basin significantly influence hydrological processes and sediment output patterns. Figure 3.5 shows that agriculture occupies 39.35% of the sub-basin primarily with crops like rice, beans and maize. Intensive agricultural practices particularly in areas with poor land management or steep gradients exacerbate soil erosion (Mdee, 2015). Agriculture is widespread in both the mountainous regions and the flat downstream portions of the river sub-basin resulting in substantial alterations to land cover and erosion rates. Bushland constitutes

33.42% of the river sub-basin, with semi-arid shrub land prevailing in the lower and middle sections of the sub basin. While bushland provides some protection against erosion, its sparse vegetation renders it particularly vulnerable to soil erosion during intense rainfall events. Furthermore, bushland regions especially those adjacent to agricultural land and grasslands facilitate sediment deposition into water bodies (Abubakari et al., 2019). Woodland makes up 13.37% of the sub-basin, predominantly located in the steeper areas. These forests stabilize the soil and reduce surface runoff thereby mitigating erosion within the river sub- basin. However, changes in land use particularly deforestation for agricultural development and other human activities have significantly reduced woodland coverage, making the upper sub-basin increasingly susceptible to erosion. More vulnerable land uses are gradually replacing the forests that once protected the soil from erosion (Gobry et al., 2023; Nguyen, 2019).

The sub-basin also features a prevalence of grasslands, despite their smaller area compared to bushland or cultivated land. The sparse canopy cover in these grasslands makes them particularly susceptible to erosion especially during the dry season. In areas with managed grazing, grasslands can help reduce surface runoff and prevent soil degradation (Mwalwiba et al., 2025). Despite their limited size built-up areas are also present within the mountainous river sub-basin. Urbanization leads to the development of impermeable surfaces which increase surface runoff and sediment transfer to water bodies. The increased surface erosion in these regions significantly impacts sediment dynamics and disrupting natural hydrological processes (Wynants et al., 2021; Yao et al., 2015). The various land uses and cover types in the Songwe River Sub-Basin illustrate the complex interactions between natural and human-induced factors affecting sediment output. Agriculture and urbanization contribute significantly to erosion especially in upper catchment areas whereas lower catchments with cultivated land and bushland typically experience sediment deposition particularly following intense rainfall. Understanding the distribution of land use and land cover is vital for modelling the impacts of climate change on sediment dynamics and for developing sustainable land management strategies to mitigate erosion and sedimentation in the river sub-basin (Arnold et al., 2012; Kimario et al., 2024;

Mbungu, Easton, et al., 2016).

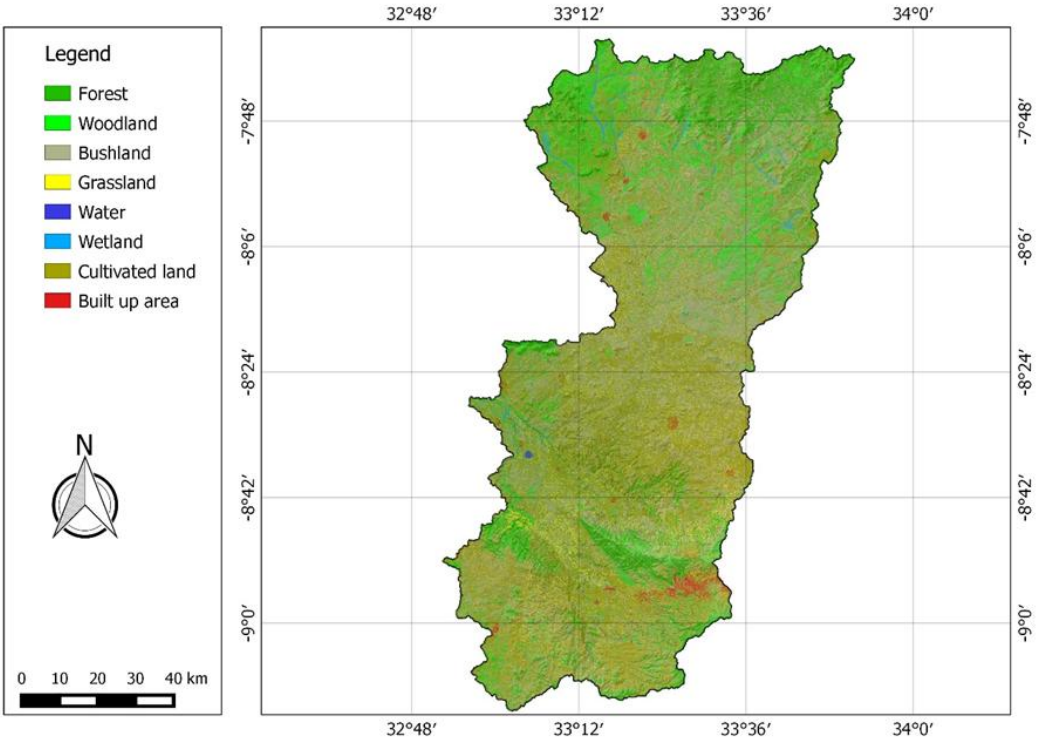

Figure 3.5 Land use/cover of Songwe River sub-basin for the year 2020 created in QGIS 2.6.1

3.4 Overview of SWAT Model

The hydrological model for the Songwe River sub-basin was constructed utilizing the Soil and Water Assessment Tool (SWAT) modelling software. SWAT was used in this research to model sediment yield in the sub-basin. This extensive, semi-distributed process-focused model forecasts the impacts of land use, management strategies and climate change on the yields of water, sediment and agricultural chemicals (Arnold et al., 2012). SWAT requires data regarding topography, land use, soil classifications and meteorological variables to conduct hydrological simulations (Addis et al., 2016; Srinivasan et al., 2012). The model was selected for its capacity to precisely simulate hydrological processes by integrating several datasets such as land use, soil characteristics and climatic variables (Akoko et al., 2021).

Moreover, SWAT is supported by extensive literature and a precisely organized database, offering a rigorous basis for model calibration and validation and thereby ensuring its reliability in hydrological simulations (Arnold et al., 2012). A significant

benefit is that SWAT is complimentary and readily available to users, facilitating its extensive usage in both research and practical watershed management (Chelkeba Tumsa, 2023). The model incorporates an integrated GIS interface augmenting its capacity to process geographical data and conduct thorough analyses thereby rendering it user-friendly and efficient for extensive hydrological modelling (Worku et al., 2017). Moreover, SWAT has been extensively used globally to assess the impacts of climate change and land use/land cover changes showcasing its adaptability and dependability across varied hydrological and climatic contexts (Chilagane et al., 2021). A significant characteristic of the SWAT model is its weather engine which generates precipitation and other meteorological variables using stochastic and probabilistic methods making it a robust tool even in data-scarce regions (Kang et al., 2019; Mdee, 2015; Sisay et al., 2017). Its ability to simulate the impacts of climate change on water and sediment yield in data scarce areas is relevant for this study, as it aimed to assess the future impacts of climate change on sediment yield in the Songwe River sub-basin. The model operates by partitioning the landscape into smaller sub-basins, each represented by Hydrological Response Units (HRUs), based on consistent land use, soil types, and slope attributes. This allows for detailed simulation of hydrological processes across different areas of the watershed. SWAT incorporates a water balance equation 2.2 to simulate the flow of water within the river sub-basin, accounting for precipitation, surface runoff, evapotranspiration, soil infiltration, and groundwater interactions. Sediment yield modelled by using the MUSLE equation 2.3, which accounts for sediment production from specific storm events, making it ideal for capturing temporal variations in sediment yield due to storm intensity (Srinivasan et al., 2012). The equation integrates runoff volume, peak runoff rate, and other factors like soil erodibility, land cover, and topography to estimate sediment yield across the river sub-basin. In this equation, sediment yield is incorporated into SWAT framework to facilitate simulation of sediment transport across the river sub -basin and identifying regions most susceptible to erosion (Arnold et al., 2012).

3.5 Input Data for SWAT Model

A complete set of data input was essential to evaluate the influence of climate change on sediment yield in the Songwe River sub-basin. The Soil and Water Assessment Tool (SWAT) model employed to simulate hydrological processes, relies on diverse information to accurately illustrate sediment yield and soil erosion dynamics within the sub-basin. Acquiring necessary hydrological variables at timescales appropriate for catchment-scale processes is frequently a complicated endeavour. Nevertheless, these challenges, such data is important for understanding the sub-basin's dynamics and its reaction to hydrological events. SWAT is an extensive model that necessitates a variety of knowledge and data for optimal functionality. This investigation necessitated many kinds of data including: The Digital Elevation Model (DEM), soil information, land use, the stream network layer and meteorological data including precipitation, temperature, solar radiation, wind speed, relative humidity and river flow (Figure 3.6). These data are crucial for hydrological modelling and calibration. The data used in this research was acquired from several organizations and agencies, with the Digital Elevation Model (DEM) and land cover satellite imagery being retrieved from the Advanced Land Observing Satellite Phased Array L-band Synthetic Aperture Radar (ALOS PALSAR) via the Alaska Satellite Facility and USGS Earth Explorer, respectively. To guarantee data reliability quality control was implemented by graphical, statistical and ground-truthing techniques. The data were crucial for the construction, calibration and operation of the Soil and Water Assessment Tool (SWAT) model which was used to predict sediment yield under various climate scenarios.

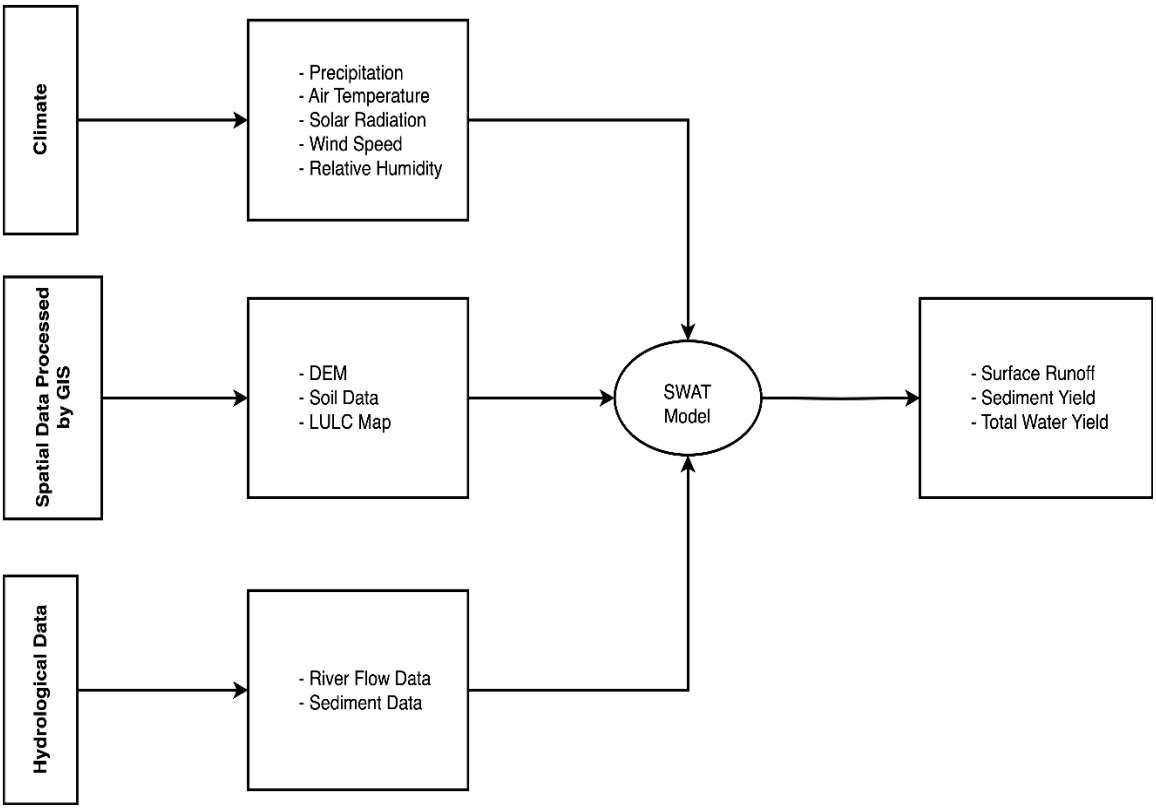

Figure 3.6: illustrates the input and output components of the SWAT model used for simulating sediment yield

3.5.1 Data Collection

The primary data source was the Digital Elevation Model (DEM) used to delineate the topography of the Songwe Sub-Basin. A 30-meter digital elevation model from ALOS PALSAR was used to precisely delineate the terrain's characteristics including drainage patterns and slope gradients. The DEM data analyzed in QGIS, enabled the extraction of hydrological characteristics, such as slope and flow direction which are essential for comprehending sediment transport dynamics (Arnold et al., 2012).

The Land Use and Land Cover (LULC) map for the year 2020 constituted another essential dataset. The LULC map was categorized into specific land cover types: cultivated land, bushland, forests, woodlands, grasslands and urban areas. This classification, crucial for the development of Hydrological Response Units (HRUs), offered a spatial depiction of land use within the river sub-basin, facilitating the categorization of regions with similar land use, soil and slope attributes. Hydrologic

Response Units (HRUs) are essential to the SWAT model as they delineate spatial units that influence runoff and sediment yield predictions. The LULC data was processed and classified using the QSWAT 1.7 interface in QGIS which facilitated its incorporation into the SWAT model (Arnold et al., 2012).

The Soil Map of the World from FAO/UNESCO was used to identify the types and attributes of soil within the sub-basin. This dataset found nine principal soil classifications in the region including Eutric Fluvisols, Chromic Cambisols and Haplic Solonetz. Soil characteristics such as texture, structure and organic matter significantly affect a soil's erodibility; hence, they directly impact sediment output forecasts. The Erodibility Factor (K-factor) an essential variable in soil erosion modelling was used to evaluate soil susceptibility to erosion. Soils exhibiting elevated K-values such as Eutric Leptosols were categorized as more susceptible to erosion particularly in regions with steep gradients or agricultural practices. The SWAT model incorporated this information to efficiently mimic the link between soil properties and erosion processes.

Meteorological data are essential for precisely modelling sediment transport and erosion processes in the Songwe River Sub-Basin. This study used daily precipitation data obtained from three meteorological stations situated inside the sub basin: Galula, Lupa Tingatinga and Maji Depo (refer to Table 3.1). These stations supplied essential rainfall data needed for modelling surface runoff and sediment yield. Furthermore, data on minimum and maximum temperatures, solar radiation, wind speed and relative humidity were obtained from the Lake Rukwa Water Basin office and the Global Weather Database for SWAT (refer to Figure 3.7). Modelling evapotranspiration and runoff processes, which significantly influence sediment transport and erosion dynamics within the sub basin requires a thorough understanding of meteorological characteristics. Alongside local meteorological records, satellite data from the Earth System Grid Federation (ESGF) were integrated into the study to augment the precision of the models.

The high-resolution (30-meter) images were obtained from the United States Geological Survey's Earth Explorer platform (https://earthexplorer.usgs.gov/) and

supplied essential data for the study. This research employed Landsat images from the following datasets: Landsat 5 (TM) for 1990 and 2000, Landsat 5 (TM BUMPER) for 2010, and Landsat 8 (OLI_TIRS) for 2020 (Table 3.2). The images were chosen according to particular path/row combinations and acquisition dates to guarantee consistent spatial and temporal coverage. This collection of images preserved spatial consistency and temporal integrity within the research region. The images were obtained in May 2022 and were crucial for establishing a temporal perspective of land use and land cover dynamics in the SongweRiver Sub-Basin. Field observations were conducted alongside satellite imagery to collect ground-truthing data for the calibration of land-use classifications. Ground-truthing entailed the establishment of exact locational points for each land use and land cover category ensuring the precision of the categorizing process.

This research used high resolution climatic simulations from four regional climate models (RCMs) that were influenced by general circulation models (GCMs) as part of the Coordinated Regional Climate Downscaling Experiment (CORDEX). CORDEX is a project of the World Climate Research Program (WCRP) seeks to produce high-resolution climate data for diverse geographical regions improving the spatial and temporal resolution of climate forecasts (Mutayoba et al., 2018a).

The chosen four Regional Climate Models data were the Climate Limited-Area Model (CCLM4), Rossby Centre Regional Climate Model (RCA4), Regional Atmospheric Climate Model (RACMO22T) and High-Resolution Limited Area Model (HIRHAM5). The future climatic data used in this study were sourced from the CORDEX-Africa dataset acquired via the Earth System Grid Federation (ESGF) site (https://esg-dn1.nsc.liu.se/projects/esgf-liu/) which offers outputs from various regional climate models (RCMs). We underwent stringent quality assessments and utilized the datasets in compliance with the CORDEX initiative usage protocols (http://wcrp-cordex.ipsl.jussieu.fr/). The spatial resolution of the CORDEX-Africa RCMs is 0.44° x 0.44° (about 50 km) providing adequate detail for regional climate forecasts in Africa (Luhunga et al., 2018; Mutayoba et al., 2018b). These models use a rotating pole coordinate system to align their grid with the equatorial region enhancing the accuracy of climate projections for the African continent. The climate

projections included historical data (1981–1992) and future forecasts (2011–2100). Climate projections were established for three specific periods: the present (2011–2040), mid-century (2041–2070) and end-century (2071–2100). The future forecasts were predicated on two Representative Concentration Pathways (RCPs): RCP4.5, indicative of a moderate greenhouse gas emissions scenario and RCP8.5, indicative of a high emissions scenario. The future predictions offer daily data on minimum and maximum temperatures and precipitation was essential for hydrological and sediment modelling as these elements affect river flow, soil erosion and sediment yield.

The four CORDEX RCMS for Africa were selected for their proven capacity to accurately simulate African climate dynamics particularly in terms of precipitation and temperature variability which are critical for hydrological modelling and sediment yield predictions (Lahunga et al., 2016a). These models are esteemed for their robustness in representing African climate variability and are ideal for examining future climate projections especially for areas such as the Songwe River sub-basin. The chosen models were previously used to simulate climate conditions in the southern highlands of Tanzania with reasonably small errors as documented by (Luhunga et al., 2018). These experiments demonstrated the models' capacity to replicate regional climatic patterns making them suitable for this investigation.

In the comparison between RCP4.5 and RCP8.5, the two scenarios represent different levels of greenhouse gas emissions and their potential impacts on climate. RCP4.5 is a moderate emissions scenario, reflecting efforts to mitigate climate change while RCP8.5 assumes high emissions and represents a "business-as-usual" scenario with limited mitigation efforts. The action taken involved using these scenarios to capture a range of possible future climate conditions in the Songwe River sub-basin. RCP4.5 typically leads to less extreme climate impacts with moderate increases in precipitation and temperature resulting in relatively lower increases in sediment yield. In contrast, RCP8.5, with its higher emissions, leads to more significant temperature and precipitation changes, exacerbating the risk of higher sediment yield due to increased rainfall intensity and altered hydrological cycles. This comparison is vital for understanding the full spectrum of potential climate impacts guiding adaptive management strategies in the sub-basin to mitigate future sedimentation risks.

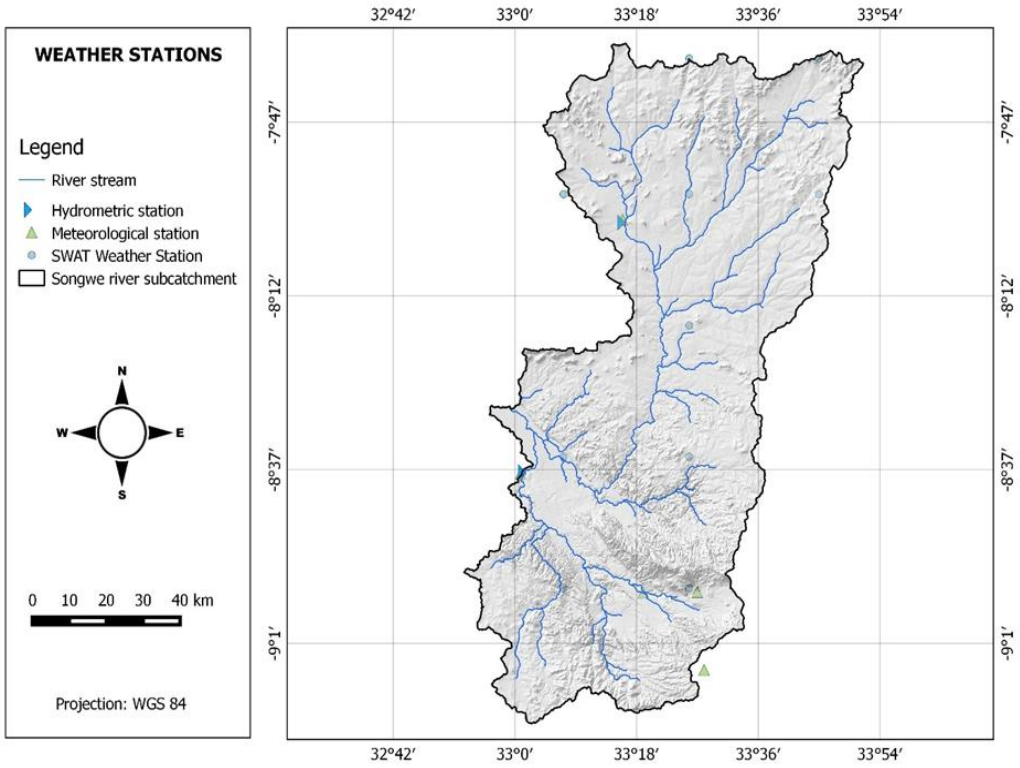

Figure 3.7: Weather data station in Songwe River sub-basin created in QSWAT version 1.7

Table 3.1: Meteorological and hydrological stations in the Songwe River sub-basin

S/N	Name	Station Type	UTM / Latitude	UTM / Longitude
1	Galula Met Station	Weather and Rain gauge	-8.62	39.014
2	Lupatingatinga Met Station	Weather	-8.02	39.266
3	Utengule Usongwe Pr. Sch	Rain gauge	-8.9	33.3166
4	Isangati Primary School	Rain gauge	-9.0833	33.4666
5	Mbeya Maji Depot	Rain gauge	-8.899	39.45
6	Songwe at Galula	Hydrometric	-8.616	33.026
7	Lupa at Lupatingatinga	Hydrometric and Rain gauge	-8.027	33.271

Table 3.2: Satellite Imagery Data

Year	Spacecraft ID	Sensor ID	Path/Row	Acquisition date	Cloud clover (%)
1990	Landsat 5	TM (SAM)	169/65	04/09/1990	0
		TM (SAM)	169/66	20/09/1990	0
		TM (SAM)	170/65	25/07/1990	0
		TM (SAM)	170/66	09/07/1990	0
2000	Landsat 5	TM (SAM)	169/66	30/08/2000	0
		TM (SAM)	169/66	30/08/2000	0
		TM (SAM)	170/65	08/10/2000	0
		TM (SAM)	170/66	08/10/2000	0
2010	Landsat 5	TM (BUMPER)	169/66	26/08/2010	3
		TM (BUMPER)	169/66	26/08/2010	8
		TM (BUMPER)	170/65	05/11/2010	1
		TM (BUMPER)	170/66	29/05/2010	1
2020	Landsat 8	OLI_TIRS	169/66	22/09/2020	0
		OLI_TIRS	169/66	22/09/2020	0
		OLI_TIRS	170/65	28/08/2020	0
		OLI_TIRS	170/66	28/08/2020	0

3.5.2 Data processing and Preparation

Data processing and preparation were executed by using QSWAT 1.7 and QGIS 2.6.1 to construct a comprehensive model database for simulation (Arnold et al., 2012). This methodology delineates the origins, processing phases and methods employed to prepare the datasets. The spatially distributed model employed in the GIS platform for the QSWAT interface necessitates essential resources, including the Digital Elevation Model (DEM), soil information, land use/land cover data, meteorological information and stream network layers. Moreover, data on river discharges was used for the calibration of streamflow.

3.5.2.1 Digital Elevation Model (DEM)

Topography is characterized by the Digital Elevation Model (DEM) which represents the elevation of each location within a specified area at a certain spatial resolution (Figure 3.2). A high-resolution Digital Elevation Model (DEM) with a spatial resolution of 30 m x 30 m was acquired from the Advanced Land Observing Satellite Phased Array L-band Synthetic Aperture Radar (ALOS PALSAR) via the Alaska Satellite Facility (accessed in May 2022). The DEM was modified in QGIS through operations including sink filling, reprojection to the WGS84/UTM coordinate system

and hydrological changes to render it appropriate for runoff and sediment modelling. The DEM was employed to define the watershed utilizing the SWAT watershed delineator tool and to compute flow accumulation, examining the drainage patterns of the land surface topography. Digital Elevation Model (DEM) facilitated the delineation of sub-basin boundaries, the identification of stream networks and the computation of slopes, all of which are essential for calculating runoff and sediment output (Abbaspour et al., 2007; Arnold et al., 2012). River sub-basin attributes, encompassing slope gradient, slope length and stream network parameters such as channel slope, length and breadth, were obtained from the DEM.

3.5.2.2 Soil Information

The SWAT model necessitates various soil textural and physicochemical characteristics, encompassing soil texture, accessible water content, hydraulic conductivity, bulk density and organic carbon content for different strata of each soil type. Soil maps for the sub-basin were sourced from the FAO-UNESCO Soil Map of the World, Volume VI, which offers comprehensive classifications of soil types (Arnold et al., 2012; FAO & UNESCO, 1977), (Figure 3.8). This map delineates nine principal soil types within the river sub basin which were used to establish essential soil characteristics in the model, including water penetration rates, surface runoff and erosion potential. The model integrated soil texture, depth, organic matter content and erodibility to improve the precision of sediment yield forecasts (Arnold et al., 2012).

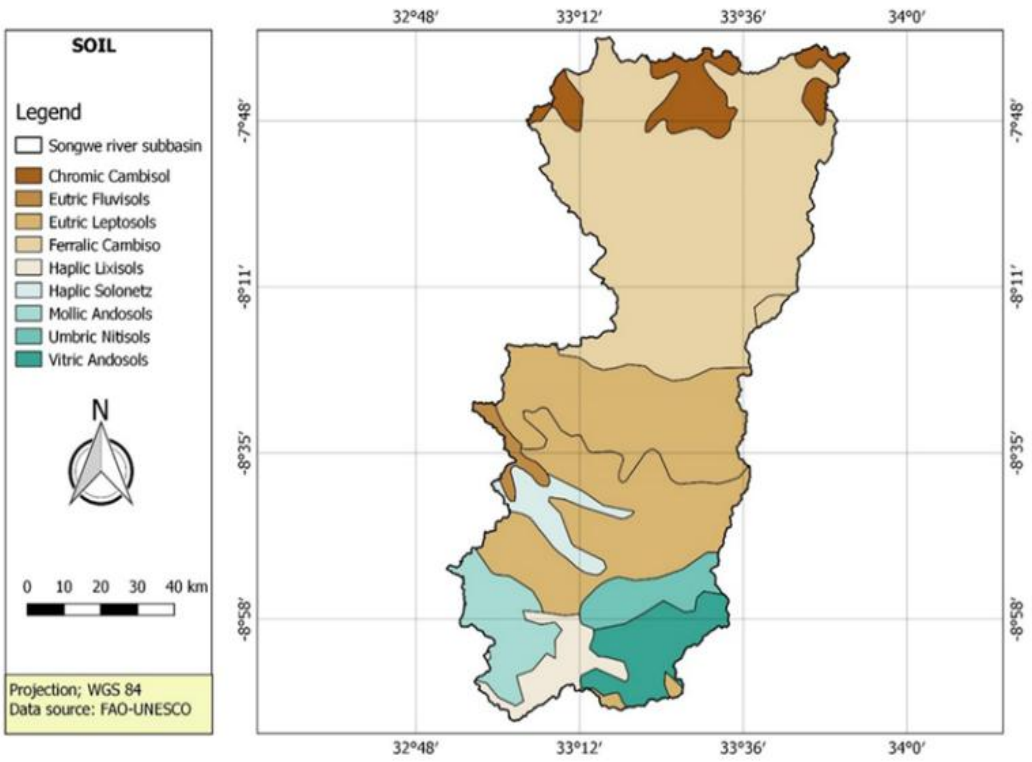

Figure 3.8: Soil map of Songwe River sub-basin

3.5.2.3 Land Use/Land Cover Data

The analysis of land use and land cover (LULC) changes throughout time is essential for comprehending the impacts of land management strategies and climate change on sediment yield. Monitoring these changes helps to evaluate the impact of anthropogenic activities and environmental fluctuations on the hydrological and sedimentary dynamics of a region. The investigation of the spatial and temporal changes in land use/land cover (LULC) within the Songwe River sub-basin employed Landsat imagery and Geographic Information System (GIS) methodologies to assess changes across four temporal intervals: 1990, 2000, 2010 and 2020. Multispectral Level-2 Landsat photos exhibiting less than 10% cloud cover were used for the analysis.

(a) Image Pre-processing and Classification

Image Rectification and Mosaicking

Prior to classification, the satellite images were subjected to geometric rectification to ensure spatial precision and uniformity. The images were aligned to the Universal Transverse Mercator (UTM) coordinate system, specifically UTM Zone 37 South utilizing the Clarke 1880 Spheroid and the Arc 1960 Datum. Image mosaicking was executed to combine images from the same year but in distinct rows, resulting a singular image that covered the full research area, hence enhancing spatial coverage (Gobry et al., 2023; Kitalika et al., 2018; Selmy et al., 2023).

Image Classification

An unsupervised classification technique, iterative self-organizing data analysis (ISODATA), was initially employed for the classification of land use and land cover (LULC) utilizing ERDAS IMAGINE 2016 (ERDAS, 2016). A total of thirty-six (36) LULC classes were produced, representing various land-cover types including forest, woodland, agricultural land and urban regions. Subsequent to the ISODATA classification, visual interpretation and field data were utilized to enhance and consolidate the classes into more significant land use and land cover categories. The categories were forest, woodland, bushland, grassland, water bodies, wetlands, cultivated land and built-up regions according to the actual land use types identified in the study area (Table 3.3). The ISODATA approach effectively identifies natural clusters in the data particularly when prior information about land cover categories is minimal (Nguyen, 2019; Selmy et al., 2023). A Maximum Likelihood Classification (MLC) method a supervised classification technique was subsequently employed to improve classification accuracy. MLC is a supervised classification technique that employs statistical probability to allocate pixels to established land cover categories; hence, it enhances the accuracy and dependability of the final classification (Nyatuame et al., 2023; Selmy et al., 2023). The CCI Global Land Cover dataset was used as a reference to improve classification accuracy (Bontemps et al., 2011). The two-step categorization approach guarantees the precision and pertinence of the final LULC map.

Table 3.3: Land use/cover classification scheme for the Songwe River Sub-basin

S/N	Land use/cover	Description
1	Forest	Area of land covered with at least 10% tree crown cover, naturally grown or planted and or 50% or more shrub and tree regeneration cover
2	Woodland	Area of land covered with low density trees with height between forming closed to open habitat with plenty of sunlight and limited shade
3	Bushland	Area dominated with bushes and shrubs with occasional short emergent trees
4	Grassland	Land area dominated by grasses
5	Water body	Area within body of land, filled with water, localized in a basin, which rivers flow into or out of them
6	Wetland	Land area that is saturated with water either permanent or seasonally including valley bottoms
7	Cultivated land	Area subjected to agricultural production farms with crops and harvested crop land
8	Built up area	Manmade infrastructure (roads and buildings) and settlement (town and villages)

Evaluation of LULC Classification Accuracy

The Kappa coefficient was used to evaluate the accuracy of the final classified images. The Kappa coefficient statistic quantifies the degree of agreement between the categorized image and reference data offering a rigorous evaluation of correctness . The Kappa value was derived from the confusion matrix, a method that compares anticipated classifications with actual ground-truth data obtained during fieldwork. The Kappa coefficient quantifies the agreement between observed and predicted classifications with values over 0.85 deemed acceptable for robust analysis. Accuracy tests were performed for each time epoch (1990, 2000, 2010 and 2020) employing ground-truthing data pertinent to each period hence, assuring temporal consistency and dependable validation of the categorization outcomes. Ground-truth data were gathered for the years 1990, 2000, 2010 and 2020 to authenticate the classification results. The accuracy for each epoch varied between 91.74% and 92.44%, yielding an overall Kappa score of 0.90 which signifies a robust concordance between the observed and predicted land cover classifications.

The equation for the Kappa statistic is as follows:

$$K = \frac{N \sum_{i=1}^{r} x_{ii} - \sum_{i=1}^{r}(x_{i+} \times x_{+i})}{N^2 - \sum_{i=1}^{r}(x_{i+} \times x_{+i})} \quad (2.1)$$

Where N is the total number of sites in the matrix; r is the number of rows in the matrix; xii is the number in row i and column I; x_{+i} is the total for row I; and x_{i+} is the total for column.

(b) Change Detection Analysis

Change detection analysis was used to measure the magnitude, velocity, and geographical distribution of land use and land cover changes across four temporal intervals (1990, 2000, 2010 and 2020) (Figure 3.9). The post-classification comparison method was employed, offering a comprehensive and systematic framework for evaluating temporal changes in land cover (Mawasha & Britz, 2022). This methodology reduces inaccuracies induced by atmospheric fluctuations or sensor discrepancies by juxtaposing categorized outputs from various temporal intervals (Mawasha & Britz, 2022). The rate of change in land cover types was calculated using the methodology outlined by (Kashaigili & Majaliwa, 2010) facilitating a precise evaluation of land use and land cover dynamics over time (Figure 3.4).

Table 3.4: The land use and land cover types and their respective proportional coverage of the Songwe River sub-basin

	1990		**2000**		**2010**		**2020**	
Class	Area [Ha]	Percentage [%]	Area [Ha]	Percentage [%]	Area [Ha]	Percentage [%]	Area [Ha]	Percentage [%]
Forest	261880	24.34	247548	23.01	200039	18.59	120428	11.19
Woodland	351771	32.69	318299	29.58	252937	23.51	143863	13.37
Bushland	297960	27.69	355733	33.06	325086	30.21	359827	33.42
Grassland	1385	0.13	6164	0.57	9573	0.89	17356	1.61
Water	3942	0.37	2882	0.27	2011	0.19	1293	0.12
Wetland	21560	2.00	4360	0.41	3760	0.35	3030	0.28
Agriculture	133560	12.41	136447	12.68	277201	25.76	423346	39.35
Built up	4019	0.37	4643	0.43	5471	0.51	6935	0.64
Total	1076078	100	1076078	100	1076078	100	1076078	100

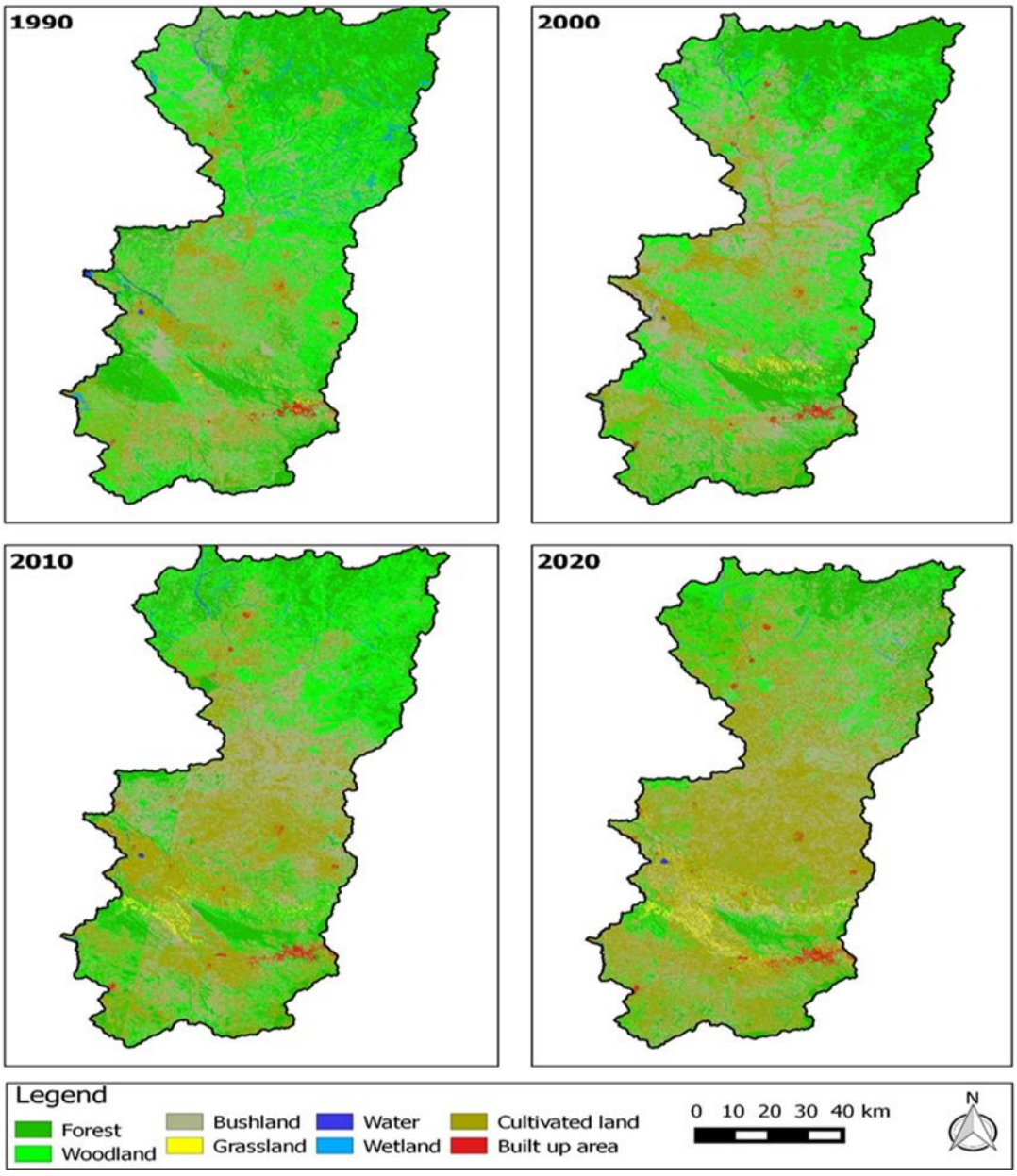

Figure 3.9: Land use Land Cover (LULC) cover maps of 1990, 2000, 2010 and 2020 created in QGIS 2.6.1

(c) Predicting Future Land Use Land Cover Change

This study projected future land use and land cover (LULC) changes for the years 2040, 2070 and 2100 based on classified LULC maps from 2010 and 2020.

The Cellular Automata-Markov Chain (CA-Markov) used for forecasting future land use and land cover (LULC) changes in the Songwe River sub-basin provides.

However, while the CA-Markov model is useful for medium-term forecasting, it has significant limitations when applied to long-term predictions because it assumes constant transition probabilities over time, overlooking potential changes driven by factors such as policy changes, technological advancements or climate change. Additionally, the model simplifies complex socio-economic, political and environmental dynamics failing to fully account for the diverse and unpredictable influences that drive land-use decisions.

The CA-Markov model integrates Markov chain analysis with cellular automata to forecast future changes in land-use categories based on past transition patterns (Azizi et al., 2016; Khawaldah et al., 2020). The Markov Chain analysis underpins the CA-Markov model by computing a transition probability matrix that measures the possibility of each land-use category migrating to another over time (Camara et al., 2020; Papa et al., 2015). This matrix is based on historical land use and land cover data, enabling the model to analyse past land-use dynamics and forecast future trends. The transition probability matrix aids in determining the potential transformation of wooded regions into agricultural land or the encroachment of urban areas on neighbouring natural landscapes. This study is essential for understanding prospective land use trajectories, which can guide planning and management methods (Arfasa et al., 2023; Selmy et al., 2023).

After generating the transition probability matrix, the next step in the modelling procedure entailed constructing a transition area matrix. This matrix evaluates the anticipated area of alteration for each LULC class throughout the predicted period. The transition areas matrix is an essential instrument for measuring the degree of alteration in each land-use category. The CA-Markov model was developed and validated using IDRISI Selva v.17.0 software. This software package is renowned for its proficiency in spatial modelling especially in predicting land use changes (Camara et al., 2020; Papa et al., 2015). The CA-Markov model in IDRISI Selva facilitates the amalgamation of cellular automata and Markov Chain methodologies, offering a versatile and dynamic framework for predicting land use and land cover changes. This software guarantees a rigorous modelling process, effectively forecasting intricate land-use shifts.

Model validation was performed to ascertain the accuracy and dependability of the model's predictions by juxtaposing the simulated LULC map for 2020 with the actual satellite-derived LULC map for that year. Kappa statistics were employed to evaluate the model's correctness, offering a quantitative assessment of the concordance between the anticipated and observed land-use categories. The Kappa index is a crucial instrument for assessing the efficacy of land-use models, as it considers both actual agreement and random occurrence. The study validated the model and evaluated its predictive capability by comparing the simulated and actual maps through the Kappa statistic. A high Kappa value (often over 0.85) signifies that the model's predictions are dependable and that the anticipated future alterations in LULC are likely to mirror actual patterns.

Upon validation of the CA-Markov model, QGIS 2.6.1 was employed to produce the final maps of projected land use/land cover (LULC) changes for the years 2040, 2070 and 2100. QGIS is prevalent open-source GIS software that facilitates diverse spatial analysis activities and map generation, providing an array of capabilities for visualizing and analyzing geospatial data (Chilagane et al., 2020). QGIS is esteemed for its adaptability and accessibility, allowing researchers to conduct intricate geographical analyses without the substantial expenses linked to proprietary GIS software (Khawaldah et al., 2020). The land cover maps predicted by the CA-Markov model for each period were imported into QGIS as raster layers. These layers were color-coded with unique schemes for each land use category, offering a clear visual depiction of how the landscape might change across different scenarios (Liping et al., 2018; Selmy et al., 2023). Various QGIS tools including the Raster Calculator (Getachew Abebe & Woldemariam, 2024; Selmy et al., 2023), were utilized to conduct change detection analysis, pinpointing regions with notable land cover changes. The final maps were exported for display purposes, enhancing the communication of the spatial patterns of anticipated LULC transformations (Gulakhmadov et al., 2020).

3.5.2.4 Meteorological Data

Meteorological data are essential for modelling the influence of climatic variables, including temperature and precipitation, on sediment yield. This study required daily meteorological data for SWAT were obtained from observed datasets supplemented

by data produced by a weather generator model. The Global Weather Database for SWAT supplied data on minimum and maximum temperatures, solar radiation, wind speed, relative humidity and wind direction (Mwalwiba et al., 2025). Furthermore, daily precipitation data from the Maji Depo, Galula, and Lupa Tingatinga stations were obtained from the Lake Rukwa Water Basin Office were used to estimate sediment yields. The data prepared in the Tables input data format for SWAT. Precipitation is fundamental in influencing runoff and erosion, rendering accurate rainfall data is vital for the exact modelling of sediment dynamics (Feyissa Negewo & Kumar Sarma, 2022; Mbungu, Heatwole, et al., 2016).

3.5.2.5 Hydrological Flow Data

Daily River flow data sourced from the Lake Rukwa Water Basin Office at the Galula and Lupa Tingatinga stations between 1981 and 2005 were essential for model calibration and validation. River flow data are essential for correlating sediment transport and erosion processes with hydrological flow dynamics (Tsegaye & Bharti, 2021). The data were used to calibrate and validate the SWAT model.

3.6 Bias Correction for Future Climate Data

To enhance reliability of the model outputs, bias correction was implemented by the linear scaling method. This approach calibrates model generated temperature and precipitation estimates to align with observed data. Rainfall data from the Galula, Lupa Tingatinga and Maji Depo stations in conjunction with temperature information from the SWAT Global Weather Database served as reference observations. The linear scaling method was chosen for its simplicity, clarity and efficacy in correcting mean climatic biases while preserving the temporal variability of model outputs (Azari et al., 2016; Mahmood et al., 2018). In contrast to more intricate techniques such as quantile mapping or delta change, linear scaling necessitates limited observational data and computational resources, rendering it especially advantageous in regions like the Songwe River sub-basin, where observational data is frequently deficient. The linear scaling method adjusts the RCM-derived data to more accurately reflect actual meteorological conditions, hence enhancing the realism of the model's results. This strategy has demonstrated reliability in hydrological research particularly in countries such as Africa where it is essential for climate models to accurately reflect observed

climatic conditions (Luo et al., 2018; Yeboah et al., 2022). The implementation of bias correction guaranteed that the RCM outputs were more precisely aligned with observed climate conditions in the Songwe River sub-basin, thereby improving the credibility of subsequent hydrological and sediment yield models. Modifying the data allows the revised climate variables temperature and precipitation to more exactly represent actual circumstances, hence facilitating more precise forecasts of runoff, erosion and sediment yield in future climatic scenarios. The modified climatic data later served as the basis for hydrological modelling and sediment production forecasts.

Linear scaling for bias correction of climate model data has several limitations. While it adjusts the model's mean values to match observed data, it does not address discrepancies in the distribution of climate variables at the extremes. The frequency and intensity of high-end events such as extreme rainfall or temperature spikes are often not corrected. As a result, the corrected data may still misrepresent key aspects of the climate system, such as the variability in rainfall patterns which are crucial for projection of sediment yield. It also assumes that the relationship between observed and modelled data remains constant across all time periods and regions which may not hold in non-stationary climate conditions.

Multiple statistical indicators were used to assess the efficiency of the Regional Climate Models (RCMs) in forecasting temperature and precipitation in the Songwe River Sub-Basin. The employed metrics comprised Bias, Correlation Coefficient (CC), Coefficient of Variation (CV), R-squared (R^2), Mean Absolute Error (MAE) and Root Mean Squared Error (RMSE). Each statistic offers significant insights into the models' accuracy and the dependability of their predictions. Bias measures the systematic differences between observed and modelled values with positive bias indicating overestimation and negative bias indicating underestimation in the model. The Correlation Coefficient (CC) quantifies the strength and direction of the association between observed and modelled data where values approaching 1 signify a robust positive correlation. The Coefficient of Variation (CV) signifies the variability or uncertainty in the model's predictions where elevated CV values denote increased uncertainty (Mishra & Coulibaly, 2009). R-squared (R^2) signifies the fraction of the observed variability elucidated by the model, with elevated R^2 values signifying

superior model fit (Legates & McCabe, 1999). Ultimately, Mean Absolute Error (MAE) and Root Mean Squared Error (RMSE) quantify the extent of discrepancies between observed and modelled data with diminished values signifying superior model efficacy (Legates & McCabe, 1999).

3.7 SWAT Model Setup

This research employed the SWAT model, customized with QSWAT version 1.7 and connected with QGIS 2.6.1 to optimize model processing and improve spatial analysis. QGIS 2.6.1 provides a stable and well-tested environment for integrating older hydrological modeling tools, such as the QSWAT 1.7 plugin. This is particularly beneficial in data-scarce regions where reliability and consistent results are essential for accurate sediment yield modelling under climate change scenarios. QSWAT, an interface for the SWAT model facilitates seamless integration with QGIS enhancing the visualization, administration and processing of input data. The setup of the SWAT (Soil and Water Assessment Tool) model for this study adhered to a systematic methodology encompassing five essential stages: (1) data preparation; (2) sub-basin discretization; (3) HRU (Hydrologic Response Unit) delineation; (4) parameter sensitivity analysis; and (5) calibration, validation and performance assessment of the model. The initial phase of the setup process entailed the preparation of the necessary spatial and temporal data for the SWAT model. The spatial datasets comprising the Digital Elevation Model (DEM), land use/land cover, soil classifications and climatic data were gathered and projected to the Universal Transverse Mercator (UTM) coordinate system specifically UTM Zone 37 South, utilizing the Clarke 1880 Spheroid and the Arc 1960 Datum.

The Digital Elevation Model (DEM) was employed to delineate the sub-basin and examine the drainage patterns of the terrestrial surface. A digital stream network layer was integrated and overlaid onto the DEM to accurately define the streams' locations. The land use/land cover spatial data was subsequently classified into categories suitable for the SWAT model's land cover classification. A user-defined lookup table was established, assigning the corresponding SWAT code for each category of land use/land cover, in accordance with the model's specified format (Arnold et al., 2012). The watershed delineation procedure had five principal steps: establishing the DEM,

delineating the stream network, identifying the outflows and inlets, selecting and defining watershed outlets and computing sub-basin characteristics. Following the configuration of the model with default parameters, preliminary streamflow simulations were performed during the calibration phase to assess the model's efficacy (Assfaw, 2019; Gyamfi et al., 2016). The default simulations established a foundation for the subsequent adjustment of model parameters to enhance precision.

3.7.1 Songwe River Sub-Basin Delineation

Songwe River Sub-basin and sub-basins delineation was conducted utilizing 30 m by 30 m resolution DEM data through the sub-basin delineation component of the QSWAT model. The SWAT project configuration was established within the QSWAT interface. The sub-basin delineation procedure has five primary steps: DEM configuration, stream identification, outlet and inlet specification, sub-basin outlet selection and sub-basin parameter computation (Arnold et al., 2012). Upon completion of the DEM setup and specification of the outlet site, the model autonomously computed the flow direction and flow accumulation (Akoko et al., 2021; Memarian et al., 2014). Subsequently, stream networks, sub watersheds, and topographic parameters were computed using the relevant tools inside the QSWAT interface. The stream definition and sub-basin dimensions were meticulously established by establishing a threshold area or minimum drainage area necessary for the formation of stream origins. The QSWAT interface proposed a threshold value resulting in the delineation of the Songwe River Sub-basin into sub basins, with an estimated total size of 10,800 km² (Figure 3.10). This approach facilitated the precise identification of hydrological units which was crucial for the subsequent modelling and analysis of water flow and sediment transport in the area.

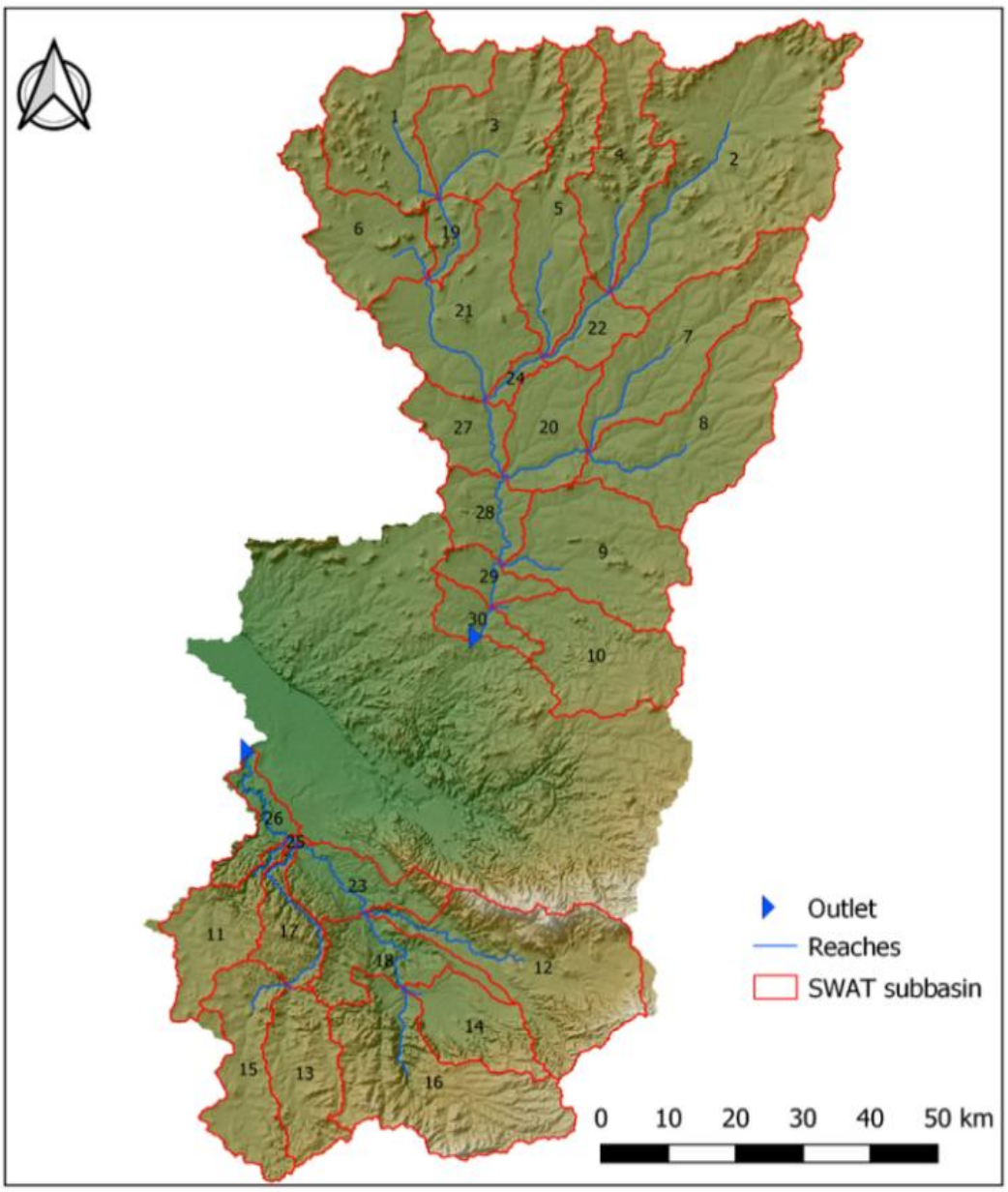

Figure 3.10: Sub-basins delineated within the study area

The river sub-basin delineation method involved generating topographic parameters, such as elevation and slope, for the river sub-basin and its sub-basins using the DEM data. The river sub-basin elevation varies from 800 to 2805 meters above the mean sea level. The maximum elevation is at Poroto Highlands and other mountainous regions and the minimum elevation is at the river sub-basin exit. Slope classification was performed according to the elevation range of the DEM utilized in the sub-basin

delineation process. The slope values of the watershed were subsequently reclassified based on the percentage size of the sub-basin (Figure 3.11) enabling a more detailed examination of the terrain's impact on hydrological processes and sediment transport.

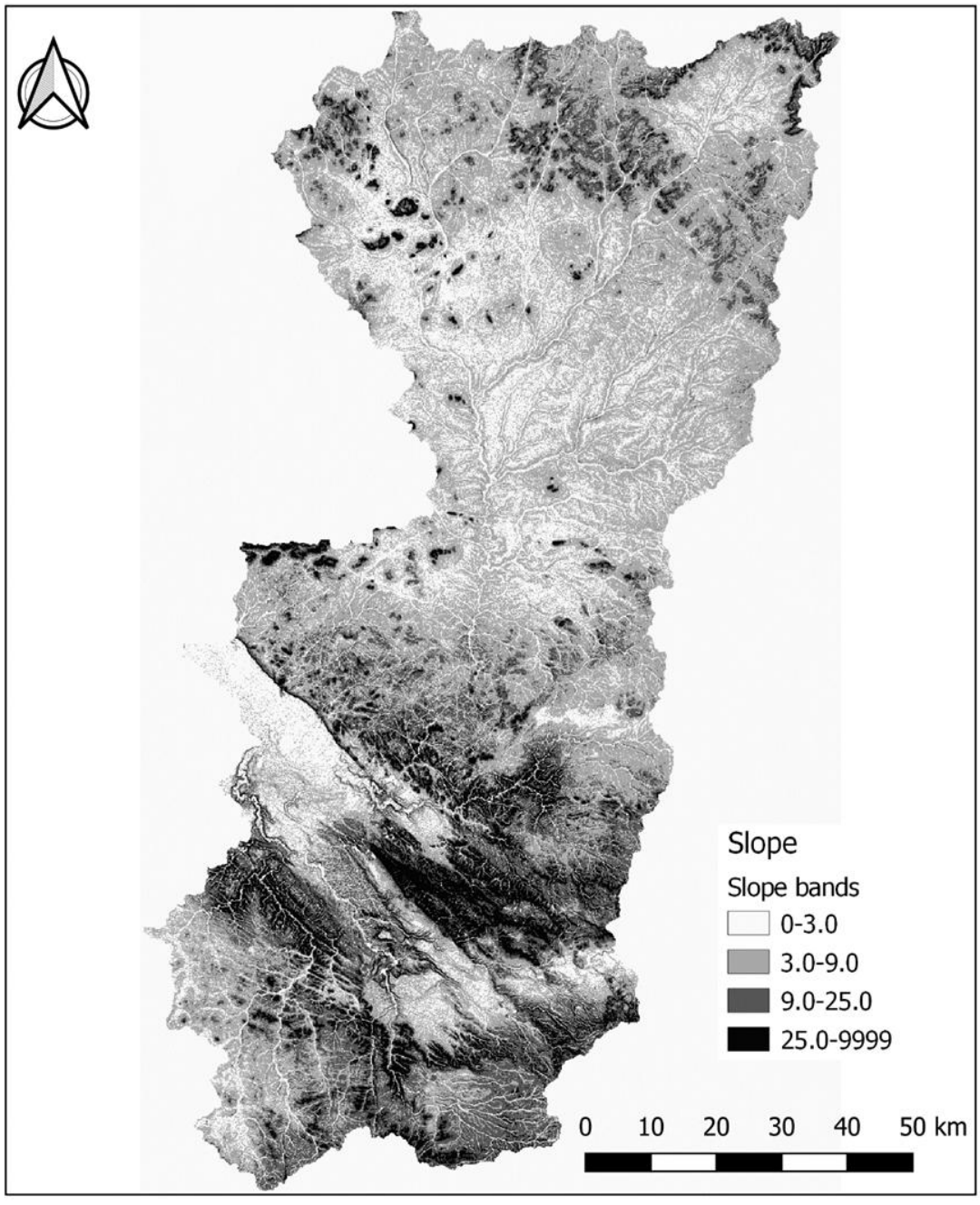

Figure 3.11: shows the slope classification of the Songwe River sub-basin

3.7.2 Hydrologic Response Units (HRU)

The sub-basin was divided into Hydrological Response Units (HRUs) by applying threshold values determined by land use/land cover, soil characteristics and slope percentage. The threshold level is employed to exclude insignificant land use/land cover types within the sub-basin, minor soil classifications within a specific land use/land cover area and minor slope categories within a soil type in designated land use/land cover areas. Subsequent to the exclusion of minor categories, the residual land use/land cover areas, soil types and slope classifications were reallocated to guarantee comprehensive representation of 100% of their respective areas inside the SWAT model. Land use, soil and slope characterization were conducted with commands from the HRU analysis menu within the QSWAT Toolbar. These technologies facilitated the integration of raster-format land use and soil maps into the current project, evaluating slope characteristics and identifying the combinations of land use, soil and slope classes within the defined sub-basins. In SWAT, HRU distribution can be defined in two ways: by assigning a single HRU to each sub-watershed or by allocating several HRUs to each sub-watershed according to predetermined threshold values. The SWAT User's Manual advises that a 20% land use threshold, a 10% soil threshold and a 20% slope threshold are sufficient for the majority of modelling applications (Neitsch et al., 2011). Employing various threshold criteria, specifically 10% land use, 20% soil and 10% slope thresholds, yields a more accurate prediction of runoff and sediment yield. This study used the concept of HRU with various thresholds: 10% land use, 20% soil and 10% slope (Setegn et al., 2008). The threshold values stipulated that only land use types comprising a minimum of 10% of the sub-watershed area and soils constituting at least 20% of the area within each designated land use were included in the HRU analysis. The Songwe River sub-basin was consequently partitioned into hydrological response units each characterized by a distinct combination of land use and soil type. The quantity of HRUs in each sub-catchment is presented in Figure 3.12

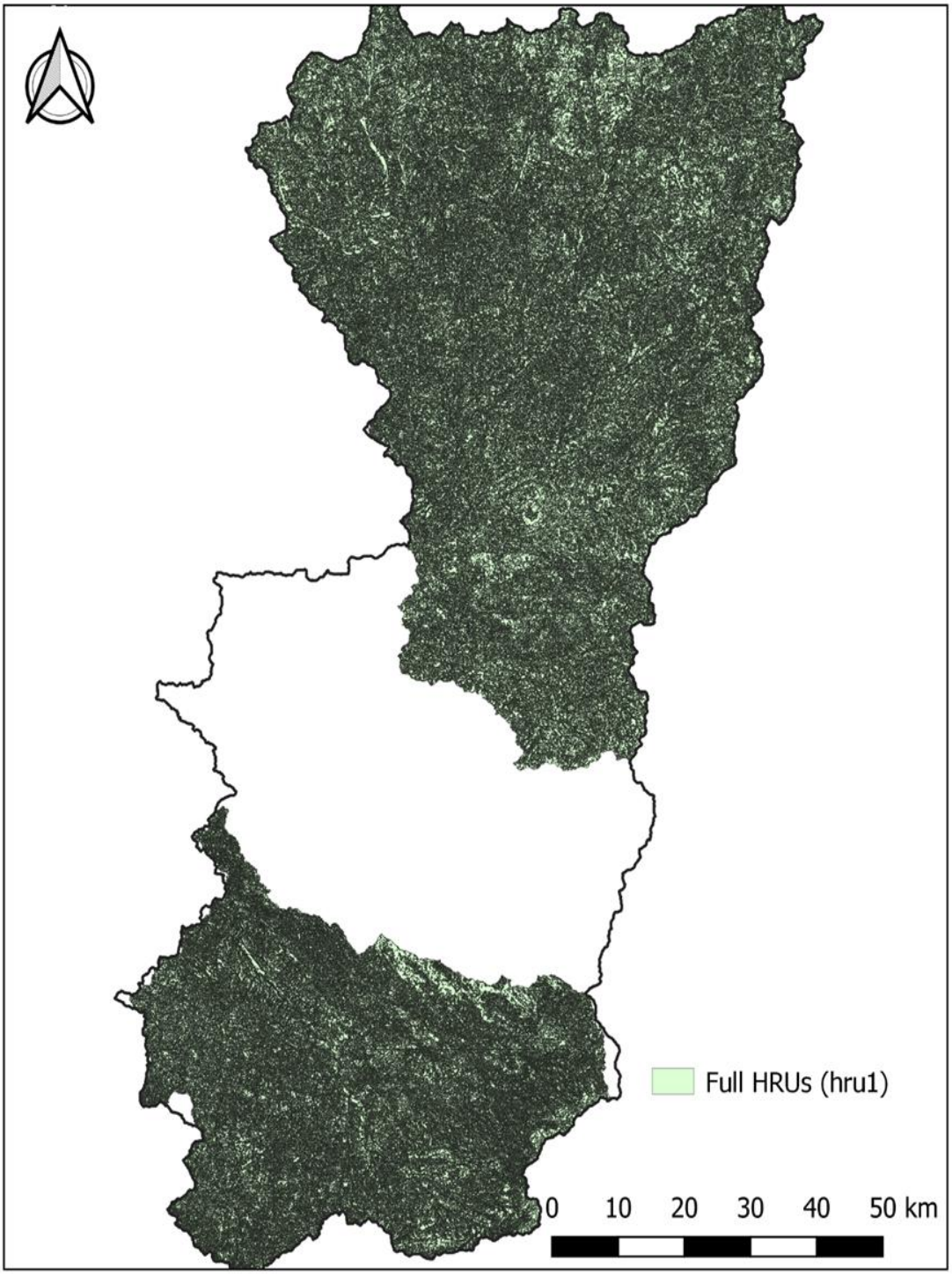

Figure 3.12: Illustrates the distribution of HRUs across the Songwe River sub-basin

3.8 Calibration and Validation of SWAT Model

The daily river discharge data from the Galula gauging station were used for the calibration and validation of the SWAT model. Calibration and validation were

conducted using SWATCUP's SUFI-2, a semi-automated tool for calibration and uncertainty assessment (Arnold et al., 2012). The process began with a sensitivity analysis, followed by the calibration procedure. The calibration iterations were carried over into the validation phase (Abbaspour et al., 2007). Sensitivity analysis was performed in QSWAT both with and without discharge data from gauging stations, and in SWAT-CUP using the SUFI techniques, executing the model 1000 times. The t-statistic and p-value were used to prioritize the sensitivity of the factors, with the most critical parameters characterized by the lowest p-values and highest absolute t-statistic values.

Since sediment data were unavailable, the SWAT model was calibrated for streamflow alone. Literature values from similar regions were used to estimate sediment-related parameters, which is a recognized limitation of the study. As a result, while streamflow calibration provides insights into hydrological behavior the lack of sediment data introduces uncertainty when simulating sediment yield. This limitation also affects the model's ability to predict future sediment dynamics with high accuracy as the sediment-related parameters may not fully reflect local conditions of the Songwe River sub-basin. The calibration aimed to minimize the difference between the model's simulated outputs and the observed values. Monthly streamflow data from 1974 to 1983 were used for calibration while data from 1984 to 1991 were employed for validation.

Four primary statistical coefficients were used to assess model performance, focusing on the goodness of fit between simulated and observed data during calibration and validation: the Nash-Sutcliffe Efficiency (NSE), Coefficient of Determination (R^2), Percent Bias (PBIAS), and the ratio of the root mean square error to observation standard deviation (RSR) (Assfaw, 2019; Begou et al., 2016; Mfwango et al., 2022). Additionally, the r-factor and p-factor were utilized to evaluate the uncertainty in model predictions. The model's overall performance was assessed based on the ratings of these objective functions (Gyamfi et al., 2016).

3.9 Characterization of Sediment Sources and Mapping Sediment Sources in the Songwe River Sub-Basin

This study focuses on the Songwe River sub-basin a crucial region for investigating soil erosion and sediment yield. Using the Soil and Water Assessment Tool (SWAT) the study conducted a detailed analysis of sediment production and identified its sources within the sub-basin. The SWAT model was integrated with QGIS tools to analyze spatial and temporal data, providing a robust framework for modeling erosion andsediment yield across the sub-basin and identifying sediment sources under various climatic scenarios.

The integration of SWAT and QGIS allowed for a comprehensive assessment of sediment dynamics, considering key factors such as land use, soil properties, slope, topography, and rainfall. This combined approach helped forecast sediment sources, pinpoint erosion hotspots, and evaluate the impacts of these factors on erosion patterns. The study also mapped areas most vulnerable to erosion, providing a clear picture of sediment transport patterns within the sub-basin.

Additionally, the study examined future scenarios for erosion and sediment yield under climate change using the calibrated SWAT model under two Representative Concentration Pathways (RCPs): RCP4.5 and RCP8.5. Bias-corrected output from four regional climate models were incorporated as input data for the SWAT model. The analysis was performed for three distinct future time periods—2011–2040, 2041–2070 and 2071–2100 to explore how climate change might influence sediment dynamics over the coming decades.

3.10 Simulation of Sediment Yield Under Different Climate Scenarios in the Songwe River Sub-Basin

To model the impacts of climate change on sediment yield in the Songwe River sub-basin, two distinct Representative Concentration Pathways (RCPs) RCP 4.5 and RCP 8.5 were chosen. The simulations were conducted based on future forecasts for the periods 2011–2040, 2041–2070 and 2071–2100. The climate projection scenario was formulated using simulations from four high-resolution regional climate models (RCMs) informed by general circulation models (GCMs) from the Coordinated

Regional Climate Downscaling Experiment (CORDEX) under the RCP 4.5 and RCP 8.5 scenarios. The chosen models were previously used to mimic climatic conditions in the southern highlands of Tanzania, with relatively little inaccuracy (Luhunga et al., 2018b).

The impacts of climate change were evaluated by employing the calibrated SWAT model with projected climate data for the periods 2011–2040, 2041–2070 and 2071–2100 under two emission scenarios (RCP 4.5 and RCP 8.5). The 2020 Land Use and Land Cover (LULC) map was used to operate the SWAT model for future projections. Bias-adjusted future precipitation data in conjunction with minimum and maximum temperature forecasts from four regional climate models (RCMs) served as inputs for operating the SWAT model. This methodology presupposes that land use and land cover classifications will remain unchanged over the forthcoming era. Furthermore, other SWAT input parameters such as soil composition and topography were maintained at fixed values. A primary assumption of this study is that the calibrated parameter set retains its validity throughout fluctuating environmental conditions. The SWAT model uses the MUSLE equation 2.3 to simulate future sediment yield.

The influence of climate projections on soil erosion and sediment yield was assessed by comparing SWAT results across four distinct RCM scenarios: CCLM4, HIRHAM5, RACMO22T and RCA4 within the sub-basin. This comparison facilitated the assessment of discrepancies in sediment yield forecasts across the various models and elucidated the impact of RCM selection on future sediment yield estimations.

3.11 Evaluating the impacts of Climate Change under Different Scenarios on Sediment Yield in the Songwe River Sub-Basin

The impacts of climate change under different future land use/land cover (LULC) scenarios were evaluated by employing the calibrated SWAT model with projected climate data for the periods 2011–2040, 2041–2070 and 2071–2100 alongside LULC forecasts for 2040, 2070 and 2100 (Figure 3.13) under two emission scenarios (RCP 4.5 and RCP 8.5). LULC maps for 2040, 2070 and 2100 were used to operate the SWAT model for the near future (2021–2040), mid-future (2041–2070) and end-of-century (2071–2100) intervals, respectively. Furthermore, prospective land use and

land cover (LULC) maps were integrated into the SWAT model to address different future scenarios across several temporal intervals under two emission scenarios: Representative Concentration Pathways (RCP) 4.5 and RCP 8.5.

The climate data used for this analysis were derived from bias-corrected forecasts of future mean precipitation as well as minimum and maximum temperatures sourced from four regional climate models (RCMs). The climate estimates were derived from the Coordinated Regional Climate Downscaling Experiment (CORDEX) under RCP 4.5 and RCP 8.5 emission scenarios offering a spectrum of potential future climatic conditions. The forecasts served as input variables in the SWAT model to simulate future sediment dynamics under various climate and different land use scenarios. The different future land use scenarios when combined with climate data facilitates an evaluation of how changes in land use and climate patterns interact. This interaction influences sediment yield.

The SWAT model simulations were conducted for each future period, and the results were examined to assess the cumulative impacts of climate change under future land use scenaros on sediment yield. The integration of prospective land use scenarios facilitates a more thorough comprehension of the influence of anthropogenic and climatic factors on water resources and sediment yields enabling the development of suitable management options to alleviate adverse effects.

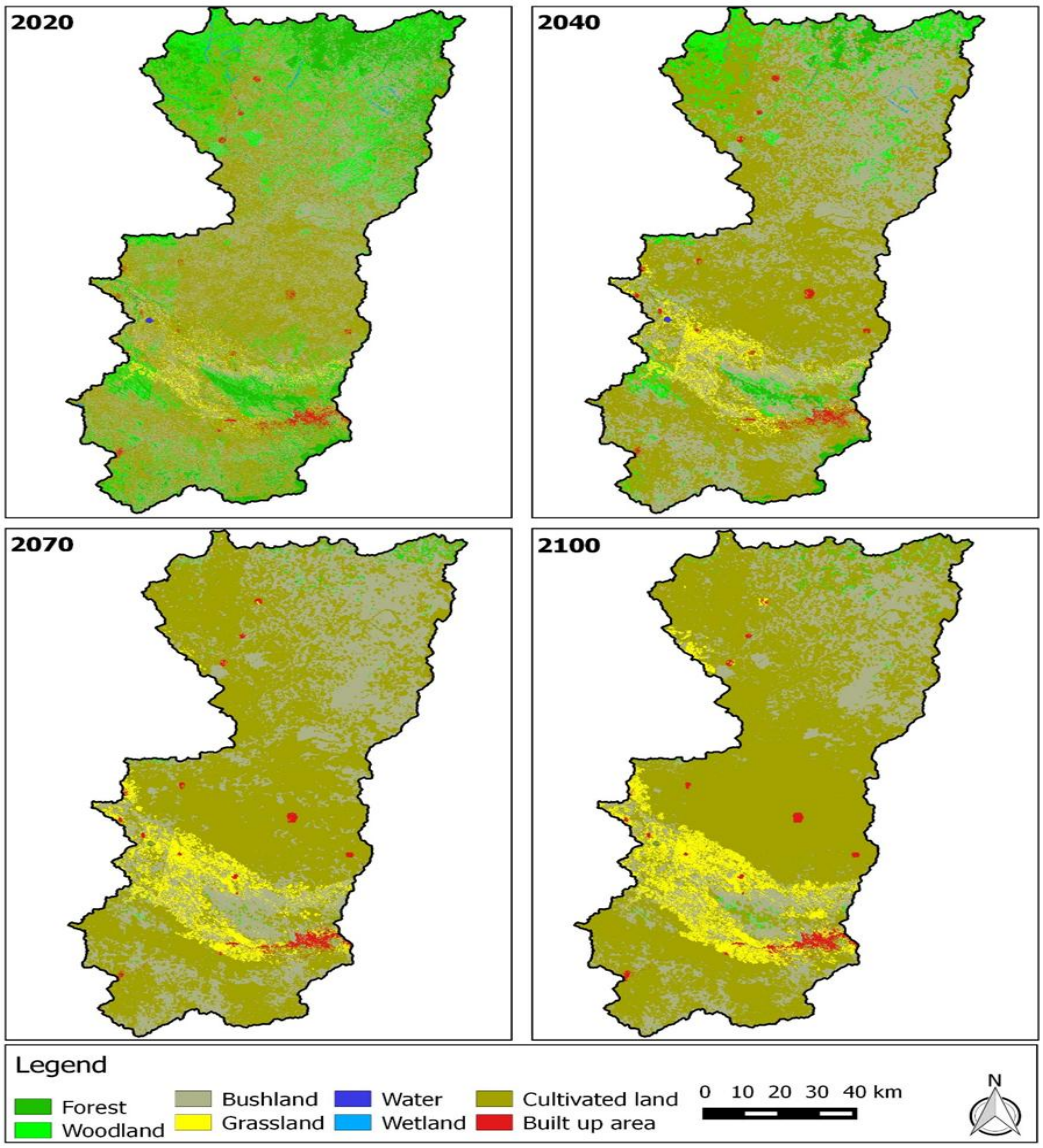

Figure 3.13: Predicted land use and land cover maps for 2040, 2070, and 2100 in the Songwe River Sub-basin created in QGIS 2.6.1

The SWAT model has limitations when applied to sediment yield predictions in the Songwe River sub-basin. Its performance heavily depends on the quality and accuracy of input data and the lack of observed sediment data for calibration means that sediment-related parameters were estimated using literature values from similar regions which not fully reflect local conditions. Additionally, the model primarily focuses on physical and environmental factors neglecting socio-economic influences which are crucial for understanding sediment dynamics in the region. Furthermore,

uncertainties in climate change projections given the limited availability of reliable local climate data and impact future sediment yield forecast. These limitations constrain the model's accuracy in predicting sediment yield and assessing the impact of future changes in the sub-basin.

3.12 Concluding Remarks

This chapter offered the methods and materials used in this study for each specific objective. The study design follows the quantitative method. To model the impacts of climate change on sediment yield in Songwe River sub-basin the study used the spatial and meteorological data as input data in the SWAT Model. The QGIS software was used to process the spatial data and mapping of sediment sources in the river sub-basin. The chapter also, outlined the method employed in developing, calibrating and validating the SWAT model. The climate data from four regional models was bias corrected and then used as an input data for the calibrated SWAT model for simulating historical and future sediment yield

CHAPTER FOUR

RESULTS AND DISCUSSIONS

4.1 Overview

The study used the SWAT model and QGIS to delineate sediment yield and assess their regional distribution. It also examines the impact of climate change on sediment yield across several climate scenarios, considering projected alterations in temperature and precipitation. The study illustrates the efficiency of the SWAT model by analyzing current and prospective land use and examines the impacts of climate change at the sub-basin level. This study underscores how land-use changes, such as agricultural expansion, urban development and deforestation interact with climatic conditions to shape sediment yield. Forecasts for the periods 2011–2040, 2041–2070 and 2071–2100 under RCP4.5 and RCP8.5 suggest that the cumulative impacts of climate change could lead to increased sediment production. This indicates increased unpredictability in sediment dynamics resulting in increasing challenges for the management of erosion, sedimentation and water quality.

4.2 Sensitivity Analysis, Model Calibration and Validation

The sensitivity analysis performed on the SWAT model in the Songwe River sub-basin found the most significant parameters influencing streamflow and sediment output. Table 4.1 enumerates the selected sensitive parameters based on their statistical significance underscoring their critical role in influencing hydrological processes within the sub-basin. The most sensitive parameters for simulating streamflow and sediment yield were the Soil Conservation Service (SCS) Curve Number for Moisture Condition II (CN2), Soil Available Water Content (SOL_AWC), Groundwater Outlet Moisture (GWOMN), Groundwater Delay (GW DELAY) and Groundwater Evapotranspiration (GW REVAP). These parameters had a substantial impact on sediment transport, runoff and base flow within the Songwe River sub-basin. The SCS Curve Number for Moisture Condition II (CN2) is the most sensitive parameter for simulating river flow and sediment yield in Songwe River Sub-basin. CN2 is vital for determining the amount of surface runoff during a rainfall event. A higher CN2 value results in greater runoff which enhances the potential for soil erosion and sediment transport. This parameter is directly tied to soil erodibility because areas with higher

runoff are more likely to erode and increase sediment yield. The Soil Available Water Content (SOL_AWC) is the second most sensitive parameter. SOL_AWC also plays a critical role in runoff generation. When soil has a low AWC, it cannot absorb water as effectively, leading to increased surface runoff that further exacerbates soil erosion and sediment yield.

Table 4.1: Sensitive parameter rank for flow and sediment modelling at the Songwe River Sub-basin

Parameter Name	t-Stat	P-Value
1:R_CN2.mgt	-30.75798222	0.0
7:R_SOL_AWC(..).sol	4.880786852	1.434e-06
4:V_GWOMN.gw	-2.975964448	0.005065941
3:V_GW_DELAY.gw	-2.878518173	0.004171187
5:V_GW_REVAP.gw	-1.628220185	0.104124918
12:R_SOL_K(..).sol	0.940189367	0.347586531
6:V_SURLAG.bsn	-0.817409884	0.414093942
5:V_ESCO.bsn	0.812802289	0.416800461
2:V_ALPHA_BF.gw	0.688072418	0.491734779
10:V_RCHRG_DP.gw	0.613550836	0.538732596
9:V_REVAPMN.gw	-0.369003489	0.716759779
11:R_SOL_BD(..).sol	0.049572681	0.960483242

The Galula gauging station in the Songwe River sub-basin served as the calibration and validation site for the semi-distributed SWAT hydrologic model which was used to simulate sediment yield. A total of seventeen years of streamflow data (1974–1991) were used to calibrate and validate the SWAT model for the Songwe River sub-basin at this station. The results are illustrated in Figure 4.1A and Figure 4.1B. A comparison between the observed and simulated streamflow data showed a positive correlation during both the calibration and validation phases. The model achieved below the accepted threshold goodness of fit metrics during calibration in the data scarce sub-basin, with a Nash-Sutcliffe Efficiency (NSE) of 0.47, a coefficient of determination (R^2) of 0.59 and a ratio of model error to standard deviation of observations (RSR) of 0.73. Performance improved in the validation phase, yielding an NSE of 0.59, an R^2 of 0.59 and an RSR of 0.64 (see Table 4.2).

Despite the lower Nash-Sutcliffe Efficiency (NSE) values (0.47 during calibration and 0.59 during validation), the model remains usable because it effectively captures the seasonal trends and overall dynamics of streamflow and sediment yield in the Songwe River sub-basin. The model's ability to simulate key hydrological patterns such as peak flows and baseflow is supported by other metrics, such as an R^2 of 0.59 and an RSR of 0.73 in calibration and 0.64 in validation, indicating acceptable error relative to the data's variability. The improvement in model performance from calibration to validation suggests that it is adaptable and reliable for predicting general trends in streamflow and sediment yield and provide valuable insights. Comparative evaluations with other studies suggest that while the model demonstrated satisfactory performance, but there is still potential for improvement particularly during the calibration phase. Research conducted in the Upper Blue Nile Basin (Lebeza et al., 2024) reported NSE values ranging from 0.71 to 0.74 indicating exceptional performance possibly due to more stable hydrological conditions improved data availability and less complex watershed characteristics. A study in the Nyando Basin (Opere et al., 2019; Opere & Okello, 2011), showed slightly lower performance compared to the Songwe River Sub-Basin; however, the trends observed were similar, highlighting common challenges such as seasonal variability and data limitations. The model for the Songwe River Sub-Basin exhibited inadequate performance (NSE = 0.47 during calibration), which can be attributed to complex hydrological dynamics including variability in precipitation and groundwater interactions compounded by potential data constraints. Nevertheless, the model's performance improved after validation (NSE = 0.59) meaning that it requires continued advancements in data accuracy and parameter calibration to more effectively represent the changing climatic and land-use conditions within the Songwe River Sub-Basin.

Due to the lack of observed sediment data, the sediment parameters in this model were not calibrated. Instead, they were derived from literature values which introduces potential uncertainty in the sediment yield results. Relying on literature-based sediment parameters means that the model may not fully capture local variations or specific site conditions, leading to a possible misrepresentation of sediment dynamics.

Therefore, sediment yield estimates should be treated with caution due to their reliance on these generalized parameters rather than site-specific calibration.

Table 4.2: Evaluation Statistics for calibration and validation

	CALIBRATION				VALIDATION				CALIBRATION		VALIDATION	
Flow Station	NSE	R^2	RSR	PBIAS	NSE	R^2	RSR	PBIAS	Ob-flow (m^3/s)	Sim-flow (m^3/s)	Ob-flow (m^3/s)	Sim-flow (m^3/s)
Galula	0.47	0.59	0.73	-35.5	0.59	0.59	0.64	3.9	33.16	44.9	33.16	31.88
Lupa	-0.09	0.01	1.04	-17.1	-0.08	0.01	1.04	9.1	93.30	109.22	93.30	84.80

Ob-flow; Observed flow Sim-flow; Simulated flow

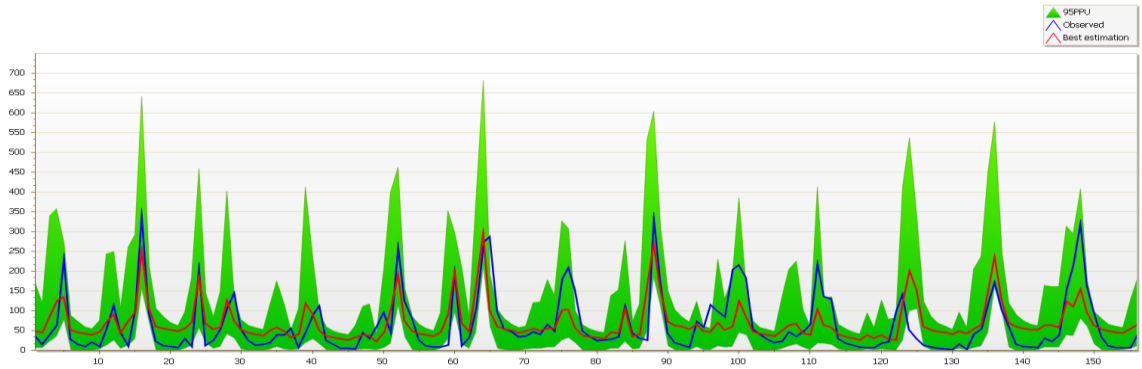

Figure 4.1A: Observed and simulated monthly flow for calibration period at Galula gauging station (1974–1991)

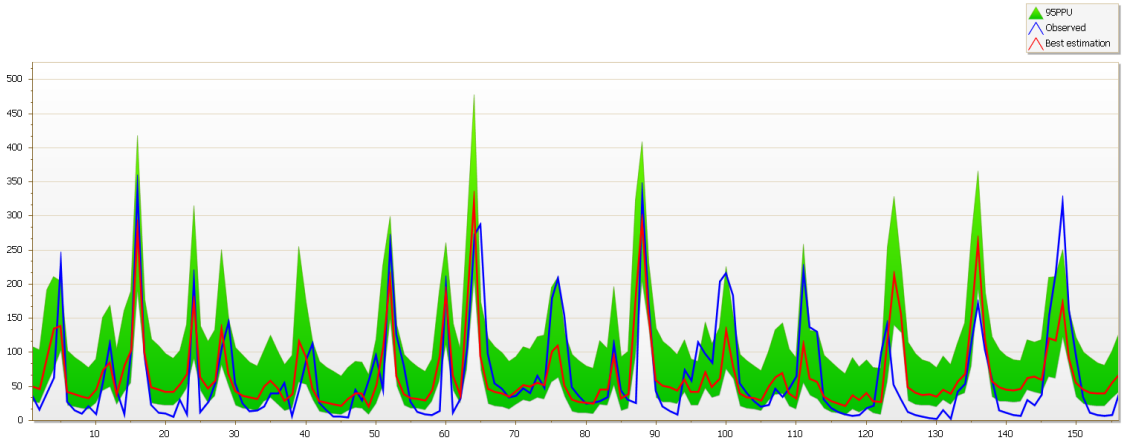

Figure 4.1B Observed and simulated monthly flow for validation period at Galula gauging station (1974–1991)

4.3 Changes in Historical and Future Precipitation and Temperature

The average monthly mean precipitation forecasts from four regional climate models (CCLM4, HIRHAM5, RACMO22T and RCA4) for the historical, near-future, mid-future and end-of-century periods were assessed against actual observations from the baseline period and meteorological data produced by the SWAT model. Most models demonstrated an overestimation of precipitation in historical simulations particularly at all stations inside the sub-basin (Figure 4.2 – Figure 4.4). The bias-corrected findings for the historical era indicated that at numerous sites the CCLM4 and HIRHAM5 models surpassed RCA4 and RACMO22T in properly representing the observed mean monthly precipitation. The overestimations may arise from the regional biases prevalent in global climate models which often struggle to represent localized precipitation patterns effectively (Jones et al., 2023).

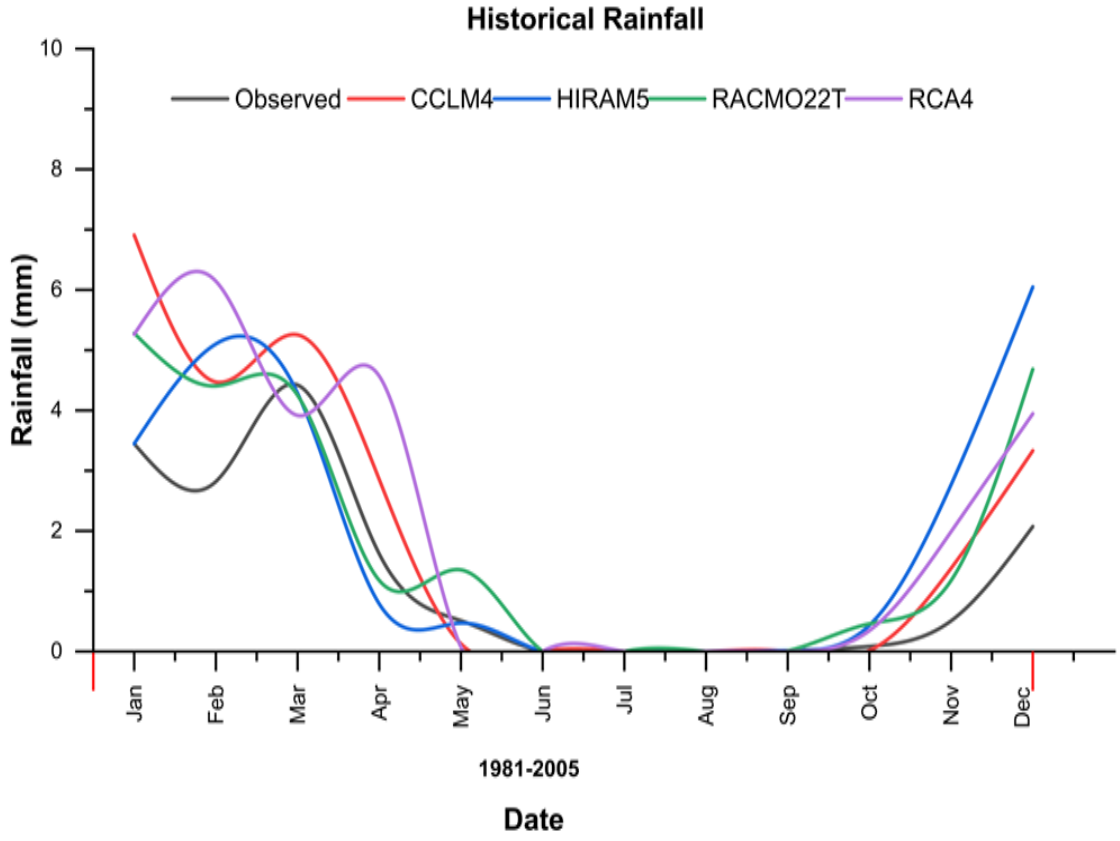

Figure 4.2: Historical Monthly mean rainfall at Galula station (1981 – 2005)

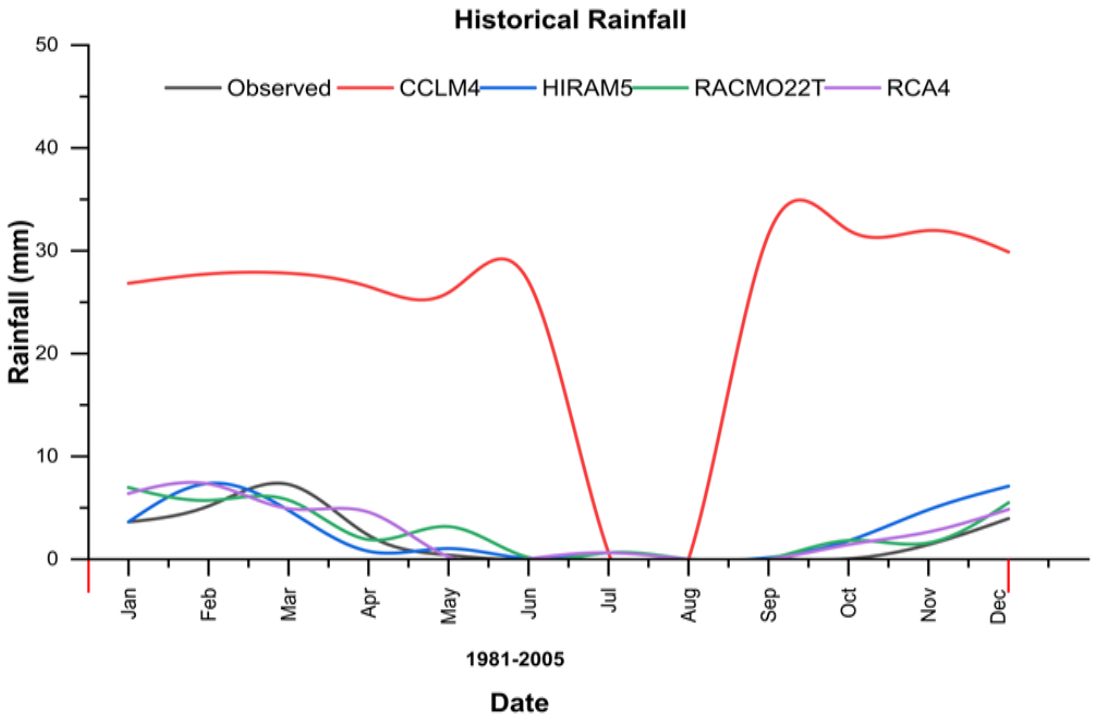

Figure 4.3: Historical Monthly mean rainfall at Lupa station (1981 – 2005)

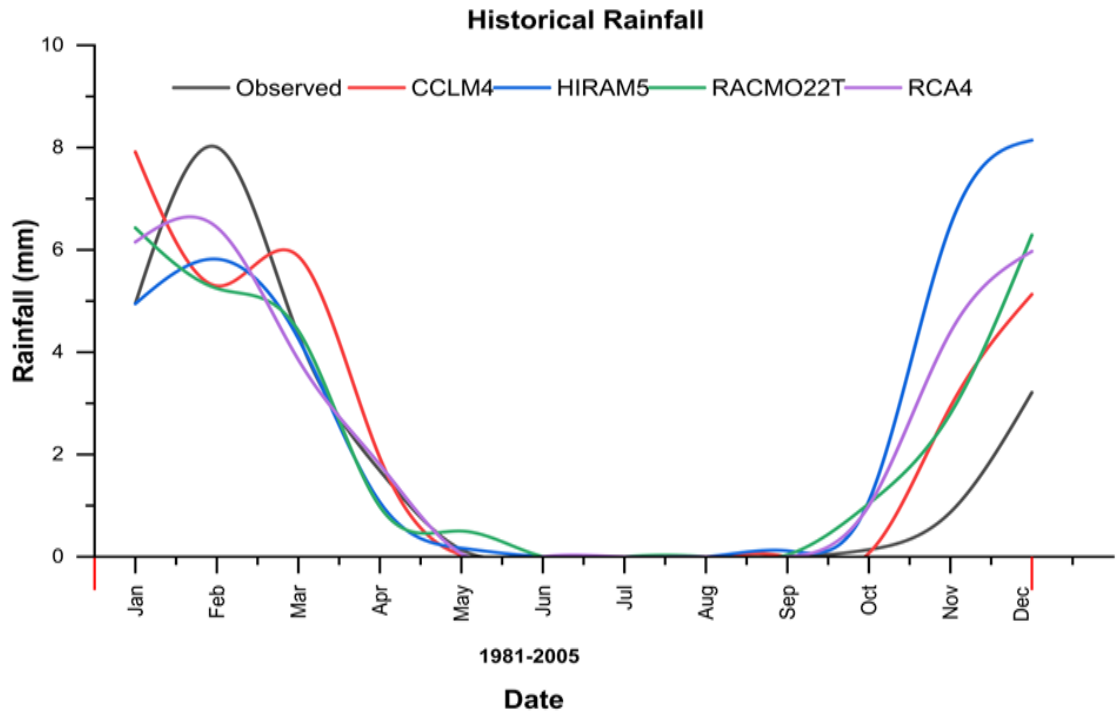

Figure 4.4: Historical Monthly mean rainfall at Mbeya maji station (1981 – 2005)

In the RCP 4.5 scenario all four regional climate models predict a consistent reduction in mean annual precipitation over the three future decades. During the near-future period (2011–2040) precipitation is anticipated to reduce by around 2% to 5% with the most significant reductions forecasted by CCLM4 (4%) and HIRHAM5 (5%) although RCA4 and RACMO22T suggest lesser decreases of about 2% to 3% (Figure 4.5 – Figure 4.7). By mid-century (2041–2070) the reductions become increasingly uniform attaining levels between 5% and 8%. During the late century (2071–2100) the drying trend intensifies exhibiting rainfall reductions of 8% to 10%. The decreases are most evident during the early rainy season (January–April) prompting worries about reduced agricultural seasons and diminished water supply. These forecasts correspond with findings from another study, wherein elevated precipitation levels under the RCP 4.5 scenario are frequently associated with regional climate models that depict more pronounced warming trends (Knutti et al., 2013). This data indicates that regional climate models such as RCA4 and RACMO22T may more effectively represent regional climatic alterations due to their increased sensitivity relative to other models.

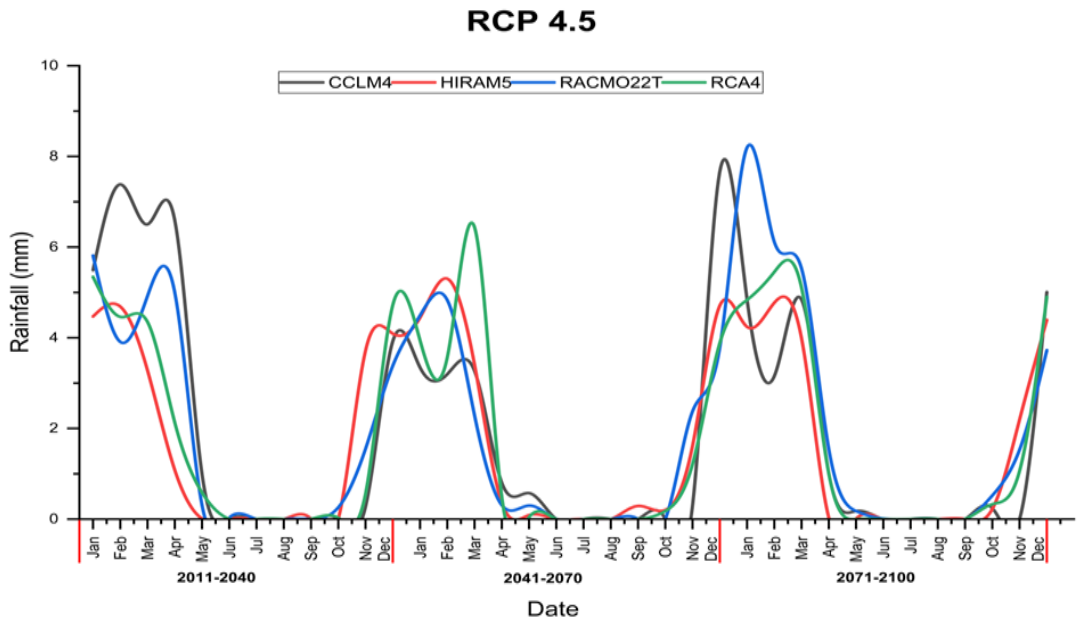

Figure 4.5: Simulated Monthly mean rainfall at Galula station (2011 – 2100) under RCP 4.5

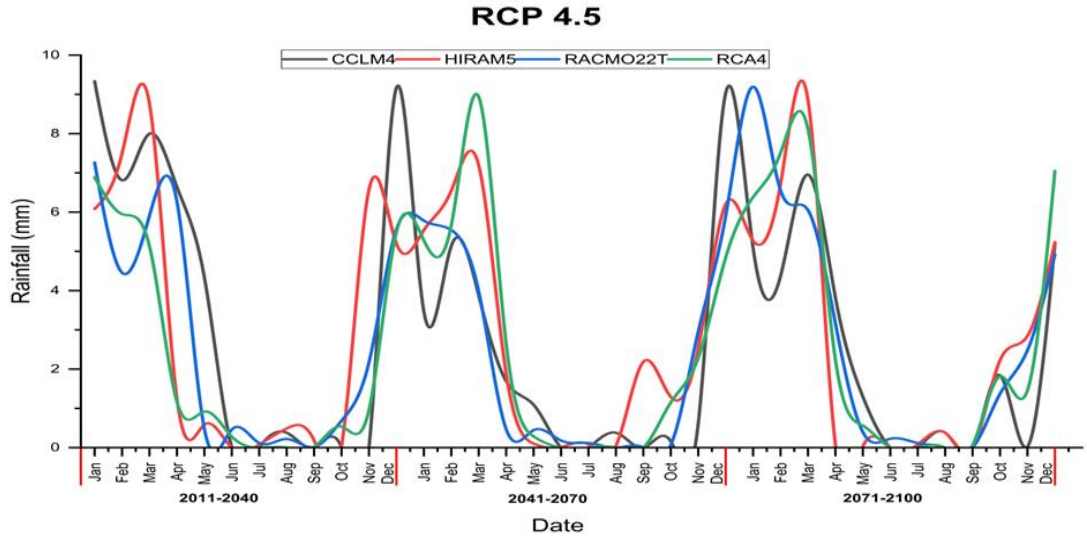

Figure 4.6: Simulated Monthly mean rainfall at Lupa station (2011 – 2100) under RCP 4.5

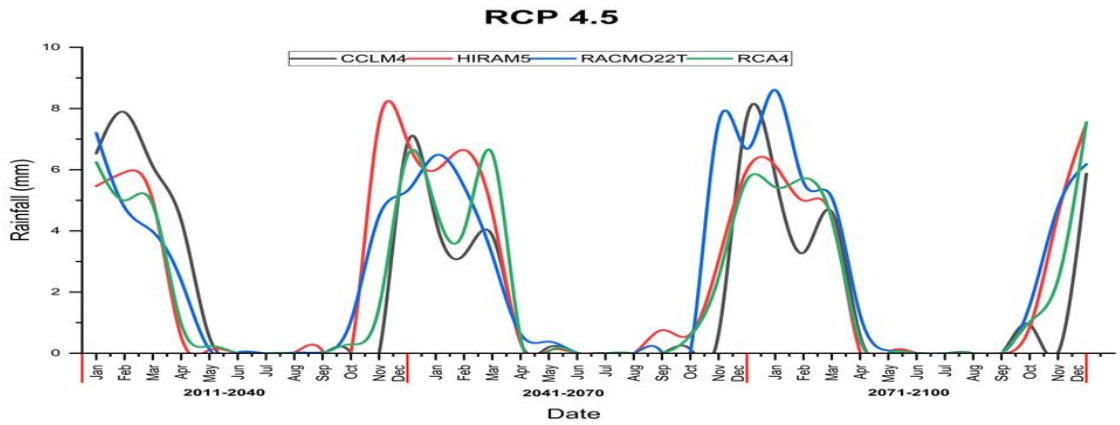

Figure 4.7: Simulated Monthly mean rainfall at Mbeya maji station (2011 – 2100) under RCP 4.5

According to the RCP 8.5 high-emission scenario, precipitation levels are expected to rise in most months particularly during the latter portion of the rainy season (November–December). Between 2010 and 2040 annual precipitation is anticipated to increase by around 3% to 6% with RCA4 and RACMO22T exhibiting the most pronounced rises relative to the more conservative models CCLM4 and HIRHAM5 (Figure 4.8 – Figure 4.10). During the mid-century period (2041–2070) these increases intensify to between 5% and 8% but regional variances become apparent. By the conclusion of the century (2071–2100) the forecast for precipitation becomes more definitive suggesting annual rises of 8% to 12%. RCA4 and RACMO22T consistently

forecast the most precipitation whereas CCLM4 and HIRHAM5 exhibit somewhat drier conditions.

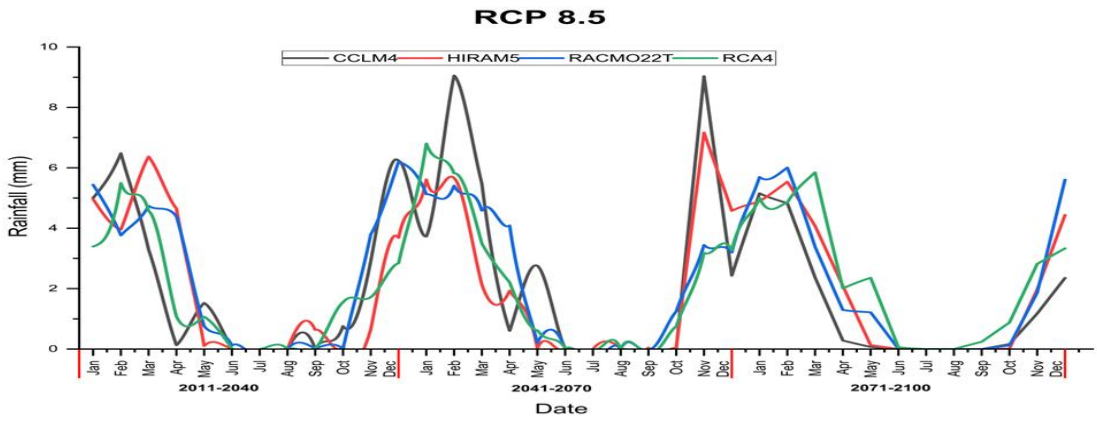

Figure 4.8: Simulated Monthly mean rainfall at Galula station (2011 – 2100) under RCP 8.5

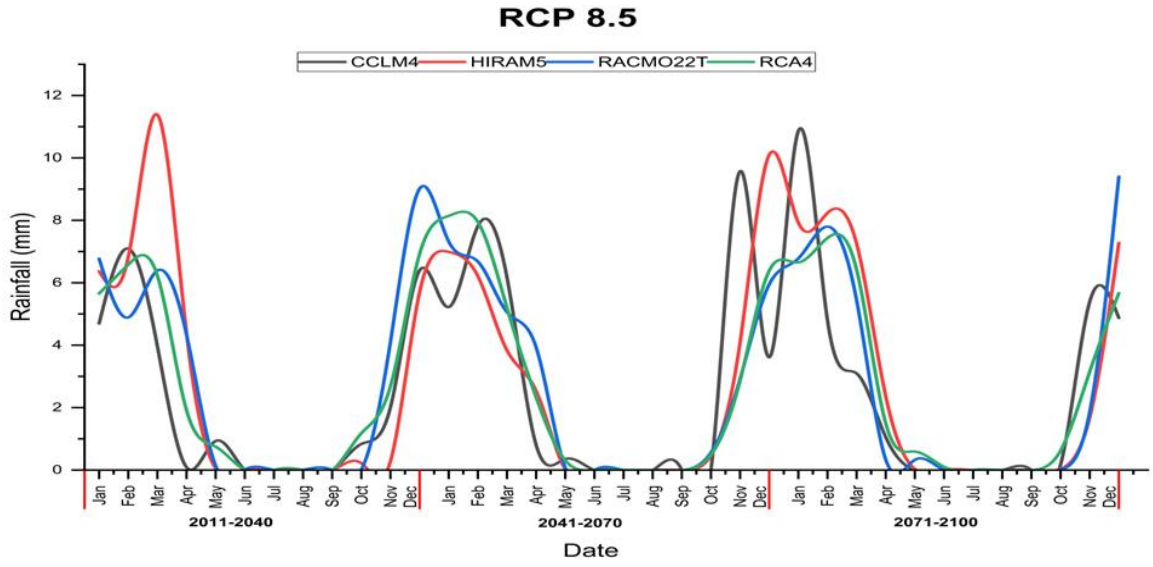

Figure 4.9: Simulated Monthly mean rainfall at Lupa station (2011 – 2100) under RCP 8.5

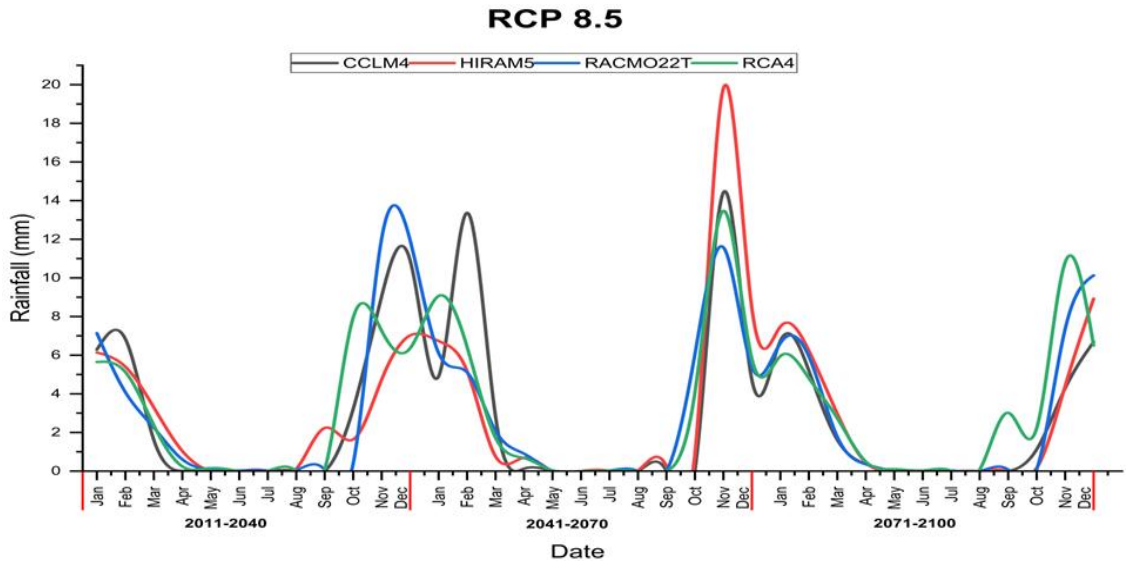

Figure 4.10: Simulated Monthly mean rainfall at Mbeya maji station (2011 – 2100) under RCP 8.5

These results demonstrate that RCP 4.5 is associated with a gradual drying of the Songwe River sub-basin (2% to 10%) but RCP 8.5 indicates a tendency towards increased moisture (3% to 12%) (Figure 4.11). The variability among models is considerable: RCA4 and RACMO22T consistently predict wetter outcomes but CCLM4 and HIRHAM5 forecast drier conditions in both scenarios. This variety underscores the uncertainty inherent in regional climate predictions and underscores the need for employing ensemble approaches. From a management perspective the varying rainfall forecasts provide two categories of risks: reduced water availability in stabilization scenarios and heightened probabilities of flooding and sedimentation in high-emission scenarios. The varying forecasts for the sub-basin may be affected by local meteorological conditions and land-use alterations around the stations that influence rainfall patterns. These discrepancies underscore the need for accounting for local climate dynamics when analyzing outcomes from global models.

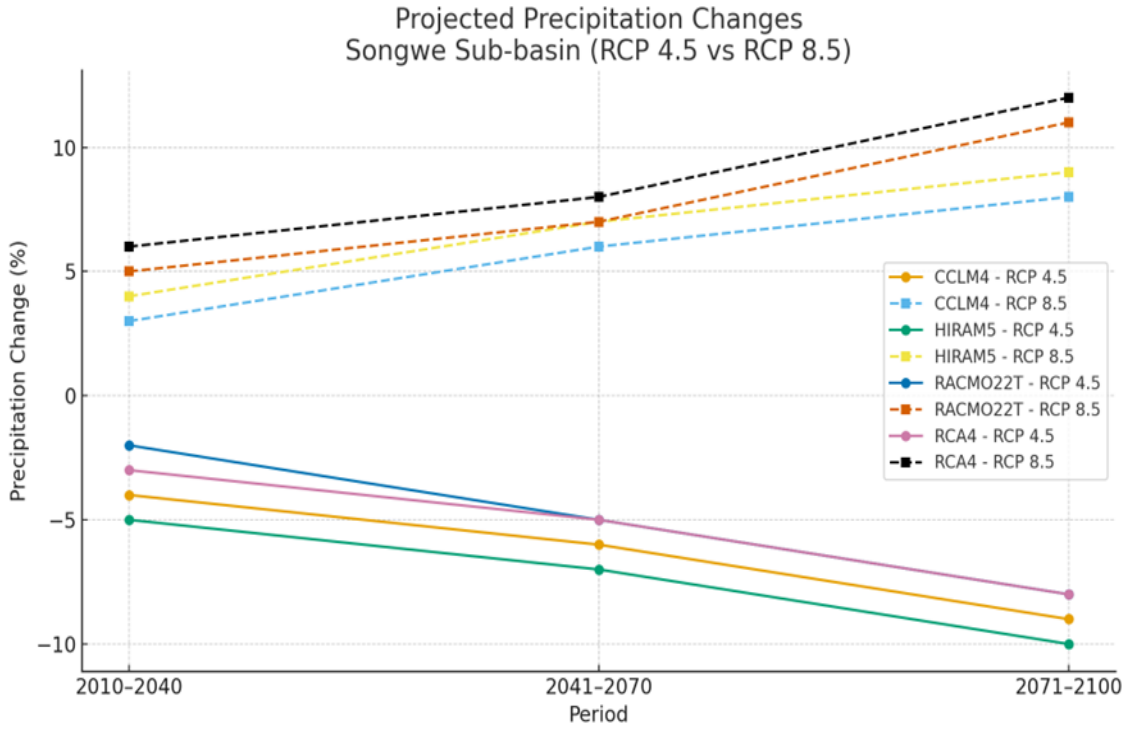

Figure 4.11: Projected rainfall changes for Songwe River Sub-basin under RCP4.5 and RCP 8.5

During the historical period all four climate models forecast a consistent rise in both minimum and maximum temperatures over the Songwe River Sub-basin (Figure 4.12 and Figure 4.13).

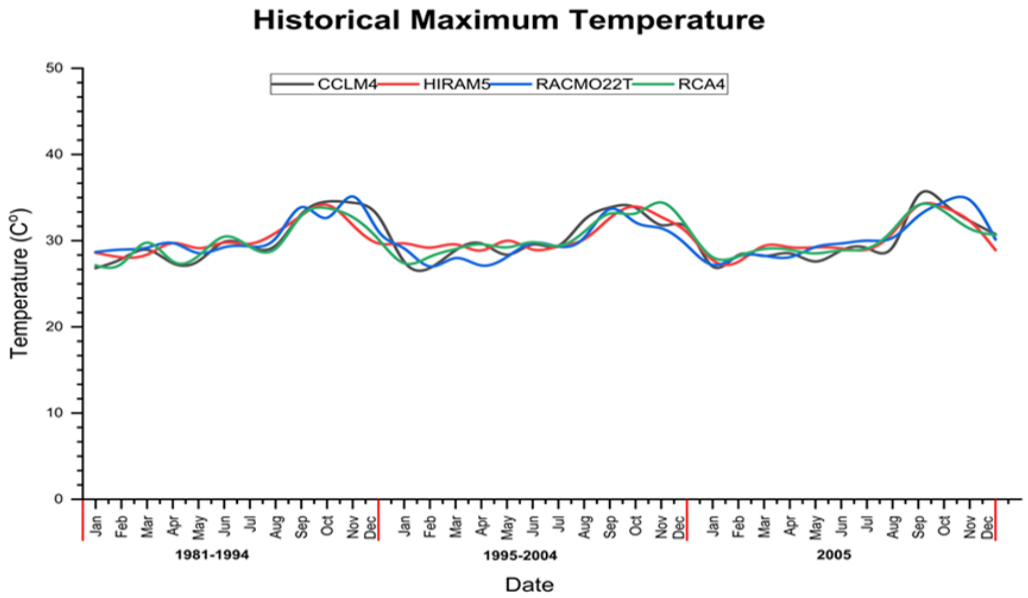

Figure 4.12: Historical Monthly mean maximum temperature at Galula station

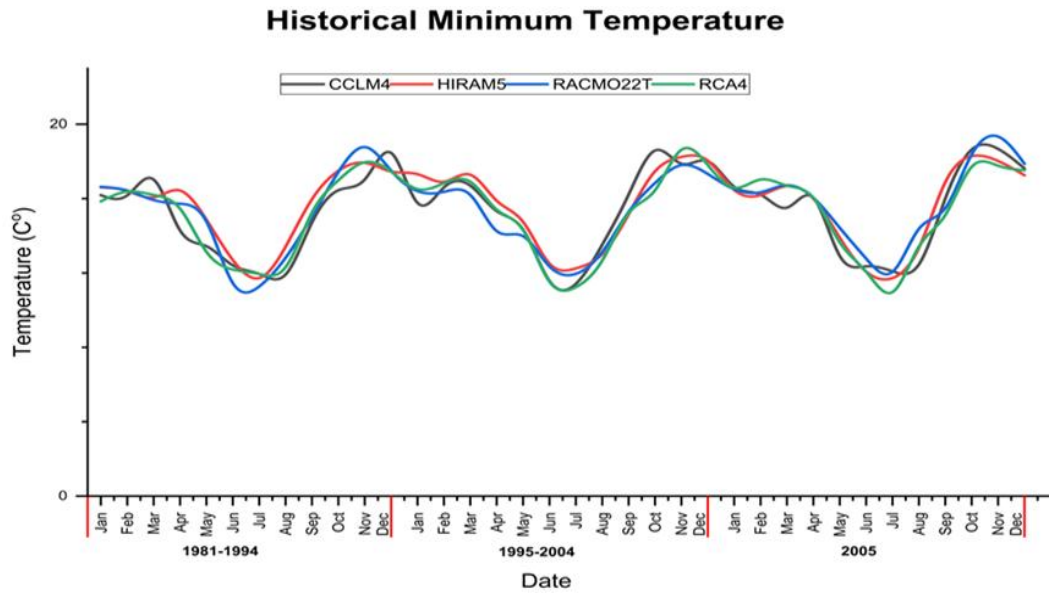

Figure 4.13: Historical Monthly mean minimum temperature at Galula station

All models forecast a consistent rise in both minimum and maximum temperatures over the sub-basin during the early, mid and late periods of the century under the RCP 4.5 and RCP 8.5 climate scenarios. This trend aligns with extensive climate change research forecasting substantial warming in East Africa especially under high-emission scenarios (Feyissa Negewo & Kumar Sarma, 2022; Lazaro et al., 2023; Mbungu, Heatwole, et al., 2016) The period from 2010 to 2040 is expected to witness a modest increase in both maximum and minimum temperatures under the RCP 4.5 scenario. Under RCP 4.5 the maximum temperature is anticipated to rise by around 0.5°C to 0.9°C and the lowest temperature may rise by 0.3°C to 0.6°C (Figure 4.14 and Figure 4.15). Despite being comparatively minor relative to anticipated future increases this temperature rises are yet substantial enough to affect both natural systems and human activities in the Songwe River Sub-Basin.

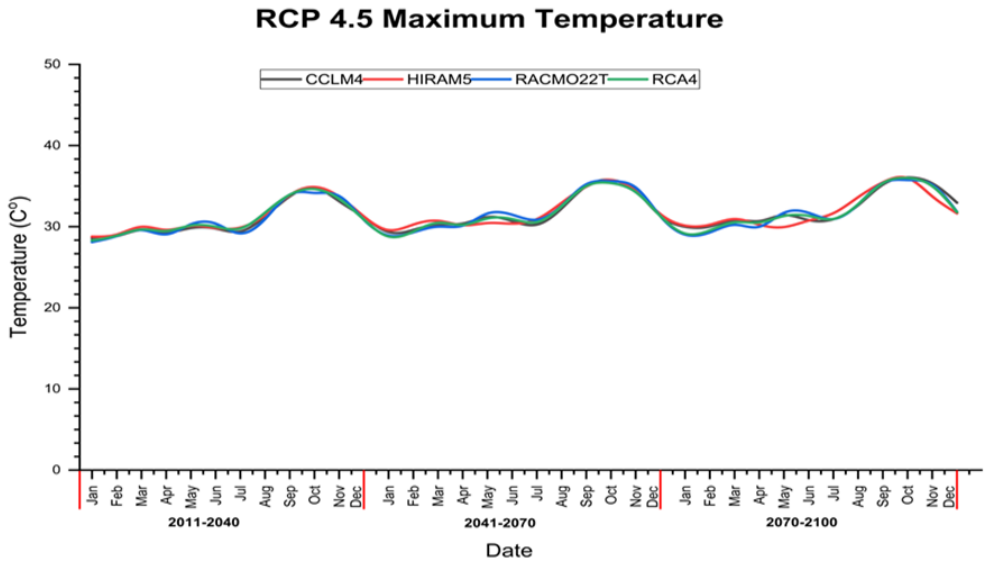

Figure 4.14: Simulated Monthly mean maximum temperature at Galula station RCP 4.5

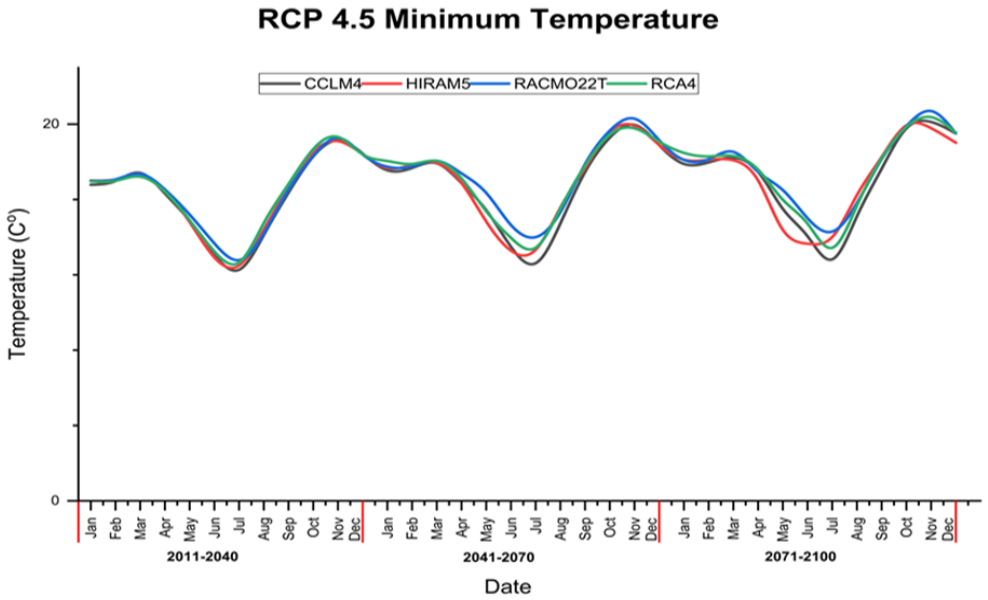

Figure 4.15: Simulated Monthly mean minimum temperature at Galula station RCP 4.5

Under RCP 8.5 the increase in temperature is more pronounced. The anticipated maximum temperature is expected to rise by 0.7°C to 1.1°C while the lowest may increase by 0.5°C to 0.8°C (Figure 4.16 and Figure 4.17). The temperature increases surpass projections associated with RCP 4.5 highlighting the risk of heightened warming in high emissions scenarios which exacerbate climate-related issues such as heatwaves resulting in significant repercussions for water supply, sediment yield,

agriculture and public health (Amasi et al., 2021; Mbungu, Easton, et al., 2016; Mfwango et al., 2022). These results align with study demonstrating pervasive temperature increases in East Africa where seasonal and yearly temperature anomalies have already been seen (Chapman et al., 2021; Eriksen et al., 2008; Lahunga et al., 2016a).

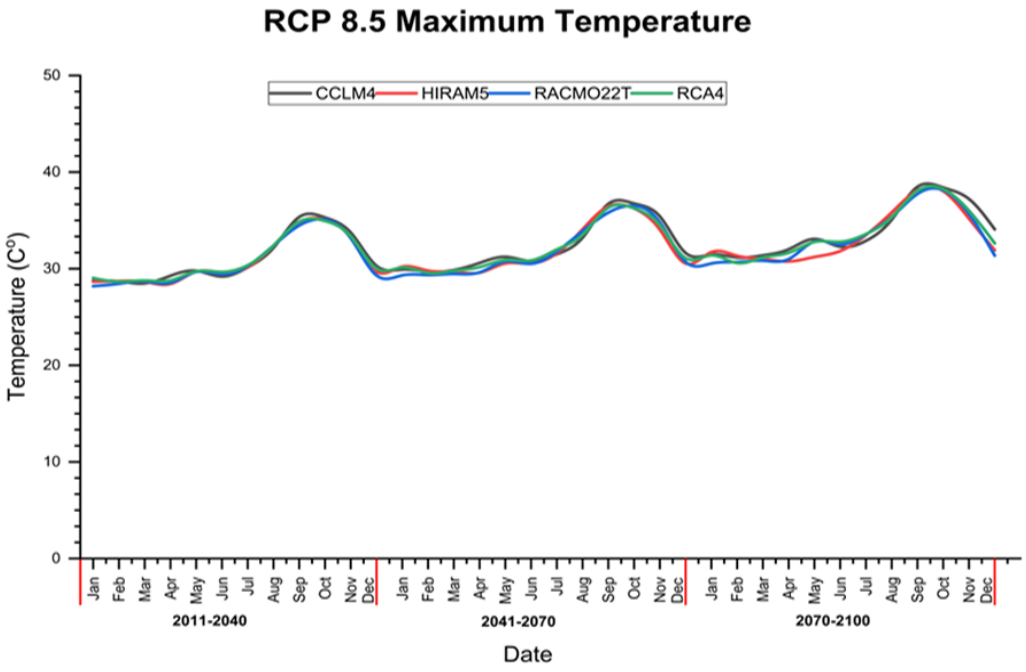

Figure 4.16: Simulated Monthly mean maximum temperature at Galula station RCP 8.5

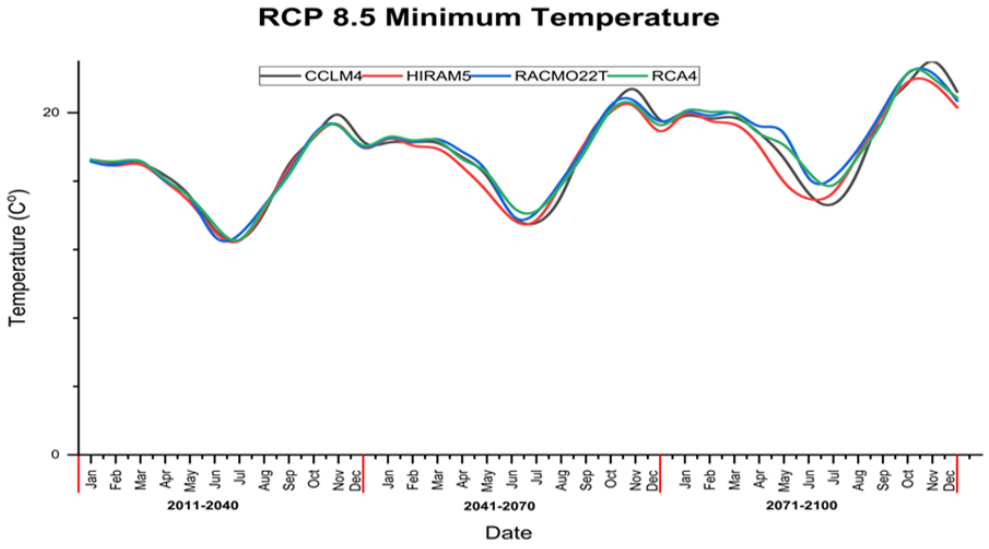

Figure 4.17: Simulated Monthly mean minimum temperature at Galula station RCP 8.5

The projections for the Songwe River Sub-Basin are consistent with wider regional analyses in East Africa. East Africa is undergoing increasing temperature trends particularly under high-emission scenarios and that precipitation patterns are anticipated to become more unpredictable with specific regions suffering heightened risks of floods and droughts (Chapman et al., 2021; Guilyardi et al., 2018; IPCC, 2021). The increased frequency and intensity of rainfall and changes in precipitation patterns may exacerbate soil erosion and sediment problems in the area (Theron et al., 2021). Moreover, similar study in the Mekong River Basin has predicted significant alterations in temperature and precipitation leading to heightened soil erosion and water resource challenges as supported by the results for the Songwe River Sub-Basin (Shrestha et al., 2012). Understanding regional climate forecasts and their local impacts are important when creating effective climate adaptation policies particularly in susceptible sub-basins (Azari et al., 2012; FAO, 2014; Shemsanga et al., 2010). Given the escalating unpredictability of precipitation and temperature patterns it is imperative to plan for extreme occurrences such as droughts and intense rainfall that may exacerbate current issues in water resource management, agriculture and infrastructure. Furthermore, these estimates highlight the imperative to strengthen climate resilience in the region to safeguard ecosystems and populations from impending climate threats.

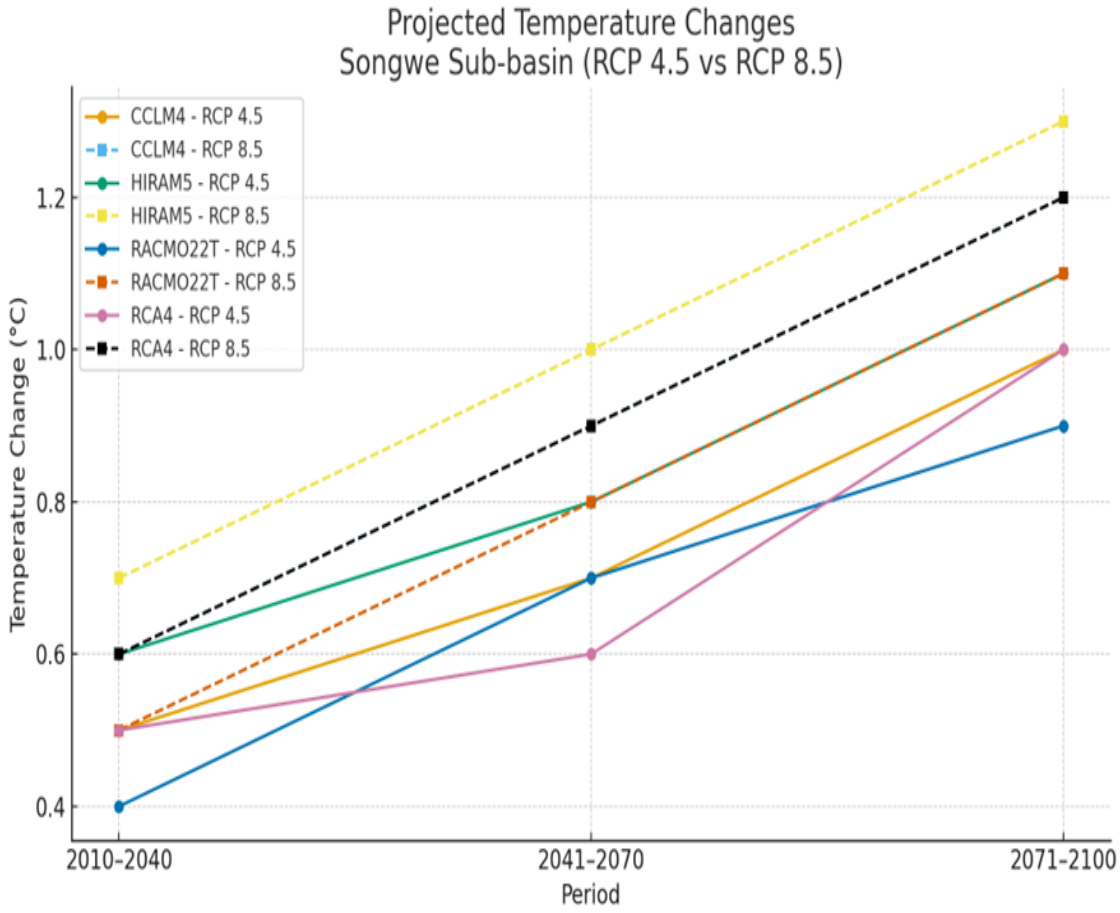

Figure 4.18: Projected temperature changes for Songwe River Sub-basin under RCP4.5 and RCP 8.5

The analysis of temperature and precipitation forecasts for the Songwe Sub-Basin reveals significant trends that align with broader climate change projections for East Africa. A notable discovery is the expected increase in temperature. The slope values for the RCP 4.5 and RCP 8.5 scenarios demonstrate a consistent rise in both maximum and minimum temperatures throughout the forthcoming decades (Figure 4.18). The significant warming trend shown under RCP 8.5 underscores the imperative to mitigate greenhouse gas emissions to avert severe temperature escalations (Assfaw et al., 2023). These findings correspond with broader global trends demonstrating significant warming in sub-Saharan Africa where temperature rises are anticipated to be more severe than in other areas (IPCC, 2021). The R-squared values are significantly high for both scenarios (0.992 for RCP 4.5 and 0.998 for RCP 8.5) further corroborate the reliability of the temperature forecasts illustrating a distinct and consistent increase in

temperature over time and suggesting that future warming in the sub-basin can be expected. Rising temperatures will substantially impact the Songwe River Sub-Basin especially for water resources and agriculture (Chapman et al., 2021).

The evaluation of the regional climate models (CCLM4, HIRHAM5, RACMO22T and RCA4) at Galula Station demonstrated considerable discrepancies in their efficiency especially with precipitation and temperature forecasts. CCLM4 was recognized as the most dependable model for predicting rainfall exhibiting a bias of 0 and indicating that its forecasted rainfall closely matched observed amounts though with little underestimation. This model attained a perfect correlation coefficient (CC = 1), signifying an exceptional alignment with observed rainfall data. This finding aligns with research by (Lebeza et al., 2024), which demonstrated CCLM4's enhanced efficacy in mimicking rainfall in the Lower Awash River Sub-Basin of Ethiopia. In contrast, the other models (HIRHAM5, RACMO22T and RCA4) demonstrated negative biases, regularly underestimating precipitation a tendency that raises concerns for water resource management and agricultural planning (Jones et al., 2023). This bias corresponds with the findings of (Mustefa Abdule et al., 2023), in the Yadot watershed of Ethiopia, where RACMO22T and RCA4 showed diminished efficacy in mimicking observed precipitation patterns. HIRHAM5 exhibited the highest coefficient of variation (CV = 2.169) signifying substantial unpredictability in its rainfall estimates whereas CCLM4 displayed the lowest CV (0.101) reflecting stability in its forecasts despite some underestimation.

All models exhibited positive biases in temperature forecasts with predictions above actual observed values underscoring the prevailing trend of global warming. The models exhibited moderate to strong positive correlations (CC values ranging from 0.5 to 0.7) illustrating their efficacy in simulating temperature changes; nevertheless, the elevated CV values signified considerable uncertainty in the temperature predictions. These findings underscore the merits and limitations of the models. CCLM4's ability to mimic actual rainfall patterns without bias and attain a perfect correlation renders it the most reliable model for rainfall predictions at Galula Station despite its small underestimation of overall amounts. Conversely, HIRHAM5, RACMO22T and RCA4 had negative biases and diminished correlations, therefore making them less reliable

for accurate rainfall predictions. Regarding temperature, although the models predominantly reflected the rising trend with adequate accuracy the positive biases and high CV values signify considerable uncertainty in temperature projections potentially leading to overestimations of temperature extremes.

4.4 Future Projections of Land Use/Land Cover Changes

4.4.1 Spatial and Temporal Variations in Land Use and Land Cover in the Songwe River Sub-basin for the years 1990, 2000, 2010 and 2020

Table 4.3 outlines comprehensive accuracy metrics including Producer's Accuracy (PA), User's Accuracy (UA), overall classification accuracies and Kappa statistics for various land use/land cover (LULC) classifications within the Songwe River Sub-basin spanning the temporal intervals of 1990, 2000, 2010 and 2020. The classification accuracies for the years 1990, 2000, 2010 and 2020 were 92.01%, 91.74%, 91.96% and 92.44% respectively (Table 4.3). The results demonstrate a significant degree of accuracy in the classification of land use and land cover across the entire study period. The overall Kappa statistic for all years was consistently 0.90 indicating strong agreement between the observed and projected categories in the Songwe River Sub-basin. The elevated Kappa value indicates few classification errors implying that the classification method was very reliable and precise over all the analyzed years.

The results correspond with other research in comparable areas where high accuracy in remote sensing classification has been documented hence, affirming the dependability of satellite-based techniques for land cover monitoring (Azizi et al., 2016; Barbosa de Souza et al., 2023; Chilagane et al., 2020; Leta et al., 2021; Selmy et al., 2023). The classification of natural land cover types including forests and wetlands attained high accuracy; however, built-up areas exhibited comparatively lower accuracy especially in the early years of 2000 and 2010. This discrepancy may be ascribed to difficulties in identifying urban areas in remote sensing data at lower spatial resolutions (Abdelmajeed & Juszczak, 2024). The high accuracy metrics and Kappa values show that the classification approach for the Songwe River sub-basin is dependable and establishes a strong basis for identifying and examining LULC changes during the study period.

Table 4.3: Accuracy assessment for 1990, 2000, 2010, and 2020 images classification at Songwe River Sub-basin

LULC	1990		2000		2010		2020	
	PA (%)	UA (%)	PA (%)	UA (%)	PA (%)	UA (%)	PA (%)	UA (%)
Forest	90.88	79.12	90.88	79.88	90.36	86.94	87.74	81.38
Woodland	82.10	73.70	82.10	73.70	86.45	72.88	81.86	78.06
Bushland	88.20	96.03	88.20	96.03	88.80	95.23	92.21	96.93
Grassland	95.93	99.87	95.93	99.87	95.93	99.87	96.06	95.88
Water	94.89	89.56	94.89	94.09	97.87	99.57	97.87	100.00
Wetland	99.06	99.66	99.69	99.66	99.08	99.69	99.64	100.00
Cultivated land	99.34	95.45	95.55	93.36	88.80	96.54	88.91	94.88
Built up area	99.56	100.00	90.63	84.65	99.56	68.36	99.14	68.69
Overall accuracy	92.01		91.74		91.96		92.44	

4.4.2 Historical Land Use/Land Cover Change in the Songwe River Sub-Basin (1990-2020)

In recent decades, the Songwe River sub-basin has experienced substantial changes in land use and land cover (LULC) predominantly influenced by population growth and agricultural development. The changes shown in LULC fluctuations from 1990 to 2020 illustrate the significant influence of both natural and anthropogenic activities on the region's ecosystem (Figure 4.19). Similar to other regions of sub-Saharan Africa these alterations significantly impact biodiversity, socioeconomic advancement and environmental sustainability (Gobry et al., 2023; Guder & Kabeta, 2025; Tekalegn and Diekkrüger, 2017).

In 1990, woodland constituted the predominant land cover in the Songwe River sub-basin at 32.69%, succeeded by bushland at 27.69%, forest at 24.34%, and agricultural land at 12.41%. This trend resembles observations in other catchments in East Africa where woodland and scrub frequently dominate rural landscapes (Mbungu, Easton, et al., 2016; Mutayoba et al., 2018b). By 2000, forest cover had diminished to 29.58% (318,299 hectares), while bushland expanded to 33.06% (355,733 hectares). The transition from forest to bushland aligns with regional trends, as deforestation and land

degradation are converting forested regions into less productive land types (Kitalika et al., 2018; Selmy et al., 2023).

The most major alteration transpired between 2000 and 2010, during which agricultural land expanded markedly by 25.76% (277,201 hectares) nearly doubling from the preceding decade. This increase in agricultural expansion reflects the trend demonstrated by various studies in East Africa, where rising food demands and economic development have resulted in the transformation of natural ecosystems into agricultural land (Gemmechis, 2022; Mbungu, Easton, et al., 2016) Throughout this era forest and woodland areas dropped by 23.51% (252,937 hectares) and 18.59% (200,039 hectares) respectively. The increase in agricultural land, primarily at the cost of natural areas illustrates a global trend in land-use transformation with agricultural intensification as a principal catalyst for deforestation (Guder & Kabeta, 2025; Mfwango et al., 2022).

Between 2010 and 2020 agricultural land maintained its dominance, growing to 39.35% (423,346 hectares), representing a 216.97% increase since 1990 (Table 4.4). Conversely, forest and woodland coverage experienced significant declines reducing to 11.19% (120,428 hectares) and 13.37% (143,863 hectares) respectively (Figure 4.19). The agricultural growth frequently results in the diminishment of forest and woodland areas in comparable sub-Saharan countries (Arfasa et al., 2023; Chawanda et al., 2024; Selmy et al., 2023). Bushland, meanwhile, remained substantial encompassing 33.42% (359,827 hectares) signifying that certain natural habitats persisted despite the continuous agricultural growth. The developed area expanded by 72.57% (2,916 hectares) indicating a persistent tendency towards urbanization in the region. Like other sub-Saharan nations urbanisation in the SongweRiver Sub-basin is intensifying frequently replacing natural landscapes with urban expansion (Chelkeba Tumsa, 2023; Gondwe et al., 2021; Mnyali & Materu, 2021).

Table 4.4: Spatial distribution of land use and land cover across the Songwe River Sub-basin from 1990 to 2020

	1990		**2000**		**2010**		**2020**	
Class	Area [Ha]	Percentage [%]	Area [Ha]	Percentage [%]	Area [Ha]	Percentage [%]	Area [Ha]	Percentage [%]
Forest	261880	24.34	247548	23.01	200039	18.59	120428	11.19
Woodland	351771	32.69	318299	29.58	252937	23.51	143863	13.37
Bushland	297960	27.69	355733	33.06	325086	30.21	359827	33.42
Grassland	1385	0.13	6164	0.57	9573	0.89	17356	1.61
Water	3942	0.37	2882	0.27	2011	0.19	1293	0.12
Wetland	21560	2.00	4360	0.41	3760	0.35	3030	0.28
Agriculture	133560	12.41	136447	12.68	277201	25.76	423346	39.35
Built up	4019	0.37	4643	0.43	5471	0.51	6935	0.64
Total	1076078	100	1076078	100	1076078	100	1076078	100

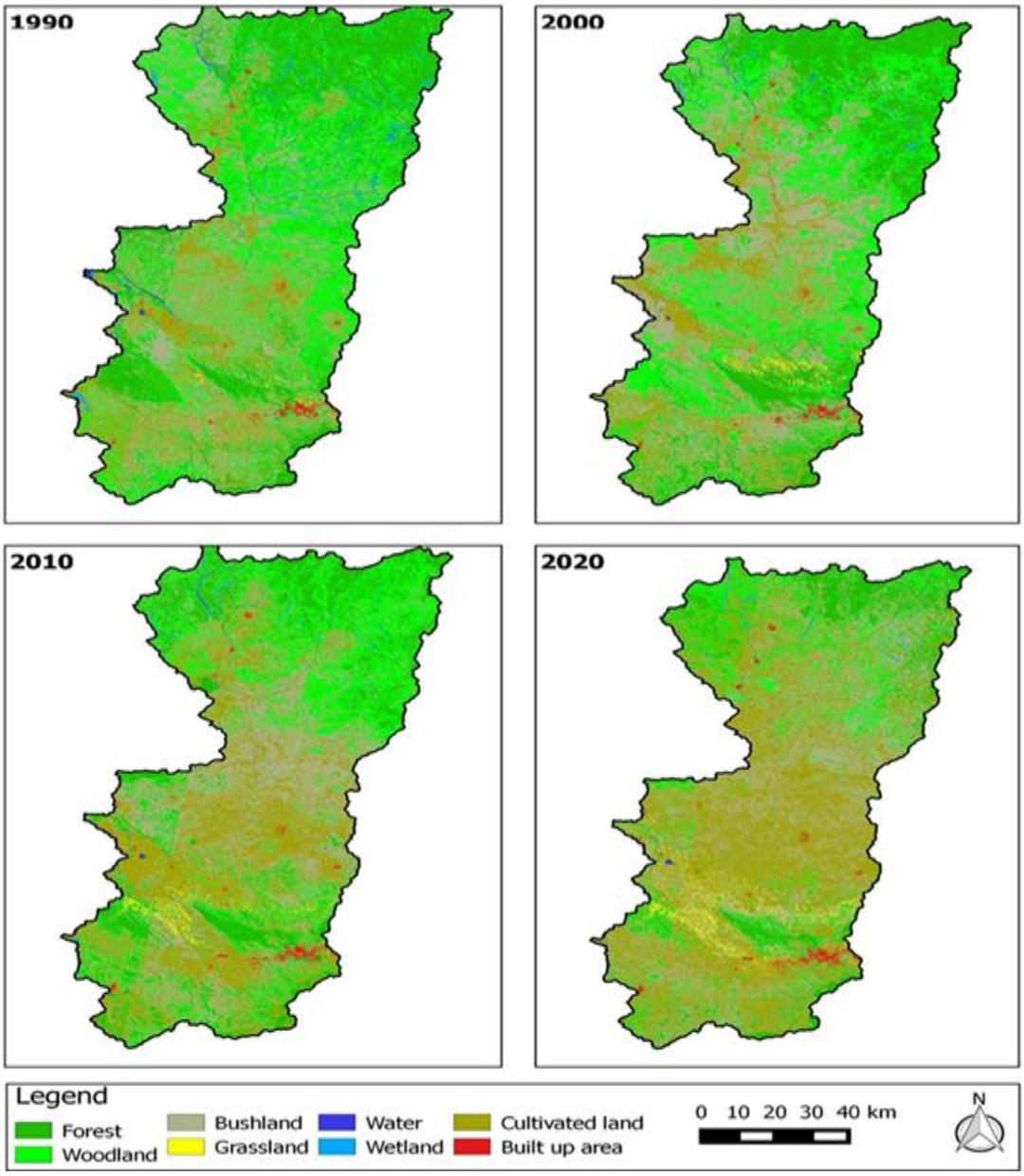

Figure 4.19: Land use/land cover maps for 1990, 2000, 2010, and 2020 at Songwe River Sub-basin

Between 1990 and 2020 the overall forest loss was substantial at 54.01% (141,452 hectares) while the cumulative forest area loss reached 59.10% (207,908 hectares). This reduction is mostly attributed to urbanisation, logging and deforestation for agricultural purposes which jeopardise essential ecosystem functions including climate control, carbon sequestration and biodiversity (Gobry et al., 2023; Selmy et al., 2023). The reduction in wetlands and water bodies was significant with wetlands

decreasing by 85.95% (18,530 hectares) and water bodies by 67.21% (2,650 hectares) (Table 4.5). These ecosystems are essential for flood mitigation, water filtration and providing habitats for many species. The losses in wetland regions emphasising the vulnerability of these ecosystems to anthropogenic activity and climate change (Kalisa et al., 2013; Karim et al., 2019). The swift decline of wetlands from 2010 to 2020 averaging an annual loss of 618 hectares indicates mounting pressure on these ecosystems, presumably attributable to heightened agricultural practices and alterations in hydrology (Ndulue & Mbajiorgu, 2018a).

The substantial increase in agricultural land, especially from 2000 to 2010, might be viewed as a reaction to escalating food demands prompted by population growth and economic advancement. This aligns with developments in other African countries where agricultural land has expanded significantly to accommodate a swiftly growing population (Chawanda et al., 2024; Mustefa Abdule et al., 2023; Nyatuame et al., 2023; Selmy et al., 2023). The expansion of agricultural land throughout this period signifies an escalating reliance on land for food security notwithstanding the detrimental impact on biodiversity and ecological integrity. The increase in grassland by 1,153.07% (15,971 hectares) and the expansion of bushland by 20.76% (61,866 hectares) indicate alterations in land management techniques specifically the transformation of other land types into grassland for grazing. Bushland had the most rapid expansion from 2010 to 2020 increasing by 2,062 hectares per year underscoring the dynamic characteristics of this land cover category notwithstanding persistent land use pressures.

The most significant loss of woodland (33,472 hectares) transpired between 1990 and 2000 succeeded by the most considerable reduction of forest cover (47,509 hectares) from 2000 to 2010 (Table 4.5). The most significant increases in agricultural land (146,146 hectares) and developed areas (1,464 hectares) occurred over the 2010–2020 period reflecting an ongoing trend of agricultural intensification and urbanization. The findings align with analogous research in the region that has identified comparable trends of deforestation and agricultural propagation influenced by socio-economic determinants such as demographic growth and economic advancement (Chang et al., 2018; Nyatuame et al., 2023).

Table 4.5: Land use/cover Changes in the Songwe River Sub-basin between 1990 and 2000, 2000 and 2010, and 2010 and 2020

	1990 - 2000			2000 - 2010			2010 - 2020		
Class	Area change (Ha)	Percentage change (%)	Annual Rate of Change (Ha/year)	Area change (Ha)	Percentage change (%)	Annual Rate of Change (Ha/year)	Area change (Ha)	Percentage change (%)	Annual Rate of Change (Ha/year)
Forest	-14332	-5.47	-1433	-47509	-19.19	-4751	-79611	-39.80	-7961
Woodland	-33472	-9.52	-3347	-65363	-20.54	-6536	-109073	-43.12	-10907
Bushland	57773	19.39	5777	-30647	-8.62	-3065	34740	10.69	3474
Grassland	4779	345.00	478	3409	55.31	341	7783	81.30	778
Water	-1060	-26.89	-106	-871	-30.22	-87	-719	-35.73	-72
Wetland	-17200	-79.78	-1720	-600	-13.77	-60	-730	-19.41	-73
Agriculture	2887	2.16	289	140753	103.16	14075	146146	52.72	14615
Built up	625	15.54	62	828	17.83	83	1464	26.75	146
Total									

4.4.3 Land Use/Land Cover Transition in the Songwe River Sub-Basin

The transition matrices (Tables 4.6-4.9) from 1990 to 2020 indicate substantial alterations in LULC within the Songwe River sub-basin, primarily attributed to agricultural growth and deforestation, a pattern noted in other sub-Saharan Africa areas (Based et al., 2018; Belay & Mengistu, 2021; Kimario et al., 2024; Lazaro et al., 2023). From 1990 to 2000 forest cover diminished by more than 100,000 hectares with notable transformations to cultivated land (3,528 hectares), bushland (27,867 hectares) and woodland (70,520 hectares). The rise in cultivated land from 7,535 hectares to 136,447 hectares significantly influenced these changes, reflecting a similar pattern observed in East Africa (Chawanda et al., 2024; Mbungu, Easton, et al., 2016; Tadese et al., 2021).

Between 2000 and 2010 forest areas had a persistent decline with significant conversions to scrub (21,766 hectares) and woodland (55,317 hectares). The bushland

region expanded to 355,733 hectares predominantly at the cost of forests and woodlands. The area of agricultural land rise considerably over this period reaching 277,202 hectares. This ongoing agricultural expansion aligns with trends observed in other African regions where rising food demands result in extensive land conversion (Mbungu, Easton, et al., 2016; Mustefa Abdule et al., 2023; Tekalegn and Diekkrüger, 2017)

From 2010 to 2020, forest areas decreased to 75,179 hectares, while woodland diminished to 61,869 hectares. The cultivated area expanded to 423,422 hectares, underscoring the dominance of agriculture in the sub-basin as observed in similar research in sub-Saharan Africa (Mbungu, Easton, et al., 2016; Mutayoba et al., 2018b; Serdeczny et al., 2017) Bushland expanded to 359,575 hectares mostly due to conversions from woodland and forest. Although wetlands and water bodies have remained reasonably stable, they are susceptible to the encroachment of agricultural land.

Urbanization has also led to changes in land use with developed areas increasing by 72.57% throughout the research period reflecting the urban expansion trends noted throughout the region. Nevertheless, the total area of developed land is minimal in comparison to agricultural and natural land cover types.

Table 4.6: Land use land cover transition in Songwe River sub-basin between 1990 - 2000

	FRST	**FRSD**	**RNGB**	**RNGE**	**WATR**	**WETN**	**AGRL**	**BULT**	**TOTAL**
FRST	141352	70520	27867	33	715	3529	3528	0	247545
FRSD	81230	135657	79976	89	885	8497	11976	0	318310
RNGB	30373	119060	139465	497	598	4191	61542	0	355727
RNGE	185	959	2506	259	157	49	2050	0	6164
WATR	487	317	427	0	1226	403	22	0	2882
WETN	693	483	406	0	73	2701	4	0	4360
AGRL	7535	24705	47108	496	287	2189	54127	0	136447
BULT	25	70	206	11	0	1	312	4020	4644
TOTAL	261880	351771	297960	1385	3942	21560	133560	4020	1076078

FRST; Forest FRSD; Woodland RNGB; Bushland RNGE; Grassland WATR; Water WETN; Wetland AGRL; Cultivated land BULT; Built up area

Table 4.7: Land use land cover transition in Songwe River sub-basin between 2000 - 2010

	FRST	**FRSD**	**RNGB**	**RNGE**	**WATR**	**WETN**	**AGRL**	**BULT**	**TOTAL**
FRST	116344	55317	21766	389	576	561	5054	47	200054
FRSD	95996	94649	52271	839	287	1034	7762	111	252948
RNGB	23406	115374	147024	2325	273	288	36024	347	325062
RNGE	2150	3011	3170	283	2	0	955	0	9572
WATR	231	119	347	46	1170	16	81	0	2011
WETN	279	143	426	0	451	2301	159	0	3759
AGRL	8950	49412	129641	2281	121	159	85963	675	277202
BULT	194	274	1088	1	1	0	449	3463	5471
TOTAL	247549	318299	355733	6163	2882	4360	136447	4643	1076078

FRST; Forest FRSD; Woodland RNGB; Bushland RNGE; Grassland WATR; Water WETN; Wetland AGRL; Cultivated land BULT; Built up area

Table 4.8: Land use land cover transition in Songwe River sub-basin between 2010- 2020

	FRST	**FRSD**	**RNGB**	**RNGE**	**WATR**	**WETN**	**AGRL**	**BULT**	**TOTAL**
FRST	75179	32482	7759	74	239	260	4528	28	120550
FRSD	46616	61869	27306	215	191	286	7373	64	143920
RNGB	43887	98747	128049	1605	166	139	86787	195	359575
RNGE	708	1015	2630	6371	4	0	6602	19	17350
WATR	127	115	134	2	761	0	154	0	1293
WETN	179	147	168	0	344	2012	188	0	3038
AGRL	33123	58171	158200	1305	305	1063	170214	1042	423422
BULT	219	390	841	0	0	0	1355	4123	6929
TOTAL	200039	252937	325086	9573	2011	3760	277201	5472	1076078

FRST; Forest FRSD; Woodland RNGB; Bushland RNGE; Grassland WATR; Water WETN; Wetland AGRL; Cultivated land BULT; Built up area

Table 4.9: Land use land cover transition in Songwe River sub-basin between 1990 - 2020

	FRST	**FRSD**	**RNGB**	**RNGE**	**WATR**	**WETN**	**AGRL**	**BULT**	**TOTAL**
FRST	76991	26317	12792	35	663	1572	2161	11	120541
FRSD	54650	49663	30428	61	526	2724	5972	29	144055
RNGB	76565	129096	100711	434	762	6491	45449	88	359595
RNGE	2672	3965	6392	118	56	42	4095	9	17349
WATR	189	126	105	1	754	25	103	0	1303
WETN	136	479	619	0	213	1580	21	0	3048
AGRL	50452	141537	145580	677	965	9121	74404	526	423261
BULT	226	588	1334	59	2	6	1356	3356	6926
TOTAL	261880	351771	297960	1385	3942	21560	133560	4019	1076078

FRST; Forest FRSD; Woodland RNGB; Bushland RNGE; Grassland WATR; Water WETN; Wetland AGRL; Cultivated land BULT; Built up area

4.4.4 Future Land Use/Land Cover Change in the Songwe River Sub-Basin

The projected land use and land cover (LULC) changes in the Songwe River sub-basin from 2020 to 2100 provide a comprehensive overview of how the region's landscape is expected to evolve under "business-as-usual" scenarios, driven primarily by agricultural expansion and urbanization. These projections reflect trends based on past and present land use patterns, but they do not account for potential policy changes, conservation efforts or other future interventions that could alter the trajectory. The projected land use and land cover (LULC) changes in the sub-basin from suggest considerable changes across many land cover categories including forest, woodland, bushland, grassland, water, wetlands, cultivated land and urban areas (Figure 4.20). These alterations show persistent pressure from agriculture and urbanization, similar to trends observed in other regions of sub-Saharan Africa, where agricultural growth and urban expansion are primary catalysts of land modification (McConnell et al., 2015).

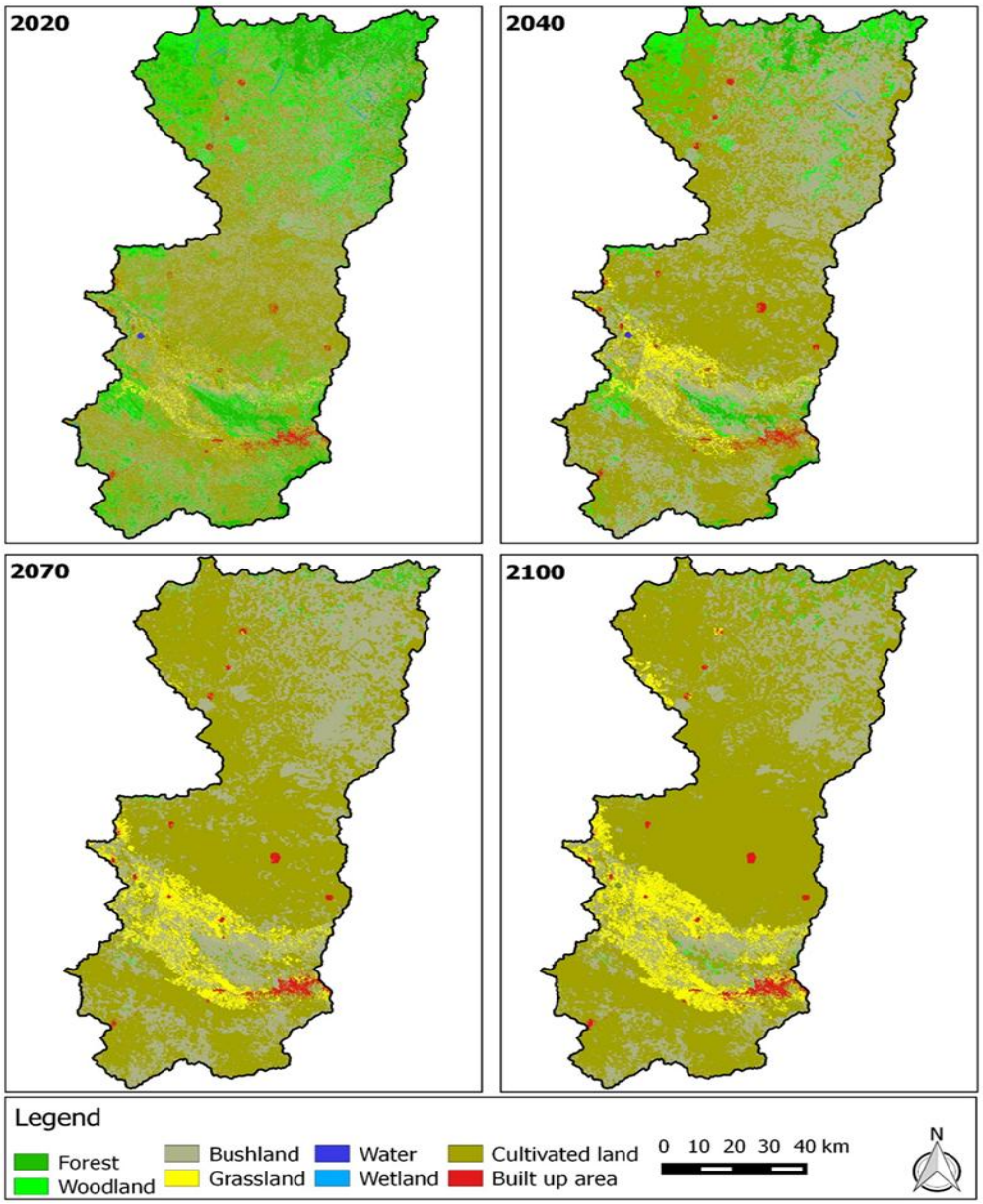

Figure 4.20: Predicted Land Use/Land Cover Maps for 2040, 2070 and 2100 in the Songwe River sub-basin

From 2020 to 2040, forest cover is projected to decrease by 88,945 hectares (8.24%), resulting in a total drop of 120,428 hectares (11.19%) ultimately leaving 31,483 hectares (2.95%) by 2040. This significant decline indicates a rapid increase in deforestation driven by agricultural development and urban growth. This deforestation pattern aligns with research in East Africa where similar trends of forest depletion from agricultural encroachment have been shown (Basheer et al., 2016). The reduction of

woodland is significant, with its area declining from 143,863 hectares (13.37%) in 2020 to 71,489 hectares (6.69%) in 2040, a decline of 72,374 hectares (6.68%). This scenario indicates a prevalent transformation of natural landscapes into modified land uses underscoring the growing prevalence of agricultural and urbanized regions in the environment (Agbola et al., 2001).

Nonetheless these reductions, bushland is projected to increase from 359,827 hectares (33.42%) in 2020 to 400,935 hectares (36.74%) by 2040. The spread of bushland may result from the degradation of forests and woods which are being transformed into less profitable land classifications. This expansion is inadequate to offset the decline of more diversified ecosystems including woodlands and forests. Grassland is anticipated to expand from 17,356 hectares (1.61%) in 2020 to 34,933 hectares (3.27%) by 2040 indicating a trend of converting forested regions into open fields frequently for grazing purposes (Agbola et al., 2001; Marhaento et al., 2018; Selmy et al., 2023). Wetlands and water bodies are anticipated to diminish during this timeframe with wetlands decreasing by 50.52% (from 3,030 hectares in 2020 to 1,528 hectares in 2040) and water bodies contracting by 52.03% (from 1,293 hectares in 2020 to 621 hectares in 2040). The observed losses are alarming given that wetlands and aquatic ecosystems are essential for flood management, water filtration and habitat support (Kalisa et al., 2013a; Taylor, 2012). Global trends suggest that agricultural expansion, industrial development and the impacts of climate change are increasingly endangering wetlands (Masson-Delmotte et al., 2019; Serdeczny et al., 2017; Shinhu et al., 2023).

The area of cultivated land is projected to rise substantially from 423,346 hectares (39.35%) in 2020 to 527,035 hectares (49.30%) by 2040 (Table 4.10). This rise signifies the escalating demand for agricultural production propelled by population expansion and the necessity for food security, a pattern also observed in other sub-Saharan nations. Urbanization is expected to persist though at a diminished rate with the developed area increasing from 6,935 hectares (0.64%) in 2020 to 8,055 hectares (0.75%) by 2040. Although developed regions are limited in size relative to other land uses and their growth signifies persistent pressures from urbanization (Gondwe et al., 2021a; Mbungu, Easton, et al., 2016; Mfwango et al., 2022a).

From 2040 to 2070, the reduction of forest and woodland areas persists. By 2070 forest cover is projected to decline significantly to 3,437 hectares (0.32%), indicating a reduction of 28,046 hectares (2.63%) over the 30-year span. Woodland experiences a significant reduction decreasing from 71,489 hectares (6.69%) in 2040 to 5,895 hectares (0.55%) in 2070 resulting in a loss of 65,594 hectares (6.14%). This amount indicates the near-complete exhaustion of forest and woodland resources due to their conversion into agricultural land and urban development. Bushland is projected to diminish by 39,951 hectares (3.73%) between 2070 and 2100 indicating further land conversion presumably for agricultural or urban purposes. Grassland is anticipated to persist in its gradual expansion attaining 61,142 hectares (5.72%) by 2070 an increase from 34,933 hectares (3.27%) in 2040. This growth is presumably prompted by the transformation of woodland and scrub into grazing fields indicative of changes in land management techniques and the rising demand for pasture. Wetlands and aquatic ecosystems experience ongoing reductions, with wetlands decreasing from 1,528 hectares (0.14%) in 2040 to 92 hectares (0.01%) by 2070. Correspondingly, water bodies will diminish from 621 hectares (0.06%) to 66 hectares (0.01%) by 2070 indicating the near-total eradication of these ecosystems before the century's end.

By 2070, the area of cultivated land is projected to expand to 634,680 hectares (59.37%) an increase of 107,645 hectares (10.07%) indicative of the ongoing demand for agricultural land to sustain the increasing population. Developed regions expand gradually attaining 9,782 hectares (0.92%) by 2070. The rise of urban areas persists, although agriculture exert the most significant strain on the landscape as shown in other sub-Saharan countries (Gemmechis, 2022a; Mfwango et al., 2022c).

By 2100, forest cover is projected to diminish significantly leaving merely 3,249 hectares (0.30%) intact. Woodland experiences a minor loss resulting in 5,817 hectares (0.54%) by the year 2100. Bushland diminish substantially by 102,875 hectares (9.63%) to 258,109 hectares (23.48%) but grassland expand to 87,328 hectares (8.17%) (Table 4.10). Wetlands and aquatic regions would nearly disappear with wetlands diminishing to 89 hectares (0.01%) and water bodies to 62 hectares (0.01%). Cultivated land prevail in the landscape encompassing 711,001 hectares (66.51%) indicative of the predominant impact of agriculture (Figure 4.21). The developed area

expands to 10,422 hectares (0.97%) indicating ongoing urbanization though at a slower pace relative to agriculture.

Table 4.10: Projected land use/cover changes in the Songwe River sub-basin for the years 2040, 2070 and 2100

LULC	2020		2040		2070		2100	
	(Ha)	(%)	(Ha)	(%)	(Ha)	(%)	(Ha)	(%)
Forest	120428	11.19	31483	2.95	3437	0.32	3249	0.30
Woodland	143863	13.37	71489	6.69	5895	0.55	5817	0.54
Bushland	359827	33.42	400935	36.84	360984	33.11	258109	23.48
Grassland	17356	1.61	34933	3.27	61142	5.72	87328	8.17
Water	1293	0.12	621	0.06	66	0.01	62	0.01
Wetland	3030	0.28	1528	0.14	92	0.01	89	0.01
Cultivated land	423346	39.35	527035	49.30	634680	59.37	711001	66.51
Built up area	6935	0.64	8055	0.75	9782	0.92	10422	0.97
Total	1076078	100	1076078	100	1076078	100	1076078	100

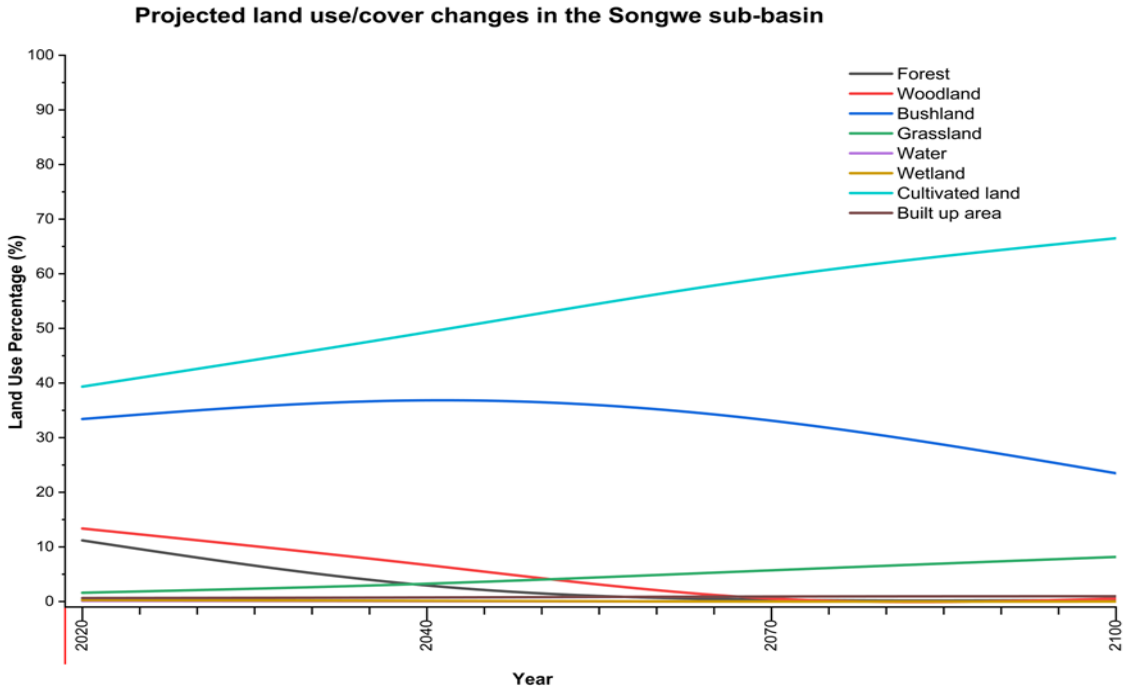

Figure 4.21: Projected Land Use Land Cover Percentage Change in the Songwe River Sub-basin

4.5 Characterization and Mapping of Sediment Sources in the Songwe River Sub-Basin

The SWAT model and QGIS analysis were employed to evaluate the impacts of various factors on sediment sources generation under baseline and future scenarios in the Songwe River Sub-basin.

The sediment sources in the Songwe River Sub-basin exhibit distinct patterns influenced by a combination of factors such as land use, soil types, vegetation cover, slope and seasonal precipitation all of which are further altered by the impacts of climate change. The results highlight that land use and land cover (LULC) classes play a significant role in sediment source production, with cultivated areas and bushland being the largest contributors. Among the LULC categories, cultivated land emerged as the greatest source of sediment, producing an average of 54.94 tons/ha annually, followed by bushland, which generated 40.6 tons/ha (Table 4.11). The continual tillage and absence of cover crops in agricultural fields leave the soil increasingly vulnerable to erosion especially during the rainy season when precipitation intensifies and surface runoff escalates (Tenaw et al., 2024). These findings align with other studies undertaken in East Africa including a study in the Simiyu River sub catchment which emphasizes the considerable influence of farming practices on sediment dynamics and erosion rates (James Shinhu, 2024). Grasslands those located on steep slopes also contributed to sediment production producing 22.91 tons/ha annually. The steep gradients of these areas coupled with increased runoff results in rapid water flow and enhanced soil erosion. This finding correlate with previous study which emphasizes the vulnerability of grasslands on steep inclines to erosion especially in the absence of sufficient root systems to stabilize the soil (Gupta, 2015; Sime & Abebe, 2022). The agricultural land, grasslands on steep slopes and forests all play crucial roles in sediment generation and erosion patterns in East Africa. However, local factors such as the specific land use practices, vegetation types, and climate change impacts reveal unique aspects of sediment production in this region.

Conversely, forests and woodlands contributed less to sediment source production. Forests in particular displayed the lowest sediment yield with woodland areas generating only 1.34tons/ha annually. This is consistent with the known protective role

of dense vegetation in mitigating soil erosion. Forests reduce surface runoff by enhancing water infiltration and by intercepting rainfall and preventing soil displacement (Based et al., 2018; Blake et al., 2018; Guder & Kabeta, 2025). The results underscore the critical function of wooded area as natural barriers to erosion which reduce sediment mobilization by absorbing precipitation and stabilizing soil (Zhang et al., 2019; Zhang et al., 2015).These findings provide clear evidence that land cover type plays a decisive role in sediment generation in the Songwe River Sub-basin with cultivated land, bushland and grasslands on steep slopes contributing the most to erosion while forests and woodlands offer significant protection against soil degradation.

Table 4.11: LULC classes contribution to mean annual surface runoff and sediment production

Land use/cover	**Surface runoff (mm)**	**Sediment yield (t/ha)**
Cultivated land	290.43	54.94
Built-up are	179.32	0.29
Woodland	173.97	1.34
Forest	110.54	5.53
Grassland	156.14	22.91
Bushland	145.29	40.60

The sediment source results underscore the influence of land use and soil types on the erosion dynamics within the Songwe River Sub-basin. The sub-basin exhibits an average annual sediment yield of 125.61 tons/ha which provides a benchmark for analyzing sediment source patterns in the area (Table 4.12).

The sediment source results from the Songwe River Sub-basin underscore the significant role of seasonal rainfall variations in influencing sediment production. The sub-basin experiences the highest sediment yield during the wet season, particularly in the months of January, February and March with sediment production ranging from 109.4 tons/ha to 171.84 tons/ha. These findings are consistent with similar studies, such as those by Golosov & Walling (2019) and Mbungu et al. (2016), which highlight the amplified sediment yield during peak rainfall events in tropical regions. The intense precipitation during the wet season leads to increased surface runoff which in

turn increases erosion rates when soil is bare. This relationship between high rainfall and sediment production is common across tropical regions where the combination of intense rainfall, low vegetation cover and land disturbance exacerbate erosion. The findings from the Songwe Sub-basin align with these broader patterns, reflecting the vulnerability of soils in areas with high rainfall and limited vegetative cover. However, differences arise when considering the specific conditions of the Songwe River Sub-basin compared to other tropical regions. For example, the soil types in the Songwe region could be more prone to erosion and local land use practices, such as intensive tillage or inadequate conservation measures in agricultural lands could contribute to higher sediment yield than observed in areas with more effective soil management.

The CCLM4 climate model projects a significant increase in sediment production due to intensified rainfall patterns in the future, forecasting a 75.37% increase in February sediment yields during the period from 2011–2040. This highlights how climate change, with its potential to increase rainfall intensity, could exacerbate erosion in the Songwe River sub-basin more than in other regions. The differences in sediment production observed across studies may, therefore, be driven by local soil conditions, land management practices and variations in climate models, all of which should be carefully considered when planning future erosion control strategies in the region.

In contrast, sediment production in the dry season was minimal which is indicative of the reduced rainfall and lower runoff typical of this period. The dominance of sediment production during the wet season particularly in February and April highlights the critical role of rainfall intensity in driving soil erosion processes. This finding aligns with previous studies which show that rainfall intensity rather than total rainfall has a disproportionate impact on sediment yield in tropical basins (Marko et al., 2023).

Table 4.12: Influence of different variables on sediment yield at sub basin level

Sub-basin	Coverage (Km2)	Dominant land use	Dominant soil	Slope	Annual mean SYLD (t/ha)
1	389	FRSD	Af3-1-2a-407	3.0-9.0	3.07
2	929	FRST	Ao66-2ab-429	3.0-9.0	5.12
3	359	RNGB	Af3-1-2a-407	3.0-9.0	5.10
4	316	FRST	Ao66-2ab-429	3.0-9.0	5.52
5	349	RNGB	Ao66-2ab-429	3.0-9.0	4.32
6	278	AGRR	Af3-1-2a-407	3.0-9.0	4.13
7	405	RNGB	Ao66-2ab-429	3.0-9.0	3.98
8	503	RNGB	Af3-1-2a-407	3.0-9.0	3.95
9	396	RNGB	Af3-1-2a-407	3.0-9.0	6.62
10	328	AGRR	Nd34-2bc-803	3.0-9.0	19.88
11	207	AGRR	Rd20-2c-932	3.0-9.0	43.43
12	527	AGRR	Tm13-2-3c-	9.0-25.0	6.97
13	234	RNGB	Rd20-2c-932	3.0-9.0	12.09
14	197	AGRR	Gp6-2-3a-633	3.0-9.0	7.78
15	263	AGRR	Ne43-2-3a-	3.0-9.0	5.74
16	527	AGRR	Tm13-2-3c-	9.0-25.0	18.84
17	132	AGRR	Rd20-2c-932	9.0-25.0	97.10
18	196	AGRR	Rd20-2c-932	9.0-25.0	29.96
19	76	AGRR	Af3-1-2a-407	3.0-9.0	7.66
20	208	RNGB	Af3-1-2a-407	0-3.0	2.66
21	407	RNGB	Af3-1-2a-407	0-3.0	3.52
22	101	RNGB	Ao66-2ab-429	3.0-9.0	4.26
23	185	AGRR	Rd20-2c-932	9.0-25.0	94.46
24	31	RNGB	Af3-1-2a-407	0-3.0	3.30
25	5	AGRR	Rd20-2c-932	0-3.0	35.01
26	100	AGRR	Rd20-2c-932	9.0-25.0	41.19
27	141	RNGB	Af3-1-2a-407	0-3.0	3.96
28	137	RNGB	Af3-1-2a-407	3.0-9.0	4.46
29	82	RNGB	Af3-1-2a-407	3.0-9.0	8.38
30	86	AGRR	Af3-1-2a-407	3.0-9.0	17.91

The regional distribution of sediment yield in the baseline scenario illustrates the substantial impacts of land use and soil types on sediment production. Sub-basins in the southern, central and lower regions of the basin exhibit particularly high sediment production. These areas are characterized by elevated agricultural activities especially farming on steep inclines which significantly contributes to erosion. For instance, Eutric Leptosols known for their shallow profiles and vulnerability to erosion in steep regions were found to exhibit very high sediment yield (Tenaw et al., 2024). The highest sediment production was observed in sub-basins 17, 18 and 23 which are predominantly agricultural and have elevated erosion rates (Figure 4.22). These findings align with studies from (Chilagane et al., 2021) and (Mbungu, Easton, et al., 2016), who identified similar issues in tropical watersheds. In these regions, changes in land use especially the conversion of forest to agricultural land have led to increased sediment discharge due to the loss of protective vegetation and the increased vulnerability of soils to erosion.

The observed patterns of sediment yield in the Songwe River Sub-basin, particularly in regions with significant forest cover, align with broader studies that emphasize the protective role of forests in mitigating soil erosion. Forests especially those in the northern sections of the sub-basin were associated with much lower sediment yield due to their ability to stabilize soil, enhance water infiltration and intercept rainfall, thus reducing surface runoff and erosion. These findings support the work of (Hailu et al., 2023) and (Rodrigues et al., 2020), which highlight the critical role that forested landscapes play in reducing sediment mobilization. Forests act as natural barriers against erosion by improving soil structure and enhancing root systems that bind the soil, preventing it from being washed away during heavy rainfall. The areas of the Songwe River Sub-basin with significant forest cover exhibit markedly lower sediment production, underscoring the importance of maintaining and expanding forested areas for sustainable land management.

However, differences in sediment production between various regions of the Songwe River sub-basin are also evident, particularly when considering the spatial distribution of sediment production under four regional climate models (RCMs) CCLM4, HIRHAM5, RCA4 and RACMO22T. The CCLM4 and HIRHAM5 models simulated higher precipitation and temperature values leading to increased sediment production in agricultural sub-basins with steep terrain. These models predicted the highest sediment yield in sub-basins 11, 13, 16, 17, 18, 23 and 26, areas characterized by intensive agricultural activities, steep slopes and vulnerable soil types like Eutric Leptosols which are shallow and prone to erosion. These findings are consistent with studies from other East African regions, such as the Upper Blue Nile Basin where similar climatic drivers intensified rainfall and temperature increases are known to exacerbate erosion in agricultural landscapes. Conversely, the RCA4 and RACMO22T models predicted somewhat lower sediment yield, which could be due to differences in their predicted precipitation intensity and temperature patterns. For instance, these models might have predicted less intense rainfall or more moderate temperature increases compared to CCLM4 and HIRHAM5 which directly influenced the erosion process in steep agricultural areas. Despite these differences, all four models consistently predicted high-risk sub-basins in the Songwe region, confirming the

vulnerability of these areas to erosion under both historical and future climate scenarios.

The differences in sediment production predictions between the models can likely be attributed to several factors. Firstly, soil types play a significant role in these variations. Eutric Leptosols, common in the high-risk areas of the Songwe River sub-basin are particularly susceptible to erosion due to their shallow profiles and low water retention capacity especially on steep slopes. In contrast, areas with more erosion-resistant soils, such as Vertisols or deeper soils with better structure, might show lower sediment yield regardless of precipitation intensity. The structure of the climate models themselves contributes to the variability in predictions. Different models have different assumptions about rainfall patterns; temperature increases and how these variables interact with local conditions like topography and land use. For example, CCLM4 and HIRHAM5 may simulate more extreme climate scenarios compared to RCA4 and RACMO22T which could explain the higher sediment yield predicted by the former models. These variations highlight the importance of considering multiple models to capture a range of potential future scenarios, which can inform more robust soil conservation strategies for regions like the Songwe Sub-basin.

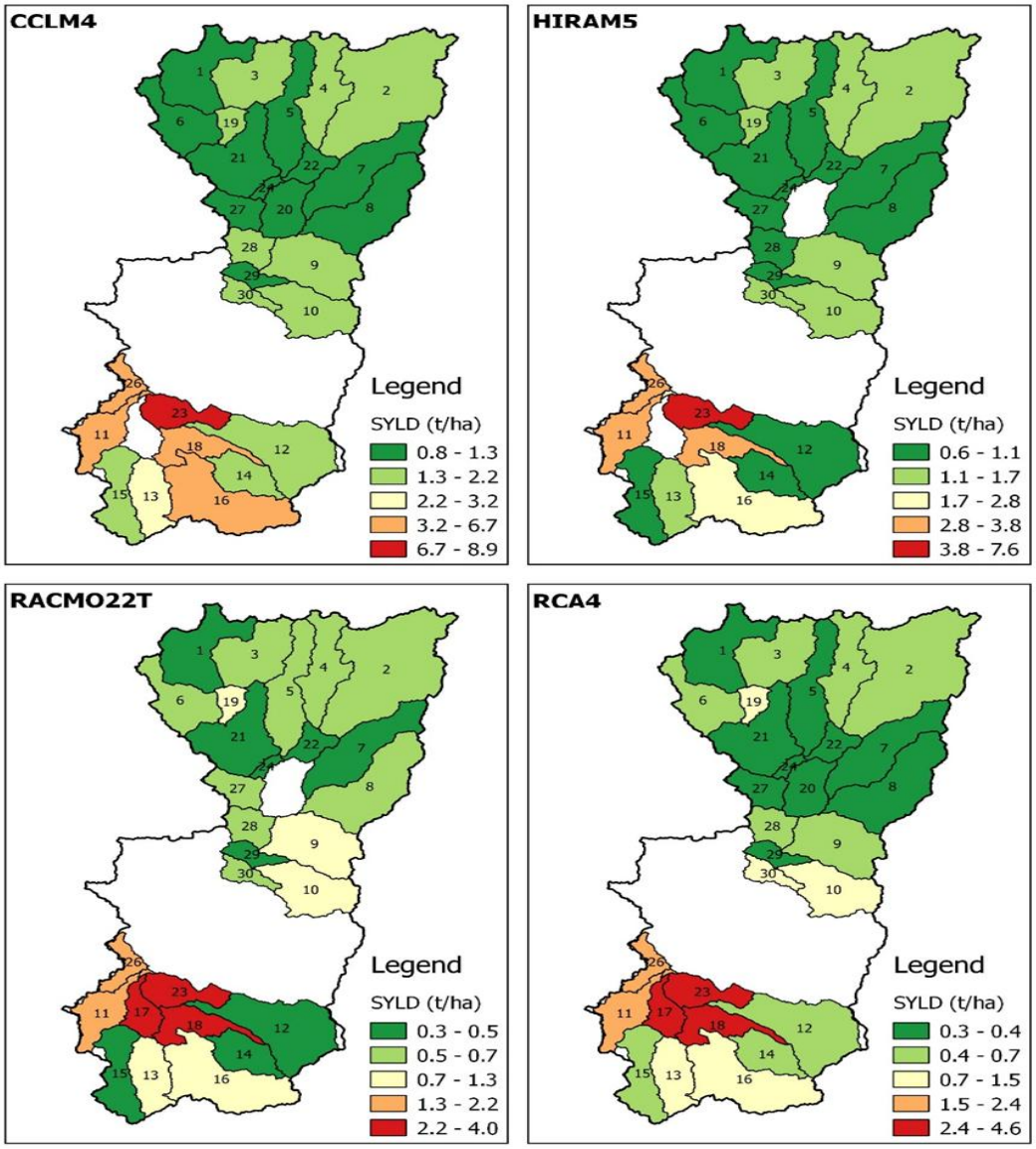

Figure 4.22: Spatial distribution of sediment yield map under Historical simulation

Projected climate change scenarios indicate a substantial increase in future sediment production within the Songwe River Sub-basin during the rainy season. This analysis utilized bias-corrected outputs from four RCMs under the RCP4.5 and RCP8.5 scenarios. The results demonstrate a consistent increase in sediment production from 2011 to 2100 with significant rises observed during the months of January, February and March which are typically characterized by elevated sediment production due to seasonal rainfall patterns. The future intensification of sediment production during

these months highlights the aggravating impact of climate change on sediment dynamics in the region. The analysis indicates that under the RCP4.5 scenario which assumes modest emissions reductions sediment production is expected to progressively increase. However, these alterations are less pronounced than those observed under the high-emissions scenario (RCP8.5) (Figure 4.3). Specifically, for the period 2011 to 2040 the CCLM4 model predicts a 75.37% increase in sediment production for February compared to historical norms. This finding is consistent with previous studies which suggest that intensified rainfall due to climate change could exacerbate erosion rates. For instance, (Rodrigues et al., 2020) found that such intensified precipitation is a key driver of increased sediment yield in tropical catchments particularly in areas with steep terrain and agricultural activity.

From 2041 to 2070 under RCP4.5, sediment production is projected to experience a considerable increase during the rainy months of January, February and March. This increase is attributed to the escalation of heavy rainfall events which are expected to become more frequent and intense due to climate change. The RCP4.5 scenario thus demonstrates the cumulative impacts of increased rainfall intensity and the rising occurrence of extreme weather events. During the 2071–2100 period sediment production is anticipated to increase significantly underscoring the long-term impacts of climate change on sediment dynamics (Figure 4.23).

In contrast, the RCP8.5 scenario which represents a high-emissions trajectory predicted a significantly greater increase in sediment production across all periods. During the 2011–2040 timeframe sedimentation increases are markedly elevated with models forecasting a substantial rise in sediment yield during the wet season. The CCLM4 model forecasts a 75.37% increase in sediment yield for February suggesting the preliminary impacts of climate change on precipitation patterns. However, the period from 2041 to 2070 is expected to witness the most significant increase in sediment production. The RCA4 model predicts a 221.85% increase in sediment production in April under RCP8.5 highlighting the escalating risk of erosion as extreme weather events become more frequent and intense (Figure 4.23).

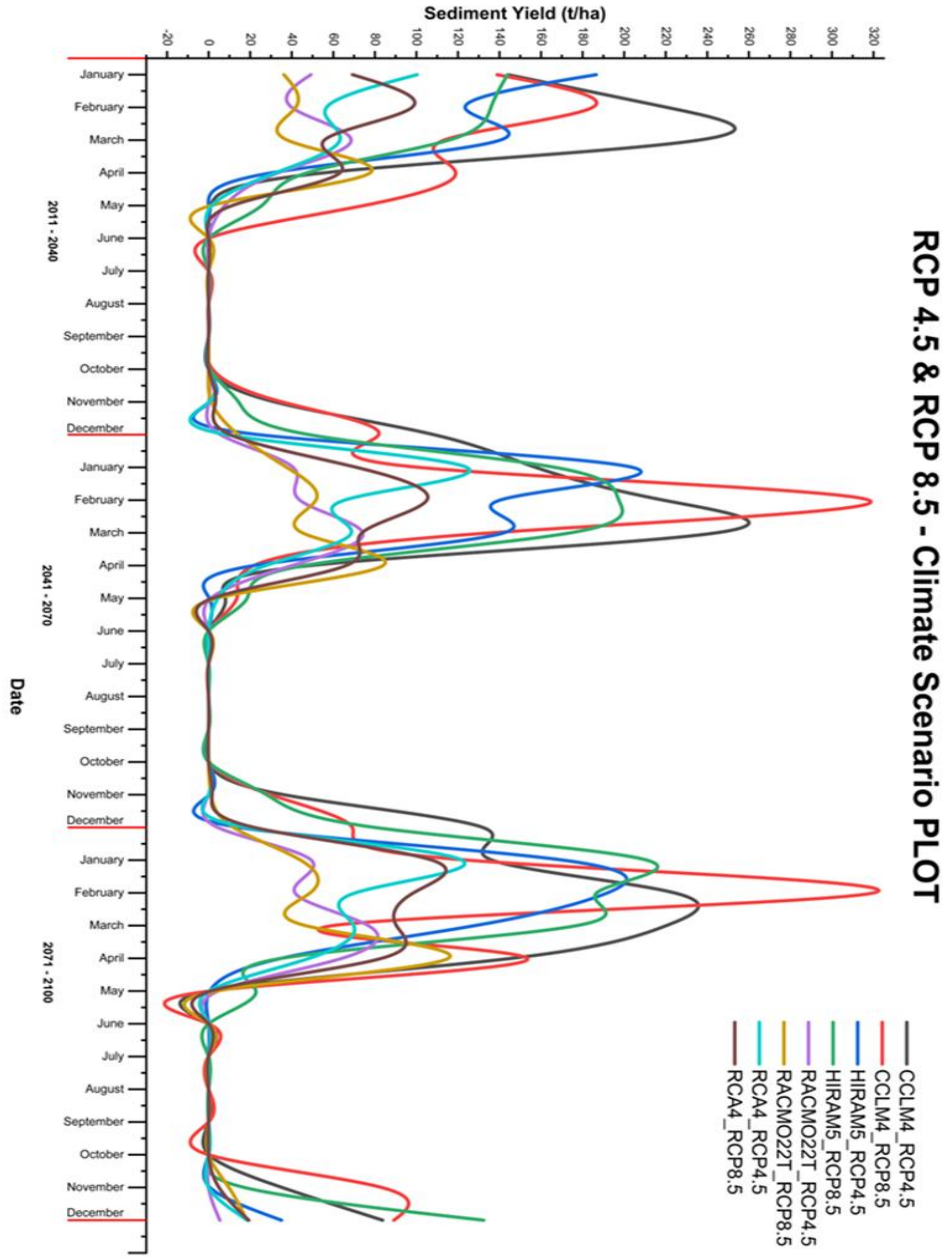

Figure 4.23: Temporal distribution of monthly sediment yield under RCP 4.5 & RCP8.5scenario (2011 – 2100)

Projections of sediment production under the RCP4.5 and RCP8.5 scenarios for the period 2011–2040 showed an increase in sediment production for both scenarios compared to the historical period. The sediment yield map for the Songwe River Sub-Basin identified key areas that are susceptible to erosion and sedimentation during the period 2011–2040 under the RCP4.5 scenario. The spatial distribution of sediment

production as simulated under four RCMs (CCLM4, HIRHAM5, RCA4 and RACMO22T) reveals that large amounts of sediment production are expected under the CCLM4 and HIRHAM5 models followed by RCA4 and RACMO22T.

Significant sediment production is observed in sub-basins 11, 16, 17, 18, 23 and 26 under the CCLM4 and HIRHAM5 models (Figure 4.24). These areas are characterized by agricultural activities, intensive precipitation, steep terrain and soils prone to erosion. These factors make the regions vulnerable to erosion. In contrast, sub-basins 11, 16 and 26 experienced only a slight increase in sediment production when simulated under the RCA4 and RACMO22T models. This suggests that the RCA4 and RACMO22T models may be less sensitive to projected changes in precipitation and temperature compared to the CCLM4 and HIRHAM5 models.

The CCLM4 and HIRHAM5 models simulated higher precipitation and temperature values both of which influence soil erosion dynamics in areas of cultivated land located on steep terrain. This aligns with findings from similar studies in East Africa which emphasize that intensified rainfall and higher temperatures in agricultural regions with steep slopes exacerbate erosion rates and increase sediment production.

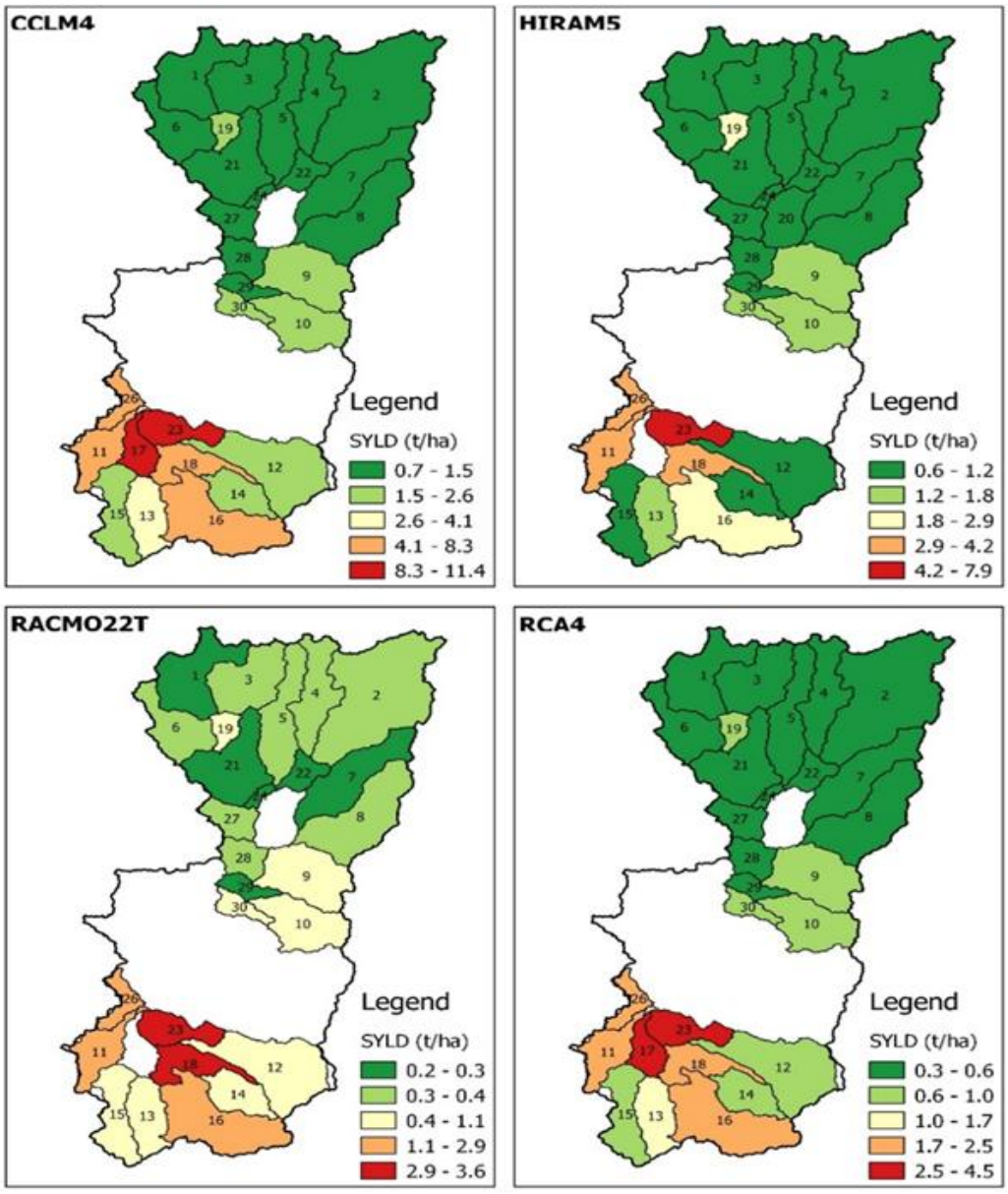

Figure 4.24: Spatial distribution of sediment yield map under RCM – RCP4.5 scenarios (2011 – 2040)

The RCP8.5 scenario indicated a significant increase in sediment production for the period 2011–2040 in sub-basins 11, 12, 13, 15, 16, 17, 18, 23 and 26 under both the CCLM4 and HIRHAM5 climate models (Figure 4.25). The highest sediment production is observed in sub-basin 18 for the CCLM4 model and in sub-basins 17, 18 and 23 for the HIRHAM5 model. These areas are characterized by agricultural

activities, intensive precipitation, steep terrain, and erodible soils such as Eutric Leptosols which make them vulnerable to erosion.

In contrast, the RCA4 and RACMO22T models showed a slightly lower increase in sediment production with sub-basins 17 and 18 experiencing the highest values under the RCA4 model. However, even in these models the sediment production increase is still significant suggesting that the overall pattern of increased erosion due to climate change remains consistent across all models although with different magnitudes. When compared to the RCP4.5 scenario the RCP8.5 scenario projects a higher increase in sediment production in several key sub-basins particularly those in the southern and central regions of the Songwe River Sub-basin. While the RCP4.5 scenario showed moderate increases in sub-basins 11, 16, 17 and 18. The RCP8.5 scenario highlights a more dramatic increase in the wet season months exacerbated by increased precipitation and higher temperatures.

The results from the RCP8.5 scenario also demonstrated a more significant shift in sediment dynamics with sub-basin 18 being a key hotspot under the CCLM4 model and sub-basins 17, 18 and 23 emerging as critical areas of concern under the HIRHAM5 model. These areas are not only subject to agricultural pressures but are also highly vulnerable to climate-induced changes in rainfall intensity and temperature which are likely to drive further increases in erosion rates and sediment yield.

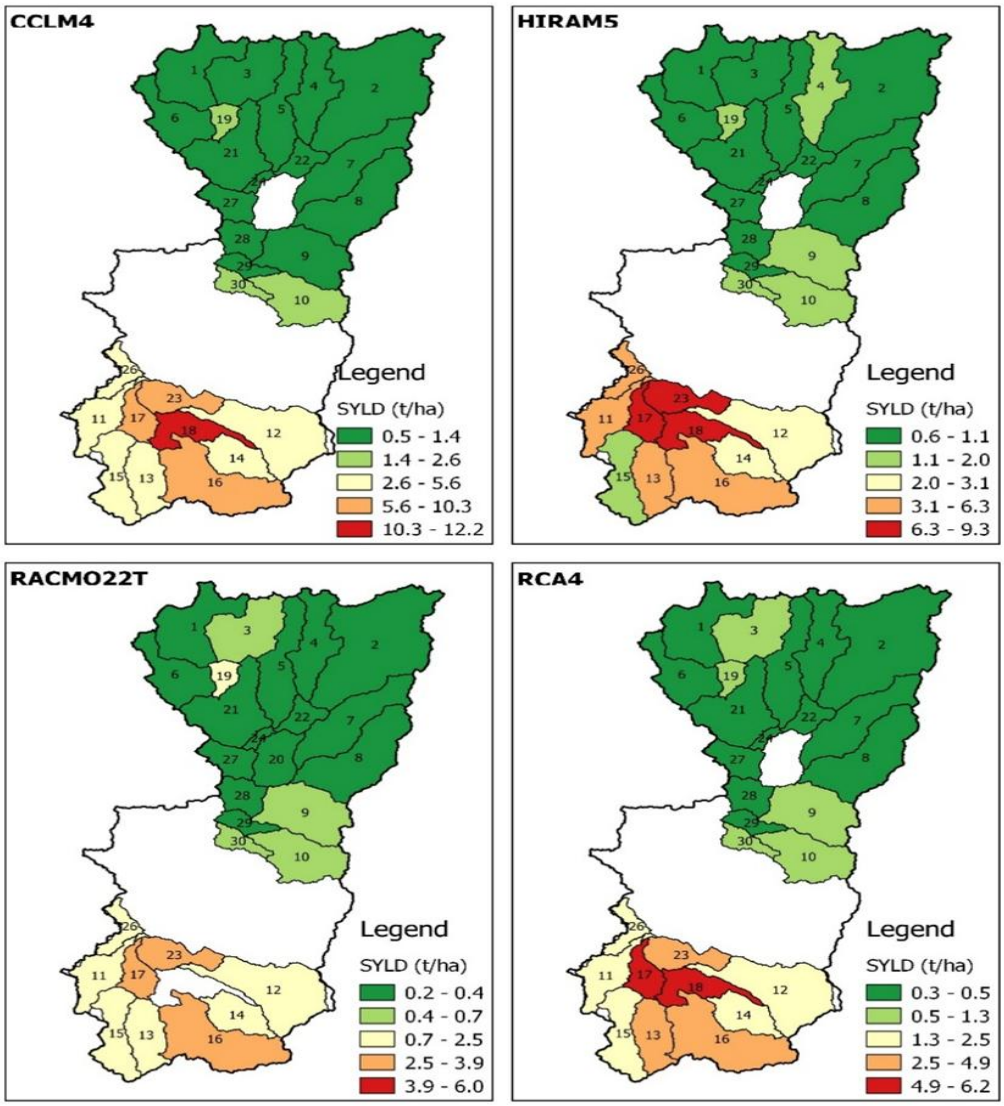

Figure 4.25: Spatial distribution of sediment yield map under RCM – RCP8.5 scenarios (2010 – 2040)

The projections for the period 2041–2070 under the RCP4.5 and RCP8.5 scenarios show a slight increase in sediment production for both scenarios compared to the historical period and the near future period of 2011–2040. The sediment yield map for the Songwe River Sub-Basin identifies key regions that are susceptible to erosion and sedimentation for the period 2041–2070 under the RCP4.5 scenario. The RCP4.5 scenario indicates moderate increase in sediment production with pronounced peaks occurring during periods of high precipitation.

The spatial distribution of sediment production under the four regional climate models (RCMs)—CCLM4, HIRHAM5, RCA4 and RACMO22T shows significant sediment production under CCLM4 and HIRHAM5 models followed by RCA4 and RACMO22T. The highest sediment production is observed in sub-basins 11, 13, 16, 17, 18, 19, 23 and 26 under the CCLM4 and HIRHAM5 models (Figure 4.26). It reflects the increasing vulnerability of these regions under both climate change scenarios. In contrast, the RCA4 and RACMO22T models show a slightly lower increase in sediment production but still identify sub-basins 17, 18 and 23 as areas with the highest sediment production across all models.

The historical sediment yield in the Songwe River Sub-Basin provides a baseline with much lower sediment production than projected for the future. The areas most susceptible to erosion during the historical period were the same as future period, but indicate further increase in sediment yield for 2041–2070 due to the combined impacts of climate change and land use changes. For the period 2011–2040 both the RCP4.5 and RCP8.5 scenarios predicted an increase in sediment production but the 2041–2070 period shows a slightly higher increase compared to 2011–2040 in sub-basins 17, 18 and 23. This suggests that future climate changes such as increased rainfall intensity and higher temperatures exacerbate sediment production even further than initially projected in the near future.

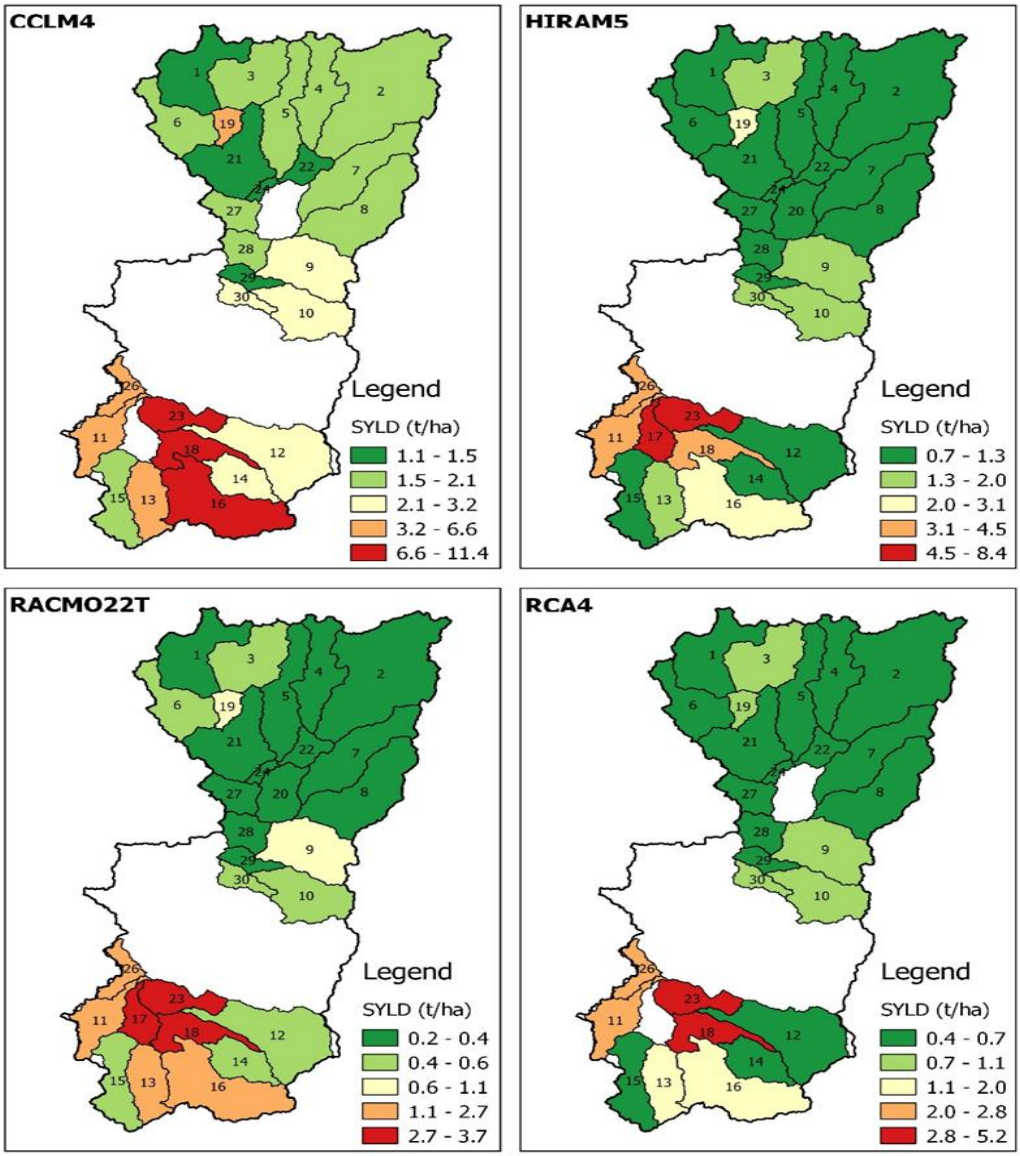

Figure 4.26: Spatial distribution of sediment yield map under RCM – RCP4.5 scenarios (2041 – 2070)

The RCP8.5 scenario indicates an increase in sediment production for the period 2041–2070 in sub-basins under the CCLM4 model and HIRHAM5 model. The CCLM4 and HIRHAM5 models continue to dominate the prediction of high sediment production particularly in sub-basins 11, 13, 16, 17, 18, 19, 23 and 26 which remain high-risk areas in all future projections (Figure 4.27). In contrast, the RACMO22T and RCA4 models predict slightly lower increases in sediment production compared to CCLM4 and HIRHAM5 models in sub-basins 11, 12 and 26. However, these models still

predict significant increases in sediment production across the entire basin in the regions most vulnerable to erosion. These results suggest that some models predict more significant impacts on sediment production reflecting the heightened climate change vulnerability of these areas.

During the historical period sediment production in the Songwe River Sub-Basin was relatively lower with specific regions exhibiting moderate erosion. The 2041–2070 period shows a marked increase in sediment production, particularly in sub-basins 17, 18, and 23, due to the intensification of rainfall and higher temperatures under the RCP8.5 scenario. By comparing the 2041–2070 period with the 2011–2040 period, it is evident that increased precipitation and temperaturewill further intensify sediment yield in the Songwe River Sub-Basin exacerbating the challenges posed by agricultural land use and steep slopes.

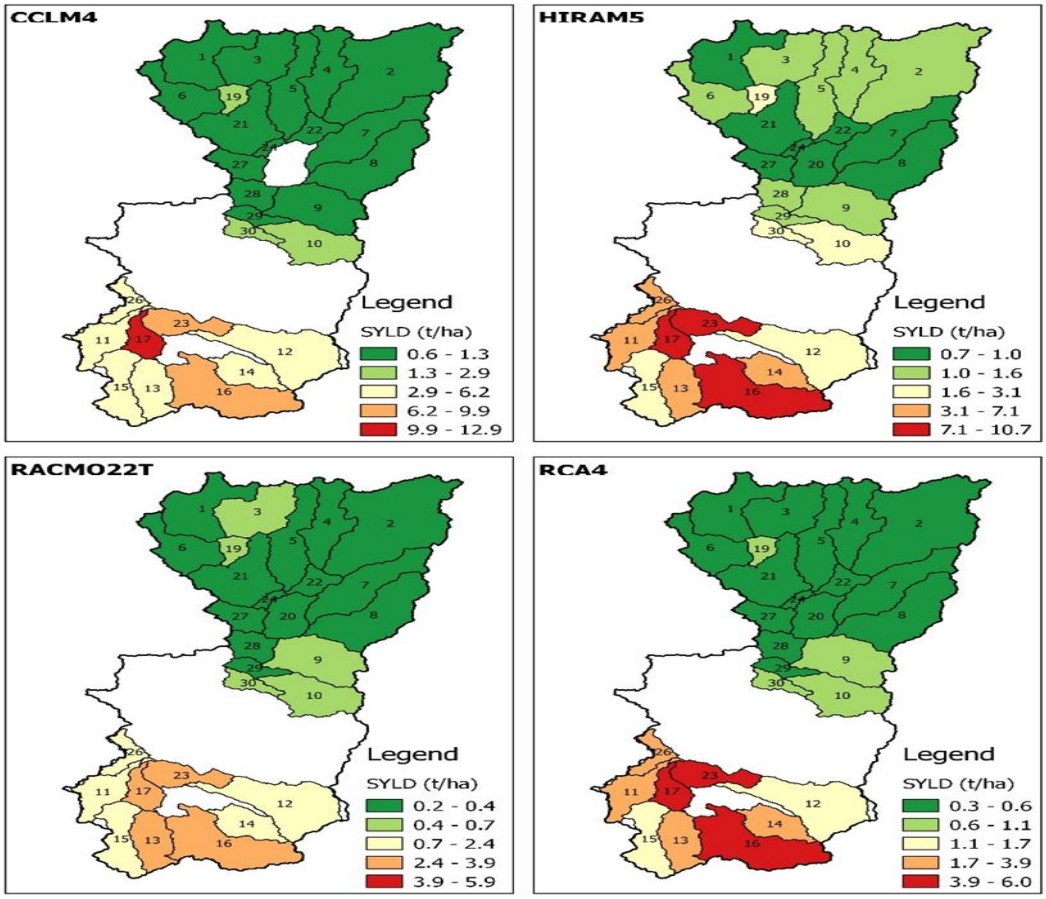

Figure 4.27: Spatial distribution of sediment yield map under RCM – RCP8.5 scenarios (2041 – 2070)

The projections for the period 2071–2100 under both the RCP4.5 and RCP8.5 scenarios indicate a significant increase in sediment production compared to the historical period and earlier future projections (2011–2040 and 2041–2070). The sediment yield map of the Songwe River Sub-Basin identifies key regions that are susceptible to erosion and sedimentation during the period 2071–2100 under the RCP4.5 scenario. The spatial distribution of sediment production as simulated under four RCMs shows that large amounts of sediment production are expected under CCLM4 and HIRHAM5 models followed by RCA4 and RACMO22T.

The highest sediment production is observed in sub-basins 11, 12, 13, 14, 15, 16, 17, 18, 23 and 26 under the CCLM4 model and in sub-basins 11, 13, 16, 18, 23 and 26 for the HIRHAM5 model (Figure 4.28). The historical sediment yield was much lower with fewer sub-basins experiencing severe erosion. However, as precipitation intensity and temperature increase the vulnerable sub-basins such as 17, 18 and 23 are projected to experience much higher sediment yield compared to historical period, 2011–2040 and 2041–2070 projections. The RCP4.5 scenario projects more extreme rainfall events and higher temperatures which increase runoff and erosion.

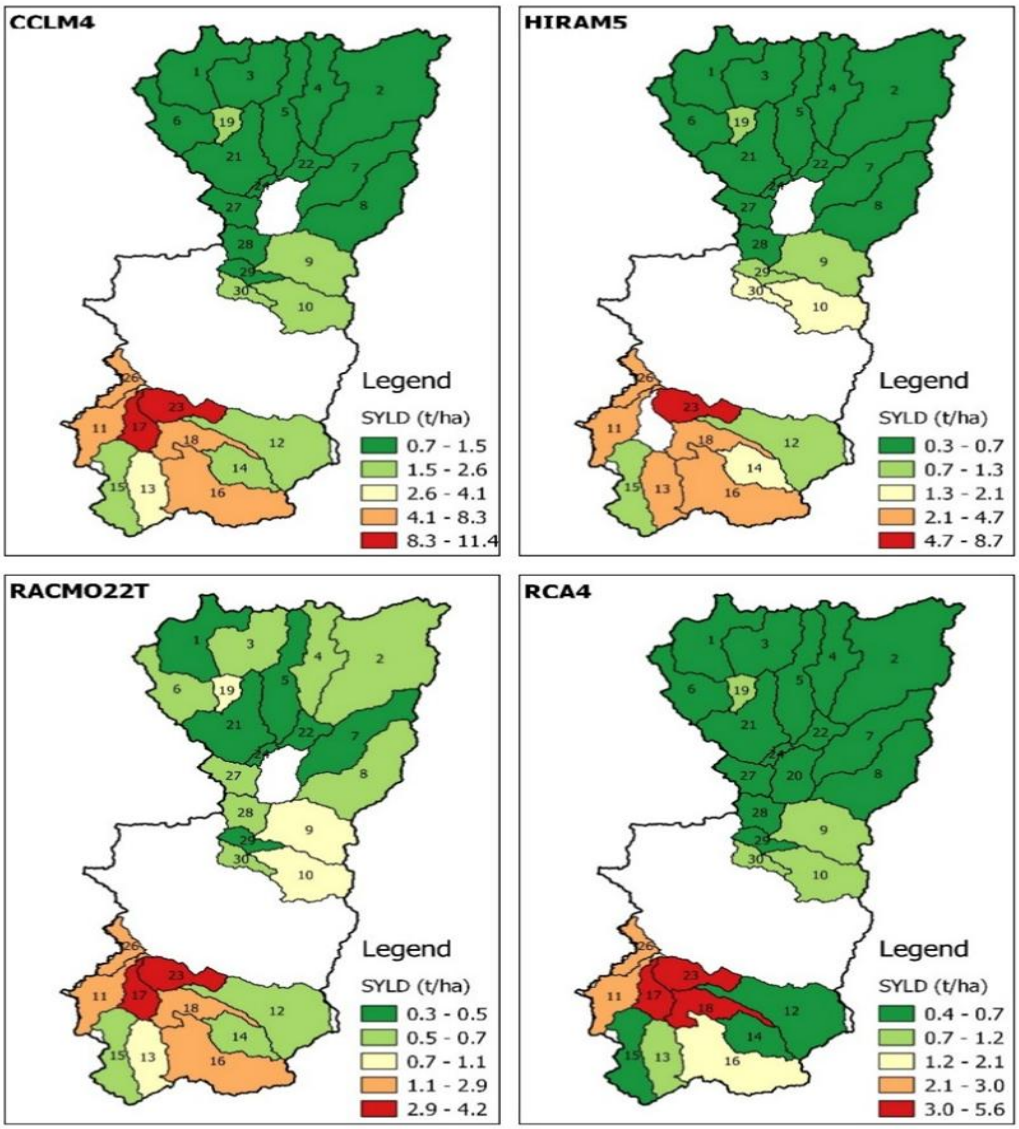

Figure 4.28: Spatial distribution of sediment yield map under RCM-RCP4.5 scenarios (2071-2100)

The RCP8.5 scenario for the period 2071–2100 indicates a significant increase in sediment production in sub-basins 2, 3, 4, 9, 10, 11, 12, 13, 15, 16, 17, 18, 23, 26, 28 and 30 under both the HIRHAM5 model and CCLM4 model (Figure 4.29). The highest sediment production is observed in sub-basin 17 for the CCLM4 model and in sub-basins 16, 17 and 23 for the HIRHAM5 model. These sub-basins are characterized by agricultural activities, intensive precipitation, steep terrain, and soils prone to erosion. There was also a noticeable increase in sediment production in sub-basins 11, 12, 13, 14, 15, 16, 17, 18, 23, and 26 under both the RACMO22T model and RCA4 model.

The RCP8.5 scenario for the 2071–2100 period shows a substantial increase in sediment production in sub-basins 17, 18 and 23 compared to the historical period and the earlier projections for 2011–2040 and 2041–2070. The marked increase in sediment production across the Sub-Basin driven by higher rainfall intensity and temperature increases. This period sees the greatest intensification in erosion due to more frequent extreme weather events and the continued increase in agricultural activities on steep slopes.

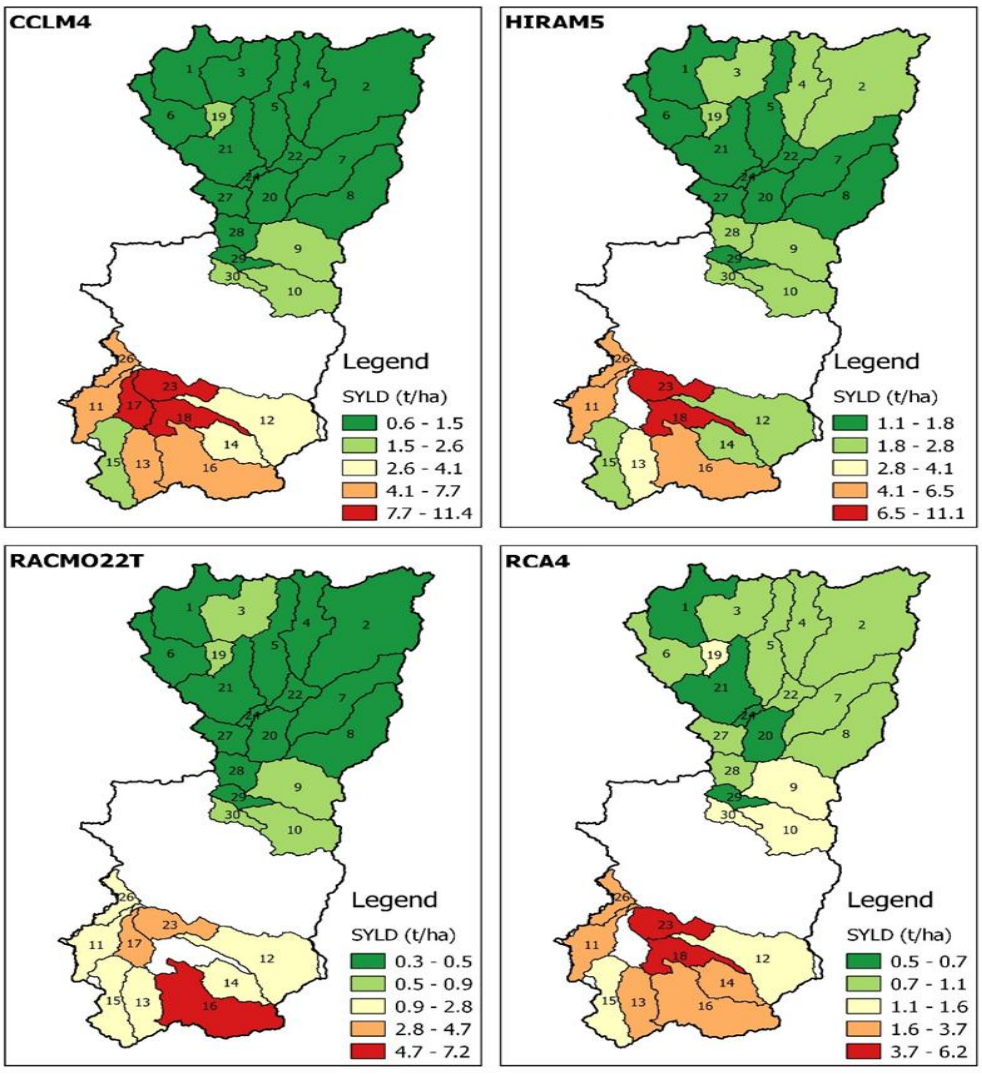

Figure 4.29: Spatial distribution of sediment yield map under RCM – RCP8.5 scenarios (2071 – 2100)

These results align with other studies from East African regions including the Upper Blue Nile Basin where steep gradients and agricultural practices have been identified as key contributors to elevated sediment production (Leta et al., 2023; Zimale et al., 2016). Similar to these areas the Songwe River Sub-Basin experiences a complex interaction of fluctuating precipitation patterns, complex hydrological processes and intensive agricultural practices all of which contribute to increased sediment generation. The presence of Eutric Leptosols in certain regions further amplifies susceptibility to soil erosion, emphasizing the urgent need for focused soil conservation initiatives to address the growing erosion risks.

To mitigate the anticipated rise in sediment production it is essential to adopt soil conservation measures in the most vulnerable regions of the Songwe River Sub-Basin. Practices such as terracing, contour farming, agroforestry and cover cropping reduce soil erosion. In areas dominated by Eutric Leptosols, enhancing soil structure and improving water retention through practices like mulching and the addition of organic materials would control soil erosion. These projections highlight the critical importance of integrating climate change into sediment management strategies. As increased precipitation and higher temperatures exacerbate erosion in agricultural areas and steep terrains. The proactive measures are required to address these challenges. Implementing climate-adaptive sediment management strategies is essential to mitigate the impacts of climate change on soil degradation.

These findings underscore the heightened risk of soil degradation under climate change and emphasize the importance of implementing targeted soil conservation measures in the most vulnerable sub-basins. This approach is critical to reduce future erosion and sedimentation impacts, preserving the ecological health of the basin and ensuring sustainable land use in the Songwe River Sub-Basin.

4.6 Projected Sediment Yield under Different Climate Scenarios and Historical Sediment yield in the Songwe River Sub-Basin

The historical sediment yield in the Songwe River Sub-Basin for the period 1981 to 2005 has been analyzed and compared against the estimated sediment yield derived from four RCMs: CCLM4, HIRHAM5, RACMO22T and RCA4. The results provide

understanding into how varying climate forecasts influence sediment transport dynamics in the sub-basin. The observed historical sediment yield for the period 1981 to 2005 based on empirical estimation indicates seasonal variations. These fluctuations reflect both natural factors such as rainfall intensity and human-induced factors including deforestation and agricultural practices. The historical sediment yield shows peak values during the rainy season which corresponds to the period of highest runoff and soil erosion rates. The sediment yield predictions from the four regional climate models (CCLM4, HIRHAM5, RACMO22T and RCA4) exhibit a range of responses when compared to historical data from 1981 to 2005. The CCLM4 model predicts slightly higher sediment yield during the wettest months due to its sensitivity to increased precipitation (Figure 4.30). In contrast, the HIRHAM5 model aligns closely with historical sediment yield but underestimates peak sediment transport during intense rainfall events. RACMO22T shows intermediate results with sediment yield slightly higher than historical values though it tends to overestimate sediment transport during transitional periods between wet and dry months and predict increased erosion during periods of lower rainfall. The RCA4 model being the most conservative closely follows historical trends suggest that sediment yield may not change drastically despite projected changes in rainfall.

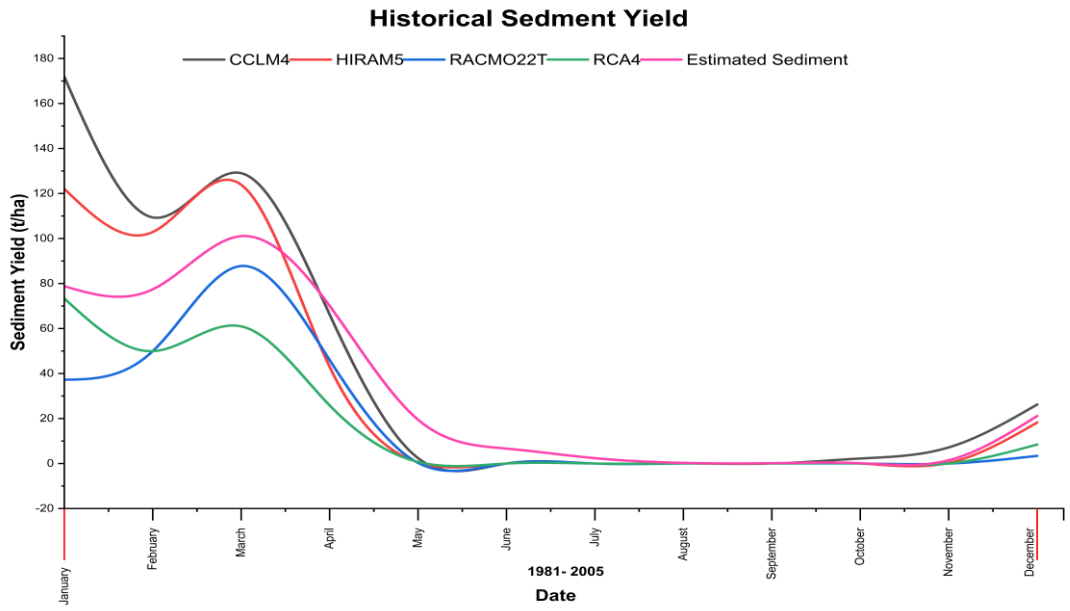

Figure 4.30: Temporal distribution of monthly sediment yield under RCM scenario (1981 – 2005

The sediment yield forecasts for the Songwe River sub-basin simulated with the SWAT model indicate a persistent upward trajectory in sediment yields over the three periods: 2011-2040, 2041-2070 and 2071-2100 under RCP 4.5 and RCP 8.5 climatic scenarios (Figure 4.31). This trend is apparent across all four climate models (CCLM4, HIRHAM5, RACMO22T, RCA4) with a more pronounced increase noted under the high-emission scenario (RCP 8.5).

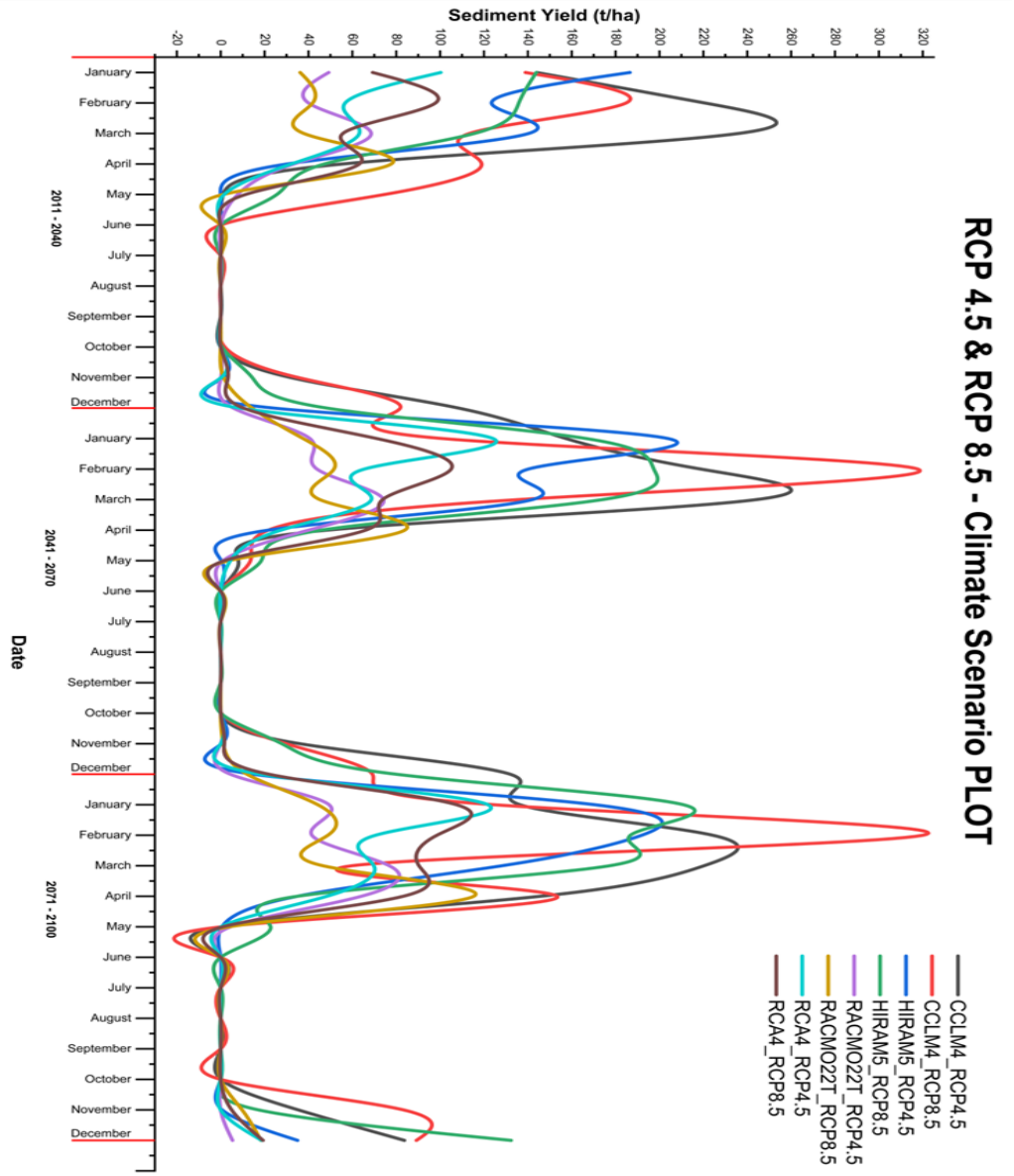

Figure 4.31: Temporal distribution of monthly sediment yield under RCM – RCP 4.5 & RCP8.5scenario (2011 – 2100)

In the initial period (2011-2040) sediment yield experiences moderate increases indicative of the preliminary impacts of climate change (Figure 4.32). SWAT simulations predict a moderate rise in sediment yield for the near-future period from 2011 to 2040 relative to historical projections. The models forecast a sediment yield increase of approximately 10–15% primarily attributed to cultivated fields which exhibit heightened soil exposure and increased runoff vulnerability. Among these models HIRHAM5 predicts the most significant rise mostly due to its consideration of more intense precipitation episodes whereas CCLM4 provides more conservative forecasts reflecting its diminished sensitivity to rainfall variability. RACMO22T and RCA4 demonstrate moderate increases indicating typical rainfall intensities while exhibiting somewhat heightened sensitivity to seasonal variations compared to CCLM4 (Figure 4.32). The results indicate that moderate climate changes pose a danger of heightened sediment movement in the Songwe sub-basin, particularly in agricultural areas.

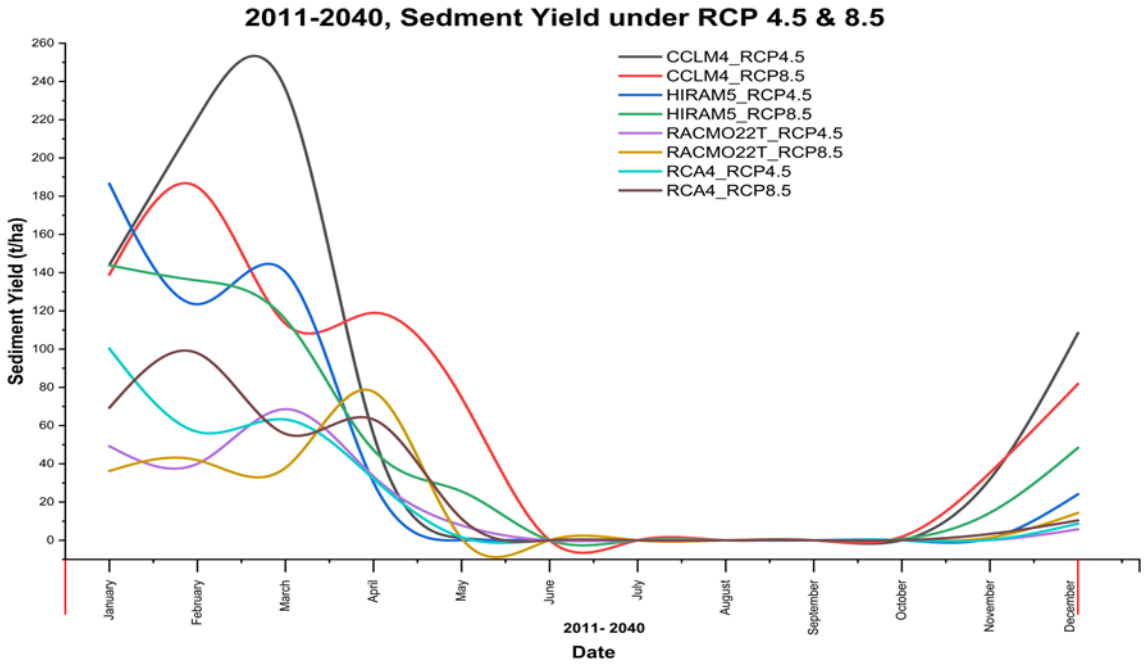

Figure 4.32: Temporal distribution of monthly sediment yield under RCM – RCP 4.5 & RCP8.5scenario (2011 – 2040)

The mid-century phase (2041-2070) witnesses' significant escalations as climate patterns intensify. During the mid-century era of 2041–2070 the anticipated sediment

yields suggest a notable increase demonstrating heightened climate impacts under both RCP 4.5 and RCP 8.5 scenarios (Figure 4.33). SWAT simulations suggest that sediment yields may grow by 20–35% relative to historical data, with the most significant increases observed in areas with steeper gradients and erodible soils. HIRHAM5 once again predicts the highest sediment yield emphasizing the crucial influence of future rainfall intensity and frequency on erosion (Figure 4.33). The RCA4 estimates indicate substantial increases illustrating the model's acute sensitivity to variations in precipitation and temperature. Conversely, CCLM4 remains the most cautious model; however, it still predicts significant increases in sediment yield. These mid-century discoveries align with regional studies in East Africa, where increased rainfall intensity coupled with human land usage has been demonstrated to exacerbate erosion. The 20–40% increase in sediment yield in the Ethiopian Highlands under similar mid-century scenarios, suggesting that the patterns found in the Songwe River sub-basin are consistent with those in other highland watersheds in the region.

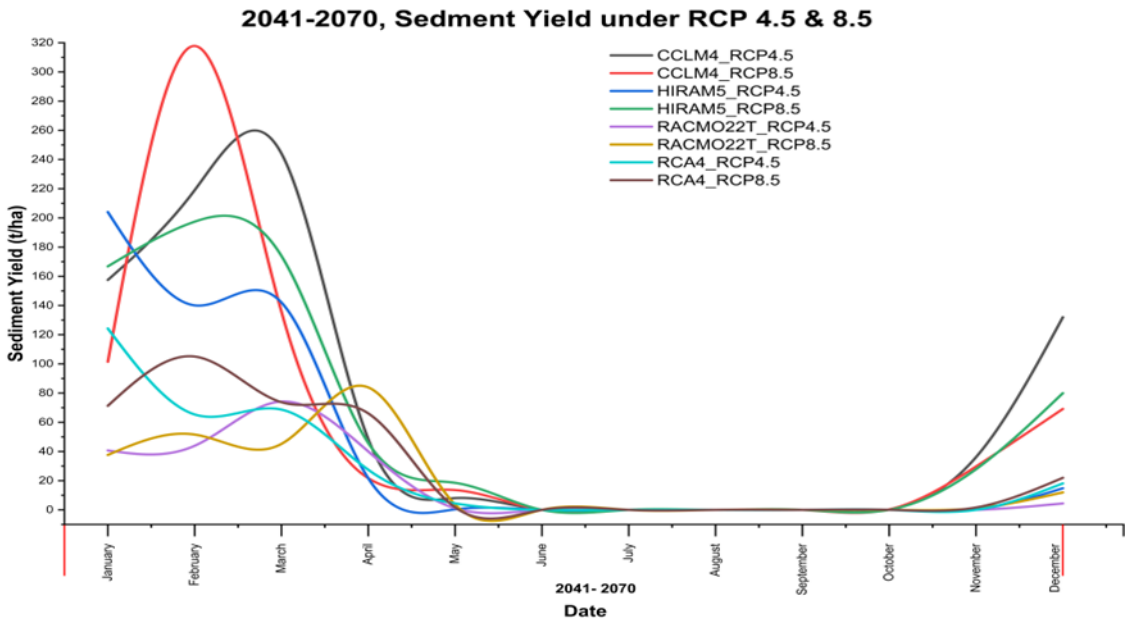

Figure 4.33: Temporal distribution of monthly sediment yield under RCM – RCP 4.5 & RCP8.5scenario (2041 – 2070)

The late-century period (2071-2100) predicts the highest increase in sediment production especially under the most severe estimates of RCP 8.5. This result

demonstrates that even minor climate change may exacerbate soil erosion particularly due to increasingly unpredictable rainfall and runoff patterns. Projections from the SWAT model indicate a substantial rise in sediment yield throughout the late-century era of 2071–2100 particularly under the high-emission RCP 8.5 scenario (Figure 4.34). Projected sediment yield is expected to increase by 35–50% relative to historical levels with severe forecasts from HIRHAM5 and RCA4 suggesting intensified storm events and enhanced runoff. RACMO22T predicts marginally reduced increments. CCLM4 consistently forecasts the minimal aggressive increments in sediment yield. While it projects a 35% rise in sediment output by 2071-2100 it adopts a more cautious methodology for modelling extreme weather events presumably owing to its diminished sensitivity to temperature-induced fluctuations in precipitation. This attribute renders CCLM4 a more cautious model for predicting unfavorable scenarios beneficial for preparing for mild climate changes; yet, it may potentially underestimate the dangers of severe erosion if extreme climatic events occur as suggested by previous models. RACMO22T and RCA4 indicates a moderate increase in sediment yield with projections somewhere between HIRHAM5 and CCLM4. This information demonstrates the model's moderate sensitivity to changes in rainfall intensity providing a balanced viewpoint that may aid in formulating adaptive management solutions. While these projections indicate an anticipated rise in sediment yields, the rate of this increase may not be as drastic as stated by many extreme models. The significant increase in sediment yield during this era underscores the risk of severe soil erosion and associated environmental repercussions, including the siltation of aquatic systems, diminished water quality, land degradation. These results correspond with studies undertaken in other regions of Africa, where end-century projections indicate that the interplay of high-intensity rainfall and land degradation may substantially increase sediment loads. The sediment production in Ethiopian watersheds could more than double under RCP 8.5 by the century's conclusion, highlighting the critical necessity for adaptive land management strategies (Bekele & Abate, 2020; Feyissa Negewo & Kumar Sarma, 2022; Guder & Kabeta, 2025; Jilo et al., 2019).

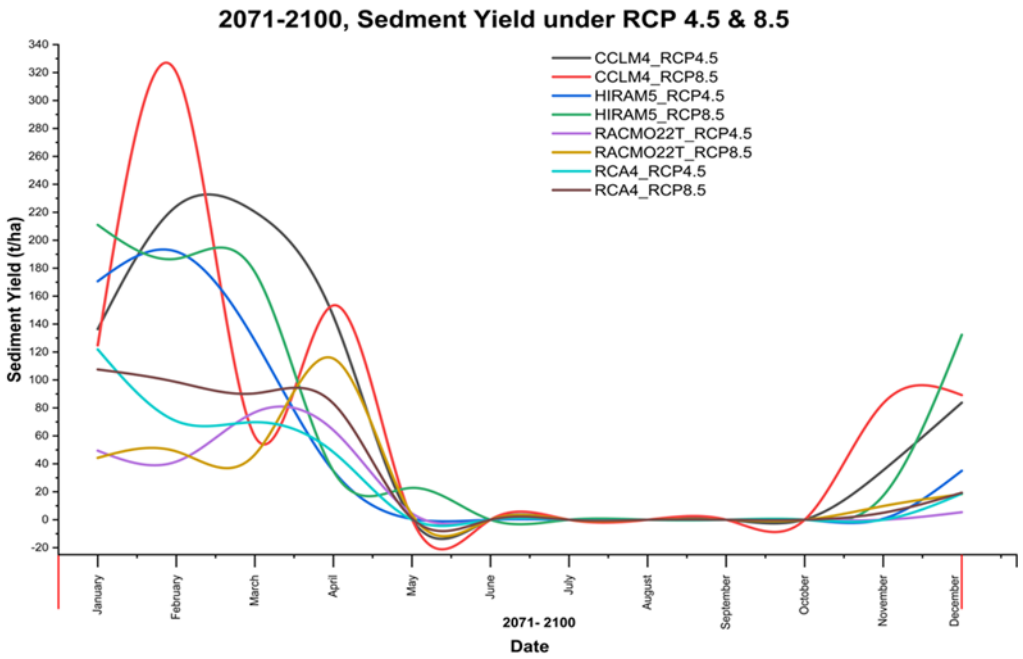

Figure 4.34: Temporal distribution of monthly sediment yield under RCM – RCP 4.5 & RCP8.5scenario (2071 – 2100)

The disparities in results among the models demonstrate the differing assumptions and techniques employed to simulate the impacts of climate change on hydrological processes. For instance, CCLM4 forecasts a more modest alteration in climatic conditions whereas models like HIRHAM5 and RCA4 exhibit heightened sensitivity to anticipated increases in extreme weather events such as intense precipitation and prolonged droughts resulting in elevated erosion rates. The RACMO22T model which incorporates increased rainfall intensity yields estimate similar to those of HIRHAM5 but emphasizes extreme occurrences to a lesser degree. The discrepancies in forecasts among different models underscore the necessity of evaluating many climate models when anticipating future climate-related effects. Relying on a singular model may result in either an overestimation or underestimation of the dangers associated with future sedimentation. Consequently, it is imperative to analyze the complete spectrum of model results and adopt adaptable, robust tactics capable of responding to numerous prospective scenarios.

4.7 Evaluating the Impacts of Climate Change under Different Scenarios on Sediment Yield in the Songwe River Sub-Basin

This study investigates the impacts of climate change on sediment yield in the Songwe River sub-basin by integrating projected land use maps for 2040, 2070 and 2100 with the results from four regional climate models under RCP 4.5 and RCP 8.5. The SWAT model was employed to predict sediment yield during these periods under diverse climate scenarios offering an in-depth investigation of the potential impacts of climate change under different future land use scenarios on sediment dynamics in this area. The future land use scenarios in the Songwe River sub-basin from 2020 to 2100 suggest a considerable transformation propelled by agricultural expansion and urbanization. Forest cover is anticipated to diminish significantly, with a fall surpassing 120,000 hectares by 2040, followed by ongoing declines thereafter. The continuous deforestation causes the increased emission of greenhouse gases such as carbon dioxide that result in modification of precipitation and temperature in the Songwe River sub-basin (Gemmechis, 2022; Mbungu, Easton, et al., 2016). The transformation of natural landscapes into agricultural and urban zones will elevate climate change impacts and risk of soil erosion and sediment yield. These alterations mirror trends identified in other areas of sub-Saharan Africa, where agricultural advancement and urbanization act as the principal catalysts for land modification and erosion (McConnell et al., 2015).

The sediment yield forecasts from the four models indicate divergent trends in reaction to climate change and land use alterations. From 2011 to 2040, sediment yields exhibit relative stability across all four models with minor increases mostly attributed to land use alterations including agricultural growth and deforestation (Figure 4.35).

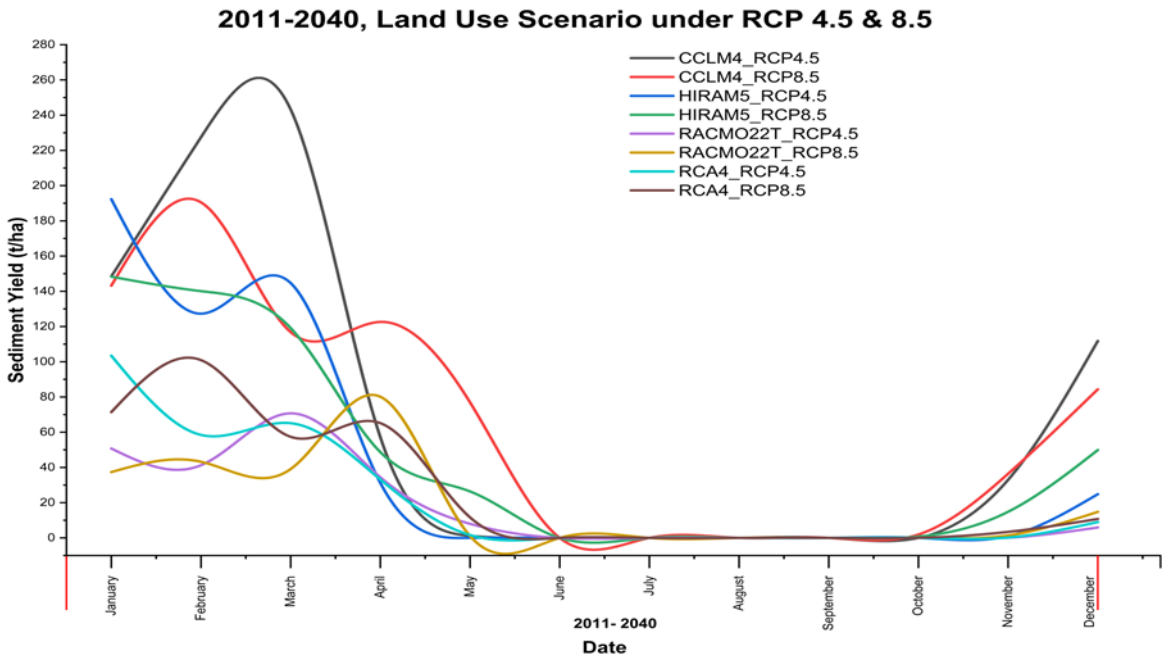

Figure 4.35: Temporal distribution of monthly sediment yield under RCM – RCP 4.5 & RCP8.5scenario (2011 – 2040)

From 2041 to 2070, the anticipated sediment yield markedly increases especially under the elevated RCP8.5 scenarios (HIRHAM5_RCP8.5 and RCA4_RCP8.5) indicate the escalating effects of intensified rainfall patterns and heightened surface runoff (Figure 4.36). These models indicate that alterations in land cover and the removal of vegetation increase the sub-basin's susceptibility to soil erosion, which is exacerbated by more intense rainfall events.

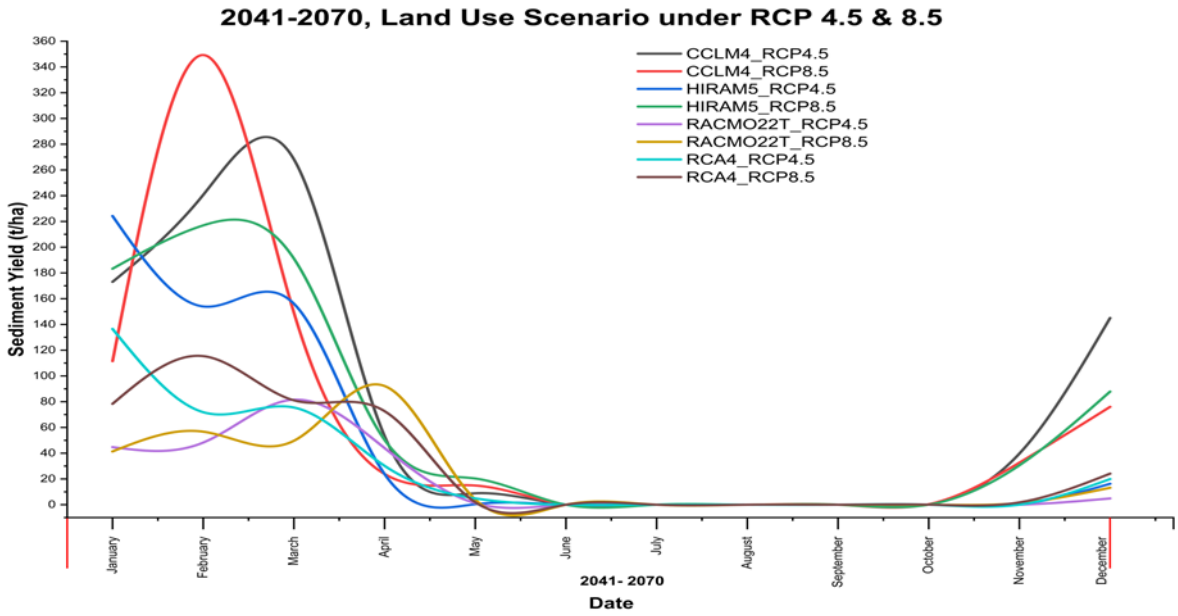

Figure 3:36 Temporal distribution of monthly sediment yield under RCM- RCP 4.5 & RCP8.5scenario (2041 – 2070)

During the concluding interval from 2071 to 2100, the cumulative impacts of climate change and land use alteration are most evident. The CCLM4_RCP4.5 and RACMO22T_RCP4.5 models forecast a consistent rise in sediment yield with increments of 20–30% indicative of ongoing landscape alteration and heightened precipitation intensity (Figure 4.37). Conversely, the HIRHAM5_RCP8.5 and RCA4_RCP8.5 models forecast significantly greater increases with sediment yield nearly doubling relative to the 2011–2040 period. This significant increase is ascribed to the impacts of intensified precipitation, augmented surface runoff, and the ongoing transformation of natural landscapes into agricultural and urban environments.

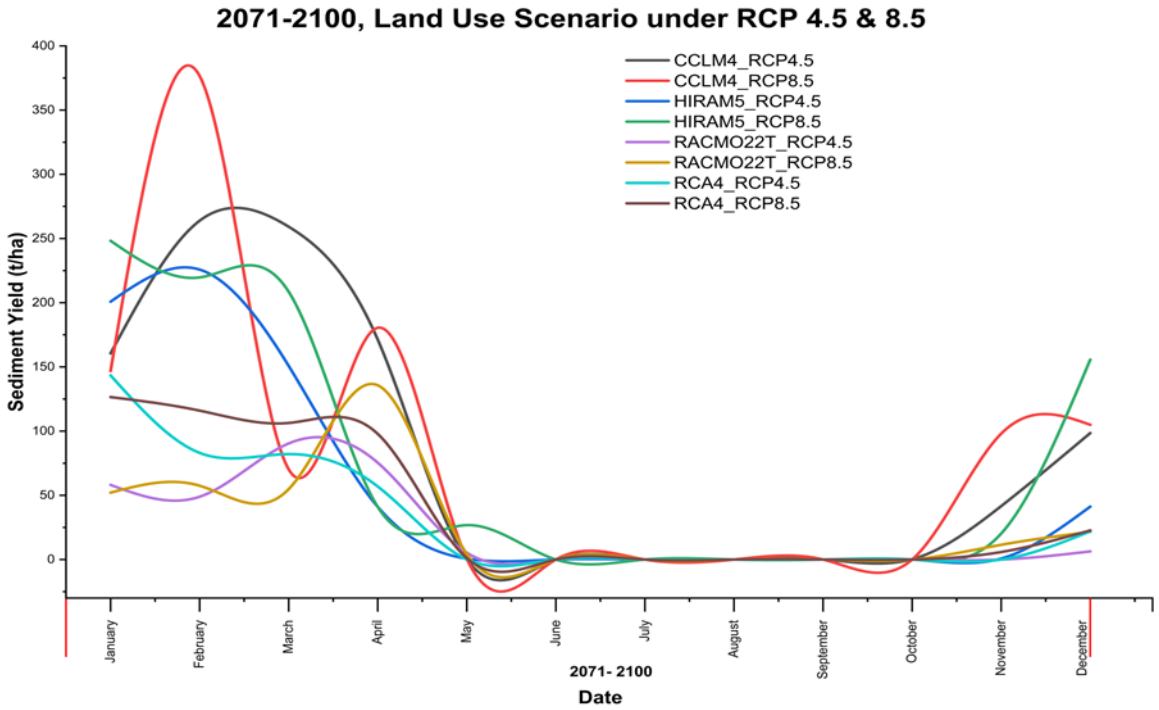

Figure 4.37: Temporal distribution of monthly sediment yield under RCM – RCP 4.5 & RCP8.5scenario (2071 – 2100)

The principal distinctions among these climate models pertain to the magnitude and frequency of precipitation and temperature escalations. The HIRHAM5_RCP8.5 and RCA4_RCP8.5 models forecast the most severe climatic alterations, as characterized by sediment yield estimates. These models indicate that intense rainfall events increase in frequency, intensifying soil erosion. In contrast, the CCLM4_RCP4.5 and RACMO22T_RCP4.5 models forecast more mild elevations in temperature and precipitation, leading to less pronounced increases in sediment yield. The diminished precipitation intensity and reduced frequency of extreme weather events in these models indicate that gains in sediment yield are more gradual, yet still significant due to persistent land use alterations such as agricultural expansion and deforestation. The regional variability in sediment yields within the sub-basin varies among the models. In extreme scenarios, regions that have had substantial agricultural development and deforestation are anticipated to witness the most dramatic increases in sediment yield, especially during the 2070–2100 decade. Conversely, under the more temperate

climate scenarios, the rise in sediment yield is more uniformly spread throughout the sub-basin, exhibiting fewer prominent concentrations of severe erosion zones.

The increases are ascribed to intensified precipitation from climate change and ongoing environmental modifications due to urbanization and agriculture, which aggravate soil erosion in regions where vegetation has been diminished by deforestation and land conversions (Feyissa Negewo & Kumar Sarma, 2022; Mbungu, Heatwole, et al., 2016; Zhang et al., 2019). This discovery aligns with studies in other African basins, like the Upper Blue Nile, where combined land use and climatic alterations led to significant variations in sediment yield (Tikuye et al., 2024). These findings underscore the necessity for resilient, adaptive management systems that account for both climate change and land use forecasts to effectively minimize the expected increase in sediment yield.

4.8 Concluding Remarks

This chapter provides the valuable insights on the critical role of climate change in shaping sediment transport processes in the Songwe River sub-basin and contribution to understanding the broader implications of climate change on sediment transport in East Africa. The projections of future climate scenarios indicate that without significant intervention sediment in the sub-basin would likely to increase and posing challenges for land and water resources management. The chapter also provides foundation for developing targeted management strategies that consider both climate and land use factors to mitigate risks of soil erosion and sedimentation.

CHAPTER FIVE

CONCLUSIONS AND RECOMMENDATIONS

5.1 Conclusions

5.1.1 General Conclusions

This study assessed the impacts of climate change on sediment yield in the Songwe River Sub-Basin using the SWAT model with four regional climate projections under RCP4.5 and RCP8.5 for the periods 2011–2040, 2041–2070 and 2071–2100. The findings indicate that climate change through altered precipitation patterns and rising temperatures impacts sediment yield in the sub-basin with the most substantial increases expected toward the end of the century under RCP8.5. The study also highlights that higher temperatures accelerate erosion particularly in areas where vegetation cover is already compromised by human activities.

The model calibration for streamflow demonstrated below the standard threshold performance with a Nash-Sutcliffe Efficiency (NSE) of 0.47, which improved during validation to an NSE of 0.59. Although the sediment yield simulations were not calibrated due to data limitations, they produced spatially plausible patterns that aligned well with land use and soil erodibility. Despite these challenges, the model remains a valuable tool as it effectively captures the seasonal trends and overall dynamics of both streamflow and sediment yield in the Songwe River sub-basinThe study emphasizes the necessity of high-resolution climate models for accurate projections in regions like the Songwe River Sub-Basin where detailed climate and sediment data are limited. These findings emphasize the need for climate change adaptation strategies in regional water and land management policies. In particular, multi-model approaches considering both climate and land-use changes are essential for accurately forecasting sediment dynamics and planning effective mitigation measures in the sub-basin.

5.1.2 Specific Conclusions

5.1.2.1 Characterization and Map of Sediment Sources in the Songwe River Sub-Basin

The characterization and mapping of sediment sources in the Songwe River sub-basin demonstrate that areas in elevated sub-basins particularly those near agricultural areas

are highly susceptible to increased sedimentation due to intensified precipitation, steep gradients, erodible soils and poor land management practices including deforestation and unregulated farming. Climate change projections indicate that by 2050, sediment yield in the higher catchment sections of the Songwe River Sub-basin may increase by 25%, while sedimentation in lower catchment areas is anticipated to rise by as much as 30% by 2100 particularly during extreme precipitation events. Agricultural expansion and urbanization further exacerbate surface runoff and soil erosion. This finding emphasizes the need for improved land management practices to mitigate sedimentation in regions vulnerable to climate change. Mapping these sources also underscores the urgency of addressing land-use impacts and supporting sustainable farming techniques.

5.1.2.2 Determination of sediment yield under different climate scenarios in the Songwe River Sub-basin

The findings indicate a consistent increase in sediment yield over time with the most significant increases observed under the RCP 8.5 scenario especially in the late-century period where sediment yield could increase by 35–50%. The models projected a 10-15% rise in sediment yield by 2040 and 20–35% increase by 2070 under RCP 8.5. Models like HIRHAM5 forecast the most significant increases owing to its higher sensitivity to rainfall intensity compared to more conservative models like CCLM4. This variability highlights the importance of using a multi-model approach to predict future sedimentation under climate change scenarios. By integrating SWAT with RCM projections, the study offered valuable insights into managing sediment transport and erosion under future climatic scenarios.

5.1.2.3 Evaluation of impacts of climate change under different scenarios on sediment yield in the Songwe River Sub-basin

The findings showed that climate change coupled with land-use changes considerably increases sediment yield. By 2050, under the RCP4.5 scenario sediment yield may increase by 15–20% potentially reaching a 30% increase under the more extreme RCP8.5 scenario by 2070. The combined impacts of rising temperatures, increased rainfall intensity and significant land use changes (like agricultural expansion and urbanization) lead to intensified soil erosion and sediment deposition in rivers and

lakes. The SWAT model showed a strong capacity for simulating sediment dynamics by incorporating changes in precipitation and temperature under future land use scenarios. Climate change, combined with land use changes significantly enhance sediment yield.

5.2 Recommendations

5.2.1 Specific Recommendations

The study acknowledges limitations, primarily the lack of detailed sediment data for model calibration and the reliance on historical land use trends to project future condition, which may not account for sudden policy changes or unexpected changes. These limitations suggest the need for improved real-time data collection, better monitoring systems and a more dynamic approach to modelling that includes adaptive management strategies. Additionally, the study recommends future research to focus on identifying Best Management Practices (BMPs) to mitigate erosion and sediment yield, as well as enhancing sustainable land and water management strategies to better manage sediment dynamics under climate change.

5.2.1.1 Characterization of sediment sources and mapping of sediment sources in the Songwe River Sub-basin

The government of Tanzania, in partnership with local extension officers and farmers should promote soil conservation effort and promote sustainable land use practices such as the adoption of terracing, contour farming, agroforestry and reforestation in areas prone to erosion and sedimentation, specifically sub-basins 17, 18, and 23 in the southern and central parts of the Songwe River sub-basin

5.2.1.2 Determination of sediment yield under different climate scenarios in the Songwe River Sub-basin

The Ministry of Water in partnership with research institutions should establish a real-time sediment yield monitoring system integrated with climate models to monitor sediment yield and forecast future trends in the Songwe River sub-basin. This effort should involve collaboration with research institutions and governmental bodies to secure funding and develop the necessary monitoring infrastructure.

The Tanzania National Water Policy 2002 version 2025 should integrate climate projections into water resource management by prioritizing the development of sediment management programs in key basins, such as the Songwe River sub-basin. This should include the implementation of targeted strategies to reduce sedimentation in water reservoirs ensuring the protection of water storage capacity and infrastructure against the impacts of climate change.

5.2.1.3 Evaluation of impacts of climate change under different scenarios on sediment yield in the Songwe River Sub-basin

The government of Tanzania through the Ministry of Water and the Ministry of Agriculture should establish erosion control structures including check dams, riparian buffers and soil stabilization projects in the Songwe River sub-basin, particularly in areas with high sediment yield, such as the upper sub-basin regions. This should be done by using available funding from national and international climate adaptation programs and collaborating with local authorities for effective implementation.

5.2.2 Future Research Works

i. Future study should concentrate on building long-term monitoring stations in critical sub-basins to collect data on sediment, climate and land use. These stations would provide real-time data and enhance the accuracy of model calibration and validation for sediment yield projections in the Songwe River sub-basin.
ii. Future study should aim to identify and simulate the most Best Management Practices (BMPs) for mitigating soil erosion and sediment yield under different climate scenarios in the Songwe River sub-basin. These practices inform the development of sustainable land and water management strategies to reduce the impacts of climate change on sedimentation.
iii. Future study should focus on developing models that account for sudden policy changes and unexpected changes in land use as the reliance on historical land use trends to project future conditions may not fully capture these dynamics.

5.3 Contribution to the Body of Knowledge

This study is the first to integrate climate projections with the SWAT model to project the impacts of climate change on future sediment yield in the Songwe River sub-basin. The results demonstrate that under a high-emissions scenario by the end of the century sediment yield could increase substantially with the most severe impacts concentrated in agricultural areas with steep gradients. By identifying areas most at risk of increased sedimentation and erosion, the study provides critical insights for sustainable land and water management. Furthermore, the findings enhance the understanding of sediment transport processes not only in the Songwe River sub-basin but also in East African river basins. The study supports the development of targeted adaptation strategies and contributes to global discussions on climate change and sediment management in developing countries, helping to inform policies and practices that address climate-induced sediment challenges.

REFERENCES

Abbaspour, K. C., Yang, J., Maximov, I., Siber, R., Bogner, K., Mieleitner, J., Zobrist, J., & Srinivasan, R. (2007). Modelling hydrology and water quality in the pre-alpine/alpine Thur watershed using SWAT. *Journal of Hydrology*, *333*(2–4), 413–430. https://doi.org/10.1016/j.jhydrol.2006.09.014

Abdelmajeed, A. Y. A., & Juszczak, R. (2024). Challenges and Limitations of Remote Sensing Applications in Northern Peatlands: Present and Future Prospects. In *Remote Sensing* (Vol. 16, Issue 3). Multidisciplinary Digital Publishing Institute (MDPI). https://doi.org/10.3390/rs16030591

Abubakari, S., Dong, X., Su, B., Hu, X., Liu, J., Li, Y., Peng, T., Ma, H., Wang, K., & Xu, S. (2019). Modelling streamflow response to climate change in data-scarce white volta river basin of West Africa using a semi-distributed hydrologic model. *Journal of Water and Climate Change*, *10*(4), 907–930. https://doi.org/10.2166/wcc.2018.193

Addis, H. K., Strohmeier, S., Ziadat, F., Melaku, N. D., & Klik, A. (2016). Modeling streamflow and sediment using SWAT in ethiopian highlands. *International Journal of Agricultural and Biological Engineering*, *9*(5), 51–66. https://doi.org/10.3965/j.ijabe.20160905.2483

Adhikari, U., & Nejadhashemi, A. P. (2016). Impacts of climate change on water resources in Malawi. *Journal of Hydrologic Engineering*, *21*(11), 1–13. https://doi.org/10.1061/(ASCE)HE.1943-5584.0001436

Agbola, S. B., Coomes, O. T., Lambin, E. F., Turner, B. L., Geist, H. J., Agbola, S. B., Angelsen, A., Bruce, J. W., Dirzo, R., Unther Fischer, G. U., Folke, C., George, P. S., Homewood, K., Imbernon, J., Leemans, R., Li, X., Moran, E. F., Mortimore, M., Ramakrishnan, P. S., … Xu, J. (2001). The causes of land-use and land-cover change: Moving beyond the myths. In *Global Environmental Change* (Vol. 11). https://www.researchgate.net/publication/40143592

Akoko, G., Le, T. H., Gomi, T., & Kato, T. (2021). A review of swat model application in africa. *Water (Switzerland)*, *13*(9). https://doi.org/10.3390/w13091313

Al-Khafaji, M. S., & Al-Mukhtar, M. (2017). *Modeling Suspended Sediment Load Using SWAT Model in Data Scarce Area-Iraq (Al-Adhaim Watershed as a Case Study) Modeling Suspended Sediment Load Using SWAT Model View project Assessment and Mitigation of Sediment Yield for Hemrin Dam Watershed View proje*. *January*.

Amasi, A. I. M., Wynants, M., Kawalla, R. A., Sawe, S., Munishi, L., Blake, W. H., & Mtei, K. M. (2021). Reconstructing the Changes in Sedimentation and Source Provenance in East African Hydropower Reservoirs: A Case Study of Nyumba ya Mungu in Tanzania. *Earth*, *2*(3), 485–514. https://doi.org/10.3390/earth2030029

Ang, R., & Oeurng, C. (2018). Simulating streamflow in an ungauged catchment of Tonlesap Lake Basin in Cambodia using Soil and Water Assessment Tool (SWAT) model. *Water Science*, *32*(1), 89–101. https://doi.org/10.1016/j.wsj.2017.12.002

Appiah, D. (2015). A sedimentologic analysis of terrace sediments from the Pawmpawm River Channel, Ghana. *Journal of Science and Technology (Ghana)*, *34*(2), 35. https://doi.org/10.4314/just.v34i2.5

Arfasa, G. F., Owusu-Sekyere, E., & Doke, D. A. (2023). Predictions of land use/land cover change, drivers, and their implications on water availability for irrigation in the Vea catchment, Ghana. *Geocarto International*, *38*(1). https://doi.org/10.1080/10106049.2023.2243093

Arnold, J. G., Kiniry, J. R., Srinivasan, R., Williams, J. R., Haney, E. B., & Neitsch, S. L. (2012). *Soil & Water Assessment Tool*.

Assfaw, A. T. (2019). Calibration, Validation and Performance Evaluation of Swat Model for Sediment Yield Modelling in Megech Reservoir Catchment, Ethiopia. *Journal of Environmental Geography*, *12*(3–4), 21–31. https://doi.org/10.2478/jengeo-2019-0009

Assfaw, M. T., Neka, B. G., & Ayele, E. G. (2023). Modeling the impact of climate change on streamflow responses in the Kessem watershed, Middle Awash sub-basin, Ethiopia. *Journal of Water and Climate Change*, *14*(12), 4837–4859. https://doi.org/10.2166/wcc.2023.541

Atef, I., Ahmed, W., & Abdel-Maguid, R. H. (2024). Future land use land cover changes in El-Fayoum governorate: a simulation study using satellite data and CA-Markov model. *Stochastic Environmental Research and Risk Assessment*, *38*(2), 651–664. https://doi.org/10.1007/s00477-023-02592-0

Augustsson, A., Gaillard, M., Peltola, P., Bergbäck, B., & Saarinen, T. (2013). *Effects of land use and climate change on erosion intensity and sediment geochemistry at Lake Lehmilampi , Finland*. https://doi.org/10.1177/0959683613484615

Azari, M., Moradi, H. R., Saghafian, B., & Faramarzi, M. (2012). *Modeling Impacts of Climate Change on Stream Flow and Sediment Yield : Implications for Adaptive Measures on Soil and Water Conservation in North of Iran*. 2012.

Azari, M., Moradi, H. R., Saghafian, B., & Faramarzi, M. (2016). Climate change impacts on streamflow and sediment yield in the North of Iran. *Hydrological Sciences Journal*, *61*(1), 123–133. https://doi.org/10.1080/02626667.2014.967695

Azim, F., Shakir, A. S., Habib-ur-Rehman, & Kanwal, A. (2016). Impact of climate change on sediment yield for Naran watershed, Pakistan. *International Journal*

of Sediment Research, *31*(3), 212–219. https://doi.org/10.1016/j.ijsrc.2015.08.002

Azizi, A., Malakmohamadi, B., & Jafari, H. R. (2016). Land use and land cover spatiotemporal dynamic pattern and predicting changes using integrated CA-markov model. *Global Journal of Environmental Science and Management*, *2*(3), 223–234. https://doi.org/10.7508/gjesm.2016.03.002

Barbosa de Souza, K., Rosa dos Santos, A., Macedo Pezzopane, J. E., Machado Dias, H., Ferrari, J. L., Machado de Oliveira Peluzio, T., Toledo, J. V., Freire Carvalho, R. de C., Rizzo Moreira, T., França Araújo, E., Gomes da Silva, R., Pósse Senhorelo, A., Azevedo Costa, G., Duarte Nader Mardeni, V., Horn Kunz, S., & Cordeiro dos Santos, E. (2023). Modeling Dynamics in Land Use and Land Cover and Its Future Projection for the Amazon Biome. *Forests*, *14*(7). https://doi.org/10.3390/f14071281

Based, P., Gharesou, C. S., Nouri, A., Saffari, A., & Karami, J. (2018). *Assessment of Land Use and Land Cover Changes on Soil Erosion Geography & Natural Disasters*. *8*(2). https://doi.org/10.4172/2167-0587.1000222

Basheer, A. K., Lu, H., Omer, A., Ali, A. B., & Abdelgader, A. M. S. (2016). Impacts of climate change under CMIP5 RCP scenarios on the streamflow in the Dinder River and ecosystem habitats in Dinder National Park, Sudan. *Hydrology and Earth System Sciences*, *20*(4), 1331–1353. https://doi.org/10.5194/hess-20-1331-2016

Begou, J. C., Jomaa, S., Benabdallah, S., Bazie, P., Afouda, A., & Rode, M. (2016). Multi-site validation of the SWAT model on the Bani catchment: Model performance and predictive uncertainty. *Water (Switzerland)*, *8*(5). https://doi.org/10.3390/w8050178

Bekele, S., & Abate, B. (2020). Estimation of Sediment Yield using Swat Model: A Case of Soke River Watershed, Ethiopia Estimation of Sediment Yield using Swat Model: A Case of Soke River Watershed, Ethiopia. *International Journal of Engineering, Research & Technology (IJERT)*, *9*(12), 685–695. www.ijert.org

Belay, T., & Mengistu, D. A. (2021). Impacts of land use/land cover and climate changes on soil erosion in Muga watershed, Upper Blue Nile basin (Abay), Ethiopia. *Ecological Processes*, *10*(1). https://doi.org/10.1186/s13717-021-00339-9

Beroho, M., Briak, H., Cherif, E. K., Boulahfa, I., Ouallali, A., Mrabet, R., Kebede, F., Bernardino, A., & Aboumaria, K. (2023). Future Scenarios of Land Use/Land Cover (LULC) Based on a CA-Markov Simulation Model: Case of a Mediterranean Watershed in Morocco. *Remote Sensing*, *15*(4). https://doi.org/10.3390/rs15041162

Betrie, G. D., Mohamed, Y. A., van Griensven, A., & Mynett, A. (n.d.). *Sediment management modelling in the Blue Nile Basin using SWAT model*.

Blake, W. H., Rabinovich, A., Wynants, M., Kelly, C., Nasseri, M., Ngondya, I., Patrick, A., Mtei, K., Munishi, L., Boeckx, P., Navas, A., Smith, H. G., Gilvear, D., Wilson, G., Roberts, N., & Ndakidemi, P. (2018). Soil erosion in East Africa: An interdisciplinary approach to realising pastoral land management change. *Environmental Research Letters*, *13*(12). https://doi.org/10.1088/1748-9326/aaea8b

Bontemps, S., Herold, M., Kooistra, L., van Groenestijn, A., Hartley, A., Arino, O., Moreau, I., & Defourny, P. (2011). *Revisiting land cover observations to address the needs of the climate modelling community*. https://doi.org/10.5194/bgd-8-7713-2011

Bussi, G., Dadson, S. J., Prudhomme, C., & Whitehead, P. G. (2016). Modelling the future impacts of climate and land-use change on suspended sediment transport in the River Thames (UK). *Journal of Hydrology*, *542*, 357–372. https://doi.org/10.1016/j.jhydrol.2016.09.010

C, C. B., & M, O. G. (2024). Effect of temperature and rainfall variability on greater kudu (Tragelaphus strepsiceros) population in Lake Bogoria landscape. In *East African Journal of Science* (Vol. 5, Issue 2).

Camara, M., Jamil, N. R. B., Abdullah, A. F. B., & Hashim, R. B. (2020). Integrating cellular automata Markov model to simulate future land use change of a tropical basin. *Global Journal of Environmental Science and Management*, *6*(3), 403–414. https://doi.org/10.22034/gjesm.2020.03.09

Catchments, P. (2005). *Sediment Yield Modeling Using SWAT Model in Tropical Regions*.

Cavalli, M., Vericat, D., & Pereira, P. (2019). Mapping water and sediment connectivity. *Science of the Total Environment*, *673*(April), 763–767. https://doi.org/10.1016/j.scitotenv.2019.04.071

Chang, Y., Hou, K., Li, X., Zhang, Y., & Chen, P. (2018). Review of Land Use and Land Cover Change research progress. *IOP Conference Series: Earth and Environmental Science*, *113*(1). https://doi.org/10.1088/1755-1315/113/1/012087

Chapman, S., Birch, C. E., Galdos, M. V., Pope, E., Davie, J., Bradshaw, C., Eze, S., & Marsham, J. H. (2021). Assessing the impact of climate change on soil erosion in East Africa using a convection-permitting climate model. *Environmental Research Letters*, *16*(8). https://doi.org/10.1088/1748-9326/ac10e1

Chawanda, C. J., Nkwasa, A., Thiery, W., & Van Griensven, A. (2024). Combined impacts of climate and land-use change on future water resources in Africa.

Hydrology and Earth System Sciences, *28*(1), 117–138. https://doi.org/10.5194/hess-28-117-2024

Chelkeba Tumsa, B. (2023). The Response of Sensitive LULC Changes to Runoff and Sediment Yield in a Semihumid Urban Watershed of the Upper Awash Subbasin Using the SWAT+ Model, Oromia, Ethiopia. *Applied and Environmental Soil Science*, *2023*. https://doi.org/10.1155/2023/6856144

Chen, C. N., Tfwala, S. S., & Tsai, C. H. (2020). Climate change impacts on soil erosion and sediment yield in a watershed. *Water (Switzerland)*, *12*(8). https://doi.org/10.3390/w12082247

Chen, N., Liu, D., & Cao, Z. (2019). Potential impacts of climate change on sediment yield in the Xunhe River basin. *Journal of Soil and Water Conservation*, *74*(3), 209–224. https://doi.org/10.2489/jswc.74.3.209

Chilagane, N. A., Kashaigili, J. J., & Mutayoba, E. (2020). Historical and Future Spatial and Temporal Changes in Land Use and Land Cover in the Little Ruaha River Catchment, Tanzania. *Journal of Geoscience and Environment Protection*, *08*(02), 76–96. https://doi.org/10.4236/gep.2020.82006

Chilagane, N. A., Kashaigili, J. J., Mutayoba, E., Lyimo, P., Munishi, P., Tam, C., & Burgess, N. (2021). Impact of Land Use and Land Cover Changes on Surface Runoff and Sediment Yield in the Little Ruaha River Catchment. *Open Journal of Modern Hydrology*, *11*(03), 54–74. https://doi.org/10.4236/ojmh.2021.113004

Chiphang, N., Golom, T., Bandyopadhyay, A., & Bhadra, A. (2022). Modeling the impact of climate change on sediment yield from an Eastern Himalayan River Basin using ArcSWAT. *Arabian Journal of Geosciences*, *15*(3). https://doi.org/10.1007/s12517-022-09562-w

Clement, M., Mwakalila, S., & Norbert, J. (2016). Implications of Land Use and Climate Change on Water Balance Components in the Sigi Catchment, Tanzania. *Journal of the Geographical Association of Tanzania*, *39*(1), 142–159.

da Fonseca, C. A. B., Al-ansari, N., da Silva, R. M., Santos, C. A. G., Zerouali, B., de Oliveira, D. B., & Elbeltagi, A. (2022). Investigating Relationships between Runoff–Erosion Processes and Land Use and Land Cover Using Remote Sensing Multiple Gridded Datasets. *ISPRS International Journal of Geo-Information*, *11*(5). https://doi.org/10.3390/ijgi11050272

da Silva, M. S., Cavalcante, R. L., E Souza Filho, P. W. M., da Silva Júnior, R. O., Pontes, P. R., Dallagnol, R., & da Rocha, E. J. P. (2021). Comparison of sediment rating curves and sediment yield in subbasins of the itacaiúnas river watershed, eastern amazon. *Revista Brasileira de Recursos Hidricos*, *26*, 1–20. https://doi.org/10.1590/2318-0331.2621202100009

Daba, M. H., & You, S. (2020). Assessment of climate change impacts on river flow regimes in the upstream of awash basin, ethiopia: Based on ipcc fifth assessment report (ar5) climate change scenarios. *Hydrology*, *7*(4), 1–22. https://doi.org/10.3390/hydrology7040098

Daniel, H., & Abate, B. (2022). Effect of climate change on streamflow in the Gelana watershed, Rift valley basin, Ethiopia. *Journal of Water and Climate Change*, *13*(5), 2205–2232. https://doi.org/10.2166/wcc.2022.059

Das, B., Jain, S. K., Thakur, P. K., & Singh, S. (2021). Assessment of climate change impact on the Gomti River basin in India under different RCP scenarios. *Arabian Journal of Geosciences*, *14*(2). https://doi.org/10.1007/s12517-020-06359-7

Ddamulira, R. (2016). Climate change and energy in East Africa. *Development (Basingstoke)*, *59*(3–4), 257–262. https://doi.org/10.1057/s41301-017-0101-1

Dibaba, W. T., Miegel, K., & Demissie, T. A. (2019). Evaluation of the CORDEX regional climate models performance in simulating climate conditions of two catchments in Upper Blue Nile Basin. *Dynamics of Atmospheres and Oceans*, *87*(May), 101104. https://doi.org/10.1016/j.dynatmoce.2019.101104

Djunarsjah, E., Julian, M. M., Putra, A. P., Nusantara, C. A. S., Lubis, N. S., Baskoro, A. A., & Alfandi, N. R. (2023). *Assessing the Impact of Land Use Change and Climate Variability on Soil Erosion Rates in Peusangan Watershed, Aceh Province, Indonesia*. https://doi.org/10.21203/rs.3.rs-3000963/v1

Echogdali, F. Z., Boutaleb, S., Taia, S., Ouchchen, M., Id-Belqas, M., Kpan, R. B., Abioui, M., Aswathi, J., & Sajinkumar, K. S. (2022). Assessment of soil erosion risk in a semi-arid climate watershed using SWAT model: case of Tata basin, South-East of Morocco. *Applied Water Science*, *12*(6). https://doi.org/10.1007/s13201-022-01664-w

Efthimiou, N., Lykoudi, E., & Karavitis, C. (2017). Comparative analysis of sediment yield estimations using different empirical soil erosion models. *Hydrological Sciences Journal*, *62*(16), 2674–2694. https://doi.org/10.1080/02626667.2017.1404068

Egberts, N. (2020). *Analyzing gully erosion in the Lake Manyara catchment–Tanzania*. http://dspace.library.uu.nl/handle/1874/404675%0Ahttp://localhost/handle/1874/404675

Ercan, M. B., Maghami, I., Bowes, B. D., Morsy, M. M., & Goodall, J. L. (2020). Estimating Potential Climate Change Effects on the Upper Neuse Watershed Water Balance Using the SWAT Model. *Journal of the American Water Resources Association*, *56*(1), 53–67. https://doi.org/10.1111/1752-1688.12813

Eriksen, S., O'Brien, K., & Rosentrater, L. (2008). *Climate change in eastern and southern Africa*.

FAO. (2014). *Adapting to climate change through land and water management in Eastern Africa*.

FAO, & UNESCO. (1977). FAO-UNESCO soil map of the world, 1:5000000. Africa. *Fao Soil Bulletin*, *VI*(1), 346.

Feger, K., Universit, T., Schmalz, B., Universit, T., Kapp, G., & Universit, T. (2017). Technische Universität Dresden *Impact of Land Management Practices on Water Balance and Sediment Transport in the Morogoro Catchment , Uluguru Mountains (Tanzania) DISSERTATION to achieve the academic degree Doctor rerum silvaticarum By Dominico Benedic*.

Feyissa Negewo, T., & Kumar Sarma, A. (2022). Evaluation of Climate Change-Induced Impact on Streamflow and Sediment Yield of Genale Watershed, Ethiopia. *The Nature, Causes, Effects and Mitigation of Climate Change on the Environment*, *June*. https://doi.org/10.5772/intechopen.98515

Gadissa, T., Nyadawa, M., Behulu, F., & Mutua, B. (2018). The effect of climate change on loss of lake volume: Case of sedimentation in Central Rift Valley Basin, Ethiopia. *Hydrology*, *5*(4). https://doi.org/10.3390/hydrology5040067

Gassman, P. W., Reyes, M. R., Green, C. H., Arnold, J. G., & Gassman, P. W. (2007). The Soil And Water Assessment Tool: Historical Development, Applications, And Future Research Directions Invited Review Series. *Transactions of the ASABE*, *50*(4), 1211–1250.

Gassman, P. W., & Yingkuan, W. (2015). IJABE SWAT Special Issue: Innovative modeling solutions for water resource problems. *International Journal of Agricultural and Biological Engineering*, *8*(3). https://doi.org/10.3965/j.ijabe.20150803.1763

Gemechu, T. M., Zhao, H., Bao, S., Yangzong, C., Liu, Y., Li, F., & Li, H. (2021). Estimation of hydrological components under current and future climate scenarios in guder catchment, upper Abbay Basin, Ethiopia, using the swat. *Sustainability (Switzerland)*, *13*(17). https://doi.org/10.3390/su13179689

Gemmechis, W. A. (2022). *Land Use Land Cover Dynamics Using CA-Markov Chain Model and Geospatial Techniques: A Case of Belete Gera Regional Forest Priority Area, South Western Ethiopia.* https://doi.org/10.21203/rs.3.rs-1805209/v1

Getachew Abebe, T., & Woldemariam, A. (2024). Erosion spatial distribution mapping and sediment yield estimation using RUSLE and Arc GIS of Ayigebire watershed, North Shewa zone of Amhara region, Ethiopia. *Water-Energy Nexus*, *7*, 124–134. https://doi.org/10.1016/j.wen.2023.12.002

Gharibdousti, S. R., Kharel, G., & Stoecker, A. (2019). Modeling the impacts of agricultural best management practices on runoff, sediment, and crop yield in an agriculture-pasture intensive watershed. *PeerJ*, *2019*(7), 1–24. https://doi.org/10.7717/peerj.7093

Gitima, G., Teshome, M., Kassie, M., & Jakubus, M. (2023). Quantifying the impacts of spatiotemporal land use and land cover changes on soil loss across agroecologies and slope categories using GIS and RUSLE model in Zoa watershed, southwest Ethiopia. *Ecological Processes*, *12*(1). https://doi.org/10.1186/s13717-023-00436-x

Gnitou, G. T., Ma, T., Tan, G., Ayugi, B., Nooni, I. K., Alabdulkarim, A., & Tian, Y. (2019). Evaluation of the rossby centre regional climate model rainfall simulations over west africa using large-scale spatial and temporal statistical metrics. *Atmosphere*, *10*(12), 1–25. https://doi.org/10.3390/ATMOS10120802

Gobry, J. J., Twisa, S. S., Ngassapa, F., & Kilulya, K. F. (2023). Impact of land-use/cover change on water quality in the Mindu Dam drainage, Tanzania. *Water Practice and Technology*, *18*(5), 1086–1098. https://doi.org/10.2166/wpt.2023.067

Gondwe, J. F., Lin, S., & Munthali, R. M. (2021). Analysis of Land Use and Land Cover Changes in Urban Areas Using Remote Sensing: Case of Blantyre City. *Discrete Dynamics in Nature and Society*, *2021*. https://doi.org/10.1155/2021/8011565

Guder, A. C., & Kabeta, W. F. (2025). Evaluation of future land use change impacts on soil erosion for holota watershed, Ethiopia. *Scientific Reports*, *15*(1). https://doi.org/10.1038/s41598-025-91381-6

Guilyardi, E., Lescarmontier, L., Matthews, R., Point, S. P., Rumjaun, anwar bhai, Schlüpmann, J., & Wilgenbus, D. (2018). IPCC special report global warming of 1 . 5 ° C. Summary for teachers coordinator. *ResearchGate*, *December*, 1–24. https://www.ipcc.ch/site/assets/uploads/sites/2/2018/12/ST1.5_OCE_LR.pdf%0Ahttps://www.researchgate.net/publication/332717759

Gulakhmadov, A., Chen, X., Gulahmadov, N., Liu, T., Anjum, M. N., & Rizwan, M. (2020). Simulation of the potential impacts of projected climate change on streamflow in the vakhsh river basin in central Asia under CMIP5 RCP Scenarios. *Water (Switzerland)*, *12*(5). https://doi.org/10.3390/w12051426

Gupta, S. (2015). *Simulating Climate Change Impact on Soil Erosion & Soil Carbon Sequestration*.

Guzman, C. D., Zimale, F. A., Tebebu, T. Y., Bayabil, H. K., Tilahun, S. A., Yitaferu, B., Rientjes, T. H. M., & Steenhuis, T. S. (2017). Modeling discharge and sediment concentrations after landscape interventions in a humid monsoon

climate: The Anjeni watershed in the highlands of Ethiopia. *Hydrological Processes*, *31*(6), 1239–1257. https://doi.org/10.1002/hyp.11092

Gwapedza, D., Nyamela, N., Hughes, D. A., Slaughter, A. R., Mantel, S. K., & van der Waal, B. (2021). Prediction of sediment yield of the Inxu River catchment (South Africa) using the MUSLE. *International Soil and Water Conservation Research*, *9*(1), 37–48. https://doi.org/10.1016/j.iswcr.2020.10.003

Gyamfi, C., Ndambuki, J. M., & Salim, R. W. (2016). Application of SWAT Model to the Olifants Basin: Calibration, Validation and Uncertainty Analysis. *Journal of Water Resource and Protection*, *08*(03), 397–410. https://doi.org/10.4236/jwarp.2016.83033

Haddadchi, A., Hicks, M., Olley, J. M., Singh, S., & Srinivasan, M. S. (2019). Grid-based sediment tracing approach to determine sediment sources. *Land Degradation and Development*, *30*(17), 2088–2106. https://doi.org/10.1002/ldr.3407

Haddadchi, A., Ryder, D. S., Evrard, O., & Olley, J. (2005). *Sediment Fingerprinting in Fluvial Systems : Review of Tracers , Sediment Sources and Mixing Models*. *8212*, 1–25.

Hailu, M. B., Mishra, S. K., & Jain, S. K. (2023). Evaluation of Spatial-Temporal Variation of Soil Loss and Best Conservation Measures in an East Africa Catchment. *Sustainability (Switzerland)*, *15*(10). https://doi.org/10.3390/su15107778

Hallouz, F., Meddi, M., Mahé, G., Alirahmani, S., & Keddar, A. (2018). Modeling of discharge and sediment transport through the SWAT model in the basin of Harraza (Northwest of Algeria). *Water Science*, *32*(1), 79–88. https://doi.org/10.1016/j.wsj.2017.12.004

Haque, M. B., Karmakar, S., Datta, S., Sajid, A. P., Mamun, M. M. A. Al, Hoque, M. E., Hossain, M. M., & Alam, M. S. (2024). Discharge and sediment load modeling using rating curve-based missing data management. *Hydrology Research*, *55*(10), 959–975. https://doi.org/10.2166/nh.2024.165

Haregeweyn, N., Poesen, J., Verstraeten, G., Govers, G., de Vente, J., Nyssen, J., Deckers, J., & Moeyersons, J. (2013). Assessing the performance of a spatially distributed soil erosion and sediment delivery model (WATEM/SEDEM) in northern ethiopia. *Land Degradation and Development*, *24*(2), 188–204. https://doi.org/10.1002/ldr.1121

Himanshu, S. K., Pandey, A., Yadav, B., & Gupta, A. (2019). Evaluation of best management practices for sediment and nutrient loss control using SWAT model. *Soil and Tillage Research*, *192*, 42–58. https://doi.org/10.1016/j.still.2019.04.016

Huon, S., Evrard, O., Gourdin, E., Lefèvre, I., Bariac, T., Reyss, J., Henry, T., Sengtaheuanghoung, O., Ayrault, S., & Ribolzi, O. (2017). *Journal of Hydrology : Regional Studies Suspended sediment source and propagation during monsoon events across nested sub-catchments with contrasted land uses in Laos*. *9*, 69–84.

Huong, H. Le, & Son, N. T. (2020). Response of streamflow and soil erosion to climate change and human activities in nam rom river basin, northwest of vietnam. *Environment and Natural Resources Journal*, *18*(4), 411–423. https://doi.org/10.32526/ennrj.18.4.2020.39

Hussain, F., Nabi, G., Wu, R., Hussain, B., & Abbas, T. (2019). *Parameter evaluation for soil erosion estimation on small watersheds using SWAT model*. *12*(1), 96–108. https://doi.org/10.25165/j.ijabe.20191201.3769

Ijaz, M. A., Ashraf, M., Hamid, S., Niaz, Y., Waqas, M. M., Tariq, M. A. U. R., Saifullah, M., Bhatti, M. T., Tahir, A. A., Ikram, K., Shafeeque, M., & Ng, A. W. M. (2022). Prediction of Sediment Yield in a Data-Scarce River Catchment at the Sub-Basin Scale Using Gridded Precipitation Datasets. *Water (Switzerland)*, *14*(9). https://doi.org/10.3390/w14091480

Imani, R., Ghasemieh, H., & Mirzavand, M. (2014). Determining and Mapping Soil Erodibility Factor (Case Study: Yamchi Watershed in Northwest of Iran). *Open Journal of Soil Science*, *04*(05), 168–173. https://doi.org/10.4236/ojss.2014.45020

IPCC. (2021). AR6 Climate Change 2021: The Physical Science Basis. Chapter 3: Human influence on the climate system. *Ipcc*, *August*, 207. https://www.ipcc.ch/report/ar6/wg1/

J. Kimwaga, R. (2012). Modelling the Impact of Land Use Changes on Sediment Loading Into Lake Victoria Using SWAT Model: A Case of Simiyu Catchment Tanzania. *The Open Environmental Engineering Journal*, *5*(1), 66–76. https://doi.org/10.2174/1874829501205010066

J. Kitalika, Aldo., L. Machunda, Revocatus., C. Komakech, Hans., & N. Njau, Karoli. (2018). Land-Use and Land Cover Changes on the Slopes of Mount Meru-Tanzania. *Current World Environment*, *13*(3), 331–352. https://doi.org/10.12944/cwe.13.3.07

Jacoby, H., Wang, C., Prinn, R., Jacoby, H., Sokolov, A., Wang, C., Xiao, X., Yang, Z., Eckhaus, R., Stone, P., Ellerman, D., Melillo, J., Fitzmaurice, J., Kicklighter, D., Holian, G., & Liu, Y. (1999). *Integrated global system model for climate policy assessment : feedbacks and sensitivity Studies Integrated Global System Model For Climate Policy Assessment: Feedbacks And Sensitivity Studies*. https://www.researchgate.net/publication/37594959

James Shinhu, R. (2024). *The Impacts Of Land Use And Climate Change On Simiyu River Discharge And The Riverine Sediment Dynamics Flowing Towards Lake Victoria*.

Jamshidi, R., Dragovich, D., & Webb, A. A. (2014). Distributed empirical algorithms to estimate catchment scale sediment connectivity and yield in a subtropical region. *Hydrological Processes*, *28*(4), 2671–2684. https://doi.org/10.1002/hyp.9805

Jcu, R. (2016). *Sedimentology and stratigraphy of the late Cenozoic lake beds succession, Rukwa Rift Basin, Tanzania: implications for hydrocarbon prospectivity*.

Jilo, N. B., Gebremariam, B., Harka, A. E., Woldemariam, G. W., & Behulu, F. (2019). Evaluation of the impacts of climate change on sediment yield from the Logiya Watershed, Lower Awash Basin, Ethiopia. *Hydrology*, *6*(3). https://doi.org/10.3390/hydrology6030081

John, E., Bunting, P., Hardy, A., Roberts, O., Giliba, R., & Silayo, D. S. (2020). Modelling the impact of climate change on Tanzanian forests. *Diversity and Distributions*, *26*(12), 1663–1686. https://doi.org/10.1111/ddi.13152

Jones, K., Nowak, A., Berglund, E., Grinnell, W., Temu, E., Paul, B., Renwick, L. L. R., Steward, P., Rosenstock, T. S., & Kimaro, A. A. (2023). Evidence supports the potential for climate-smart agriculture in Tanzania. *Global Food Security*, *36*. https://doi.org/10.1016/j.gfs.2022.100666

K, G. E. (2025). Modeling Spatial and Temporal Dynamics of Land use and Land cover in the Songwe Sub-basin Tanzani, using Cellular Automata Markov Model. *East African Journal of Science*, *6*(2).

Kahimba, C., Sife, A. S., Maliondo, S. M. S., Mpeta, E. J., & Olson, J. (2015). Climate change and food security in Tanzania: analysis of current knowledge and research gaps. *Tanzania Journal of Agricultural Sciences*, *14*(1), 21–33.

Kalisa, D., Majule, A., & Lyimo, J. G. (2013). *African Journal of Agricultural Research Role of wetlands resource utilisation on community livelihoods: The case of Songwe River Basin, Tanzania*. *8*(49), 6457–6467. https://doi.org/10.5897/AJAR09.573

Kang, W., Yang, C. Y., Lee, J., & Julien, P. Y. (2019). Sediment Yield for Ungauged Watersheds in South Korea. *KSCE Journal of Civil Engineering*, *23*(12), 5109–5120. https://doi.org/10.1007/s12205-019-0085-3

Kangalawe, R. Y. M. (2017). Climate change impacts on water resource management and community livelihoods in the southern highlands of Tanzania. *Climate and Development*, *9*(3), 191–201. https://doi.org/10.1080/17565529.2016.1139487

Kanito, D., Bedadi, B., & Feyissa, S. (2023). Sediment yield estimation in GIS environment using RUSLE and SDR model in Southern Ethiopia. *Geomatics, Natural Hazards and Risk*, *14*(1). https://doi.org/10.1080/19475705.2023.2167614

Karakoyun, E., & Kaya, N. (2022). Hydrological simulation and prediction of soil erosion using the SWAT model in a mountainous watershed: a case study of Murat River Basin, Turkey. *Journal of Hydroinformatics*, *24*(6), 1175–1193. https://doi.org/10.2166/hydro.2022.056

Karim, M., Maanan, M., Maanan, M., Rhinane, H., & Rueff, H. (2019). Assessment of water body change and sedimentation rate in Moulay Bousselham wetland , Morocco , using geospatial technologies. *International Journal of Sediment Research*, *34*(1), 65–72. https://doi.org/10.1016/j.ijsrc.2018.08.007

Kashaigili, J. J., & Majaliwa, A. M. (2010). Integrated assessment of land use and cover changes in the Malagarasi river catchment in Tanzania. *Physics and Chemistry of the Earth*, *35*(13–14), 730–741. https://doi.org/10.1016/j.pce.2010.07.030

Kassian, L. M., Tenywa, M., Liwenga, E. T., Dyer, K. W., & Bamutaze, Y. (2017). Implication of climate change and variability on stream flow in Iringa region, Tanzania. *Journal of Water and Climate Change*, *8*(2), 336–347. https://doi.org/10.2166/wcc.2016.238

Khawaldah, H. A., Farhan, I., & Alzboun, N. M. (2020). Simulation and prediction of land use and land cover change using GIS, remote sensing and CA-Markov model. *Global Journal of Environmental Science and Management*, *6*(2), 215–232. https://doi.org/10.22034/gjesm.2020.02.07

Kido, R., Inoue, T., Hatono, M., & Yamanoi, K. (2023). Assessing the impact of climate change on sediment discharge using a large ensemble rainfall dataset in Pekerebetsu River basin, Hokkaido. *Progress in Earth and Planetary Science*, *10*(1). https://doi.org/10.1186/s40645-023-00580-0

Kimario, I. C., Mkonda, M. Y., & Materu, S. F. (2024). Monitoring Land Use and Land Cover Changes in the Lower Mara River Basin, using Google Earth Engine. *East African Journal of Environment and Natural Resources*, *7*(1), 475–493. https://doi.org/10.37284/eajenr.7.1.2223

Kimwaga, R. J., Bukirwa, F., Banadda, N., Wali, U. G., Nhapi, I., & Mashauri, D. A. (2012). Modelling the Impact of Land Use Changes on Sediment Loading Into Lake Victoria Using SWAT Model: A Case of Simiyu Catchment Tanzania. In *The Open Environmental Engineering Journal* (Vol. 5).

Kishiwa, P., Nobert, J., Kongo, V., & Ndomba, P. (2018). Assessment of impacts of climate change on surface water availability using coupled SWAT and WEAP models: Case of upper Pangani River Basin, Tanzania. *Proceedings of the*

International Association of Hydrological Sciences, *378*, 23–27. https://doi.org/10.5194/piahs-378-23-2018

Kolli, M. K., Opp, C., & Groll, M. (2021). Estimation of soil erosion and sediment yield concentration across the Kolleru Lake catchment using GIS. *Environmental Earth Sciences*, *80*(4). https://doi.org/10.1007/s12665-021-09443-7

Krysanova, V., & White, M. (2015). Aperçu des progrès de l'évaluation des ressources en eau avec SWAT. *Hydrological Sciences Journal*, *60*(5), 771–783. https://doi.org/10.1080/02626667.2015.1029482

Kumar, S., Mishra, A., & Raghuwanshi, N. S. (2012). Estimating catchment sediment yield, reservoir sedimentation and reservoir effective life using SWAT Model. *Proceedings of SWAT International Conference*, *April 2015*, 18–20.

Lahunga, P., Luhunga, P., Botai, J., & Kahimba, F. (2016a). Evaluation of the performance of CORDEX regional climate models in simulating present climate conditions of Tanzania. In *Journal of Southern Hemisphere Earth Systems Science* (Vol. 66).

Lahunga, P., Luhunga, P., Botai, J., & Kahimba, F. (2016b). Evaluation of the performance of CORDEX regional climate models in simulating present climate conditions of Tanzania. In *Journal of Southern Hemisphere Earth Systems Science* (Vol. 66).

Lalika, M. C. S., Meire, P., Ngaga, Y. M., & Chang'a, L. (2015). Understanding watershed dynamics and impacts of climate change and variability in the Pangani River Basin, Tanzania. *Ecohydrology and Hydrobiology*, *15*(1), 26–38. https://doi.org/10.1016/j.ecohyd.2014.11.002

Lazaro, B. H., Hagai, M. M., & Mato, R. R. (2023). Effects of Climate Change, Land Use and Land Cover Variability on Green and Blue Water in Wami/Ruvu Basin, Tanzania. *Tanzania Journal of Science*, *49*(1), 250–262. https://doi.org/10.4314/tjs.v49i1.22

Lebeza, T. M., Gashaw, T., Bayabil, H. K., van Oel, P. R., Worqlul, A. W., Dile, Y. T., & Chukalla, A. D. (2024). Performance of specific CMIP6 GCMs for simulating the historical rainfall and temperature climatology of Lake Tana sub-basin, Ethiopia. *Scientific African*, *26*. https://doi.org/10.1016/j.sciaf.2024.e02387

Legates, D. R., & McCabe, G. J. (1999). Evaluating the use of 'goodness-of-fit' measures in hydrologic and hydroclimatic model validation. *Water Resources Research*, *35*(1), 233–241. https://doi.org/10.1029/1998WR900018

Leta, M. K., Demissie, T. A., & Tränckner, J. (2021). Modeling and prediction of land use land cover change dynamics based on land change modeler (Lcm) in nashe

watershed, upper blue nile basin, Ethiopia. *Sustainability (Switzerland)*, *13*(7). https://doi.org/10.3390/su13073740

Leta, M. K., Waseem, M., Rehman, K., & Tränckner, J. (2023). Sediment yield estimation and evaluating the best management practices in Nashe watershed, Blue Nile Basin, Ethiopia. *Environmental Monitoring and Assessment*, *195*(6). https://doi.org/10.1007/s10661-023-11337-z

Lèye, I., Sambou, S., Landing Sané, M., Ndiaye, I., Maria Ndione, D., Kane, S., Diatta, S., Diédhiou, R., & Talla Cissé, M. (2020). Hydrological Modeling of an Ungauged River Basin Using SWAT Model for Water Resource Management Case of Kayanga River Upstream Niandouba Dam. *Journal of Water Resources and Ocean Science*, *9*(1), 29. https://doi.org/10.11648/j.wros.20200901.14

Liping, C., Yujun, S., & Saeed, S. (2018). Monitoring and predicting land use and land cover changes using remote sensing and GIS techniques—A case study of a hilly area, Jiangle, China. *PLoS ONE*, *13*(7). https://doi.org/10.1371/journal.pone.0200493

Loague, K., & Vanderkwaak, J. E. (2002). Simulating hydrological response for the R-5 catchment: Comparison of two models and the impact of the roads. *Hydrological Processes*, *16*(5), 1015–1032. https://doi.org/10.1002/hyp.316

Luhunga, P. M., Kijazi, A. L., Chang'a, L., Kondowe, A., Ng'ongolo, H., & Mtongori, H. (2018). Climate change projections for Tanzania Based on high-resolution regional climate models from the Coordinated Regional Climate Downscaling Experiment (CORDEX)-Africa. *Frontiers in Environmental Science*, *6*(OCT). https://doi.org/10.3389/fenvs.2018.00122

Luo, M., Liu, T., Meng, F., Duan, Y., Frankl, A., Bao, A., & De Maeyer, P. (2018). Comparing bias correction methods used in downscaling precipitation and temperature from regional climate models: A case study from the Kaidu River Basin in Western China. *Water (Switzerland)*, *10*(8). https://doi.org/10.3390/w10081046

Magang, D. S., Ojara, M. A., Yunsheng, L., & King'uza, P. H. (2024). Future climate projection across Tanzania under CMIP6 with high-resolution regional climate model. *Scientific Reports*, *14*(1). https://doi.org/10.1038/s41598-024-63495-w

Mahmood, R., Jia, S., Tripathi, N. K., & Shrestha, S. (2018). Precipitation extended linear scaling method for correcting GCM precipitation and its evaluation and implication in the transboundary Jhelum River basin. *Atmosphere*, *9*(5). https://doi.org/10.3390/atmos9050160

Marco Ndomba, P. (2010). Modelling of Sedimentation Upstream of Nyumba Ya Mungu Reservoir in Pangani River Basin. In *Nile Basin Water Science& Engineering Journal* (Vol. 3).

Marco Ndomba, P., & Mtalo, F. (2016). *The Suitability of SWAT Model in Sediment Yield Modeling for Ungauged Catchments. A Case of Simiyu River Subcatchment, Tanzania African hydrology View project HydroPeak View project*. https://www.researchgate.net/publication/299627818

Marco, P., & van, A. (2011). Suitability of SWAT Model for Sediment Yields Modelling in the Eastern Africa. *Advances in Data, Methods, Models and Their Applications in Geoscience*, *December 2011*. https://doi.org/10.5772/39013

Maref, N., Baahmed, D., Bemmoussat, K., & Mahfoud, Z. (2022). *SWAT model application for sediment yield modeling and parameters analysis in Wadi K'sob (Northeast of Algeria)*.

Marhaento, H., Booij, M. J., & Hoekstra, A. Y. (2018). Hydrological response to future land-use change and climate change in a tropical catchment. *Hydrological Sciences Journal*, *63*(9), 1368–1385. https://doi.org/10.1080/02626667.2018.1511054

Marko, O., Gjoka, K., Shkodrani, N., & Gjipalaj, J. (2023). Climate Change Effect on Soil Erosion in Vjosa River Basin. *Journal of Ecological Engineering*, *24*(2), 92–100. https://doi.org/10.12911/22998993/156831

Masson-Delmotte, V., Zhai, P., Pörtner, H.-O., Roberts, D., Skea, J., Calvo, E., Priyadarshi, B., Shukla, R., Ferrat, M., Haughey, E., Luz, S., Neogi, S., Pathak, M., Petzold, J., Pereira, J. P., Vyas, P., Huntley, E., Kissick, K., Belkacemi, M., & Malley, J. (2019). *Climate Change and Land An IPCC Special Report on climate change, desertification, land degradation, sustainable land management, food security, and greenhouse gas fluxes in terrestrial ecosystems Head of TSU (Operations) IT/Web Manager Senior Administrator*. www.ipcc.ch

Mawasha, T., & Britz, W. (2022). Detecting land use and land cover change for a 28-year period using multi-temporal Landsat satellite images in the Jukskei River catchment, Gauteng, South Africa. *South African Journal of Geomatics*, *11*(1). https://doi.org/10.4314/sajg.v11i1.2

Mbungu, W. B., Easton, Z. M., & Galbraith, J. M. (2016). *Impacts of Land Use and Land Cover Changes , and Climate Variability on Hydrology and Soil Erosion in the Upper Ruvu Watershed , Tanzania*.

Mbungu, W. B., Heatwole, C. D., Chair, ;, Easton, Z. M., Galbraith, J. M., & Sridhar, V. (2016). *Impacts of Land Use and Land Cover Changes, and Climate Variability on Hydrology and Soil Erosion in the Upper Ruvu Watershed, Tanzania*.

McConnell, W. J., Viña, A., Kull, C., & Batko, C. (2015). Forest transition in Madagascar's highlands: Initial evidence and implications. *Land*, *4*(4), 1155–1181. https://doi.org/10.3390/land4041155

Mcnulty, S., Ph, D., Swift, L., Hays, J., Clingenpeel, A., & Predicting, A. (1995). *Predicting Watershed Erosion Production And Over-Land Sediment Transport Using A GIS*. 397–406.

Mdee, O. J. (2015). Spatial distribution of runoff in ungauged catchments in Tanzania. *Water Utility Journal*, *9*, 61–70. http://repository.udom.ac.tz/handle/20.500.12661/2199

Melchioly, S. R. (2021). Effects of Climate Changes on Water Resources: A Case of Mindu Dam in Morogoro Municipality, Tanzania. *Tanzania Journal of Science*, *47*(3), 1252–1265. https://doi.org/10.4314/tjs.v47i3.33

Melesse, A. M., & Abtew, W. (2015). Landscape Dynamics, Soils and Hydrological Processes in Varied Climates. *Landscape Dynamics, Soils and Hydrological Processes in Varied Climates*, 1–839. https://doi.org/10.1007/978-3-319-18787-7

Memarian, H., Balasundram, S. K., Abbaspour, K. C., Talib, J. B., Teh, C., Sung, B., Sood, A. M., Memarian, H., Balasundram, S. K., Abbaspour, K. C., Jamal, B., Memarian, H., Balasundram, S. K., Abbaspour, K. C., Talib, J. B., & Teh, C. (2014). SWAT-based hydrological modelling of tropical land-use scenarios. *Hydrological Sciences Journal – Journal Des Sciences Hydrologiques*, *59*(10), 1808–1829. https://doi.org/10.1080/02626667.2014.892598

Mengistu, A. G., van Rensburg, L. D., & Woyessa, Y. E. (2019). Techniques for calibration and validation of SWAT model in data scarce arid and semi-arid catchments in South Africa. *Journal of Hydrology: Regional Studies*, *25*. https://doi.org/10.1016/j.ejrh.2019.100621

Mengistu, A. G., Woldesenbet, T. A., & Dile, Y. T. (2021). Evaluation of the performance of bias-corrected CORDEX regional climate models in reproducing Baro–Akobo basin climate. *Theoretical and Applied Climatology*, *144*(1–2), 751–767. https://doi.org/10.1007/s00704-021-03552-w

Mfwango, L. H., Ayenew, T., & Mahoo, H. F. (2022). Impacts of climate and land use/cover changes on streamflow at Kibungo sub-catchment, Tanzania. *Heliyon*, *8*(11). https://doi.org/10.1016/j.heliyon.2022.e11285

Miller, B. W., & Doyle, M. W. (2014). Rangeland management and fluvial geomorphology in northern Tanzania. *Geomorphology*, *214*, 366–377. https://doi.org/10.1016/j.geomorph.2014.02.018

Mishra, A. K., & Coulibaly, P. (2009). Developments in hydrometric network design: A review. In *Reviews of Geophysics* (Vol. 47, Issue 2). https://doi.org/10.1029/2007RG000243

Mnyali, E. T., & Materu, S. F. (2021). Analysis of the Current and Future Land Use/Land Cover Changes in Peri-Urban Areas of Dar es Salaam City, Tanzania

using Remote Sensing and GIS Techniques. *Tanzania Journal of Science*, *47*(5), 1622–1636. https://doi.org/10.4314/tjs.v47i5.12

Mollel, G. R., Mulungu, D. M. M., Nobert, J., & Alexander, A. C. (2023). Assessment of climate change impacts on hydrological processes in the Usangu catchment of Tanzania under CMIP6 scenarios. *Journal of Water and Climate Change*, *14*(11), 4162–4182. https://doi.org/10.2166/wcc.2023.542

Morgan, R. P. C., Quinton, J. N., Smith, R. E., Govers, G., Poesen, J. W. A., Chisci, G., & Torri, D. (1998). The EUROSEM Model. In *Modelling Soil Erosion by Water* (pp. 389–398). Springer Berlin Heidelberg. https://doi.org/10.1007/978-3-642-58913-3_29

Moriasi, D. N., Arnold, J. G., Liew, M. W. Van, Bingner, R. L., Harmel, R. D., & Veith, T. L. (1983). Model Evaluation Guidelines For Systematic Quantification Of Accuracy In Watershed Simulations. In *Transactions of the ASABE* (Vol. 50, Issue 3).

Mrad, D., Boukhari, S., Dairi, S., & Djebbar, Y. (2024). Modeling the sediment yield and estimating the best management practices in the Seybouse basin, Northeastern Algeria. *Water Science and Technology*, *89*(6), 1497–1511. https://doi.org/10.2166/wst.2024.067

Msadala, V. C., & Basson, G. R. (2017). Revised regional sediment yield prediction methodology for ungauged catchments in South Africa. *Journal of the South African Institution of Civil Engineering*, *59*(2), 28–36. https://doi.org/10.17159/2309-8775/2017/v59n2a4

Msaghaa, J. J. (2012). *Sediment Yield Modeling and Identification of Erosion Hotspots in Tropical Watersheds: The Case of Upper Ruvu Catchment in Tanzania* [Florida International University]. https://doi.org/10.25148/etd.FI12080633

Mtelela, C. (2018). *Preliminary Sedimentology And Stratigraphy Of The Enigmatic Middle Lake Beds Succession (Pleistocene ?) In The Rukwa Rift Basin , Tanzania*. *44*(1), 75–96.

Mueller-Warrant, G. W., Phillips, C. L., & Trippe, K. M. (2019). Use of SWAT to Model Impact of Climate Change on Sediment Yield and Agricultural Productivity in Western Oregon, USA. *Open Journal of Modern Hydrology*, *09*(02), 54–88. https://doi.org/10.4236/ojmh.2019.92004

Mustefa Abdule, A., Muluneh, A., & Woldemichael, A. (2023). Impact of Climate and Land Use/Cover Changes on Streamflow in Yadot Watershed, Genale Dawa Basin, Ethiopia. *Air, Soil and Water Research*, *16*. https://doi.org/10.1177/11786221231200106

Mutayoba, E., Kashaigili, J. J., Kahimba, F. C., Mbungu, W., & Chilagane, N. A. (2018a). Assessing the Impacts of Land Use and Land Cover Changes on

Hydrology of the Mbarali River Sub-Catchment. The Case of Upper Great Ruaha Sub-Basin, Tanzania. *Engineering*, *10*(09), 616–635. https://doi.org/10.4236/eng.2018.109045

Mutayoba, E., Kashaigili, J. J., Kahimba, F. C., Mbungu, W., & Chilagane, N. A. (2018b). Assessment of the Impacts of Climate Change on Hydrological Characteristics of the Mbarali River Sub Catchment Using High Resolution Climate Simulations from CORDEX Regional Climate Models. *Applied Physics Research*, *10*(5), 61. https://doi.org/10.5539/apr.v10n5p61

Mwalwiba, L. G., Kifanyi, G. E., Mutayoba, E., Ndambuki, J. M., & Chilagane, N. (2023). Assessment of Climate Change's Impacts on River Flows in the Songwe Sub-Basin. *Open Journal of Modern Hydrology*, *13*(02), 141–164. https://doi.org/10.4236/ojmh.2023.132008

Mwalwiba, L. G., Kifanyi, G. E., Mutayoba, E., Ndambuki, J. M., Chilagane, N., & Molla, W. O. (2025). Assessing and mapping sediment yield response under climate projections in Songwe Watershed ,. *Journal of Future Sustainability*, *5*(3), 153–164. https://doi.org/10.5267/j.jfs.2025.8.001

Nachmany, M. (2018). Climate change governance in Tanzania: challenges and opportunities. *London School of Economics and Political Science*, *October*. http://www.lse.ac.uk/GranthamInstitute/wp-content/uploads/2018/10/Climate-change-governance-in-Tanzania-challenges-and-opportunities.pdf

Nagireddy, N. R., Keesara, V. R., Venkata Rao, G., Sridhar, V., & Srinivasan, R. (2023). Assessment of the Impact of Climate Change on Streamflow and Sediment in the Nagavali and Vamsadhara Watersheds in India. *Applied Sciences (Switzerland)*, *13*(13), 1–22. https://doi.org/10.3390/app13137554

Narsimlu, B., Gosain, A. K., Chahar, B. R., Singh, S. K., & Srivastava, P. K. (2015). SWAT Model Calibration and Uncertainty Analysis for Streamflow Prediction in the Kunwari River Basin, India, Using Sequential Uncertainty Fitting. *Environmental Processes*, *2*(1), 79–95. https://doi.org/10.1007/s40710-015-0064-8

Näschen, K., Diekkrüger, B., Leemhuis, C., Seregina, L. S., & van der Linden, R. (2019). Impact of climate change on water resources in the Kilombero Catchment in Tanzania. *Water (Switzerland)*, *11*(4). https://doi.org/10.3390/w11040859

Ndomba, P. M. (2013). Validation of PSIAC Model for Sediment Yields Estimation in Ungauged Catchments of Tanzania. *International Journal of Geosciences*, *04*(07), 1101–1115. https://doi.org/10.4236/ijg.2013.47104

Ndomba, P. M., Mtalo, F. W., & Killingtveit, Å. (2008). A guided SWAT model application on sediment yield modeling in Pangani river basin: Lessons learnt. *Journal of Urban and Environmental Engineering*, *2*(2), 53–62. https://doi.org/10.4090/juee.2008.v2n2.053062

Ndulue, E. L., & Mbajiorgu, C. C. (2018a). Modeling climate and landuse change impacts on streamflow and sediment yield of an agricultural watershed using SWAT. *Agricultural Engineering International: CIGR Journal*, *20*(4), 15–25.

Ndulue, E. L., & Mbajiorgu, C. C. (2018b). *Modeling climate and landuse change impacts on streamflow and sediment yield of an agricultural watershed using SWAT*. http://www.cigrjournal.org

Negussie, K. G., Wyss, D., Knox, N., Vallejo, O. M., Corral-Pazos-de-Provens, E., & Kappas, M. (2022). Evaluating SWAT model for streamflow estimation in the semi-arid Okavango-Omatako catchment, Namibia. *African Journal of Environmental Science and Technology*, *16*(11), 385–403. https://doi.org/10.5897/ajest2022.3155

Neitsch, S. L., Arnold, J. G., Kiniry, J. R., & Williams, J. R. (2011). *COLLEGE OF AGRICULTURE AND LIFE SCIENCES Soil and Water Assessment Tool Theoretical Documentation Version 2009*.

Neverman, A. J., Donovan, M., Smith, H. G., Ausseil, A. G., & Zammit, C. (2023). Climate change impacts on erosion and suspended sediment loads in New Zealand. *Geomorphology*, *427*(January), 108607. https://doi.org/10.1016/j.geomorph.2023.108607

Ngo Thanh, S., Le Huong Vnua, H., Phuong Tran, T., Duc Loc, N., Le Huong, H., & Thanh Son, N. (2020). Application of SWAT model to Assess Land Use and Climate Changes Impacts on Hydrology of Nam Rom River Basin in Vietnam Use of ICT to Assess Climate and Land Use Changes Impacts on Hydrological Responses and Sediment Yield for future Land Use Planning and Sustainable Water Management-A Case Study in the Upper Response of Streamflow and Soil Erosion to Climate Change and Human Activities in Nam Rom River Basin, Northwest of Vietnam ARTICLE INFO ABSTRACT. *Environment and Natural Resources Journal*, *18*(4), 411–423. https://doi.org/10.20944/preprints202001.0362.v1

Nguyen, H. H. (2019). *Modelling effects of land-use and climate changes on catchment streamflow, sediment and nutrient loads by means of alternative and integrated models*.

Nilawar, A. P., & Waikar, M. L. (2019). Impacts of climate change on streamflow and sediment concentration under RCP 4.5 and 8.5: A case study in Purna river basin, India. *Science of the Total Environment*, *650*, 2685–2696. https://doi.org/10.1016/j.scitotenv.2018.09.334

Nkwasa, A., Chawanda, C. J., & van Griensven, A. (2022). Regionalization of the SWAT+ model for projecting climate change impacts on sediment yield: An application in the Nile basin. *Journal of Hydrology: Regional Studies*, *42*. https://doi.org/10.1016/j.ejrh.2022.101152

Nobert, J. (2022). Assessment of the Impact of Climate Change on Stream Flow: The Case of Little Ruaha Catchment, Rufiji Basin, Tanzania. *Tanzania Journal of Science*, *48*(1), 170–184. https://doi.org/10.4314/tjs.v48i1.16

Noel, S. (2014). Climate-resilient development. *Climate Resilience in Development Planning*, 13–22. https://doi.org/10.1787/9789264209503-4-en

Nyatuame, M., Agodzo, S., Amekudzi, L. K., & Mensah-Brako, B. (2023). Assessment of past and future land use/cover change over Tordzie watershed in Ghana. *Frontiers in Environmental Science*, *11*. https://doi.org/10.3389/fenvs.2023.1139264

Ojija, F., Abihudi, S., Mwendwa, B., Leweri, C. M., & Chisanga, K. (2017). The Impact of Climate Change on Agriculture and Health Sectors in Tanzania: A review. *International Journal of Environment, Agriculture and Biotechnology*, *2*(4), 1758–1766. https://doi.org/10.22161/ijeab/2.4.37

Op de Hipt, F., Diekkrüger, B., Steup, G., Yira, Y., Hoffmann, T., Rode, M., & Näschen, K. (2019). Modeling the effect of land use and climate change on water resources and soil erosion in a tropical West African catch-ment (Dano, Burkina Faso) using SHETRAN. *Science of the Total Environment*, *653*, 431–445. https://doi.org/10.1016/j.scitotenv.2018.10.351

Opere, A. O., & Okello, B. N. (2011). *Hydrologic analysis for river Nyando using SWAT*. https://doi.org/10.5194/hessd-8-1765-2011

Opere, A., Omwoyo, A., Mueni, P., & Arango, M. (2019). Impact of climate change on water resources in Eastern Africa. *Hydrology and Water Resources Management in Arid, Semi-Arid, and Tropical Regions*, 199–227. https://doi.org/10.4018/978-1-7998-0163-4.ch010

Osman, M. A. A., Abdel-Rahman, E. M., Onono, J. O., Olaka, L. A., Elhag, M. M., Adan, M., & Tonnang, H. E. Z. (2023). Mapping, intensities and future prediction of land use/land cover dynamics using google earth engine and CA- artificial neural network model. *PLoS ONE*, *18*(7 JULY). https://doi.org/10.1371/journal.pone.0288694

Papa, R., Ali, M., De Kerckhove, D., Deakin, M., Kellerman, A., Levinson, D. M., Malanima, P., Nuzzolo, A., Battarra, R., Anna, R., Rocca, L., & Mazzeo, G. (2015). TeMA Journal of Land Use, Mobility and Environment EDITOR IN-CHIEF EDITORIAL ADVISORY BOARD. In *TeMA Journal of Land Use Mobility and Environment* (Vol. 3). https://www.pexels.com/photo/london-telephone-booth-long-exposure-lights-6618/

Parajuli, P. B., & Risal, A. (2021). Evaluation of climate change on streamflow, sediment, and nutrient load at watershed scale. *Climate*, *9*(11). https://doi.org/10.3390/cli9110165

Pedrosa-Pàmies, R., Parinos, C., Sanchez-Vidal, A., Gogou, A., Calafat, A., Canals, M., Bouloubassi, I., & Lampadariou, N. (2015). Composition and sources of sedimentary organic matter in the deep eastern Mediterranean Sea. *Biogeosciences*, *12*(24), 7379–7402. https://doi.org/10.5194/bg-12-7379-2015

Qi, J., Zhang, X., Yang, Q., Srinivasan, R., Arnold, J. G., Li, J., Waldholf, S. T., & Cole, J. (2020). SWAT ungauged: Water quality modeling in the Upper Mississippi River Basin. *Journal of Hydrology*, *584*. https://doi.org/10.1016/j.jhydrol.2020.124601

Raigani, Z. M., Nosrati, K., & Collins, A. L. (2019). Fingerprinting sub-basin spatial sediment sources in a large Iranian catchment under dry-land cultivation and rangeland farming: Combining geochemical tracers and weathering indices. *Journal of Hydrology: Regional Studies*, *24*(May), 100613. https://doi.org/10.1016/j.ejrh.2019.100613

Rodrigues, A. R., Botequim, B., Tavares, C., Pécurto, P., & Borges, J. G. (2020). Addressing soil protection concerns in forest ecosystem management under climate change. *Forest Ecosystems*, *7*(1). https://doi.org/10.1186/s40663-020-00247-y

Schuller, P., Walling, D. E., Iroumé, A., Quilodrán, C., & Castillo, A. (2021). Quantifying the temporal variation of the contribution of fine sediment sources to sediment yields from Chilean forested catchments during harvesting operations. *Bosque (Valdivia)*, *42*(2), 231–244. https://doi.org/10.4067/s0717-92002021000200231

Selmy, S. A. H., Kucher, D. E., Mozgeris, G., Moursy, A. R. A., Jimenez-Ballesta, R., Kucher, O. D., Fadl, M. E., & Mustafa, A. rahman A. (2023). Detecting, Analyzing, and Predicting Land Use/Land Cover (LULC) Changes in Arid Regions Using Landsat Images, CA-Markov Hybrid Model, and GIS Techniques. *Remote Sensing*, *15*(23). https://doi.org/10.3390/rs15235522

Serdeczny, O., Adams, S., Baarsch, F., Coumou, D., Robinson, A., Hare, W., Schaeffer, M., Perrette, M., & Reinhardt, J. (2017). Climate change impacts in Sub-Saharan Africa: from physical changes to their social repercussions. *Regional Environmental Change*, *17*(6), 1585–1600. https://doi.org/10.1007/s10113-015-0910-2

Serpa, D., Nunes, J. P., Santos, J., Sampaio, E., Jacinto, R., Veiga, S., Lima, J. C., Moreira, M., Corte-Real, J., Keizer, J. J., & Abrantes, N. (2015). Impacts of climate and land use changes on the hydrological and erosion processes of two contrasting Mediterranean catchments. *Science of the Total Environment*, *538*, 64–77. https://doi.org/10.1016/j.scitotenv.2015.08.033

Setegn, S. G., Srinivasan, R., & Dargahi, B. (2008). Hydrological Modelling in the Lake Tana Basin, Ethiopia Using SWAT Model. In *The Open Hydrology Journal* (Vol. 2).

Setti, S., Barik, K. K., & Maheswaran, R. (2024). A Review of Attribution of Land Use and Climate Change on River Hydrology. *Current Agriculture Research Journal*, *12*(2), 498–514. https://doi.org/10.12944/carj.12.2.02

Shemsanga, C., Omambia, A. N., & Gu, Y. (2010). The Cost of Climate Change in Tanzania: Impacts and Adaptations. *Journal of American ScienceJournal of American Science*, *6*(63), 182–196. http://www.americanscience.org

Shinhu, R. J., Amasi, A. I., Wynants, M., Nobert, J., Mtei, K. M., & Njau, K. N. (2023). Assessing the Impacts of Land Use and Climate Changes on River Discharge towards Lake Victoria. *Earth (Switzerland)*, *4*(2), 365–383. https://doi.org/10.3390/earth4020020

Shivhare, N., Dikshit, P. K. S., & Dwivedi, S. B. (2018). A Comparison of SWAT Model Calibration Techniques for Hydrological Modeling in the Ganga River Watershed. *Engineering*, *4*(5), 643–652. https://doi.org/10.1016/j.eng.2018.08.012

Shrestha, B., Babel, M. S., Maskey, S., Griensven, A. Van, Uhlenbrook, S., Green, A., Akkharath, I., Engineering, H., Brussels, V. U., River, M., Secretariat, C., Chak, S., Krom, A., Menachey, K., & Penh, P. (2013). *Impact of climate change on sediment yield in the Mekong River basin : a case study of the Nam Ou basin , Lao PDR*. *2008*, 1–20. https://doi.org/10.5194/hess-17-1-2013

Shrestha, B., Babel, M. S., Maskey, S., van Griensven, A., Uhlenbrook, S., Green, A., & Akkharath, I. (2012). Impact of climate change on sediment yield in the Mekong River Basin: a case study of the Nam Ou Basin, Lao PDR. *Hydrology and Earth System Sciences Discussions*, *9*(3), 3339–3384. https://doi.org/10.5194/hessd-9-3339-2012

Shrestha, N. K., & Wang, J. (2018). Predicting sediment yield and transport dynamics of a cold climate region watershed in changing climate. *Science of the Total Environment*, *625*, 1030–1045. https://doi.org/10.1016/j.scitotenv.2017.12.347

Sigalla, O. Z., Twisa, S., Chilagane, N. A., Mwabumba, M. F., Selemani, J. R., & Valimba, P. (2024). Future Trade-Off for Water Resource Allocation: The Role of Land Cover/Land Use Change. *Water (Switzerland)*, *16*(3). https://doi.org/10.3390/w16030493

Sime, C. H., & Abebe, W. T. (2022). Sediment Yield Modeling and Mapping of the Spatial Distribution of Soil Erosion-Prone Areas. *Applied and Environmental Soil Science*, *2022*. https://doi.org/10.1155/2022/4291699

Sisay, E., Halefom, A., Khare, D., Singh, L., & Worku, T. (2017). Hydrological modelling of ungauged urban watershed using SWAT model. *Modeling Earth Systems and Environment*, *3*(2), 693–702. https://doi.org/10.1007/s40808-017-0328-6

Smetanová, A., Müller, A., Zargar, M., Suleiman, M. A., Gholami, F. R., & Mousavi, M. (2020). Mesoscale mapping of sediment source hotspots for dam sediment management in data-sparse semi-arid catchments. *Water (Switzerland)*, *12*(2). https://doi.org/10.3390/w12020396

Srinivasan, R. (2009). Swat Application: Global Applications. *World*. http://crsps.net/wp-content/downloads/SANREM VT/Documents from SKB for Archive Purposes/4- Scholarly Articles/10-2009-4-1058.pdf#page=18

Srinivasan, R., Santhi, C., Harmel, R. D., & Griensven, A. Van. (2012). *Swat: m*. *55*(4), 1491–1508.

Ssewankambo, G., Kabenge, I., Nakawuka, P., Wanyama, J., Zziwa, A., Bamutaze, Y., Gwapedza, D., Palmer, C. T., Tanner, J., Mantel, S., & Tessema, B. (2023). Assessing soil erosion risk in a peri-urban catchment of the Lake Victoria basin. *Modeling Earth Systems and Environment*, *9*(2), 1633–1649. https://doi.org/10.1007/s40808-022-01565-6

Stone, D. P. (2015). The Intergovernmental Panel on Climate Change (IPCC). *The Changing Arctic Environment*, 307–308. https://doi.org/10.1017/cbo9781316146705.014

Strauch, M., Bernhofer, C., Koide, S., Volk, M., Lorz, C., & Makeschin, F. (2012). Using precipitation data ensemble for uncertainty analysis in SWAT streamflow simulation. *Journal of Hydrology*, *414–415*, 413–424. https://doi.org/10.1016/j.jhydrol.2011.11.014

Sulaiman, S. O., Al-Ansari, N., Shahadha, A., Ismaeel, R., & Mohammad, S. (2021). Evaluation of sediment transport empirical equations: case study of the Euphrates River West Iraq. *Arabian Journal of Geosciences*, *14*(10). https://doi.org/10.1007/s12517-021-07177-1

Tabarestani, E. S., Afzalimehr, H., & Sui, J. (2022). Assessment of Annual Erosion and Sediment Yield Using Empirical Methods and Validating with Field Measurements—A Case Study. *Water (Switzerland)*, *14*(10). https://doi.org/10.3390/w14101602

Tadese, S., Soromessa, T., & Bekele, T. (2021). Analysis of the Current and Future Prediction of Land Use/Land Cover Change Using Remote Sensing and the CA-Markov Model in Majang Forest Biosphere Reserves of Gambella, Southwestern Ethiopia. *Scientific World Journal*, *2021*. https://doi.org/10.1155/2021/6685045

Tekalegn and Diekkrüger. (2017). *Assessing Impacts of Land Use/Cover and Climate Changes on Hydrological Regime in the Headwater Region of the Upper Blue Nile River Basin, Ethiopia*. https://core.ac.uk/download/pdf/226123558.pdf

Tenaw, W. G., Tadesse, K. B., & Kerebih, M. S. (2024). Estimation of Sediment Yield and Evaluation of Management Options in the Watershed Using SWAT Model. *Air, Soil and Water Research*, *17*. https://doi.org/10.1177/11786221241284461

Tesfahunegn, G. B., Tamene, L., & Vlek, P. L. G. (2012). Modeling soil erosion by water using SWAT in northern Ethiopia. In *East African Journal of Science and Technology* (Vol. 2, Issue 1). http://www.eajscience.com

Tessema, N., Kebede, A., & Yadeta, D. (2021). Modelling the effects of climate change on streamflow using climate and hydrological models: the case of the Kesem sub-basin of the Awash River basin, Ethiopia. *International Journal of River Basin Management*, *19*(4), 469–480. https://doi.org/10.1080/15715124.2020.1755301

Theron, S. N., Weepener, H. L., Le Roux, J. J., & Engelbrecht, C. J. (2021). Modelling potential climate change impacts on sediment yield in the Tsitsa river catchment, South Africa. *Water SA*, *47*(1), 67–75. https://doi.org/10.17159/wsa/2021.v47.i1.9446

Tian, P., Mu, X., Liu, J., Hu, J., & Gu, C. (2016). Impacts of Climate Variability and Human Activities on the Changes of Runoff and Sediment Load in a Catchment of the Loess Plateau, China. *Advances in Meteorology*, *2016*. https://doi.org/10.1155/2016/4724067

Tibangayuka, N., Mulungu, D. M. M., & Izdori, F. (2022). Assessing the potential impacts of climate change on streamflow in the data-scarce Upper Ruvu River watershed, Tanzania. *Journal of Water and Climate Change*, *13*(9), 3496–3513. https://doi.org/10.2166/wcc.2022.208

Tikuye, B. G., Ray, R. L., Gebeyehu, K., & Teshome, M. (2024). Assessing the influence of land use/land cover dynamics and climate change on water resources in Upper Blue Nile, Ethiopia. *Journal of Water and Climate Change*, *15*(9), 4745–4774. https://doi.org/10.2166/wcc.2024.319

Toma, M. B., Belete, M. D., & Ulsido, M. D. (2023). Hydrological Components and Sediment Yield Response to Land Use Land Cover Change in The Ajora-Woybo Watershed of Omo-Gibe Basin, Ethiopia. *Air, Soil and Water Research*, *16*. https://doi.org/10.1177/11786221221150186

Tsegaye, L., & Bharti, R. (2021). Soil erosion and sediment yield assessment using RUSLE and GIS-based approach in Anjeb watershed, Northwest Ethiopia. *SN Applied Sciences*, *3*(5). https://doi.org/10.1007/s42452-021-04564-x

Valimba, P. C. (2019). *Development of Improved Characteristic Equations for Lake Rukwa in Tanzania*. *38*(1), 83–96.

Vanmaercke, M., Poesen, J., Broeckx, J., & Nyssen, J. (2014). Sediment yield in Africa. In *Earth-Science Reviews* (Vol. 136, pp. 350–368). Elsevier. https://doi.org/10.1016/j.earscirev.2014.06.004

Walling, D. E., & Collins, A. L. (2005). *Suspended sediment sources in British rivers*. *1*(April).

Worku, T., Khare, D., & Tripathi, S. K. (2017). Modeling runoff–sediment response to land use/land cover changes using integrated GIS and SWAT model in the Beressa watershed. *Environmental Earth Sciences*, *76*(16), 1–14. https://doi.org/10.1007/s12665-017-6883-3

Wynants, M., Patrick, A., Munishi, L., Mtei, K., Bodé, S., Taylor, A., Millward, G., Roberts, N., Gilvear, D., Ndakidemi, P., Boeckx, P., & Blake, W. H. (2021). Soil erosion and sediment transport in Tanzania: Part II – sedimentological evidence of phased land degradation. *Earth Surface Processes and Landforms*, *46*(15), 3112–3126. https://doi.org/10.1002/esp.5218

Xu, M., Dong, X., Yang, X., Chen, X., Zhang, Q., Liu, Q., Id, R. W., Yao, M., Id, T. A. D., & Jeppesen, E. (2017). *Recent Sedimentation Rates of Shallow Lakes in the Middle and Lower Reaches of the Yangtze River : Patterns , Controlling Factors and Implications for Lake Management*. 1–18. https://doi.org/10.3390/w9080617

Xu, Z., Zhang, S., & Yang, X. (2021). Water and sediment yield response to extreme rainfall events in a complex large river basin: A case study of the Yellow River Basin, China. *Journal of Hydrology*, *597*. https://doi.org/10.1016/j.jhydrol.2021.126183

Yao, H., Shi, C., Shao, W., Bai, J., & Yang, H. (2015). Impacts of Climate Change and Human Activities on Runoff and Sediment Load of the Xiliugou Basin in the Upper Yellow River. *Advances in Meteorology*, *2015*. https://doi.org/10.1155/2015/481713

Yeboah, K. A., Akpoti, K., Kabo-bah, A. T., Ofosu, E. A., Siabi, E. K., Mortey, E. M., & Okyereh, S. A. (2022). Assessing climate change projections in the Volta Basin using the CORDEX-Africa climate simulations and statistical bias-correction. *Environmental Challenges*, *6*(August 2021), 100439. https://doi.org/10.1016/j.envc.2021.100439

Yu, Z., Chen, X., & Wu, J. (2022). Calibrating a Hydrological Model in an Ungauged Mountain Basin with the Budyko Framework. *Water (Switzerland)*, *14*(19). https://doi.org/10.3390/w14193112

Zettam, A., Taleb, A., Sauvage, S., Boithias, L., Belaidi, N., & Sánchez-Pérez, J. M. (2017). Modelling hydrology and sediment transport in a semi-arid and anthropized catchment using the swat model: The case of the Tafna River (Northwest Algeria). *Water (Switzerland)*, *9*(3). https://doi.org/10.3390/w9030216

Zhang, S., Li, Z., Hou, X., & Yi, Y. (2019). Impacts on watershed-scale runoff and sediment yield resulting from synergetic changes in climate and vegetation. *Catena*, *179*(April), 129–138. https://doi.org/10.1016/j.catena.2019.04.007

Zhang, X. ke, Fan, J. hui, & Cheng, G. wei. (2015). Modelling the effects of land-use change on runoff and sediment yield in the Weicheng River watershed, Southwest China. *Journal of Mountain Science*, *12*(2), 434–445. https://doi.org/10.1007/s11629-013-2762-x

Zhang, Y., You, Q., Chen, C., & Ge, J. (2016). Impacts of climate change on streamflows under RCP scenarios: A case study in Xin River Basin, China. *Atmospheric Research*, *178–179*, 521–534. https://doi.org/10.1016/j.atmosres.2016.04.018

Zhou, Y., Xu, Y. J., Xiao, W., Wang, J., Huang, Y., & Yang, H. (2017). Climate change impacts on flow and suspended sediment yield in headwaters of high-latitude regions-A case study in China's far Northeast. *Water (Switzerland)*, *9*(12). https://doi.org/10.3390/w9120966

Zimale, Moges, M. A., Alemu, M. L., Ayana, E. K., Demissie, S. S., & Tilahun, S. A. (2016). Calculating the sediment budget of a tropical lake in the Blue Nile basin: Lake Tana. *SOIL Discussions*, *January*, 1–32. https://doi.org/10.5194/soil-2015-84

APPENDICES

Appendix A: Research Proposal Approval Letter

MBEYA UNIVERSITY OF SCIENCE AND TECHNOLOGY

OFFICE OF THE DEPUTY VICE CHANCELLOR - ACCADEMIC, RESEARCH AND CONSULTANCY

DIRECTORATE OF POSTGRADUATE STUDIES, RESEARCH AND PUBLICATIONS

Telephone: +255 (0) 25 2957541/4
Fax: + 255 (0) 25 2957552
E-mail: drp@must.ac.tz
Website: www.must.ac.tz

P.O. Box 131,
Mbeya,
Tanzania.

28th Oct 2025

RE: APPROVAL FOR DATA COLLECTION

Dear Lupakisyo George,

I am pleased to inform you that your research proposal titled "*Modelling the Impacts of Climate Change on Sediment Yield: A Case Study of Songwe Sub Basin, Tanzania*" has been approved for data collection.

You are now authorised to proceed with collecting data in accordance with the approved methodology and ethical guidelines. We wish you success in this final phase of your study and look forward to the timely completion of your research.

MBEYA UNIVERSITY OF SCIENCE AND TECHNOLOGY
DIRECTOR OF POSTGRADUATE STUDIES, RESEARCH AND PUBLICATIONS
P.O.BOX 131 MBEYA

Dr. Fredrick Ojija (PhD)

Director Postgraduate Studies, Research and Publications

CC:

1. Principal- CET
2. HoD-Civil Engineering Department
3. Postgraduate Coordinator-CET
4. HoD-Postgraduate Studies

Appendix B: Journal Published Papers

Journal of Future Sustainability 5 (2025) 153–164

Contents lists available at GrowingScience

Journal of Future Sustainability

homepage: www.GrowingScience.com/jfs

Assessing and mapping sediment yield response under climate projections in Songwe Watershed

Lupakisyo G. Mwalwiba[a*], Gislar E. Kifanyi[a], Edmund Mutayoba[b], Julius M. Ndambuki[c], Nyemo Chilagane[d] and Wilfred O. Molla[e]

[a]*College of Engineering and Technology, Mbeya University of Science and Technology, Mbeya, Tanzania*
[b]*Department of Water Supply and Sanitation Engineering, Water Institute, Dar es Salaam, Tanzania*
[c]*Tshwane University of Technology, Pretoria, South Africa*
[d]*Tanzania Research and Conservation Organization, P.O Box 6873 Morogoro, Tanzania*
[e]*MALK Consultants Limited, P.O Box 2839 Mbeya, Tanzania*

C H R O N I C L E

Article history:
Received: January 10, 2024
Received in revised format: February 21, 2024
Accepted: August 7, 2024
Available online: August 7, 2024

Keywords:
SWAT Model
Sediment
Climate change
Watershed

A B S T R A C T

Climate change creates considerable issues for watershed management, especially in areas prone to erosion and sediment production. The purpose of this study was to examine and map the sediment yield response to future climatic scenarios in the Songwe Watershed. The Soil and Water Assessment Tool (SWAT), which is integrated with Regional Climate Models (RCM) under Representative Concentration Pathways (RCPs) 8.5, was used to evaluate the possible consequences on sediment transport dynamics within the watershed. The simulated results from the four Regional Climate Models (CCLM4, HIRAM5, RACMO22T, and RCA4 RCMs) showed that sediment yields increased for future estimates from 2011 to 2100 under RCP 8.5, owing mostly to increased rainfall and altered hydrological cycles. The results reveal that the average annual sediment yield could increase by 30-50% under RCP 8.5. scenario. Sediment yield mapping highlights crucial hotspots, notably in steep terrain and places with minimal vegetation cover, that are extremely susceptible to erosion, providing useful insights for focused intervention measures. The study emphasized the need for adaptive watershed management methods to counteract the negative effects of climate change on soil erosion and sediment crusade.

1. Introduction

Sediment yield is a critical factor in river basin management, influencing water quality and the longevity of hydraulic structures such as dams and reservoirs. Various factors, including climate, land use, topography, and soil type, affect sediment transport in rivers (Mwalwiba et al., 2023; Ranjan & Mishra, 2023; Santos et al., 2021).With changing climate patterns, it's vital to assess how future conditions might alter sediment yield, particularly in regions prone to soil erosion and sedimentation (Neverman et al., 2023). Numerous studies have explored sediment yield in different watersheds using models like the Soil and Water Assessment Tool (SWAT) to predict future scenarios (Zhang, & Yang, 2021; Tadesse et al., 2024; Zhang et al., 2019). Tanzania and other African countries have experienced significant shifts in precipitation and temperature due to climate change, impacting river flow, soil erosion, sediment movement, and watershed hydrology (Luhunga et al., 2018; Tibangayuka et al., 2022).Tanzania's diverse topography, soil composition, climate changes, and land use dynamics result in significant river flows and sediment discharges (Chilagane et al., 2021; Mfwango et al., 2022; Nilawar & Waikar, 2019). Human activities, such as deforestation and fossil fuel use, contribute to global warming and increasing greenhouse gas levels (Kassian et al., 2017; Ndulue & Mbajiorgu, 2018). The Intergovernmental Panel on Climate Change predicts global warming will reach 1.5 degrees Celsius between 2030 and 2052, with East African temperatures expected to rise by 1-4 degrees Celsius by the 2090s, potentially increasing rainfall by 48% (Guilyardi et al., 2018).

* Corresponding author.
E-mail address: lupakisyog@yahoo.co.uk (L. G. Mwalwiba)

ISSN 2816-8151 (Online) - ISSN 2816-8143 (Print)

doi: 10.5267/j.jfs.2025.8.001

The Songwe Watershed in Tanzania faces pressures from environmental changes and human activities like mining, deforestation, and agriculture(Mwalwiba et al., 2023). Understanding sediment yield response in this watershed is crucial for effective water resource management and sustainable development. Using hydrological models and QGIS, this study assessed and mapped sediment yield under projected climate scenarios for the Songwe Watershed. The research used Regional Climate Models under RCP 8.5 and the SWAT hydrological model to assess sediment yield over three time periods: 2041-2040, 2041-2070, and 2071-2100. Based on simulations of the 2020 land use land cover map and future climatic forecasts, the study found substantial sub-basins prone to soil erosion and sediment yield. The results provide insights into climate change's impact on sediment processes, informing local and global efforts to manage and mitigate these effects on riverine systems. This study highlights the importance of incorporating climate projections into watershed management strategies to address future sediment yield challenges. The detailed maps and data generated provide valuable insights for designing targeted intervention measures, such as reforestation, terracing, and improved agricultural practices, to mitigate erosion and enhance watershed resilience. The research highlighted the necessity for adaptive watershed management practices to preserve the ecological integrity and sustainability of the Songwe Watershed in the face of a changing climate. By combining robust climate projections with sediment yield modeling, this research contributes to a deeper understanding of hydrological responses to climate change and offers a basis for developing resilient watershed management plans.

2. Materials and methods

2.1 Study area

Fig. 1 shows the 10,800-square-kilometer Songwe watershed in eastern Lake Rukwa Basin, southern-western Tanzania. The position is between $07^{0}40'$S and $09^{0}20'$S and $33^{0}00'$E and $33^{0}50'$E(Mwalwiba et al., 2023). The region has many hills that cross fertile valleys at 600–2400 meters above sea level. The watershed has good soils, ample precipitation, temperate temperatures, and excellent agricultural potential. The Songwe watershed is one of Tanzania's most productive. The watershed includes Mbeya City, a major commercial and industrial hub. The watershed has a tropical climate with a protracted rainy season from October to May. A dry season occurs between June and September. The highlands receive 2600mm of yearly precipitation, while the lowlands receive 650mm. Height affects average temperature, which ranges from 16°C to 30°C. The Lupa, Songwe, and Zira rivers drain the Songwe watershed. These rivers divide the watershed into north, middle, and south. In the gold mining zone, rivers converge and discharge into Lake Rukwa after crossing vast, flat plains. All watershed rivers have strong seasonality, with high flows in the rainy season and low flows otherwise. River flows peak in February and March and drop between July and November, with September being the driest.

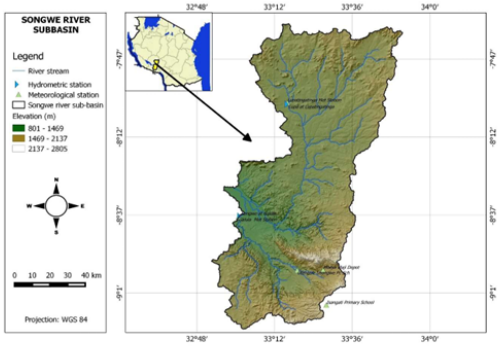

Fig. 1. Map of the study area

2.2 Data used

The Ministry of Water Tanzania's Lake Rukwa Water Basin, office provided the daily streamflow information for the Songwe watershed at Galula station. In this study, a Digital Elevation Model (DEM) with a 30-meter spatial resolution was acquired from the Advanced Land Observing Satellite Phased Array L-band Synthetic Aperture Radar (ALOS PALSAR) (Mwalwiba et al., 2023). This data, available from the Alaska Satellite Facility (ASF) at http://www.asf.alaska.edu, was used to delineate the watershed and analyze its topographic features. Land use and land cover (LULC) LULC data for the year 2020 were downloaded from the United States Geological Survey (USGS) Earth Explorer platform at https://earthexplorer.usgs.gov (Mwalwiba et al., 2023). The data were categorized to match the input requirements of the

SWAT model, providing an accurate representation of the watershed's surface characteristics. Soil information was extracted from the FAO-UNESCO Soil Map of the World, Volume VI, available online at https://swat.tamu.edu/data/. This data was essential for defining soil properties and distribution within the SWAT model.

Data on the everyday rainfall were collected from Lake Rukwa Water Basin office. Additional meteorological parameters, including minimum and maximum temperatures, solar radiation, wind speed, relative humidity, and wind direction, were obtained from the updated Global Weather Database for SWAT (Mwalwiba et al., 2023). Daily streamflow information for the baseline scenario (1981-2005) was provided by the Lake Rukwa Water Basin office for the Lupa tinga tinga and Galula stations (Mwalwiba et al., 2023). This data was crucial for model calibration and validation.

There are eight dominant land use and land cover types in the Songwe watershed as shown in Figure 2. The large area of the watershed is covered by cultivated land 39.35%, bushland 33.42%, and woodland 13.37%. The mountainous area of the sub-basin is covered by woodland, cultivated land, and built-up areas. The land downstream of the sub-basin is cultivated land, bushland, and grassland. The soil type used in this study was extracted from the FAO-UNESCO Soil Map of the World soil database (Mwalwiba et al., 2023). The Songwe watershed contains nine major soil types, Eutric Fluvisol, Chromic Cambisols, Mollic Andosols, Vitric Andosols, Haplic lixisols, Eutric leptosols, Haplic solonetz, Ferralic Cambisol, and Umbric Nitisol.

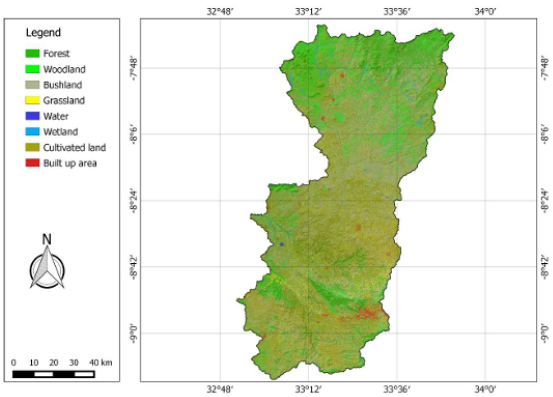

Fig. 2. Land use/cover of Songwe watershed

2.3 SWAT Model

The SWAT Model was used to accomplish this objective. SWAT model is a continuous, long-term, physical-based distributed model developed by Agricultural Research Services of the United States Department of Agriculture to predict the impact of land management practices on water, sediment, and agriculture chemical yields in large and complex watersheds with varying soil, land use, and management conditions over long periods (Akoko et al., 2021). The SWAT model includes a weather engine capable of generating precipitation and other weather parameters for un-gauged watersheds using stochastic (randomly determined) and probabilistic methods (Chilagane et al., 2021). This weather generation relies on global data sets like the CFSR (Climate Forecast System Reanalysis) to ensure accurate weather simulations.

The SWAT model developed by (Mwalwiba et al., 2023) was used to accomplish this study. The model was built on the QGIS 2.6.1 interface, which is an open-source geographic information system. The model incorporates relative humidity, solar radiation, wind speed, and temperature data (both minimum and maximum) from the CFSR Global Weather Data for SWAT (https://swat.tamu.edu/data/cfsr), Rainfall data obtained from the Tanzania Meteorological Agency (TMA), water discharge data from the Songwe sub-basin, specifically at the Galula and Lupa gauging stations, provided by the Lake Ruka Basin Water Office (Mwalwiba et al., 2023).

Modified Universal Soil Loss Equation (MUSLE) was employed to model soil erosion processes. whereas the Bagnold equation was utilized to characterize channel transport(Srinivasan, 2009). Unlike the Universal Soil Loss Equation (USLE), which predicts long-term average annual soil loss, MUSLE can predict sediment yield from individual storm events, making it more suitable for dynamic watershed modeling. The MUSLE sediment model is as follows:

$$Sed = 11.811.8b(Q_{surf}\ x\ q_{peak}\ x\ Area_{HRU})^2\ x\ K_{USLE}\ x\ C_{USLE}\ x\ P_{USLE}\ xLS_{USLE}\ x\ CFRG2$$

where Sed is the sediment yield (metric ton day^{-1}), Qsurf is the surface runoff volume (mm ha^{-1}), peak is the peak runoff rate in m^3 s^{-1}, Area HRU is the area of HRU in ha, KUSLE is the soil erodibility factor, CUSLE is the cover and management factor, PUSLE is the support practice factor, LS is a topographic factor, and CFRG is the course fragment factor, in the universal soil loss equation (USLE).

2.4 Model calibration and simulation analysis

Model calibration and validation to reduce prediction uncertainty were conducted using the Sequential Uncertainty Fitting (SUFI-2) algorithm within the SWAT-CUP framework (Abbaspour et al., 2007). The calibration and validation processes utilized monthly flow data spanning from 1981 to 1992. A five-year warm-up period prior to 1981 was implemented to achieve steady-state conditions and mitigate the impact of unknown initial conditions on the model.

Four objective functions were employed to evaluate the model's performance: Nash-Sutcliffe Efficiency (NSE), Coefficient of Determination (R^2), Probability Bias (PBIAS), and Root Mean Square Error (RSR) (Chilagane et al., 2021; Mazengo et al., 2022). The general performance rating statistics for these objective functions, as suggested by Gyamfi et al., (2016), were used to determine the model's performance. The results of this calibration and validation indicate how well the model simulates the observed data, providing confidence in its predictive capabilities and helping to reduce the uncertainties associated with the model's predictions.

2.5 Scenario analysis

The study utilized climate projections for the Songwe watershed developed by Mwalwiba (2023). The climate projection scenario was created using simulations from four high-resolution regional climate models (RCMs) driven by general circulation models (GCMs) from the Coordinated Regional Climate Downscaling Experiment (CORDEX). These were assessed under two Representative Concentration Pathways (RCP): RCP 4.5 and RCP 8.5. Table 1 lists the RCMs and their respective driving GCMs used in this study. The selected models were previously employed to simulate climate conditions over the southern highlands of Tanzania with relatively minimal errors (Luhunga et al., 2018; Mwalwiba et al., 2023).

A fixed change scenario was employed to assess the influence of climate projections from different regional climate models on soil erosion and sediment yield. In this scenario, the calibrated and validated Soil and Water Assessment Tool (SWAT) model was run with modified climate projection data while maintaining constant physical variables. The impact of the climate projection on soil erosion, sediment yield, and other hydrological components was quantified by comparing SWAT outputs for the four different RCM scenarios: CLM4, HIRAM5, RACMO2T, and RCA4. The simulated sediment yield results for these four RCM scenarios were then compared to determine the sediment yield response under varying climate projections. The study evaluated the impacts of climate change on sediment production in the Songwe watershed by comparing sediment yields between historical (1981–2005) and future periods under the RCP 8.5 scenario (Nilawar & Waikar, 2019; Srinivasan et al, 2023)). The SWAT model's simulations under current subbasin management systems projected sediment yields in response to climate change scenarios.

Table 1
The CORDEX RCMs and their driving GCMs

S/N	RCM	Mode Center	Short name	GCMs
1	DMI HIRHAM5	Denmarks Meteoroliske Institute (DMI), Denmark	HIRHAMS	ICHEC
2	CLMcom COSMO-CLM (CCLM4)	Climate Limited-Area Modelling (CLM) Community	CCLM4	MPI ICHEC CNRM
3	KNMI Regional Atmospheric Climate Model, Version (RACMO2.2T)	Kininklijk Nederlands Meteorologisch Institute (SMHI), Swiden	RACMO99T	ICHEC
4	SMHIRossby Center Regional Atmospheric Model (RCA4)	Sweriges Meteorologiska OchHydrologiska Institut (SMHI), Sweden	RCA4	MPI ICHEC CNRM

3. Results

3.1 Model calibration and validation results

The model calibration and validation results were presented by Mwalwiba (2023). The model showed the goodness of fit with NSE 0.45, R2 0.59, and RSR 0.73 for the calibration period and NSE 0.59, R2 0.59, and RSR 0.64 for the validation period. The curve number (CN2) which indicates the runoff response of a catchment was found to be the most sensitive parameter followed by the Available water capacity of the soil layer (SOL_AWC), the Threshold depth of water in the shallow aquifer required for return flow to occur (GWQMN), Groundwater delay (GW_DELAY) and Groundwater “revap” coefficient (GW_REVAP).

3.2 The influence of different variables on sediment yield generation under the baseline scenario

The sediment output in subbasins covered with bushland and cultivated land is significant, as highlighted by the SWAT model and QGIS analysis. The erosion of farmed land leads to faster depletion of topsoil. Cultivated land contributes 54.94 tons/ha of sediment annually, while bushland contributes 40.6 tons/ha, and grassland on steep slopes contributes 22.91 tons/ha (Tables 2 and 3). In the subbasin, these land uses resulted in an average annual sediment output of 125.61 tons/ha. In the Songwe watershed, historical data indicates that average monthly sediment production peaks in January, February, and March, with estimates of 171.84 tons/ha, 109.4 tons/ha, and 129.04 tons/ha, respectively (Figure 6). Agricultural fields and bushland in the southern, middle, and lower regions of the Songwe subbasin, with soils such as eutric leptosols, eutric fluvisols, vitric andosols, haplic lixisols, and umbric nitisols on steep slopes, are estimated to yield higher sediment (Table 3). Eutric leptosols, being extremely shallow and found on hard rock or unconsolidated, very gravelly materials, are particularly prone to erosion (Tadesse et al., 2024).

The agricultural land and bushland in the Songwe watershed contribute approximately 76.1% of the sediment output. Forest and woodland regions, due to their heavy vegetation cover, do not significantly contribute to sediment output (Table 2)

Table 2
LULC classes contribution to mean annual surface runoff and sediment yield

Land use/cover	Surface runoff (mm)	Sediment yield (t/ha)
Cultivated land	290.43	54.94
Built-up are	179.32	0.29
Woodland	173.97	1.34
Forest	110.54	5.53
Grassland	156.14	22.91
Bushland	145.29	40.60

Table 3
Influence of different variables on sediment yield at sub-basin level

Sub-basin	Coverage (Km2)	Dominant land use	Dominant soil	Slope	Annual mean SYLD (t/ha)
1	389	FRSD	Af3-1-2a-407	3.0-9.0	3.07
2	929	FRST	Ao66-2ab-429	3.0-9.0	5.12
3	359	RNGB	Af3-1-2a-407	3.0-9.0	5.10
4	316	FRST	Ao66-2ab-429	3.0-9.0	5.52
5	349	RNGB	Ao66-2ab-429	3.0-9.0	4.32
6	278	AGRR	Af3-1-2a-407	3.0-9.0	4.13
7	405	RNGB	Ao66-2ab-429	3.0-9.0	3.98
8	503	RNGB	Af3-1-2a-407	3.0-9.0	3.95
9	396	RNGB	Af3-1-2a-407	3.0-9.0	6.62
10	328	AGRR	Nd34-2bc-803	3.0-9.0	19.88
11	207	AGRR	Rd20-2c-932	3.0-9.0	43.43
12	527	AGRR	Tm13-2-3c-945	9.0-25.0	6.97
13	234	RNGB	Rd20-2c-932	3.0-9.0	12.09
14	197	AGRR	Gp6-2-3a-633	3.0-9.0	7.78
15	263	AGRR	Ne43-2-3a-839	3.0-9.0	5.74
16	527	AGRR	Tm13-2-3c-945	9.0-25.0	18.84
17	132	AGRR	Rd20-2c-932	9.0-25.0	97.10
18	196	AGRR	Rd20-2c-932	9.0-25.0	29.96
19	76	AGRR	Af3-1-2a-407	3.0-9.0	7.66
20	208	RNGB	Af3-1-2a-407	0-3.0	2.66
21	407	RNGB	Af3-1-2a-407	0-3.0	3.52
22	101	RNGB	Ao66-2ab-429	3.0-9.0	4.26
23	185	AGRR	Rd20-2c-932	9.0-25.0	94.46
24	31	RNGB	Af3-1-2a-407	0-3.0	3.30
25	5	AGRR	Rd20-2c-932	0-3.0	35.01
26	100	AGRR	Rd20-2c-932	9.0-25.0	41.19
27	141	RNGB	Af3-1-2a-407	0-3.0	3.96
28	137	RNGB	Af3-1-2a-407	3.0-9.0	4.46
29	82	RNGB	Af3-1-2a-407	3.0-9.0	8.38
30	86	AGRR	Af3-1-2a-407	3.0-9.0	17.91

3.3 Spatial distribution of sediment yield under different RCM scenarios

To assess future sediment yields in the watershed, the SWAT model was employed using bias-corrected data from four regional climate models (RCMs): CCLM4, HIRAM5, RACMO22T, and RCA4. These models were used to project sediment yields for the period 2011–2100 under the RCP8.5 scenario, which assumes a high greenhouse gas concentration pathway. The RCP 8.5 scenario reflects the socioeconomic activities within the subbasin, such as intensive agriculture and land use changes, which influence erosion rates (Mwalwiba et al., 2023). Historically, the mean annual sediment output in the Songwe watershed was estimated at 514.58 tons/ha for CCLM4, 411.012 tons/ha for HIRAM5, 203.514 tons/ha for RACMO22T, and 219.3 tons/ha for RCA4 RCMs (Figure 6). The analysis further showed that the months of January,

February, and March exhibited the highest average monthly sediment outputs historically. For the CCLM4 model, these outputs were 171.84 tons/ha, 109.4 tons/ha, and 129.04 tons/ha, respectively. For the HIRAM5 model, the outputs were 122.10 tons/ha, 102.92 tons/ha, and 123.9 tons/ha, respectively. The RACMO22T model indicated outputs of 37.27 tons/ha, 28.76 tons/ha, and 87.78 tons/ha, respectively, while the RCA4 RCMs projected 73.37 tons/ha, 49.96 tons/ha, and 60.97 tons/ha, respectively (Table 4).

The highest increase in future average monthly sediment yield in the 2011 – 2040 period was 32% in February for the HIRAM5, 79.49%,68.96% and 221.85% in April for the CCLM4, RACMO22T, andRCA4 RCMs respectively. For the mid period the future sediment yield increased by 190.51, and 91.84% in February for the CCLM4, and HIRAM5 respectively, 82.37%, and 144.6% in April for the RACMO22T, andRCA4 RCMs respectively. For the last period the future sediment yield increased by 192.57, and 81.47% in February for the CCLM4, and HIRAM5 respectively, 150.74%, and 155.8% in April for the RACMO22T, andRCA4 RCMs respectively (Table 4). According to the results of the SWAT model running under the RCP 8.5 scenario, the Songwe watershed's sediment yields will rise in the future during the rainy season (Figures 6, 7, 8, and 9). The model findings show that, for all future projection periods, the maximum sediment yields were observed in January, February, March, and April (Figs. 7,8 and Fig. 9).

Table 4
Future Sediment yield results under four regional climate models at watershed level

Range	Date	CCLM4	Increase/ Decrease	% + -	HIRAM5	Increase/ Decrease	% + -	RACMO 22T	Increase/ Decrease	% + -	RCA4	Increase/ Decrease	% + -
2011 - 2040	January	138.9	-32.94	-19.17	143.87	+21.77	+17.83	36.24	-1.01	-2.71	107.53	+34.16	+46.56
	February	184.77	+75.37	+68.9	135.9	+32.98	+32	41.92	+13.17	+45.78	98.57	+48.61	+97.3
	March	113.34	-15.7	-12.17	115.56	-8.34	-6.73	37.95	-49.84	-56.77	90.40	+29.43	+48.27
	April	118.95	+52.68	+79.49	47.244	+4.244	+9.87	77.72	+31.72	+68.96	83.17	+57.33	+221.85
2041 - 2070	January	101.45	-70.39	-40.96	166.8	+44.70	+36.61	37.63	+6.4	+1.1	69.29	-4.08	-5.56
	February	317.82	+208.42	+192.57	197.44	+94.52	+91.84	51.61	+22.85	+79.46	97.89	+55.07	+95.94
	March	135.69	+6.65	+5.15	173.93	+50	+40.35	45.22	-42.57	-48.37	55.68	-5.29	-8.68
	April	21.70	-44.57	-67.26	45.81	+2.81	+6.54	83.89	+37.89	+82.37	63.21	+37.37	+144.6
2071 - 2100	January	124.78	-47.06	-27.39	210.97	+88.874	+72.79	44.287	+7.037	+18.89	71.289	-2.08	-2.84
	February	320.07	+210.67	+192.57	186.76	+83.84	+81.47	48.88	+20.13	+68	105.03	+55.07	110.23
	March	59.69	-69.35	-53.74	177.22	+53.32	+43	46.65	-41.14	-46.86	73.77	12.8	21
	April	153.41	+87.13	+131.48	34.86	-8.138	-18.93	115.34	+69.34	+150.74	66.095	40.26	+155.8

The sediment output for the Songwe watershed is highly concentrated in four months, accounting for approximately 78.88% of the annual total. Climate change has significantly impacted the region, leading to high rates of soil erosion and sediment output. The Songwe watershed's sub-basins have been analyzed for future soil erosion hotspots based on predicted average yearly sediment outputs.

From 2011 to 2040, sub-basins 17, 18, and 23 exhibited the highest simulated sediment yield. For 2041 to 2070, the highest yields were found in sub-basins 16, 17, and 23. For 2071 to 2100, sub-basins 16, 17, 18, and 23 showed the highest yields across all four regional climate models (RCMs) (Figure 3, 4 and 5). The highest simulated average sediment yield ranged from 3.7 tons/ha to 12.9 tons/ha in these sub-basins. Moderate sediment yields were observed in sub-basins 11, 12, 13, 14, 15, and 26, located in the upstream southern parts and lowlands of the watershed, areas characterized by agricultural activities, mining, urbanization, and bushlands. Sub-basins in the upstream northern regions, covered by dense forests, showed the lowest sediment yields. Low sediment outputs were strongly correlated with excellent plant cover in these areas. The study on the Songwe watershed using the SWAT Model under the RCP 8.5 scenario reveals significant insights into sediment yields over the 21st century. The predictions are based on four regional climate models (RCMs): CCLM4, HIRAM5, RACMO22T, and RCA4.

The total average annual sediment yields predicted by the SWAT Model under RCP 8.5 were anticipated to be 749.65 tons/ha, 555.85 tons/ha, 210.63 tons/ha, 404.91 for CCLM4, HIRAM5, RACMO22T, and RCA4 RCMs respectively for the years 2011 to 2040, 689.44 tons/ha, 760.87 tons/ha, 235.12 tons/ha, 311.23 tons/ha for CCLM4, HIRAM5, RACMO22T, and RCA4 RCMs respectively for the years 2041 to 2070, and 831.44 tons/ha, 782.17 tons/ha, 286.92 tons/ha, 341.56 tons/ha for CCLM4, HIRAM5, RACMO22T, and RCA4 RCMs respectively for the years 2071 to 2100 (Figure 7, 8 and 9). All four RCMs predict that the greatest sediment yields will occur in January, February, March, and April across all future periods. In contrast, sediment yields during the dry season are predicted to be minimal or nonexistent. According to the findings, sediment yields increased by 45.68%, 35.24%, 3.5%, 84.64% for CCLM4, HIRAM5, RACMO22T, and RCA4 RCMs respectively between 2011 and 2040, 34%, 85.12%, 15.53%, 41.92% for CCLM4, HIRAM5, RACMO22T, and RCA4 RCMs respectively between 2041 and 2070, and 61.58%, 112.2%, 40.99%, 51.19% between 2071 and 2100 under RCP 8.5. These predictions indicate a notable increase in sediment yields under the RCP 8.5 scenario, particularly

during the wet season months. The data show significant variability among the different RCMs, underscoring the potential impacts of climate change on sediment transport in the Songwe watershed.

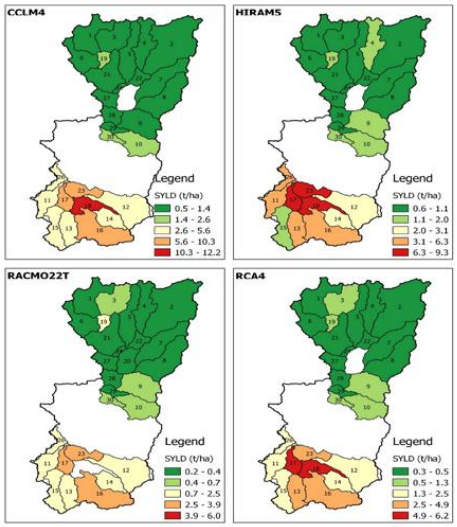

Fig. 3. Spatial distribution of sediment yield map under RCM – RCP8.5 scenario (2011 – 2040)

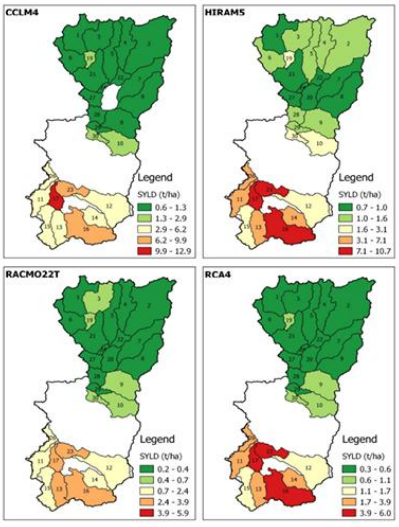

Fig. 4. Spatial distribution of sediment yield under RCM – RCP 8.5 scenario (2041 – 2070)

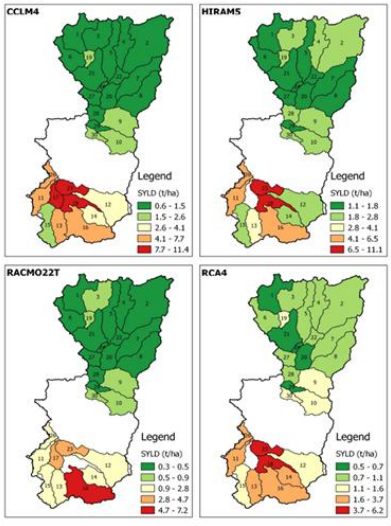

Fig. 5. Spatial distribution of sediment yield under RCM – RCP 8.5 scenario (2071 – 2100)

160

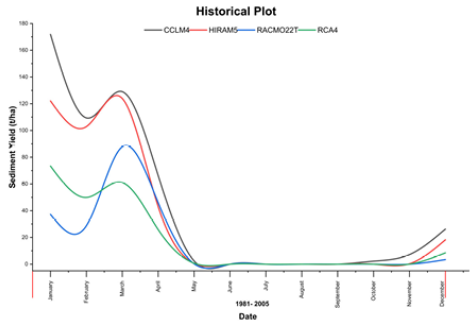

Fig. 6. Spatial distribution of monthly sediment yield under RCM scenario (1981 – 2005)

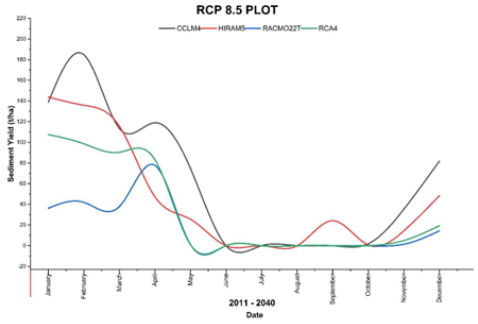

Fig. 7. Spatial distribution of monthly sediment yield under RCM – RCP 8.5 scenario (2011– 2040)

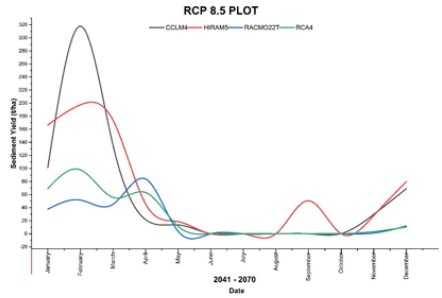

Fig. 8. Spatial distribution of monthly sediment yield under RCM – RCP 8.5 scenario (2041 – 2070)

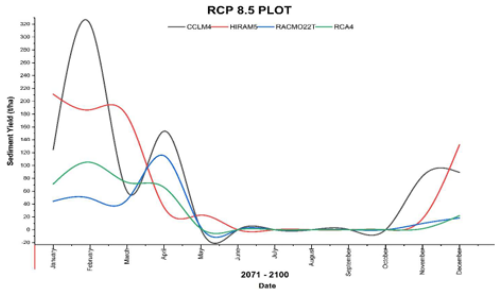

Fig. 9. Spatial distribution of monthly sediment yield under RCM – RCP 8.5 scenario (2071 – 2100)

4. Discussion

Mwalwiba's (2023) study provides a thorough examination of the calibration and validation of hydrological models, with particular attention paid to important performance indicators like the Ratio of the Root Mean Square Error to the Standard Deviation of the Measured Data (RSR), the Coefficient of Determination (R^2), and the Nash-Sutcliffe Efficiency (NSE). The findings show a reasonable degree of predictive performance, which offers important information about how well the model can replicate the hydrological processes in catchments. The prediction accuracy and dependability of the model are revealed by the performance metrics during both the calibration and validation phases. The model appears to have a moderate capacity for prediction during the calibration phase, based on the NSE value of 0.45. During the calibration phase, the model explains around 59% of the variance in the observed runoff data, according to an R2 value of 0.59. This points to the possible need for further improvement while also indicating a reasonable correlation between the simulated and observed values. With an RSR value of 0.73, the observed data's standard deviation is 73% of the RMSE, indicating a significant degree of error in the model's predictions. A large variance is indicated by an RSR value near 0.7, but it is within tolerable bounds for early modeling attempts. During the validation period, the NSE improved to 0.59, indicating improved predicted accuracy and model reliability. This improvement suggests that the post-calibration model tweaks were successful in improving the model's representation of the watershed area's hydrological processes. The R2 value of 0.59 during validation shows a persistent degree of correlation between observed and predicted values, which is consistent with the calibration period. This consistency highlights the applicability and dependability of the model. The parameters that have a substantial impact on the model's performance are identified by the sensitivity analysis carried out as part of Mwalwiba's study. It is essential to comprehend how these factors affect the model's output in order to improve and optimize the model for use in the future. The most sensitive metric was shown to be the CN2, which represents a catchment's runoff reaction. This sensitivity emphasizes how crucial a role it plays in affecting the formation of surface runoff and emphasizes how crucial precise CN2 estimation is for model calibration. River flow and sediment output forecasts are greatly impacted by antecedent moisture conditions, soil types, and changes in land use, according to the CN2. As a result, increasing the accuracy of data pertaining to these variables might enhance model performance. Its effect on the model's capacity to replicate soil moisture dynamics and water availability for plant uptake is shown by the SOL_AWC. Predictions of river flow, sediment production, and groundwater recharge depend on the accurate modeling of soil qualities and water retention traits, which are essential for evapotranspiration and infiltration processes.

Based on the SWAT model and QGIS analysis, the sediment yield in the Songwe watershed provides important insights into the dynamics of soil erosion and sedimentation under various land cover types. With an annual input of 54.94 tons/ha, farmed land is the largest contributor to sediment yield. The amount of time that rain and wind may erode soil is increased by frequent tilling and insufficient cover crops. Fertilizer and pesticide applications in the watershed erode the structure of the soil and increase its susceptibility to erosion. Soil loss is also exacerbated by the absence of cover crops, contour farming, or terracing. Bushland is a major source of sediment, contributing 40.6 tons/ha yearly. Although there is some plant cover in bushland, it is not dense enough to completely protect the soil. Slope-facing grassland adds 22.91 tons of silt per hectare each year. The possibility for erosion is increased by the slope angle, which also speeds up water flow. Grass roots are not strong or deep enough to keep the soil in place when water moves quickly. Because of their lush vegetation, forest and woodland regions contribute the least amount of silt. Rainfall is captured, lessening its immediate effect on soil erosion. The historical average monthly sediment production of the Songwe watershed was estimated to be higher in January, February, and March (171.84 tons/ha, 109.4 tons/ha, and 129.04 tons/ha, respectively). The peak months line up with the rainy season, which raises sediment output in watersheds, soil erosion, and river flow. Planting and farming at certain times of the year may expose more soil to erosion. Higher sediment yields are found in the watershed's Southern, Middle, and Lower Regions as a result of a mix of steep slopes, intensive farming methods, and soil types such eutric leptosols that are prone to erosion. Extremely shallow and prone to soil erosion, eutric leptosol soils can be found in unconsolidated, highly gravelly materials or scattered over hard rocks (Tadesse et al.,2023). High sediment production is most often due to a lack of vegetation, poor land management, and intensive agriculture activities. The study indicates sub-basins 16, 17, 18, and 23 as potential soil erosion hotspots, with the largest sediment production. Intensive agriculture, mining, urbanization, and wildland areas are more prone to erosion due to diminished vegetation cover and increased surface runoff. In contrast, sub-basins with extensive forest

The results of this work, which used the SWAT model with bias-corrected data from four RCMs (CCLM4, HIRAM5, RACMO22T, and RCA4) under the RCP8.5 scenario, provide a detailed knowledge of sediment yield dynamics in the Songwe watershed from 2011 to 2100. Our findings show considerable differences in sediment yield forecasts between RCMs, emphasizing the relevance of model selection and bias correction in hydrological investigations. The study's forecasts show a large rise in sediment yields throughout the twenty-first century, particularly during the wet season months of January, February, March, and April. This is constant across all RCMs, demonstrating the impact of increased rainfall and land use changes on erosion processes. The larger sediment yields during the wet season are most likely due to increased rainfall intensity, which causes more surface runoff and erosion. Because sediment transport is so closely tied to precipitation patterns, soil conservation activities should be concentrated during these months. This emphasizes the significance of including climate change scenarios in hydrological models to better anticipate future erosion dynamics. The sediment yield forecasts for the Songwe watershed show a significant rise over three future periods: 2011-2040, 2041-2070, and 2071-2100. Sediment yields are much larger under the RCP 8.5 scenario than they are today, demonstrating a direct association with the expected climate changes. These patterns indicate a large rise in sediment production, particularly during the rainy season, emphasizing the importance of adaptive management measures to limit the effects on the watershed. The seasonal patterns in sediment output show that the majority of sediment transport takes place during the wet months of January, February, March, and April. This is constant across all RCMs and time periods, implying that heavy rainfall and runoff during these months contribute significantly to sediment displacement. During the dry season, however, sediment outputs are small or nonexistent, reflecting the lower precipitation and runoff that are typical of these months. This seasonal trend implies that peak sediment yields occur during the wettest months, underscoring the importance of precipitation in driving erosion processes in the region. The disparities between models may also be due to variances in the geographical and temporal resolution of climatic data, soil properties, and land use changes reflected by each model.

The examination of sediment yield from 2011 to 2100 demonstrates considerable temporal variations throughout the watershed. Initially, from 2011 to 2040, subbasins 17, 18, and 23 had the highest sediment yields. This pattern shifted slightly in the mid-century era (2041–2070), with sub-basins 16, 17, and 23 showing elevated yields, and then expanded to encompass sub-basin 18 by the end of the century (2071–2100). These patterns indicate that sediment yield hotspots are changing, possibly due to climate-induced changes in rainfall intensity and distribution, which are known to have a direct impact on erosion and sediment transport mechanisms. High sediment production is concentrated in various subbasins, most notably 16, 17, 18, and 23. These places appear to be particularly prone to erosion, potentially due to a combination of steep slopes, soil type, and land use practices that increase sediment mobilization. The highest sediment yields, which ranged from 3.7 to 12.9 tons/ha, show the importance of tailored erosion control strategies in these sensitive sites. Moderate sediment production in subbasins 11, 12, 13, 14, 15, and 26 are associated with agricultural activities, mining, urbanization, and bushlands. These land activities often disrupt the soil and reduce plant cover, resulting in increased sediment runoff. Agricultural operations, in example, can considerably increase sediment outputs through soil tillage, deforestation for farmland expansion, and poor land management. Mining activities disturb the soil structure and contribute to increased silt flow into waterways. The upstream northern subbasins with thick forest cover had the lowest sediment production. The substantial association between low sediment discharges and high plant cover highlights trees' importance in soil stabilization and erosion reduction. Simulated sediment yield patterns have significant consequences for watershed management. High-yield areas, notably sub-basins 16, 17, 18, and 23, should be prioritized for erosion control measures such as reforestation, terracing, and the adoption of sustainable agriculture methods. These techniques can help reduce sediment production, preserve soil

fertility, and safeguard downstream water quality. Our findings are consistent with prior research that has emphasized the impact of climate change and land use practices on sediment dynamics in tropical watersheds. Similar studies in other African basins have found similar results, with greater precipitation and warmth under high emission scenarios leading to higher sediment production (Gyamfi et al., 2021; Leta et al., 2023).

5. Conclusions and Recommendations

The study of sediment yield in the Songwe Watershed under various climate forecasts demonstrates a strong relationship between climate change and sediment yield. The expected increases in temperature and precipitation variability contribute to higher erosion rates, which leads to increased sediment production. The sensitivity of sediment output to climate projections emphasizes the necessity of knowing regional hydrological systems and how they interact with climate change. The use of several climate models and scenarios emphasizes the uncertainty involved in estimating sediment output under future climate circumstances. However, models consistently forecast an increase in extreme weather events, such as heavy rainfall, which worsens soil erosion and sediment transport. The study stresses the need of region-specific climate models in effectively representing local climatic fluctuations and their effects on sediment movements. Land use and cover changes in the Songwe Watershed have a substantial impact on sediment output. Deforestation, agricultural development, and urbanization make soil more susceptible to erosion. The interaction between land use changes and climate forecasts increases sediment yield, emphasizing the importance of sustainable land management techniques in sediment mitigation. The Songwe Watershed's hydrological response to climate forecasts implies changing flow regimes, which may have implications for water resource management. Increased sedimentation has an impact on water quality, reservoir capacity, and aquatic ecosystems, providing issues for downstream communities who rely on these resources.

Understanding sediment yield response under climate change scenarios is critical for sustainable water resource management in the Songwe Watershed. According to the findings, sedimentation will continue to affect water infrastructure, agricultural output, and ecosystem health unless adequate actions are implemented. To counteract the effects of increased sediment output, it is critical to undertake soil conservation methods such as contour farming, terracing, and reforestation. These methods help to stabilize the soil, prevent erosion, and improve water infiltration, hence limiting sediment transport. Promoting climate-resilient agriculture methods like agroforestry and conservation tillage can help prevent soil erosion and increase soil health. Encouraging farmers to implement these methods through education and incentives will be critical to lowering sediment yield.

Acknowledgements

This research did not receive any specific fund from funding agencies in the public, commercial, or not-for-profit sectors. This paper is the outcome of a research project supported by the Mbeya University of Science and Technology Research Fund through post-graduate studies.

References

Abbaspour, K. C., Yang, J., Maximov, I., Siber, R., Bogner, K., Mieleitner, J., … Srinivasan, R. (2007). Modeling hydrology and water quality in the pre-alpine/alpine Thur watershed using SWAT. *Journal of Hydrology*, *333*(2–4), 413–430. https://doi.org/10.1016/j.jhydrol.2006.09.014

Akoko, G., Le, T. H., Gomi, T., & Kato, T. (2021). A review of swat model application in Africa. *Water (Switzerland)*, *13*(9). https://doi.org/10.3390/w13091313

Chilagane, N. A., Kashaigili, J. J., Mutayoba, E., Lyimo, P., Munishi, P., Tam, C., & Burgess, N. (2021). Impact of Land Use and Land Cover Changes on Surface Runoff and Sediment Yield in the Little Ruaha River Catchment. *Open Journal of Modern Hydrology*, *11*(03), 54–74. https://doi.org/10.4236/ojmh.2021.113004

Guilyardi, E., Lescarmontier, L., Matthews, R., Point, S. P., Rumjaun, anwar bhai, Schlüpmann, J., & Wilgenbus, D. (2018). IPCC special report global warming of 1 . 5 ° C. Summary for teachers coordinator. *ResearchGate*, (December), 1–24. Retrieved from https://www.ipcc.ch/site/assets/uploads/sites/2/2018/12/ST1.5_OCE_LR.pdf%0Ahttps://www.researchgate.net/publication/332717759

Gyamfi, C., Ndambuki, J. M., & Salim, R. W. (2016). Application of SWAT Model to the Olifants Basin: Calibration, Validation and Uncertainty Analysis. *Journal of Water Resource and Protection*, *08*(03), 397–410. https://doi.org/10.4236/jwarp.2016.83033

Kassian, L. M., Tenywa, M., Liwenga, E. T., Dyer, K. W., & Bamutaze, Y. (2017). Implication of climate change and variability on stream flow in Iringa region, Tanzania. *Journal of Water and Climate Change*, *8*(2), 336–347. https://doi.org/10.2166/wcc.2016.238

Leta, M. K., Waseem, M., [illegible] (2023). [illegible] management practices in Nashe watershed, Blue Nile Basin, Ethiopia. *Environmental Monitoring and Assessment*, *195*(6). https://doi.org/10.1007/s10661-023-11337-z

Luhunga, P. M., Kijazi, A. L., Chang'a, L., Kondowe, A., Ng'ongolo, H., & Mtongori, H. (2018). Climate change projections for Tanzania Based on high-resolution regional climate models from the Coordinated Regional Climate Downscaling Experiment (CORDEX)-Africa. *Frontiers in Environmental Science*, *6*(OCT), 1–20. https://doi.org/10.3389/fenvs.2018.00122

Mazengo, M., Kifanyi, G. E., Mutayoba, E., & Chilagane, N. (2022). Modeling Surface Water Availability for Irrigation Development in Mbarali River Sub-Catchment Mbeya, Tanzania. *Journal of Geoscience and Environment Protection*, *10*(04), 1–14. https://doi.org/10.4236/gep.2022.104001

Mfwango, L. H., Ayenew, T., & Mahoo, H. F. (2022). Impacts of climate and land use/cover changes on streamflow at Kibungo sub-catchment, Tanzania. *Heliyon*, *8*(11), e11285. https://doi.org/10.1016/j.heliyon.2022.e11285

Mwalwiba, L. G., Kifanyi, G. E., Mutayoba, E., Ndambuki, J. M., & Chilagane, N. (2023). Assessment of Climate Change's Impacts on River Flows in the Songwe Sub-Basin. *Open Journal of Modern Hydrology*, *13*(02), 141–164. https://doi.org/10.4236/ojmh.2023.132008

Nagireddy, N. R., Keesara, V. R., Venkata Rao, G., Sridhar, V., & Srinivasan, R. (2023). Assessment of the Impact of Climate Change on Streamflow and Sediment in the Nagavali and Vamsadhara Watersheds in India. *Applied Sciences (Switzerland)*, *13*(13), 1–22. https://doi.org/10.3390/app13137554

Ndulue, E. L., & Mbajiorgu, C. C. (2018). Modeling climate and land use change impacts on streamflow and sediment yield of an agricultural watershed using SWAT. *Agricultural Engineering International: CIGR Journal*, *20*(4), 15–25.

Neverman, A. J., Donovan, M., Smith, H. G., Russell, A. G., & Zammit, C. (2023). Climate change impacts erosion and suspended sediment loads in New Zealand. *Geomorphology*, *427*(January), 108607. https://doi.org/10.1016/j.geomorph.2023.108607

Nilawar, A. P., & Waikar, M. L. (2019). Impacts of climate change on streamflow and sediment concentration under RCP 4.5 and 8.5: A case study in Purna river basin, India. *Science of the Total Environment*, *650*, 2685–2696. https://doi.org/10.1016/j.scitotenv.2018.09.334

Ranjan, R., & Mishra, A. (2023). Climate change impacts streamflow and suspended sediment load in the flood-prone river basin. *Journal of Water and Climate Change*, *14*(7), 2260–2276. https://doi.org/10.2166/wcc.2023.037

Santos, J. Y. G. dos, Montenegro, S. M. G. L., Silva, R. M. da, Santos, C. A. G., Quinn, N. W., Dantas, A. P. X., & Ribeiro Neto, A. (2021). Modeling the impacts of future LULC and climate change on runoff and sediment yield in a strategic basin in the Caatinga/Atlantic forest ecotone of Brazil. *Catena*, *203*. https://doi.org/10.1016/j.catena.2021.105308

Srinivasan, R. (2009). Swat Application: Global Applications. *World*. Retrieved from http://crsps.net/wp-content/downloads/SANREM VT/Documents from SKB for Archive Purposes/4- Scholarly Articles/10-2009-4-1058.pdf#page=18

Tibangayuka, N., Mulungu, D. M. M., & Izdori, F. (2022). Assessing the potential impacts of climate change on streamflow in the data-scarce Upper Ruvu River watershed, Tanzania. *Journal of Water and Climate Change*, *13*(9), 3496–3513. https://doi.org/10.2166/wcc.2022.208

Xu, Z., Zhang, S., & Yang, X. (2021). Water and sediment yield response to extreme rainfall events in a complex large river basin: A case study of the Yellow River Basin, China. *Journal of Hydrology*, *597*(September 2020), 126183. https://doi.org/10.1016/j.jhydrol.2021.126183

Zewde, N. T., Denboba, M. A., Tadesse, S. A., & Getahun, Y. S. (2024). Predicting runoff and sediment yields using soil and water assessment tool (SWAT) model in the Jemma Subbasin of Upper Blue Nile, Central Ethiopia. *Environmental Challenges*, *14*(December 2023), 100806. https://doi.org/10.1016/j.envc.2023.100806

Zhang, S., Li, Z., Hou, X., & Yi, Y. (2019). Impacts on watershed-scale runoff and sediment yield resulting from synergetic changes in climate and vegetation. *Catena*, *179*(April), 129–138. https://doi.org/10.1016/j.catena.2019.04.007

EISSN: 2707-0425

East African Journal of Science, Technology and Innovation, Vol. 6 (2): March 2025

Modeling Spatial and Temporal Dynamics of Land use and Land cover in the Songwe Sub-basin, Tanzania, using Cellular Automata Markov Model

[1*]*MWALWIBA L*, [1]*GISLAR E. K*, [2]*MUTAYOBA E*, [3]*NDAMBUKI J*, [4]*NYEMO C*

[1]Mbeya University of Science and Technology, Tanzania
[2]***Department of Water Supply and Sanitation Engineering, Water Institute, Dar es Salaam, Tanzania***
[3]***Tshwane University of Technology, Pretoria, South Africa***
[4]***Tanzania Research and Conservation Organization, P.O Box 6873 Morogoro, Tanzania***

***Corresponding Author**: lupakisyog@yahoo.co.uk*

Abstract

Using the Cellular Automata (CA) Markov Model in combination with Geographic Information System (GIS) and Remote Sensing (RS) technologies, this study examines the spatial and temporal dynamics of land use and land cover (LULC) in the Songwe sub-basin, Tanzania. By combining historical data spanning from 1990 to 2020 at a spatial resolution of 30 meters, the study aims to forecast future LULC changes up to the year 2100. GIS technologies made it easier to spatially analyze and visualize these changes, and LULC data was used to calibrate the CA-Markov model with transition probabilities taken from the historical era. The results highlight significant land use transitions, with significant transitions from woodland and natural vegetation to agricultural land and urban areas. These changes are largely driven by population growth and the rising demand for food production. Forest cover and woodland areas have notably decreased by 54.01% and 59.10%, respectively, while agricultural land has increased by 216.97%. Projections indicate that by 2100, forests and woodlands will largely disappear, being replaced by agricultural land. Additionally, significant reductions in wetlands and water bodies are expected. Rapid urbanization is anticipated to intensify the degradation of natural ecosystems, leading to further strain on hydrological systems. The study recommends the implementation of stronger conservation policies, including the expansion of protected areas for vital habitats, and the promotion of sustainable agricultural practices such as agroforestry and conservation tillage. To enhance long-term ecological resilience, the study also emphasizes the need for ecosystem-based management approaches that prioritize water resource preservation and biodiversity. Additionally, involving local communities in land management decisions is crucial for ensuring the sustainability of natural resources and ecosystem services in the Songwe sub-basin.

Keywords: *Cellular Automata -Markov model; Landsat images; Land use land cover change; Spatial and temporal dynamics; Remote sensing*

Received: 16/08/24
Accepted: 11/03/25
Published: 28/03/25

Cite as, *Mwalwiba (2025)*. Modeling Spatial and Temporal Dynamics of Land use and Land cover in the Songwe Sub-basin Tanzani, using Cellular Automata Markov Model. *East African Journal of Science, Technology and Innovation 6(2).*

Introduction

Sustainable development is dependent on the preservation of environmental sustainability, which is endangered by changes in land use and land cover (LULC) (Dammag *et al.,* 2023). LULC refers to the way in which the Earth's surface is utilized by humans, such as for agriculture, urban development, forestry, or conservation, as well as the natural cover of the land, such as forests, grasslands, and wetlands (Dammag *et al.,* 2023). LULC alterations are among the most significant land surface modifications, with far-reaching implications for ecosystems and environmental processes. These changes impact hydrology, soil erosion, sedimentation, ecosystem dynamics, biodiversity, climate, and biogeochemical cycles (Leta *et al.,* 2021). The spatial temporal interaction of biophysical and human elements is the basis for land use change (Sigalla *et al.,* 2024), human activities such as deforestation, urbanization, and agricultural growth. These disturbances affect biodiversity, soil erosion, climate change, environmental conservation, pollution, and water resources (Gemmechis, 2022). LULC dynamics are influenced by a variety of factors such as government activities, natural disasters, economic activity, and population shifts (Beroho *et al.,* 2023). Therefore, understanding these changes is critical for evaluating their environmental and socio-economic implications (Beshir *et al.,* 2023).

In recent years, Tanzania has experienced significant shifts in LULC, with notable consequences for ecosystem function and hydrological processes. Studies in East Africa indicate that these changes impact catchment conditions, leading to soil erosion, sedimentation, freshwater scarcity, and water contamination. Particularly in regions such as the Songwe sub-basin, LULC changes have been linked to declining water quality, increasing sedimentation, and land degradation, posing significant challenges to long-term environmental sustainability. The complex relationship between LULC change and environmental degradation underscores the necessity of assessing human-environment interactions at a sub -basin scale (Beroho *et al.,* 2023).

Despite the extensive studies on LULC changes by using GIS, Remote Sensing (RS), and CA-Markov models in land use modeling in various locations, including the Songwe sub-basin there is a lack of literature on their application to simulating and forecasting future LULC trends in the Songwe sub-basin, with an emphasis on both historical dynamics and potential future scenarios. Using GIS and remote sensing methods, this study intends to examine past land use and land cover (LULC) changes in the Songwe sub-basin from 1990 to 2020. It also uses the Cellular Automata-Markov (CA-Markov) model to predict future LULC trends for 2040, 2070, and 2100. This work adds to our understanding of how land use transformation affects ecosystem services in the Songwe sub-basin by providing a thorough analysis of past, current, and future LULC changes. This study aims to provide solutions for enhancing ecosystem sustainability and mitigating hydrological and soil degradation, thereby supporting broader sustainable development initiatives.

Materials and Methods

Study Area

The Songwe catchment, encompassing approximately 10,800 km², is located within the eastern Lake Rukwa Basin in the southwestern region of Tanzania. Geographically, it stretches between latitudes 07°40'S and 09°20'S and longitudes 33°00'E and 33°50'E, as detailed by Mwalwiba *et al.,* (2023). This region is characterized by a diverse topography, with numerous hills ranging in elevation from 600 to 2,400 meters above sea level. The catchment area is known for its fertile land and favorable agricultural potential, supported by a tropical climate that brings abundant rainfall and moderate temperatures. The long rainy season, extending from October to May, contributes to the region's agricultural productivity. In contrast, the dry season occurs from June to September. Precipitation levels vary significantly across the catchment, with the highlands receiving an average annual rainfall of 2,600 mm, while the lowlands receive approximately 650 mm. The average temperature within the Songwe catchment ranges from 16°C to 30°C, with variations largely influenced by altitude. The

catchment is drained by three primary rivers: Lupa, Songwe, and Zira. These rivers flow across expansive plains before converging and ultimately discharging into Lake Rukwa. The river systems exhibit notable seasonality, with peak flows observed during the wet season and diminished flows during the dry months. River flows typically reach their peak in February and March, while the driest period is recorded in September, with a reduction in flow from July to November. The Songwe catchment serves as a vital source of freshwater for the surrounding regions, including Mbeya City, Songwe District, and Chunya District.

A variety of activities that are essential to the livelihoods of the nearby communities, such as Mbeya City, Songwe District, and Chunya District, are supported by the catchment. The main economic activity is agriculture, especially the production of crops like coffee, tobacco, and maize. The area is home to both large- and small-scale mining operations, industrial operations, and fishing in addition to agriculture. The high speed of urbanization, notably in and around Mbeya City, is further pushing changes in land use and adding to the region's environmental issues. Although the Songwe catchment supports a variety of plants and animals and offers vital ecosystem services like soil fertility, water filtration, and biodiversity support, changes in land use brought about by mining, urbanization, and agricultural growth have resulted in environmental pressures like sedimentation, soil erosion, and deterioration of water quality. These socio-economic activities, combined with the catchment's ecological significance, highlights the importance of understanding the dynamics of land use and land cover changes in the region. Such an understanding is crucial for managing the competing demands of development, environmental sustainability, and water resource conservation.

Figure 1

Map of Songwe District Tanzania the Study Area

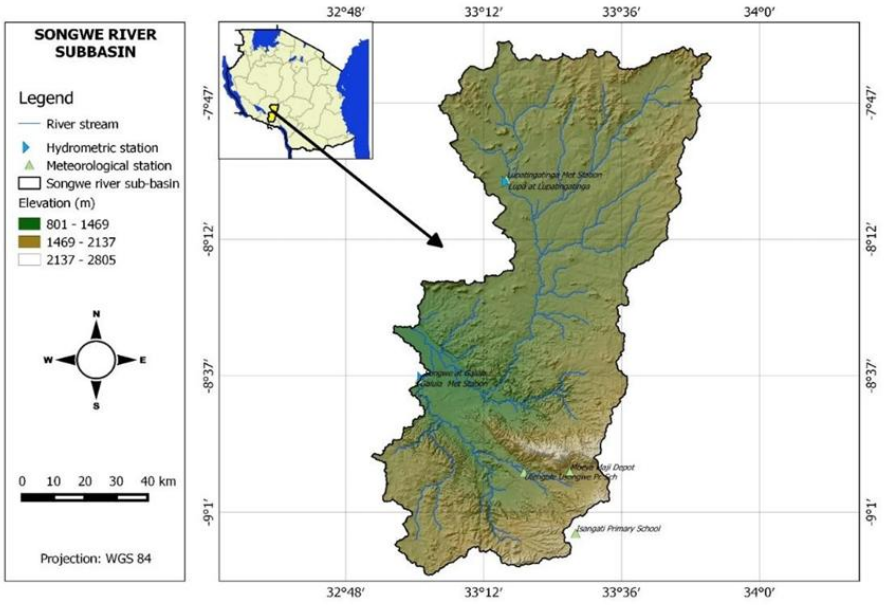

Data Collection, Tools and Techniques

Assessing land use land cover change

Data acquisition

The study on the spatial and temporal land use/cover transformation of the Songwe sub-basin utilized Landsat imagery and GIS to analyze changes across four-time epochs: 1990, 2000, 2010, and 2020. In particular, the study used multispectral level-2 data with less than 10% cloud cover from 30-meter-resolution Landsat images. Landsat 5 (TM) from 1990 and 2000, Landsat 5 (TM BUMPER) from 2010, and Landsat 8 (OLI_TIRS) from 2020 are among the chosen images. For these images, the equivalent path/row combinations in various years are 169/65, 169/66, 170/65, and 170/66. The images taken on April 9 (169/65), September 20 (169/66), July 25 (170/65), and September 7 (170/66) of 1990 (Landsat 5-TM (SAM)) showed no cloud cover. Images with 169/66 (August 30), 170/65 (August 10), and 170/66 (August 10) with no cloud cover were utilized in 2000 (Landsat 5-TM (SAM)). Images from 170/65 (May 11) and 170/66 (May 29) were included since they had only 1% cloud cover in 2010 (Landsat 5-TM (BUMPER)). Finally, 169/66 (September 22), 170/65 (August 28), and 170/66 (August 28) 2020 (Landsat 8-OLI_TIRS) images with 0% cloud cover were chosen. This choice preserves a high-quality dataset for analysis while guaranteeing uniformity in temporal and spatial coverage. These images were sourced from the United States Geological Survey's Earth Explorer website (https://earthexplorer.usgs.gov/). For the purpose of establishing precise locational point data for each land-use and land-cover class included in the classification, field observations were conducted before image classification.

Image pre-processing and classification

Images were geometrically rectified to ensure geometric compatibility and registered to the UTM map coordinate system UTM zone 37 South, Spheroid Clarke 1880, Datum Arc 1960. Image mosaic was conducted to merge together images of the same year with same path and different row so as to create a single image that covers the entire clusters. The unsupervised (Iterative Self- Organizing Data Analysis – ISODATA) image classification was conducted for all images using ERDAS IMAGINE 2016. Maximum of thirty-six (36) land use/cover classes were formulated. The formulated classes were visually interpreted and confirmed through the use of ground truthing data correspond to the images acquisition and hybrid google maps. Using ground truthing data, related classifications were then combined and recorded into main land-use/cover classes following the unsupervised ISODATA classification. This stage guarantees that the classification is more meaningful for analysis and in line with actual data. The ISODATA result was then added to the Maximum Likelihood Classification (MLC) for further refining after the related classes were combined. As a supervised classification technique, the MLC increases accuracy by classifying each pixel according to the most likely land-use/cover class determined by statistical analysis. In this instance, a CCI Global classification method was used, most likely using the Climate Change Initiative Global Land Cover dataset. The main land use/covers classifications covered by the MLC were: forest, woodland, bushland, grassland, water bodies, wetland, cultivated land and built-up areas. Forest: Area of land covered with at least 10% tree crown cover, naturally grown or planted and or 50% or more shrub and tree regeneration cover, Woodland: Area of land covered with low density trees with height between forming closed to open habitat with plenty of sunlight and limited shade, Bushland: Area dominated with bushes and shrubs with occasional short emergent trees, Grassland: Land area dominated by grasses, Water body: Area within body of land, filled with water, localized in a basin, which rivers flow into or out of them, Wetland: Land area that is saturated with water either permanent or seasonally including valley bottoms, Cultivated land: Area subjected to agricultural production farms with crops and harvested crop land, and Built-up Areas: Areas where human infrastructure has been developed, such as urban centers, residential areas, roads, and industrial zones.

Accuracy assessment

Kappa coefficient statistics was used to assess the accuracy of final classified image. Reference images for accuracy assessment were developed based on ground truthing data. Confusion matrix techniques was also used to estimate the classification accuracy. Accuracy assessment was

conducted for each epoch (1990, 2000, 2010, and 2020) with ground truthing data specific to each period to ensure temporal consistency and reliable validation of the classification results.

$$K = \frac{N \sum_{i=1}^{r} x_{ii} - \sum_{i=1}^{r} (x_{i+} \times x_{+i})}{N^2 - \sum_{i=1}^{r} (x_{i+} \times x_{+i})} \quad \ldots\ldots\ldots\ldots\ldots\ldots\ldots\ldots (1)$$

Where N is the total number of sites in the matrix, r is the number of rows in the matrix, xii is the number in row i and column i, x_{+i} is the total for row i, and x_{i+} is the total for column.

Change detection analysis

This study employed change detection analysis to quantify the extent, rate, and spatial distribution of land use/land cover (LULC) changes across different time periods. The assessment was conducted using a post-classification comparison approach, ensuring a detailed and systematic evaluation of temporal variations in land cover. The study employed post-classification comparisons to identify LULC changes in order to get more accurate and trustworthy results. The estimation for the rate of change for the different land covers was computed based on Kashaigili and Majaliwa, (2010). Satellite images from various time periods were independently classified using this method, and the classified outputs were then compared. This method reduces classification errors that could result from spectrum fluctuations brought on by atmospheric or sensor perturbations by examining classified images rather than raw pixel values.

Predicting future land use land cover change

The study used classified land use and land cover (LULC) maps for 2010 and 2020 to generate conversion probabilities and forecast future changes in LULC. CA-Markov model (Cellular Automata-Markov Chain) was employed to analyze past land use transitions and predict future changes. First, Markov Chain analysis was used to compute a transition probability matrix, which quantified the likelihood of each land use category converting into another over time. The transition areas matrix was generated to estimate the total expected change in each LULC class. IDRISI Selva v.17.0 software facilitated the development and validation of the CA-Markov model, ensuring accurate future predictions. For model validation, the simulated land-use/cover map for 2020 was compared with the actual satellite- derived land-use/cover map based on the Kappa statistics. Then, the standard Kappa index was used to check whether the model is valid

Results

Accuracy

The overall land use land cover classification accuracy for the years 1990, 2000, 2010, and 2020 is 92.01%, 91.74%, 91.96%, and 92.44%, respectively. The overall kappa statistic for all years is 0.90, indicating a strong agreement between the observed and predicted classifications in the Songwe sub basin.

Historical Land Use Land Cover change in Songwe sub basin

Over the past few decades, the Songwe sub-basin has experienced considerable changes in land use and land cover (LULC), mostly due to population growth and agricultural expansion. Significant changes in several land categories are revealed by the examination of Land Use/Land Cover (LULC) variations from 1990 to 2020 (Figure 2). Over the course of the 30-year study period, these changes represent the effects that both natural and human activities had on the terrain. Changes in land use have a significant impact on biodiversity, socioeconomic development, and environmental sustainability. With 32.69% (351,771 ha) of the Songwe sub-basin covered by woodland in 1990, it was the most common land cover. Bushland (27.69%), forest (24.34%), and agricultural land (12.41%) were the next most common land covers. There were notable developments during the next ten years. In 2000, forest cover declined to 29.58% (318,299 hectares) and bushland rose to 33.06% (355,733 ha) as the primary land cover (Table 1). The percentage of forest lands decreased as well, reaching 23.01% (247,548 hectares). The start of the significant agricultural growth began during this time, and it climbed slightly to 12.68% (136,447 ha). The decade spanning from 2000 to 2010 saw a surge in agricultural growth. By 2010, the percentage of land used for agriculture had increased to 25.76% (277,201 ha), almost doubling from the previous ten years. Bushland exhibited a modest decline, but remained considerable at 30.21% (325,086 ha). With a decrease of 23.51% (252,937 ha) and

18.59% (200,039 ha), respectively, woodland and forest areas continued to drop. In line with urbanization tendencies, there was also a discernible rise in built-up areas and grasslands during this time. Agricultural land cover continued to dominate in the most recent decade, 2010–2020, reaching 39.35% (423,346 hectares) at that time.

Table 1

Land Use Land Cover Spatial Coverage in Songwe Sub Basin, Tanzania

Class	1990		2000		2010		2020		1990 - 2000			2000 - 2010			2010 - 2020		
	Area [Ha]	Percentage [%]	Area [Ha]	Percentage [%]	Area [Ha]	Percentage [%]	Area [Ha]	Percentage [%]	Area change (Ha)	Percentage change (%)	Annual Rate of Change (Ha/year)	Area change (Ha)	Percentage change (%)	Annual Rate of Change (Ha/year)	Area change (Ha)	Percentage change (%)	Annual Rate of Change (Ha/year)
Forest	261880	24.34	247548	23.01	200039	18.59	120428	11.19	-14332	-5.47	-1433	-47509	-19.19	-4751	-79611	-39.80	-7961
Woodland	351771	32.69	318299	29.58	252937	23.51	143863	13.37	-33472	-9.52	-3347	-65363	-20.54	-6536	-109073	-43.12	-10907
Bushland	297960	27.69	355733	33.06	325086	30.21	359827	33.42	57773	19.39	5777	-30647	-8.62	-3065	34740	10.69	3474
Grassland	1385	0.13	6164	0.57	9573	0.89	17356	1.61	4779	345.00	478	3409	55.31	341	7783	81.30	778
Water	3942	0.37	2882	0.27	2011	0.19	1293	0.12	-1060	-26.89	-106	-871	-30.22	-87	-719	-35.73	-72
Wetland	21560	2.00	4360	0.41	3760	0.35	3030	0.28	-17200	-79.78	-1720	-600	-13.77	-60	-730	-19.41	-73
Agriculture	133560	12.41	136447	12.68	277201	25.76	423346	39.35	2887	2.16	289	140753	103.16	14075	146146	52.72	14615
Built up	4019	0.37	4643	0.43	5471	0.51	6935	0.64	625	15.54	62	828	17.83	83	1464	26.75	146
Total	1076078	100	107607 8	100	107607 8	100	107607 8	100									

While woodland and forest areas saw considerable declines, falling to 13.37% (143,863 ha) and 11.19% (120,428 ha), respectively, bushland remained sizable at 33.42% (359,827 ha). At 6,935 ha, or 0.64% of the total, the built-up area has increased, indicating the sub-basin's continued urbanization

Figure 2

Land Use/Land Cover Maps for 1990, 2000, 2010, and 2020 at Songwe Sub Basin, Tanzania

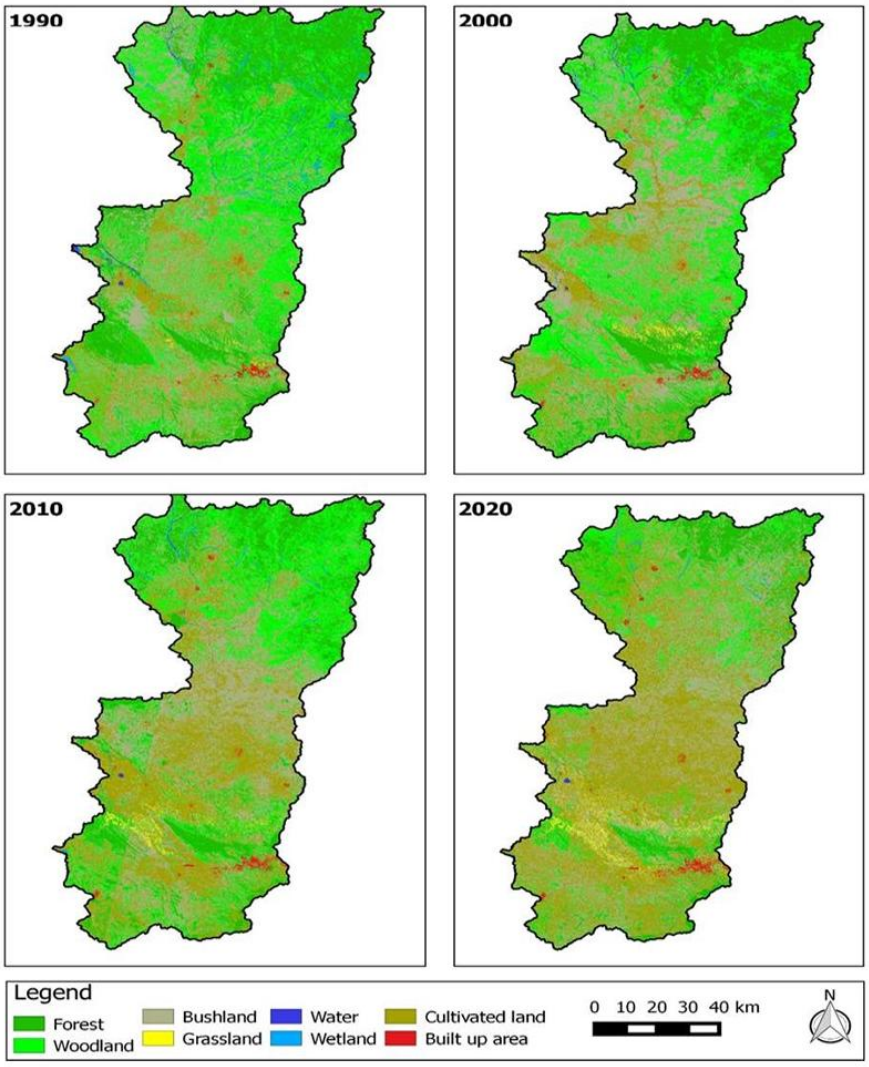

Land use/ land cover transition Matrix in the Songwe Sub basin

A thorough understanding of the alterations in land use and land cover (LULC) within the Songwe sub-basin over a three-decade period (1990-2020 is offered by the transition matrices (Table 2, Table 3, Table 4, and Table 5). These matrices show notable changes, particularly with regard to the expansion of agriculture and deforestation. This pattern emphasizes how deforestation and increased agriculture production affect natural ecosystems. Between 1990 and 2000, Deforestation was evident as the forest area shrank from 247,545 hectares to 141,352 hectares. A significant amount of the forest area was converted to cultivated land (3,528 ha), bushland (27,867

ha), and woodland (70,520 ha). Conversion from forest (70,520 ha), bushland (79,976 ha), and grassland (2,506 ha) resulted in an increase in woodland. A significant amount of bushland was converted into woodland (79,976 ha) and cultivated land (61,542 ha). Large-scale increase of farmed land (from 7,535 ha to 136,447 ha), mostly at the expense of bushland, woodland, and forests. The amount of forest cover decreased steadily between 2000 and 2010, reaching 116,344 hectares. significant conversion to scrub (21,766 ha) and woodland (55,317 ha). decrease in woodland as a result of its conversion to bushland (52,271 ha) and farmed land (49,412 ha). The area of bushland grew from 297,960 hectares to 355,733 ha as a result of the conversion of woods. Having undergone substantial conversion from bushland, woodland, and forest, the cultivated land area grew to 277,202 ha. The forest area decreased significantly to 75,179 hectares between 2010 and 2020. continuous conversion of land to different uses, primarily agriculture and forest areas. Forestry was reduced to 61,869 hectares as a result of being turned into wilderness and agricultural land. The area of bushland grew to 359,575 hectares, primarily from woodland and forest. The area under cultivation increased to 423,422 hectares, maintaining the pattern of agricultural growth at the expense of natural ecosystems.

Table 2

Land use land cover transition in Songwe sub-basin Tanzania between 1990 - 2000

	FRST	**FRSD**	**RNGB**	**RNGE**	**WATR**	**WETN**	**AGRL**	**BULT**	**TOTAL**
FRST	141352	70520	27867	33	715	3529	3528	0	247545
FRSD	81230	135657	79976	89	885	8497	11976	0	318310
RNGB	30373	119060	139465	497	598	4191	61542	0	355727
RNGE	185	959	2506	259	157	49	2050	0	6164
WATR	487	317	427	0	1226	403	22	0	2882
WETN	693	483	406	0	73	2701	4	0	4360
AGRL	7535	24705	47108	496	287	2189	54127	0	136447
BULT	25	70	206	11	0	1	312	4020	4644
TOTAL	261880	351771	297960	1385	3942	21560	133560	4020	1076078

FRST; Forest FRSD; Woodland RNGB; Bushland RNGE; Grassland WATR; Water
WETN; Wetland AGRL; Cultivated land BULT; Built up area

Table 3

Land use land cover transition in Songwe sub-basin, Tanzania between 2000 - 2010

	FRST	**FRSD**	**RNGB**	**RNGE**	**WATR**	**WETN**	**AGRL**	**BULT**	**TOTAL**
FRST	116344	55317	21766	389	576	561	5054	47	200054
FRSD	95996	94649	52271	839	287	1034	7762	111	252948
RNGB	23406	115374	147024	2325	273	288	36024	347	325062
RNGE	2150	3011	3170	283	2	0	955	0	9572
WATR	231	119	347	46	1170	16	81	0	2011
WETN	279	143	426	0	451	2301	159	0	3759
AGRL	8950	49412	129641	2281	121	159	85963	675	277202
BULT	194	274	1088	1	1	0	449	3463	5471
TOTAL	247549	318299	355733	6163	2882	4360	136447	4643	1076078

FRST; Forest FRSD; Woodland RNGB; Bushland RNGE; Grassland WATR; Water
WETN; Wetland AGRL; Cultivated land BULT; Built up area

Table 4

Land use land cover transition in Songwe sub-basin, Tanzania between 2010 - 2020

	FRST	FRSD	RNGB	RNGE	WATR	WETN	AGRL	BULT	TOTAL
FRST	75179	32482	7759	74	239	260	4528	28	120550
FRSD	46616	61869	27306	215	191	286	7373	64	143920
RNGB	43887	98747	128049	1605	166	139	86787	195	359575
RNGE	708	1015	2630	6371	4	0	6602	19	17350
WATR	127	115	134	2	761	0	154	0	1293
WETN	179	147	168	0	344	2012	188	0	3038
AGRL	33123	58171	158200	1305	305	1063	170214	1042	423422
BULT	219	390	841	0	0	0	1355	4123	6929
TOTAL	200039	252937	325086	9573	2011	3760	277201	5472	1076078

FRST; Forest FRSD; Woodland RNGB; Bushland RNGE; Grassland WATR; Water
WETN; Wetland AGRL; Cultivated land BULT; Built up area

Table 5

Land use land cover transition in Songwe sub-basin, Tanzania between 1990 - 2020

	FRST	FRSD	RNGB	RNGE	WATR	WETN	AGRL	BULT	TOTAL
FRST	76991	26317	12792	35	663	1572	2161	11	120541
FRSD	54650	49663	30428	61	526	2724	5972	29	144055
RNGB	76565	129096	100711	434	762	6491	45449	88	359595
RNGE	2672	3965	6392	118	56	42	4095	9	17349
WATR	189	126	105	1	754	25	103	0	1303
WETN	136	479	619	0	213	1580	21	0	3048
AGRL	50452	141537	145580	677	965	9121	74404	526	423261
BULT	226	588	1334	59	2	6	1356	3356	6926
TOTAL	261880	351771	297960	1385	3942	21560	133560	4019	1076078

FRST; Forest FRSD; Woodland RNGB; Bushland RNGE; Grassland WATR; Water
WETN; Wetland AGRL; Cultivated land BULT; Built up area

Future land use land cover change in Songwe sub basin

In many categories, including forest, woodland, bushland, grassland, water, wetland, cultivated land, and built-up area, the results show the expected distribution of land use and land cover (LULC) from 2020 to 2100 (see Figure 3). Significant variations in land use patterns have been documented over time, especially in the areas of cultivated land, forest cover, and other LULC categories. The expected drop in the forest area between 2020 and 2040 is estimated to be 88,945 hectares (8.24%), or a significant decrease of 120,428 hectares (11.19%) to 31,483 hectares (2.95%). In addition, the woodland area drastically decreases over time, going from 143,863 hectares (13.37%) in 2020 to 71,489 hectares (6.69%) by 2040, a decrease of 72,374 hectares (6.68%). This indicates a widespread shift of natural landscapes into various land uses. Between 2020 and 2040, bushland grew somewhat, from 359,827 hectares (33.42%) to 400,935 hectares (36.74. From 17,356 hectares (1.61%) in 2020 to 34,933 hectares (3.27%) in 2040, the area covered by grasslands grows. Despite its moderate growth, this indicates a trend toward open land area expansion brought about by the conversion of formerly wooded areas into grasslands. During this time, wetlands and bodies of water both declines. There is a decline in both water areas and wetlands from 1,293

hectares (0.12%) to 621 hectares (0.06%) and 3,030 hectares (0.28%) to 1,528 hectares (0.14%). Between 2020 and 2040, the amount of land under cultivation increases dramatically, from 423,346 hectares (39.35%) to 527,035 hectares (49.30%). The increased need for agricultural output, which is probably being driven by population growth and the need for food security, is reflected in this rise of 103,689 hectares (9.95%). Additionally, by 2040, the built-up area will grow, rising from 6,935 hectares (0.64%) to 8,055 hectares (0.75%). Between 2040 and 2070, the amount of forest land decreases even more, with the forest cover decreasing from 31,483 hectares (2.95%) to 3,437 hectares (0.32%). This represents a sharp decline of 28,046 hectares (2.63%) during a 30-year period, suggesting that forest resources are almost depleted and that by 2070 there would be very little forest cover left. A more dramatic decrease occurs in the woodland area, which goes from 71,489 hectares (6.69%) in 2040 to 5,895 hectares (0.55%) in 2070. The majority of woodland areas appear to have been transferred to other land uses, based on the loss of 65,594 hectares (6.14%). In 2070, there will be 360,984 hectares (33.11%) of bushland, down from 400,935 hectares (36.84%) in 2040. This decline of 39,951 hectares (3.73%) shows that even bushland areas are being converted to other land uses, even though they are still the major land cover type. During this time, grassland continues to grow, reaching 61,142 hectares (5.72%) in 2070 from 34,933 hectares (3.27%) in 2040. Wetlands and water bodies are still diminishing; in 2070, wetlands will have shrunk from 1,528 hectares (0.14%) to 92 hectares (0.01%), and water areas will have decreased from 621 hectares (0.06%) in 2040 to 66 hectares (0.01%). The likelihood of these ecosystems disappearing entirely by 2070 suggests extreme environmental stress. There is a significant increase in the amount of land under cultivation, going from 527,035 hectares (49.30%) in 2040 to 634,680 hectares (59.37%) in 2070. The necessity to support a growing population is driving the continued conversion of natural landscapes into agricultural land, as evidenced by the growth of 107,645 hectares (10.07%). The built-up area shows evidence of ongoing urbanization and infrastructure development, growing from 8,055 hectares (0.75%) in 2040 to 9,782 hectares (0.92%) in 2070. The period from 2041 to 2070 sees a continuation of the patterns witnessed in the previous era, with additional losses in forest and woodland areas. By 2070, forests have mostly been converted to other land uses, and the amount of forest cover is almost completely gone. With only 3,249 hectares (0.30%) of forest cover left by 2100 a modest decrease from 3,437 hectares (0.32%) in 2070 forest cover had virtually completely vanished by that time. The fact that forests are almost certain to disappear by 2100 emphasizes how urgent conservation actions must be taken to stop additional loss. From 5,895 hectares (0.55%) in 2070 to 5,817 hectares (0.54%) in 2100, the amount of woodland continues to decrease slightly. The small amount of woodland that remains suggests that this sort of land is no longer an important part of the landscape. From 360,984 hectares (33.11%) in 2070 to 258,109 hectares (23.48%) in 2100 a decrease of 102,875 hectares (9.63%) bushland experiences a steep fall. This notable decline points to additional land conversion, most likely for urban or agricultural uses. By 2100, both wetlands and water bodies will be almost dead; wetlands will have shrunk from 92 hectares (0.01%) to 89 hectares (0.01%), and water areas will have decreased somewhat from 66 hectares (0.01%) to 62 hectares (0.01%) in 2070. Severe environmental degradation is suggested by the almost complete extinction of these habitats. With an increase from 634,680 hectares (59.37%) in 2070 to 711,001 hectares (66.51%) in 2100, arable land continues to be the majority. The increase of 76,321 hectares (7.14%) reflects the ongoing demand for agricultural land, probably at the expense of natural ecosystems. The built-up area shows a slight increase, rising from 9,782 hectares (0.92%) in 2070 to 10,422 hectares (0.97%) in 2100, indicating continued urban development.

Figure 3

Predicted Future Land Use Land Cover Maps for 2040, 2070, and 2100, at Songwe Sub Basin, Tanzania

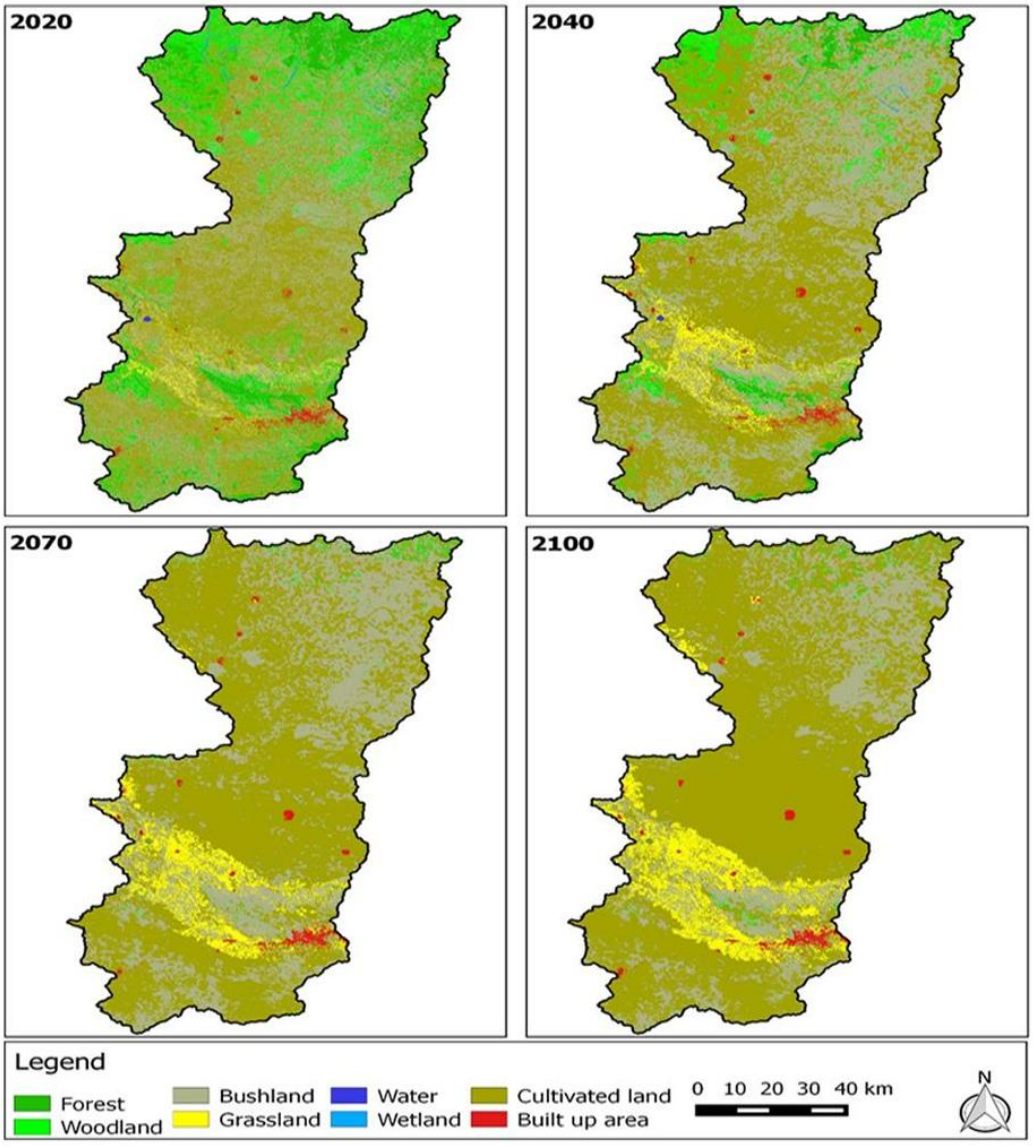

Discussion

Historical Land Use Land Cover change in Songwe sub- basin

An interesting case study of how human activity and natural processes affect Sub-Saharan African landscapes is the changes in land use and land cover (LULC) in the Songwe sub-basin over the last three decades. Significant trends that not only have local effects but also reflect larger regional and worldwide patterns of environmental change are shown by the analysis of LULC fluctuations from 1990 to 2020. The 0.90 kappa average value indicating a strong agreement between the observed and predicted classifications in the Songwe sub- basin. This value signifies a strong agreement, reinforcing the reliability of our classification process. High kappa values suggest minimal classification errors, providing confidence in the detected LULC changes. Similar patterns of deforestation and agricultural intensification have been reported by studies carried out in other parts of East Africa, including Tanzania's Kilombero Valley and Kenya's Upper Tana River basin. In the Ethiopian Highlands, for example, a recent study by Beshir *et al.,* (2023) found that over a 30-year period, logging and agricultural expansion were the main causes of a 42.76% decline in forest cover. This demonstrates the widespread effect of agricultural operations on woodland areas throughout the region, as evidenced by the 54.01% drop in woodland and the 59.10% reduction in forest cover noted in the Songwe sub-basin. Among the most noteworthy developments during the 30-year period was the tremendous expansion in agricultural land in the Songwe sub-basin, which increased by 216.97%. This development appears to be putting more strain on the Songwe sub-basin's land resources than has been documented in other Sub-Saharan African locations. Increases in built-up areas of 72.57% in the Songwe sub-basin indicate tendencies in urbanization that are representative of larger Sub-Saharan African processes. Rapid urban expansion in the region is attributed to population increase and rural-to-urban migration (Mnyali and Materu, 2021). Consistent with these results is the Songwe sub-basin's growing built-up area, especially the acceleration from 2010 to 2020, which points to a tendency toward more concentrated urban development. The reduction in wetlands and water bodies in the Songwe sub-basin is alarming since these ecosystems play crucial ecological roles; wetlands have shrunk by 85.95% and water bodies by 67.21%. Reports of comparable decreases have been made in other parts of Africa. The growth of 1,153.07% and 20.76%, respectively, in grassland and bushland areas contrasts with patterns in certain other regions where grasslands are frequently turned into agricultural land. The Songwe sub-basin's noticeable increase in grassland, however, would point to changes in land management techniques, perhaps in relation to grazing and other agricultural activities. The historical examination of LULC changes shows clear trends over the decades, with the largest reductions in woodland and forest cover taking place between 1990 and 2010, and then huge increases in agricultural production and urbanization in the decade that followed. These patterns align with the conclusions of recent research conducted by Osman *et al.,* (2023) which emphasized the quickening rate of changes in land cover in emerging countries due to population expansion and economic development. In conclusion, the Songwe sub-basin's LULC changes between 1990 and 2020 are indicative of larger regional and worldwide patterns in the transition of land use. Significant environmental issues faced by many emerging regions are reflected in the sub-basin's extensive deforestation, increased agricultural production, urbanization, and loss of wetlands. Land management techniques and conservation initiatives urgently need to be prioritized in light of these changes' significant effects on biodiversity, climate regulation, and sustainable development.

Land use/ land cover transition in the Songwe Sub- basin

Over the past three decades, there has been a notable decrease in the amount of forest and woodland regions. The main causes of this decrease are conversions to bushland and agricultural land. Climate regulation, carbon sequestration, and biodiversity are all severely impacted by the loss of forest cover. Over all time periods, the amount of land under cultivation has increased steadily and significantly. This trend highlights the increasing strain that agricultural activities driven by population development and

the demand for food security are placing on natural environments. Although agricultural growth boosts livelihoods, it endangers the sub-basin's sustainability and ecological balance. Both inflows and outflows have occurred in bushland. Bushland first grew as a result of conversion from woods and forests. The constant change from bushland to agricultural land, however, demonstrated the dynamic character of this land cover type. Wetlands and submerged places have not changed much. Although these ecosystems are still comparatively stable, they are nonetheless susceptible to degradation and invasion from growing agricultural lands. The amount of land that is built up has steadily increased due to infrastructure development and urbanization. Even while the overall area is still tiny in comparison to other land uses, the trend points to growing pressures from development and human settlement.

Future land use land cover change in Songwe sub-basin

The study highlights a significant transformation in land use and land cover within the Songwe sub-basin, driven primarily by urbanization and agricultural expansion. A striking reduction in forest cover from 8.24% in 2020 to just 0.30% by 2100 indicate a severe loss of biodiversity and ecosystem integrity. This tendency is in line with larger worldwide trends, according to which the loss of biodiversity and the degradation of ecosystems are mostly caused by deforestation and land conversion for agriculture (Sigalla *et al.,* 2024). Similarly, woodland areas are expected to decline from 13.37% to 0.54%, reflecting global trends where forests are increasingly converted into farmland to support a growing population. According to Liping *et al.,* (2018), this reflects comparable patterns seen in other areas where forests and woodlands are being destroyed to accommodate an expanding human population. The rapid expansion of cultivated and built-up areas suggests an urgent need to balance food security and environmental conservation (Barbosa de Souza *et al.,* 2023). While grasslands are projected to increase from 3.27% in 2040 to 8.17% in 2100, this rise is likely due to land degradation or grazing needs and is insufficient to compensate for the loss of more complex ecosystems. The near-total disappearance of wetlands and water bodies by 2100 is particularly alarming, as these ecosystems play a crucial role in maintaining water quality, supporting biodiversity, and regulating climate impacts. Without intervention, the projected land use and land cover changes in the Songwe sub-basin could lead to severe environmental challenges, including increased vulnerability to climate change. To mitigate these effects, it is essential to implement targeted strategies such as reforestation programs, which could help restore lost forest cover and enhance carbon sequestration. Promoting agroforestry and sustainable agricultural practices, such as conservation tillage, crop rotation, and integrated land-use planning, would support both food security and environmental conservation.

Despite the valuable insights gained from this study, the study has several limitations, such as the reliance on 30-meter resolution Landsat imagery, while effective for broad-scale LULC analysis, may not fully capture finer land-use details, the CA-Markov model assumes that historical trends will continue, potentially overlooking the influence of unexpected policy interventions, climate variability, and socio-economic shifts. The absence of extensive field validation across different seasons further restricts classification accuracy. To address these limitations, future research should incorporate higher-resolution satellite imagery, develop multi-scenario projections, integrate socio-economic data with LULC models, and quantify the economic value of ecosystem services. Furthermore, participatory GIS approaches involving local communities in land-use planning and management should be explored to enhance sustainable development strategies in Songwe sub-basin.

Conclusion

This study provided the detailed analysis of the spatial and temporal dynamics of land use and land cover (LULC) in the Songwe Sub-Basin, contributing to a deeper understanding of how land use patterns have changed over time in this specific region. With its accurate representation of the sub-basin's dynamic processes, the CA Markov model provides a trustworthy forecast for LULC changes in the future. The findings show a significant change in the patterns of land

use, with observable transitions from natural vegetation and wooded regions to agricultural land and urban growth. The growing population and greater need for food production led to a large expansion in the area under cultivation. The growth of urban areas is a sign of increasing pressure from development and human settlement. Flood control, water purification, and wildlife habitats are all seriously threatened by the degradation of wetlands and other bodies of water. Forests and woodlands will almost completely disappear by 2100. The landscape is anticipated to be dominated by agricultural land, which will increase environmental pressure. To balance agricultural expansion with the preservation of natural ecosystems, sustainable land management strategies must be put into place immediately. In order to safeguard the remaining forests, woodlands, wetlands, and water bodies, tougher conservation regulations are urgently needed. Monitoring Land Use and Change (LULC) changes continuously is necessary to assess the success of conservation and land management initiatives in the Songwe sub- basin.

Acknowledgement

This paper is the outcome of a research project supported by the Mbeya University of Science and Technology Research Fund through post-graduate studies.

References

Barbosa de Souza, K., Rosa dos Santos, A., Macedo Pezzopane, J. E., Machado Dias, H., Ferrari, J. L., Machado de Oliveira Peluzio, T., Toledo, J. V., Freire Carvalho, R. de C., Rizzo Moreira, T., França Araújo, E., Gomes da Silva, R., Pósse Senhorelo, A., Azevedo Costa, G., Duarte Nader Mardeni, V., Horn Kunz, S., & Cordeiro dos Santos, E. (2023). Modeling Dynamics in Land Use and Land Cover and Its Future Projection for the Amazon Biome. Forests, 14(7). https://doi.org/10.3390/f14071281

Beroho, M., Briak, H., Cherif, E. K., Boulahfa, I., Ouallali, A., Mrabet, R., Kebede, F., Bernardino, A., & Aboumaria, K. (2023). Future Scenarios of Land Use/Land Cover (LULC) Based on a CA-Markov Simulation Model: Case of a Mediterranean Watershed in Morocco. Remote Sensing, 15(4). https://doi.org/10.3390/rs15041162

Beshir, S., Moges, A., & Dananto, M. (2023). Trend analysis, past dynamics and future prediction of land use and land cover change in upper Wabe-Shebele river basin. Heliyon, 9(9). https://doi.org/10.1016/j.heliyon.2023.e19128

Chilagane, N. A., Kashaigili, J. J., & Mutayoba, E. (2020). Historical and Future Spatial and Temporal Changes in Land Use and Land Cover in the Little Ruaha River Catchment, Tanzania. Journal of Geoscience and Environment Protection, 08(02), 76–96. https://doi.org/10.4236/gep.2020.82006

Dammag, A. Q., Jian, D., Cong, G., Derhem, B. Q., & Latif, H. Z. (2023). Predicting spatio-temporal land use / land cover changes and their drivers forces based on a cellular automated Markov model in Ibb City, Yemen. Geocarto International, 38(1). https://doi.org/10.1080/10106049.2023.2268059

Gemmechis, W. A. (2022). Land Use Land Cover Dynamics Using CA-Markov Chain Model and Geospatial Techniques: A Case of Belete Gera Regional Forest Priority Area, South Western Ethiopia. Modeling Earth Systems and Environment Land Use Land Cover Dynamics Using CA-Markov Chain Model and Geospatial Techniques: A Case of Belete Gera Regional Forest Priority Area, South Western Ethiopia. https://doi.org/10.21203/rs.3.rs-1805209/v1

Gobry, J. J., Twisa, S. S., Ngassapa, F., & Kilulya, K. F. (2023). Impact of land-use/cover change on water quality in the Mindu Dam drainage, Tanzania. Water Practice and

Technology, 18(5), 1086–1098. https://doi.org/10.2166/wpt.2023.067

Leta, M. K., Demissie, T. A., & Tränckner, J. (2021). Modeling and prediction of land use land cover change dynamics based on land change modeler (Lcm) in nashe watershed, upper blue nile basin, Ethiopia. Sustainability (Switzerland), 13(7). https://doi.org/10.3390/su13073740

Liping, C., Yujun, S., & Saeed, S. (2018). Monitoring and predicting land use and land cover changes using remote sensing and GIS techniques—A case study of a hilly area, Jiangle, China. PLoS ONE, 13(7). https://doi.org/10.1371/journal.pone.0200493

Mnyali, E. T., & Materu, S. F. (2021). Analysis of the Current and Future Land Use/Land Cover Changes in Peri-Urban Areas of Dar es Salaam City, Tanzania using Remote Sensing and GIS Techniques. Tanzania Journal of Science, 47(5), 1622–1636. https://doi.org/10.4314/tjs.v47i5.12

Mutayoba, E., Kashaigili, J. J., Kahimba, F. C., Mbungu, W., & Chilagane, N. A. (2018). Assessing the Impacts of Land Use and Land Cover Changes on Hydrology of the Mbarali River Sub-Catchment. The Case of Upper Great Ruaha Sub-Basin, Tanzania. Engineering, 10(09), 616–635. https://doi.org/10.4236/eng.2018.109045

Mwalwiba, L. G., Kifanyi, G. E., Mutayoba, E., Ndambuki, J. M., & Chilagane, N. (2023). Assessment of Climate Change's Impacts on River Flows in the Songwe Sub-Basin. Open Journal of Modern Hydrology, 13(02), 141–164. https://doi.org/10.4236/ojmh.2023.132008

Nyatuame, M., Agodzo, S., Amekudzi, L. K., & Mensah-Brako, B. (2023). Assessment of past and future land use/cover change over Tordzie watershed in Ghana. Frontiers in Environmental Science, 11. https://doi.org/10.3389/fenvs.2023.1139264

Osman, M. A. A., Abdel-Rahman, E. M., Onono, J. O., Olaka, L. A., Elhag, M. M., Adan, M., & Tonnang, H. E. Z. (2023). Mapping, intensities and future prediction of land use/land cover dynamics using google earth engine and CA- artificial neural network model. PLoS ONE, 18(7 JULY). https://doi.org/10.1371/journal.pone.0288694

Sigalla, O. Z., Twisa, S., Chilagane, N. A., Mwabumba, M. F., Selemani, J. R., & Valimba, P. (2024). Future Trade-Off for Water Resource Allocation: The Role of Land Cover/Land Use Change. Water (Switzerland), 16(3). https://doi.org/10.3390/w16030493

Open Journal of Modern Hydrology, 2023, 13, 141-164
https://www.scirp.org/journal/ojmh
ISSN Online: 2163-0496
ISSN Print: 2163-0461

Assessment of Climate Change's Impacts on River Flows in the Songwe Sub-Basin

Lupakisyo G. Mwalwiba[1*], Gislar E. Kifanyi[1], Edmund Mutayoba[2], Julius M. Ndambuki[3], Nyemo Chilagane[4]

[1]College of Engineering and Technology, Mbeya University of Science and Technology, Mbeya, Tanzania
[2]Department of Irrigation and Water Supply Engineering, Water Institute, Dar es Salaam, Tanzania
[3]Tshwane University of Technology, Pretoria, South Africa
[4]Tanzania Research and Conservation Organization, Morogoro, Tanzania
Email: *lupakisyog@yahoo.co.uk

How to cite this paper: Mwalwiba, L.G., Kifanyi, G.E., Mutayoba, E., Ndambuki, J.M. and Chilagane, N. (2023) Assessment of Climate Change's Impacts on River Flows in the Songwe Sub-Basin. *Open Journal of Modern Hydrology*, **13**, 141-164.
https://doi.org/10.4236/ojmh.2023.132008

Received: January 17, 2023
Accepted: April 25, 2023
Published: April 28, 2023

Abstract

River flow in the Songwe sub-basin is predicted to alter due to climate change, which would have an impact on aquatic habitats, infrastructure, and people's way of life. Therefore, the influence of climate change should be taken into account when making decisions about the sustainable management of water resources in the sub-basin. This study looked into how river discharge would react to climate change in the future. By contrasting hydrological characteristics simulated under historical climate (1981-2010) with projected climate (2011-2040, 2041-2070, and 2071-2100) under two emission scenarios, the effects of climate change on river flow were evaluated (RCP 4.5 and RCP 8.5). The ensemble average of four CORDEX regional climate models was built to address the issue of uncertainty introduced by the climate models. The SWAT model was force-calibrated using the results from the generated ensemble average for the RCP 4.5 and RCP 8.5 emission scenarios in order to mimic the river flow during past (1981-2010) and future (2011-2100) events. The increase in river flows for the Songwe sub-basin is predicted to be largest during the rainy season by both the RCP 4.5 and RCP 8.5 scenarios. Under RCP 8.5, the abrupt decrease in river flow is anticipated to reach its maximum in March 2037, when the discharge will be 44.84 m^3/sec, and in March 2027, when the discharge will be 48 m^3/sec. The extreme surge in river flow will peak, according to the RCA4, in February 2023, in April 2083 under RCP 4.5, and, according to the CCLM4 and RCA4, in November 2027 and November 2046, respectively. The expected decrease and increase in river flow throughout both the dry and wet seasons may have an impact on the management of the sub-water basin's resources, biodiversity, and hydraulic structures. The right adaptations and mitigation strategies should be adopted in order to lessen the negative consequences of climate change on precipita-

tion, temperature, and river flow in the sub-basin.

Keywords

Climate Change, Climate Models, Songwe River Sub-Basin, River Flow, SWAT

1. Introduction

The world is dealing with an increase in sediment output and a shortage of water resources for social-economic activities as a result of rising population and land use activities [1]. The hydrological cycle is altered as a result of climate change, which also has an impact on the environment and human life worldwide [2]. The Intergovernmental Panel on Climate Change (IPCC) anticipated that the world's temperature will rise by 1.5˚C in its Sixth Assessment Report (AR6) [3]. It is beyond dispute that human activity is driving climate change, resulting in extreme weather events like heatwaves, torrential downpours, and droughts, and impacting every corner of the planet in various ways [3]. Tanzania is one of the developing nations that are experiencing the effects of climate change on its water, sediment yield and agricultural industries [4]. These effects result in modifications to the catchment's runoff volume, streamflow volume, soil moisture, soil erosion, and sediment yield [5]. One of the most noticeable aspects of the changing climate that directly affects all hydrological responses in the catchments is the rise in surface air temperature and rainfall patterns [6]. Small alterations in the global climate across eastern and southern Africa have a significant impact on the regional climate [7]. Most regions are subject to variations in temperature and rainfall patterns because hydrological conditions vary from region to region [8]. Strong agreement was found between the 34 climate models used in Future Climate for Africa (FCFA) 2017 regarding Tanzania's continued warming in the range of 0.80 C to 1.80 C by the 2040s [9], which will cause an increase in annual evapotranspiration, unbalanced atmospheric moisture, and changes in the hydrological cycle of the ecosystems [10].

Currently, it is crucial to evaluate how climate change may affect local and regional water resources. Changing river flow conditions are a key effect of climate change on Tanzania's water resources [9]. River flow changes are mostly brought on by variations in the water balance, such as precipitation and temperature [11]. Many researchers have combined future projected climate data from climate models with hydrological models to assess how future runoff would respond to climate change [12]. Studying the effects of climate change on river flows involves using global climate model (GCM) or regional climate model (RCM) climate change scenarios [13]. In the Little Ruaha catchment, Nobert (2022) evaluated the expected changes in streamflow brought on by upcoming climate change for the years 2025-2060. The RCP4.5 and RCP8.5 greenhouse gas concentration scenarios and General Circulation Model (GCM) datasets from

the ACCESS1.0, CNRM-CM5, and BCC-CSM1 models were chosen as the representative scenarios. The calibrated NAM hydrological model was used to analyze the effect of climate change on stream flows. The impact assessment findings indicate that for both the RCP4.5 and RCP8.5 scenarios, the monthly maximum and minimum temperatures will rise in the range of 0.8˚C to 2˚C under the climate change scenario (2025-2060). In the case of rainfall, an average yearly increase in rainfall of around 10% over the baseline is anticipated. The inter-annual variability of rainfall for the years 2025 to 2060, however, indicates a declining trend for RCP 8.5. According to the simulation results, streamflow for RCP4.5 and RCP8.5 will fall by around 30% and 6%, respectively.

The effects of climate change on hydrological responses and sediment yield in the Songwe sub-basin and Lake Rukwa Basin have not been discussed in any of the research. This study used high-resolution climate and spatial data, as well as the Soil and Water Assessment Tool (SWAT), to evaluate the effects of climate change on the streamflow of the Songwe sub-basin in the Lake Rukwa Basin. In this work, data from the ensemble of the CORDEX Africa regional climate model (RCM) have been conducted under RCP 4.5 and 8.5 out of four potential emission scenarios of RCP 2.0, RCP 4.5, RCP 6.0, and RCP 8.5. These were added to the hydrological model once they had been calibrated and verified. The RCP 4.5 scenario depicts the approach to the radiative forcing trajectory that stabilizes without overshoot and leads to a peak level of 4.5 W/m^2 [14]. According to the RCP 8.5, the radiative forcing will increase and reach 8.5 W/m^2 by 2100 [2]. The focus of this study was therefore to assess the impacts of climate change on river flows under RCP 4.5 and 8.5.

2. Materials and Method

2.1. Description of the Study Area

The Songwe sub-basin (**Figure 1**) covers an area of roughly 10,800 km^2 and is situated in the eastern portion of the Lake Rukwa Basin in southern-western Tanzania. It is found between latitudes 07˚40'S and 09˚20'S and longitudes 33˚00'E and 33˚50'E. All river catchments that pour into Lake Rukwa have one outlet, describing an internal drainage system. There are various hills in the area that cuts through fertile valleys, and their elevations range from 600 to 2400 masl. The catchment is distinguished by generally healthy, fertile soils, consistent, and copious amounts of precipitation, mild temperatures, and excellent agricultural potential. According to the 2012 National Census, the sub-basin has a population of roughly 843,278 people, 40% of whom reside in Mbeya City and the adjacent peri-urban areas. By 2035, the sub-basin population is expected to increase to around 1,643,629 people. One of Tanzania's most productive regions is the Songwe watershed. About 80% of the population works in agriculture is the primary industry. Mbeya City, a significant regional economic and industrial hub, is also located within the watershed.

Due to topographical height, differences in rainfall distribution based on time

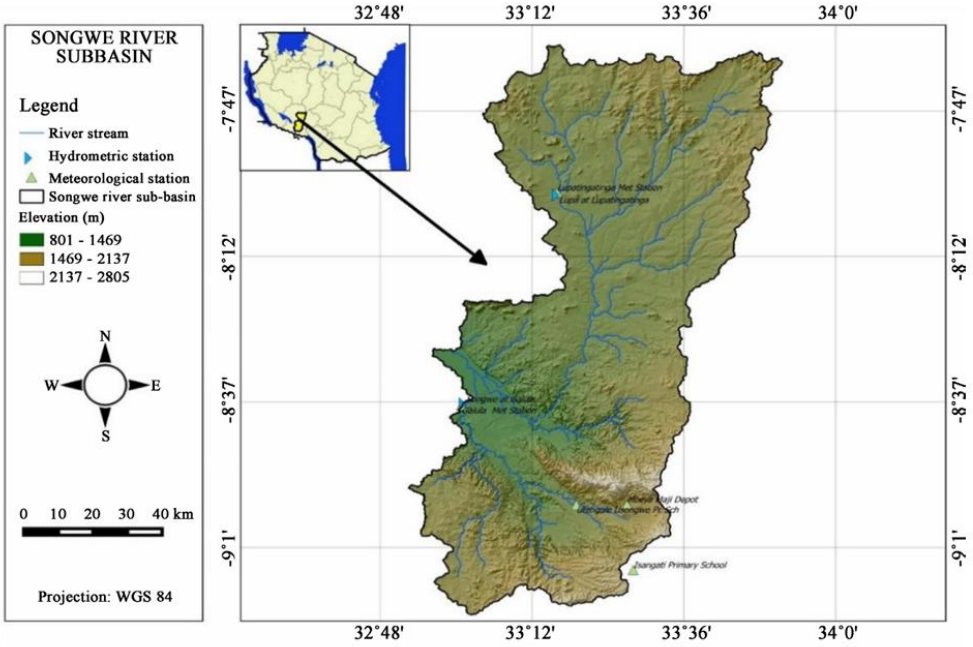

Figure 1. Location of the Songwe sub-basin.

and place, and related land use activities that occurred in the sub-basin that influenced river flow, soil erosion, and sediment yield to rivers and Lake Rukwa, the Songwe sub-basin has a diverse bioclimate. The sub-basin primarily has a tropical climate and has one extended rainy season (October to May). From about June to September, there is a dry period. The lowlands receive 650 mm of annual precipitation, while the highlands receive 2600 mm. The altitude-dependent mean temperature ranges from about 16˚C in the highlands to roughly 30˚C in the lowlands. Three significant rivers drain the northern, central, and southern portions of the Songwe Sub-basin: the River Lupa, the River Songwe, and the River Zira, which originate in the Poroto Mountains and drain the southern portion. The rivers travel through the gold mine area, crossing wide flat lowlands, combining, and then emptying into Lake Rukwa. Strong seasonality is present in all sub-basin rivers, with high flows during the rainy season and low flows during the rest of the year. The rivers see their highest flows between February and March and their lowest flows between July and November, with September being the driest month. Climate change, which has led to significant fluctuations in temperature and precipitation and has serious effects on the management and use of the sub-basin water resources, has made the issue worse.

2.2. Spatial, Meteorological, and Hydrological Datasets

The stream network and hydrologic response units are easier to define in the

SWAT model simulation due to the streamflow data, topographic features, and spatial distribution of land cover/use and soil types. The Ministry of Water Tanzania's Lake Rukwa Water Basin office provided the daily streamflow information for the Songwe sub-basin at Galula station. One of the essential inputs used by SWAT to divide the sub-basin into smaller sub-basins and to examine the sub-drainage basin's pattern, slope, stream length, and channel width is the Digital Elevation Model (DEM). In this investigation, a DEM with a 30 m spatial resolution was collected from the Advanced Land Observing Satellite Phased Array L-band Synthetic Aperture Radar (ALOS PALSAR) at the Alaska Satellite Facility, which may be found online at http://www.asf.alaska.edu. Images of land use and land cover (LULC) for the year 2020 used in this study were downloaded for free from the United States Geological Survey (USGS) website at https://earthexplorer.usgs.gov/, and categorized in line with the input specifications of the SWAT model. From the FAO-UNESCO Soil Map of the World, Volume VI at https://swat.tamu.edu/data/ online, a soil map was constructed. The water balance model in SWAT depends on data on daily precipitation, maximum and minimum air temperatures, relative humidity, wind speed, and solar radiation. Data on the daily rainfall, were gathered from the Ministry of Water's Lake Rukwa Water Basin office. While data on the minimum and maximum temperatures, solar radiation, wind speed, relative humidity, and wind direction were obtained from the updated Global Weather Database for SWAT. The Lake Rukwa Water Basin office provided daily baseline data for the Lupa tinga tinga and Galula stations. The baseline scenario was examined and calibrated using data from the baseline era, which ran from 1981 to 1992.

2.3. Climate Change Data output and Bias Correction

The CORDEX-Africa runs of the Climate Model Intercomparison Project Phase 5 (CMIP5) were downscaled from GCMs utilized in this study [8]. The Consortium for Small-scale Modeling (COSMO), Climate Limited-Area Model (CCLM), SMHI Ross by Centre Regional Climate Model (RCA4), Max Planck Institute Regional Model (REMO), KNMI-Regional Atmospheric Climate Model (RACMO22T), and High-Resolution Limited Area Model (HIRHAM5) are some of the most well-known CORDEX RCMs used in Africa [7]. For this investigation, the four RCMs produced through the CORDEX-Africa Data Search (HIRHAM5, CCLM4, RACMO22T, and RCA4) were employed (**Table 1**). RCMs used in this work have a 0.44 degree grid spacing (50 km of resolution). The reference period is changed to reflect the period of observations that are available (1981-1992). Using the spatial resolution of 0.44˚ and the RCP4.5 and RCP8.5 emission scenario paths, an ensemble mean from the regional climate models CORDEX Africa [15] was taken at the model boundaries. The Earth System Grid Federation-Lawrence Livermore National Laboratory website, https://esgf-node.llnl.gov/projects/esgf-llnl/, is where the CORDEX data were obtained. In the context of the Coordinated Regional Climate Downscaling

Table 1. The CORDEX-RCMs and their driving GCMs.

S/N	RCM	Mode Centre	Short name	GCMs
1	DMI HIRHAM5	Danmarks Meteorologiske Institut (DMI), Denmark	HIRHAM5	ICHEC
2	CLMcom COSMO-CLM (CCLM4)	Climate Limited-Area Modelling (CLM) Community	CCLM4	MPI ICHEC CNRM
3	KNMI Regional Atmospheric Climate Model, version (RACMO2.2T)	Koninklijk Nederlands Meteorologisch Instituut (KNMI), Netherlands	RACMO22T	ICHEC
4	SMHIRossby Center Regional Atmospheric Model (RCA4)	Sveriges Meteorologiska OchHydrologiska Institut (SMHI), Sweden	RCA4	MPI ICHEC CNRM

Experiment [12], the ensemble means data are available over Africa at 0.44˚ resolution, and they have already been used over Africa. The studies of the data concentrated on the future eras and the reference period (1981-1992) (2011-2100). Climate model data for hydrologic modeling (CMhyd) for four RCMs outputs and give climate data for the SWAT model were bias-corrected by the linear scaling method because precipitation and temperature are the main drivers of the hydrological regime of climate change. For the bias correction of the four RCMs' output of climate data, data on precipitation measured at gauging stations in the sub-basin and the on minimum and maximum temperature gathered from SWAT Global Weather Data were used.

2.4. Hydrological Modeling

SWAT Model Selection, Set up, and Calibration

In vast catchments with changing soils, land use/land cover, and management conditions, the SWAT model uses a physically-based, semi-distributed approach to anticipate the effects of land management methods on water, sediment, and nutrients [16]. Comprehensive data on the weather, soil characteristics, and terrain, vegetation, and land management techniques are required for the SWAT model [17]. The SWAT model was used to simulate the water balance for the chosen period and under changing climatic conditions [18]. [16] provides a thorough explanation of the SWAT model. The DEM-derived drainage patterns that the model uses to construct small sub-basins that are then divided into smaller sub-basins by a threshold that specifies the required amount of drainage to create a stream [19]. Hydrologic response units (HRU) with unique LULC classes, soil types, and slope classes are created from these small sub-basins [20]. Each hydrologic response unit runoff is anticipated independently and routed to determine the sub-overall basin's runoff. In general, the SWAT model integrates climatic station data at the sub-basin while solving the water balance equation

for each HRU and adding the HRU calculations for each sub-basin [16]. For each HRU, the hydrological balance is simulated using the water balance equation [16]. The Songwe sub-basin, which has an extent of around 10,800 km^2, is one of the catchment that the SWAT model can be applied to. The application addresses the bias-correction of RCMs temperature and precipitation, as well as the development, calibration, and validation of the SWAT model for the Songwe sub-basin and the forced simulation of the model using a set of bias-corrected RCM outputs to evaluate future climatic and river flow change for the years 2011-2100. Galula station streamflow data from 1981 to 1992 were used to assess the model's calibration and performance. Due to its ability to physically foundation and continually simulate hydrological processes, the SWAT model was chosen for this study. These characteristics are crucial for modeling the effects of climate change on streamflow. The model can calculate the basin's hydrologic water cycle by integrating various spatial data, observed data, and anticipated climatic data (Arnold *et al.*, 2012), which makes it valuable for catchment management. The SWAT is a hydrological model with a physical foundation that integrates with QGIS. For the model setup in this study, QSWAT 1.7 version, compatible with QGIS 2.6.1 interface, was employed. Spatial, hydrological, meteorological, and projected climate data were among the inputs gathered to create the model. Figure 2 shows satellite pictures of land use and land cover,

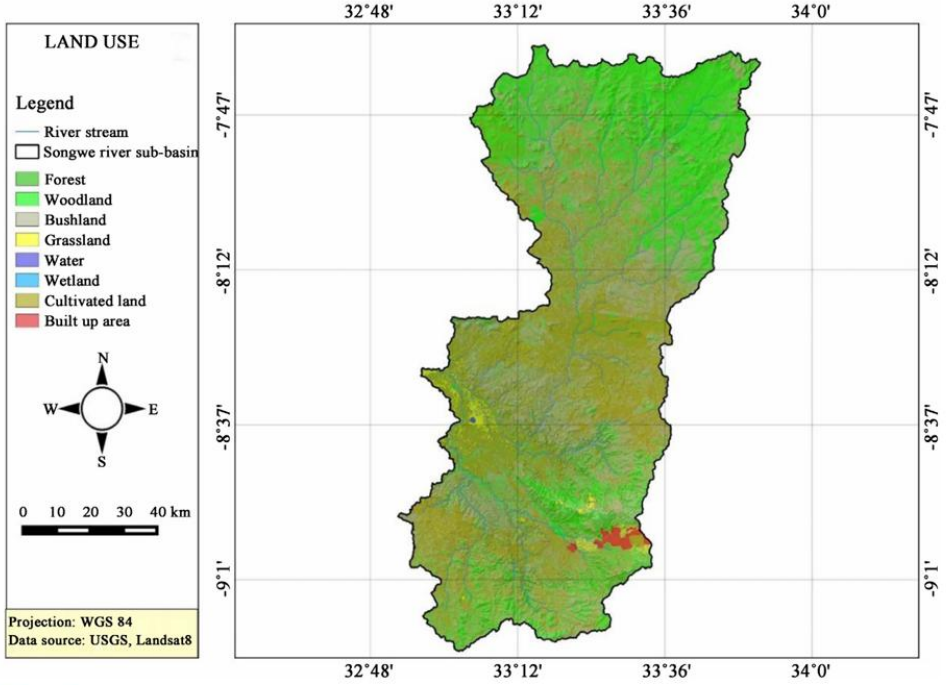

Figure 2. Land use/cover of Songwe sub-basin.

Figure 3 shows a digital elevation model with a 30 m resolution, and Figure 4 shows a soil map of the Songwe sub-basin. Figure 5 depicts the placement of the metrological and hydrological stations. Table 2 in Figure 2 displays the land use/cover in the Songwe sub-basin. The DEM and river channels of the study area served as the foundation for the model setup.

Water Balance Equation;

$$SW_t = SW_o + \sum_{i=1}^{t}\left(R_{day} - Q_{surf} - E_a - W_{sweep} - W_{gw}\right)t \quad (1)$$

SW_t is the final soil water content,

SW_o is the initial soil water content on day i in mm,

R_{day} is the amount of precipitation on day in mm,

Q_{surf} is the amount of surface runoff on day i in mm,

E_a is the amount of evapotranspiration on day i in mm,

W_{sweep} is the amount of water entering the vadose zone from the soil profile on day i in mm,

W_{gw} is the amount of return flow on day i in mm,

t is the time in da.

The land phase of the hydrological cycle and the water phase of the hydrological cycle are the two stages of the SWAT. The process of water transportation through the stream network was chosen for this study's focus area: the water

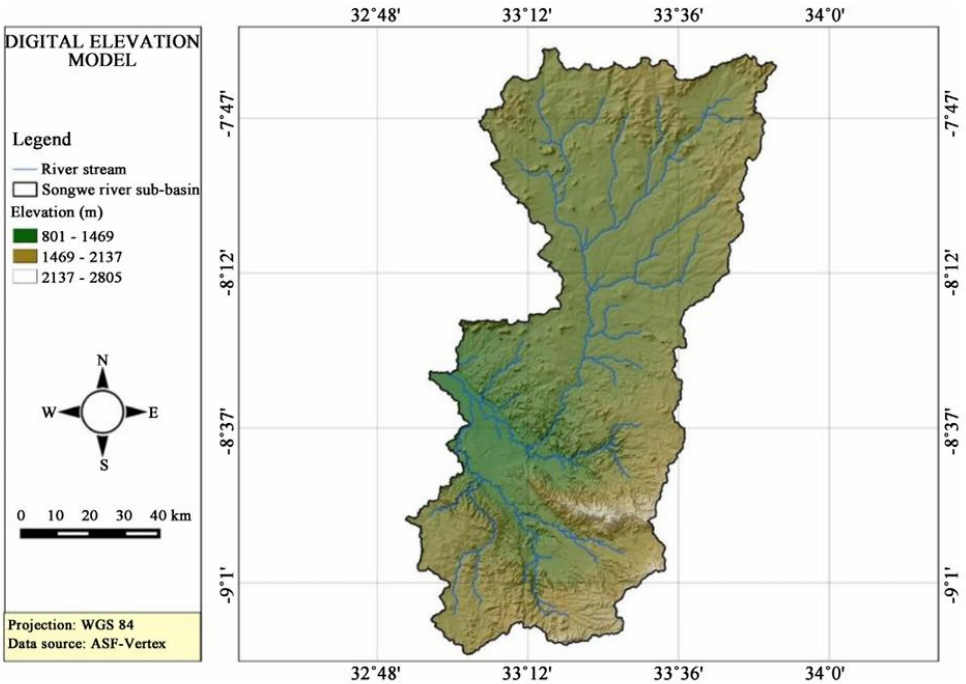

Figure 3. Digital Elevation Model of Songwe sub-basin.

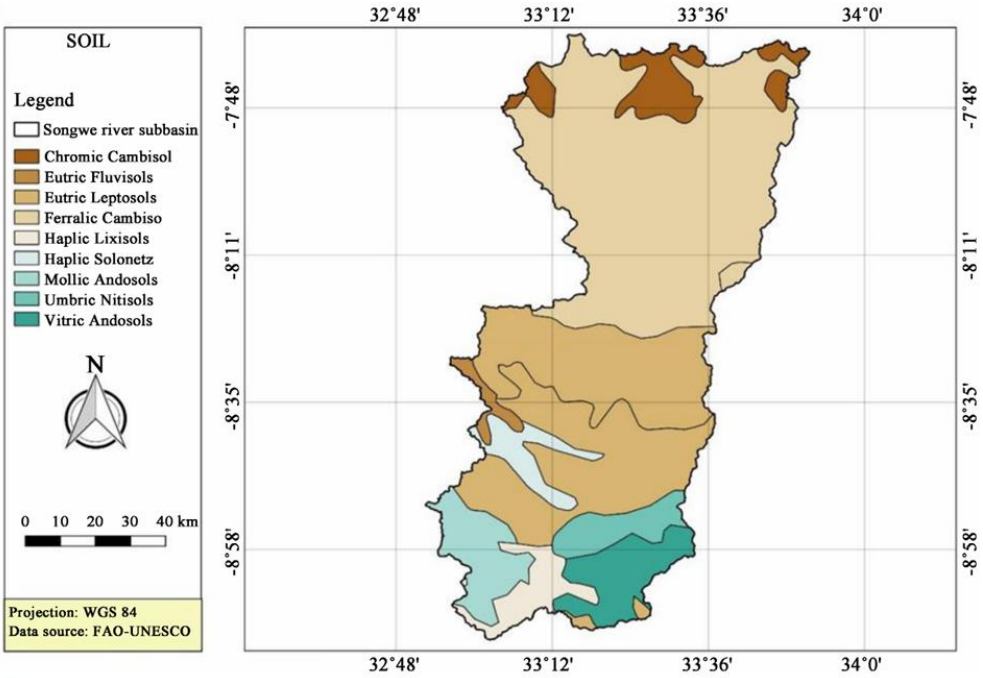

Figure 4. Soil map of Songwe sub-basin.

phase. Additionally, the SWAT model employed the Penman-Monteith model to estimate potential evapotranspiration [14]. The total volume of surface runoff was calculated using The Curve Number (CN), which requires daily precipitation data. The Songwe sub-basin was divided into several smaller sub-basins for the SWAT model, and these smaller sub-basins were then separated into units with distinctive soil and land use characteristics called hydrological response units (HRUs). These HRUs are described as homogeneous spatial units with comparable hydrological and geomorphological characteristics [1]. The sub-basins were then divided into a total of 345 hydrologic response units based on land use, soil type, and slope (HRUs). The model was first filled with the reclassified land use, land cover, and soil data before the HRUs were specified. The climatic data were entered into the model and written using the SWAT Model's Write SWAT Input Tables interface. The Write SWAT Input Tables interface of the SWAT Model was used to load and write the model's climate data, which included precipitation (pcp), temperature (tmp), relative humidity (rh), solar radiation, and wind speed. The SWAT model was run once the model's settings were modified and tables for observed weather data had been produced.

The goal of model calibration is to optimize the model's agreement with a collection of experimental data by adjusting a set of parameters. It involves changing model parameters based on comparing outcomes to observations in

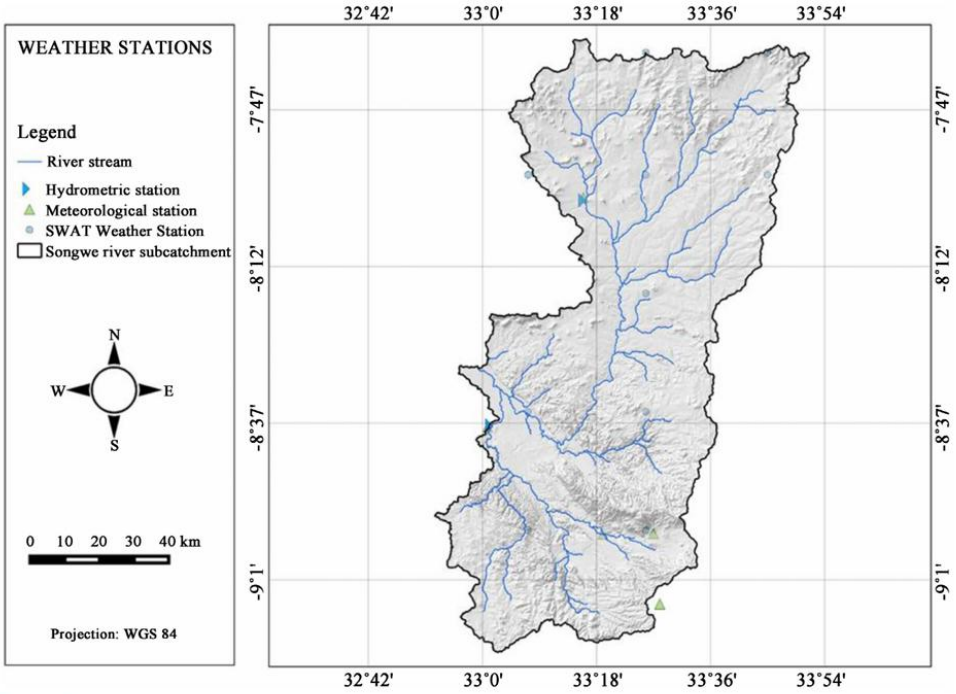

Figure 5. Weather data station in Songwe sub-basin.

Table 2. Land use/cover coverage in Songwe sub-basin.

Land use/cover	Coverage (Ha)	Percentage (%)
Forest	19,721	1.83
Woodland	326,133	30.30
Bushland	375,031	34.84
Grassland	13,441	1.25
Water	365	0.03
Wetland	190	0.02
Cultivated land	333,252	30.96
Built up area	8326	0.77

order to maintain the same response over time. From the standpoint of the model's intended usage, validation is the act of assessing how accurately a model represents the real world. Using observed streamflow data from Galula station for the years 1981 to 1992, the model was calibrated and validated. The SWAT-Calibration and Uncertainty Program's Sequential Uncertainty Fitting version 2 technique (SUFI-2) was used to identify and calibrate the SWAT model's sensitive parameters (SWAT-CUP). The SWAT model had to simulate flows with bi-

as-corrected temperature and rainfall over the future periods and in the baseline period after being calibrated and validated using data on observed stream flows. In accordance with four regional climate models, the simulated stream flows for the 2040s, 2070s, and 20100s correspond to two scenarios.

3. Results and Discussion

3.1. SWAT Model Calibration, Validation, and Performance

The Galula gauging station in the Songwe sub-basin served as the calibration and validation site for the semi-distributed SWAT hydrologic model. With goodness-of-fit values of NSE 0.45, R^2 0.59, and RSR 0.73 for the calibration period and NSE 0.59, R^2 0.59, and RSR 0.64 for the validation period, the model was able to mimic stream flows. Table 3 shows that stream flows from the Songwe sub-basin could be simulated by the model.

The parameters utilized for the SWAT model's calibration were subjected to a global sensitivity analysis using the SWAT-CUP. The findings demonstrated that the stream flow calibration's sensitive parameters included CN2, SOL AWC, GWQWN, GW DELAY, and GW REVAP (Table 4).

3.2. Climate Change Impact in the Songwe Sub-Basin

3.2.1. Changes in Future Precipitation and Temperature

The four regional climate models' projections of average monthly mean precipitation for the historical, near-future, mid-future, and end-of-century periods were contrasted with actual observations from the base period and meteorological data produced by SWAT. Most months of the year in CCLM4, HIRAM5, RACMO22T, and RCA4 for the historical simulation of climate models in the

Table 3. Evaluation statistics for calibration and validation.

Flow Station	CALIBRATION				VALIDATION				CALIBRATION		VALIDATION	
	NSE	R^2	RSR	PBIAS	NSE	R^2	RSR	PBIAS	Ob-flow (m^3/s)	Sim-flow (m^3/s)	Ob-flow (m^3/s)	Sim-flow (m^3/s)
Galula	0.47	0.59	0.73	−35.5	0.59	0.59	0.64	3.9	33.16	44.9	33.16	31.88
Lupa	−0.09	0.01	1.04	−17.1	−0.08	0.01	1.04	9.1	93.30	109.22	93.30	84.80

Ob-flow; Observed flow. Sim-flow; Simulated flow.

Table 4. Most sensitive parameters and their fitted values.

Rank	Parameter	Parameter definition	Fitted value
1	CN2.mgt	SCS runoff curve number	0.00000000
2	SOL_AWC.sol	Available water capacity of the soil layer	0.00000143
3	GWQWN.gw	Threshold depth of water in the shallow aquifer required for return flow to occur	0.00306594
4	GW_DELAY.gw	Groundwater delay	0.00417118
5	GW_REVAP	Groundwater "revap" coefficient	0.10412491

sub-basin are characterized by an overestimation of the observed precipitation in all stations (Figure 6). The bias-corrected Regional climate models output for historical revealed that, in the majority of the stations under study, the CCLM4 and HIRAM5 models outperformed the RCA4 and the RACMO22T models in terms of their ability to replicate the observed mean monthly rainfall. In accordance with the RCP 4.5 climate scenarios, the four climate models predict that the amount of precipitation over the sub-basin will decrease in the months of January, February, March, April, and November, increase in the month of December during the early part of the century, and decrease in the month of December for the mid and late parts of the century. Under RCP 4.5, the RCA4 and RACMO22T models predicted more precipitation than the CCLM4 and HIRAM5 RCMs (Figure 7). All four climate models predict a rise in precipitation over the sub-basin in January, February, March, April, November, and December under the RCP 8.5 warming scenarios, and a decrease in April. Also, except for January, March, and April for the Galula Station, drop for January, February, March, and November. Increase for December for the mid- and end-century periods for all four RCMs. Under RCP 8.5, the RCA4 and RACMO22T models predicted more precipitation than the CCLM4 and HIRAM5 RCMs (Figure 8). All four climate models predict an increase in temperature over the sub-basin during the early, mid, and end periods of the century under both the RCP 4.5 and RCP 8.5 climate scenarios. For Galula station in the Songwe sub-basin, all regional climate models predicted a rise in the lowest and maximum temperature in both the historical and future climate (Figure 9). Future months with high temperatures include September, October, November, and December.

3.2.2. Climate Change Impacts on River Flow

River flows alter as a result of climate change's impact on various water balance components. Accordingly, under the two RCP scenarios, changes in river flows are anticipated in the sub-basin following the change in temperature. The calibrated SWAT model was used to simulate the anticipated river flows for the first, middle, and last decades of the century using the output from the four Regional Climate Models that had been bias-corrected. In the sub-basin, the effects of the changing climate were evaluated. It has been shown how the river flows under RCPs 4.5 and 8.5 between the historical and future periods (Figure 10). Both the RCP 4.5 and RCP 8.5 scenarios predict that the rise in river flows for the Songwe sub-basin will be greatest during the rainy season. However, it is anticipated that the dramatic reduction in river flow would be at its peak in March 2037, when the discharge will be 44.84 m^3/sec, and in March 2027, when the discharge will be 48 m^3/sec, under RCP 8.5. (Figure 10(b) and Figure 10(c)). According to the RCA4 regional climate model, the extreme rise in river flow will reach its peak in February 2023, in April 2083 under RCP 4.5, and in November 2027 and November 2046 by the CCLM4 and RCA4 regional climate models, respectively. The management of the sub-basin's water resources,

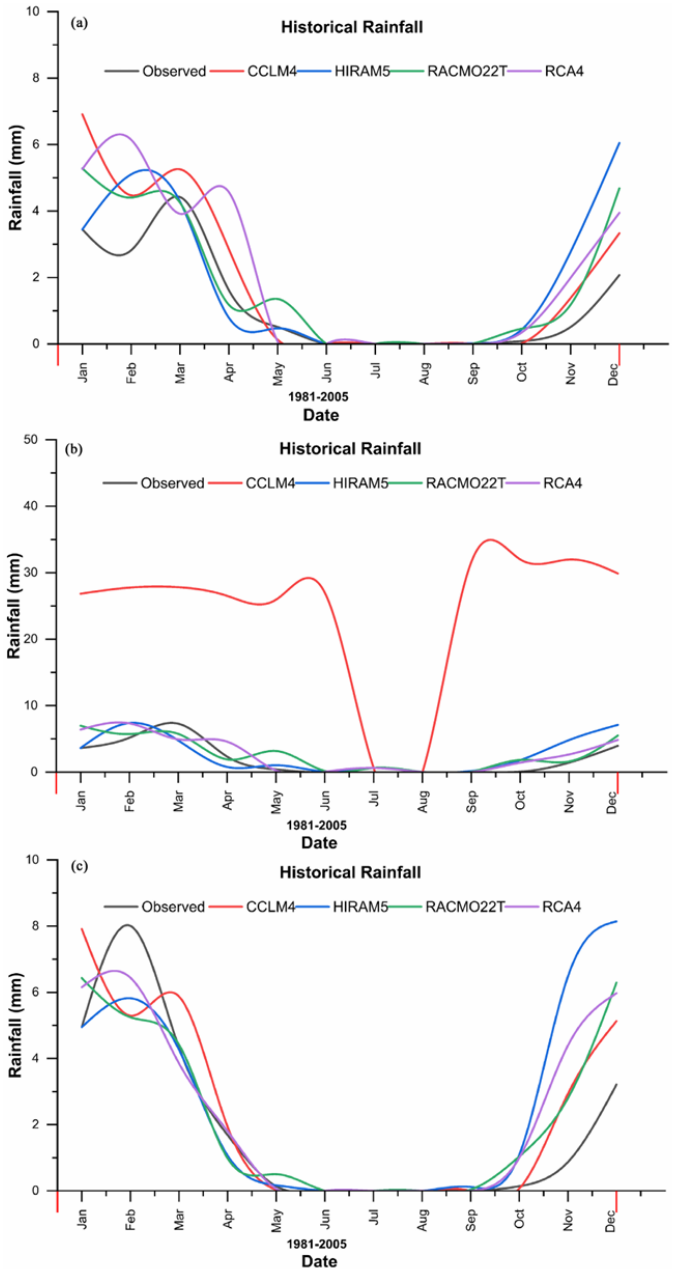

Figure 6. (a) Historical Monthly mean rainfall at Galula station (1981-2005); (b) Historical Monthly mean rainfall at Lupa station (1981-2005); (c) Historical Monthly mean rainfall at Mbeya maji station (1981-2005).

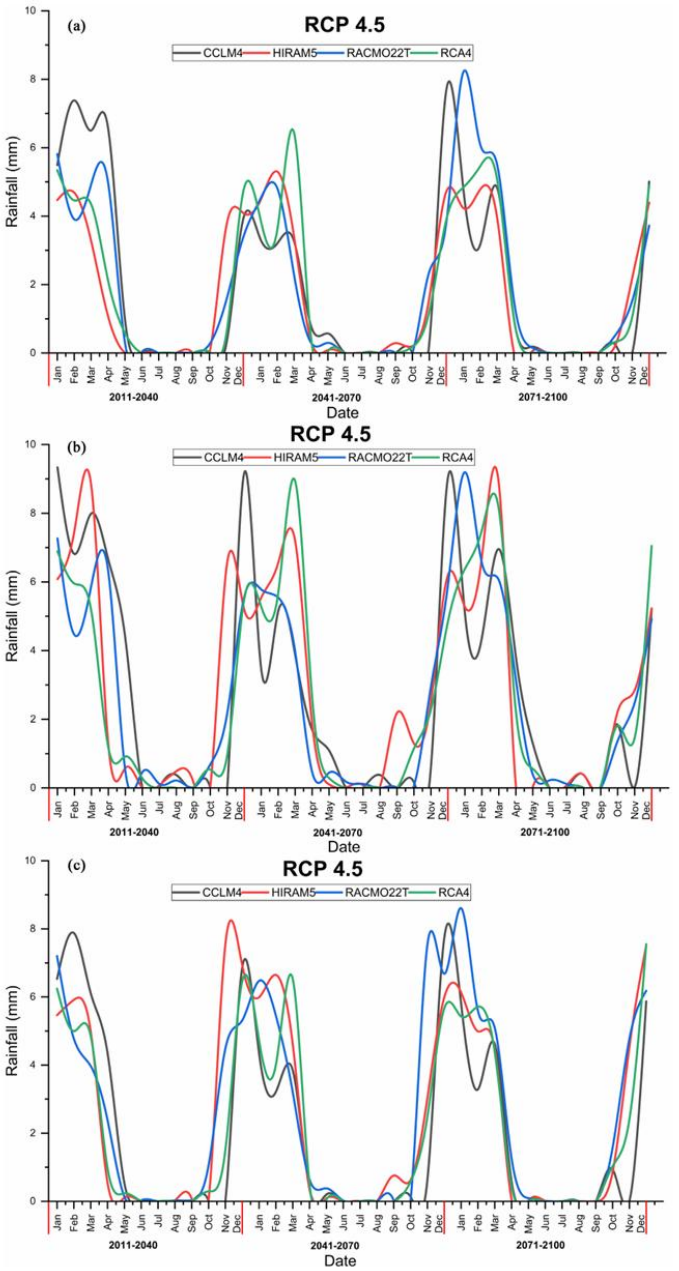

Figure 7. (a) Simulated Monthly mean raifall at Galula station (2011-2100) under RCP 4.5; (b) Simulated Monthly mean raifall at Lupa station (2011-2100) under RCP 4.5; (c) Simulated Monthly mean raifall at Mbeya maji station (2011-2100) under RCP 4.5.

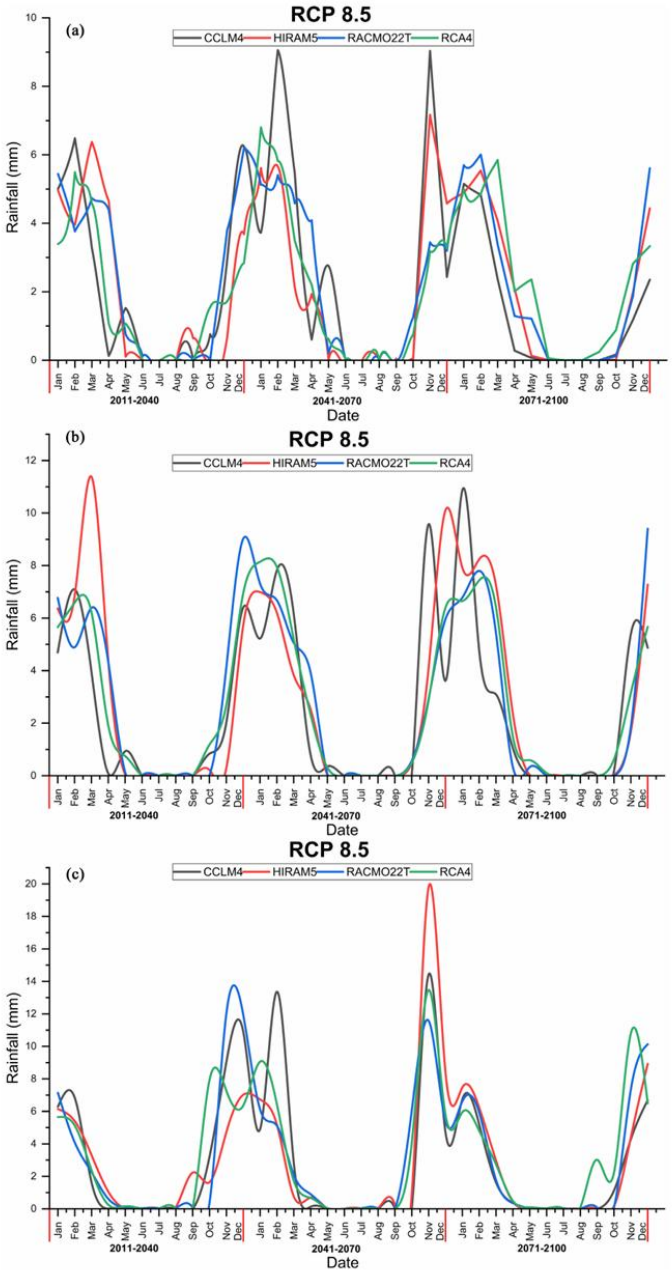

Figure 8. (a) Simulated Monthly mean raifall at Galula station (2011-2100) under RCP 8.5; (b) Simulated Monthly mean raifall at Lupa station (2011-2100) under RCP 8.5; (c) Simulated Monthly mean raifall at Mbeya maji station (2011-2100) under RCP 8.5.

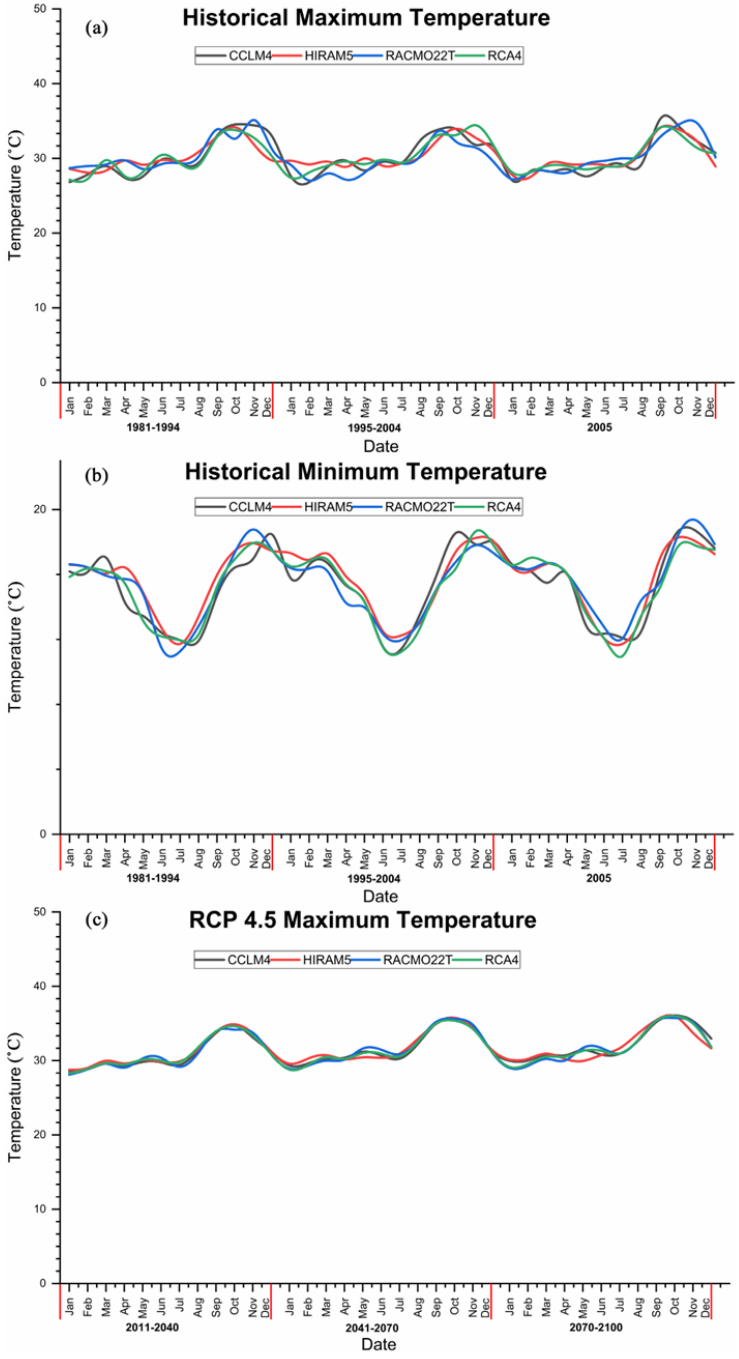
(a)
Historical Maximum Temperature
CCLM4
HIRAM5
RACMO22T
RCA4
Temperature (˚C)
1981-1994
1995-2004
2005
Date
(b)
Historical Minimum Temperature
CCLM4
HIRAM5
RACMO22T
RCA4
Temperature (˚C)
1981-1994
1995-2004
2005
Date
(c)
RCP 4.5 Maximum Temperature
CCLM4
HIRAM5
RACMO22T
RCA4
Temperature (˚C)
2011-2040
2041-2070
2070-2100
Date

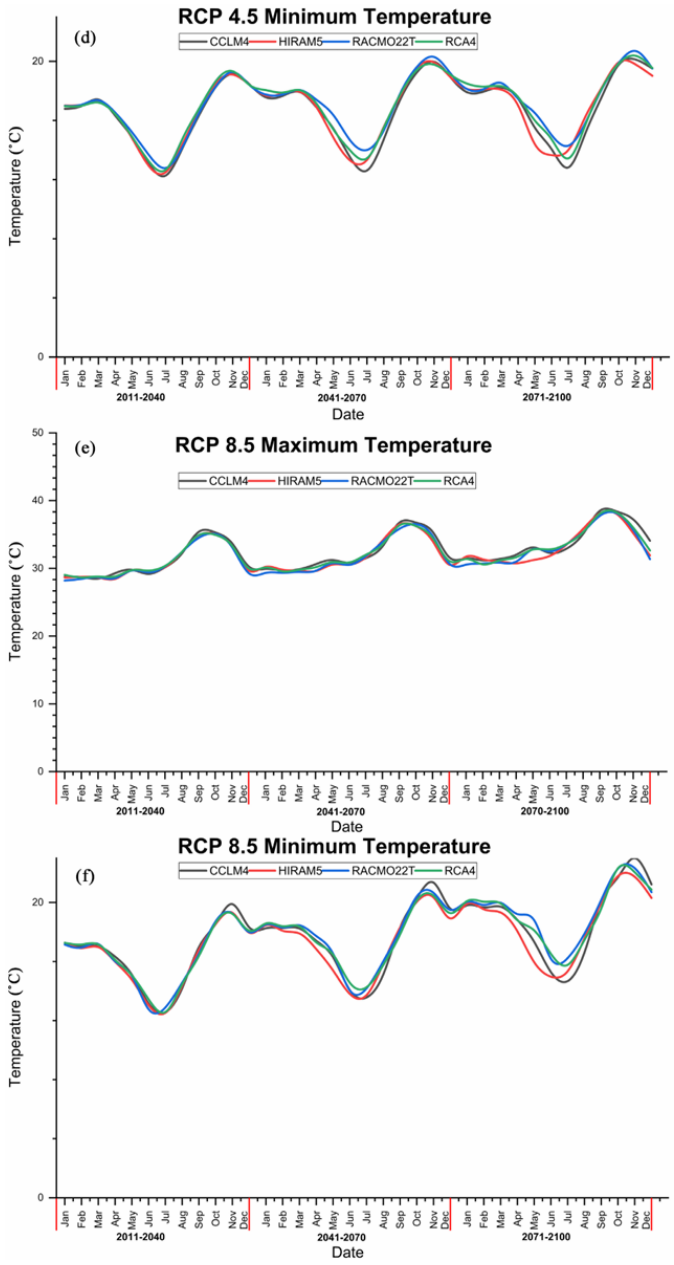

Figure 9. (a) Historical Monthly mean maximum temperature at Galula station; (b) Historical Monthly mean minimum temperature at Galula station; (c) Simulated Monthly mean maximum temperature at Galula station RCP 4.5; (d) Simulated Monthly mean minimum temperature at Galula station RCP 4.5; (e) Simulated Monthly mean maximum temperature at Galula station RCP 8.5; (f) Simulated Monthly mean minimum temperature at Galula station RCP 8.5.

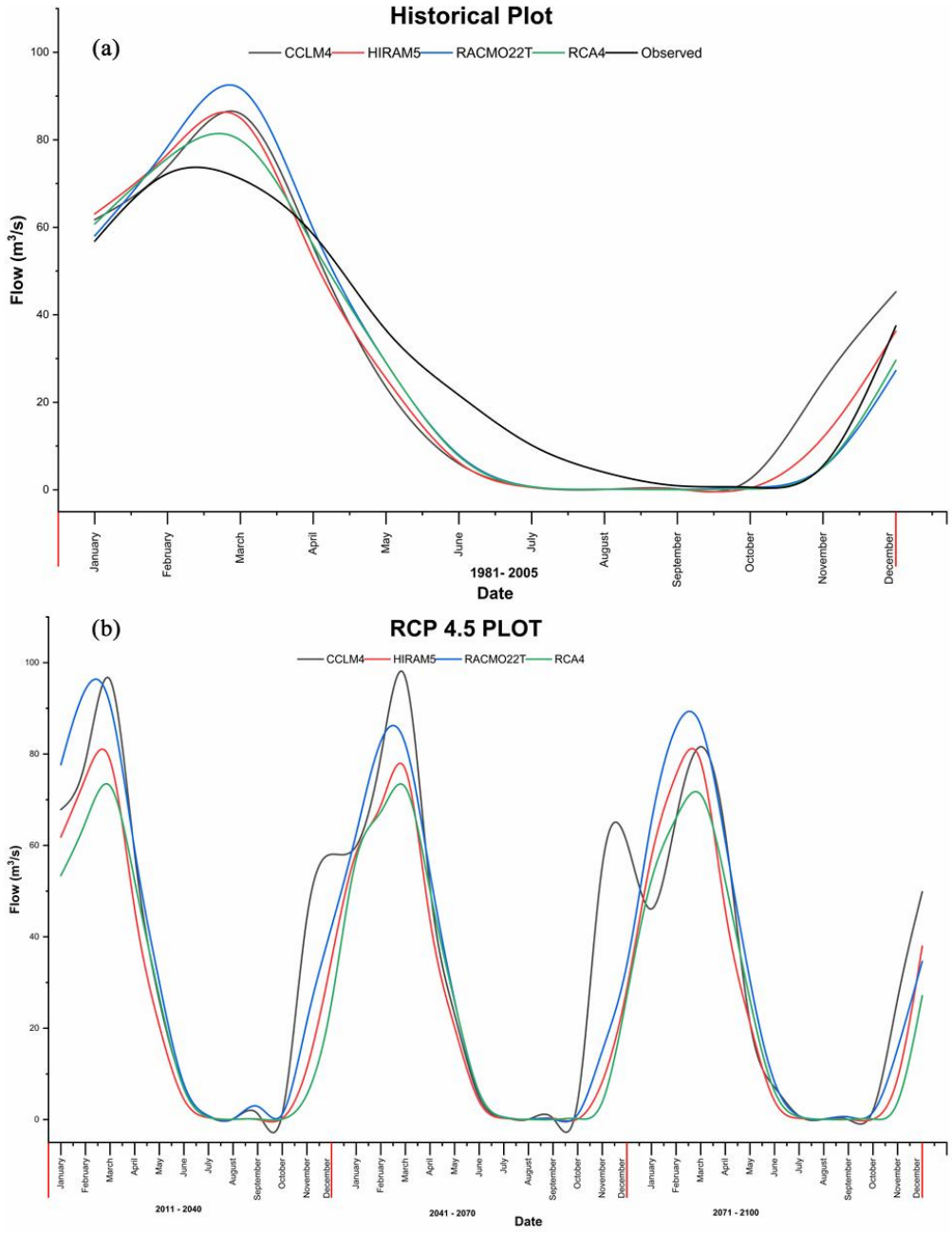
Historical Plot
(a)
CCLM4
HIRAM5
RACMO22T
RCA4
Observed
Flow (m³/s)
1981- 2005
Date
(b)
RCP 4.5 PLOT
CCLM4
HIRAM5
RACMO22T
RCA4
Flow (m³/s)
2011 - 2040
2041 - 2070
2071 - 2100
Date

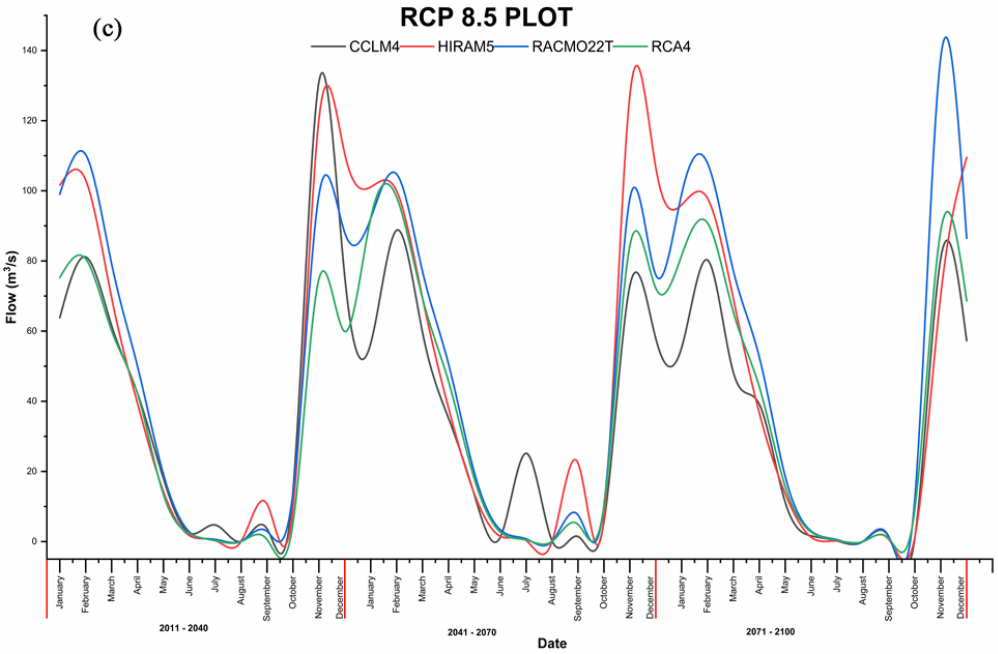

Figure 10. (a) Historical Monthly mean discharge at Galula station (1981-2005); (b) Simulated Monthly mean discharge under RCP 4.5 at Galula station (2011-2100); (c) Simulated Monthly mean discharge under RCP 8.5 at Galula station (2011-2100).

biodiversity, and hydraulic structures may be impacted by the anticipated reduction and rise in river flow throughout both the dry and wet seasons.

3.2.3. Climate Change Impacts on Water Components

The simulated average monthly stream flow for the two climate change scenarios was used to examine the effects of climate change on various water balance components. For the sub-basin, differences between the baseline and future period forecasts in the average annual precipitation, evaporation, surface runoff, lateral flow, groundwater, percolation, and total water yield were estimated. Early and mid-century annual precipitation increased by 67.6 mm under RCP 4.5, while annual precipitation decreased by 13.4 mm under RCP 4.5 for the CCLM4 regional climate model. These changes were observed in surface runoff, lateral flow, groundwater, total water yield, percolation, and evaporation (Table 5). According to RCP 4.5, the HIRAM5 regional climate model, annual precipitation decreased by 189.6 mm, as did surface runoff, lateral flow, groundwater, total water yield, percolation, and evaporation for each of the three time periods of the century (Table 6). For the RACMO22T regional climate model, the increase in annual precipitation, surface runoff, lateral flow, groundwater, total water yield, percolation, and evaporation for the early and end of the century and the decrease in annual precipitation, runoff, lateral flow, groundwater, total

Table 5. Simulated Water balance under CCLM4 RCM.

Hydrologic unit	Annual averages						
	Baseline (1981-2005)	Present century (2011-2040		Mid-century (2041-2071)		End century (2071-2100)	
		RCP 4.5	RCP 8.5	RCP 4.5	RCP 8.5	RCP 4.5	RCP 8.5
Precipitation (mm)	974	996.3	920.2	1064.6	868.3	960.6	853.7
Surface runoff (mm)	153.63	178.88	168.81	233.73	136.9	198.66	141.18
Lateral flow (mm)	13.17	13.51	12.94	13.45	12.08	11.98	11.22
Groundwater (mm)	14.94	15.4	13.48	15.68	12.43	13.08	12.08
Total water yield (mm)	432.4	466.21	416.45	525.77	361.38	436.07	355.65
Percolation (mm)	300.81	308.68	271.96	316.07	252.35	262.08	242.05
Evaporation (mm)	503.9	494.7	464.4	499.1	464.9	488.4	458.2

Table 6. Simulated Water balance under HIRAM5 RCM.

Hydrologic unit	Annual averages						
	Baseline (1981-2005)	Present century (2011-2040		Mid-century (2041-2071)		End century (2071-2100)	
		RCP 4.5	RCP 8.5	RCP 4.5	RCP 8.5	RCP 4.5	RCP 8.5
Precipitation (mm)	972.6	930.4	1014.1	906	1020.6	729.6	1025.6
Surface runoff (mm)	123.4	117.23	179.3	119.1	195.52	80.45	203.56
Lateral flow (mm)	13.69	13.02	16.19	12.43	15.77	11.53	14.78
Groundwater (mm)	15.51	14.55	16.91	13.88	16.6	9.1	16.09
Total water yield (mm)	418.88	390.91	501.87	377.69	509.37	239.18	504.38
Percolation (mm)	315.98	291.94	342.44	278.92	334.02	182.44	327.1
Evaporation (mm)	516.8	506.8	474.2	494.1	472.6	455.9	477.9

water yield, percolation, and evaporation for the middle of the century under RCP 4.5 (Table 7). The reduction in yearly precipitation, surface runoff, groundwater, total water yield, percolation, and evaporation under RCP 4.5, as well as the reduction in precipitation, lateral flow, groundwater, percolation, and evaporation for the middle of the century. Additionally, the RCA4 regional climate model predicts a decrease in lateral flow, percolation, and evaporation at the end of the century under RCP 4.5. (Table 8). HIRAM5, RACMO22T, and RAC4 regional climate models projected higher annual precipitation, surface runoff, lateral flow, groundwater, total water yield, and decreased evaporation and percolation for all time periods of the century under RCP 8.5 (Tables 6-8); however, the CCLM4 climate model projected lower annual precipitation, surface runoff, lateral flow, groundwater, total water yield, percolation, and evaporation under RCP 8.5 for (Table 5). Towards the end of future periods, a major change in both water balance components is anticipated as a result of the

Table 7. Simulated Water balance under RACMO22T RCM.

Hydrologic unit	Annual averages						
	Baseline (1981-2005)	Present century (2011-2040		Mid-century (2041-2071)		End century (2071-2100)	
		RCP 4.5	RCP 8.5	RCP 4.5	RCP 8.5	RCP 4.5	RCP 8.5
Precipitation (mm)	974.4	996.9	999.1	955.4	1016	1017	1065.7
Surface runoff (mm)	76.56	68.9	97.21	64.46	97.58	76.01	116.6
Lateral flow (mm)	14.57	16.29	17.94	14.89	17.52	15.77	18.41
Groundwater (mm)	17.77	18.87	19.96	17.61	20	19.06	20.68
Total water yield (mm)	418.49	433.25	484.33	400.83	483.38	441.93	515.24
Percolation (mm)	358.2	378.52	403.66	354.85	402.01	384.44	417.32
Evaporation (mm)	522.2	531.4	478.1	519	497.2	538.9	511.2

Table 8. Simulated Water balance under RCA4 RCM.

Hydrologic unit	Annual averages						
	Baseline (1981-2005)	Present century (2011-2040		Mid-century (2041-2071)		End century (2071-2100)	
		RCP 4.5	RCP 8.5	RCP 4.5	RCP 8.5	RCP 4.5	RCP 8.5
Precipitation (mm)	974	953.2	973.2	971.5	985.3	990.5	1024.9
Surface runoff (mm)	70.51	69.18	99.41	78.24	100.6	84.28	117.7
Lateral flow (mm)	14.14	13.41	16.38	13.47	15.83	13.49	15.02
Groundwater (mm)	16.73	16.15	16.82	16.56	17.01	17.07	17.81
Total water yield (mm)	389.26	374.07	420.68	390.72	423.79	406.3	454.17
Percolation (mm)	366.76	324.07	340.1	333.42	344.06	343.3	360.06
Evaporation (mm)	550.2	545.1	515.1	544.5	522.6	547.4	529.9

changing climate.

4. Discussion

In the Songwe sub-basin, climate variability has had a significant impact on the hydrological processes. The decrease in river flow in the Songwe sub-basin and Lake Rukwa's water levels downstream are clear signs of the impacts of human activity and climate change [2]. The management of water resources and planning in this sub-basin are both projected to be impacted by climate change. The application of a hydrologic SWAT model and bias correction of the output from the four regional climate models used in the simulation is required for the assessment of how climate change would affect river flows. To get the most out of the bias correction of the output from the Regional Climate Models, observed meteorological data, as well as weather-generated data by SWAT in data-scarce

areas, were necessary.

In places with a lack of data, the lack of long-term observations has a significant impact on studies of climate change. To enable regional climate change impact evaluations at regional scales, high-resolution climate model output is used [21]. To evaluate the effect of climate change on river flows in the Songwe sub-basin, we chose four regional climate models from the CORDEX-AFRICA. The model performances for temperature, precipitation, and hydrology were compared to previously recorded data. To determine the effect of climate change on river flows in the Songwe sub-basin, the regional climate models (RCMs) were bias-corrected using meteorological data that was observed and weather data that the SWAT model generated in the sub-basin. The bias-corrected RCM output was then used directly as input data in the calibrated SWAT model. The hydrological processes in the sub-basin may be impacted by the predicted increase in runoff during the early, middle, and end of the century under RCP 8.5 and a decrease in surface runoff under RCP 4.5. The RCP 8.5 scenario predicts that the flow will increase throughout the entire century. The conflict over the use of the water resource in the sub-basin is anticipated to significantly grow as a result of the simulated decrease in river flows during the dry season.

5. Conclusion

One of the major difficulties in managing the hydrological components in the Songwe sub-basin is the impact of climate change. In this investigation, we evaluate how climate change may affect river flows in the sub-basin. For the purpose of predicting precipitation, minimum and maximum temperatures, and river flows for historical and future periods of the century, four regional climate models, which produced their output under two different climate change scenarios, RCP 4.5 and RCP 8.5, were employed. The parameters established for the hydrologic evaluation of the reference period and estimated future river flows serve as the foundation for choosing the climate model. This project's objective was to use four regional climate models to analyze the effects of climate change on river flows in the Songwe sub-basin. In general, the majority of the scenarios suggest a drop in mean monthly precipitation and an increase in mean monthly temperature for the next century. There was little agreement in the scenarios' projections of the mean monthly rainfall, even though they all projected rising mean monthly temperatures and mean annual temperatures for the study periods. But for the three future eras, the mean annual rainfall was universally predicted to decline in all scenarios. The hydrological components of the sub-basin may be negatively influenced by climate change, according to SWAT model simulation results. Under the RCP 4.5 and RCP 8.5 scenarios compared to the baseline period, the annual precipitation, surface runoff, lateral flow, groundwater, and total water production may increase or decrease in evaporation and percolation for all periods early and mid-century. The relationship between temperature and evaporation was reciprocal, and the relationship between pre-

cipitation and temperature and other hydrological components was reciprocal as well. This implies that the sub-basin may see both a decline and an increase in water balance components in the ensuing century. Therefore, to lessen the detrimental effects of climate change on precipitation, temperature, and river flow in the Songwe sub-basin, proper adaptation, and mitigation methods should be put in place.

Acknowledgements

The author acknowledges funding from the Mbeya University of Science and Technology Research Fund through the post graduate studies. Special thanks to Lake Rukwa Basin Water Office, Mbeya for providing with necessary data for this study.

Conflicts of Interest

The authors declare no conflicts of interest regarding the publication of this paper.

References

[1] Uzbekov, U., Pulatov, B., Alikhanov, B. and Pulatov, A. (2021) Predicting the Impact of Future Climate Change on Streamflow in the Ugam River Watershed. *GeoScape*, **15**, 159-172. https://doi.org/10.2478/geosc-2021-0013

[2] Negewo, T.F. and Sarma, A.K. (2022) Evaluation of Climate Change-Induced Impact on Streamflow and Sediment Yield of Genale Watershed, Ethiopia. In: Harris, S.A. Ed., *The Nature, Causes, Effects and Mitigation of Climate Change on the Environment*, IntechOpen. https://doi.org/10.5772/intechopen.98515

[3] Intergovernmental Panel on Climate Change (2021) AR6 Climate Change 2021: The Physical Science Basis. Chapter 3: Human Influence on the Climate System.

[4] Mbungu, W.B., Easton, Z.M. and Galbraith, J.M. (2016) Impacts of Land Use and Land Cover Changes, and Climate Variability on Hydrology and Soil Erosion in the Upper Ruvu Watershed, Tanzania. Master's Thesis, Virginia Polytechnic Institute and State University, Blacksburg.

[5] Kishiwa, P., Nobert, J., Kongo, V. and Ndomba, P. (2018) Assessment of Impacts of Climate Change on Surface Water Availability Using Coupled SWAT and WEAP Models: Case of Upper Pangani River Basin, Tanzania. *Proceedings of the International Association of Hydrological Sciences*, **378**, 23-27. https://doi.org/10.5194/piahs-378-23-2018

[6] Yeboah, K.A., *et al.* (2022) Assessing Climate Change Projections in the Volta Basin Using the CORDEX-Africa Climate Simulations and Statistical Bias-Correction. *Environmental Challenges*, **6**, Article ID: 100439. https://doi.org/10.1016/j.envc.2021.100439

[7] Gemechu, T.M., *et al.* (2021) Estimation of Hydrological Components under Current and Future Climate Scenarios in Guder Catchment, Upper Abbay Basin, Ethiopia, Using the Swat. *Sustainability*, **13**, Article 9689. https://doi.org/10.3390/su13179689

[8] Luhunga, P.M., Kijazi, A.L., Chang'a, L., Kondowe, A., Ng'ongolo, H. and Mtongori, H. (2018) Climate Change Projections for Tanzania Based on High-Resolution

Regional Climate Models from the Coordinated Regional Climate Downscaling Experiment (CORDEX)-Africa. *Frontiers in Environmental Science*, **6**, 1-20. https://doi.org/10.3390/su13179689

[9] Nobert, J. (2022) Assessment of the Impact of Climate Change on Stream Flow : The Case of Little Ruaha Catchment, Rufiji Basin, Tanzania. *Tanzania Journal of Science*, **48**, 170-184. https://doi.org/10.4314/tjs.v48i1.16

[10] Tarekegn, N., Abate, B., Muluneh, A. and Dile, Y. (2022) Modeling the Impact of Climate Change on the Hydrology of Andasa Watershed. *Modeling Earth Systems and Environment*, **8**, 103-119. https://doi.org/10.1007/s40808-020-01063-7

[11] Azari, M., Moradi, H.R., Saghafian, B. and Faramarzi, M. (2016) Climate Change Impacts on Streamflow and Sediment Yield in the North of Iran. *Hydrological Sciences Journal*, **61**, 123-133. https://doi.org/10.1080/02626667.2014.967695

[12] Musie, M., Sen, S. and Srivastava, P. (2020) Application of CORDEX-AFRICA and NEX-GDDP Datasets for Hydrologic Projections under Climate Change in Lake Ziway Sub-Basin, Ethiopia. *Journal of Hydrology*: *Regional Studies*, **31**, Article ID: 100721. https://doi.org/10.1016/j.ejrh.2020.100721

[13] Awotwi, A., *et al.* (2021) Climate Change Impact on Streamflow in a Tropical Basin of Ghana, West Africa. *Journal of Hydrology*: *Regional Studies*, **34**, Article ID: 100805. https://doi.org/10.1016/j.ejrh.2020.100721

[14] Shrestha, N.K. and Wang, J. (2018) Predicting Sediment Yield and Transport Dynamics of a Cold Climate Region Watershed in Changing Climate. *Science of the Total Environment*, **625**, 1030-1045. https://doi.org/10.1016/j.scitotenv.2017.12.347

[15] Mengistu, A.G., Woldesenbet, T.A. and Dile, Y.T. (2021) Evaluation of the Performance of Bias-Corrected CORDEX Regional Climate Models in Reproducing Baro-Akobo Basin Climate. *Theoretical and Applied Climatology*, **144**, 751-767. https://doi.org/10.1007/s00704-021-03552-w

[16] Arnold, J.G., Kiniry, J.R., Srinivasan, R., Williams, J.R., Haney, E.B. and Neitsch, S.L. (2012) Soil & Water Assessment Tool.

[17] Tian, P., Mu, X., Liu, J., Hu, J. and Gu, C. (2016)Impacts of Climate Variability and Human Activities on the Changes of Runoff and Sediment Load in a Catchment of the Loess Plateau, China. *Advances in Meteorology*, **2016**, Article ID: 4724067. https://doi.org/10.1155/2016/4724067

[18] Nilawar, A.P. and Waikar, M.L. (2019) Impacts of Climate Change on Streamflow and Sediment Concentration under RCP 4.5 and 8.5: A Case Study in Purna River Basin, India. *Science of the Total Environment*, **650**, 2685-2696. https://doi.org/10.1016/j.scitotenv.2018.09.334

[19] Hallouz, F., Meddi, M., Mahé, G., Alirahmani, S. and Keddar, A. (2018) Modeling of Discharge and Sediment Transport through the SWAT Model in the Basin of Harraza (Northwest of Algeria). *Water Science*, **32**, 79-88. https://doi.org/10.1016/j.wsj.2017.12.004

[20] Ndhlovu, G.Z. and Woyessa, Y.E. (2021) Evaluation of Streamflow under Climate Change in the Zambezi River Basin of Southern Africa. *Water* (*Switzerland*), **13**, Article 3114. https://doi.org/10.3390/w13213114

[21] Shrestha, B., *et al.* (2021) Impact of Climate Change on Sediment Yield in the Mekong River Basin: A Case Study of the Nam Ou Basin, Lao PDR. *Hydrology and Earth System Sciences Discussions*, **9**, 3339-3384. https://doi.org/10.5194/hessd-9-3339-2012

Appendix C: Historical and Projected Sediment Yield under RCP4.5 and RCP8.5 Climate scenarios

Historical projected sediment yield

Date	CCLM4	HIRAM5	RACMO22T	RCA4
Jan-81	10.751	1.226	0.465	3.422
Feb-81	2.956	16.852	1.202	5.532
Mar-81	9.599	7.843	2.08	1.308
Apr-81	2.897	0.319	0	4.266
May-81	0	0.021	0.295	0
Jun-81	0	0	0	0
Jul-81	0	0	0	0
Aug-81	0	0	0	0
Sept-81	0	0	0	0
Oct-81	0	0	0	0
Nov-81	0	0.046	0	0
Dec-81	0.031	0.461	0.027	0.095
Jan-82	1.067	5.551	0.438	4.4
Feb-82	0.29	1.689	0.581	2.264
Mar-82	2.648	6.94	2.814	3.313
Apr-82	1	4.16	0	1.476
May-82	0	0	0	0
Jun-82	0	0	0	0
Jul-82	0	0	0	0
Aug-82	0	0	0	0
Sept-82	0	0	0	0
Oct-82	0	0	0	0
Nov-82	0.008	0.141	0	0
Dec-82	0.294	0.692	0.082	0.092
Jan-83	0.9	4.295	0.536	4.008
Feb-83	0.805	2.061	0.526	3.468

Mar-83	10.317	5.089	2.231	1.689
Apr-83	0.765	2.472	0.007	1.29
May-83	0	0	0	0
Jun-83	0	0	0	0
Jul-83	0	0	0	0
Aug-83	0	0	0	0
Sept-83	0	0	0	0
Oct-83	0	0	0	0
Nov-83	0	0.068	0	0
Dec-83	0.272	1.924	0.167	1.429
Jan-84	4.495	2.105	3.054	0.73
Feb-84	4.206	1.691	2.195	2.05
Mar-84	2.462	7.116	0.954	8.569
Apr-84	0	0.029	0	0
May-84	0	0	0	0
Jun-84	0	0	0	0
Jul-84	0	0	0	0
Aug-84	0	0	0	0
Sept-84	0	0	0	0
Oct-84	0	0	0	0
Nov-84	0	0	0	0
Dec-84	0.32	0.525	0.76	0.052
Jan-85	1.979	6.281	3.664	1.077
Feb-85	1.468	3.227	1.185	1.136
Mar-85	14.728	7.973	4.355	0.664
Apr-85	5.126	3.028	1.651	0.151
May-85	0	0	0	0
Jun-85	0	0	0	0
Jul-85	0	0	0	0
Aug-85	0	0	0	0
Sept-85	0	0	0	0

Oct-85	0	0	0	0
Nov-85	0	0	0	0
Dec-85	1.215	0.314	0.022	0.203
Jan-86	13.077	3.257	0.864	1.424
Feb-86	6.899	2.78	0.685	1.378
Mar-86	0.879	5.974	4.67	1.071
Apr-86	0.104	0	0.086	0.99
May-86	0	0	0	0
Jun-86	0	0	0	0
Jul-86	0	0	0	0
Aug-86	0	0	0	0
Sept-86	0	0	0	0
Oct-86	0	0	0	0
Nov-86	0	0	0	0
Dec-86	0.047	0.839	0.01	0.438
Jan-87	0.665	6.003	0.933	0.126
Feb-87	0.409	3.472	0.74	0.581
Mar-87	0.978	2.093	2.264	0.684
Apr-87	0	1.524	0.244	0.484
May-87	0.321	0	0	0
Jun-87	0	0	0	0
Jul-87	0	0	0	0
Aug-87	0	0	0	0
Sept-87	0	0	0	0
Oct-87	0.024	0	0	0
Nov-87	0.058	0	0	0
Dec-87	2.545	0.409	0.002	0.161
Jan-88	1.649	7.604	0.711	2.146
Feb-88	1.408	1.964	1.182	2.217
Mar-88	0.396	6.906	3.922	1.135
Apr-88	0	2.96	0.006	0

May-88	0	0	0	0
Jun-88	0	0	0	0
Jul-88	0	0	0	0
Aug-88	0	0	0	0
Sept-88	0	0	0	0
Oct-88	0	0	0	0
Nov-88	0.019	0.044	0	0
Dec-88	1.542	0.751	0.073	0.64
Jan-89	0.409	4.583	0.44	2.981
Feb-89	43.065	2.615	0.511	1.11
Mar-89	3.947	2.183	5.217	3.357
Apr-89	0	0.985	3.067	0.784
May-89	0	0	0	0
Jun-89	0	0	0	0
Jul-89	0	0	0	0
Aug-89	0	0	0	0
Sept-89	0	0	0	0
Oct-89	2.213	0	0	0
Nov-89	0	0	0.002	0
Dec-89	0.424	0	0.28	0.335
Jan-90	13.33	4.065	1.034	1.052
Feb-90	0.532	8.446	0.708	0.53
Mar-90	3.943	4.212	1.935	0.82
Apr-90	0.105	1.056	0.516	0.521
May-90	0	0	0	0
Jun-90	0	0	0	0
Jul-90	0	0	0	0
Aug-90	0	0	0	0
Sept-90	0	0	0	0
Oct-90	0	0	0	0
Nov-90	0	0	0	0

Dec-90	0.026	0.949	0.082	0.161
Jan-91	0.533	5.227	2.042	3.256
Feb-91	7.052	1.123	0.925	0.474
Mar-91	0.512	4.212	5.079	0.774
Apr-91	0	0.156	0.185	1.809
May-91	0	0	0	0
Jun-91	0	0	0	0
Jul-91	0	0	0	0
Aug-91	0	0	0	0
Sept-91	0	0	0	0
Oct-91	0	0	0	0
Nov-91	1.51	0	0	0
Dec-91	3.764	0.228	0.703	0
Jan-92	22.274	5.137	1.274	1.674
Feb-92	0.63	4.144	0.473	1.544
Mar-92	8.929	0.602	1.628	2.334
Apr-92	0.797	1.013	0.785	0.072
May-92	0	0	0	0
Jun-92	0	0	0	0
Jul-92	0	0	0	0
Aug-92	0	0	0	0
Sept-92	0	0	0	0
Oct-92	0	0	0	0
Nov-92	0.738	0	0	0
Dec-92	0.477	0.522	0.119	0.497
Jan-93	0.873	10.995	1.707	5.572
Feb-93	0.292	2.603	1.34	1.888
Mar-93	12.22	8.249	1.754	1.463
Apr-93	0.001	11.994	0.052	0.916
May-93	0	0	0	0
Jun-93	0	0	0	0

Jul-93	0	0	0	0
Aug-93	0	0	0	0
Sept-93	0	0	0	0
Oct-93	0	0	0	0
Nov-93	0	0	0	0
Dec-93	0.001	0.591	0.044	0
Jan-94	17.678	4.703	1.738	2.429
Feb-94	0.606	3.91	1.58	0.447
Mar-94	2.775	5.706	5.116	1.279
Apr-94	2.851	4.342	9.266	0.335
May-94	0	0	0	0
Jun-94	0	0	0	0
Jul-94	0	0	0	0
Aug-94	0	0	0	0
Sept-94	0	0	0	0
Oct-94	0	0	0	0
Nov-94	0	0.01	0	0
Dec-94	0.339	0.018	0	1.057
Jan-95	0.858	1.153	0.152	4.031
Feb-95	15.231	0.644	1.644	3.143
Mar-95	1.008	5.228	7.199	3.124
Apr-95	0.183	0.251	5.056	0.001
May-95	0	0	0	0
Jun-95	0	0	0	0
Jul-95	0	0	0	0
Aug-95	0	0	0	0
Sept-95	0	0	0	0
Oct-95	0	0	0	0
Nov-95	0.002	0	0	0
Dec-95	0.057	0.147	0.306	0.126
Jan-96	5.916	2.401	1.72	3.95

Feb-96	5.009	4.423	0.805	2.653
Mar-96	0.133	5.889	3.204	0.61
Apr-96	4.262	0.107	10.842	1.805
May-96	0	0.536	0	0
Jun-96	0	0	0	0
Jul-96	0	0	0	0
Aug-96	0	0	0	0
Sept-96	0	0	0	0
Oct-96	0	0	0	0
Nov-96	0	0	0	0
Dec-96	1.147	0.628	0.024	0.03
Jan-97	42.497	4.848	1.04	2.943
Feb-97	6.009	5.237	1.47	1.438
Mar-97	17.64	2.77	3.859	4.258
Apr-97	11.329	4.394	0	1.417
May-97	0	0	0	0
Jun-97	0	0	0	0
Jul-97	0	0	0	0
Aug-97	0	0	0	0
Sept-97	0	0	0	0
Oct-97	0	0	0	0
Nov-97	0	0	0	0.03
Dec-97	0.012	0.764	0.011	0.017
Jan-98	1.697	8.844	0.926	3.759
Feb-98	3.391	2.16	1.279	0.739
Mar-98	0.894	2.95	2.566	1.804
Apr-98	22.822	0.05	3.465	0.039
May-98	1.477	0	0	0
Jun-98	0	0	0	0
Jul-98	0	0	0	0
Aug-98	0	0	0	0

Sept-98	0	0	0	0
Oct-98	0	0	0	0
Nov-98	0.018	0	0	0
Dec-98	0.476	0.537	0.073	1.082
Jan-99	5.114	5.561	2.742	2.642
Feb-99	5.511	4.653	0.842	0.467
Mar-99	0.243	4.955	2.14	2.748
Apr-99	0.083	0.094	4.18	1.232
May-99	0	0	0	0.706
Jun-99	0	0	0	0
Jul-99	0	0	0	0
Aug-99	0	0	0	0
Sept-99	0	0	0	0
Oct-99	0	0	0	0
Nov-99	0	0	0	0
Dec-99	1.928	0.797	0.124	0.03
Jan-00	1.621	2.058	1.152	4.556
Feb-00	0.366	5.215	1.044	0.433
Mar-00	1.44	10.8	4.308	1.407
Apr-00	0	0	4.274	0
May-00	0	0	0	0
Jun-00	0	0	0	0
Jul-00	0	0	0	0
Aug-00	0	0	0	0
Sept-00	0	0	0	0
Oct-00	0	0	0	0
Nov-00	0.021	0	0	0
Dec-00	7.578	0.218	0.027	0.644
Jan-01	5.402	9.384	3.309	10.819
Feb-01	0.293	10.824	3.238	1.53
Mar-01	6.521	2.151	3.4	2.171

Apr-01	0.037	3.102	0.005	0.028
May-01	0	0	0	0
Jun-01	0	0	0	0
Jul-01	0	0	0	0
Aug-01	0	0	0	0
Sept-01	0	0	0	0
Oct-01	0	0	0	0
Nov-01	4.701	0	0	0.003
Dec-01	1.631	0.496	0.046	0.495
Jan-02	5.568	3.848	2.925	1.361
Feb-02	1.299	1.341	1.149	12.618
Mar-02	12.804	0.397	4.395	3.689
Apr-02	1.894	0.163	0.684	3.974
May-02	0.61	0	0	0
Jun-02	0	0	0	0
Jul-02	0	0	0	0
Aug-02	0	0	0	0
Sept-02	0	0	0	0
Oct-02	0	0	0	0
Nov-02	0	0	0	0
Dec-02	0	1.065	0.029	0.144
Jan-03	0.035	6.319	0.751	1.279
Feb-03	0.886	5.366	0.855	0.616
Mar-03	4.878	4.613	4.527	6.232
Apr-03	0	0.74	1.291	0.291
May-03	0.006	0	0	0.009
Jun-03	0	0	0	0
Jul-03	0	0	0	0
Aug-03	0	0	0	0
Sept-03	0	0	0	0
Oct-03	0	0	0	0

Nov-03	0.051	0	0	0
Dec-03	0.094	0.021	0.063	0.587
Jan-04	4.548	0.813	1.272	1.002
Feb-04	0.363	3.424	1.379	0.256
Mar-04	7.443	5.294	1.546	2.608
Apr-04	2.427	0.018	0.125	1.104
May-04	0	0	0	0
Jun-04	0	0	0	0
Jul-04	0	0	0	0
Aug-04	0	0	0	0
Sept-04	0	0	0	0
Oct-04	0	0	0	0
Nov-04	0	0	0	0
Dec-04	1.616	0.573	0.206	0.092
Jan-05	8.901	5.835	2.362	2.728
Feb-05	0.421	3.052	1.217	1.447
Mar-05	1.701	3.758	6.622	3.858
Apr-05	9.582	0.052	0.231	2.855
May-05	0	0	0	0
Jun-05	0	0	0	0
Jul-05	0	0	0	0
Aug-05	0	0	0	0
Sept-05	0	0	0	0
Oct-05	0	0	0	0
Nov-05	0.044	0.004	0	0
Dec-05	0.386	4.749	0.128	0.051

Projected sediment yield (2010-2040) under RCP4.5

Date	CCLM4	HIRAM5	RACMO22T	RCA4
Jan-11	0.768	1.107	1.215	1.273
Feb-11	9.299	9.673	1.779	1.904
Mar-11	11.328	8.155	3.98	2.948
Apr-11	5.628	0.307	2.96	0.377
May-11	0.154	0	0	0
Jun-11	0	0	0	0
Jul-11	0	0	0	0
Aug-11	0	0	0	0
Sept-11	0	0	0	0
Oct-11	0	0	0	0
Nov-11	0	0.257	0	0
Dec-11	0.19	0.541	0.002	0.159
Jan-12	0.786	4.654	0.713	1.488
Feb-12	0.646	2.646	0.919	1.577
Mar-12	11.977	7.064	2.422	0.986
Apr-12	1.468	3.293	0	0.095
May-12	0	0	0	0
Jun-12	0	0	0	0
Jul-12	0	0	0	0
Aug-12	0	0	0	0
Sept-12	0	0	0	0
Oct-12	0	0	0	0
Nov-12	0.127	0.008	0	0
Dec-12	1.096	0.084	0.325	0.103
Jan-13	19.117	3.816	0.961	5.06
Feb-13	0.036	4.413	0.499	0.693
Mar-13	3.874	3.078	3.178	2.754
Apr-13	0.019	0	0.006	0
May-13	0	0	1.303	0
Jun-13	0	0	0	0
Jul-13	0	0	0	0
Aug-13	0	0	0	0
Sept-13	0	0	0	0
Oct-13	0	0	0	0
Nov-13	1.321	0.019	0	0
Dec-13	2.432	2.678	0.445	0.661
Jan-14	2.386	7.781	2.026	1.717
Feb-14	0.214	4.076	0.839	0.769
Mar-14	1.727	0.04	2.053	1.654
Apr-14	5.668	0.28	0.688	0.01
May-14	0	0	0	0
Jun-14	0	0	0	0
Jul-14	0	0	0	0
Aug-14	0	0	0	0
Sept-14	0	0	0	0
Oct-14	0	0	0	0
Nov-14	11.91	0	0	0.06
Dec-14	0.529	0.082	0.196	0.542
Jan-15	4.09	3.231	1.494	1.813
Feb-15	1.693	8.746	1.599	0.676

Mar-15	1.453	5.029	1.566	2.52
Apr-15	0.041	0.002	7.305	1.273
May-15	0	0	0	0
Jun-15	0	0	0	0
Jul-15	0	0	0	0
Aug-15	0	0	0	0
Sept-15	0	0	0	0
Oct-15	0	0	0	0
Nov-15	0	0	0	0
Dec-15	5.556	0.002	0.119	0.153
Jan-16	11.027	4.553	0.587	0.57
Feb-16	2.193	2.094	0.697	0.724
Mar-16	0.243	6.815	3.609	2.515
Apr-16	0	1.858	1.754	0.917
May-16	0	0	0	0.013
Jun-16	0	0	0	0
Jul-16	0	0	0	0
Aug-16	0	0	0	0
Sept-16	0	0	0	0.016
Oct-16	0.003	0	0	0
Nov-16	1.431	0	0	0
Dec-16	5.689	2.059	0.208	0.006
Jan-17	2.346	2.258	0.925	1.228
Feb-17	28.322	3.098	0.628	0.961
Mar-17	28.494	5.014	3.139	4.261
Apr-17	0.02	0.183	0.002	2.646
May-17	0	0	0	0
Jun-17	0	0	0	0
Jul-17	0	0	0	0
Aug-17	0	0	0	0
Sept-17	0	0	0	0
Oct-17	0	0	0	0
Nov-17	4.748	0	0	0
Dec-17	34.056	0.036	0.242	0.147
Jan-18	1.508	3.59	1.178	2.378
Feb-18	65.07	0.75	1.152	0.275
Mar-18	9.692	2.003	1.161	0.573
Apr-18	9.523	0	1.98	1.15
May-18	0.408	0	0	0
Jun-18	0	0	0	0
Jul-18	0	0	0	0
Aug-18	0	0	0	0
Sept-18	0	0	0	0
Oct-18	0	0	0	0
Nov-18	0	0.045	0	0
Dec-18	2.321	0.738	0.015	0.317
Jan-19	2.249	6.737	0.385	6.612
Feb-19	13.517	12.326	0.242	1.627
Mar-19	2.105	7.482	0.267	4.269
Apr-19	0.949	3.283	0	0.094
May-19	0	0	0	0
Jun-19	0	0	0	0
Jul-19	0	0	0	0
Aug-19	0	0	0	0

Sept-19	0	0	0	0
Oct-19	0	0	0	0
Nov-19	0	0	0	0
Dec-19	0.096	0.065	0.209	0.016
Jan-20	2.866	4.323	3.512	2.01
Feb-20	0.325	4.729	3.167	0.578
Mar-20	1.616	22.303	3.975	0.367
Apr-20	0.513	0	1.174	0
May-20	0	0	3.115	0
Jun-20	0	0	0	0
Jul-20	0	0	0	0
Aug-20	0	0	0	0
Sept-20	0	0	0	0
Oct-20	0	0	0	0
Nov-20	0	0	0	0
Dec-20	0.205	0.843	0.015	0.229
Jan-21	0.208	6.219	0.866	4.847
Feb-21	2.971	7.215	0.466	3.133
Mar-21	2.128	2.351	2.022	1.264
Apr-21	0.408	0.448	1.274	1.106
May-21	0	0	0	0
Jun-21	0	0	0	0
Jul-21	0	0	0	0
Aug-21	0	0	0	0
Sept-21	0	0	0	0
Oct-21	0	0	0	0
Nov-21	0.315	0	0	0
Dec-21	0.691	2.57	0.095	0.359
Jan-22	0.068	5.951	1.625	0.721
Feb-22	19.212	4.17	0.749	0.748
Mar-22	6.344	1.558	0.041	0.91
Apr-22	0	0	0	0.501
May-22	0	0	0	0
Jun-22	0	0	0	0
Jul-22	0	0	0	0
Aug-22	0	0	0	0
Sept-22	0	0	0	0
Oct-22	0	0	0	0
Nov-22	0.038	0.012	0	0
Dec-22	0.697	0.464	0.237	1.648
Jan-23	3.333	7.787	2.533	21.427
Feb-23	5.921	2.483	1.273	2.989
Mar-23	6.731	8.437	2.316	3.589
Apr-23	0.056	0.277	0.051	0.056
May-23	0	0	0	0
Jun-23	0	0	0	0
Jul-23	0	0	0	0
Aug-23	0	0	0	0
Sept-23	0	0	0	0
Oct-23	0	0	0	0
Nov-23	0.013	0	0	0
Dec-23	2.269	0.15	0.575	0.149
Jan-24	1.654	3.065	3.15	3.396
Feb-24	4.785	3.537	0.903	1.461

Mar-24	0.217	1.624	3.173	2.195
Apr-24	0	12.032	0.005	2.968
May-24	0	0	2.26	0
Jun-24	0	0	0	0
Jul-24	0	0	0	0
Aug-24	0	0	0	0
Sept-24	0	0	0	0.122
Oct-24	0	0	0	0
Nov-24	0.006	0	0	0
Dec-24	3.805	0.754	0.084	0.19
Jan-25	0.903	2.526	0.371	0.9
Feb-25	0.637	1.493	0.565	0.855
Mar-25	2.757	0.601	1.116	2.505
Apr-25	0.022	0.744	0.304	0
May-25	0	0	0.966	0
Jun-25	0	0	0	0
Jul-25	0	0	0	0
Aug-25	0	0	0	0
Sept-25	0	0	0	0
Oct-25	0	0	0	0
Nov-25	0.064	0	0	0.001
Dec-25	1.93	0.548	0.049	0
Jan-26	11.465	10.439	1.02	4.445
Feb-26	0.891	2.665	0.603	1.279
Mar-26	7.519	2.721	0.941	1.961
Apr-26	10.758	0.235	7.307	0.75
May-26	0	0	0	0.096
Jun-26	0	0	0	0
Jul-26	0	0	0	0
Aug-26	0	0	0	0
Sept-26	0	0	0	0
Oct-26	0	0	0	0
Nov-26	0	0	0	0
Dec-26	0.272	0.033	0.003	0.073
Jan-27	0.939	1.02	0.874	0.281
Feb-27	0.91	2.224	1.059	1.062
Mar-27	0.751	3.854	0.817	1.256
Apr-27	0.407	1.17	0.074	0.55
May-27	0	0	0	0
Jun-27	0	0	0	0
Jul-27	0	0	0	0
Aug-27	0	0	0	0
Sept-27	0	0	0	0
Oct-27	0	0	0	0
Nov-27	0.328	0.005	0.099	0
Dec-27	18.545	0.685	0.174	0.314
Jan-28	0.321	1.789	1.159	2.375
Feb-28	1.015	7.242	3.153	3.599
Mar-28	3.786	1.199	2.669	0.355
Apr-28	9.431	0	0	4.06
May-28	0	0	0	1.484
Jun-28	0	0	0	0
Jul-28	0	0	0	0
Aug-28	0	0	0	0

Sept-28	0	0	0	0
Oct-28	0	0	0	0
Nov-28	0	0.229	0	0
Dec-28	0.095	1.67	0.278	0.13
Jan-29	1.935	13.071	2.595	0.883
Feb-29	1.684	0.8	1.173	0.683
Mar-29	1.815	0.086	2.428	0.75
Apr-29	0.047	0	0.152	1.425
May-29	0	0	0	0
Jun-29	0	0	0	0
Jul-29	0	0	0	0
Aug-29	0	0	0	0
Sept-29	0	0	0	0
Oct-29	0	0	0	0
Nov-29	0	0	0	0
Dec-29	2.135	1.399	0.138	0.017
Jan-30	6.144	9.202	2.081	1.087
Feb-30	2.405	1.957	0.628	0.098
Mar-30	17.038	2.642	2.321	2.095
Apr-30	2.331	0	0	4.109
May-30	0.604	0	0	0
Jun-30	0	0	0	0
Jul-30	0	0	0	0
Aug-30	0	0	0	0
Sept-30	0	0	0	0
Oct-30	0	0	0	0
Nov-30	0.156	0	0	0
Dec-30	0.423	0.368	0.04	0.146
Jan-31	22.073	6.189	2.465	7.22
Feb-31	6.083	4.99	1.594	2.453
Mar-31	25.33	7.302	4.246	1.753
Apr-31	0.022	0	2.022	4.639
May-31	0	0	0	0
Jun-31	0	0	0	0
Jul-31	0	0	0	0
Aug-31	0	0	0	0
Sept-31	0	0	0	0
Oct-31	0	0	0	0
Nov-31	0.004	0	0	0
Dec-31	0	0.164	0.209	0.203
Jan-32	0.808	7.117	0.942	11.513
Feb-32	1.466	4.149	2.061	0.877
Mar-32	8.85	2.437	0.908	4.911
Apr-32	0	0	0.005	0
May-32	0	0	0	0
Jun-32	0	0	0	0
Jul-32	0	0	0	0
Aug-32	0	0	0	0
Sept-32	0	0	0	0
Oct-32	0	0	0	0
Nov-32	1.733	0	0.001	0
Dec-32	1.92	0.014	0.497	1.83
Jan-33	13.426	38.132	3.237	5.801
Feb-33	4.314	4.608	2.479	2.853

Mar-33	12.205	8.934	4.028	2.948
Apr-33	3.342	0.684	0.528	1.12
May-33	0	0	0	0
Jun-33	0	0	0	0
Jul-33	0	0	0	0
Aug-33	0	0	0	0
Sept-33	0.437	0	0	0
Oct-33	0	0	0	0
Nov-33	2.769	0.065	0	0
Dec-33	10.442	2.542	0.409	0.006
Jan-34	5.278	4.825	2.603	1.473
Feb-34	0.444	4.386	1.454	0.568
Mar-34	1.687	4.378	2.257	1.605
Apr-34	0.028	0.129	0.013	2.951
May-34	0	0	0	0
Jun-34	0	0	0	0
Jul-34	0	0	0	0
Aug-34	0	0	0	0
Sept-34	0	0	0	0
Oct-34	0	0	0	0
Nov-34	0	0.04	0	0
Dec-34	0.62	0.1	0.251	0.241
Jan-35	0.591	3.247	0.931	2.945
Feb-35	7.61	2.421	0.674	0.103
Mar-35	5.03	4.173	1.226	0.86
Apr-35	2.811	1.244	0.276	0
May-35	0	0	0	0
Jun-35	0	0	0	0
Jul-35	0	0	0	0
Aug-35	0	0	0	0
Sept-35	0	0	0	0
Oct-35	0	0	0	0
Nov-35	0	0	0	0.144
Dec-35	0.663	0.045	0.273	0.368
Jan-36	6.045	6.693	1.463	2.51
Feb-36	28.332	2.641	3.692	4.759
Mar-36	5.37	4.218	1.176	3.257
Apr-36	0.041	1.406	0.018	0.025
May-36	0	0	0	0
Jun-36	0	0	0	0
Jul-36	0	0	0	0
Aug-36	0	0	0	0
Sept-36	0	0	0	0
Oct-36	0	0	0	0
Nov-36	0	0	0	0
Dec-36	0	2.594	0.1	0
Jan-37	0.802	2.246	1.595	0.284
Feb-37	0.14	2.151	1.674	2.876
Mar-37	1.564	5.581	2.511	2.157
Apr-37	0	2.077	0	0.031
May-37	0	0	0.131	0
Jun-37	0	0	0	0
Jul-37	0	0	0	0
Aug-37	0	0	0	0

Sept-37	0	0	0	0
Oct-37	0	0	0	0
Nov-37	1.037	0.036	0	0
Dec-37	10.008	0.701	0.147	0.15
Jan-38	2.333	4.989	2.897	1.401
Feb-38	0.604	5.076	1.374	0.154
Mar-38	4.293	4.121	2.607	1.399
Apr-38	1.108	0.606	0.118	0.004
May-38	0	0	0	0
Jun-38	0	0	0	0
Jul-38	0	0	0	0
Aug-38	0	0	0	0
Sept-38	0	0	0	0
Oct-38	0	0	0	0
Nov-38	0	0	0	0
Dec-38	0.684	0.283	0.256	0.348
Jan-39	5.88	5.688	1.706	1.607
Feb-39	1.01	3.023	1.253	11.852
Mar-39	35.046	4.949	5.291	2.535
Apr-39	0.775	0.008	5.337	1.23
May-39	0	0	0	0
Jun-39	0	0	0	0
Jul-39	0	0	0	0
Aug-39	0	0	0	0
Sept-39	0	0	0	0
Oct-39	0	0	0	0
Nov-39	5.987	0.01	0	0
Dec-39	1.068	0.85	0.113	0.004
Jan-40	12.665	4.288	2.122	1.054
Feb-40	8.943	3.701	1.704	4.551
Mar-40	14.933	2.188	1.154	2.028
Apr-40	0	0.002	0	0.075
May-40	0	0	0	0
Jun-40	0	0	0	0
Jul-40	0	0	0	0
Aug-40	0	0	0	0
Sept-40	0	0	0	0
Oct-40	0	0	0	0
Nov-40	0	0.264	0	0
Dec-40	0	1.038	0.055	0.224

Projected sediment yield (2041-2070) under RCP4.5

Date	CCLM4	HIRAM5	RACMO22T	RCA4
Jan-41	0.109	2.58	0.31	0.715
Feb-41	0.128	9.422	1.133	0.487
Mar-41	2.94	4.997	0.834	4.617
Apr-41	0.005	0	0	0
May-41	0	0	0	0
Jun-41	0	0	0	0
Jul-41	0	0	0	0
Aug-41	0	0	0	0
Sept-41	0	0	0	0
Oct-41	0	0	0	0
Nov-41	0	0	0	0
Dec-41	4.899	0.957	0.105	0.117
Jan-42	3.749	5.893	1.616	3.494
Feb-42	0.314	0.459	0.83	0.748
Mar-42	2.855	3.51	1.112	2.335
Apr-42	0.034	0	0.004	1.129
May-42	0	0	0	0
Jun-42	0	0	0	0
Jul-42	0	0	0	0
Aug-42	0	0	0	0
Sept-42	0	0	0	0
Oct-42	0	0	0	0
Nov-42	0.06	0	0	0
Dec-42	1.495	0.37	0.047	0.091
Jan-43	10.348	4.768	4.045	1.186
Feb-43	10.898	1.82	1.514	1.614
Mar-43	1.5	3.641	3.87	0.717
Apr-43	0.327	0	3.2	1.727
May-43	0	0	0	0
Jun-43	0	0	0	0
Jul-43	0	0	0	0
Aug-43	0	0	0	0
Sept-43	0	0	0	0
Oct-43	0	0	0	0
Nov-43	0	0	0	0
Dec-43	0.503	0.224	0.067	0.589
Jan-44	3.796	2.861	1.168	4.391
Feb-44	3.064	7.65	0.328	0.91
Mar-44	0.144	8.078	1.844	1.686
Apr-44	3.195	1.408	0.413	0.691
May-44	7.725	0	0	0
Jun-44	0	0	0	0
Jul-44	0	0	0	0
Aug-44	0	0	0	0
Sept-44	0	0	0	0
Oct-44	0	0	0	0
Nov-44	0.307	0	0	0
Dec-44	9.594	0.023	0.179	1.233
Jan-45	14.588	3.521	1.656	2.62
Feb-45	0.66	1.599	1.365	2.454
Mar-45	17.698	0.869	2.015	4.12
Apr-45	0	0.171	0.49	0

May-45	0	0	0.395	0
Jun-45	0	0	0	0
Jul-45	0	0	0	0
Aug-45	0	0	0	0
Sept-45	0	0	0	0
Oct-45	0	0	0	0
Nov-45	1.058	0.011	0	0
Dec-45	7.047	0.297	0.265	0.69
Jan-46	31.751	8.371	1.091	10.387
Feb-46	1.658	2.675	1.069	2.161
Mar-46	1.521	2.309	2.422	3.569
Apr-46	0	4.075	0.457	0.001
May-46	0	0.315	0	0
Jun-46	0	0	0	0
Jul-46	0	0	0	0
Aug-46	0	0	0	0
Sept-46	0	0	0	0
Oct-46	0	0	0	0
Nov-46	3.951	0	0	0
Dec-46	0.007	0.062	0.414	0.036
Jan-47	0.696	5.259	0.962	4.889
Feb-47	1.708	5.784	0.923	4.106
Mar-47	4.865	2.152	3.559	3.639
Apr-47	0.039	0.582	2.079	0.524
May-47	0	0	0	0.006
Jun-47	0	0	0	0
Jul-47	0	0	0	0
Aug-47	0	0	0	0
Sept-47	0	0	0	0
Oct-47	0	0	0	0
Nov-47	0.031	0	0	0
Dec-47	0.247	0.242	0.13	0.336
Jan-48	8.123	2.991	1.793	1.121
Feb-48	2.787	2.543	1.42	1.731
Mar-48	3.702	8.258	2.621	1.451
Apr-48	0.001	0.062	0	0.656
May-48	0	0	0	0
Jun-48	0	0	0	0
Jul-48	0	0	0	0
Aug-48	0	0	0	0
Sept-48	0	0.238	0	0
Oct-48	0	0	0	0
Nov-48	0	0	0	0
Dec-48	0.573	0.543	0.32	0.254
Jan-49	4.699	3.886	1.319	1.627
Feb-49	3.822	6.591	0.733	1.237
Mar-49	82.836	6.288	1.46	4.488
Apr-49	9.549	1.605	11.371	1.782
May-49	0	0.027	0	2.436
Jun-49	0	0	0	0
Jul-49	0	0	0	0
Aug-49	0	0	0	0
Sept-49	0	0	0	0
Oct-49	0	0	0	0

Nov-49	0.006	0	0	0
Dec-49	0.21	0.517	0.147	0.269
Jan-50	17.17	4.477	0.842	3.014
Feb-50	2.022	6.446	2.126	2.207
Mar-50	5.328	2.626	2.766	4.008
Apr-50	0	0.137	0.093	0.012
May-50	0	0	0	0.002
Jun-50	0	0	0	0
Jul-50	0	0	0	0
Aug-50	0	0	0	0
Sept-50	0	0	0	0
Oct-50	0	0	0	0
Nov-50	0	0	0	0
Dec-50	3.151	0.035	0.018	0.083
Jan-51	4.358	6.761	1.313	1.079
Feb-51	0.44	3.979	3.961	0.609
Mar-51	0.105	1.561	5.313	0.183
Apr-51	0.017	0.083	0	0.125
May-51	0	0	0	0
Jun-51	0	0	0	0
Jul-51	0	0	0	0
Aug-51	0	0	0	0
Sept-51	0	0	0	0
Oct-51	0	0	0	0
Nov-51	0	0	0.002	0
Dec-51	0.369	0.022	0.276	3.016
Jan-52	0.676	11.276	1.482	5.772
Feb-52	1.403	7.698	1.477	6.762
Mar-52	0.014	4.132	4.153	0.649
Apr-52	0	1.092	0.186	0
May-52	0	0	0	0
Jun-52	0	0	0	0
Jul-52	0	0	0	0
Aug-52	0	0	0	0
Sept-52	0	0	0	0
Oct-52	0	0	0	0
Nov-52	18.872	0.007	0	0
Dec-52	1.912	0.188	0.391	0.231
Jan-53	1.199	2.539	0.752	0.934
Feb-53	5.799	0.575	0.305	0.513
Mar-53	3.175	6.565	1.316	1.854
Apr-53	0.005	0	0	1.088
May-53	0	0	0	0
Jun-53	0	0	0	0
Jul-53	0	0	0	0
Aug-53	0	0	0	0
Sept-53	0	0	0	0
Oct-53	0	0	0	0
Nov-53	0.246	0	0	0
Dec-53	0.422	0.46	0.001	0
Jan-54	2.046	6.273	0.873	5.224
Feb-54	1.519	4.344	1.729	1.407
Mar-54	0.315	7.616	3.725	2.99
Apr-54	0.019	0	3.317	0.073

May-54	0	0	0	0
Jun-54	0	0	0	0
Jul-54	0	0	0	0
Aug-54	0	0	0	0
Sept-54	0	0	0	0
Oct-54	0	0	0	0
Nov-54	0.207	0	0	0
Dec-54	7.182	0.048	0.151	0.008
Jan-55	0.598	0.522	2.054	2.885
Feb-55	1.844	4.29	2.144	3.73
Mar-55	1.809	5.268	2.855	2.469
Apr-55	0	0.029	0.815	0
May-55	0	0	0	0
Jun-55	0	0	0	0
Jul-55	0	0	0	0
Aug-55	0	0	0	0
Sept-55	0	0	0	0
Oct-55	0	0	0	0
Nov-55	2.089	0	0	0
Dec-55	1.857	1.266	0.063	0.774
Jan-56	3.208	8.691	1.103	4.935
Feb-56	2.915	9.337	0.76	1.931
Mar-56	0.203	1.034	3.799	1.906
Apr-56	0	1.876	2.109	0.237
May-56	0	0	0	0
Jun-56	0	0	0	0
Jul-56	0	0	0	0
Aug-56	0	0	0	0
Sept-56	0	0	0	0
Oct-56	0	0	0	0
Nov-56	0	0.004	0	0
Dec-56	1.272	0.261	0.001	0.015
Jan-57	3.597	2.843	0.515	3.125
Feb-57	6.089	3.368	2.176	2.005
Mar-57	13.542	0.846	2.423	0.732
Apr-57	0	0	2.79	0.731
May-57	0	0	0	0.327
Jun-57	0	0	0	0
Jul-57	0	0	0	0
Aug-57	0	0	0	0
Sept-57	0	0	0	0
Oct-57	0	0	0	0
Nov-57	0	0	0	0
Dec-57	0.417	0.659	0.064	0.03
Jan-58	2.816	5.035	1.1	1.918
Feb-58	32.862	6.594	1.579	3.323
Mar-58	27.907	1.642	0.878	1.072
Apr-58	0.025	0	1.776	0
May-58	0	0	0	0
Jun-58	0	0	0	0
Jul-58	0	0	0	0
Aug-58	0	0	0	0
Sept-58	0	0	0	0
Oct-58	0	0	0	0

Nov-58	0.068	0	0	0
Dec-58	0.018	0.87	0.282	0.643
Jan-59	0.266	9.061	1.579	6.984
Feb-59	26.927	5.212	0.537	0.613
Mar-59	14.396	6.731	0.997	1.571
Apr-59	4.594	0	0.06	1.058
May-59	0	0	0	0.001
Jun-59	0	0	0	0
Jul-59	0	0	0	0
Aug-59	0	0	0	0
Sept-59	0	0	0	0
Oct-59	0	0	0	0
Nov-59	0.819	0	0	0
Dec-59	3.417	0.01	0.062	0.138
Jan-60	0.356	1.751	3.024	1.452
Feb-60	3.97	3.912	3.17	0.954
Mar-60	4.479	8.054	2.364	1.224
Apr-60	0	0	1.87	0
May-60	0	0	0	0
Jun-60	0	0	0	0
Jul-60	0	0	0	0
Aug-60	0	0	0	0
Sept-60	0	0	0	0
Oct-60	0.239	0	0	0
Nov-60	0.138	0	0	0
Dec-60	3.995	0.125	0.087	0.012
Jan-61	2.366	13.011	1.926	5.247
Feb-61	18.54	2.344	0.88	3.827
Mar-61	5.054	5.272	3.914	5.611
Apr-61	0.002	0	0.39	0
May-61	0	0	0	0
Jun-61	0	0	0	0
Jul-61	0	0	0	0
Aug-61	0	0	0	0
Sept-61	0	0	0	0
Oct-61	0	0	0	0
Nov-61	0	0	0	0
Dec-61	6.198	0.214	0.054	0.298
Jan-62	2.135	5.832	1.169	5.611
Feb-62	0.866	1.854	0.637	2.592
Mar-62	0.617	7.227	0.916	2.647
Apr-62	0	1.194	0.063	0.99
May-62	0	0	0	0
Jun-62	0	0	0	0
Jul-62	0	0	0	0
Aug-62	0	0	0	0
Sept-62	0	0	0	0
Oct-62	0	0	0	0
Nov-62	0	0	0	0
Dec-62	5.951	0.503	0.165	2.088
Jan-63	2.846	12.019	0.777	3.022
Feb-63	1.333	9.611	0.764	1.567
Mar-63	5.285	12.942	4.023	1.953
Apr-63	0.253	0.514	1.878	4.15

May-63	0	0	0	1.027
Jun-63	0	0	0	0
Jul-63	0	0	0	0
Aug-63	0	0	0	0
Sept-63	0	0	0	0
Oct-63	0	0	0	0
Nov-63	5.759	0.004	0	0
Dec-63	0.872	0.586	0.438	1.848
Jan-64	8.33	12.319	0.931	6.631
Feb-64	4.007	7.425	2.048	0.627
Mar-64	1.928	1.941	1.226	1.218
Apr-64	0	0.109	0.527	2.187
May-64	0	0	0	0
Jun-64	0	0	0	0
Jul-64	0	0	0	0
Aug-64	0	0	0	0
Sept-64	0	0	0	0
Oct-64	0	0	0	0
Nov-64	0	0	0	0
Dec-64	0.351	1.509	0.038	0.507
Jan-65	6.649	15.395	1.545	1.415
Feb-65	41.812	4.551	2.323	1.691
Mar-65	13.305	9.828	1.62	2.838
Apr-65	0.213	0.576	0.399	0.823
May-65	0	0	0	0
Jun-65	0	0	0	0
Jul-65	0	0	0	0
Aug-65	0	0	0	0
Sept-65	0	0	0	0
Oct-65	0	0	0	0
Nov-65	0	0	0	0
Dec-65	0.036	0.382	0.038	0.627
Jan-66	0.488	7.776	0.59	6.886
Feb-66	7.994	2.46	0.7	7.353
Mar-66	17.084	0.422	1.225	2.526
Apr-66	1.109	0	0	3.911
May-66	0	0	0	0
Jun-66	0	0	0	0
Jul-66	0	0	0	0
Aug-66	0	0	0	0
Sept-66	0	0	0	0
Oct-66	0	0	0	0
Nov-66	1.896	0	0	0
Dec-66	4.119	2.05	0.082	0.352
Jan-67	5.566	14.316	2.181	2.021
Feb-67	20.526	3.655	1.277	3.558
Mar-67	6.185	9.685	1.982	1.723
Apr-67	0.175	0.015	0	0.525
May-67	0	0	0.704	0
Jun-67	0	0	0	0
Jul-67	0	0	0	0
Aug-67	0	0	0	0
Sept-67	0	0	0	0
Oct-67	0	0	0	0

Nov-67	0	0.043	0	0
Dec-67	10.012	0.996	0.082	0.026
Jan-68	1.289	11.133	1.056	4.159
Feb-68	0.731	3.887	0.904	0.881
Mar-68	1.674	3.82	1.843	2.164
Apr-68	0.255	0	0.127	0.407
May-68	0	0	0	0
Jun-68	0	0	0	0
Jul-68	0	0	0	0
Aug-68	0	0	0	0
Sept-68	0	0	0	0
Oct-68	0	0	0	0
Nov-68	0	0	0	0
Dec-68	50.5	0.144	0.045	3.729
Jan-69	4.738	3.19	0.923	15.279
Feb-69	0.436	2.354	3.991	2.06
Mar-69	0.165	0.3	2.266	0.901
Apr-69	26.68	0	4.975	4.145
May-69	0.339	0	0	0.64
Jun-69	0	0	0	0
Jul-69	0	0	0	0
Aug-69	0	0	0	0
Sept-69	0	0	0	0
Oct-69	0	0	0	0
Nov-69	0.623	0.277	0	0
Dec-69	0.917	0.904	0.19	0.023
Jan-70	8.949	9.706	1.01	6.234
Feb-70	11.931	7.677	1.123	1.721
Mar-70	3.484	4.42	4.888	1.821
Apr-70	1.926	8.088	0.62	0.476
May-70	0	0	0	0
Jun-70	0	0	0	0
Jul-70	0	0	0	0
Aug-70	0	0	0	0
Sept-70	0	0	0	0
Oct-70	0	0	0	0
Nov-70	0	0	0	0.02
Dec-70	4.442	0.335	0.209	0.061

Projected sediment yield (2071-2100) under RCP4.5

Date	CCLM4	HIRAM5	RACMO22T	RCA4
Jan-71	0.436	7.729	5.094	1.601
Feb-71	0.316	4.523	2.291	2.404
Mar-71	7.047	0.528	4.066	2.401
Apr-71	0.236	0	0.152	0.392
May-71	0	0	0	0
Jun-71	0	0	0	0
Jul-71	0	0	0	0
Aug-71	0	0	0	0
Sept-71	0	0	0	0
Oct-71	0	0	0	0
Nov-71	0	0	0	0
Dec-71	0.204	1.713	0.021	0.368
Jan-72	2.502	8.722	2.323	3.601
Feb-72	1.819	2.561	1.943	3.201
Mar-72	2.952	8.405	1.802	5.195
Apr-72	0	0.013	4.088	3.914
May-72	0	0	0	0
Jun-72	0	0	0	0
Jul-72	0	0	0	0
Aug-72	0	0	0	0
Sept-72	0	0	0	0
Oct-72	0	0	0	0
Nov-72	11.203	0.029	0	0
Dec-72	0.634	1.283	0.134	1.817
Jan-73	1.879	9.104	1.415	1.371
Feb-73	0.195	3.273	1.15	3.288
Mar-73	2.855	3.542	0.2	1.144
Apr-73	2.967	0	6.904	0.288
May-73	0	0	0.012	0
Jun-73	0	0	0	0
Jul-73	0	0	0	0
Aug-73	0	0	0	0
Sept-73	0	0	0	0
Oct-73	0.005	0	0	0
Nov-73	0	0	0	0
Dec-73	4.456	0.191	0.156	0.151
Jan-74	0.947	3.953	1.617	1.607
Feb-74	4.896	1.549	1.252	1.296
Mar-74	1.533	0.163	2.842	1.183
Apr-74	0.105	0	15.371	0.152
May-74	0	0	0	0
Jun-74	0	0	0	0
Jul-74	0	0	0	0
Aug-74	0	0	0	0
Sept-74	0	0	0	0
Oct-74	0	0	0	0
Nov-74	0.856	0.19	0	0
Dec-74	1.66	0.784	0.388	1.313
Jan-75	1.472	9.439	1.406	1.833
Feb-75	7.81	6.274	1.181	1.747
Mar-75	3.524	4.303	3.976	1.503

Apr-75	0	7.435	2.754	0
May-75	0	0	0	0
Jun-75	0	0	0	0
Jul-75	0	0	0	0
Aug-75	0	0	0	0
Sept-75	0	0	0	0
Oct-75	0	0	0	0
Nov-75	0.148	0	0	0
Dec-75	0.166	0.208	0.33	0.521
Jan-76	1.07	2.577	1.237	12.173
Feb-76	0.508	4.271	1.687	0.462
Mar-76	22.504	2.717	2.814	3.901
Apr-76	0	0	1.589	0.134
May-76	0	0	0	0
Jun-76	0	0	0	0
Jul-76	0	0	0	0
Aug-76	0	0	0	0
Sept-76	0	0	0	0
Oct-76	0	0	0	0
Nov-76	0.003	0	0	0
Dec-76	4.439	0.802	0.132	0.313
Jan-77	3.257	4.829	2.163	3.47
Feb-77	0.068	2.315	1.088	1.425
Mar-77	1.728	10.707	0.855	2.985
Apr-77	0	0.001	0.393	3.562
May-77	0.001	0.008	0	0
Jun-77	0	0	0	0
Jul-77	0	0	0	0
Aug-77	0	0	0	0
Sept-77	0	0	0	0
Oct-77	0	0	0	0
Nov-77	0.178	0	0	0
Dec-77	0	0.07	0.195	0.007
Jan-78	0.392	1.016	2.777	1.431
Feb-78	0.155	0.907	2.754	2.109
Mar-78	0.659	4.251	1.885	0.749
Apr-78	0.596	0.019	0.003	0
May-78	0	0	4.045	0
Jun-78	0	0	0	0
Jul-78	0	0	0	0
Aug-78	0	0	0	0
Sept-78	0	0	0	0
Oct-78	0	0	0	0
Nov-78	0	0.147	0	0
Dec-78	0.325	1.335	0.008	0.019
Jan-79	12.414	14.089	0.851	2.643
Feb-79	6.379	2.882	1.505	1.94
Mar-79	40.757	5.139	2.1	2.087
Apr-79	1.15	5.939	0	0.429
May-79	0	0.001	0	0
Jun-79	0	0	0	0
Jul-79	0	0	0	0
Aug-79	0	0	0	0
Sept-79	0	0	0	0

Oct-79	0	0	0	0
Nov-79	0	0	0	0
Dec-79	0.925	2.042	0.256	1.745
Jan-80	0.935	2.476	2.471	10.779
Feb-80	1.245	2.234	0.963	6.545
Mar-80	3.42	5.705	2.397	4.102
Apr-80	0	0.123	5.803	0.976
May-80	0	0	0	0
Jun-80	0	0	0	0
Jul-80	0	0	0	0
Aug-80	0	0	0	0
Sept-80	0	0	0	0
Oct-80	0	0	0	0
Nov-80	0	0	0	0
Dec-80	0	4.593	0	0.462
Jan-81	1.305	2.953	0.469	1.402
Feb-81	0.403	4.964	0.963	1.879
Mar-81	0.609	1.146	0.881	0.978
Apr-81	0	4.218	0.273	0
May-81	0	0	0.344	0
Jun-81	0	0	0	0
Jul-81	0	0	0	0
Aug-81	0	0	0	0
Sept-81	0	0	0	0
Oct-81	0	0	0	0
Nov-81	0	0.044	0	0
Dec-81	20.635	0.67	0.15	1.321
Jan-82	0.895	10.123	0.746	2.972
Feb-82	33.769	39.385	1.329	6.296
Mar-82	5.063	3.677	1.279	5.24
Apr-82	9.735	0	1.901	15.145
May-82	0	0	0	0
Jun-82	0	0	0	0
Jul-82	0	0	0	0
Aug-82	0	0	0	0
Sept-82	0	0	0	0
Oct-82	0	0	0	0
Nov-82	0	0.013	0	0
Dec-82	0.055	1.406	0.024	1.891
Jan-83	0.119	3.94	1.254	1.843
Feb-83	28.94	3.496	1.82	1.713
Mar-83	4.151	2.87	3.73	2.419
Apr-83	100.774	1.521	0.772	2.74
May-83	0	0	0	0
Jun-83	0	0	0	0
Jul-83	0	0	0	0
Aug-83	0	0	0	0
Sept-83	0	0	0	0
Oct-83	0	0	0	0
Nov-83	0.032	0	0	0
Dec-83	0	0.278	0.26	0.256
Jan-84	0.05	4.487	2.976	4.619
Feb-84	12.128	4.233	1.243	2.298
Mar-84	1.646	2.439	3.396	1.461

Apr-84	0.755	7.206	2.358	0.615
May-84	0	0	0	0
Jun-84	0	0	0	0
Jul-84	0	0	0	0
Aug-84	0	0	0	0
Sept-84	0	0	0	0
Oct-84	0	0	0.01	0
Nov-84	0.15	0.002	0	0
Dec-84	2.066	2.316	0.31	1.806
Jan-85	14.2	4.684	3.716	8.031
Feb-85	28.063	4.514	0.743	2.912
Mar-85	1.884	3.153	1.233	2.019
Apr-85	12.798	0.903	2.298	0
May-85	0	0	0	0
Jun-85	0	0	0	0
Jul-85	0	0	0	0
Aug-85	0	0	0	0
Sept-85	0	0	0	0
Oct-85	0	0	0	0
Nov-85	0	0.051	0	0
Dec-85	5.747	0.001	0.146	1.953
Jan-86	15.082	2.957	3.766	7.035
Feb-86	31.291	4.842	0.709	2.268
Mar-86	3.64	2.259	3.754	1.275
Apr-86	11.482	0.189	0.85	0.014
May-86	0	0.6	0	0
Jun-86	0	0	0	0
Jul-86	0	0	0	0
Aug-86	0	0	0	0
Sept-86	0	0	0	0
Oct-86	0	0	0	0
Nov-86	0	0	0	0
Dec-86	2.522	1.725	0.247	1.47
Jan-87	17.96	4.426	1.483	8.199
Feb-87	0.24	3.946	0.596	4.896
Mar-87	15.157	6.399	2.916	1.685
Apr-87	0	0	3.241	2.638
May-87	0	0	0	0
Jun-87	0	0	0	0
Jul-87	0	0	0	0
Aug-87	0	0	0	0
Sept-87	0	0	0	0
Oct-87	0	0	0	0
Nov-87	0.233	0	0	0
Dec-87	2.836	0.038	0.178	0.296
Jan-88	11.139	8.543	0.796	1.835
Feb-88	0.329	8.358	1.012	1.577
Mar-88	25.801	7.661	2.413	2.815
Apr-88	0	3.827	0	0.209
May-88	0	0	0	0
Jun-88	0	0	0	0
Jul-88	0	0	0	0
Aug-88	0	0	0	0
Sept-88	0	0	0	0

Oct-88	0	0	0	0
Nov-88	0	0	0	0
Dec-88	10.542	0.055	0.083	0.002
Jan-89	2.693	4.809	0.843	2.824
Feb-89	9.221	13.271	1.855	0.568
Mar-89	4.737	4.511	3.065	1.757
Apr-89	0.012	0.61	3.096	0.562
May-89	0	0	0	0
Jun-89	0	0	0	0
Jul-89	0	0	0	0
Aug-89	0	0	0	0
Sept-89	0	0	0	0
Oct-89	0	0	0	0
Nov-89	0.027	0	0	0
Dec-89	0.597	2.461	0.188	0.496
Jan-90	2.473	5.853	0.723	2.635
Feb-90	18.545	7.687	0.758	0.623
Mar-90	2.944	4.303	2.578	0.857
Apr-90	3.178	0	0.394	4.92
May-90	0	0	0	0
Jun-90	0	0	0	0
Jul-90	0	0	0	0
Aug-90	0	0	0	0
Sept-90	0	0	0	0
Oct-90	0	0	0	0
Nov-90	0	0	0	0
Dec-90	0.041	0.043	0.48	0.04
Jan-91	1.848	2.247	1.36	2.471
Feb-91	10.479	5.434	1.62	1.393
Mar-91	6.002	5.636	3.47	2.164
Apr-91	0	0	0	0.141
May-91	0	0	0	0
Jun-91	0	0	0	0
Jul-91	0	0	0	0
Aug-91	0	0	0	0
Sept-91	0	0	0	0
Oct-91	0	0	0	0
Nov-91	16.497	0	0	0
Dec-91	7.766	1.129	0.626	0.015
Jan-92	26.331	5.355	1.735	0.32
Feb-92	0.212	3.677	2.343	2.115
Mar-92	3.73	4.282	2.761	1.38
Apr-92	0.952	0.573	3.332	1.412
May-92	0	0	0	0
Jun-92	0	0	0	0
Jul-92	0	0	0	0
Aug-92	0	0	0	0
Sept-92	0	0	0	0
Oct-92	0	0	0	0
Nov-92	0.001	0	0	0
Dec-92	3.041	0.132	0.12	0.02
Jan-93	0.949	2.354	1.03	2.534
Feb-93	0.31	3.596	0.721	3.664
Mar-93	1.607	3.118	2.309	3.432

Apr-93	0.312	0.091	0.34	0.574
May-93	0	0	0	0
Jun-93	0	0	0	0
Jul-93	0	0	0	0
Aug-93	0	0	0	0
Sept-93	0	0	0	0
Oct-93	0	0	0	0
Nov-93	0	0	0	0
Dec-93	12.254	0.795	0.148	0.005
Jan-94	1.107	17.068	1.551	1.394
Feb-94	1.908	2.499	1	2.07
Mar-94	1.534	8.668	5.189	2.157
Apr-94	0	0	0.599	2.084
May-94	0	0	0	0
Jun-94	0	0	0	0
Jul-94	0	0	0	0
Aug-94	0	0	0	0
Sept-94	0	0	0	0
Oct-94	0	0	0	0
Nov-94	0	0	0	0
Dec-94	1.725	1.881	0.039	0.106
Jan-95	1.078	7.989	1.531	1.95
Feb-95	2.244	6.771	1.236	0.798
Mar-95	0.016	6.01	1.115	1.103
Apr-95	0	0	3.303	3.305
May-95	0	0	0	0
Jun-95	0	0	0	0
Jul-95	0	0	0	0
Aug-95	0	0	0	0
Sept-95	0	0	0	0
Oct-95	0	0	0	0
Nov-95	6.044	0.128	0	0
Dec-95	0.068	1.871	0.001	0.301
Jan-96	1.087	3.994	0.257	6.913
Feb-96	6.743	8.63	0.784	1.377
Mar-96	3.47	6.429	0.432	2.664
Apr-96	0	0.006	0.755	0.345
May-96	0	0	0.136	0
Jun-96	0	0	0	0
Jul-96	0	0	0	0
Aug-96	0	0	0	0
Sept-96	0	0	0	0
Oct-96	0.188	0	0	0
Nov-96	0	0	0	0
Dec-96	0.528	0.127	0.106	0.459
Jan-97	1.321	1.49	1.832	2.295
Feb-97	12.01	6.922	2.545	2.7
Mar-97	14.947	2.305	4.271	1.933
Apr-97	0.002	0	2.07	0.001
May-97	0	0	0	0
Jun-97	0	0	0	0
Jul-97	0	0	0	0
Aug-97	0	0	0	0
Sept-97	0	0	0	0

Oct-97	0	0	0	0
Nov-97	0	0.001	0	0
Dec-97	0.468	1.564	0.04	1.053
Jan-98	6.128	2.744	0.864	9.701
Feb-98	0.724	9.301	1.232	4.421
Mar-98	1.115	4.453	3.035	2.153
Apr-98	0.027	0.638	0.698	1.678
May-98	0	0	0	0
Jun-98	0	0	0	0
Jul-98	0	0	0	0
Aug-98	0	0	0	0
Sept-98	0	0	0	0
Oct-98	0	0	0	0
Nov-98	0	0.071	0	0
Dec-98	0	4.85	0.065	0
Jan-99	0	1.105	0.595	7.59
Feb-99	0.206	6.323	2.251	2.215
Mar-99	34.008	2.543	5.828	2.3
Apr-99	0.137	1.583	0.61	1.894
May-99	0	0	0	0.134
Jun-99	0	0	0	0
Jul-99	0	0	0	0
Aug-99	0	0	0	0
Sept-99	0	0	0	0
Oct-99	0	0	0	0
Nov-99	0	0.008	0	0
Dec-99	0.001	0.677	0.403	0.406
Jan-00	5.362	9.635	0.529	4.821
Feb-00	3.127	13.278	1.011	0.405
Mar-00	1.253	0.835	0.264	4.759
Apr-00	0.344	0	0.135	0.231
May-00	0	0	0	0
Jun-00	0	0	0	0
Jul-00	0	0	0	0
Aug-00	0	0	0	0
Sept-00	0	0	0	0
Oct-00	0	0	0	0
Nov-00	0	0	0	0
Dec-00	0.035	0.006	0.164	0.042

Projected sediment yield (2010-2040) under RCP8.5

Date	CCLM4	HIRAM5	RACMO22T	RCA4
Jan-11	9.766	2.156	0.686	0.914
Feb-11	4.409	3.993	1.173	3.369
Mar-11	2.093	6.647	2.936	5.124
Apr-11	0	4.738	6.137	0.249
May-11	0	0	0.145	0.819
Jun-11	0	0	0	0
Jul-11	0	0	0	0
Aug-11	0	0	0	0
Sept-11	0	0	0	0
Oct-11	0	0	0	0
Nov-11	0.186	0	0.034	0.016
Dec-11	3.624	0.188	1.144	0.091
Jan-12	2.459	1.663	0.68	2.109
Feb-12	4.588	3.754	1.087	0.686
Mar-12	1.33	1.665	0.921	1.263
Apr-12	3.698	0.103	0	0.153
May-12	0	0	0	0
Jun-12	0	0	0	0
Jul-12	0	0	0	0
Aug-12	0	0	0	0
Sept-12	0	0	0	0
Oct-12	0	0	0	0
Nov-12	0.96	0.011	0.025	0.05
Dec-12	6.928	0.363	0.26	0.054
Jan-13	8.103	3.657	3.259	7.716
Feb-13	0.438	3.77	0.638	2.343
Mar-13	7.667	3.024	0.574	2.011
Apr-13	1.043	1.209	0.063	0.393
May-13	0	0	0	0.108
Jun-13	0	0	0	0
Jul-13	0	0	0	0
Aug-13	0	0	0	0
Sept-13	0	0	0	0
Oct-13	0	0	0	0
Nov-13	0.613	0.426	0	0.03
Dec-13	1.823	1.815	0.137	0.384
Jan-14	5.51	15.298	0.564	0.456
Feb-14	4.96	1.814	0.815	0.781
Mar-14	3.209	4.423	1.057	0.841
Apr-14	15.548	1.477	1.093	0
May-14	0	0	0	0
Jun-14	0	0	0	0
Jul-14	0	0	0	0
Aug-14	0	0	0	0
Sept-14	0	0	0	0
Oct-14	0	0	0	0
Nov-14	0	0	0	1.347
Dec-14	0	0.436	1.705	0.499
Jan-15	1.043	4.423	0.791	4.446
Feb-15	0.683	4.769	3.441	6.806
Mar-15	0.18	4.614	0.815	5.208

Apr-15	5.906	0.47	2.477	4.64
May-15	0	7.397	0	0
Jun-15	0	0	0	0
Jul-15	0	0	0	0
Aug-15	0	0	0	0
Sept-15	0	0	0	0
Oct-15	0	0	0	0
Nov-15	0.006	0.034	0	0.006
Dec-15	2.807	0.946	0.351	0.228
Jan-16	1.258	5.403	0.707	1.449
Feb-16	0.778	2.271	0.662	3.218
Mar-16	0.901	2.555	0.629	3.703
Apr-16	0.084	0	0.283	0.766
May-16	29.674	0	0	0
Jun-16	0	0	0	0
Jul-16	0	0	0	0
Aug-16	0	0	0	0
Sept-16	0	0.002	0	0
Oct-16	1.887	0	0.004	0
Nov-16	2.682	0	0.158	0.259
Dec-16	0.273	0.519	0.437	0.175
Jan-17	1.161	8.451	0.605	0.187
Feb-17	17.028	6.145	1.107	6.686
Mar-17	2.442	2.51	1.219	3.4
Apr-17	0.652	4.698	1.146	10.779
May-17	0	0	0	0
Jun-17	0	0	0	0
Jul-17	0	0	0	0
Aug-17	0	0	0	0
Sept-17	0	0	0	0
Oct-17	0	0	0	0
Nov-17	0.539	0.807	0.15	0.001
Dec-17	0.236	1.89	0.479	0.177
Jan-18	10.613	4.733	1.703	0.62
Feb-18	1.511	6.558	0.703	3.517
Mar-18	8.626	0.992	0.784	0.372
Apr-18	6.089	4.725	1.682	1.816
May-18	0	0.651	0	0
Jun-18	0	0	0	0
Jul-18	0	0	0	0
Aug-18	0	0	0	0
Sept-18	0	0	0	0
Oct-18	0	0	0	0
Nov-18	0	0.014	0	0.15
Dec-18	1.383	1.193	0.376	0.255
Jan-19	1.492	3.853	1.619	5.421
Feb-19	9.351	6.515	1.478	2.737
Mar-19	14.236	3.992	2.212	0.976
Apr-19	0.479	0.352	4.345	12.286
May-19	2.781	0	0.077	0
Jun-19	0	0	0	0
Jul-19	0	0	0	0
Aug-19	0	0	0	0
Sept-19	0	0	0	0

Oct-19	0	0	0	0
Nov-19	0	0	0.128	0
Dec-19	0	1.241	0.346	0.078
Jan-20	2.324	4.924	0.751	4.392
Feb-20	0.856	3.1	0.967	2.306
Mar-20	0.296	0.211	1.413	3.845
Apr-20	1.82	0	0.029	3.029
May-20	0	0	0	0
Jun-20	0	0	0	0
Jul-20	0	0	0	0
Aug-20	0	0	0	0
Sept-20	0	0	0	0
Oct-20	0	0	0	0
Nov-20	0.063	1.087	0.225	0.004
Dec-20	8.488	2.01	0.679	0.188
Jan-21	2.904	6.597	0.524	3.274
Feb-21	1.968	6.926	1.558	0.486
Mar-21	4.062	2.712	1.044	1.36
Apr-21	0	0.53	5.698	0.03
May-21	0	0	0	0
Jun-21	0	0	0	0
Jul-21	0	0	0	0
Aug-21	0	0	0	0
Sept-21	0	0	0	0
Oct-21	0	0	0	0
Nov-21	0	0.104	0.042	0.066
Dec-21	0	2.152	0.592	0.047
Jan-22	0.075	4.733	1.295	0.336
Feb-22	0.533	6.621	0.815	2.541
Mar-22	8.78	6.645	2.91	3.229
Apr-22	0.498	0.861	5.755	3.027
May-22	0	0	0	0
Jun-22	0	0	0	0
Jul-22	0	0	0	0
Aug-22	0	0	0	0
Sept-22	0	0	0	0
Oct-22	0	0.001	0	0
Nov-22	0.006	2.464	0	0.709
Dec-22	0.01	2.101	0.18	2.34
Jan-23	45.691	0.97	0.982	1.498
Feb-23	2.225	1.776	0.372	8.546
Mar-23	4.281	4.626	0.546	1.448
Apr-23	0	5.667	20.691	3.37
May-23	0	0	0	0
Jun-23	0	0	0	0
Jul-23	0	0	0	0
Aug-23	0	0	0	0
Sept-23	0	22.989	0	0
Oct-23	0	0.016	0	0
Nov-23	0	0.021	0.131	0
Dec-23	19.342	1.043	0.963	0.631
Jan-24	13.163	1.563	0.96	2.417
Feb-24	14.308	1.432	1.56	0.99
Mar-24	0.628	0.853	1.261	1.475

Apr-24	0.126	0	0	3.975
May-24	7.919	0	0	0
Jun-24	0	0	0	0
Jul-24	0	0	0	0
Aug-24	0	0	0	0
Sept-24	0	0	0	0
Oct-24	0	0	0	0
Nov-24	0	0	0.017	0.084
Dec-24	0	1.064	0.43	1.484
Jan-25	1.834	5.313	1.194	2.686
Feb-25	25.481	5.459	2.697	2.265
Mar-25	0.665	0.396	3.798	2.338
Apr-25	0.455	3.874	3.119	2.137
May-25	0	2.512	0	0
Jun-25	0	0	0	0
Jul-25	0	0	0	0
Aug-25	0	0	0	0
Sept-25	0	0	0	0
Oct-25	0	0	0	0
Nov-25	0.005	0	0.055	0
Dec-25	0.392	0.662	0.465	0.097
Jan-26	7.316	2.036	0.823	0.442
Feb-26	21.049	4.422	1.919	7.389
Mar-26	0.174	3.141	1.959	0.441
Apr-26	1.831	0	0	2.757
May-26	0	0	0	0.003
Jun-26	0	0	0	0
Jul-26	0	0	0	0
Aug-26	0	0	0	0
Sept-26	0	0	0	0
Oct-26	0	0	0	0
Nov-26	0	2.671	0.003	0.016
Dec-26	0.01	3.588	0.107	0.024
Jan-27	0.328	1.019	0.332	1.941
Feb-27	43.37	4.203	1.474	2.809
Mar-27	3.19	9.363	2.139	0.832
Apr-27	46.042	0	0.17	0.363
May-27	0.001	0	0	0
Jun-27	0	0	0	0
Jul-27	0	0	0	0
Aug-27	0	0	0	0
Sept-27	0	0	0	0
Oct-27	0	0	0	0
Nov-27	7.92	2.067	0.002	0.244
Dec-27	0.419	2.629	0.289	0.607
Jan-28	0.62	2.245	1.233	5.732
Feb-28	0.702	3.888	1.489	3.546
Mar-28	0.465	4.477	0.633	2.837
Apr-28	0.692	0.093	7.277	0.01
May-28	0	0	0.038	0
Jun-28	0	0	0	0
Jul-28	0	0	0	0
Aug-28	0	0	0	0
Sept-28	0	0.036	0	0

Oct-28	0	0	0	0
Nov-28	0	0.065	0	0
Dec-28	0.089	0.07	0.108	0.034
Jan-29	1.65	2.503	1.25	9.603
Feb-29	0.183	1.431	1.112	4.664
Mar-29	0.699	2.781	1.055	1.91
Apr-29	0	0.001	0.342	3.936
May-29	0	9.146	0.001	0
Jun-29	0	0	0	0
Jul-29	0	0	0	0
Aug-29	0	0	0	0
Sept-29	0	1.146	0	0
Oct-29	0	0.463	0	0
Nov-29	0	1.144	0.009	0.007
Dec-29	0.024	1.984	0.337	0.502
Jan-30	2.582	11.177	0.714	4.119
Feb-30	5.594	3.962	0.742	1.022
Mar-30	1.471	1.628	0.071	8.677
Apr-30	5.697	0.042	1.234	9.341
May-30	7.036	0.01	0	0
Jun-30	0	0	0	0
Jul-30	0	0	0	0
Aug-30	0	0	0	0
Sept-30	0	0	0	0
Oct-30	0	0.245	0	0
Nov-30	18.661	0.081	0	0
Dec-30	10.151	3.349	0.866	1.777
Jan-31	0.889	2.172	1.31	0.823
Feb-31	0.793	8.238	1.17	3.368
Mar-31	0.297	1.046	0.045	1.51
Apr-31	0	2.657	0.137	0.462
May-31	0	0.001	0	0
Jun-31	0	0	0	0
Jul-31	0	0	0	0
Aug-31	0	0	0	0
Sept-31	0	0	0	0
Oct-31	0	0	0	0
Nov-31	0	0.274	0	0
Dec-31	0	0.918	0.337	1.981
Jan-32	1.228	3.838	1.562	1.837
Feb-32	0.545	4.029	1.8	0.88
Mar-32	20.681	0.402	0.555	4.323
Apr-32	1.113	0	0.483	2.106
May-32	0	0	0	0
Jun-32	0	0	0	0
Jul-32	0	0	0	0
Aug-32	0	0	0	0
Sept-32	0	0	0	0
Oct-32	0	0	0	0
Nov-32	0	0	0.034	0.107
Dec-32	0.109	0.53	0.537	1.907
Jan-33	0.036	1.195	1.626	7.27
Feb-33	0.649	4.661	1.635	1.303
Mar-33	9.381	6.724	2.401	4.033

Apr-33	0.012	0.357	3.614	0.053
May-33	0	0	0	0
Jun-33	0	0	0	0
Jul-33	0	0	0	0
Aug-33	0	0	0	0
Sept-33	0	0	0	0
Oct-33	0	0	0	0
Nov-33	0	0.506	0	0.136
Dec-33	2.117	2.069	0.22	0.542
Jan-34	0.443	5.297	1.905	2.338
Feb-34	8.444	4.119	1.188	3.645
Mar-34	1.51	2.317	1.186	5.751
Apr-34	0.293	0.354	4.287	2.831
May-34	0	5.524	0	0
Jun-34	0	0	0	0
Jul-34	0	0	0	0
Aug-34	0	0	0	0
Sept-34	0	0	0	0
Oct-34	0	0	0	0
Nov-34	0.485	0.633	0	0.009
Dec-34	0.029	2.097	0.037	0.269
Jan-35	3.462	6.29	1.715	16.937
Feb-35	1.298	1.389	1.117	0.794
Mar-35	0.199	4.425	0.497	5.041
Apr-35	2.77	0	0.814	0
May-35	0	0	0.778	0
Jun-35	0	0	0	0
Jul-35	0	0	0	0
Aug-35	0	0	0	0
Sept-35	0	0	0	0
Oct-35	0	0	0	0
Nov-35	0	0.306	0.078	0.027
Dec-35	22.176	2.416	0.145	0.004
Jan-36	7.51	7.578	2.246	1.796
Feb-36	1.396	2.559	0.701	5.799
Mar-36	9.006	4.615	1.449	5.232
Apr-36	4.639	0	6.31	2.871
May-36	0	0	0	0
Jun-36	0	0	0	0
Jul-36	0	0	0	0
Aug-36	0	0	0	0
Sept-36	0	0	0	0
Oct-36	0	0	0	0.018
Nov-36	0.014	0.594	0.002	0
Dec-36	0.192	4.905	1.651	1.442
Jan-37	3.3	2.864	1.48	0.371
Feb-37	2.54	12.497	2.963	3.152
Mar-37	1.109	11.729	0.106	2.028
Apr-37	0.692	0	0.063	1.352
May-37	0	0	0	0
Jun-37	0	0	0	0
Jul-37	0	0	0	0
Aug-37	0	0	0	0
Sept-37	0	0	0	0

Oct-37	0	0	0	0
Nov-37	0	0.037	0.001	0.013
Dec-37	0.365	0.443	0.011	0.403
Jan-38	1.692	10.616	0.942	7.768
Feb-38	3.865	9.44	1.852	5.109
Mar-38	2.829	9.214	1.489	5.305
Apr-38	10.485	1.062	0.268	4.969
May-38	0	0.345	0	0
Jun-38	0	0	0	0
Jul-38	0	0	0	0
Aug-38	0	0	0	0
Sept-38	0	0	0	0
Oct-38	0	0	0	0
Nov-38	0.138	0.126	0	0.017
Dec-38	0.001	0.968	0.052	0.019
Jan-39	0.288	3.354	1.067	1.997
Feb-39	0.765	4.749	2.372	3.015
Mar-39	1.758	0.557	1.677	0.271
Apr-39	8.038	11.748	0.164	4.354
May-39	27.211	0	0	0
Jun-39	0	0	0	0
Jul-39	0	0	0	0
Aug-39	0	0	0	0
Sept-39	0	0	0	0
Oct-39	0	0	0	0
Nov-39	0	0.863	0.181	1.664
Dec-39	0.024	1.031	0.45	2.829
Jan-40	0.16	7.947	1.713	6.636
Feb-40	4.464	1.408	1.316	4.799
Mar-40	1.172	7.274	0.568	5.62
Apr-40	0.249	2.226	0.043	1.11
May-40	0	0	0	0
Jun-40	0	0	0	0
Jul-40	0	0	0	0
Aug-40	0	0	0	0
Sept-40	0	0	0	0
Oct-40	0	0	0	0
Nov-40	3.067	0.067	0.127	0.027
Dec-40	0.82	3.774	0.663	0.236

Projected sediment yield (2041-2070) under RCP8.5

Date	CCLM4	HIRAM5	RACMO22T	RCA4
Jan-41	0.077	3.274	0.325	0.064
Feb-41	43.709	8.745	1.983	4.889
Mar-41	2.634	8.352	1.978	2.994
Apr-41	0	0.022	3.206	0.203
May-41	1.396	0	0	0
Jun-41	0	0	0	0
Jul-41	0	0	0	0
Aug-41	0	0	0	0
Sept-41	0	0	0	0
Oct-41	0	0	0	0
Nov-41	16.857	3.218	0.05	0.001
Dec-41	0.032	1.053	0.188	0.017
Jan-42	1.003	7.711	0.725	2.807
Feb-42	1.256	4.235	0.76	4.38
Mar-42	0.999	0.614	0.784	1.737
Apr-42	1.325	0.312	0.37	0.17
May-42	0	0	0	0
Jun-42	0	0	0	0
Jul-42	0	0	0	0
Aug-42	0	0	0	0
Sept-42	0	50.364	0	0
Oct-42	0	0.02	0	0
Nov-42	0.11	0.198	0.02	0
Dec-42	0.649	2.34	0.479	0.371
Jan-43	0.748	5.191	0.913	2.362
Feb-43	0.632	0.355	1.346	0.642
Mar-43	0.471	0	0.872	1.781
Apr-43	0	0	2.548	2.163
May-43	0	0	0	0
Jun-43	0	0	0	0
Jul-43	0	0	0	0
Aug-43	0	0	0	0
Sept-43	0	0	0	0
Oct-43	0	0	0	0
Nov-43	0	0.004	0.055	0.148
Dec-43	0	0.29	0.2	0.565
Jan-44	0.899	2.113	0.555	2.438
Feb-44	7.757	28.967	0.388	4.477
Mar-44	0.506	6.728	1.253	2.579
Apr-44	0	0.402	1.31	3.027
May-44	0	0	0	0

Jun-44	0	0	0	0
Jul-44	0	0	0	0
Aug-44	0	0	0	0
Sept-44	0	0	0	0
Oct-44	0	0	0	0
Nov-44	2.32	0.496	0	0
Dec-44	0.034	3.471	0.084	0.225
Jan-45	0	7.932	1.323	4.653
Feb-45	3.393	4.876	1.39	2.944
Mar-45	4.488	2.312	1.284	0.396
Apr-45	1.129	1.499	0.079	0.726
May-45	0	0	0	0
Jun-45	0	0	0	0
Jul-45	0	0	0	0
Aug-45	0	0	0	0
Sept-45	0	0.079	0	0
Oct-45	0	0	0	0
Nov-45	0.011	0.307	0.179	0.095
Dec-45	0	3.123	0.451	1.056
Jan-46	0.218	9.775	0.899	2.024
Feb-46	0.396	3.442	1.755	2.039
Mar-46	0.822	5.396	4.097	0.86
Apr-46	0	1.726	0	0.076
May-46	8.128	0.016	0	0
Jun-46	0	0	0	0
Jul-46	0	0	0	0
Aug-46	0	0	0	0
Sept-46	0	0	0	0
Oct-46	0	0	0	0.083
Nov-46	0.01	0	0.049	2.057
Dec-46	0.126	3.037	0.569	0.197
Jan-47	0.801	2.306	1.153	6.364
Feb-47	6.341	2.454	1.888	0.54
Mar-47	15.974	4.294	0.949	1.304
Apr-47	4.382	6.342	0.052	4.862
May-47	0	0.02	0	0
Jun-47	0	0	0	0
Jul-47	0	0	0	0
Aug-47	0	0	0	0
Sept-47	0	0	0	0
Oct-47	0	0	0	0
Nov-47	0.001	1.125	0.219	0.023
Dec-47	16.103	4.662	1.018	0.993

Jan-48	2.517	4.586	1.043	1.321
Feb-48	0.566	4.16	1.777	0.505
Mar-48	0.131	6.3	0.988	1.944
Apr-48	0.026	0	0	0.322
May-48	0	0	0	0
Jun-48	0	0	0	0
Jul-48	0	0	0	0
Aug-48	0	0	0	0
Sept-48	0	0	0	0
Oct-48	0	0	0	0
Nov-48	0	0.874	0.022	0
Dec-48	0.414	2.964	0.451	0.056
Jan-49	3.324	7.859	0.968	0.387
Feb-49	24.734	6.082	0.705	1.27
Mar-49	1.957	5.118	0.901	1.529
Apr-49	1.725	1.169	1.085	1.582
May-49	0	0	0	0
Jun-49	0	0	0	0
Jul-49	0	0	0	0
Aug-49	0	0	0	0
Sept-49	0	0	0	0
Oct-49	0	0	0	0
Nov-49	0	0.002	0.001	0.101
Dec-49	0.014	2.019	0.336	0.631
Jan-50	10.393	0.332	2.576	3.115
Feb-50	1.611	2.304	1.416	3.068
Mar-50	9.004	1.918	1.78	2.419
Apr-50	0	0.004	5.17	8.4
May-50	0	0	0	0
Jun-50	0	0	0	0
Jul-50	0	0	0	0
Aug-50	0	0	0	0
Sept-50	0	0	0	0
Oct-50	0	0	0	0
Nov-50	0.02	0.159	0.003	0.436
Dec-50	9.728	4.463	0.188	0.137
Jan-51	3.5	12.739	1.201	4.965
Feb-51	1.808	6.451	0.264	0.459
Mar-51	2.711	14.685	2.732	3.498
Apr-51	0	0	9.498	5.029
May-51	0	0	0	0
Jun-51	0	0	0	0
Jul-51	0	0	0	0

Aug-51	0	0	0	0
Sept-51	0	0	0	0
Oct-51	0	0	0	0
Nov-51	0	1.252	0	0
Dec-51	0	3.771	0.341	0.283
Jan-52	0.412	4.458	1.849	1.685
Feb-52	107.611	5.041	0.884	1.692
Mar-52	0.547	1.773	1.816	1.74
Apr-52	0	0.05	1.774	0.361
May-52	0	3.65	0	0
Jun-52	0	0	0	0
Jul-52	0	0	0	0
Aug-52	0	0	0	0
Sept-52	0	0.036	0	0
Oct-52	0	0	0	0
Nov-52	0	0.096	0	0
Dec-52	0	2.403	0.033	0.758
Jan-53	0.003	5.199	0.347	2.953
Feb-53	12.421	3.039	0.565	5.107
Mar-53	0.494	10.967	0.391	0.979
Apr-53	0.05	0.021	0.087	0.481
May-53	0	0	0	0
Jun-53	0	0	0	0
Jul-53	0	0	0	0
Aug-53	0	0	0	0
Sept-53	0	0	0	0
Oct-53	0	0	0	0
Nov-53	0.003	2.927	0.178	0.001
Dec-53	6.165	4.689	1.09	1.14
Jan-54	9.683	10.335	0.714	4.084
Feb-54	7.521	2.717	4.616	6.939
Mar-54	53.992	4.161	1.845	1.272
Apr-54	0	0	0.032	1.047
May-54	0	3.579	0	2.94
Jun-54	0	0	0	0
Jul-54	0	0	0	0
Aug-54	0	0	0	0
Sept-54	0	0	0	0
Oct-54	0	0	0	0
Nov-54	2.007	0.625	0.038	0
Dec-54	1.572	1.094	0.79	0.119
Jan-55	2.194	3.225	2.332	3.364
Feb-55	3.361	4.354	2.235	0.525

Mar-55	2.992	5.885	1.65	1.535
Apr-55	0.195	0.208	5.09	1.819
May-55	0	0	0	0
Jun-55	0	0	0	0
Jul-55	0	0	0	0
Aug-55	0	0	0	0
Sept-55	0	0	0	0
Oct-55	0	0	0	0
Nov-55	0	2.042	0	0
Dec-55	0.198	0.915	0.259	0.025
Jan-56	0.637	15.578	1.252	1.634
Feb-56	1.113	6.525	1.851	4.659
Mar-56	5.53	4.404	1.996	0.489
Apr-56	3.693	0.949	2.125	0.124
May-56	0	7.067	0	0
Jun-56	0	0	0	0
Jul-56	0	0	0	0
Aug-56	0	0	0	0
Sept-56	0	0	0	0
Oct-56	0	0	0	0
Nov-56	0.085	0.11	0.015	0.026
Dec-56	0	1.517	0.683	0.129
Jan-57	0.465	7.039	1.146	1.701
Feb-57	3.615	1.219	1.085	10.463
Mar-57	0.505	1.729	1.401	2.3
Apr-57	0.446	0.02	1.816	0
May-57	1.059	0	0.293	4.138
Jun-57	0	0	0	0
Jul-57	0	0	0	0
Aug-57	0	0	0	0
Sept-57	0	0	0	0
Oct-57	0	0	0	0
Nov-57	0	0.073	0.006	0.288
Dec-57	0	1.158	0.079	0.898
Jan-58	0.136	1.176	0.598	0.333
Feb-58	9.361	6.165	1.267	3.602
Mar-58	1.165	10.741	0.834	3.969
Apr-58	6.469	1.348	1.135	1.817
May-58	0	1.546	0	2.007
Jun-58	0	0	0	0
Jul-58	0	0	0	0
Aug-58	0	0	0	0
Sept-58	0	0	0	0

Oct-58	0	0	0	0
Nov-58	0.045	0.522	0	0
Dec-58	5.191	3.062	0.006	0.303
Jan-59	1.362	4.32	2.421	0.367
Feb-59	29.237	8.652	5.774	3.649
Mar-59	0.413	13.188	1.025	1.59
Apr-59	0	3.82	0.757	1.725
May-59	0	0	0	0
Jun-59	0	0	0	0
Jul-59	0	0	0	0
Aug-59	0	0	0	0
Sept-59	0	0	0	0
Oct-59	0	0	0	0
Nov-59	0.338	0.1	0.002	0
Dec-59	0.264	1.694	0.871	0.009
Jan-60	0.489	4.258	3.067	1.535
Feb-60	3.491	8.737	1.68	2.518
Mar-60	0.918	8.065	1.169	2.283
Apr-60	0.307	0.197	3.407	4.298
May-60	0	0	0.3	0
Jun-60	0	0	0	0
Jul-60	0	0	0	0
Aug-60	0	0	0	0
Sept-60	0	0.025	0	0
Oct-60	0	0	0	0
Nov-60	0.004	4.069	0.079	0.128
Dec-60	3.132	6.431	0.211	0.36
Jan-61	1.741	7.398	0.551	2.741
Feb-61	1.098	5.687	0.612	3.759
Mar-61	1.456	0.886	1.818	0.598
Apr-61	0.043	5.47	1.514	2.192
May-61	0.706	2.638	0	0
Jun-61	0	0	0	0
Jul-61	0	0	0	0
Aug-61	0	0	0	0
Sept-61	0	0	0	0
Oct-61	0	0	0	0
Nov-61	0	1.92	0.002	0.001
Dec-61	8.312	2.673	0.255	0.397
Jan-62	6.432	1.354	0.899	3.193
Feb-62	2.285	5.819	0.963	2.503
Mar-62	1.224	3.527	4.124	0.831
Apr-62	0	0.015	1.619	0

May-62	0	0	0	0
Jun-62	0	0	0	0
Jul-62	0	0	0	0
Aug-62	0	0	0	0
Sept-62	0	0	0	0
Oct-62	0	0	0	0
Nov-62	6.588	0.203	0.008	0
Dec-62	1.13	2.021	0.343	0.022
Jan-63	0.933	1.935	1.872	0.479
Feb-63	12.091	10.758	2.697	1.49
Mar-63	0.996	8.731	0.479	6.224
Apr-63	0.066	9.345	4.467	0.391
May-63	2.279	0	0	0
Jun-63	0	0	0	0
Jul-63	0	0	0	0
Aug-63	0	0	0	0
Sept-63	0	0	0	0
Oct-63	0.321	0	0	0
Nov-63	0.212	0.705	0	0
Dec-63	4.021	1.921	0.014	0.201
Jan-64	2.138	4.785	0.758	1.015
Feb-64	1.411	13.558	3.562	3.455
Mar-64	0.594	16.226	0.923	0.528
Apr-64	0.28	0.046	22.454	6.999
May-64	0	0	0.001	1.403
Jun-64	0	0	0	0
Jul-64	0	0	0	0
Aug-64	0	0	0	0
Sept-64	0	0	0	0
Oct-64	0	0	0	0
Nov-64	0	2.812	0	0
Dec-64	0.006	2.492	0.066	0.209
Jan-65	0.128	5.437	0.741	1.296
Feb-65	6.813	20.533	1.055	3.639
Mar-65	2.535	10.004	1.148	0.481
Apr-65	0	2.271	6.643	1.495
May-65	0	0	0	0.822
Jun-65	0	0	0	0
Jul-65	0	0	0	0
Aug-65	0	0	0	0
Sept-65	0	0	0	0
Oct-65	0	0	0	0
Nov-65	0	2.124	0.104	0.002

Dec-65	0	6.572	0.515	0.126
Jan-66	35.964	1.715	2.054	1.464
Feb-66	4.924	4.966	1.386	0.44
Mar-66	17.357	3.304	1.716	1.573
Apr-66	0	1.554	4.872	4.221
May-66	0	0	0	0
Jun-66	0	0	0	0
Jul-66	0	0	0	0
Aug-66	0	0	0	0
Sept-66	0	0	0	0
Oct-66	0	0	0	0
Nov-66	0.009	0.112	0.002	0
Dec-66	1.999	2.909	0.455	0.014
Jan-67	0.558	7.113	0.69	1.423
Feb-67	0.475	5.675	1.593	4.671
Mar-67	0.147	1.907	0.832	1.807
Apr-67	0	1.348	2.586	5.764
May-67	0	0	0	0
Jun-67	0	0	0	0
Jul-67	0	0	0	0
Aug-67	0	0	0	0
Sept-67	0	0	0	0
Oct-67	0	0	0	0
Nov-67	0.102	0	0	0.002
Dec-67	0.087	0.69	0.48	0.374
Jan-68	0.867	5.234	1.964	2.841
Feb-68	11.57	6.146	2.493	1.109
Mar-68	3.523	0.135	1.648	0.383
Apr-68	0	0.129	0.137	0
May-68	0	0	0.599	0
Jun-68	0	0	0	0
Jul-68	0	0	0	0
Aug-68	0	0	0	0
Sept-68	0.006	0	0	0
Oct-68	0	0.022	0	0
Nov-68	0.001	0.142	0	0
Dec-68	3.611	3.746	0.043	0.596
Jan-69	13.557	10.799	1.061	2.012
Feb-69	2.546	2.506	1.471	6.979
Mar-69	1.276	9.526	1.444	1.462
Apr-69	1.563	4.435	0.059	0
May-69	0	0	2.437	0
Jun-69	0	0	0	0

Jul-69	0	0	0	0
Aug-69	0	0	0	0
Sept-69	0	0	0	0
Oct-69	0	0	0	0.002
Nov-69	0.373	0.911	0.113	0.007
Dec-69	0.001	1.251	1.316	0.056
Jan-70	0.273	1.623	1.636	4.671
Feb-70	4.67	3.267	2.145	5.481
Mar-70	0.332	3.057	1.338	4.596
Apr-70	0	3.112	0.002	3.913
May-70	0	0	0	0
Jun-70	0	0	0	0
Jul-70	0	0	0	0
Aug-70	0	0	0	0
Sept-70	0	0	0	0
Oct-70	0	0	0	0
Nov-70	0.631	0.731	0.017	0.016
Dec-70	6.372	1.54	0.167	0.161

Projected sediment yield (2071-2100) under RCP8.5

Date	CCLM4	HIRAM5	RACMO22T	RCA4
Jan-71	0.503	2.184	1.161	5.253
Feb-71	1.629	8.661	2.423	4.654
Mar-71	0.389	2.363	1.101	2.143
Apr-71	0	1.46	0.506	0.193
May-71	0	0	0.069	0.001
Jun-71	0	0	0	0
Jul-71	0	0	0	0
Aug-71	0	0	0	0
Sept-71	0	0	0	0
Oct-71	0	0	0	0
Nov-71	0	0.286	0	0.01
Dec-71	0	1.06	0.353	0.099
Jan-72	13.984	2.018	0.96	1.049
Feb-72	1.957	3.615	0.696	2.211
Mar-72	2.327	2.672	0.218	3.77
Apr-72	0.232	0	9.008	1.525
May-72	0	0	1.243	0
Jun-72	0	0	0	0
Jul-72	0	0	0	0
Aug-72	0	0	0	0
Sept-72	0	0	0	0
Oct-72	0	0	0	0
Nov-72	0	0.125	0.876	0.009
Dec-72	0.005	4.575	0.137	0.068
Jan-73	5.876	5.529	1.053	1.788
Feb-73	0.427	9.362	1.295	3.285
Mar-73	6.022	1.032	1.142	0.454
Apr-73	0.098	4.578	2.92	1.134
May-73	0	0.385	0	0
Jun-73	0	0	0	0
Jul-73	0	0	0	0
Aug-73	0	0	0	0
Sept-73	0	0	0	0
Oct-73	0	0	0	0.018
Nov-73	0	0	0	0.001
Dec-73	0.047	4.298	0.012	0.163
Jan-74	0.045	2.754	0.408	1.454
Feb-74	0.745	2.657	0.585	0.932
Mar-74	2.099	2.13	0.937	1.119
Apr-74	0.009	0.992	0	0.377
May-74	0	0	0	0
Jun-74	0	0	0	0
Jul-74	0	0	0	0
Aug-74	0	0	0	0
Sept-74	0	0	0	0
Oct-74	0	0	0	0
Nov-74	0	0.838	0.05	0.027
Dec-74	3.928	0.285	0.375	0.471
Jan-75	6.353	2.623	2.033	1.901
Feb-75	1.952	1.982	1.599	2.836
Mar-75	1.385	5.722	2.455	1.43

Apr-75	0.107	3.929	9.839	0.512
May-75	0	1.181	1.519	0
Jun-75	0	0	0	0
Jul-75	0	0	0	0
Aug-75	0	0	0	0
Sept-75	0	0	0	0
Oct-75	0	0	0	0
Nov-75	0.65	0	0.159	0
Dec-75	3.195	0.582	0.482	0.124
Jan-76	1.161	1.718	1.606	1.259
Feb-76	0.862	1.882	1.213	7.834
Mar-76	2.024	8.815	0.504	0.809
Apr-76	0	0	0.864	0.442
May-76	0	11.825	0	0.092
Jun-76	0	0	0	0
Jul-76	0	0	0	0
Aug-76	0	0	0	0
Sept-76	0	0	0	0
Oct-76	0	0	0	0
Nov-76	2.806	0.67	0.087	0.003
Dec-76	1.034	1.919	0.106	0.454
Jan-77	9.121	1.686	1.293	1.516
Feb-77	4.812	5.927	1.01	2.471
Mar-77	3.124	4.853	3.75	3.065
Apr-77	46.118	5.203	0	2.678
May-77	0	0	0	0
Jun-77	0	0	0	0
Jul-77	0	0	0	0
Aug-77	0	0	0	0
Sept-77	0	0	0	0
Oct-77	0	0	0	0
Nov-77	0	0.662	0.212	0
Dec-77	0	5.41	1.09	0.351
Jan-78	0.358	11.386	1.757	3.671
Feb-78	5.815	6.772	0.718	0.879
Mar-78	3.027	8.48	2.306	2.85
Apr-78	7.967	1.619	1.778	0.079
May-78	0	1.457	0	0
Jun-78	0	0	0	0
Jul-78	0	0	0	0
Aug-78	0	0	0	0
Sept-78	0	0	0	0
Oct-78	0	0	0	0
Nov-78	1.694	0.176	0.026	0.002
Dec-78	11.808	0.999	2.155	0.13
Jan-79	2.133	12	2.931	1.213
Feb-79	1.038	4.875	0.839	6.888
Mar-79	2.118	5.031	0.025	2.931
Apr-79	0	0.628	12.46	1
May-79	0	0	0	0
Jun-79	0	0	0	0
Jul-79	0	0	0	0
Aug-79	0	0	0	0
Sept-79	0	0	0	0

Oct-79	0	0	0	0
Nov-79	0	0.195	0.004	0.117
Dec-79	0	1.864	0.376	0.239
Jan-80	0.038	7.195	4.244	0.462
Feb-80	0.729	14.205	1.032	1.403
Mar-80	0.771	5.591	1.232	2.51
Apr-80	0.388	0.572	1.953	4.035
May-80	0	0	0	0
Jun-80	0	0	0	0
Jul-80	0	0	0	0
Aug-80	0	0	0	0
Sept-80	0	0	0	0
Oct-80	0	0	0	0
Nov-80	0.031	1.334	1.121	0.137
Dec-80	18.094	3.18	1.074	0.819
Jan-81	1.126	13.327	0.688	3.95
Feb-81	87.909	8.534	1.025	1.676
Mar-81	4.557	3.991	0.975	1.958
Apr-81	10.787	0.261	0	1.737
May-81	0	0.065	0	0
Jun-81	0	0	0	0
Jul-81	0	0	0	0
Aug-81	0	0	0	0
Sept-81	0	0	0	0
Oct-81	0	0	0	0
Nov-81	0	0.122	0.006	0
Dec-81	0.001	0.845	0.97	0.92
Jan-82	42.369	4.151	1.237	1.485
Feb-82	6.292	4.342	1.327	10.044
Mar-82	3.124	4.772	0.703	2.177
Apr-82	6.008	1.573	6.031	1.089
May-82	0	0.311	0	0
Jun-82	0	0	0	0
Jul-82	0	0	0	0
Aug-82	0	0	0	0
Sept-82	0	0	0	0
Oct-82	0	0	0	0.022
Nov-82	10.185	0.284	0.881	0
Dec-82	3.251	3.788	0.458	0.004
Jan-83	2.383	7.188	0.507	1.388
Feb-83	1.56	7.473	1.097	1.065
Mar-83	0.478	1.015	0.833	2.694
Apr-83	0.618	0.034	3.885	4.234
May-83	0	0	0	0
Jun-83	0	0	0	0
Jul-83	0	0	0	0
Aug-83	0	0	0	0
Sept-83	0	0	0	0
Oct-83	0	0	0	0
Nov-83	0	0.131	0	0.27
Dec-83	0.021	7.327	0.066	0.451
Jan-84	0.239	8.736	0.955	3.714
Feb-84	0.397	9.479	2.457	4.735
Mar-84	0.029	0.928	1.661	1.583

Apr-84	0	0	0	1.01
May-84	0	0	0	0
Jun-84	0	0	0	0
Jul-84	0	0	0	0
Aug-84	0	0	0	0
Sept-84	0	0	0	0
Oct-84	0	0	0	0
Nov-84	0	0.013	0.299	0.022
Dec-84	0	1.408	1.754	0.543
Jan-85	8.048	5.77	2.908	2.166
Feb-85	23.621	4.118	3.202	7.295
Mar-85	5.617	9.889	0.785	3.104
Apr-85	6.795	1.831	0.106	2.172
May-85	0	0	0	0
Jun-85	0	0	0	0
Jul-85	0	0	0	0
Aug-85	0	0	0	0
Sept-85	0	0	0	0
Oct-85	0	0	0	0
Nov-85	0	3.617	2.859	0.001
Dec-85	0.004	8.071	0.583	0.111
Jan-86	1.894	8.519	0.809	1.282
Feb-86	3.298	7.964	1.782	1.246
Mar-86	3.575	5.02	1.641	1.421
Apr-86	2.089	0.001	2.903	1.572
May-86	0	0	0	0
Jun-86	0	0	0	0
Jul-86	0	0	0	0
Aug-86	0	0	0	0
Sept-86	0	0	0	0
Oct-86	0	0	0	0
Nov-86	0	0.014	0.146	0.039
Dec-86	0.966	0.164	0.575	0.295
Jan-87	1.124	1.869	0.743	9.284
Feb-87	77.638	4.564	0.365	2.573
Mar-87	1.211	6.911	1.826	2.378
Apr-87	0.412	2.147	9.284	6.825
May-87	0	2.099	0	0
Jun-87	0	0	0	0
Jul-87	0	0	0	0
Aug-87	0	0	0	0
Sept-87	0	0	0	0
Oct-87	0	0	0	0
Nov-87	0	0.964	0.041	0
Dec-87	0	2.846	0.54	0.134
Jan-88	0.007	6.759	0.556	1.419
Feb-88	5.521	6.103	2.664	1.939
Mar-88	1.008	20.606	1.234	1.15
Apr-88	0	0.629	0	2.213
May-88	0	0	0	0
Jun-88	0	0	0	0
Jul-88	0	0	0	0
Aug-88	0	0	0	0
Sept-88	0	0	0	0

Oct-88	0	0	0	0
Nov-88	0.001	0	1.769	0.005
Dec-88	0	0.923	0.993	0.554
Jan-89	0	6.187	0.818	4.733
Feb-89	67.694	12.18	4.091	1.997
Mar-89	0.501	1.506	4.17	1.019
Apr-89	0	0	0.116	0
May-89	0	0.011	0.788	0.008
Jun-89	0	0	0	0
Jul-89	0	0	0	0
Aug-89	0	0	0	0
Sept-89	0	0	0	0
Oct-89	0	0	0	0
Nov-89	0.744	6.105	0.055	0.034
Dec-89	1.803	9	0.618	0.297
Jan-90	0.748	9.62	1.165	3.474
Feb-90	2.831	2.919	2.72	6.222
Mar-90	0.315	11.319	1.322	4.114
Apr-90	66.065	0.163	4.864	0
May-90	0	0	0.048	0
Jun-90	0	0	0	0
Jul-90	0	0	0	0
Aug-90	0	0	0	0
Sept-90	0	0	0	0
Oct-90	0	0	0	0
Nov-90	0	0.366	0.027	0.006
Dec-90	3.075	6.057	0.129	0
Jan-91	12.16	22.95	3.435	0.309
Feb-91	1.943	4.278	1.061	1.059
Mar-91	4.009	9.266	1.554	0.208
Apr-91	2.245	0.088	4.791	1.431
May-91	0	0	0.001	1.4
Jun-91	0	0	0	0
Jul-91	0	0	0	0
Aug-91	0	0	0	0
Sept-91	0	0	0	0
Oct-91	0	0	0	0
Nov-91	15.235	0	0.016	0
Dec-91	10.227	23.717	0.257	5.36
Jan-92	0.972	9.637	1.384	0.665
Feb-92	0.044	0.981	2.337	2.262
Mar-92	1.215	8.588	1.616	15.404
Apr-92	0	0	3.196	2.798
May-92	0	0	0	0.054
Jun-92	0	0	0	0
Jul-92	0	0	0	0
Aug-92	0	0	0	0
Sept-92	0	0	0	0
Oct-92	0	0	0	0
Nov-92	0	0	0	0
Dec-92	1.949	15.427	0.331	0.263
Jan-93	0.509	3.873	1.594	0.592
Feb-93	1.341	5.939	1.864	4.802
Mar-93	0.442	5.601	1.138	0.776

Apr-93	0.002	0	5.505	0
May-93	0	0	0	0.149
Jun-93	0	0	0	0
Jul-93	0	0	0	0
Aug-93	0	0	0	0
Sept-93	0	0	0	0
Oct-93	0	0	0	0
Nov-93	0	0	0.062	0.028
Dec-93	0	0	0.959	0.114
Jan-94	0.106	5.263	2.937	1.025
Feb-94	2.183	11.858	1.741	7.083
Mar-94	0.381	6.223	0.453	0.895
Apr-94	0	1.848	6.698	2.048
May-94	0.524	0	0	0
Jun-94	0	0	0	0
Jul-94	0	0	0	0
Aug-94	0	0	0	0
Sept-94	0	0	0	0
Oct-94	0	0	0	0
Nov-94	28.959	0.559	0.055	0.198
Dec-94	0.05	4.004	0.763	7.105
Jan-95	1.597	15.224	1.14	2.714
Feb-95	0.677	8.999	1.542	5.874
Mar-95	0.459	14.59	3.528	1.212
Apr-95	0	2.607	4.487	8.075
May-95	0	0	0	0.004
Jun-95	0	0	0	0
Jul-95	0	0	0	0
Aug-95	0	0	0	0
Sept-95	0	0	0	0
Oct-95	0	0	0	0
Nov-95	15.507	0	0.006	0
Dec-95	1.52	8.319	1.017	0.212
Jan-96	8.387	6.648	0.556	2.13
Feb-96	2.706	8.621	0.756	1.559
Mar-96	2.878	4.989	1.177	1.114
Apr-96	0.019	0.041	17.337	2.666
May-96	0	0	0	0
Jun-96	0	0	0	0
Jul-96	0	0	0	0
Aug-96	0	0	0	0
Sept-96	0	0	0	0
Oct-96	0	0.02	0	0
Nov-96	0	0.014	0.852	0.063
Dec-96	6.172	4.078	1.133	0.951
Jan-97	0.397	8.465	0.952	1.422
Feb-97	8.342	8.916	0.925	0.306
Mar-97	4.092	3.776	0.482	2.247
Apr-97	0	2.893	0.633	0
May-97	0	0.003	0	0
Jun-97	0	0	0	0
Jul-97	0	0	0	0
Aug-97	0	0	0	0
Sept-97	0	0	0	0

Oct-97	0	0	0	0
Nov-97	0	0.088	0	0.01
Dec-97	0	1.692	0.023	0.107
Jan-98	1.793	7.111	1.23	1.182
Feb-98	2.979	3.363	0.654	5.072
Mar-98	1.938	5.191	1.3	4.054
Apr-98	1.14	1.147	4.204	1.918
May-98	0	0	0	0
Jun-98	0	0	0	0
Jul-98	0	0	0	0
Aug-98	0	0	0	0
Sept-98	0	0	0	0
Oct-98	0	0	0	0
Nov-98	7.505	0	0.164	0.632
Dec-98	22.056	0.322	0.281	0.885
Jan-99	0.183	4.008	1.845	6.965
Feb-99	2.129	5.624	2.923	2.071
Mar-99	0.214	5.047	0.649	1.162
Apr-99	0.19	0.618	1.396	4.982
May-99	0	5.439	0	0
Jun-99	0	0	0	0
Jul-99	0	0	0	0
Aug-99	0	0	0	0
Sept-99	0.432	0	0	0
Oct-99	0	0	0	0
Nov-99	0.002	0.001	0	0.034
Dec-99	0	3.266	0.524	0.01
Jan-00	1.167	6.575	1.382	1.824
Feb-00	1	0.565	2.939	2.758
Mar-00	0.361	1.304	5.933	4.021
Apr-00	2.122	0	0.574	9.35
May-00	0	0	0	0.002
Jun-00	0	0	0	0
Jul-00	0	0	0	0
Aug-00	0	0	0	0
Sept-00	0	0	0	0
Oct-00	0	0	0	0
Nov-00	0	0.637	0.001	0
Dec-00	0.003	6.933	0.184	0.738

Appendix D: Projected Sediment Yield under RCP4.5 and RCP8.5 Climate Scenarios Combined with Future Land Use Maps.

Climate scenarios Combined with future land use Maps

Date	2011 - 2040 Land use scenarios							
	CCLM4_RCP4.5	CCLM4_RCP8.5	HIRAM5_RCP4.5	HIRAM5_RCP8.5	RACMO22T_RCP4.5	RACMO22T_RCP8.5	RCA4_RCP4.5	RCA4_RCP8.5
Jan-11	0.792	10.068	1.141	2.223	1.253	0.707	1.312	0.066
Feb-11	9.587	4.545	9.972	4.116	1.834	1.209	1.963	5.040
Mar-11	11.678	2.158	8.407	6.853	4.103	3.027	3.039	3.087
Apr-11	5.802	0.000	0.316	4.885	3.052	6.327	0.389	0.209
May-11	0.159	0.000	0.000	0.000	0.000	0.149	0.000	0.000
Jun-11	0.000	0.000	0.000	0.000	0.000	0.000	0.000	0.000
Jul-11	0.000	0.000	0.000	0.000	0.000	0.000	0.000	0.000
Aug-11	0.000	0.000	0.000	0.000	0.000	0.000	0.000	0.000
Sept-11	0.000	0.000	0.000	0.000	0.000	0.000	0.000	0.000
Oct-11	0.000	0.000	0.000	0.000	0.000	0.000	0.000	0.000
Nov-11	0.000	0.192	0.265	0.000	0.000	0.035	0.000	0.001
Dec-11	0.196	3.736	0.558	0.194	0.002	1.179	0.164	0.018
Jan-12	0.810	2.535	4.798	1.714	0.735	0.701	1.534	2.894
Feb-12	0.666	4.730	2.728	3.870	0.947	1.121	1.626	4.515
Mar-12	12.347	1.371	7.282	1.716	2.497	0.949	1.016	1.791
Apr-12	1.513	3.812	3.395	0.106	0.000	0.000	0.098	0.175

May-12	0.000	0.000	0.000	0.000	0.000	0.000	0.000	0.000
Jun-12	0.000	0.000	0.000	0.000	0.000	0.000	0.000	0.000
Jul-12	0.000	0.000	0.000	0.000	0.000	0.000	0.000	0.000
Aug-12	0.000	0.000	0.000	0.000	0.000	0.000	0.000	0.000
Sept-12	0.000	0.000	0.000	0.000	0.000	0.000	0.000	0.000
Oct-12	0.000	0.000	0.000	0.000	0.000	0.000	0.000	0.000
Nov-12	0.131	0.990	0.008	0.011	0.000	0.026	0.000	0.000
Dec-12	1.130	7.142	0.087	0.374	0.335	0.268	0.106	0.382
Jan-13	19.708	8.354	3.934	3.770	0.991	3.360	5.216	2.435
Feb-13	0.037	0.452	4.549	3.887	0.514	0.658	0.714	0.662
Mar-13	3.994	7.904	3.173	3.118	3.276	0.592	2.839	1.836
Apr-13	0.020	1.075	0.000	1.246	0.006	0.065	0.000	2.230
May-13	0.000	0.000	0.000	0.000	1.343	0.000	0.000	0.000
Jun-13	0.000	0.000	0.000	0.000	0.000	0.000	0.000	0.000
Jul-13	0.000	0.000	0.000	0.000	0.000	0.000	0.000	0.000
Aug-13	0.000	0.000	0.000	0.000	0.000	0.000	0.000	0.000
Sept-13	0.000	0.000	0.000	0.000	0.000	0.000	0.000	0.000
Oct-13	0.000	0.000	0.000	0.000	0.000	0.000	0.000	0.000
Nov-13	1.362	0.632	0.020	0.439	0.000	0.000	0.000	0.153

Dec-13	2.507	1.879	2.761	1.871	0.459	0.141	0.681	0.582
Jan-14	2.460	5.680	8.022	15.771	2.089	0.581	1.770	2.513
Feb-14	0.221	5.113	4.202	1.870	0.865	0.840	0.793	4.615
Mar-14	1.780	3.308	0.041	4.560	2.116	1.090	1.705	2.659
Apr-14	5.843	16.029	0.289	1.523	0.709	1.127	0.010	3.121
May-14	0.000	0.000	0.000	0.000	0.000	0.000	0.000	0.000
Jun-14	0.000	0.000	0.000	0.000	0.000	0.000	0.000	0.000
Jul-14	0.000	0.000	0.000	0.000	0.000	0.000	0.000	0.000
Aug-14	0.000	0.000	0.000	0.000	0.000	0.000	0.000	0.000
Sept-14	0.000	0.000	0.000	0.000	0.000	0.000	0.000	0.000
Oct-14	0.000	0.000	0.000	0.000	0.000	0.000	0.000	0.000
Nov-14	12.278	0.000	0.000	0.000	0.000	0.000	0.062	0.000
Dec-14	0.545	0.000	0.085	0.449	0.202	1.758	0.559	0.232
Jan-15	4.216	1.075	3.331	4.560	1.540	0.815	1.869	4.797
Feb-15	1.745	0.704	9.016	4.916	1.648	3.547	0.697	3.035
Mar-15	1.498	0.186	5.185	4.757	1.614	0.840	2.598	0.408
Apr-15	0.042	6.089	0.002	0.485	7.531	2.554	1.312	0.748
May-15	0.000	0.000	0.000	7.626	0.000	0.000	0.000	0.000
Jun-15	0.000	0.000	0.000	0.000	0.000	0.000	0.000	0.000

Jul-15	0.000	0.000	0.000	0.000	0.000	0.000	0.000	0.000
Aug-15	0.000	0.000	0.000	0.000	0.000	0.000	0.000	0.000
Sept-15	0.000	0.000	0.000	0.000	0.000	0.000	0.000	0.000
Oct-15	0.000	0.000	0.000	0.000	0.000	0.000	0.000	0.000
Nov-15	0.000	0.006	0.000	0.035	0.000	0.000	0.000	0.098
Dec-15	5.728	2.894	0.002	0.975	0.123	0.362	0.158	1.089
Jan-16	11.368	1.297	4.694	5.570	0.605	0.729	0.588	2.087
Feb-16	2.261	0.802	2.159	2.341	0.719	0.682	0.746	2.102
Mar-16	0.251	0.929	7.026	2.634	3.721	0.648	2.593	0.887
Apr-16	0.000	0.087	1.915	0.000	1.808	0.292	0.945	0.078
May-16	0.000	30.592	0.000	0.000	0.000	0.000	0.013	0.000
Jun-16	0.000	0.000	0.000	0.000	0.000	0.000	0.000	0.000
Jul-16	0.000	0.000	0.000	0.000	0.000	0.000	0.000	0.000
Aug-16	0.000	0.000	0.000	0.000	0.000	0.000	0.000	0.000
Sept-16	0.000	0.000	0.000	0.002	0.000	0.000	0.016	0.000
Oct-16	0.003	1.945	0.000	0.000	0.000	0.004	0.000	0.086
Nov-16	1.475	2.765	0.000	0.000	0.000	0.163	0.000	2.121
Dec-16	5.865	0.281	2.123	0.535	0.214	0.451	0.006	0.203
Jan-17	2.419	1.197	2.328	8.712	0.954	0.624	1.266	6.561

Feb-17	29.198	17.555	3.194	6.335	0.647	1.141	0.991	0.557
Mar-17	29.375	2.518	5.169	2.588	3.236	1.257	4.393	1.344
Apr-17	0.021	0.672	0.189	4.843	0.002	1.181	2.728	5.012
May-17	0.000	0.000	0.000	0.000	0.000	0.000	0.000	0.000
Jun-17	0.000	0.000	0.000	0.000	0.000	0.000	0.000	0.000
Jul-17	0.000	0.000	0.000	0.000	0.000	0.000	0.000	0.000
Aug-17	0.000	0.000	0.000	0.000	0.000	0.000	0.000	0.000
Sept-17	0.000	0.000	0.000	0.000	0.000	0.000	0.000	0.000
Oct-17	0.000	0.000	0.000	0.000	0.000	0.000	0.000	0.000
Nov-17	4.895	0.556	0.000	0.832	0.000	0.155	0.000	0.024
Dec-17	35.109	0.243	0.037	1.948	0.249	0.494	0.152	1.024
Jan-18	1.555	10.941	3.701	4.879	1.214	1.756	2.452	1.362
Feb-18	67.082	1.558	0.773	6.761	1.188	0.725	0.284	0.521
Mar-18	9.992	8.893	2.065	1.023	1.197	0.808	0.591	2.004
Apr-18	9.818	6.277	0.000	4.871	2.041	1.734	1.186	0.332
May-18	0.421	0.000	0.000	0.671	0.000	0.000	0.000	0.000
Jun-18	0.000	0.000	0.000	0.000	0.000	0.000	0.000	0.000
Jul-18	0.000	0.000	0.000	0.000	0.000	0.000	0.000	0.000
Aug-18	0.000	0.000	0.000	0.000	0.000	0.000	0.000	0.000

Sept-18	0.000	0.000	0.000	0.000	0.000	0.000	0.000	0.000
Oct-18	0.000	0.000	0.000	0.000	0.000	0.000	0.000	0.000
Nov-18	0.000	0.000	0.046	0.014	0.000	0.000	0.000	0.000
Dec-18	2.393	1.426	0.761	1.230	0.015	0.388	0.327	0.058
Jan-19	2.319	1.538	6.945	3.972	0.397	1.669	6.816	0.399
Feb-19	13.935	9.640	12.707	6.716	0.249	1.524	1.677	1.309
Mar-19	2.170	14.676	7.713	4.115	0.275	2.280	4.401	1.576
Apr-19	0.978	0.494	3.385	0.363	0.000	4.479	0.097	1.631
May-19	0.000	2.867	0.000	0.000	0.000	0.079	0.000	0.000
Jun-19	0.000	0.000	0.000	0.000	0.000	0.000	0.000	0.000
Jul-19	0.000	0.000	0.000	0.000	0.000	0.000	0.000	0.000
Aug-19	0.000	0.000	0.000	0.000	0.000	0.000	0.000	0.000
Sept-19	0.000	0.000	0.000	0.000	0.000	0.000	0.000	0.000
Oct-19	0.000	0.000	0.000	0.000	0.000	0.000	0.000	0.000
Nov-19	0.000	0.000	0.000	0.000	0.000	0.132	0.000	0.104
Dec-19	0.099	0.000	0.067	1.279	0.215	0.357	0.016	0.651
Jan-20	2.955	2.396	4.457	5.076	3.621	0.774	2.072	3.211
Feb-20	0.335	0.882	4.875	3.196	3.265	0.997	0.596	3.163
Mar-20	1.666	0.305	22.993	0.218	4.098	1.457	0.378	2.494

Apr-20	0.529	1.876	0.000	0.000	1.210	0.030	0.000	8.660
May-20	0.000	0.000	0.000	0.000	3.211	0.000	0.000	0.000
Jun-20	0.000	0.000	0.000	0.000	0.000	0.000	0.000	0.000
Jul-20	0.000	0.000	0.000	0.000	0.000	0.000	0.000	0.000
Aug-20	0.000	0.000	0.000	0.000	0.000	0.000	0.000	0.000
Sept-20	0.000	0.000	0.000	0.000	0.000	0.000	0.000	0.000
Oct-20	0.000	0.000	0.000	0.000	0.000	0.000	0.000	0.000
Nov-20	0.000	0.065	0.000	1.121	0.000	0.232	0.000	0.449
Dec-20	0.211	8.751	0.869	2.072	0.015	0.700	0.236	0.141
Jan-21	0.214	2.994	6.411	6.801	0.893	0.540	4.997	5.119
Feb-21	3.063	2.029	7.438	7.140	0.480	1.606	3.230	0.473
Mar-21	2.194	4.188	2.424	2.796	2.085	1.076	1.303	3.606
Apr-21	0.421	0.000	0.462	0.546	1.313	5.874	1.140	5.185
May-21	0.000	0.000	0.000	0.000	0.000	0.000	0.000	0.000
Jun-21	0.000	0.000	0.000	0.000	0.000	0.000	0.000	0.000
Jul-21	0.000	0.000	0.000	0.000	0.000	0.000	0.000	0.000
Aug-21	0.000	0.000	0.000	0.000	0.000	0.000	0.000	0.000
Sept-21	0.000	0.000	0.000	0.000	0.000	0.000	0.000	0.000
Oct-21	0.000	0.000	0.000	0.000	0.000	0.000	0.000	0.000

Nov-21	0.325	0.000	0.000	0.107	0.000	0.043	0.000	0.000
Dec-21	0.712	0.000	2.649	2.219	0.098	0.610	0.370	0.292
Jan-22	0.070	0.077	6.135	4.879	1.675	1.335	0.743	1.737
Feb-22	19.806	0.549	4.299	6.826	0.772	0.840	0.771	1.744
Mar-22	6.540	9.052	1.606	6.851	0.042	3.000	0.938	1.794
Apr-22	0.000	0.513	0.000	0.888	0.000	5.933	0.516	0.372
May-22	0.000	0.000	0.000	0.000	0.000	0.000	0.000	0.000
Jun-22	0.000	0.000	0.000	0.000	0.000	0.000	0.000	0.000
Jul-22	0.000	0.000	0.000	0.000	0.000	0.000	0.000	0.000
Aug-22	0.000	0.000	0.000	0.000	0.000	0.000	0.000	0.000
Sept-22	0.000	0.000	0.000	0.000	0.000	0.000	0.000	0.000
Oct-22	0.000	0.000	0.000	0.001	0.000	0.000	0.000	0.000
Nov-22	0.039	0.006	0.012	2.540	0.000	0.000	0.000	0.000
Dec-22	0.719	0.010	0.478	2.166	0.244	0.186	1.699	0.781
Jan-23	3.436	47.104	8.028	1.000	2.611	1.012	22.090	3.044
Feb-23	6.104	2.294	2.560	1.831	1.312	0.384	3.081	5.265
Mar-23	6.939	4.413	8.698	4.769	2.388	0.563	3.700	1.009
Apr-23	0.058	0.000	0.286	5.842	0.053	21.331	0.058	0.496
May-23	0.000	0.000	0.000	0.000	0.000	0.000	0.000	0.000

Jun-23	0.000	0.000	0.000	0.000	0.000	0.000	0.000	0.000
Jul-23	0.000	0.000	0.000	0.000	0.000	0.000	0.000	0.000
Aug-23	0.000	0.000	0.000	0.000	0.000	0.000	0.000	0.000
Sept-23	0.000	0.000	0.000	23.700	0.000	0.000	0.000	0.000
Oct-23	0.000	0.000	0.000	0.016	0.000	0.000	0.000	0.000
Nov-23	0.013	0.000	0.000	0.022	0.000	0.135	0.000	0.001
Dec-23	2.339	19.940	0.155	1.075	0.593	0.993	0.154	1.175
Jan-24	1.705	13.570	3.160	1.611	3.247	0.990	3.501	4.210
Feb-24	4.933	14.751	3.646	1.476	0.931	1.608	1.506	7.154
Mar-24	0.224	0.647	1.674	0.879	3.271	1.300	2.263	1.311
Apr-24	0.000	0.130	12.404	0.000	0.005	0.000	3.060	1.079
May-24	0.000	8.164	0.000	0.000	2.330	0.000	0.000	3.031
Jun-24	0.000	0.000	0.000	0.000	0.000	0.000	0.000	0.000
Jul-24	0.000	0.000	0.000	0.000	0.000	0.000	0.000	0.000
Aug-24	0.000	0.000	0.000	0.000	0.000	0.000	0.000	0.000
Sept-24	0.000	0.000	0.000	0.000	0.000	0.000	0.126	0.000
Oct-24	0.000	0.000	0.000	0.000	0.000	0.000	0.000	0.000
Nov-24	0.006	0.000	0.000	0.000	0.000	0.018	0.000	0.000
Dec-24	3.923	0.000	0.777	1.097	0.087	0.443	0.196	0.123

Jan-25	0.931	1.891	2.604	5.477	0.382	1.231	0.928	3.468
Feb-25	0.657	26.269	1.539	5.628	0.582	2.780	0.881	0.541
Mar-25	2.842	0.686	0.620	0.408	1.151	3.915	2.582	1.582
Apr-25	0.023	0.469	0.767	3.994	0.313	3.215	0.000	1.875
May-25	0.000	0.000	0.000	2.590	0.996	0.000	0.000	0.000
Jun-25	0.000	0.000	0.000	0.000	0.000	0.000	0.000	0.000
Jul-25	0.000	0.000	0.000	0.000	0.000	0.000	0.000	0.000
Aug-25	0.000	0.000	0.000	0.000	0.000	0.000	0.000	0.000
Sept-25	0.000	0.000	0.000	0.000	0.000	0.000	0.000	0.000
Oct-25	0.000	0.000	0.000	0.000	0.000	0.000	0.000	0.000
Nov-25	0.066	0.005	0.000	0.000	0.000	0.057	0.001	0.000
Dec-25	1.990	0.404	0.565	0.682	0.051	0.479	0.000	0.026
Jan-26	11.820	7.542	10.762	2.099	1.052	0.848	4.582	1.685
Feb-26	0.919	21.700	2.747	4.559	0.622	1.978	1.319	4.803
Mar-26	7.752	0.179	2.805	3.238	0.970	2.020	2.022	0.504
Apr-26	11.091	1.888	0.242	0.000	7.533	0.000	0.773	0.128
May-26	0.000	0.000	0.000	0.000	0.000	0.000	0.099	0.000
Jun-26	0.000	0.000	0.000	0.000	0.000	0.000	0.000	0.000
Jul-26	0.000	0.000	0.000	0.000	0.000	0.000	0.000	0.000

Aug-26	0.000	0.000	0.000	0.000	0.000	0.000	0.000	0.000
Sept-26	0.000	0.000	0.000	0.000	0.000	0.000	0.000	0.000
Oct-26	0.000	0.000	0.000	0.000	0.000	0.000	0.000	0.000
Nov-26	0.000	0.000	0.000	2.754	0.000	0.003	0.000	0.027
Dec-26	0.280	0.010	0.034	3.699	0.003	0.110	0.075	0.133
Jan-27	0.968	0.338	1.052	1.051	0.901	0.342	0.290	1.754
Feb-27	0.938	44.711	2.293	4.333	1.092	1.520	1.095	10.787
Mar-27	0.774	3.289	3.973	9.653	0.842	2.205	1.295	2.371
Apr-27	0.420	47.466	1.206	0.000	0.076	0.175	0.567	0.000
May-27	0.000	0.001	0.000	0.000	0.000	0.000	0.000	4.266
Jun-27	0.000	0.000	0.000	0.000	0.000	0.000	0.000	0.000
Jul-27	0.000	0.000	0.000	0.000	0.000	0.000	0.000	0.000
Aug-27	0.000	0.000	0.000	0.000	0.000	0.000	0.000	0.000
Sept-27	0.000	0.000	0.000	0.000	0.000	0.000	0.000	0.000
Oct-27	0.000	0.000	0.000	0.000	0.000	0.000	0.000	0.000
Nov-27	0.338	8.165	0.005	2.131	0.102	0.002	0.000	0.297
Dec-27	19.119	0.432	0.706	2.710	0.179	0.298	0.324	0.926
Jan-28	0.331	0.639	1.844	2.314	1.195	1.271	2.448	0.343
Feb-28	1.046	0.724	7.466	4.008	3.251	1.535	3.710	3.713

Mar-28	3.903	0.479	1.236	4.615	2.752	0.653	0.366	4.092
Apr-28	9.723	0.713	0.000	0.096	0.000	7.502	4.186	1.873
May-28	0.000	0.000	0.000	0.000	0.000	0.039	1.530	2.069
Jun-28	0.000	0.000	0.000	0.000	0.000	0.000	0.000	0.000
Jul-28	0.000	0.000	0.000	0.000	0.000	0.000	0.000	0.000
Aug-28	0.000	0.000	0.000	0.000	0.000	0.000	0.000	0.000
Sept-28	0.000	0.000	0.000	0.037	0.000	0.000	0.000	0.000
Oct-28	0.000	0.000	0.000	0.000	0.000	0.000	0.000	0.000
Nov-28	0.000	0.000	0.236	0.067	0.000	0.000	0.000	0.000
Dec-28	0.098	0.092	1.722	0.072	0.287	0.111	0.134	0.312
Jan-29	1.995	1.701	13.475	2.580	2.675	1.289	0.910	0.378
Feb-29	1.736	0.189	0.825	1.475	1.209	1.146	0.704	3.762
Mar-29	1.871	0.721	0.089	2.867	2.503	1.088	0.773	1.639
Apr-29	0.048	0.000	0.000	0.001	0.157	0.353	1.469	1.778
May-29	0.000	0.000	0.000	9.429	0.000	0.001	0.000	0.000
Jun-29	0.000	0.000	0.000	0.000	0.000	0.000	0.000	0.000
Jul-29	0.000	0.000	0.000	0.000	0.000	0.000	0.000	0.000
Aug-29	0.000	0.000	0.000	0.000	0.000	0.000	0.000	0.000
Sept-29	0.000	0.000	0.000	1.181	0.000	0.000	0.000	0.000

Oct-29	0.000	0.000	0.000	0.477	0.000	0.000	0.000	0.000
Nov-29	0.000	0.000	0.000	1.179	0.000	0.009	0.000	0.000
Dec-29	2.201	0.025	1.442	2.045	0.142	0.347	0.018	0.009
Jan-30	6.334	2.662	9.487	11.523	2.145	0.736	1.121	1.582
Feb-30	2.479	5.767	2.018	4.085	0.647	0.765	0.101	2.596
Mar-30	17.565	1.516	2.724	1.678	2.393	0.073	2.160	2.354
Apr-30	2.403	5.873	0.000	0.043	0.000	1.272	4.236	4.431
May-30	0.623	7.254	0.000	0.010	0.000	0.000	0.000	0.000
Jun-30	0.000	0.000	0.000	0.000	0.000	0.000	0.000	0.000
Jul-30	0.000	0.000	0.000	0.000	0.000	0.000	0.000	0.000
Aug-30	0.000	0.000	0.000	0.000	0.000	0.000	0.000	0.000
Sept-30	0.000	0.000	0.000	0.000	0.000	0.000	0.000	0.000
Oct-30	0.000	0.000	0.000	0.253	0.000	0.000	0.000	0.000
Nov-30	0.161	19.238	0.000	0.084	0.000	0.000	0.000	0.132
Dec-30	0.436	10.465	0.379	3.453	0.041	0.893	0.151	0.371
Jan-31	22.756	0.916	6.380	2.239	2.541	1.351	7.443	2.826
Feb-31	6.271	0.818	5.144	8.493	1.643	1.206	2.529	3.875
Mar-31	26.113	0.306	7.528	1.078	4.377	0.046	1.807	0.616
Apr-31	0.023	0.000	0.000	2.739	2.085	0.141	4.782	2.260

May-31	0.000	0.000	0.000	0.001	0.000	0.000	0.000	0.000
Jun-31	0.000	0.000	0.000	0.000	0.000	0.000	0.000	0.000
Jul-31	0.000	0.000	0.000	0.000	0.000	0.000	0.000	0.000
Aug-31	0.000	0.000	0.000	0.000	0.000	0.000	0.000	0.000
Sept-31	0.000	0.000	0.000	0.000	0.000	0.000	0.000	0.000
Oct-31	0.000	0.000	0.000	0.000	0.000	0.000	0.000	0.000
Nov-31	0.004	0.000	0.000	0.282	0.000	0.000	0.000	0.001
Dec-31	0.000	0.000	0.169	0.946	0.215	0.347	0.209	0.409
Jan-32	0.833	1.266	7.337	3.957	0.971	1.610	11.869	3.292
Feb-32	1.511	0.562	4.277	4.154	2.125	1.856	0.904	2.580
Mar-32	9.124	21.321	2.512	0.414	0.936	0.572	5.063	0.857
Apr-32	0.000	1.147	0.000	0.000	0.005	0.498	0.000	0.000
May-32	0.000	0.000	0.000	0.000	0.000	0.000	0.000	0.000
Jun-32	0.000	0.000	0.000	0.000	0.000	0.000	0.000	0.000
Jul-32	0.000	0.000	0.000	0.000	0.000	0.000	0.000	0.000
Aug-32	0.000	0.000	0.000	0.000	0.000	0.000	0.000	0.000
Sept-32	0.000	0.000	0.000	0.000	0.000	0.000	0.000	0.000
Oct-32	0.000	0.000	0.000	0.000	0.000	0.000	0.000	0.000
Nov-32	1.787	0.000	0.000	0.000	0.001	0.035	0.000	0.000

Dec-32	1.979	0.112	0.014	0.546	0.512	0.554	1.887	0.023
Jan-33	13.841	0.037	39.311	1.232	3.337	1.676	5.980	0.494
Feb-33	4.447	0.669	4.751	4.805	2.556	1.686	2.941	1.536
Mar-33	12.582	9.671	9.210	6.932	4.153	2.475	3.039	6.416
Apr-33	3.445	0.012	0.705	0.368	0.544	3.726	1.155	0.403
May-33	0.000	0.000	0.000	0.000	0.000	0.000	0.000	0.000
Jun-33	0.000	0.000	0.000	0.000	0.000	0.000	0.000	0.000
Jul-33	0.000	0.000	0.000	0.000	0.000	0.000	0.000	0.000
Aug-33	0.000	0.000	0.000	0.000	0.000	0.000	0.000	0.000
Sept-33	0.451	0.000	0.000	0.000	0.000	0.000	0.000	0.000
Oct-33	0.000	0.000	0.000	0.000	0.000	0.000	0.000	0.000
Nov-33	2.855	0.000	0.067	0.522	0.000	0.000	0.000	0.000
Dec-33	10.765	2.182	2.621	2.133	0.422	0.227	0.006	0.207
Jan-34	5.441	0.457	4.974	5.461	2.684	1.964	1.519	1.046
Feb-34	0.458	8.705	4.522	4.246	1.499	1.225	0.586	3.562
Mar-34	1.739	1.557	4.513	2.389	2.327	1.223	1.655	0.544
Apr-34	0.029	0.302	0.133	0.365	0.013	4.420	3.042	7.215
May-34	0.000	0.000	0.000	5.695	0.000	0.000	0.000	1.446
Jun-34	0.000	0.000	0.000	0.000	0.000	0.000	0.000	0.000

Jul-34	0.000	0.000	0.000	0.000	0.000	0.000	0.000	0.000
Aug-34	0.000	0.000	0.000	0.000	0.000	0.000	0.000	0.000
Sept-34	0.000	0.000	0.000	0.000	0.000	0.000	0.000	0.000
Oct-34	0.000	0.000	0.000	0.000	0.000	0.000	0.000	0.000
Nov-34	0.000	0.500	0.041	0.653	0.000	0.000	0.000	0.000
Dec-34	0.639	0.030	0.103	2.162	0.259	0.038	0.248	0.215
Jan-35	0.609	3.569	3.347	6.485	0.960	1.768	3.036	1.336
Feb-35	7.845	1.338	2.496	1.432	0.695	1.152	0.106	3.752
Mar-35	5.186	0.205	4.302	4.562	1.264	0.512	0.887	0.496
Apr-35	2.898	2.856	1.282	0.000	0.285	0.839	0.000	1.541
May-35	0.000	0.000	0.000	0.000	0.000	0.802	0.000	0.847
Jun-35	0.000	0.000	0.000	0.000	0.000	0.000	0.000	0.000
Jul-35	0.000	0.000	0.000	0.000	0.000	0.000	0.000	0.000
Aug-35	0.000	0.000	0.000	0.000	0.000	0.000	0.000	0.000
Sept-35	0.000	0.000	0.000	0.000	0.000	0.000	0.000	0.000
Oct-35	0.000	0.000	0.000	0.000	0.000	0.000	0.000	0.000
Nov-35	0.000	0.000	0.000	0.315	0.000	0.080	0.148	0.002
Dec-35	0.684	22.862	0.046	2.491	0.281	0.149	0.379	0.130
Jan-36	6.232	7.742	6.900	7.812	1.508	2.315	2.588	1.509

Feb-36	29.208	1.439	2.723	2.638	3.806	0.723	4.906	0.454
Mar-36	5.536	9.285	4.348	4.758	1.212	1.494	3.358	1.622
Apr-36	0.042	4.782	1.449	0.000	0.019	6.505	0.026	4.352
May-36	0.000	0.000	0.000	0.000	0.000	0.000	0.000	0.000
Jun-36	0.000	0.000	0.000	0.000	0.000	0.000	0.000	0.000
Jul-36	0.000	0.000	0.000	0.000	0.000	0.000	0.000	0.000
Aug-36	0.000	0.000	0.000	0.000	0.000	0.000	0.000	0.000
Sept-36	0.000	0.000	0.000	0.000	0.000	0.000	0.000	0.000
Oct-36	0.000	0.000	0.000	0.000	0.000	0.000	0.000	0.000
Nov-36	0.000	0.014	0.000	0.612	0.000	0.002	0.000	0.000
Dec-36	0.000	0.198	2.674	5.057	0.103	1.702	0.000	0.014
Jan-37	0.827	3.402	2.315	2.953	1.644	1.526	0.293	1.467
Feb-37	0.144	2.619	2.218	12.884	1.726	3.055	2.965	4.815
Mar-37	1.612	1.143	5.754	12.092	2.589	0.109	2.224	1.863
Apr-37	0.000	0.713	2.141	0.000	0.000	0.065	0.032	5.942
May-37	0.000	0.000	0.000	0.000	0.135	0.000	0.000	0.000
Jun-37	0.000	0.000	0.000	0.000	0.000	0.000	0.000	0.000
Jul-37	0.000	0.000	0.000	0.000	0.000	0.000	0.000	0.000
Aug-37	0.000	0.000	0.000	0.000	0.000	0.000	0.000	0.000

Sept-37	0.000	0.000	0.000	0.000	0.000	0.000	0.000	0.000
Oct-37	0.000	0.000	0.000	0.000	0.000	0.000	0.000	0.000
Nov-37	1.069	0.000	0.037	0.038	0.000	0.001	0.000	0.002
Dec-37	10.318	0.376	0.723	0.457	0.152	0.011	0.155	0.386
Jan-38	2.405	1.744	5.143	10.944	2.987	0.971	1.444	2.929
Feb-38	0.623	3.985	5.233	9.732	1.416	1.909	0.159	1.143
Mar-38	4.426	2.916	4.248	9.499	2.688	1.535	1.442	0.395
Apr-38	1.142	10.809	0.625	1.095	0.122	0.276	0.004	0.000
May-38	0.000	0.000	0.000	0.356	0.000	0.000	0.000	0.000
Jun-38	0.000	0.000	0.000	0.000	0.000	0.000	0.000	0.000
Jul-38	0.000	0.000	0.000	0.000	0.000	0.000	0.000	0.000
Aug-38	0.000	0.000	0.000	0.000	0.000	0.000	0.000	0.000
Sept-38	0.000	0.000	0.000	0.000	0.000	0.000	0.000	0.000
Oct-38	0.000	0.000	0.000	0.000	0.000	0.000	0.000	0.000
Nov-38	0.000	0.142	0.000	0.130	0.000	0.000	0.000	0.000
Dec-38	0.705	0.001	0.292	0.998	0.264	0.054	0.359	0.614
Jan-39	6.062	0.297	5.864	3.458	1.759	1.100	1.657	2.074
Feb-39	1.041	0.789	3.116	4.896	1.292	2.445	12.219	7.195
Mar-39	36.130	1.812	5.102	0.574	5.455	1.729	2.613	1.507

Apr-39	0.799	8.287	0.008	12.111	5.502	0.169	1.268	0.000
May-39	0.000	28.053	0.000	0.000	0.000	0.000	0.000	0.000
Jun-39	0.000	0.000	0.000	0.000	0.000	0.000	0.000	0.000
Jul-39	0.000	0.000	0.000	0.000	0.000	0.000	0.000	0.000
Aug-39	0.000	0.000	0.000	0.000	0.000	0.000	0.000	0.000
Sept-39	0.000	0.000	0.000	0.000	0.000	0.000	0.000	0.000
Oct-39	0.000	0.000	0.000	0.000	0.000	0.000	0.000	0.002
Nov-39	6.172	0.000	0.010	0.890	0.000	0.187	0.000	0.007
Dec-39	1.101	0.025	0.876	1.063	0.116	0.464	0.004	0.058
Jan-40	13.057	0.165	4.421	8.193	2.188	1.766	1.087	4.815
Feb-40	9.220	4.602	3.815	1.452	1.757	1.357	4.692	5.651
Mar-40	15.395	1.208	2.256	7.499	1.190	0.586	2.091	4.738
Apr-40	0.000	0.257	0.002	2.295	0.000	0.044	0.077	4.034
May-40	0.000	0.000	0.000	0.000	0.000	0.000	0.000	0.000
Jun-40	0.000	0.000	0.000	0.000	0.000	0.000	0.000	0.000
Jul-40	0.000	0.000	0.000	0.000	0.000	0.000	0.000	0.000
Aug-40	0.000	0.000	0.000	0.000	0.000	0.000	0.000	0.000
Sept-40	0.000	0.000	0.000	0.000	0.000	0.000	0.000	0.000
Oct-40	0.000	0.000	0.000	0.000	0.000	0.000	0.000	0.000

Nov-40	0.000	3.162	0.272	0.069	0.000	0.131	0.000	0.016
Dec-40	0.000	0.845	1.070	3.891	0.057	0.684	0.231	0.166

ate	**2041 - 2070 Land use Scenarios**							
	CCLM4_RCP4.5	**CCLM4_RCP8.5**	**HIRAM5_RCP4.5**	**RAM5_RCP8.5**	**RACMO22T_RCP4.5**	**RACMO22T_RCP8.5**	**A4_RCP4.5**	**CA4_RCP8.5**
an-41	0.120	0.085	2.835	3.598	0.341	0.357	0.786	5.773
Feb-41	0.141	48.032	10.354	9.610	1.245	2.179	0.535	5.114
Mar-41	3.231	2.895	5.491	9.178	0.916	2.174	5.074	2.355
Apr-41	0.005	0.000	0.000	0.024	0.000	3.523	0.000	0.212
May-41	0.000	1.534	0.000	0.000	0.000	0.000	0.000	0.001
Jun-41	0.000	0.000	0.000	0.000	0.000	0.000	0.000	0.000
Jul-41	0.000	0.000	0.000	0.000	0.000	0.000	0.000	0.000
Aug-41	0.000	0.000	0.000	0.000	0.000	0.000	0.000	0.000
Sept-41	0.000	0.000	0.000	0.000	0.000	0.000	0.000	0.000
Oct-41	0.000	0.000	0.000	0.000	0.000	0.000	0.000	0.000
Nov-41	0.000	18.524	0.000	3.536	0.000	0.055	0.000	0.011
Dec-41	5.384	0.035	1.052	1.157	0.115	0.207	0.129	0.109

Jan-42	4.120	1.102	6.476	8.474	1.776	0.797	3.840	1.153
Feb-42	0.345	1.380	0.504	4.654	0.912	0.835	0.822	2.430
Mar-42	3.137	1.098	3.857	0.675	1.222	0.862	2.566	4.143
Apr-42	0.037	1.456	0.000	0.343	0.004	0.407	1.241	1.676
May-42	0.000	0.000	0.000	0.000	0.000	0.000	0.000	0.000
Jun-42	0.000	0.000	0.000	0.000	0.000	0.000	0.000	0.000
Jul-42	0.000	0.000	0.000	0.000	0.000	0.000	0.000	0.000
Aug-42	0.000	0.000	0.000	0.000	0.000	0.000	0.000	0.000
Sept-42	0.000	0.000	0.000	55.345	0.000	0.000	0.000	0.000
Oct-42	0.000	0.000	0.000	0.022	0.000	0.000	0.000	0.000
Nov-42	0.066	0.121	0.000	0.218	0.000	0.022	0.000	0.010
Dec-42	1.643	0.713	0.407	2.571	0.052	0.526	0.100	0.075
Jan-43	11.371	0.822	5.240	5.704	4.445	1.003	1.303	1.965
Feb-43	11.976	0.695	2.000	0.390	1.664	1.479	1.774	3.610
Mar-43	1.648	0.518	4.001	0.000	4.253	0.958	0.788	0.499
Apr-43	0.359	0.000	0.000	0.000	3.516	2.800	1.898	1.246
May-43	0.000	0.000	0.000	0.000	0.000	0.000	0.000	0.000
Jun-43	0.000	0.000	0.000	0.000	0.000	0.000	0.000	0.000
Jul-43	0.000	0.000	0.000	0.000	0.000	0.000	0.000	0.000

Aug-43	0.000	0.000	0.000	0.000	0.000	0.000	0.000	0.000
Sept-43	0.000	0.000	0.000	0.000	0.000	0.000	0.000	0.000
Oct-43	0.000	0.000	0.000	0.000	0.000	0.000	0.000	0.020
Nov-43	0.000	0.000	0.000	0.004	0.000	0.060	0.000	0.001
Dec-43	0.553	0.000	0.246	0.319	0.074	0.220	0.647	0.179
Jan-44	4.171	0.988	3.144	2.322	1.284	0.610	4.825	1.598
Feb-44	3.367	8.524	8.407	31.832	0.360	0.426	1.000	1.024
Mar-44	0.158	0.556	8.877	7.393	2.026	1.377	1.853	1.230
Apr-44	3.511	0.000	1.547	0.442	0.454	1.440	0.759	0.414
May-44	8.489	0.000	0.000	0.000	0.000	0.000	0.000	0.000
Jun-44	0.000	0.000	0.000	0.000	0.000	0.000	0.000	0.000
Jul-44	0.000	0.000	0.000	0.000	0.000	0.000	0.000	0.000
Aug-44	0.000	0.000	0.000	0.000	0.000	0.000	0.000	0.000
Sept-44	0.000	0.000	0.000	0.000	0.000	0.000	0.000	0.000
Oct-44	0.000	0.000	0.000	0.000	0.000	0.000	0.000	0.000
Nov-44	0.337	2.549	0.000	0.545	0.000	0.000	0.000	0.030
Dec-44	10.543	0.037	0.025	3.814	0.197	0.092	1.355	0.518
Jan-45	16.031	0.000	3.869	8.716	1.820	1.454	2.879	2.089
Feb-45	0.725	3.729	1.757	5.358	1.500	1.527	2.697	3.116

Mar-45	19.448	4.932	0.955	2.541	2.214	1.411	4.527	1.571
Apr-45	0.000	1.241	0.188	1.647	0.538	0.087	0.000	0.563
May-45	0.000	0.000	0.000	0.000	0.434	0.000	0.000	0.000
Jun-45	0.000	0.000	0.000	0.000	0.000	0.000	0.000	0.000
Jul-45	0.000	0.000	0.000	0.000	0.000	0.000	0.000	0.000
Aug-45	0.000	0.000	0.000	0.000	0.000	0.000	0.000	0.000
Sept-45	0.000	0.000	0.000	0.087	0.000	0.000	0.000	0.000
Oct-45	0.000	0.000	0.000	0.000	0.000	0.000	0.000	0.000
Nov-45	1.163	0.012	0.012	0.337	0.000	0.197	0.000	0.000
Dec-45	7.744	0.000	0.326	3.432	0.291	0.496	0.758	0.136
Jan-46	34.891	0.240	9.199	10.742	1.199	0.988	####	1.384
Feb-46	1.822	0.435	2.940	3.782	1.175	1.929	2.375	8.609
Mar-46	1.671	0.903	2.537	5.930	2.662	4.502	3.922	0.889
Apr-46	0.000	0.000	4.478	1.897	0.502	0.000	0.001	0.486
May-46	0.000	8.932	0.346	0.018	0.000	0.000	0.000	0.101
Jun-46	0.000	0.000	0.000	0.000	0.000	0.000	0.000	0.000
Jul-46	0.000	0.000	0.000	0.000	0.000	0.000	0.000	0.000
Aug-46	0.000	0.000	0.000	0.000	0.000	0.000	0.000	0.000
Sept-46	0.000	0.000	0.000	0.000	0.000	0.000	0.000	0.000

Oct-46	0.000	0.000	0.000	0.000	0.000	0.000	0.000	0.000
Nov-46	4.342	0.011	0.000	0.000	0.000	0.054	0.000	0.003
Dec-46	0.008	0.138	0.068	3.337	0.455	0.625	0.040	0.499
Jan-47	0.765	0.880	5.779	2.534	1.057	1.267	5.373	1.666
Feb-47	1.877	6.968	6.356	2.697	1.014	2.075	4.512	2.715
Mar-47	5.346	17.554	2.365	4.719	3.911	1.043	3.999	3.368
Apr-47	0.043	4.815	0.640	6.969	2.285	0.057	0.576	2.943
May-47	0.000	0.000	0.000	0.022	0.000	0.000	0.007	0.000
Jun-47	0.000	0.000	0.000	0.000	0.000	0.000	0.000	0.000
Jul-47	0.000	0.000	0.000	0.000	0.000	0.000	0.000	0.000
Aug-47	0.000	0.000	0.000	0.000	0.000	0.000	0.000	0.000
Sept-47	0.000	0.000	0.000	0.000	0.000	0.000	0.000	0.000
Oct-47	0.000	0.000	0.000	0.000	0.000	0.000	0.000	0.000
Nov-47	0.034	0.001	0.000	1.236	0.000	0.241	0.000	0.000
Dec-47	0.271	17.696	0.266	5.123	0.143	1.119	0.369	0.386
Jan-48	8.926	2.766	3.287	5.040	1.970	1.146	1.232	4.034
Feb-48	3.063	0.622	2.795	4.571	1.560	1.953	1.902	0.966
Mar-48	4.068	0.144	9.075	6.923	2.880	1.086	1.595	3.132
Apr-48	0.001	0.029	0.068	0.000	0.000	0.000	0.721	0.087

May-48	0.000	0.000	0.000	0.000	0.000	0.000	0.000	0.000
Jun-48	0.000	0.000	0.000	0.000	0.000	0.000	0.000	0.000
Jul-48	0.000	0.000	0.000	0.000	0.000	0.000	0.000	0.000
Aug-48	0.000	0.000	0.000	0.000	0.000	0.000	0.000	0.000
Sept-48	0.000	0.000	0.262	0.000	0.000	0.000	0.000	0.000
Oct-48	0.000	0.000	0.000	0.000	0.000	0.000	0.000	0.000
Nov-48	0.000	0.000	0.000	0.960	0.000	0.024	0.000	0.002
Dec-48	0.630	0.455	0.597	3.257	0.352	0.496	0.279	0.143
Jan-49	5.164	3.653	4.270	8.636	1.449	1.064	1.788	1.333
Feb-49	4.200	27.180	7.243	6.684	0.805	0.775	1.359	7.569
Mar-49	91.029	2.151	6.910	5.624	1.604	0.990	4.932	3.221
Apr-49	10.493	1.896	1.764	1.285	12.496	1.192	1.958	1.099
May-49	0.000	0.000	0.030	0.000	0.000	0.000	2.677	0.000
Jun-49	0.000	0.000	0.000	0.000	0.000	0.000	0.000	0.000
Jul-49	0.000	0.000	0.000	0.000	0.000	0.000	0.000	0.000
Aug-49	0.000	0.000	0.000	0.000	0.000	0.000	0.000	0.000
Sept-49	0.000	0.000	0.000	0.000	0.000	0.000	0.000	0.000
Oct-49	0.000	0.000	0.000	0.000	0.000	0.000	0.000	0.000
Nov-49	0.007	0.000	0.000	0.002	0.000	0.001	0.000	0.129

Dec-49	0.231	0.015	0.568	2.219	0.162	0.369	0.296	0.263
Jan-50	18.868	11.421	4.920	0.365	0.925	2.831	3.312	0.508
Feb-50	2.222	1.770	7.084	2.532	2.336	1.556	2.425	1.542
Mar-50	5.855	9.895	2.886	2.108	3.040	1.956	4.404	2.758
Apr-50	0.000	0.000	0.151	0.004	0.102	5.681	0.013	4.434
May-50	0.000	0.000	0.000	0.000	0.000	0.000	0.002	0.000
Jun-50	0.000	0.000	0.000	0.000	0.000	0.000	0.000	0.000
Jul-50	0.000	0.000	0.000	0.000	0.000	0.000	0.000	0.000
Aug-50	0.000	0.000	0.000	0.000	0.000	0.000	0.000	0.000
Sept-50	0.000	0.000	0.000	0.000	0.000	0.000	0.000	0.000
Oct-50	0.000	0.000	0.000	0.000	0.000	0.000	0.000	0.000
Nov-50	0.000	0.022	0.000	0.175	0.000	0.003	0.000	0.151
Dec-50	3.463	10.690	0.038	4.904	0.020	0.207	0.091	0.900
Jan-51	4.789	3.846	7.430	13.999	1.443	1.320	1.186	4.341
Feb-51	0.484	1.987	4.373	7.089	4.353	0.290	0.669	1.842
Mar-51	0.115	2.979	1.715	16.137	5.838	3.002	0.201	2.152
Apr-51	0.019	0.000	0.091	0.000	0.000	10.437	0.137	1.909
May-51	0.000	0.000	0.000	0.000	0.000	0.000	0.000	0.000
Jun-51	0.000	0.000	0.000	0.000	0.000	0.000	0.000	0.000

Jul-51	0.000	0.000	0.000	0.000	0.000	0.000	0.000	0.000
Aug-51	0.000	0.000	0.000	0.000	0.000	0.000	0.000	0.000
Sept-51	0.000	0.000	0.000	0.000	0.000	0.000	0.000	0.000
Oct-51	0.000	0.000	0.000	0.000	0.000	0.000	0.000	0.000
Nov-51	0.000	0.000	0.000	1.376	0.002	0.000	0.000	0.000
Dec-51	0.405	0.000	0.024	4.144	0.303	0.375	3.314	1.011
Jan-52	0.743	0.453	12.391	4.899	1.629	2.032	6.343	1.632
Feb-52	1.542	######	8.459	5.540	1.623	0.971	7.431	####
Mar-52	0.015	0.601	4.541	1.948	4.564	1.996	0.713	2.392
Apr-52	0.000	0.000	1.200	0.055	0.204	1.949	0.000	1.197
May-52	0.000	0.000	0.000	4.011	0.000	0.000	0.000	0.000
Jun-52	0.000	0.000	0.000	0.000	0.000	0.000	0.000	0.000
Jul-52	0.000	0.000	0.000	0.000	0.000	0.000	0.000	0.000
Aug-52	0.000	0.000	0.000	0.000	0.000	0.000	0.000	0.000
Sept-52	0.000	0.000	0.000	0.040	0.000	0.000	0.000	0.000
Oct-52	0.000	0.000	0.000	0.000	0.000	0.000	0.000	0.024
Nov-52	20.738	0.000	0.008	0.105	0.000	0.000	0.000	0.000
Dec-52	2.101	0.000	0.207	2.641	0.430	0.036	0.254	0.004
Jan-53	1.318	0.003	2.790	5.713	0.826	0.381	1.026	1.525

Feb-53	6.373	13.649	0.632	3.340	0.335	0.621	0.564	1.170
Mar-53	3.489	0.543	7.214	12.052	1.446	0.430	2.037	2.960
Apr-53	0.005	0.055	0.000	0.023	0.000	0.096	1.196	4.653
May-53	0.000	0.000	0.000	0.000	0.000	0.000	0.000	0.000
Jun-53	0.000	0.000	0.000	0.000	0.000	0.000	0.000	0.000
Jul-53	0.000	0.000	0.000	0.000	0.000	0.000	0.000	0.000
Aug-53	0.000	0.000	0.000	0.000	0.000	0.000	0.000	0.000
Sept-53	0.000	0.000	0.000	0.000	0.000	0.000	0.000	0.000
Oct-53	0.000	0.000	0.000	0.000	0.000	0.000	0.000	0.000
Nov-53	0.270	0.003	0.000	3.216	0.000	0.196	0.000	0.297
Dec-53	0.464	6.775	0.505	5.153	0.001	1.198	0.000	0.496
Jan-54	2.248	10.641	6.893	11.357	0.959	0.785	5.741	4.081
Feb-54	1.669	8.265	4.774	2.986	1.900	5.073	1.546	5.203
Mar-54	0.346	59.332	8.369	4.573	4.093	2.027	3.286	1.740
Apr-54	0.021	0.000	0.000	0.000	3.645	0.035	0.080	1.110
May-54	0.000	0.000	0.000	3.933	0.000	0.000	0.000	0.000
Jun-54	0.000	0.000	0.000	0.000	0.000	0.000	0.000	0.000
Jul-54	0.000	0.000	0.000	0.000	0.000	0.000	0.000	0.000
Aug-54	0.000	0.000	0.000	0.000	0.000	0.000	0.000	0.000

Sept-54	0.000	0.000	0.000	0.000	0.000	0.000	0.000	0.000
Oct-54	0.000	0.000	0.000	0.000	0.000	0.000	0.000	0.000
Nov-54	0.227	2.205	0.000	0.687	0.000	0.042	0.000	0.024
Dec-54	7.892	1.727	0.053	1.202	0.166	0.868	0.009	0.597
Jan-55	0.657	2.411	0.574	3.544	2.257	2.563	3.170	2.380
Feb-55	2.026	3.693	4.714	4.785	2.356	2.456	4.099	8.016
Mar-55	1.988	3.288	5.789	6.467	3.137	1.813	2.713	3.411
Apr-55	0.000	0.214	0.032	0.229	0.896	5.593	0.000	2.387
May-55	0.000	0.000	0.000	0.000	0.000	0.000	0.000	0.000
Jun-55	0.000	0.000	0.000	0.000	0.000	0.000	0.000	0.000
Jul-55	0.000	0.000	0.000	0.000	0.000	0.000	0.000	0.000
Aug-55	0.000	0.000	0.000	0.000	0.000	0.000	0.000	0.000
Sept-55	0.000	0.000	0.000	0.000	0.000	0.000	0.000	0.000
Oct-55	0.000	0.000	0.000	0.000	0.000	0.000	0.000	0.000
Nov-55	2.296	0.000	0.000	2.244	0.000	0.000	0.000	0.001
Dec-55	2.041	0.218	1.391	1.005	0.069	0.285	0.851	0.122
Jan-56	3.525	0.700	9.551	17.119	1.212	1.376	5.423	1.409
Feb-56	3.203	1.223	10.260	7.170	0.835	2.034	2.122	1.369
Mar-56	0.223	6.077	1.136	4.840	4.175	2.193	2.095	1.562

Apr-56	0.000	4.058	2.062	1.043	2.318	2.335	0.260	1.727
May-56	0.000	0.000	0.000	7.766	0.000	0.000	0.000	0.000
Jun-56	0.000	0.000	0.000	0.000	0.000	0.000	0.000	0.000
Jul-56	0.000	0.000	0.000	0.000	0.000	0.000	0.000	0.000
Aug-56	0.000	0.000	0.000	0.000	0.000	0.000	0.000	0.000
Sept-56	0.000	0.000	0.000	0.000	0.000	0.000	0.000	0.000
Oct-56	0.000	0.000	0.000	0.000	0.000	0.000	0.000	0.000
Nov-56	0.000	0.093	0.004	0.121	0.000	0.016	0.000	0.043
Dec-56	1.398	0.000	0.287	1.667	0.001	0.751	0.016	0.324
Jan-57	3.953	0.511	3.124	7.735	0.566	1.259	3.434	####
Feb-57	6.691	3.973	3.701	1.340	2.391	1.192	2.203	2.827
Mar-57	14.881	0.555	0.930	1.900	2.663	1.540	0.804	2.613
Apr-57	0.000	0.490	0.000	0.022	3.066	1.996	0.803	7.500
May-57	0.000	1.164	0.000	0.000	0.000	0.322	0.359	0.000
Jun-57	0.000	0.000	0.000	0.000	0.000	0.000	0.000	0.000
Jul-57	0.000	0.000	0.000	0.000	0.000	0.000	0.000	0.000
Aug-57	0.000	0.000	0.000	0.000	0.000	0.000	0.000	0.000
Sept-57	0.000	0.000	0.000	0.000	0.000	0.000	0.000	0.000
Oct-57	0.000	0.000	0.000	0.000	0.000	0.000	0.000	0.000

Nov-57	0.000	0.000	0.000	0.080	0.000	0.007	0.000	0.000
Dec-57	0.458	0.000	0.724	1.273	0.070	0.087	0.033	0.147
Jan-58	3.095	0.149	5.533	1.292	1.209	0.657	2.108	1.559
Feb-58	36.112	10.287	7.246	6.775	1.735	1.392	3.652	2.131
Mar-58	30.667	1.280	1.804	11.803	0.965	0.916	1.178	1.264
Apr-58	0.027	7.109	0.000	1.481	1.952	1.247	0.000	2.432
May-58	0.000	0.000	0.000	1.699	0.000	0.000	0.000	0.000
Jun-58	0.000	0.000	0.000	0.000	0.000	0.000	0.000	0.000
Jul-58	0.000	0.000	0.000	0.000	0.000	0.000	0.000	0.000
Aug-58	0.000	0.000	0.000	0.000	0.000	0.000	0.000	0.000
Sept-58	0.000	0.000	0.000	0.000	0.000	0.000	0.000	0.000
Oct-58	0.000	0.000	0.000	0.000	0.000	0.000	0.000	0.000
Nov-58	0.075	0.049	0.000	0.574	0.000	0.000	0.000	0.005
Dec-58	0.020	5.704	0.956	3.365	0.310	0.007	0.707	0.609
Jan-59	0.292	1.497	9.957	4.747	1.735	2.660	7.675	5.201
Feb-59	29.590	32.129	5.727	9.508	0.590	6.345	0.674	2.195
Mar-59	15.820	0.454	7.397	14.492	1.096	1.126	1.726	1.120
Apr-59	5.048	0.000	0.000	4.198	0.066	0.832	1.163	0.000
May-59	0.000	0.000	0.000	0.000	0.000	0.000	0.001	0.009

Jun-59	0.000	0.000	0.000	0.000	0.000	0.000	0.000	0.000
Jul-59	0.000	0.000	0.000	0.000	0.000	0.000	0.000	0.000
Aug-59	0.000	0.000	0.000	0.000	0.000	0.000	0.000	0.000
Sept-59	0.000	0.000	0.000	0.000	0.000	0.000	0.000	0.000
Oct-59	0.000	0.000	0.000	0.000	0.000	0.000	0.000	0.000
Nov-59	0.900	0.371	0.000	0.110	0.000	0.002	0.000	0.037
Dec-59	3.755	0.290	0.011	1.862	0.068	0.957	0.152	0.326
Jan-60	0.391	0.537	1.924	4.679	3.323	3.370	1.596	3.818
Feb-60	4.363	3.836	4.299	9.601	3.484	1.846	1.048	6.837
Mar-60	4.922	1.009	8.851	8.863	2.598	1.285	1.345	4.521
Apr-60	0.000	0.337	0.000	0.216	2.055	3.744	0.000	0.000
May-60	0.000	0.000	0.000	0.000	0.000	0.330	0.000	0.000
Jun-60	0.000	0.000	0.000	0.000	0.000	0.000	0.000	0.000
Jul-60	0.000	0.000	0.000	0.000	0.000	0.000	0.000	0.000
Aug-60	0.000	0.000	0.000	0.000	0.000	0.000	0.000	0.000
Sept-60	0.000	0.000	0.000	0.027	0.000	0.000	0.000	0.000
Oct-60	0.263	0.000	0.000	0.000	0.000	0.000	0.000	0.000
Nov-60	0.152	0.004	0.000	4.471	0.000	0.087	0.000	0.007
Dec-60	4.390	3.442	0.137	7.067	0.096	0.232	0.013	0.000

Jan-61	2.600	1.913	14.298	8.130	2.116	0.605	5.766	0.340
Feb-61	20.374	1.207	2.576	6.249	0.967	0.673	4.205	1.164
Mar-61	5.554	1.600	5.793	0.974	4.301	1.998	6.166	0.229
Apr-61	0.002	0.047	0.000	6.011	0.429	1.664	0.000	1.573
May-61	0.000	0.776	0.000	2.899	0.000	0.000	0.000	1.538
Jun-61	0.000	0.000	0.000	0.000	0.000	0.000	0.000	0.000
Jul-61	0.000	0.000	0.000	0.000	0.000	0.000	0.000	0.000
Aug-61	0.000	0.000	0.000	0.000	0.000	0.000	0.000	0.000
Sept-61	0.000	0.000	0.000	0.000	0.000	0.000	0.000	0.000
Oct-61	0.000	0.000	0.000	0.000	0.000	0.000	0.000	0.000
Nov-61	0.000	0.000	0.000	2.110	0.000	0.002	0.000	0.000
Dec-61	6.811	9.134	0.235	2.937	0.059	0.280	0.327	5.890
Jan-62	2.346	7.068	6.409	1.488	1.285	0.988	6.166	0.731
Feb-62	0.952	2.511	2.037	6.395	0.700	1.058	2.848	2.486
Mar-62	0.678	1.345	7.942	3.876	1.007	4.532	2.909	####
Apr-62	0.000	0.000	1.312	0.016	0.069	1.779	1.088	3.075
May-62	0.000	0.000	0.000	0.000	0.000	0.000	0.000	0.059
Jun-62	0.000	0.000	0.000	0.000	0.000	0.000	0.000	0.000
Jul-62	0.000	0.000	0.000	0.000	0.000	0.000	0.000	0.000

Aug-62	0.000	0.000	0.000	0.000	0.000	0.000	0.000	0.000
Sept-62	0.000	0.000	0.000	0.000	0.000	0.000	0.000	0.000
Oct-62	0.000	0.000	0.000	0.000	0.000	0.000	0.000	0.000
Nov-62	0.000	7.240	0.000	0.223	0.000	0.009	0.000	0.000
Dec-62	6.540	1.242	0.553	2.221	0.181	0.377	2.295	0.289
Jan-63	3.127	1.025	13.208	2.126	0.854	2.057	3.321	0.651
Feb-63	1.465	13.287	10.562	11.822	0.840	2.964	1.722	5.277
Mar-63	5.808	1.095	14.222	9.595	4.421	0.526	2.146	0.853
Apr-63	0.278	0.073	0.565	10.269	2.064	4.909	4.560	0.000
May-63	0.000	2.504	0.000	0.000	0.000	0.000	1.129	0.164
Jun-63	0.000	0.000	0.000	0.000	0.000	0.000	0.000	0.000
Jul-63	0.000	0.000	0.000	0.000	0.000	0.000	0.000	0.000
Aug-63	0.000	0.000	0.000	0.000	0.000	0.000	0.000	0.000
Sept-63	0.000	0.000	0.000	0.000	0.000	0.000	0.000	0.000
Oct-63	0.000	0.353	0.000	0.000	0.000	0.000	0.000	0.000
Nov-63	6.329	0.233	0.004	0.775	0.000	0.000	0.000	0.031
Dec-63	0.958	4.419	0.644	2.111	0.481	0.015	2.031	0.125
Jan-64	9.154	2.349	13.537	5.258	1.023	0.833	7.287	1.126
Feb-64	4.403	1.551	8.159	14.899	2.251	3.914	0.689	7.784

Mar-64	2.119	0.653	2.133	17.831	1.347	1.014	1.338	0.984
Apr-64	0.000	0.308	0.120	0.051	0.579	24.675	2.403	2.251
May-64	0.000	0.000	0.000	0.000	0.000	0.001	0.000	0.000
Jun-64	0.000	0.000	0.000	0.000	0.000	0.000	0.000	0.000
Jul-64	0.000	0.000	0.000	0.000	0.000	0.000	0.000	0.000
Aug-64	0.000	0.000	0.000	0.000	0.000	0.000	0.000	0.000
Sept-64	0.000	0.000	0.000	0.000	0.000	0.000	0.000	0.000
Oct-64	0.000	0.000	0.000	0.000	0.000	0.000	0.000	0.000
Nov-64	0.000	0.000	0.000	3.090	0.000	0.000	0.000	0.218
Dec-64	0.386	0.007	1.658	2.738	0.042	0.073	0.557	7.808
Jan-65	7.307	0.141	16.918	5.975	1.698	0.814	1.555	2.982
Feb-65	45.947	7.487	5.001	22.564	2.553	1.159	1.858	6.455
Mar-65	14.621	2.786	10.800	10.993	1.780	1.262	3.119	1.332
Apr-65	0.234	0.000	0.633	2.496	0.438	7.300	0.904	8.874
May-65	0.000	0.000	0.000	0.000	0.000	0.000	0.000	0.004
Jun-65	0.000	0.000	0.000	0.000	0.000	0.000	0.000	0.000
Jul-65	0.000	0.000	0.000	0.000	0.000	0.000	0.000	0.000
Aug-65	0.000	0.000	0.000	0.000	0.000	0.000	0.000	0.000
Sept-65	0.000	0.000	0.000	0.000	0.000	0.000	0.000	0.000

Oct-65	0.000	0.000	0.000	0.000	0.000	0.000	0.000	0.000
Nov-65	0.000	0.000	0.000	2.334	0.000	0.114	0.000	0.000
Dec-65	0.040	0.000	0.420	7.222	0.042	0.566	0.689	0.233
Jan-66	0.536	39.521	8.545	1.885	0.648	2.257	7.567	2.341
Feb-66	8.785	5.411	2.703	5.457	0.769	1.523	8.080	1.713
Mar-66	18.774	19.074	0.464	3.631	1.346	1.886	2.776	1.224
Apr-66	1.219	0.000	0.000	1.708	0.000	5.354	4.298	2.930
May-66	0.000	0.000	0.000	0.000	0.000	0.000	0.000	0.000
Jun-66	0.000	0.000	0.000	0.000	0.000	0.000	0.000	0.000
Jul-66	0.000	0.000	0.000	0.000	0.000	0.000	0.000	0.000
Aug-66	0.000	0.000	0.000	0.000	0.000	0.000	0.000	0.000
Sept-66	0.000	0.000	0.000	0.000	0.000	0.000	0.000	0.000
Oct-66	0.000	0.000	0.000	0.000	0.000	0.000	0.000	0.000
Nov-66	2.084	0.010	0.000	0.123	0.000	0.002	0.000	0.069
Dec-66	4.526	2.197	2.253	3.197	0.090	0.500	0.387	1.045
Jan-67	6.116	0.613	15.732	7.816	2.397	0.758	2.221	1.563
Feb-67	22.556	0.522	4.016	6.236	1.403	1.751	3.910	0.336
Mar-67	6.797	0.162	10.643	2.096	2.178	0.914	1.893	2.469
Apr-67	0.192	0.000	0.016	1.481	0.000	2.842	0.577	0.000

May-67	0.000	0.000	0.000	0.000	0.774	0.000	0.000	0.000
Jun-67	0.000	0.000	0.000	0.000	0.000	0.000	0.000	0.000
Jul-67	0.000	0.000	0.000	0.000	0.000	0.000	0.000	0.000
Aug-67	0.000	0.000	0.000	0.000	0.000	0.000	0.000	0.000
Sept-67	0.000	0.000	0.000	0.000	0.000	0.000	0.000	0.000
Oct-67	0.000	0.000	0.000	0.000	0.000	0.000	0.000	0.000
Nov-67	0.000	0.112	0.047	0.000	0.000	0.000	0.000	0.011
Dec-67	11.002	0.096	1.095	0.758	0.090	0.527	0.029	0.118
Jan-68	1.416	0.953	12.234	5.752	1.160	2.158	4.570	1.299
Feb-68	0.803	12.714	4.271	6.754	0.993	2.740	0.968	5.574
Mar-68	1.840	3.871	4.198	0.148	2.025	1.811	2.378	4.455
Apr-68	0.280	0.000	0.000	0.142	0.140	0.151	0.447	2.108
May-68	0.000	0.000	0.000	0.000	0.000	0.658	0.000	0.000
Jun-68	0.000	0.000	0.000	0.000	0.000	0.000	0.000	0.000
Jul-68	0.000	0.000	0.000	0.000	0.000	0.000	0.000	0.000
Aug-68	0.000	0.000	0.000	0.000	0.000	0.000	0.000	0.000
Sept-68	0.000	0.007	0.000	0.000	0.000	0.000	0.000	0.000
Oct-68	0.000	0.000	0.000	0.024	0.000	0.000	0.000	0.000
Nov-68	0.000	0.001	0.000	0.156	0.000	0.000	0.000	0.695

Dec-68	55.495	3.968	0.158	4.116	0.049	0.047	4.098	0.973
Jan-69	5.207	14.898	3.505	11.867	1.014	1.166	####	7.654
Feb-69	0.479	2.798	2.587	2.754	4.386	1.616	2.264	2.276
Mar-69	0.181	1.402	0.330	10.468	2.490	1.587	0.990	1.277
Apr-69	29.319	1.718	0.000	4.874	5.467	0.065	4.555	5.475
May-69	0.373	0.000	0.000	0.000	0.000	2.678	0.703	0.000
Jun-69	0.000	0.000	0.000	0.000	0.000	0.000	0.000	0.000
Jul-69	0.000	0.000	0.000	0.000	0.000	0.000	0.000	0.000
Aug-69	0.000	0.000	0.000	0.000	0.000	0.000	0.000	0.000
Sept-69	0.000	0.000	0.000	0.000	0.000	0.000	0.000	0.000
Oct-69	0.000	0.000	0.000	0.000	0.000	0.000	0.000	0.000
Nov-69	0.685	0.410	0.304	1.001	0.000	0.124	0.000	0.037
Dec-69	1.008	0.001	0.993	1.375	0.209	1.446	0.025	0.011
Jan-70	9.834	0.300	10.666	1.784	1.110	1.798	6.851	2.004
Feb-70	13.111	5.132	8.436	3.590	1.234	2.357	1.891	3.031
Mar-70	3.829	0.365	4.857	3.359	5.371	1.470	2.001	4.419
Apr-70	2.116	0.000	8.888	3.420	0.681	0.002	0.523	####
May-70	0.000	0.000	0.000	0.000	0.000	0.000	0.000	0.002
Jun-70	0.000	0.000	0.000	0.000	0.000	0.000	0.000	0.000

Jul-70	0.000	0.000	0.000	0.000	0.000	0.000	0.000	0.000
Aug-70	0.000	0.000	0.000	0.000	0.000	0.000	0.000	0.000
Sept-70	0.000	0.000	0.000	0.000	0.000	0.000	0.000	0.000
Oct-70	0.000	0.000	0.000	0.000	0.000	0.000	0.000	0.000
Nov-70	0.000	0.693	0.000	0.803	0.000	0.019	0.022	0.000
Dec-70	4.881	7.002	0.368	1.692	0.230	0.184	0.067	0.811

Date	**2071 - 2100 land use scenarios**							
	CCLM4_RCP4.5	**CCLM4_RCP8.5**	**HIRAM5_RCP4.5**	**HIRAM5_RCP8.5**	**RACMO22T_RCP4.5**	**RACMO22T_RCP8.5**	**RCA4_RCP4.5**	**RCA4_RCP8.5**
Jan-71	0.513	0.592	9.093	2.569	5.993	1.366	1.884	1.075
Feb-71	0.372	1.916	5.321	10.189	2.695	2.851	2.828	3.964
Mar-71	8.291	0.458	0.621	2.780	4.784	1.295	2.825	6.028
Apr-71	0.278	0.000	0.000	1.718	0.179	0.595	0.461	0.293
May-71	0.000	0.000	0.000	0.000	0.000	0.081	0.000	0.964
Jun-71	0.000	0.000	0.000	0.000	0.000	0.000	0.000	0.000
Jul-71	0.000	0.000	0.000	0.000	0.000	0.000	0.000	0.000
Aug-71	0.000	0.000	0.000	0.000	0.000	0.000	0.000	0.000
Sept-71	0.000	0.000	0.000	0.000	0.000	0.000	0.000	0.000
Oct-71	0.000	0.000	0.000	0.000	0.000	0.000	0.000	0.000
Nov-71	0.000	0.000	0.000	0.336	0.000	0.000	0.000	0.019

Dec-71	0.240	0.000	2.015	1.247	0.025	0.415	0.433	0.107
Jan-72	2.944	16.452	10.261	2.374	2.733	1.129	4.236	2.481
Feb-72	2.140	2.302	3.013	4.253	2.286	0.819	3.766	0.807
Mar-72	3.473	2.738	9.888	3.144	2.120	0.256	6.112	1.486
Apr-72	0.000	0.273	0.015	0.000	4.809	10.598	4.605	0.180
May-72	0.000	0.000	0.000	0.000	0.000	1.462	0.000	0.000
Jun-72	0.000	0.000	0.000	0.000	0.000	0.000	0.000	0.000
Jul-72	0.000	0.000	0.000	0.000	0.000	0.000	0.000	0.000
Aug-72	0.000	0.000	0.000	0.000	0.000	0.000	0.000	0.000
Sept-72	0.000	0.000	0.000	0.000	0.000	0.000	0.000	0.000
Oct-72	0.000	0.000	0.000	0.000	0.000	0.000	0.000	0.000
Nov-72	13.180	0.000	0.034	0.147	0.000	1.031	0.000	0.059
Dec-72	0.746	0.006	1.509	5.382	0.158	0.161	2.138	0.064
Jan-73	2.211	6.913	10.711	6.505	1.665	1.239	1.613	9.078
Feb-73	0.229	0.502	3.851	11.014	1.353	1.524	3.868	2.756
Mar-73	3.359	7.085	4.167	1.214	0.235	1.344	1.346	2.366
Apr-73	3.491	0.115	0.000	5.386	8.122	3.435	0.339	0.462
May-73	0.000	0.000	0.000	0.453	0.014	0.000	0.000	0.127
Jun-73	0.000	0.000	0.000	0.000	0.000	0.000	0.000	0.000

Jul-73	0.000	0.000	0.000	0.000	0.000	0.000	0.000	0.000
Aug-73	0.000	0.000	0.000	0.000	0.000	0.000	0.000	0.000
Sept-73	0.000	0.000	0.000	0.000	0.000	0.000	0.000	0.000
Oct-73	0.006	0.000	0.000	0.000	0.000	0.000	0.000	0.000
Nov-73	0.000	0.000	0.000	0.000	0.000	0.000	0.000	0.035
Dec-73	5.242	0.055	0.225	5.056	0.184	0.014	0.178	0.452
Jan-74	1.114	0.053	4.651	3.240	1.902	0.480	1.891	0.536
Feb-74	5.760	0.876	1.822	3.126	1.473	0.688	1.525	0.919
Mar-74	1.804	2.469	0.192	2.506	3.344	1.102	1.392	0.989
Apr-74	0.124	0.011	0.000	1.167	18.084	0.000	0.179	0.000
May-74	0.000	0.000	0.000	0.000	0.000	0.000	0.000	0.000
Jun-74	0.000	0.000	0.000	0.000	0.000	0.000	0.000	0.000
Jul-74	0.000	0.000	0.000	0.000	0.000	0.000	0.000	0.000
Aug-74	0.000	0.000	0.000	0.000	0.000	0.000	0.000	0.000
Sept-74	0.000	0.000	0.000	0.000	0.000	0.000	0.000	0.000
Oct-74	0.000	0.000	0.000	0.000	0.000	0.000	0.000	0.000
Nov-74	1.007	0.000	0.224	0.986	0.000	0.059	0.000	1.585
Dec-74	1.953	4.621	0.922	0.335	0.456	0.441	1.545	0.587
Jan-75	1.732	7.474	11.105	3.086	1.654	2.392	2.156	5.231

Feb-75	9.188	2.296	7.381	2.332	1.389	1.881	2.055	8.007
Mar-75	4.146	1.629	5.062	6.732	4.678	2.888	1.768	6.127
Apr-75	0.000	0.126	8.747	4.622	3.240	11.575	0.000	5.459
May-75	0.000	0.000	0.000	1.389	0.000	1.787	0.000	0.000
Jun-75	0.000	0.000	0.000	0.000	0.000	0.000	0.000	0.000
Jul-75	0.000	0.000	0.000	0.000	0.000	0.000	0.000	0.000
Aug-75	0.000	0.000	0.000	0.000	0.000	0.000	0.000	0.000
Sept-75	0.000	0.000	0.000	0.000	0.000	0.000	0.000	0.000
Oct-75	0.000	0.000	0.000	0.000	0.000	0.000	0.000	0.000
Nov-75	0.174	0.765	0.000	0.000	0.000	0.187	0.000	0.007
Dec-75	0.195	3.759	0.245	0.685	0.388	0.567	0.613	0.268
Jan-76	1.259	1.366	3.032	2.021	1.455	1.889	#####	1.705
Feb-76	0.598	1.014	5.025	2.214	1.985	1.427	0.544	3.786
Mar-76	26.475	2.381	3.196	10.371	3.311	0.593	4.589	4.356
Apr-76	0.000	0.000	0.000	0.000	1.869	1.016	0.158	0.901
May-76	0.000	0.000	0.000	13.912	0.000	0.000	0.000	0.000
Jun-76	0.000	0.000	0.000	0.000	0.000	0.000	0.000	0.000
Jul-76	0.000	0.000	0.000	0.000	0.000	0.000	0.000	0.000
Aug-76	0.000	0.000	0.000	0.000	0.000	0.000	0.000	0.000

Sept-76	0.000	0.000	0.000	0.000	0.000	0.000	0.000	0.000
Oct-76	0.000	0.000	0.000	0.000	0.000	0.000	0.000	0.000
Nov-76	0.004	3.301	0.000	0.788	0.000	0.102	0.000	0.305
Dec-76	5.222	1.216	0.944	2.258	0.155	0.125	0.368	0.206
Jan-77	3.832	10.731	5.681	1.984	2.545	1.521	4.082	0.220
Feb-77	0.080	5.661	2.724	6.973	1.280	1.188	1.676	7.866
Mar-77	2.033	3.675	12.596	5.709	1.006	4.412	3.512	4.000
Apr-77	0.000	54.256	0.001	6.121	0.462	0.000	4.191	12.681
May-77	0.001	0.000	0.009	0.000	0.000	0.000	0.000	0.000
Jun-77	0.000	0.000	0.000	0.000	0.000	0.000	0.000	0.000
Jul-77	0.000	0.000	0.000	0.000	0.000	0.000	0.000	0.000
Aug-77	0.000	0.000	0.000	0.000	0.000	0.000	0.000	0.000
Sept-77	0.000	0.000	0.000	0.000	0.000	0.000	0.000	0.000
Oct-77	0.000	0.000	0.000	0.000	0.000	0.000	0.000	0.000
Nov-77	0.209	0.000	0.000	0.779	0.000	0.249	0.000	0.001
Dec-77	0.000	0.000	0.082	6.365	0.229	1.282	0.008	0.208
Jan-78	0.461	0.421	1.195	13.395	3.267	2.067	1.684	0.729
Feb-78	0.182	6.841	1.067	7.967	3.240	0.845	2.481	4.138
Mar-78	0.775	3.561	5.001	9.976	2.218	2.713	0.881	0.438

Apr-78	0.701	9.373	0.022	1.905	0.004	2.092	0.000	2.136
May-78	0.000	0.000	0.000	1.714	4.759	0.000	0.000	0.000
Jun-78	0.000	0.000	0.000	0.000	0.000	0.000	0.000	0.000
Jul-78	0.000	0.000	0.000	0.000	0.000	0.000	0.000	0.000
Aug-78	0.000	0.000	0.000	0.000	0.000	0.000	0.000	0.000
Sept-78	0.000	0.000	0.000	0.000	0.000	0.000	0.000	0.000
Oct-78	0.000	0.000	0.000	0.000	0.000	0.000	0.000	0.000
Nov-78	0.000	1.993	0.173	0.207	0.000	0.031	0.000	0.176
Dec-78	0.382	13.892	1.571	1.175	0.009	2.535	0.022	0.300
Jan-79	14.605	2.509	16.575	14.118	1.001	3.448	3.109	6.378
Feb-79	7.505	1.221	3.391	5.735	1.771	0.987	2.282	3.220
Mar-79	47.949	2.492	6.046	5.919	2.471	0.029	2.455	1.148
Apr-79	1.353	0.000	6.987	0.739	0.000	14.659	0.505	14.454
May-79	0.000	0.000	0.001	0.000	0.000	0.000	0.000	0.000
Jun-79	0.000	0.000	0.000	0.000	0.000	0.000	0.000	0.000
Jul-79	0.000	0.000	0.000	0.000	0.000	0.000	0.000	0.000
Aug-79	0.000	0.000	0.000	0.000	0.000	0.000	0.000	0.000
Sept-79	0.000	0.000	0.000	0.000	0.000	0.000	0.000	0.000
Oct-79	0.000	0.000	0.000	0.000	0.000	0.000	0.000	0.000

Nov-79	0.000	0.000	0.000	0.229	0.000	0.005	0.000	0.000
Dec-79	1.088	0.000	2.402	2.193	0.301	0.442	2.053	0.092
Jan-80	1.100	0.045	2.913	8.465	2.907	4.993	#####	5.167
Feb-80	1.465	0.858	2.628	16.712	1.133	1.214	7.700	2.713
Mar-80	4.024	0.907	6.712	6.578	2.820	1.449	4.826	4.524
Apr-80	0.000	0.456	0.145	0.673	6.827	2.298	1.148	3.564
May-80	0.000	0.000	0.000	0.000	0.000	0.000	0.000	0.000
Jun-80	0.000	0.000	0.000	0.000	0.000	0.000	0.000	0.000
Jul-80	0.000	0.000	0.000	0.000	0.000	0.000	0.000	0.000
Aug-80	0.000	0.000	0.000	0.000	0.000	0.000	0.000	0.000
Sept-80	0.000	0.000	0.000	0.000	0.000	0.000	0.000	0.000
Oct-80	0.000	0.000	0.000	0.000	0.000	0.000	0.000	0.000
Nov-80	0.000	0.036	0.000	1.569	0.000	1.319	0.000	0.005
Dec-80	0.000	21.287	5.404	3.741	0.000	1.264	0.544	0.221
Jan-81	1.535	1.325	3.474	15.679	0.552	0.809	1.649	3.852
Feb-81	0.474	103.422	5.840	10.040	1.133	1.206	2.211	0.572
Mar-81	0.716	5.361	1.348	4.695	1.036	1.147	1.151	1.600
Apr-81	0.000	12.691	4.962	0.307	0.321	0.000	0.000	0.035
May-81	0.000	0.000	0.000	0.076	0.405	0.000	0.000	0.000

Jun-81	0.000	0.000	0.000	0.000	0.000	0.000	0.000	0.000
Jul-81	0.000	0.000	0.000	0.000	0.000	0.000	0.000	0.000
Aug-81	0.000	0.000	0.000	0.000	0.000	0.000	0.000	0.000
Sept-81	0.000	0.000	0.000	0.000	0.000	0.000	0.000	0.000
Oct-81	0.000	0.000	0.000	0.000	0.000	0.000	0.000	0.000
Nov-81	0.000	0.000	0.052	0.144	0.000	0.007	0.000	0.078
Dec-81	24.276	0.001	0.788	0.994	0.176	1.141	1.554	0.055
Jan-82	1.053	49.846	11.909	4.884	0.878	1.455	3.496	0.395
Feb-82	39.728	7.402	46.335	5.108	1.564	1.561	7.407	2.989
Mar-82	5.956	3.675	4.326	5.614	1.505	0.827	6.165	3.799
Apr-82	11.453	7.068	0.000	1.851	2.236	7.095	#####	3.561
May-82	0.000	0.000	0.000	0.366	0.000	0.000	0.000	0.000
Jun-82	0.000	0.000	0.000	0.000	0.000	0.000	0.000	0.000
Jul-82	0.000	0.000	0.000	0.000	0.000	0.000	0.000	0.000
Aug-82	0.000	0.000	0.000	0.000	0.000	0.000	0.000	0.000
Sept-82	0.000	0.000	0.000	0.000	0.000	0.000	0.000	0.000
Oct-82	0.000	0.000	0.000	0.000	0.000	0.000	0.000	0.000
Nov-82	0.000	11.982	0.015	0.334	0.000	1.036	0.000	0.834
Dec-82	0.065	3.825	1.654	4.456	0.028	0.539	2.225	2.753

Jan-83	0.140	2.804	4.635	8.456	1.475	0.596	2.168	1.762
Feb-83	34.047	1.835	4.113	8.792	2.141	1.291	2.015	10.054
Mar-83	4.884	0.562	3.376	1.194	4.388	0.980	2.846	1.704
Apr-83	118.558	0.727	1.789	0.040	0.908	4.571	3.224	3.965
May-83	0.000	0.000	0.000	0.000	0.000	0.000	0.000	0.000
Jun-83	0.000	0.000	0.000	0.000	0.000	0.000	0.000	0.000
Jul-83	0.000	0.000	0.000	0.000	0.000	0.000	0.000	0.000
Aug-83	0.000	0.000	0.000	0.000	0.000	0.000	0.000	0.000
Sept-83	0.000	0.000	0.000	0.000	0.000	0.000	0.000	0.000
Oct-83	0.000	0.000	0.000	0.000	0.000	0.000	0.000	0.000
Nov-83	0.038	0.000	0.000	0.154	0.000	0.000	0.000	0.000
Dec-83	0.000	0.025	0.327	8.620	0.306	0.078	0.301	0.742
Jan-84	0.059	0.281	5.279	10.278	3.501	1.124	5.434	2.844
Feb-84	14.268	0.467	4.980	11.152	1.462	2.891	2.704	1.165
Mar-84	1.936	0.034	2.869	1.092	3.995	1.954	1.719	1.735
Apr-84	0.888	0.000	8.478	0.000	2.774	0.000	0.724	4.676
May-84	0.000	0.000	0.000	0.000	0.000	0.000	0.000	0.000
Jun-84	0.000	0.000	0.000	0.000	0.000	0.000	0.000	0.000
Jul-84	0.000	0.000	0.000	0.000	0.000	0.000	0.000	0.000

Aug-84	0.000	0.000	0.000	0.000	0.000	0.000	0.000	0.000
Sept-84	0.000	0.000	0.000	0.000	0.000	0.000	0.000	0.000
Oct-84	0.000	0.000	0.000	0.000	0.012	0.000	0.000	0.000
Nov-84	0.176	0.000	0.002	0.015	0.000	0.352	0.000	0.099
Dec-84	2.431	0.000	2.725	1.656	0.365	2.064	2.125	1.746
Jan-85	16.706	9.468	5.511	6.788	4.372	3.421	9.448	3.160
Feb-85	33.015	27.789	5.311	4.845	0.874	3.767	3.426	2.665
Mar-85	2.216	6.608	3.709	11.634	1.451	0.924	2.375	2.751
Apr-85	15.056	7.994	1.062	2.154	2.704	0.125	0.000	2.514
May-85	0.000	0.000	0.000	0.000	0.000	0.000	0.000	0.000
Jun-85	0.000	0.000	0.000	0.000	0.000	0.000	0.000	0.000
Jul-85	0.000	0.000	0.000	0.000	0.000	0.000	0.000	0.000
Aug-85	0.000	0.000	0.000	0.000	0.000	0.000	0.000	0.000
Sept-85	0.000	0.000	0.000	0.000	0.000	0.000	0.000	0.000
Oct-85	0.000	0.000	0.000	0.000	0.000	0.000	0.000	0.000
Nov-85	0.000	0.000	0.060	4.255	0.000	3.364	0.000	0.000
Dec-85	6.761	0.005	0.001	9.495	0.172	0.686	2.298	0.114
Jan-86	17.744	2.228	3.479	10.022	4.431	0.952	8.276	0.520
Feb-86	36.813	3.880	5.696	9.369	0.834	2.096	2.668	8.693

Mar-86	4.282	4.206	2.658	5.906	4.416	1.931	1.500	0.519
Apr-86	13.508	2.458	0.222	0.001	1.000	3.415	0.016	3.244
May-86	0.000	0.000	0.706	0.000	0.000	0.000	0.000	0.004
Jun-86	0.000	0.000	0.000	0.000	0.000	0.000	0.000	0.000
Jul-86	0.000	0.000	0.000	0.000	0.000	0.000	0.000	0.000
Aug-86	0.000	0.000	0.000	0.000	0.000	0.000	0.000	0.000
Sept-86	0.000	0.000	0.000	0.000	0.000	0.000	0.000	0.000
Oct-86	0.000	0.000	0.000	0.000	0.000	0.000	0.000	0.000
Nov-86	0.000	0.000	0.000	0.016	0.000	0.172	0.000	0.019
Dec-86	2.967	1.136	2.029	0.193	0.291	0.676	1.729	0.028
Jan-87	21.129	1.322	5.207	2.199	1.745	0.874	9.646	2.284
Feb-87	0.282	91.339	4.642	5.369	0.701	0.429	5.760	3.305
Mar-87	17.832	1.425	7.528	8.131	3.431	2.148	1.982	0.979
Apr-87	0.000	0.485	0.000	2.526	3.813	10.922	3.104	0.427
May-87	0.000	0.000	0.000	2.469	0.000	0.000	0.000	0.000
Jun-87	0.000	0.000	0.000	0.000	0.000	0.000	0.000	0.000
Jul-87	0.000	0.000	0.000	0.000	0.000	0.000	0.000	0.000
Aug-87	0.000	0.000	0.000	0.000	0.000	0.000	0.000	0.000
Sept-87	0.000	0.000	0.000	0.000	0.000	0.000	0.000	0.000

Oct-87	0.000	0.000	0.000	0.000	0.000	0.000	0.000	0.000
Nov-87	0.274	0.000	0.000	1.134	0.000	0.048	0.000	0.287
Dec-87	3.336	0.000	0.045	3.348	0.209	0.635	0.348	0.714
Jan-88	13.105	0.008	10.051	7.952	0.936	0.654	2.159	6.744
Feb-88	0.387	6.495	9.833	7.180	1.191	3.134	1.855	4.172
Mar-88	30.354	1.186	9.013	24.242	2.839	1.452	3.312	3.338
Apr-88	0.000	0.000	4.502	0.740	0.000	0.000	0.246	0.012
May-88	0.000	0.000	0.000	0.000	0.000	0.000	0.000	0.000
Jun-88	0.000	0.000	0.000	0.000	0.000	0.000	0.000	0.000
Jul-88	0.000	0.000	0.000	0.000	0.000	0.000	0.000	0.000
Aug-88	0.000	0.000	0.000	0.000	0.000	0.000	0.000	0.000
Sept-88	0.000	0.000	0.000	0.000	0.000	0.000	0.000	0.000
Oct-88	0.000	0.000	0.000	0.000	0.000	0.000	0.000	0.000
Nov-88	0.000	0.001	0.000	0.000	0.000	2.081	0.000	0.000
Dec-88	12.402	0.000	0.065	1.086	0.098	1.168	0.002	0.040
Jan-89	3.168	0.000	5.658	7.279	0.992	0.962	3.322	11.298
Feb-89	10.848	79.640	15.613	14.329	2.182	4.813	0.668	5.487
Mar-89	5.573	0.589	5.307	1.772	3.606	4.906	2.067	2.247
Apr-89	0.014	0.000	0.718	0.000	3.642	0.136	0.661	4.631

May-89	0.000	0.000	0.000	0.013	0.000	0.927	0.000	0.000
Jun-89	0.000	0.000	0.000	0.000	0.000	0.000	0.000	0.000
Jul-89	0.000	0.000	0.000	0.000	0.000	0.000	0.000	0.000
Aug-89	0.000	0.000	0.000	0.000	0.000	0.000	0.000	0.000
Sept-89	0.000	0.000	0.000	0.000	0.000	0.000	0.000	0.000
Oct-89	0.000	0.000	0.000	0.000	0.000	0.000	0.000	0.000
Nov-89	0.032	0.875	0.000	7.182	0.000	0.065	0.000	0.008
Dec-89	0.702	2.121	2.895	10.588	0.221	0.727	0.584	0.591
Jan-90	2.909	0.880	6.886	11.318	0.851	1.371	3.100	4.846
Feb-90	21.818	3.331	9.044	3.434	0.892	3.200	0.733	1.202
Mar-90	3.464	0.371	5.062	13.316	3.033	1.555	1.008	10.208
Apr-90	3.739	77.724	0.000	0.192	0.464	5.722	5.788	10.989
May-90	0.000	0.000	0.000	0.000	0.000	0.056	0.000	0.000
Jun-90	0.000	0.000	0.000	0.000	0.000	0.000	0.000	0.000
Jul-90	0.000	0.000	0.000	0.000	0.000	0.000	0.000	0.000
Aug-90	0.000	0.000	0.000	0.000	0.000	0.000	0.000	0.000
Sept-90	0.000	0.000	0.000	0.000	0.000	0.000	0.000	0.000
Oct-90	0.000	0.000	0.000	0.000	0.000	0.000	0.000	0.000
Nov-90	0.000	0.000	0.000	0.431	0.000	0.032	0.000	0.000

Dec-90	0.048	3.618	0.051	7.126	0.565	0.152	0.047	2.091
Jan-91	2.174	14.306	2.644	27.000	1.600	4.041	2.907	0.968
Feb-91	12.328	2.286	6.393	5.033	1.906	1.248	1.639	3.962
Mar-91	7.061	4.716	6.631	10.901	4.082	1.828	2.546	1.776
Apr-91	0.000	2.641	0.000	0.104	0.000	5.636	0.166	0.544
May-91	0.000	0.000	0.000	0.000	0.000	0.001	0.000	0.000
Jun-91	0.000	0.000	0.000	0.000	0.000	0.000	0.000	0.000
Jul-91	0.000	0.000	0.000	0.000	0.000	0.000	0.000	0.000
Aug-91	0.000	0.000	0.000	0.000	0.000	0.000	0.000	0.000
Sept-91	0.000	0.000	0.000	0.000	0.000	0.000	0.000	0.000
Oct-91	0.000	0.000	0.000	0.000	0.000	0.000	0.000	0.000
Nov-91	19.408	17.924	0.000	0.000	0.000	0.019	0.000	0.000
Dec-91	9.136	12.032	1.328	27.902	0.736	0.302	0.018	2.331
Jan-92	30.978	1.144	6.300	11.338	2.041	1.628	0.376	2.161
Feb-92	0.249	0.052	4.326	1.154	2.756	2.749	2.488	1.035
Mar-92	4.388	1.429	5.038	10.104	3.248	1.901	1.624	5.086
Apr-92	1.120	0.000	0.674	0.000	3.920	3.760	1.661	2.478
May-92	0.000	0.000	0.000	0.000	0.000	0.000	0.000	0.000
Jun-92	0.000	0.000	0.000	0.000	0.000	0.000	0.000	0.000

Jul-92	0.000	0.000	0.000	0.000	0.000	0.000	0.000	0.000
Aug-92	0.000	0.000	0.000	0.000	0.000	0.000	0.000	0.000
Sept-92	0.000	0.000	0.000	0.000	0.000	0.000	0.000	0.000
Oct-92	0.000	0.000	0.000	0.000	0.000	0.000	0.000	0.000
Nov-92	0.001	0.000	0.000	0.000	0.000	0.000	0.000	0.126
Dec-92	3.578	2.293	0.155	18.149	0.141	0.389	0.024	2.244
Jan-93	1.116	0.599	2.769	4.556	1.212	1.875	2.981	8.553
Feb-93	0.365	1.578	4.231	6.987	0.848	2.193	4.311	1.533
Mar-93	1.891	0.520	3.668	6.589	2.716	1.339	4.038	4.745
Apr-93	0.367	0.002	0.107	0.000	0.400	6.476	0.675	0.062
May-93	0.000	0.000	0.000	0.000	0.000	0.000	0.000	0.000
Jun-93	0.000	0.000	0.000	0.000	0.000	0.000	0.000	0.000
Jul-93	0.000	0.000	0.000	0.000	0.000	0.000	0.000	0.000
Aug-93	0.000	0.000	0.000	0.000	0.000	0.000	0.000	0.000
Sept-93	0.000	0.000	0.000	0.000	0.000	0.000	0.000	0.000
Oct-93	0.000	0.000	0.000	0.000	0.000	0.000	0.000	0.000
Nov-93	0.000	0.000	0.000	0.000	0.000	0.073	0.000	0.160
Dec-93	14.416	0.000	0.935	0.000	0.174	1.128	0.006	0.638
Jan-94	1.302	0.125	20.080	6.192	1.825	3.455	1.640	2.751

Feb-94	2.245	2.568	2.940	13.951	1.176	2.048	2.435	4.288
Mar-94	1.805	0.448	10.198	7.321	6.105	0.533	2.538	6.766
Apr-94	0.000	0.000	0.000	2.174	0.705	7.880	2.452	3.331
May-94	0.000	0.616	0.000	0.000	0.000	0.000	0.000	0.000
Jun-94	0.000	0.000	0.000	0.000	0.000	0.000	0.000	0.000
Jul-94	0.000	0.000	0.000	0.000	0.000	0.000	0.000	0.000
Aug-94	0.000	0.000	0.000	0.000	0.000	0.000	0.000	0.000
Sept-94	0.000	0.000	0.000	0.000	0.000	0.000	0.000	0.000
Oct-94	0.000	0.000	0.000	0.000	0.000	0.000	0.000	0.000
Nov-94	0.000	34.069	0.000	0.658	0.000	0.065	0.000	0.011
Dec-94	2.029	0.059	2.213	4.711	0.046	0.898	0.125	0.316
Jan-95	1.268	1.879	9.399	17.911	1.801	1.341	2.294	19.926
Feb-95	2.640	0.796	7.966	10.587	1.454	1.814	0.939	0.934
Mar-95	0.019	0.540	7.071	17.165	1.312	4.151	1.298	5.931
Apr-95	0.000	0.000	0.000	3.067	3.886	5.279	3.888	0.000
May-95	0.000	0.000	0.000	0.000	0.000	0.000	0.000	0.000
Jun-95	0.000	0.000	0.000	0.000	0.000	0.000	0.000	0.000
Jul-95	0.000	0.000	0.000	0.000	0.000	0.000	0.000	0.000
Aug-95	0.000	0.000	0.000	0.000	0.000	0.000	0.000	0.000

Sept-95	0.000	0.000	0.000	0.000	0.000	0.000	0.000	0.000
Oct-95	0.000	0.000	0.000	0.000	0.000	0.000	0.000	0.000
Nov-95	7.111	18.244	0.151	0.000	0.000	0.007	0.000	0.032
Dec-95	0.080	1.788	2.201	9.787	0.001	1.196	0.354	0.005
Jan-96	1.279	9.867	4.699	7.821	0.302	0.654	8.133	2.113
Feb-96	7.933	3.184	10.153	10.142	0.922	0.889	1.620	6.822
Mar-96	4.082	3.386	7.564	5.869	0.508	1.385	3.134	6.155
Apr-96	0.000	0.022	0.007	0.048	0.888	20.396	0.406	3.378
May-96	0.000	0.000	0.000	0.000	0.160	0.000	0.000	0.000
Jun-96	0.000	0.000	0.000	0.000	0.000	0.000	0.000	0.000
Jul-96	0.000	0.000	0.000	0.000	0.000	0.000	0.000	0.000
Aug-96	0.000	0.000	0.000	0.000	0.000	0.000	0.000	0.000
Sept-96	0.000	0.000	0.000	0.000	0.000	0.000	0.000	0.000
Oct-96	0.221	0.000	0.000	0.024	0.000	0.000	0.000	0.021
Nov-96	0.000	0.000	0.000	0.016	0.000	1.002	0.000	0.000
Dec-96	0.621	7.261	0.149	4.798	0.125	1.333	0.540	1.696
Jan-97	1.554	0.467	1.753	9.959	2.155	1.120	2.700	0.436
Feb-97	14.129	9.814	8.144	10.489	2.994	1.088	3.176	3.708
Mar-97	17.585	4.814	2.712	4.442	5.025	0.567	2.274	2.386

Apr-97	0.002	0.000	0.000	3.404	2.435	0.745	0.001	1.591
May-97	0.000	0.000	0.000	0.004	0.000	0.000	0.000	0.000
Jun-97	0.000	0.000	0.000	0.000	0.000	0.000	0.000	0.000
Jul-97	0.000	0.000	0.000	0.000	0.000	0.000	0.000	0.000
Aug-97	0.000	0.000	0.000	0.000	0.000	0.000	0.000	0.000
Sept-97	0.000	0.000	0.000	0.000	0.000	0.000	0.000	0.000
Oct-97	0.000	0.000	0.000	0.000	0.000	0.000	0.000	0.000
Nov-97	0.000	0.000	0.001	0.104	0.000	0.000	0.000	0.015
Dec-97	0.551	0.000	1.840	1.991	0.047	0.027	1.239	0.474
Jan-98	7.209	2.109	3.228	8.366	1.016	1.447	#####	9.139
Feb-98	0.852	3.505	10.942	3.956	1.449	0.769	5.201	6.011
Mar-98	1.312	2.280	5.239	6.107	3.571	1.529	2.533	6.241
Apr-98	0.032	1.341	0.751	1.349	0.821	4.946	1.974	5.846
May-98	0.000	0.000	0.000	0.000	0.000	0.000	0.000	0.000
Jun-98	0.000	0.000	0.000	0.000	0.000	0.000	0.000	0.000
Jul-98	0.000	0.000	0.000	0.000	0.000	0.000	0.000	0.000
Aug-98	0.000	0.000	0.000	0.000	0.000	0.000	0.000	0.000
Sept-98	0.000	0.000	0.000	0.000	0.000	0.000	0.000	0.000
Oct-98	0.000	0.000	0.000	0.000	0.000	0.000	0.000	0.000

Nov-98	0.000	8.829	0.084	0.000	0.000	0.193	0.000	0.020
Dec-98	0.000	25.948	5.706	0.379	0.076	0.331	0.000	0.022
Jan-99	0.000	0.215	1.300	4.715	0.700	2.171	8.929	2.349
Feb-99	0.242	2.505	7.439	6.616	2.648	3.439	2.606	3.547
Mar-99	40.009	0.252	2.992	5.938	6.856	0.764	2.706	0.319
Apr-99	0.161	0.224	1.862	0.727	0.718	1.642	2.228	5.122
May-99	0.000	0.000	0.000	6.399	0.000	0.000	0.158	0.000
Jun-99	0.000	0.000	0.000	0.000	0.000	0.000	0.000	0.000
Jul-99	0.000	0.000	0.000	0.000	0.000	0.000	0.000	0.000
Aug-99	0.000	0.000	0.000	0.000	0.000	0.000	0.000	0.000
Sept-99	0.000	0.508	0.000	0.000	0.000	0.000	0.000	0.000
Oct-99	0.000	0.000	0.000	0.000	0.000	0.000	0.000	0.000
Nov-99	0.000	0.002	0.009	0.001	0.000	0.000	0.000	1.958
Dec-99	0.001	0.000	0.796	3.842	0.474	0.616	0.478	3.328
Jan-00	6.308	1.373	11.335	7.735	0.622	1.626	5.672	7.807
Feb-00	3.679	1.176	15.621	0.665	1.189	3.458	0.476	5.646
Mar-00	1.474	0.425	0.982	1.534	0.311	6.980	5.599	6.612
Apr-00	0.405	2.496	0.000	0.000	0.159	0.675	0.272	1.306
May-00	0.000	0.000	0.000	0.000	0.000	0.000	0.000	0.000

Jun-00	0.000	0.000	0.000	0.000	0.000	0.000	0.000	0.000
Jul-00	0.000	0.000	0.000	0.000	0.000	0.000	0.000	0.000
Aug-00	0.000	0.000	0.000	0.000	0.000	0.000	0.000	0.000
Sept-00	0.000	0.000	0.000	0.000	0.000	0.000	0.000	0.000
Oct-00	0.000	0.000	0.000	0.000	0.000	0.000	0.000	0.000
Nov-00	0.000	0.000	0.000	0.749	0.000	0.001	0.000	0.032
Dec-00	0.041	0.004	0.007	8.156	0.193	0.216	0.049	0.278